

**SPIRODIEPOXIDE-BASED CASCADE STRATEGIES TO THE UPPER HEMISPHERE OF
PECTENOTOXIN-4**

by

Da Xu

A dissertation submitted to the

Graduate School-New Brunswick

Rutgers, The State University of New Jersey

In partial fulfillment of the requirements

For the degree of

Doctor of Philosophy

Graduate Program in Chemistry and Chemical Biology

Written under the direction of

Lawrence J. Williams

And approved by

New Brunswick, New Jersey

October, 2014

ABSTRACT OF THE DISSERTATION

Spirodiepoxide-based Cascade Strategies to the Upper Hemisphere of Pectenotoxin-4

By Da Xu

Dissertation Director:

Professor Lawrence J. Williams

Disclosed are studies on allene oxidations and functionally diverse motif. The utilization of spirodiepoxide based methodologies in the synthesis of highly functionalized α -tetrahydrofuranyl- α' -hydroxy ketones led to a cascade strategy to the upper hemisphere of pectenotoxin-4. Remarkably, an advanced allene intermediate with six stereo centers and one epoxide was converted to a C1-C19 sector of pectenotoxin-4 with 9 stereo centers including 3 rings in one pot and 26% yield. It is also shown that electrophile capture with osmium enolates resulted in anti- α -halo- α' -hydroxyketone products. This method complements our spirodiepoxide chemistry in stereoselective conversion of chiral allenes. Finally, we envisioned that a cyclodecatrienone, prepared via C-C fragmentation of a *cis*-decalin derivative, could be built up to Vernonia allenes and other structurally related germacrane by taking advantage of our allene chemistry.

Acknowledgements

I would like to express my sincere gratitude to my advisor Professor Lawrence J. Williams. He has been a great mentor. Through him, I have learned a tremendous amount of knowledge and skill. It has been a great pleasure working for him during the past five years.

I would also like to thank Professor Roger A. Jones, Professor Daniel Seidel and Dr. Hong Zhao for being on my thesis defense committee. I thank them for their participation and helpful suggestions.

I would like to thank all the former and current members in the Williams group. Dr. Madhuri Manpadi and Dr. Michael Drahl are thanked for introducing me to the lab and helping me with my first project. From there, I started my journey. For my last project in the group, I worked with Dr. Rojita Sharama. It was a great pleasure to work with her. Dr. Kai Liu, Libing Yu, and Huan Wang are thanked for their friendship, accompany, and help I am also greatly appreciated that Michael Patrick and Chris Sowa helped reading and correcting the manuscripts.

I would also like to give my sincere thanks to friends in the Seidel group. Chang Min and Chenfei Zhao are thanked for their help with the product characterization.

I would also like to thank Dr. Peng Liu for his inspiring discussions and helpful suggestions.

Finally, I would like to give my deepest gratitude to my wife, parents, sister, and brother-in-law, for their love and support through all these years.

Table of Contents

Abstract	ii
Acknowledgements	iii
List of Figures	vi
List of Schemes	vii
List of Tables	x

Chapter 1: Toward an Integrated Route to the Vernonia Allenes and Related

Sesquiterpenoids

1.1. Background	1
1.2. Result and discussion	5
1.3. Summary	10
1.4. References	10

Chapter 2: Spirodiepoxide-based Cascade Strategies to the Upper Hemisphere of

Pectenotoxin-4

2.1. Background	14
2.2. A Spirodiepoxide(SDE) strategy to PTX-4	34
2.3. Synthetic approach towards C1-C19 sector of PTX-4	46
2.4. Summary	60
2.5. References	60

Chapter 3: Allene Osmylation

3.1. Background	63
3.2. Result and discussion	84
3.3. Summary	98
3.4. References	101

Chapter 4: Experimental Data

4.1. General	107
4.2. Chapter 1	108
4.3. Chapter 2	137
4.4. Chapter 3	178

Appendix: Spectral Data

Spectra of Compounds	203
----------------------------	-----

List of Figures

Figure 1.1	Known natural endocyclic allenes and some related germacrane 2
Figure 2.1	Selected members in the pectenotoxin family 15
Figure 2.2	Acid-catalyzed interconversions between PTXs 16
Figure 2.3	Selected approaches to the ring systems in PTXs 35
Figure 2.4	Catalysts for olefin cross metathesis and observed side products 48
Figure 3.1	Osmium complexes for olefin dihydroxylation in the secondary cycle .. 68
Figure 3.2	Structure of oxo-osmium(VI) pyridine complex 69
Figure 3.3	Proposed osmium enolate and other reported metal enolates 76
Figure 3.4	Common ligands used for olefin osmylation 89

List of Schemes

Scheme 1.1	Enantioselective synthesis of germacrenes and related sesquiterpenes	3
Scheme 1.2	An integrated routing strategy to the xeniolide, xenibellol, and florldide cores.....	4
Scheme 1.3	C-C fragmentation to endocyclic allene 17	5
Scheme 1.4	Synthesis of endocyclic allene 1.47	8
Scheme 1.5	Bromoolefination products from diketone aldehyde 1.41	9
Scheme 2.1	Brimble's synthesis of ABC rings	17
Scheme 2.2	Brimble's synthesis of FG rings	18
Scheme 2.3	Brimble's synthesis of CDE rings	19
Scheme 2.4	Donohoe's oxidative cyclization strategy to ABC Rings of PTX-4	20
Scheme 2.5	Paquette's directed hydrogenation approach to F ring	21
Scheme 2.6	Paquette's synthesis of ABCE rings	22
Scheme 2.7	Pihko's synthesis of ABCD rings	23
Scheme 2.8	Pihko's synthesis of F ring	24
Scheme 2.9	Roush's synthesis of CDE rings	25
Scheme 2.10	Micalizio's synthesis of ABCDE rings	26
Scheme 2.11	Rychnovsky's synthesis of AB spiroketal ring	27
Scheme 2.12	Evans' synthesis of the upper hemisphere of PTX-4	28
Scheme 2.13	Evans' synthesis of the lower hemisphere of PTX-4	28
Scheme 2.14	Finally coupling of PTX-4	29
Scheme 2.15	Murai and Fujiwara's synthesis of C31-C40 fragment	30

Scheme 2.16	Murai and Fujiwara's synthesis of C ring	32
Scheme 2.17	Fujiwara's synthesis of E ring	33
Scheme 2.18	Final coupling of PTX-2	34
Scheme 2.19	Allene diepoxidation to the tetrahydrofuran motif	36
Scheme 2.20	Spirodiepoxide strategy to PTX-4	37
Scheme 2.21	Synthesis of the C21-C29 segment of PTX-4	38
Scheme 2.22	Synthesis of the C30-C40 segment of PTX-4	39
Scheme 2.23	Synthesis of the lower hemisphere of PTX-4	40
Scheme 2.24	A spirodiepoxide-based strategy to the AB ring system of PTX-4	42
Scheme 2.25	A spirodiepoxide-based strategy to the C ring of PTX-4	43
Scheme 2.26	A spirodiepoxide-based strategy to the ABC rings of PTX-4	44
Scheme 2.27	Synthesis of a C1-C10 Weinreb amide	47
Scheme 2.28	Synthesis of a C11-C19 alkyne	49
Scheme 2.29	Convergent assembling of a C1-C19 epoxy allene	50
Scheme 2.30	Synthesis of <i>m</i> -FBn ether protected olefin 2.213	51
Scheme 2.31	Synthesis of a C11-C19 alkyne	51
Scheme 2.32	Preparation of α,β -unsaturated aldehydes via olefin metathesis	53
Scheme 2.33	Catalytic epoxidation of α,β -unsaturated aldehydes	53
Scheme 2.34	Synthesis of C1-C19 epoxy allenyl ketone 2.227	54
Scheme 2.35	Synthesis of the C1-C6 chlorohydrin	55
Scheme 2.36	Synthesis of the C1-C19 epoxy allenyl ketone	56
Scheme 2.37	Oxidative cyclization C1-C19 epoxy allenyl ketone 2.227	58

Scheme 2.38	Oxidative cyclization of a model allenyl ketone.....	59
Scheme 3.1	Proposed mechanism for the Os(VIII)-catalyzed dihydroxylation of olefins	64
Scheme 3.2	The conversion of monoester to diester in solution	65
Scheme 3.3	Selected examples for OsO ₄ promoted oxidative decomposition	67
Scheme 3.4	Stoichiometric allene osmylation by Crabtree and related osmium complexes	70
Scheme 3.5	Face selective DMDO oxidation and allene osmylation	77
Scheme 3.6	Osmylation elimination	80
Scheme 3.7	Osmium addition to an enantiomerically enriched allene	86
Scheme 3.8	Osmium addition to an enantiomerically enriched allene	86
Scheme 3.9	Osmylation/Fluorination of disubstituted allenes	88
Scheme 3.10	Mechanistic framework for the Os(VIII)-catalyzed oxidation of allenes	94
Scheme 3.11	Stoichiometric allene osmylation using 2 equiv of OsO ₄	95
Scheme 3.12	Revised mechanistic framework for osmylation/bromo-addition of trisubstituted allenes	100

Lists of Tables

Table 1.1	Computed torsion angles for potential C-C fragmentation substrates	7
Table 2.1	DMDO oxidation of allenyl aldehydes/ketones	41
Table 3.1	Catalytic allene osmylation	71
Table 3.2	Asymmetric allene osmylation of mono and disubstituted allenes	72
Table 3.3	Asymmetric allene osmylation of trisubstituted aryl allene	72
Table 3.4	Ruthenium catalyzed allene dihydroxylation	75
Table 3.5	Stoichiometric osmylation of cyclic bisallenes	79
Table 3.6	Stoichiometric osmylation of acyclic allenes	81
Table 3.7	Catalytic osmylation of acyclic allene	82
Table 3.8	Initial mechanistic framework for osmylation of trisubstituted allenes with aminohydroxylation reagent	84
Table 3.9	Osmylation/Fluorination of trisubstituted allenes	87
Table 3.10	The effect of additives on osmylation of trisubstituted allenes	91
Table 3.11	Osmylation/Fluorination of trisubstituted allenes under basic conditions	92
Table 3.12	Osmylation/Fluorination of trisubstituted allenes under acidic conditions	93
Table 3.13	Catalytic osmylation using H ₂ O ₂ and <i>t</i> -BuOOH	97
Table 3.14	Osmylation/bromo-addition of trisubstituted allenes	99
Table 3.15	Product derivatization	100

Chapter 1 Toward an Integrated Route to the Vernonia Allenes and Related Sesquiterpenoids¹

1.1 Background

To date, there are well over 200 allene containing natural products are known.²⁻¹¹ Among these, bicyclic germacranolides **1.1-1.3** are the only known endocyclic allene-containing natural products (Figure 1.1). They were isolated by the Bohlmann group from the aerial parts of *Vernonia lilacina* Mart. about 30 years ago.¹²⁻¹⁴ To date, there has been only one synthetic studies toward these interesting 10-membered cyclic allenenes. One possible reason might be the lack of methods for cyclic allene formation which can be applied to complex structure. However, the interest in vernonia allenenes is not only limited to the stereoselective formation of endocyclic ring systems. Our motive was to identify and simplify access to a cluster of selective bioactive sesquiterpenes as well as vernonia.

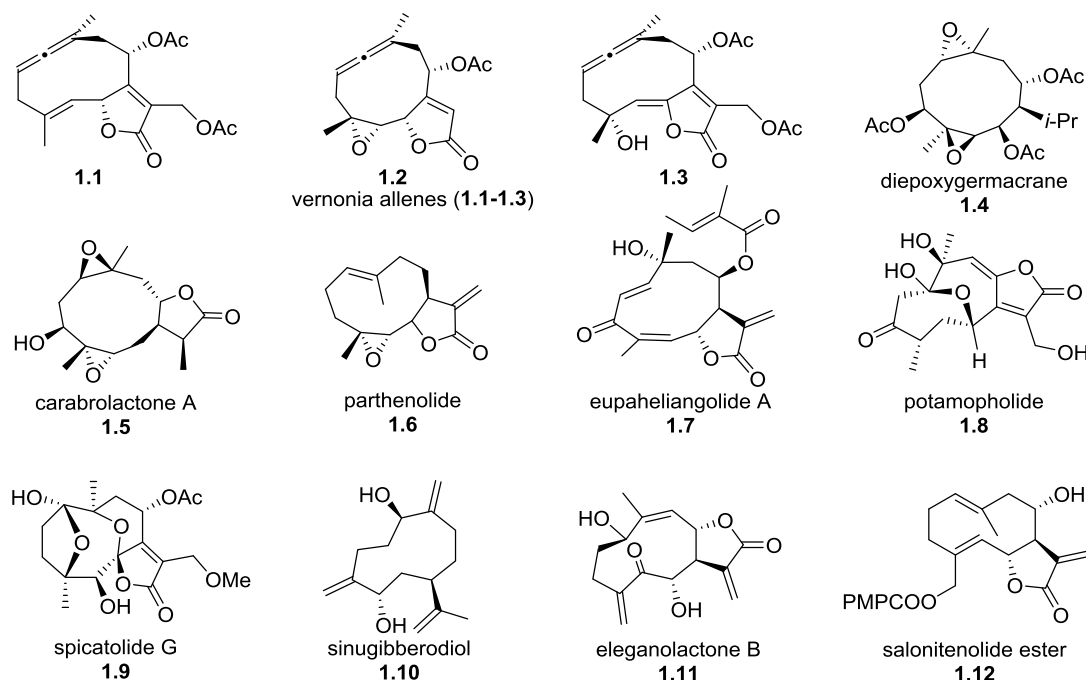
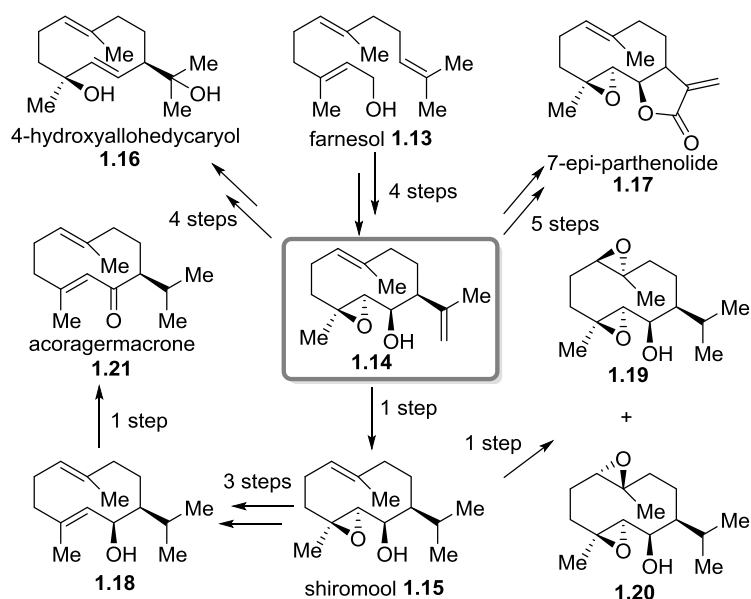


Figure 1.1 Known natural endocyclic allenes and some related germacranes

Germacranes are a large group of sesquiterpenes widely occurring in animals, plants and micro-organisms with anti-inflammatory activities, antibacterial and antifungal activities, anti-cancer activities and other various biological activities, for example (Figure 1.1): parthenolide **1.6** has anti-inflammatory and anti-hyperalgesic effects and induces apoptosis of human acute myelogenous leukemia stem and progenitor cells;^{15,16} eupaheliangolide A **1.7** is cytotoxic to human oral epidermoid (KB), cervical epitheloid (Hela), and liver (hepa59T/VGH) carcinoma cells;¹⁷ sinugibberodiol **1.10** has a potent effect in inhibiting multidrug resistance activity of mammalian tumor cells;¹⁸ elegantolactone B **1.11** inhibits the proliferation of HL-60 human promyelocytic leukemia cell line in a dose-dependent manner;¹⁹ and ester derivatives of salonitenolide **1.12** show promising antibacterial activity.²⁰

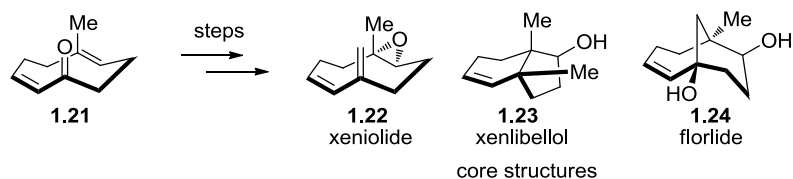
Because of their unique structures, general occurrence, and important roles in biology sesquiterpenes and sesquiterpenoids have received much attention in organic synthesis.²¹

One recent example was provided by the Baran group. In 2012, they advanced an efficient route to 6 structurally related sesquiterpene natural products via chemo- and stereoselective oxidations of a key intermediate **1.14** (Scheme 1.1).²²



Scheme 1.1 Enantioselective synthesis of germacrenes and related sesquiterpenes²²

We have also been exploring an integrated route would enable direct access to a cluster of selective bioactive compounds in a structure space, rather than a single route that targets a specific molecule. This integrated route would be highly useful and offer many advantages, especially in terms of step economy. Recently we reported an integrated routing strategy to access members of the xenicane superfamily. The core ring systems of the xeniolide, xenibellol, and florlide natural products were constructed stereoselectively from an enantioenriched cyclononadienone (Scheme 1.2).²³

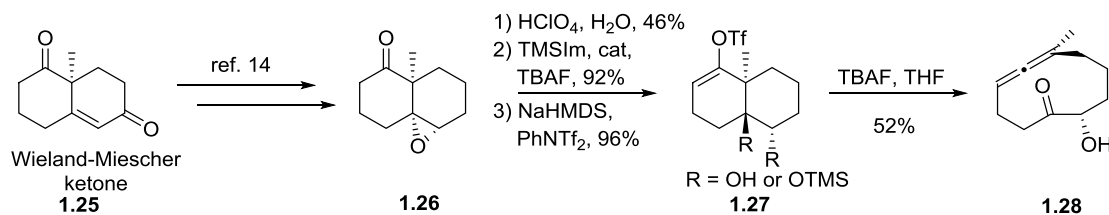


Scheme 1.2 An integrated routing strategy to the xeniolide, xenibellol, and florlide cores²³

Our interest in the vernonia allenes is motivated in part by a desire to identify, and simplify access to, useful bioactive compounds in this germacrane sesquiterpenes structure space. Moreover, functionalized allenes would be great intermediates for an integrated routing strategy, taking advantage of methods for transforming allenes to diverse motifs. Stereoselective preparation of endocyclic allenes in complex settings is not trivial. Several methods for the preparation of endocyclic allenes are known,^{24–28} but the reliability of these methods in preparing advanced endocyclic allene intermediates bearing various functional groups is an issue. Hence, our primary goal was to demonstrate, in a feasibility study, that endo cyclic allenes are readily available.

We extended Eschenmoser's C–C fragmentation method to stereospecifically obtain allenes. In the original report, an endocyclic allene was prepared via fragmentation of a dianion generated from a trans-decalin derivative **1.27** (R = OTMS, Scheme 1.3).^{29,30} The reaction conditions for allene formation are sufficiently mild. But this route suffered from inefficient functional group manipulations, also oxidation prior to fragmentation is not preferred. In principle, this strategy can be used to access endocyclic allene intermediates for an integrated routing strategy that aims to access the structure space represented by a variety of germacrane natural products; however, we needed an improved route to a

better substrate.



Scheme 1.3 C-C fragmentation to endocyclic allene 17^{29,30}

1.2 Result and discussion

1. Computational analysis of C–C fragmentation

For anionic C–C fragmentation reactions to proceed, ideally the bond connecting the leaving group and the C–C bond that is to be cleaved need to occupy an antiperiplanar conformation. This is completely analogous to the E2 elimination. E2 eliminations seem to be more frequently applied in systems with flexibility, where stereochemical requirements can usually be met. C–C fragmentation reactions are more often seen in cyclic systems, where the substrates' reactivities are more sensitive to structural constraints. Designing substrates for C–C fragmentation is considered to be non-trivial. The conformational tolerance and the participation of other functionalities in fragmentation have not yet been fully established. Computational mechanistic studies might provide useful stereoelectronic information about selected fragmentation candidates and increase the reliability of proposed fragmentations.³¹

Our computational studies for selected C–C fragmentation substrates are shown in Table 1.1. The dihedral angles for bonds (shown in blue) from the alcohols ($R/R' = \text{OH}$) and the corresponding alkoxide anions ($R/R' = \text{O}^-$) were taken to approximate the torsion angle of bonds involved in C–C fragmentation from the anionic fragmentation intermediates. For each substrate, the energies of several conformers were minimized (in vacuum) by Gaussian 03 using the B3LYP functional and the 6-31G(d,p) basis set.^{32–40} The results for the relatively low energy conformers with the largest dihedral angles are listed. Entry 1 shows a trans-decalin system, the dihedral angles for which are around 155° , deviate significantly from the ideal 180° . Attempts to optimize the ground state geometries of dianion **1.31** were not successful. Experimentally, the vinyl triflate (**1.27**, $R = \text{OH}$) resisted fragmentation under standard basic conditions. But, the silyl ether (**1.27**, $R = \text{OTMS}$) underwent smooth fragmentation upon exposure to TBAF, presumably via the dianion **1.31** (Scheme 1.3). Entry 2 shows a cis-decalin system containing two double bonds. The dihedral angles for this entry are around 175° , much closer to 180° . For comparison, a cis-hydrindane system was shown in entry 3. The dihedral angles for this entry are around 163° . Importantly, alcohol **1.34** in this entry fragments to give the E-alkene in 60% yield upon treatment with NaH in DMSO.⁴¹ Entry 4 and 5 show some substrates with a methyl ester substituent at the olefin double bond. The ester was chosen as a prototype for substitutions at C–C fragmentation substrates, and it can also serve as a starting point for product derivatization. All substrates in these two entries gave dihedral angles larger than that of entry 3. We also expect alcohol **1.36** and **1.38** to undergo smooth C–C fragmentation under suitable reaction conditions. However, in this case, there appears to be a stereo/electronic difference between the alcohol and anion (**1.36** vs **1.37** and **1.38**

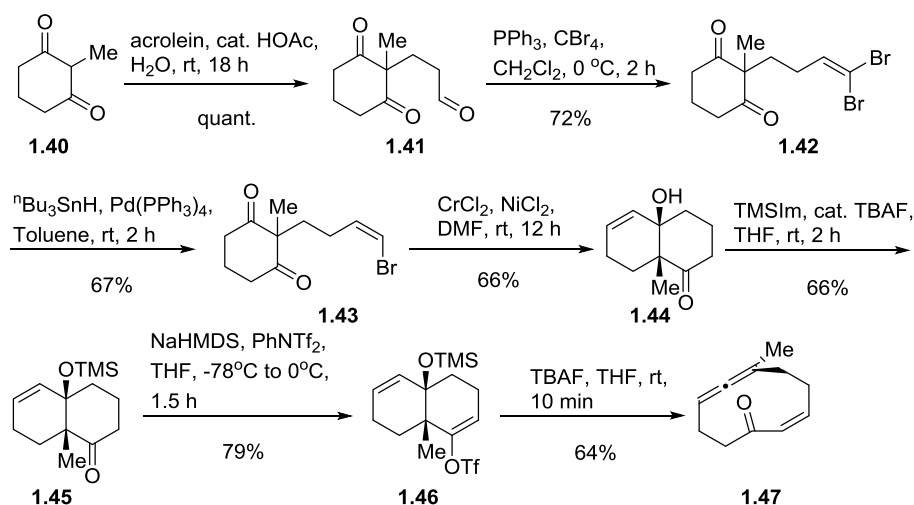
vs **1.39**). The ester is coplanar with the double bond for the alcohols, whereas the ester is slightly twisted out of plane for the alkoxides. This change in conformation implicates some interaction between the alkoxide and ester group which might affect C–C fragmentation.

Table 1.1 Computed torsion angles for potential C–C fragmentation substrates

entry	substrate	R(R')	torsion angle
1		1.27: OH (OH)	153°
		1.29: OH (O-)	155°
		1.30: O- (OH)	156°
		1.31: O- (O-)	see text
2		1.32: OH	175°
		1.33: O-	176°
3		1.34: OH	164°
		1.35: O-	162°
4		1.36: OH	174°
		1.37: O-	177°
5		1.38: OH	171°
		1.39: O-	170°

2. Preparation of the two substrates: bicyclic vinyl triflates

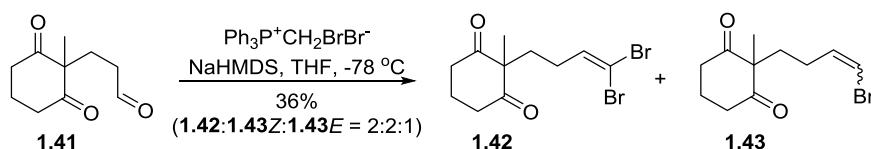
Due to the concern of the alkoxide interacting with the methyl ester, we finally targeted compound **1.46** (Scheme 1.4) as a model for our synthetic studies. Upon treatment with TBAF, the newly formed anion **1.33** should be able to adopt conformers with the proper orientation for fragmentation, as suggested by our computational studies.



Scheme 1.4 Synthesis of endocyclic allene **1.47**

Preparation of the model compound **1.46** commenced from the commercial diketone **1.40** (Scheme 1.4). Alkylation of **1.40** can be easily achieved with bases and activated halides such as allyl bromides or propargyl bromides. However, when reacting with alkyl halides, major products are usually the O-alkylation compounds.⁴² The side chain was then installed using a three step sequence: acid promoted Michael addition with acrolein⁴³ (**1.40**→**1.41**), then Corey-Fuchs dibromoolefination with the aldehyde⁴⁴ (**1.41**→**1.42**), followed by Pd(PPh₃)₄ catalyzed selective reduction of the E-bromo atom using n-Bu₃SnH⁴⁵ (**1.42**→**1.43**). Initially, we prepared vinyl bromide **1.43** using the Wittig reaction with bromomethyl triphenylphosphorane (Scheme 1.5).⁴⁶ 14% yield was obtained when aldehyde **1.41** was treated with equal amounts of the bromomethyl triphenylphosphonium bromide and NaHMDS in THF. Under basic conditions, bromomethyl triphenylphosphorane did not behave well, and both E-vinyl bromo olefin and dibromo olefin were obtained in the product mixture. Bromo group scrambling for related systems under basic conditions is known.^{46,47} To improve the yield, we first evaluated the

influence of the reaction conditions, including the ratio of Wittig reagent relative to aldehyde (1-3 equiv), solvent (tetrahydrofuran and toluene), and aldehyde concentration (0.035-0.09 M). Under all conditions tested, the yield was between 13 and 26%. A different base t-BuOK was then examined, which was suggested to promote the formation of phosphorane efficiently and minimize dihaloolefin formation.⁴⁶ The influence of HMPA and idomethyl triphenylphosphrane was also examined, since they had been shown to increase the Z/E ratio by the Stork group.⁴⁸ However, these conditions all failed to improve the yield of **1.43**.



Scheme 1.5 Bromoolefination products from diketone aldehyde **1.41**

Finally, under mild Nozaki-Hiyama-Kishi conditions vinyl bromide **1.43** cyclized to form the bicyclic alcohol **1.44** in good yield. Intramolecular cyclization of ketones under the Nozaki-Hiyama-Kishi conditions is not usually seen, and the reaction behaved well in this case. TMS protection of tertiary alcohol **1.44** competed with enone ether formation, but a 66% yield of the desired ether was obtained. The installation of the nucleofuge was achieved by preparing the vinyl triflate from ketone **1.45**. Under anhydrous conditions, **1.46** generated an alkoxide anion which promptly underwent C-C fragmentation to give the ten membered endocyclic allene **1.47** that is functionalized with a double bond and a ketone in 64% yield.

1.3 Summary

In principle, the Vernonia allenes and structurally related germacranes are accessible from a ten-membered endocyclic allenes of type **1.47**. To explore a mild and facile method of producing such structures, the C-C fragmentation of selected bicyclic systems were studied by computation, and the resulted strategic target was prepared and evaluated. Out of the candidates studied (**1.27**, **1.29** – **1.39**), a *cis*-decalin derivative **1.46** was chosen. Pleasingly, we prepared allene **1.47** in seven steps *via* cyclodecadienone **1.40** under mild reaction conditions. With all the methodologies involving allene transformations developed by our group^{49–59}, this cyclodecatrienone strategy represents a viable intermediate or intermediate-type, which can be built up to more complex ten membered ring based natural products and natural product-related bioactive compounds.

1.4 References

- (1) Xu, D.; Drahl, M. A.; Williams, L. J. *Beilstein J. Org. Chem.* **2011**, 7, 937.
- (2) Hoffmann-Röder, A.; Krause, N. *Angew. Chem. Int. Ed.* **2004**, 43, 1196.
- (3) Krause, N.; Hoffmann-Röder, A. *Allenic Natural Products and Pharmaceuticals. In Modern Allene Chemistry*; Krause, N.; Hashmi, A. S. K., Eds.; Wiley-VCH: Weinheim, Germany, 2004; pp. 997–1040.
- (4) Since 2003, more than 50 additional allene-containing natural products have been reported, see the following eight recent references for example: Umezawa, T.; Oguri, Y.; Matsuura, H.; Yamazaki, S.; Suzuki, M.; Yoshimura, E.; Furuta, T.; Nogata, Y.; Serisawa, Y.; Matsuyama-Serisawa, K.; Abe, T.; Matsuda, F.; Suzuki, M.; Okino, T. *Angew. Chem. Int. Ed.* **2014**, 53, 3909.
- (5) Zhang, Y.; Fang, H.; Xie, Q.; Sun, J.; Liu, R.; Hong, Z.; Yi, R.; Wu, H. *Molecules* **2014**, 19, 2100.

- (6) Ahn, J. H.; Kim, E. S.; Lee, C.; Kim, S.; Cho, S.-H.; Hwang, B. Y.; Lee, M. K. *Bioorg. Med. Chem. Lett.* **2013**, *23*, 3604.
- (7) Jones, T. H.; Adams, R. M. M.; Spande, T. F.; Garraffo, H. M.; Kaneko, T.; Schultz, T. R. *J. Nat. Prod.* **2012**, *75*, 1930.
- (8) Xie, H.-H.; Yoshikawa, M. *J. Asian Nat. Prod. Res.* **2012**, *14*, 503.
- (9) Gutiérrez-Cepeda, A.; Fernández, J. J.; Norte, M.; Souto, M. L. *Org. Lett.* **2011**, *13*, 2690.
- (10) Maoka, T.; Akimoto, N.; Terada, Y.; Komemushi, S.; Harada, R.; Sameshima, N.; Sakagami, Y. *J. Nat. Prod.* **2010**, *73*, 675.
- (11) Shaker, K. H.; Müller, M.; Ghani, M. A.; Dahse, H.-M.; Seifert, K. *Chem. Biodivers.* **2010**, *7*, 2007.
- (12) Jakupovic, J.; Schmeda-hirschmann, G.; Schuster, A.; Zdero, C.; Bohlmann, F.; King, R. M.; Robinson, H.; Pickardt, J. *Phytochemistry* **1985**, *25*, 145.
- (13) Bohlmann, F.; Zdero, C.; King, R. M.; Robinson, H. *Phytochemistry* **1982**, *21*, 695.
- (14) Bohlmann, F.; Jakupovic, J.; Gupta, R. K.; King, R. M.; Robinson, H. *Phytochemistry* **1981**, *20*, 473.
- (15) Feltenstein, M. W.; Schühly, W.; Warnick, J. E.; Fischer, N. H.; Sufka, K. J. *Pharmacol. Biochem. Behav.* **2004**, *79*, 299.
- (16) Guzman, M. L.; Rossi, R. M.; Karnischky, L.; Li, X.; Peterson, D. R.; Howard, D. S.; Jordan, C. T. *Blood* **2005**, *105*, 4163.
- (17) Shen, Y.-C.; Lo, K.-L.; Kuo, Y. H.; Khalil, A. T. *J. Nat. Prod.* **2005**, *68*, 745.
- (18) Li, N.; Wu, J.; Hasegawa, T.; Sakai, J.; Bai, L.; Wang, L.; Kakuta, S.; Furuya, Y.; Ogura, H.; Kataoka, T.; Tomida, A.; Tsuruo, T.; Ando, M. *J. Nat. Prod.* **2007**, *70*, 998.
- (19) Triana, J.; López, M.; Rico, M.; González-Platas, J.; Quintana, J.; Estévez, F.; León, F.; Bermejo, J. *J. Nat. Prod.* **2003**, *66*, 943.
- (20) Bruno, M.; Rosselli, S.; Maggio, A.; Raccuglia, R. A.; Napolitano, F.; Senatore, F. *Planta Med.* **2003**, *69*, 277.
- (21) Minnaard, A. J.; Wijnberg, J. B. P. A.; de Groot, A. *Tetrahedron* **1999**, *55*, 2115.
- (22) Foo, K.; Usui, I.; Götz, D. C. G.; Werner, E. W.; Holte, D.; Baran, P. S. *Angew. Chem. Int. Ed.* **2012**, *51*, 11491.

- (23) Drahl, M. A.; Akhmedov, N. G.; Williams, L. J. *Tetrahedron Lett.* **2011**, 52, 325.
- (24) Price, J. D.; Johnson, R. P. *Tetrahedron Lett.* **1986**, 27, 4679.
- (25) Christl, M.; Braun, M.; Fischer, H.; Groetsch, S.; Muller, G.; Leusser, D.; Deuerlein, S.; Stalke, D.; Arnone, M.; Engels, B. *European J. Org. Chem.* **2006**, 5045.
- (26) Norbert Krause and Anja Hoffmann-Röder. *Chem. Commun.* **2009**, 5707.
- (27) Brody, M. S.; Williams, R. M.; Finn, M. G. *J. Am. Chem. Soc.* **1997**, 119, 3429.
- (28) Ogasawara, M.; Okada, A.; Nakajima, K.; Takahashi, T. *Org. Lett.* **2009**, 11, 177.
- (29) KAMETANI, T.; FURUYAMA, H.; SUZUKI, Y.; HONDA, T.; TAKAHASHI, H. *J. Pharm. Soc. Japan* **1984**, 104, 147.
- (30) Kolakowski, R. V; Manpadi, M.; Zhang, Y.; Emge, T. J.; Williams, L. J. *J. Am. Chem. Soc.* **2009**, 131, 12910.
- (31) Drahl, M. A.; Manpadi, M.; Williams, L. J. *Angew. Chem. Int. Ed.* **2013**, 52, 11222.
- (32) Ditchfield, R. *J. Chem. Phys.* **1971**, 54, 724.
- (33) Hariharan, P. C.; Pople, J. A. *Theor. Chim. Acta* **1973**, 28, 213.
- (34) Hariharan, P. C.; Pople, J. A. *Mol. Phys.* **1974**, 27, 209.
- (35) McLean, A. D.; Chandler, G. S. *J. Chem. Phys.* **1980**, 72, 5639.
- (36) Vosko, S. H.; Wilk, L.; Nusair, M. *Can. J. Phys.* **1980**, 58, 1200.
- (37) Lee, C.; Yang, W.; Parr, R. G. *Phys. Rev. B* **1988**, 37, 785.
- (38) Becke, A. D. *J. Chem. Phys.* **1993**, 98, 5648.
- (39) Stephens, P. J.; Devlin, F. J.; Chabalowski, C. F.; Frisch, M. J. *J. Phys. Chem.* **1994**, 98, 11623.
- (40) Gaussian 03, 2004.
- (41) Zhang, Y.; Lotesta, S. D.; Emge, T. J.; Williams, L. J. *Tetrahedron Lett.* **2009**, 50, 1882.
- (42) Bedekar, A. V; Watanabe, T.; Tanaka, K.; Fuji, K. *Synthesis-Stuttgart* **1995**, 1069.
- (43) Huddleston, R. R.; Krische, M. J. *Org. Lett.* **2003**, 5, 1143.

- (44) Corey, E. J.; Fuchs, P. L. *Tetrahedron Lett.* **1972**, *13*, 3769.
- (45) Uenishi, J.; Kawahama, R.; Shiga, Y.; Yonemitsu, O.; Tsuji, J. *Tetrahedron Lett.* **1996**, *37*, 6759.
- (46) Matsumoto, M.; Kuroda, K. *Tetrahedron Lett.* **1980**, *21*, 4021.
- (47) Lakhriissi, Y.; Taillefumier, C.; Chretien, F.; Chapleur, Y. *Tetrahedron Lett.* **2001**, *42*, 7265.
- (48) Stork, G.; Zhao, K. *Tetrahedron Lett.* **1989**, *30*, 2173.
- (49) Ghosh, P.; Cusick, J. R.; Inghrim, J.; Williams, L. J. *Org. Lett.* **2009**, *11*, 4672.
- (50) Ghosh, P.; Lotesta, S. D.; Williams, L. J. *J. Am. Chem. Soc.* **2007**, *129*, 2438.
- (51) Ghosh, P.; Zhang, Y.; Emge, T. J.; Williams, L. J. *Org. Lett.* **2009**, *11*, 4402.
- (52) Joyasawal, S.; Lotesta, S. D.; Akhmedov, N. G.; Williams, L. J. *Org. Lett.* **2010**, *12*, 988.
- (53) Katukojvala, S.; Barlett, K. N.; Lotesta, S. D.; Williams, L. J. *J. Am. Chem. Soc.* **2004**, *126*, 15348.
- (54) Liu, K.; Kim, H.; Ghosh, P.; Akhmedov, N. G.; Williams, L. J. *J. Am. Chem. Soc.* **2011**, *133*, 14968.
- (55) Lotesta, S. D.; Hou, Y. Q.; Williams, L. J. *Org. Lett.* **2007**, *9*, 869.
- (56) Sharma, R.; Manpadi, M.; Zhang, Y.; Kim, H.; Ahkmedov, N. G.; Williams, L. J. *Org. Lett.* **2011**, *13*, 3352.
- (57) Sharma, R.; Williams, L. J. *Org. Lett.* **2013**, *15*, 2202.
- (58) Wang, Z. H.; Shangguan, N.; Cusick, J. R.; Williams, L. J. *Synlett* **2008**, 213.
- (59) Yue, Z.; Cusick, J. R.; Ghosh, P.; Ning, S. G.; Katukojvala, S.; Inghrim, J.; Emge, T. J.; Williams, L. J. *J. Org. Chem.* **2009**, *74*, 7707.

Chapter 2 Spirodiepoxide-based Cascade Strategies to the Upper Hemisphere of Pectenotoxin-4

2.1 Background

1. Isolation, structure and biological activity

Pectenotoxin (PTX, Figure 2.1) is a family of lipophilic polyether phycotoxins produced by the marine dinoflagellate genus *Dinophysis*, which has been described as accumulating in certain foods and possibly causing poisoning in human.¹ **PTX-1** to **-5** were first isolated from the hepatopancreas (digestive glands) of the scallop *Patinopecten yessoensis* by Yasumoto and co-workers in 1984.^{2,3} The structure assignment of **PTX-1** is supported by X-ray crystallographic studies and other characterization methods, but the absolute configuration was not confirmed until 1997, by NMR spectroscopy using a chiral anisotropic reagent.⁴

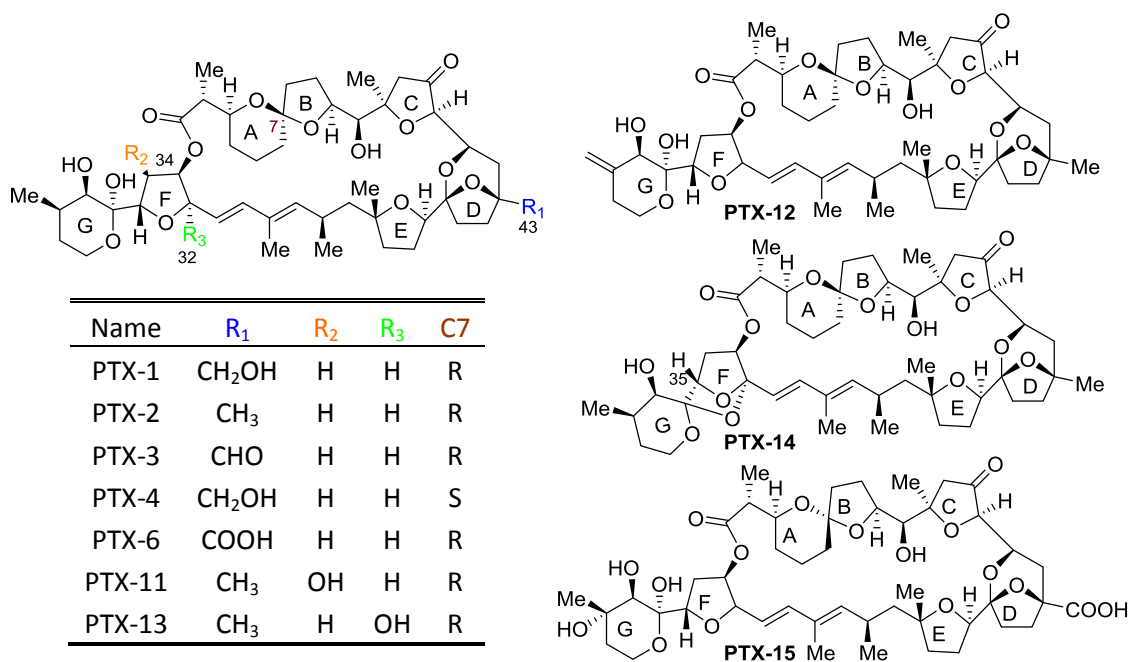


Figure 2.1 Selected members in the pectenotoxin family

PTXs are 34-membered macrolides featuring four substituted tetrahydrofuran rings, a 1,3-diene and several ketals. Currently, there are more than 14 members in the pectenotoxin family. The structures of **PTX-5** and **PTX-10** have not yet been determined. All PTXs absorb UV light between 235 and 239 nm, which is between the wavelength of the maximum absorption for 1,3-butadiene (217nm) and 1,3,5-hexatriene (258nm). **PTX-7**, **PTX-6**, **PTX-9** and **PTX-4**, **PTX-1**, **PTX-8** are inter convertible when treated with diluted acids (Figure 2.2),⁵ and **PTX-2** is stable for more than 24 h in phosphate buffers between pH 4.5 and 9.1.⁶ Some of the PTXs such as **PTX-1**, **PTX-3**, **PTX-6**, and **PTX-2** seco acid (**PTX-2sa**) are suggested to be shellfish metabolites or artifacts of **PTX-2**. There are two known metabolic pathways for **PTX-2**. It can be oxidized progressively at C43 to an alcohol (**PTX-1**), aldehyde (**PTX-3**), and carboxylic acid (**PTX-6**). The oxidation of the methyl group leads to reduced toxicity. It can also be hydrolyzed by enzymes in scallops to **PTX-2sa**, which is much less toxic.¹

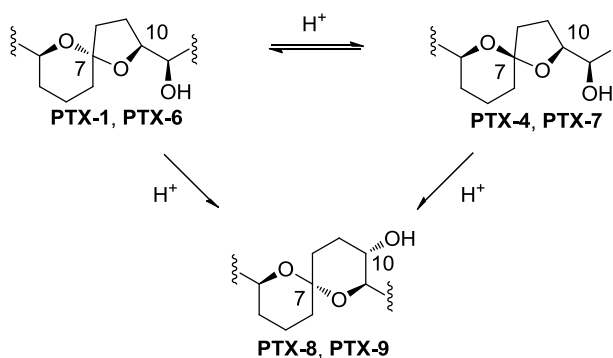


Figure 2.2 Acid-catalyzed interconversions between PTXs⁵

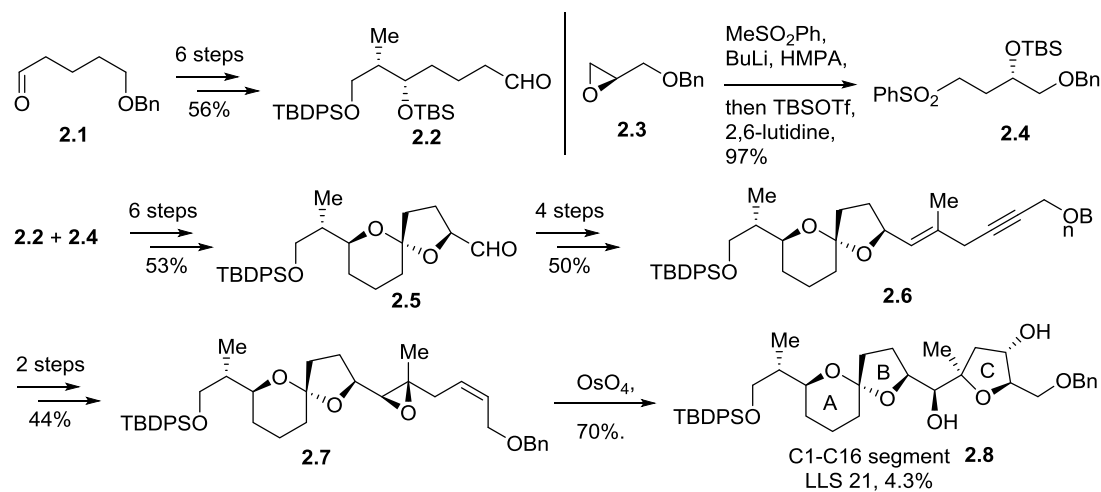
PTXs were initially categorized as a group of diarrhetic shellfish poisoning (DSP) toxins. Since no human poisonings from PTXs have been confirmed, nor do they induce diarrhea in animal studies, they were later removed from the DSP toxin group, however, some are potent bioactive compounds. PTXs are highly toxic to mice via intraperitoneal injection.¹ **PTX-1**, **PTX-6**, and **PTX-9** can induce damage in the actin cytoskeleton and reduce viability of primary cultured rat hepatocytes.⁷ **PTX-2** can form a complex with G-actin, and effectively inhibit actin polymerization.⁸ **PTX-2** was also reported to display cytotoxicity in certain human cancer cells.⁹

2. Previous synthetic approaches

The structural complexity of PTXs, along with their interesting bioactivities, has generated much attention. To date, 11 research groups have been involved in the pursuit of total syntheses of the PTXs. Their work is summarized below.

PTX-2 segments synthesized by the Brimble group

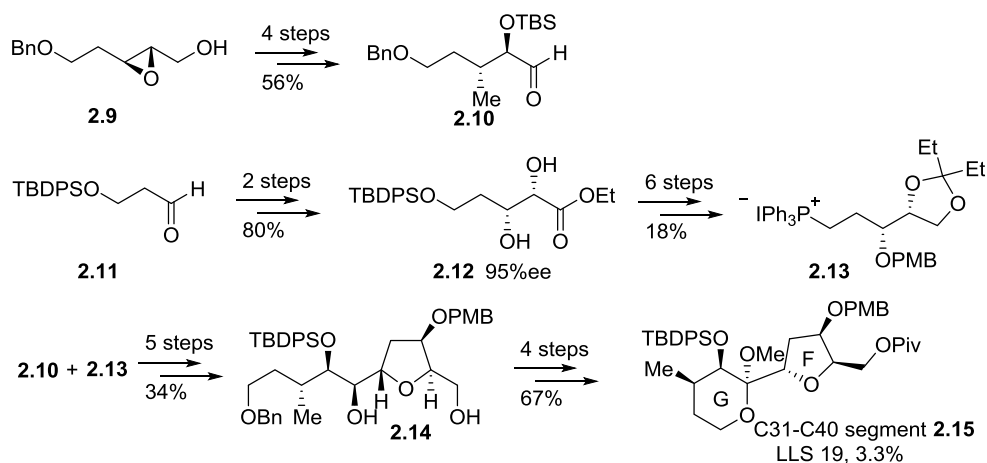
The Brimble group published syntheses of the C1-C16 ABC ring, C12-C28 CDE ring and C31-C40 FG ring segments.¹⁰⁻¹⁴ In their synthesis of the C1-C16 segment (Scheme 2.1),¹⁰⁻¹² the AB spiroketal rings were prepared via a four step sequence, including coupling of aldehyde **2.2** and sulfone **2.4**, oxidation of the resulting α -hydroxysulfone, reductive desulfonylation of the α -sulfonylketone, and acid promoted bicyclic ketal formation. The C ring backbone was constructed by Wittig olefination of the aldehyde **2.5** ($E:Z = 100:1$), transferring the α,β -unsaturated ester into the corresponding allylic iodide and coupling of the unstable allylic iodide and lithium acetylide ($E:Z = 3.1:1$). The epoxide in bicycle **2.7** was formed via Shi oxidation (37% yield). Finally, spontaneous cyclization of the Sharpless asymmetric dihydroxylation product obtained from **2.7** completed the synthesis of the C1-C16 segment **2.8**.



Scheme 2.1 Brimble's synthesis of ABC rings¹⁰⁻¹²

In 2007, the Brimble group reported a synthesis of the C31-C40 FG ring segment (Scheme 2.2).¹³ The backbone was assembled via Z-selective Wittig reaction between aldehyde **2.10**

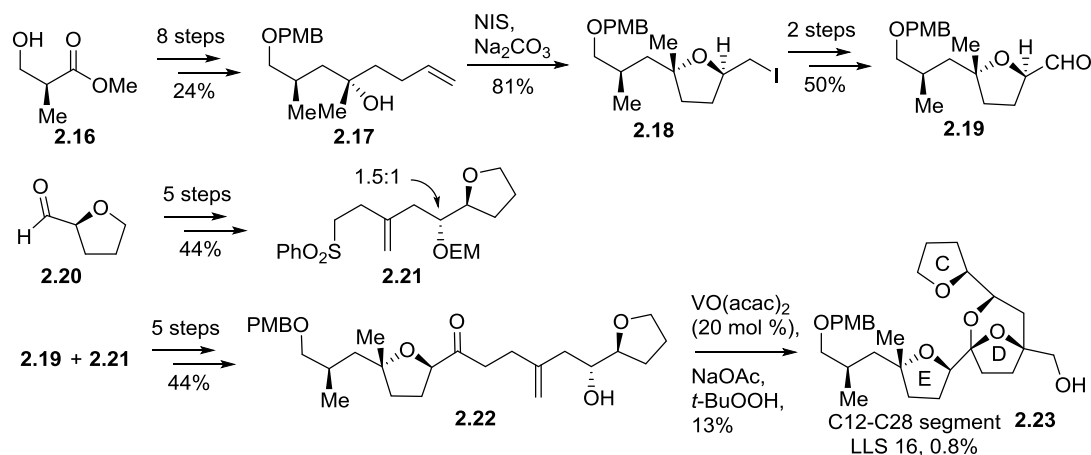
and phosphonium salt **2.13**. The olefin was then oxidized via a hydroxyl group directed stereoselective epoxidation using *m*-CPBA after deprotection of the secondary OTBS group. Acid promoted 5-*exo*-tet cyclization of the epoxide yielded the F ring. Dess–Martin periodinane oxidation of the newly formed secondary alcohol in **2.14** provided the appropriately functionalized acyclic framework. Lastly, the intermediate hemiacetal was protected as the methoxy ketal **2.15**.



Scheme 2.2 Brimble's synthesis of FG rings¹³

The Brimble group also reported a synthesis of the C12-C28 CDE ring segment (Scheme 2.3).¹⁴ It was constructed via a cascade cyclization of a triol generated from VO(acac)₂ promoted epoxidation of the homoallylic alcohol **2.22**. The alcohol **2.22** was assembled using the same strategy as in their AB ring segment synthesis, via the union of the E ring aldehyde **2.19** which was synthesized from Roche ester **2.16**, with the C ring sulfone **2.21**. The carbon skeleton of **2.16** was elongated via cyanide displacement and addition of a homoallyl Grignard reagent, and the E ring was constructed via iodoetherification. The sulfone **2.21** was prepared by addition of a functionalized allyl indium reagent to (S)-

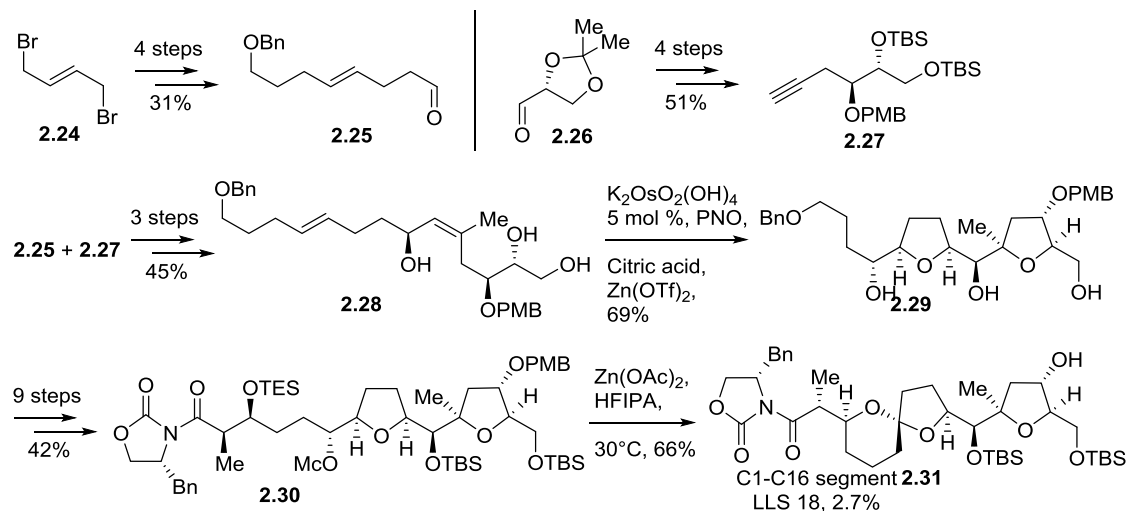
tetrahydrofuran aldehyde **2.20**, followed by subsequent standard functional group manipulations.



Scheme 2.3 Brimble's synthesis of CDE rings¹⁴

PTX-4 segments synthesized by the Donohoe group

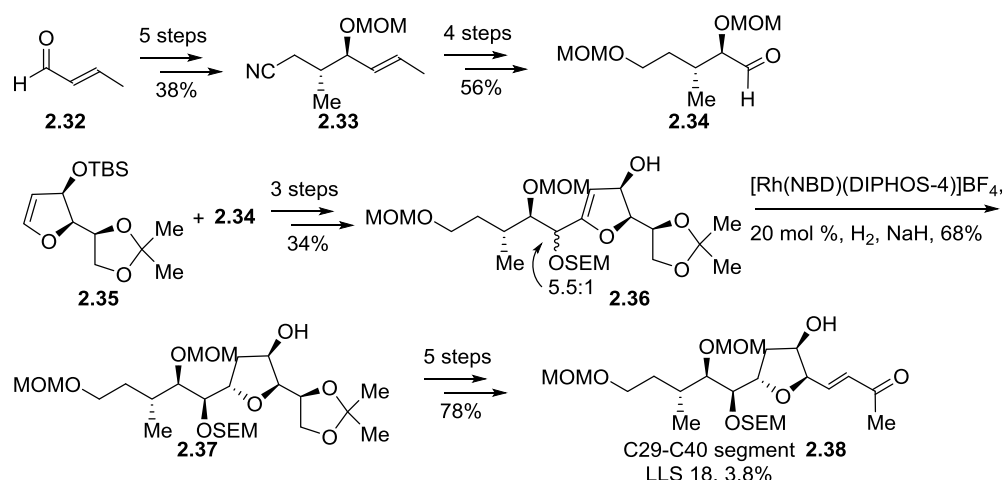
In 2013, the Donohoe group reported an efficient synthesis of C1-C16 segment of PTX-4, using their osmium catalyzed oxidative cyclization method in the construction of the BC rings (Scheme 2.4).¹⁵ The substrate for oxidative cyclization **2.28** was prepared via Carreira reaction between alkyne **2.27** and aldehyde **2.25** followed by catalytic regio- and stereoselective methylation and desilylation. Treatment of **2.28** with $\text{K}_2[\text{OsO}_2(\text{OH})_4]$, pyridine *N*-oxide and $\text{Zn}(\text{OTf})_2$ at 80°C in acetonitrile and buffer gave the desired bis-cycle **2.29** in 69% yield. Finally, the hydride-shift-initiated spiroketalization of **2.30** was promoted by $\text{Zn}(\text{OAc})_2$ in a polar solvent, hexafluoroisopropanol, giving the final C1-C16 ABC ring segment **2.31** of PTX-4.



Scheme 2.4 Donohoe's oxidative cyclization strategy to ABC Rings of PTX-4¹⁵

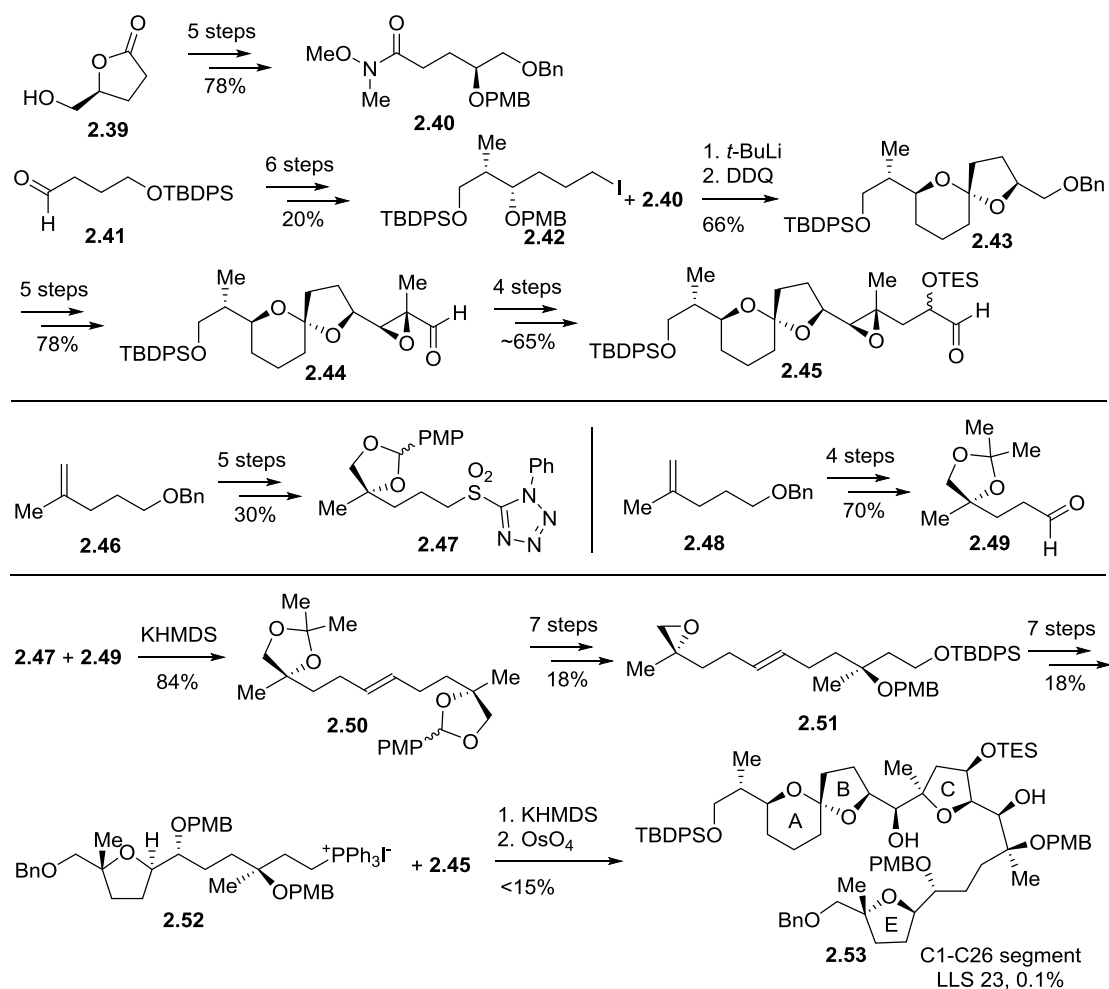
PTX-2 segments synthesized by the Paquette group

In 2002, the Paquette group reported a synthesis of the C29-C40 F ring fragment **2.38** (Scheme 2.5),^{16,17} featuring an alkoxide-directed hydrogenation to form the F ring with a rhodium based cationic catalyst. The substrate for hydrogenation, enol ether **2.36**, was prepared by coupling dihydrofuran **2.35** with aldehyde **2.34**, which was prepared from *E*-crotonaldehyde via Evans' *anti*-aldol reaction, cyanide displacement, ozonolysis, and subsequent protection/deprotection.



Scheme 2.5 Paquette's directed hydrogenation approach to F ring^{16,17}

The preparation of C1-C26 ABCE ring fragment was reported by the Paquette group in 2007 (Scheme 2.6).^{18,19} Segment **2.53** was assembled from the subunits AB ring aldehyde **2.45** and E ring phosphonium salt **2.52**. The AB spiroketal was formed from convergent coupling of an alkyl iodide **2.42** with a Weinreb amide **2.40**, followed by two chain extensions using Wittig reactions. The Julia olefination product from the sulfone **2.47** and aldehyde **2.49** was converted to an epoxy olefin **2.51** in 7 steps. Subsequent Sharpless asymmetric dihydroxylation of **2.51** followed by acid promoted epoxide opening gave the E ring. It was then derivatized to phosphonium salt **2.52**, which was then combined with aldehyde **2.52**. Stoichiometric osmylation of the Wittig reaction product was accompanied by spontaneous cyclization to give the C1-C26 segment **2.53** as the final product.

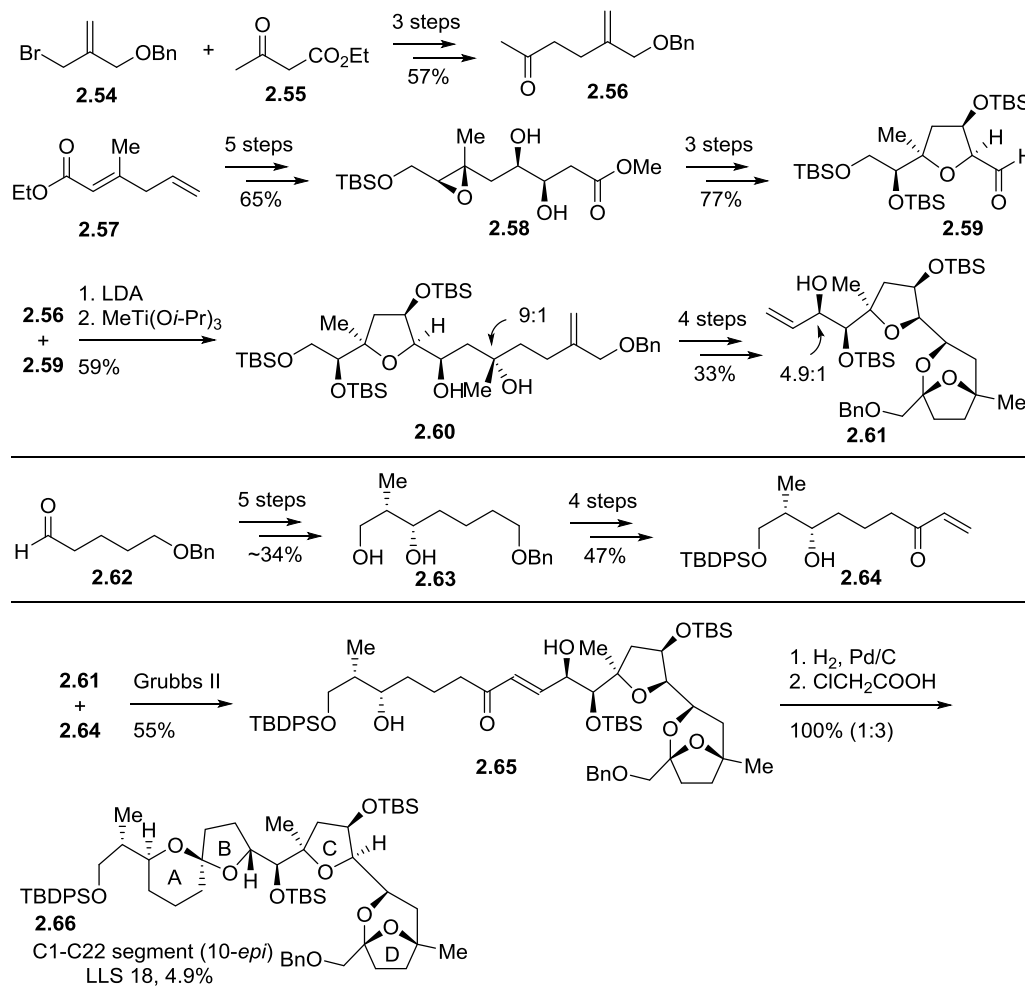


Scheme 2.6 Paquette's synthesis of ABCE rings^{18,19}

PTX-2 segments synthesized by the Pihko group

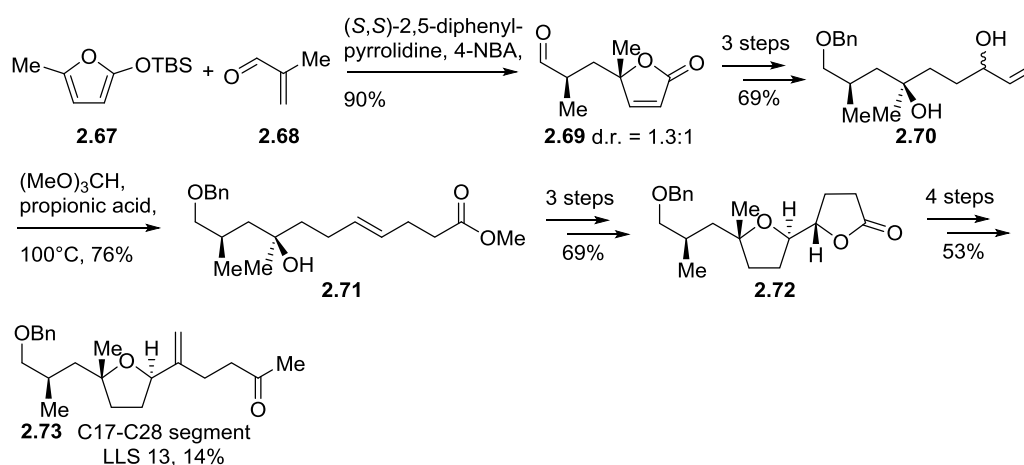
The Pihko group presented 10-epi ABCD ring, C10-C26 CDE ring and C17-C28 F ring segment syntheses (Scheme 2.7).^{20–24} Their route to the 10-epi ABCD ring segment **2.66** features an olefin cross metathesis of vinyl alcohol **2.61** and enone **2.64**.²³ Synthesis of vinyl alcohol **2.61** is shown on the top part of Scheme 2.7. Following a Cornforth-selective aldol reaction using ketone **2.56** and C ring aldehyde **2.59**, an *anti* diol **2.60** was obtained by methyl addition by $\text{MeTi}(\text{O}i\text{-Pr})_3$. **2.60** was then converted into a bicyclic ketal after ozonolysis of the double

bond. Finally, vinyl magnesium bromide addition to an aldehyde in the last step of this sequence gave the vinyl alcohol **2.61** in 4.9:1 dr, favoring the undesired product. The preparation of enone **2.64** was accessed via aldehyde **2.62** in 9 steps, including an Evans' *syn*-aldol reaction and vinylmagnesium bromide addition to a lactone intermediate. The cross metathesis between **2.64** and **2.61** was achieved using the Grubbs 2nd generation catalyst to afford a *trans*-olefin in 48–55% yield. After hydrogenation, the spiroketalization was achieved under different acidic conditions.



Scheme 2.7 Pihko's synthesis of 10-*epi*-ABCD rings^{20–23}

In 2007, the Pihko group revealed their enantioselective synthesis of C17-C28 F ring segment **2.73** using a catalytic enantioselective Mukaiyama-Michael reaction as the key step (Scheme 2.8). Firstly, the Mukaiyama-Michael product aldehyde **2.69** was converted to allylic alcohol **2.70**. The following Johnson-Claisen rearrangement cleanly afforded olefin **2.71** as an essentially pure *E*-isomer. Sharpless asymmetric dihydroxylation led to diol formation and spontaneous lactone formation. After activating the C23 secondary alcohol via selective mesylation, the F ring was formed by treating the mesylate with 2,6-lutidine at 120°C, giving compound **2.72**. Finally, a four step sequence converted the lactone to a methyl ketone with a terminal olefin (**2.73**).

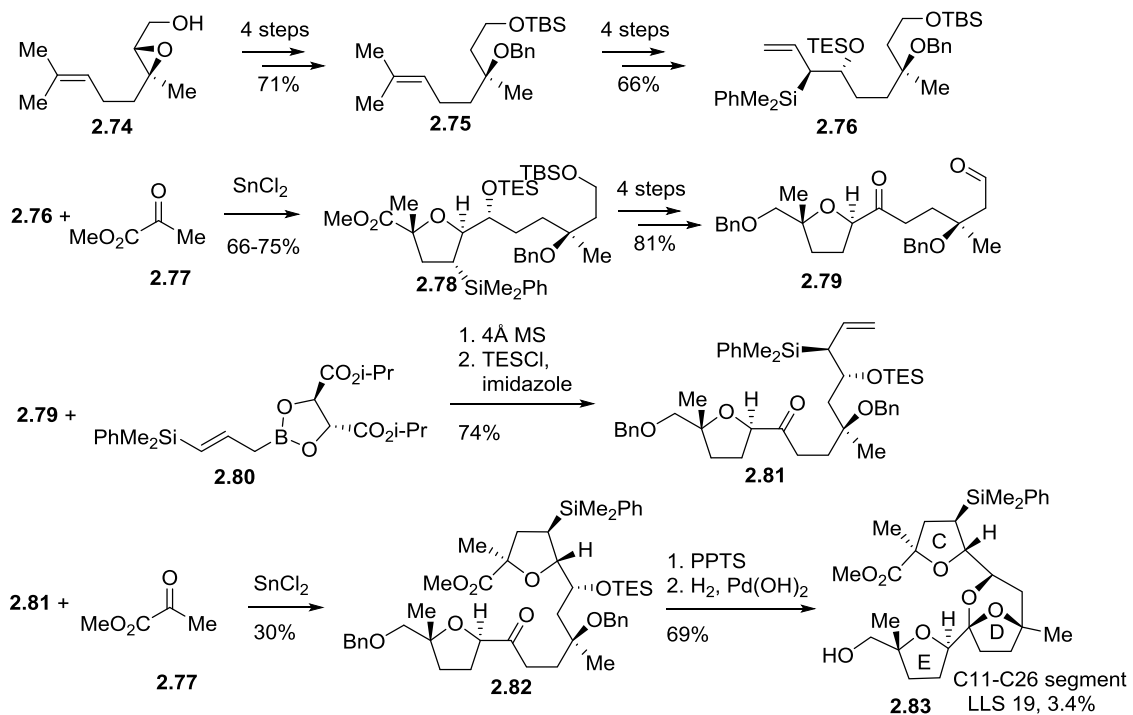


Scheme 2.8 Pihko's synthesis of F ring²⁴

PTX-2 segments synthesized by the Roush and Micalizio group

In 2001, Micalizio and Roush reported their synthesis of the **PTX-2** C11-C26 CDE ring segment (**2.83**) utilizing their allylsilane chemistry (Scheme 2.9).²⁵ The first chelation controlled stereoselective [3 + 2] annulation between allylsilane **2.76** and methyl pyruvate

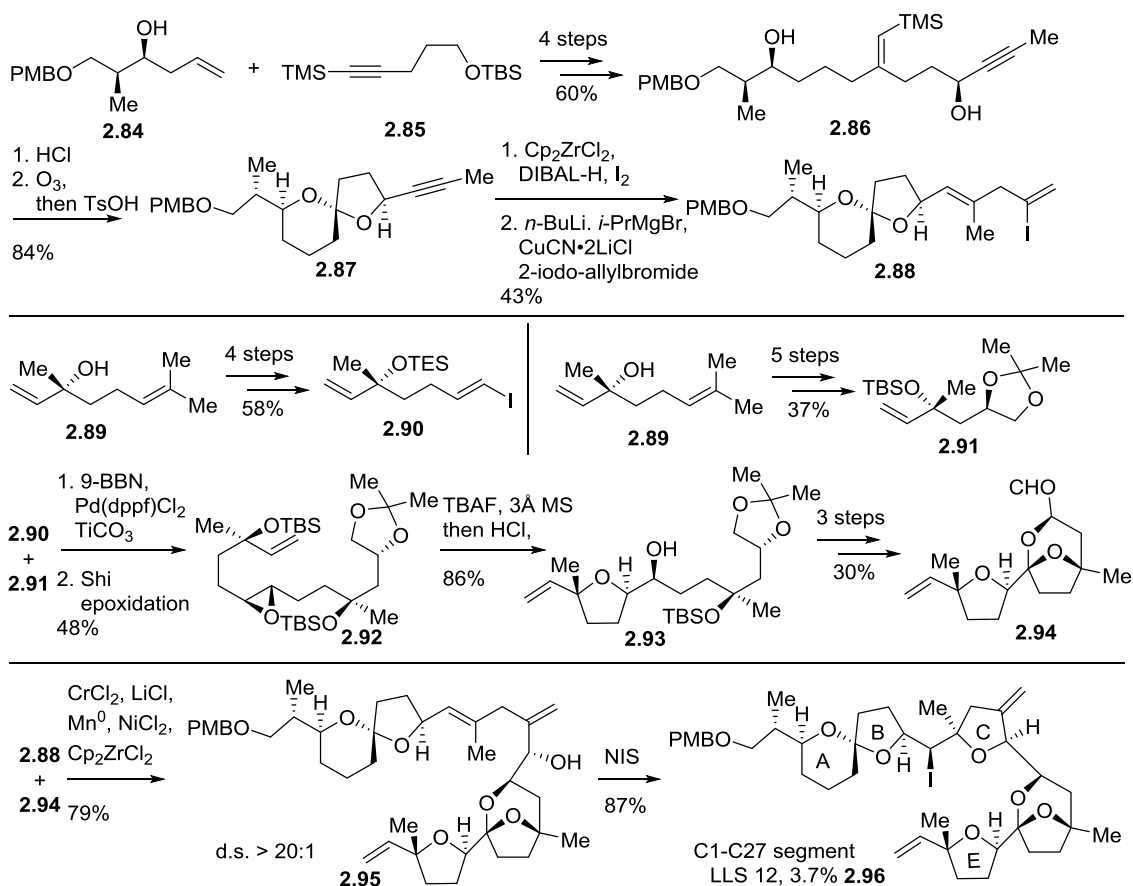
2.77 afforded the E ring product **2.78** in 66-75% yield (>20:1 ds). The second annulation between allylsilane **2.81** and methyl pyruvate provided a 1:1 mixture of C ring product **2.82** and an allylated product in 60% yield. But the stereochemistry at C15 is opposite to that of the natural product. Allylsilanes **2.76** and **2.81** were synthesized by asymmetric silylallylboration of the corresponding aldehydes with γ -silylallylboranes.



Scheme 2.9 Roush's synthesis of CDE rings²⁵

Micalizio reported an independent approach to the total synthesis of **PTX-2**. His strategy for the C11-C27 ABCDE ring segment **2.96** involved an asymmetric Nozaki-Hiyama-Kishi coupling of two subunits vinyl iodide **2.88** and aldehyde **2.94** (Scheme 2.10).^{26,27} The vinyl iodide piece **2.88** was prepared from titanium-mediated hydroxyl-directed reductive cross coupling between alkene **2.84** and alkyne **2.85**. Protodesilylation of propargyl alcohol **2.86**,

followed by ozonolysis and acid-promoted dehydration produced the AB spiroketal ring. Aldehyde **2.94** was obtained through hydroboration/Suzuki coupling of vinyl iodine **2.90** and terminal olefin **2.91**. The following Shi epoxidation, selective desilylation and acid promoted cyclization, delivered the E ring intermediate **2.93**, which was subsequently functionalized to the tricyclic aldehyde **2.94**.

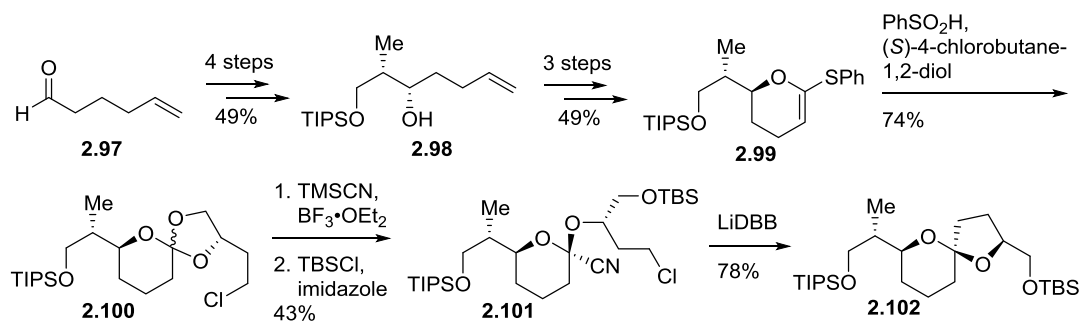


Scheme 2.10 Micalizio's synthesis of ABCDE rings^{26,27}

PTX-2 segments synthesized by the Rychnovsky group

The Rychnovsky group provided a new strategy for stereoselective generation of the non-

anomeric AB spiroketal ring in **PTX-2** (Scheme 2.11).^{28,29} Taking advantage of axial-selective reductive lithiation of the 2-cyano tetrahydropyran ring in **2.101**, the spiroacetal center with desired non-anomeric conformation was formed with high diastereoselectivity (**2.101**→**2.102**). Upon treatment of CSA in CH₂Cl₂, **2.102** was converted to the more stable anomeric spiroketal in 83% yield.

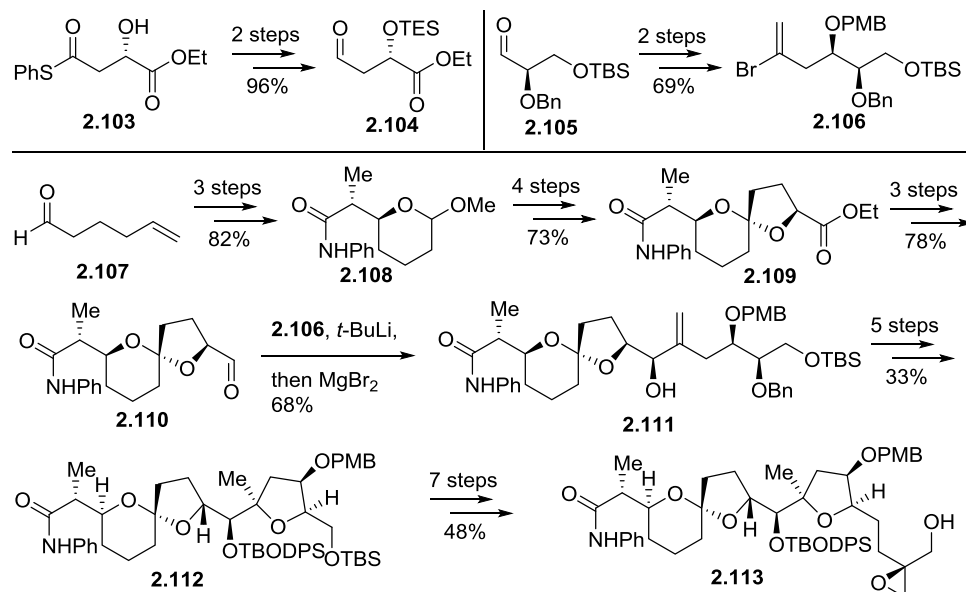


Scheme 2.11 Rychnovsky's synthesis of AB spiroketal ring^{28,29}

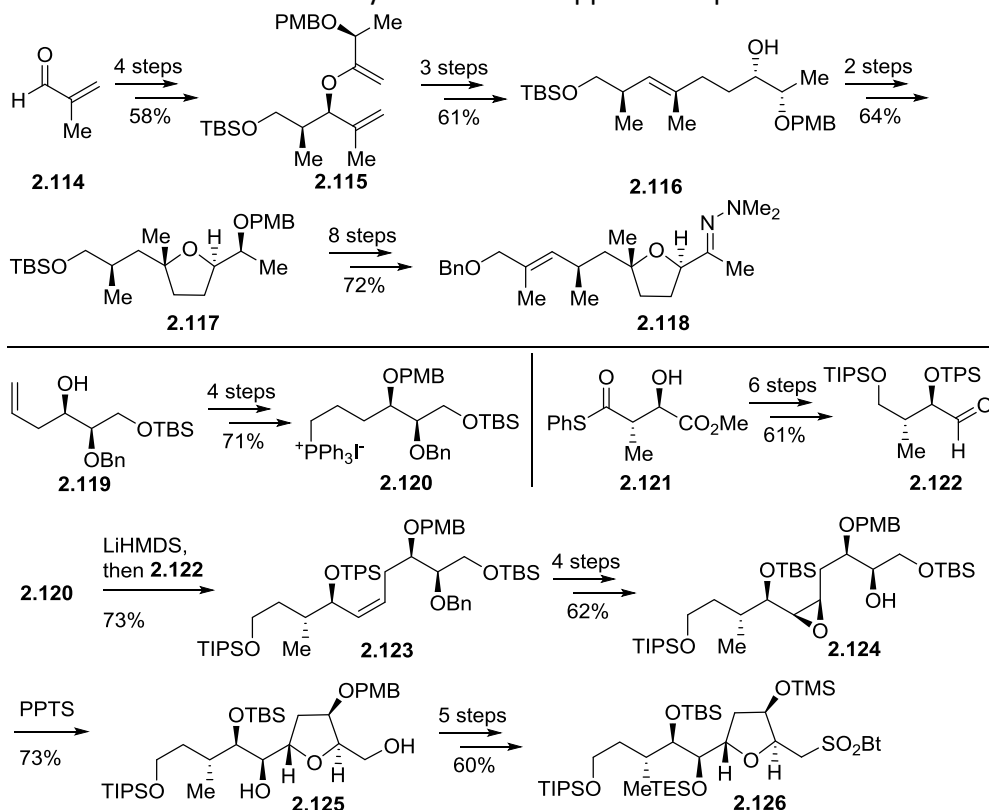
Evans' total synthesis of PTX-4 and PTX-8

The first total synthesis in the PTX family was achieved by the Evans group in 2002.^{30,31} Their strategy included disconnections across the C1-O33 ester bond, the C19-C20 C-C bond and the C30-C31 olefin bond, resulting in three advanced intermediates: C1-C19 ABC ring segment **2.113**, C20-C30 E ring segment **2.118** and C31-C40 F ring segment **2.126**. The C1-C19 segment **2.113** was synthesized via sequential coupling of four pieces: methoxy ketal **2.108**, aldehyde **2.104**, vinyl bromide **2.106** and 2-(benzyloxymethyl)allyltributylstannane (Scheme 2.12). In particular, the Wittig reaction between the phosphonium salt generated from **2.108** and aldehyde **2.104** delivered the AB spiroketal with high yield and diastereoselectivity. Scheme 2.13 shows the synthesis for the other two segments. The C20-

C30 backbone was prepared efficiently via Claisen rearrangement of 1,5-diene **2.115**, followed by chelation controlled $\text{Zn}(\text{BH})_4$ reduction. The C31-C40 backbone was assembled by Wittig reaction of phosphonium salt **2.120** and aldehyde **2.122** with high stereoselectivity.

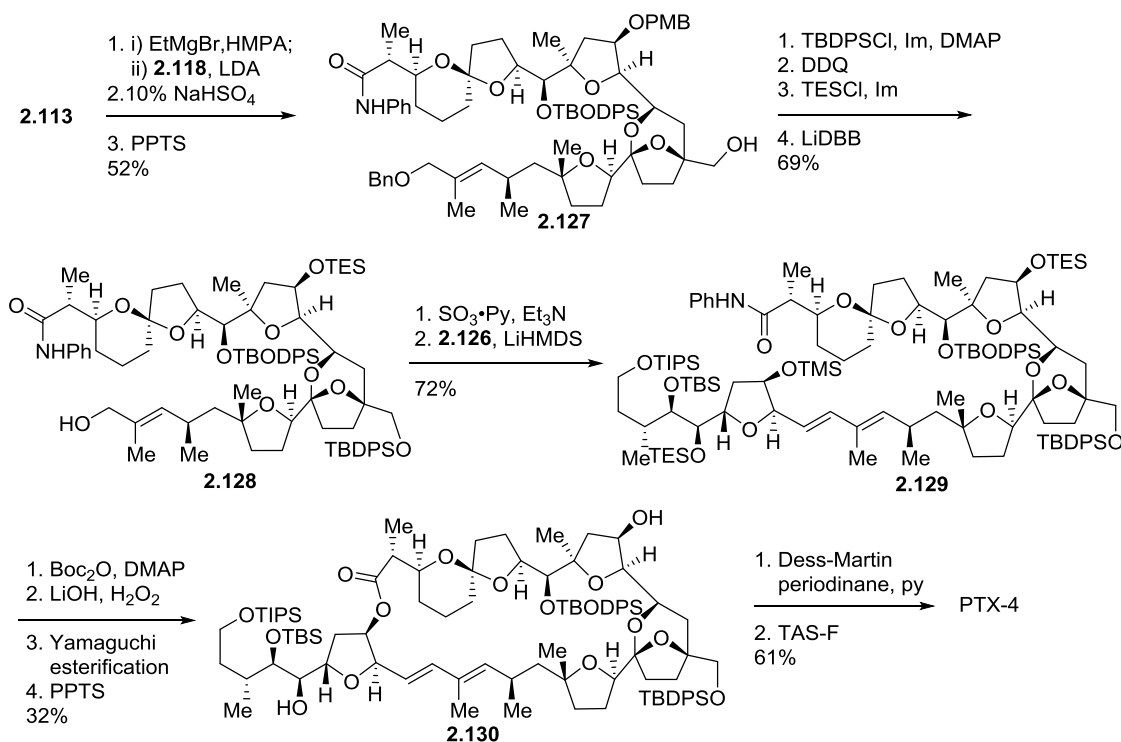


Scheme 2.12 Evans' synthesis of the upper hemisphere of **PTX-4**



Scheme 2.13 Evans' synthesis of the lower hemisphere of **PTX-4**

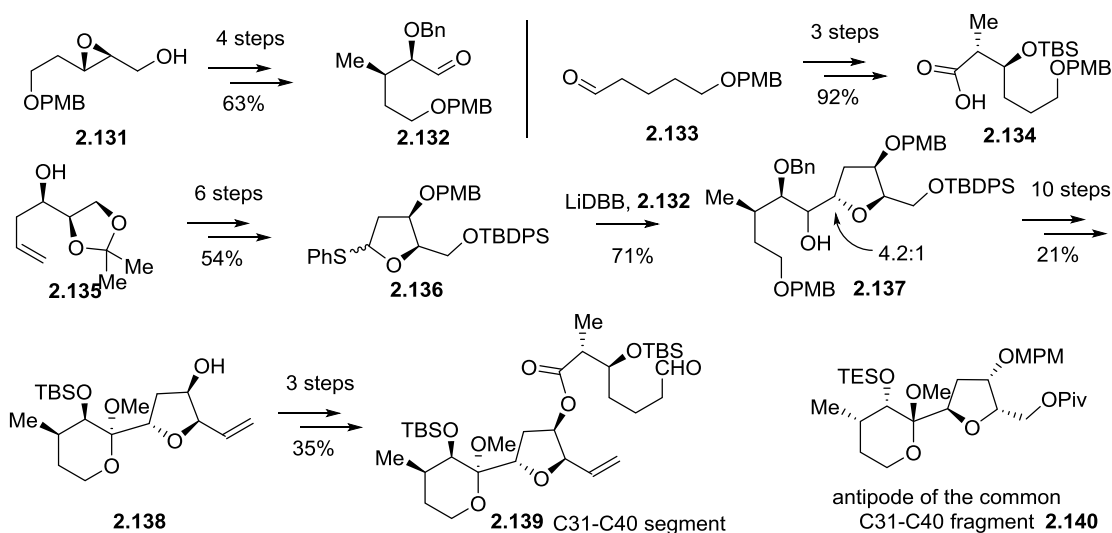
In the final coupling stage, the metalloenamine derived from **2.118** was coupled with the MgBr_2 activated epoxy alcohol **2.113** to give a hydrazinyl lactol intermediate which was then hydrolyzed to yield the ABCDE segment **2.127**. **2.127** was then converted into an aldehyde and coupled with sulfone **2.126** via Julia olefination. Subsequent macrolactonization was achieved under Yamaguchi conditions; however, this transformation is not well-described, and appears to be highly inefficient. Selective desilylation and oxidation of **2.130** afforded the final G ring. Finally, global deprotection completed the total synthesis of **PTX-4** in 36 steps (longest linear sequence) and 0.3% overall yield. **PTX-8** was also obtained via acid promoted isomerization of **PTX-4**.



Scheme 2.14 Finally coupling of **PTX-4**

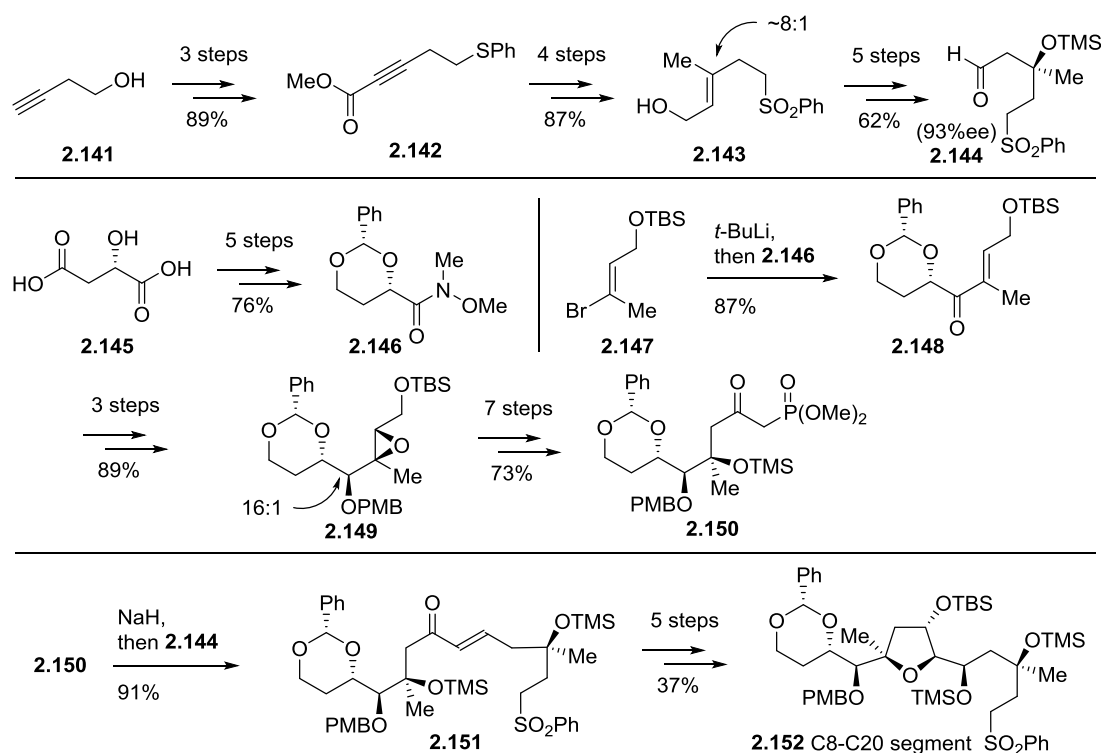
Fujiwara' total synthesis of PTX-2

Murai, Fujiwara, and coworkers were the first to report their total synthesis towards the natural product **PTX-2**. And in 2014, the Fujiwara group also reported the first total synthesis of **PTX-2**. They first published the synthesis of the FG ring common segment **2.140** in 1997 (Scheme 2.15).³² Due to the lack of information about the absolute configuration at that time, the synthesized structure is antipodal to the natural product; however synthesis of the correct enantiomer was reported in 2005.³³ In their revised route, the C31-C40 FG rings segment **2.139** was prepared via the coupling of three pieces: α -phenylthiotetrahydrofuran **2.136** prepared from D-glyceraldehyde acetonide derived homoallyl alcohol **2.135**, aldehyde **2.132** prepared in 4 steps from the known epoxide **2.131**, and carboxylic acid **2.134** prepared via Evan's *syn*-aldol reaction. The first coupling was achieved via α -lithiation of **2.136** and subsequent addition to aldehyde **2.132**, giving a 4.2:1 mixture of diastereomers at C-35 favoring the desired one. The second coupling was promoted by DCC/DMAP after selective PMB ether cleavage.



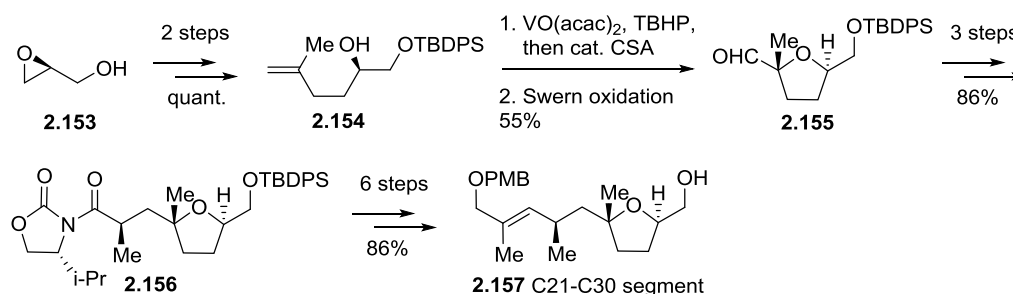
Scheme 2.15 Murai and Fujiwara's synthesis of C31-C40 fragment

The Murai and Fujiwara groups reported three synthetic routes for C ring segments.^{34–36} The most recent one involves a Horner-Wadsworth-Emmons reaction of a functionalized C16–C20 aldehyde **2.144** and a phosphonate **2.150** (Scheme 2.16). Firstly, aldehyde **2.144** was prepared from 3-butyn-1-ol **2.141**. The stereochemistry at C18 was setup by Sharpless asymmetric epoxidation followed by LiAlH_4 mediated epoxide opening. The allyl alcohol substrate **2.143** was formed via Z-selective addition of thiophenol **2.142** and subsequent methyl cuprate addition. Then, phosphonate **2.150** was accessed via coupling of Weinreb amide **2.146** and a known bromoalkene **2.147**. The direct coupling product, enone **2.148**, was reduced diastereoselectively by chelation controlled $\text{Zn}(\text{BH}_4)_2$ reduction. The stereochemistry at C12 was setup in a similar way as for C18. Lastly, a similar sequence, ketone reduction and alkene epoxidation, was employed in converting the aldehyde and phosphonate to the coupling product enone **2.151**. However, the stereoselectivity is not satisfying, being 9.7:1 at C16 via DIBAL-H reduction and only 3.7:1 at C18 via *m*CPBA oxidation.



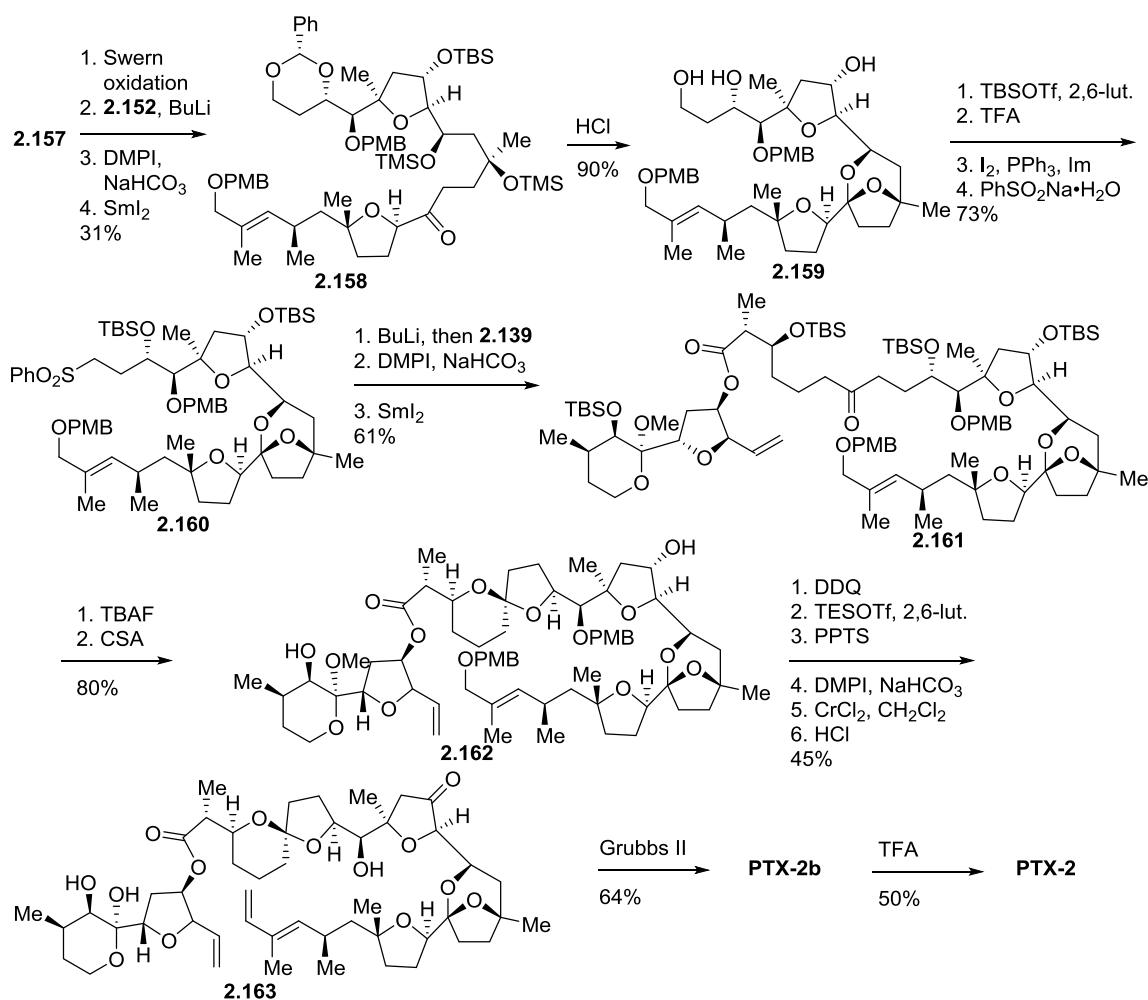
Scheme 2.16 Murai and Fujiwara's synthesis of C ring

In 2007, the Fujiwara group reported the synthesis of the C21-C30 F ring fragment **2.157** (Scheme 2.17).³⁵ **2.157** was assembled in 13 steps from (*S*)-glycidol **2.153**, which include epoxide opening with 2-methyl-3-propenylmagnesium chloride (\rightarrow **2.154**), epoxidation using TBHP/ $\text{VO}(\text{acac})_2$ with a selectivity of 3.2:1 followed by acid promoted 5-*exo*-tet epoxide opening (\rightarrow **2.155**), and stereoselective methylation at C27 using Evans' chiral auxiliary (\rightarrow **2.156**).



Scheme 2.17 Fujiwara's synthesis of E ring

The first total synthesis of PTX-2 was published by the Fujiwara group in 2014, involving coupling of the above three segments: C31-C40 FG ring segment **2.139**, C8-C20 C ring segment **2.152** and C21-C30 E ring segment **2.157** (Scheme 2.18).³⁷ The coupling strategy is the same as that was used by the Brimble group, which involves coupling between an aldehyde and a sulfone, oxidation of the resultant alcohol and subsequent reductive desulfonylation. Firstly, segment **2.152** and segment **2.157** were coupled together to give ketone **2.158**. Treatment with aqueous HCl in THF led to formation of bicyclic ketal **2.159**. Then, sulfone **2.160** was coupled with segment **2.152** to give ketone **2.161**. Subsequent desilylation and acid treatment gave the anomeric AB spiroketal **2.162**. DDQ deprotection of C30 PMB ether followed by Dess–Martin oxidation and Takai olefination set the stage for the final ring closing metathesis (\rightarrow **2.163**). The anomeric AB spiroketal product **PTX-2b** was obtained in 42 steps (longest linear sequence) and 0.7% overall yield. The nonanomeric AB spiroketal product **PTX-2** was prepared from **PTX-2b** in 50% yield by brief treatment with dilute TFA.



Scheme 2.18 Final coupling of **PTX-2**

2.2 A Spirodiepoxide(SDE) strategy to PTX-4

Take together the complexity of the PTXs inspired diverse structures and many new chemical transformations. PTX-2/PTX-4 contain 34-membered macrolides featuring 19 stereocenters, a 1,3-diene and 7 rings, including a spiroketal AB ring, a bicyclic ketal D ring, a hemiketal G ring, and 3 functionalized tetrahydrofuran CEF rings. As described above, the approaches to the ring systems include acid promoted cyclization of hydroxyl ketones to spiroketals and bicyclic ketals, 5-*exo*-tet cyclization of epoxy alcohols or iodoetherification of

olefinic alcohols to substituted tetrahydrofurans. New methods have also been developed, including reductive cyclization, osmium catalyzed oxidative cyclization, reduction of dihydrofuran, and stereoselective [3+2] annulation between allylsilanes and methyl pyruvate.

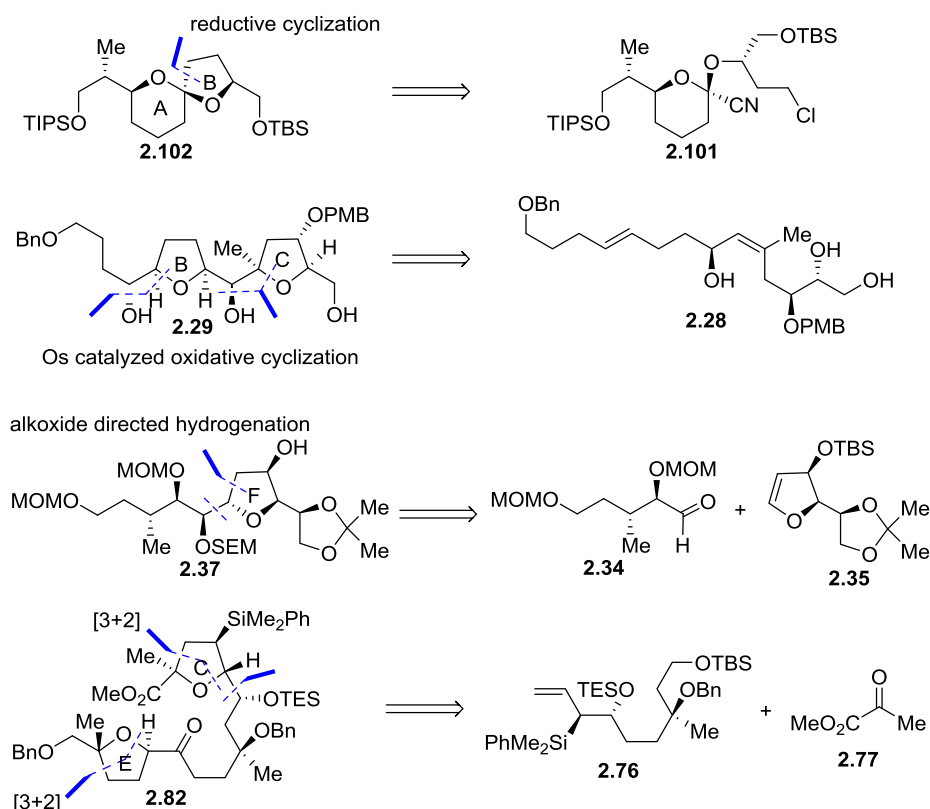
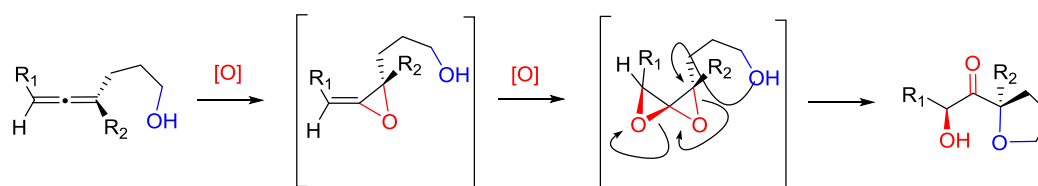


Figure 2.3 Selected approaches to the ring systems in PTXs

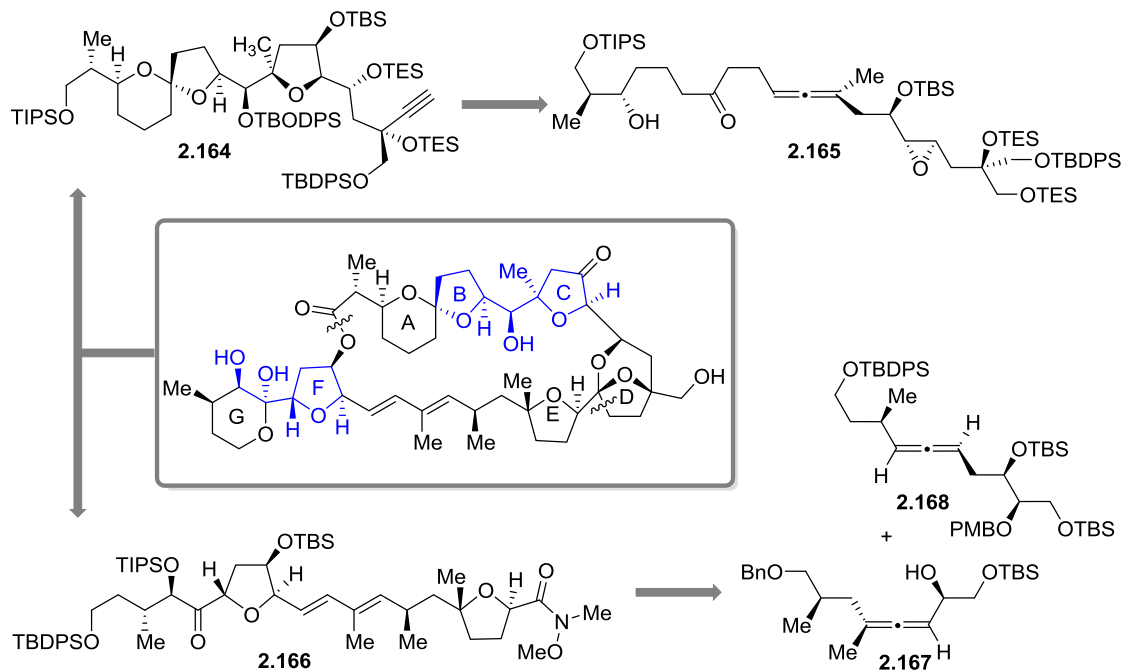
Our endeavor in pursuing the total synthesis of **PTX-4** aimed to develop superior strategies and direct methods by studying the intrinsic reactivity of SDEs and solving the problems encountered in constructing such a stereo-complex molecule. Spirodiepoxide based transformations offer new routes of entry to highly enantioenriched and densely functionalized structural motifs. Especially, tetrahydrofuran containing triads can be

obtained from allenyl alcohol substrates (Scheme 2.19). Our studies of DMDO oxidation of allenes have shown that the first epoxidation occurs at the more substituted double bond with excellent facial selectivity ($> 20:1$), resulting in a highly reactive allene oxide intermediate that is then rapidly oxidized to afford the SDE. The second oxidation occurs faster and is less selective. Subsequent intramolecular ring opening gives the α -tetrahydrofuanyl- α' -hydroxy ketone product. In principle, this strategy can provide access to the B, C, E, and F rings of **PTX-4**, as well as the adjacent oxygenated substituents, and perhaps more if cascade sequence can be realized, thereby facilitating the construction of **PTX-4**.



Scheme 2.19 Allene diepoxidation to the tetrahydrofuran motif

The route to **PTX-4** described here, focused on the preparation of a C1-C20 alkyne segment **2.164** for union with a C21-C40 Weinreb amide segment **2.166** (Scheme 2.20). We envisioned construction of **PTX-4** from convergent coupling of these two pieces. Subsequent copper hydride reduction of the resultant alkynone using Lipshutz's condition and acid promoted ketalization should give the bicyclic ketal D ring.³⁸ Finally, Yamaguchi macrolactonization followed by global deprotection should achieve our target, as shown by Evans in his total synthesis of **PTX-4** (Scheme 2.14). To date, the synthesis of the lower hemisphere of **PTX-4** has been completed by former graduate students Dr. R. V. Kolakowski and Dr. R. Sharma.³⁹ Their results are briefly outlined below.



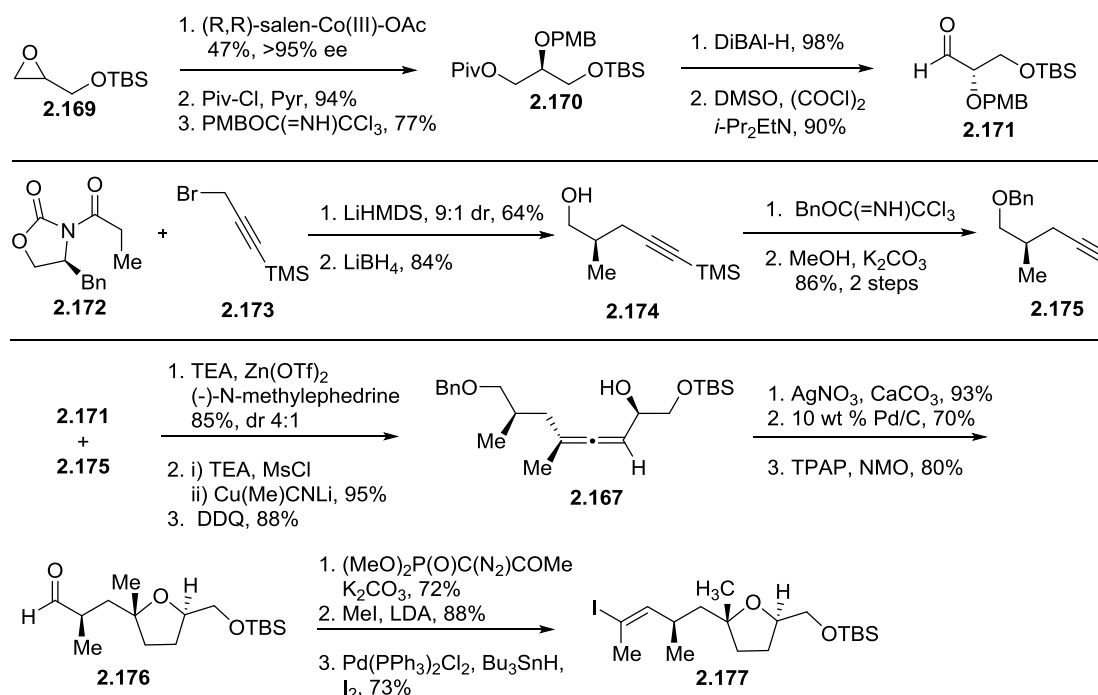
Scheme 2.20 Spirodiepoxide strategy to PTX-4

1. Access to the lower hemisphere of PTX-4 via functionalized allene intermediates

A convergent synthesis to the lower hemisphere of PTX-4 was realized via coupling of two advanced intermediates vinyl iodide **2.177** and vinyl stannane **2.185**, derived from allene **2.167** and **2.168** respectively. Both allenes were prepared from convergent coupling of the corresponding aldehyde and alkyne.

The synthesis of C21-C29 E ring vinyl iodide **2.177** is shown in Scheme 2.21. Jacobsen hydrolytic kinetic resolution of the silyl ether of glycidol **2.169** followed by a protection/deprotection/oxidation sequence gave the enantiomeric pure aldehyde **2.171**. Alkyne **2.175** was prepared from Evans' oxazolidinone **2.172** and TMS protected propargyl bromide **2.173** in 3 steps. These two compartments were coupled together under Carreira

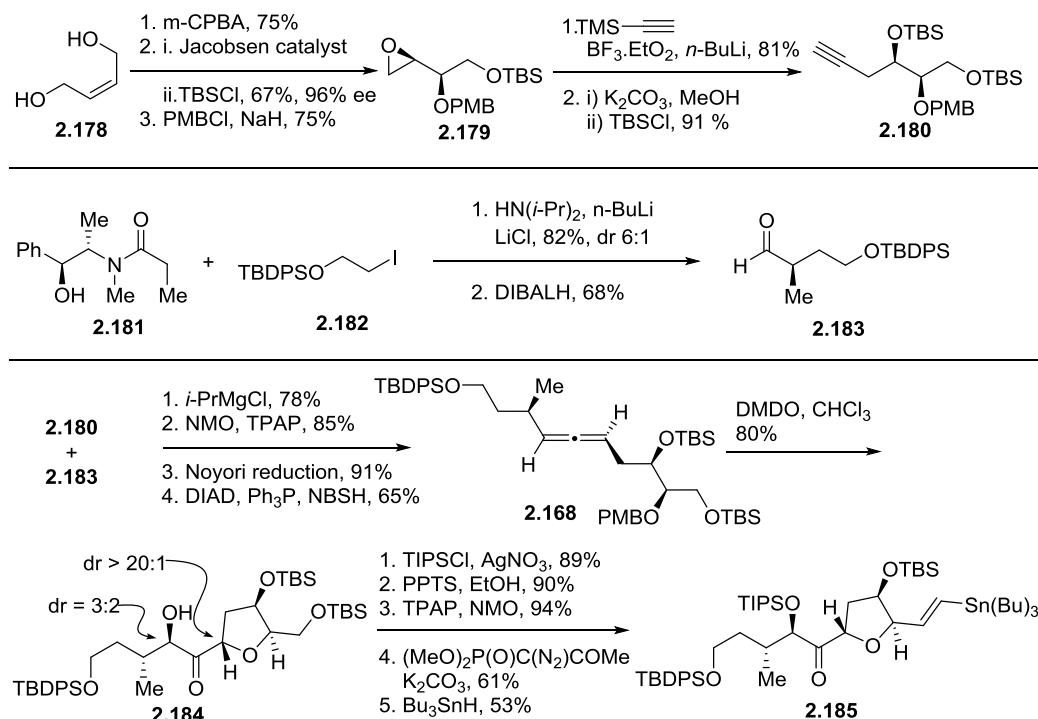
conditions. An oxidation/Noyori reduction sequence was used to improve the diastereoisomeric purity. Allene intermediate **2.167** was obtained utilizing our one pot allene synthesis procedure including mesylation and SN2' methyl cuprate addition. The E ring was formed by Marshall cyclization and hydrogenation. The final vinyl iodide **2.177** was accomplished by another standard four step sequence.



Scheme 2.21 Synthesis of the C21-C29 segment of **PTX-4**

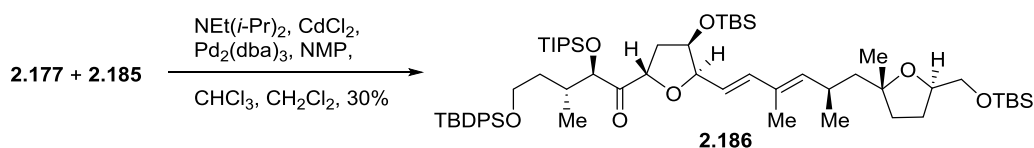
The other allene intermediate **2.168** was synthesized using Myers' stereospecific allene synthesis from a propargylic alcohol (Scheme 2.22). The alkyne component **2.180** was prepared by TMS acetylene mediated epoxide opening of a fully protected epoxy diol **2.179**, which in turn was prepared by Payne rearrangement of a symmetric epoxy diol mediated by Jacobsen's catalyst. The aldehyde component **2.183** was obtained in two steps from alkylation of Myers' amide enolates using a TBDPS protected 2-iodoethanol **2.182**. The

coupling product from alkyne **2.180** and aldehyde **2.183** was first oxidized and then reduced to give a single diastereoisomer. Myers allene synthesis then gave the functionalized product **2.168**. Hydrogen bond directed DMDO oxidation of **2.168** gave the F ring product **2.184** with 1.5:1 dr at C37. Another five step sequence produced vinyl stannane **2.185**, setting the stage for the coupling reaction.



Scheme 2.22 Synthesis of the C30-C40 segment of **PTX-4**

The final Stille coupling of vinyl iodide **2.177** and vinyl stannane **2.185** employed the condition used in Evans' total synthesis of (+)-Lepicidin, where CdCl₂ served as a transmetalation cocatalyst. CdCl₂ can help in preventing homodimerization of coupling partners.⁴⁰ By applying their conditions, we were able to isolate the cross coupling product **2.186** in 30% yield.



Scheme 2.23 Synthesis of the lower hemisphere of **PTX-4**

2. Spirodiepoxide strategy to the AB spiroketal ring

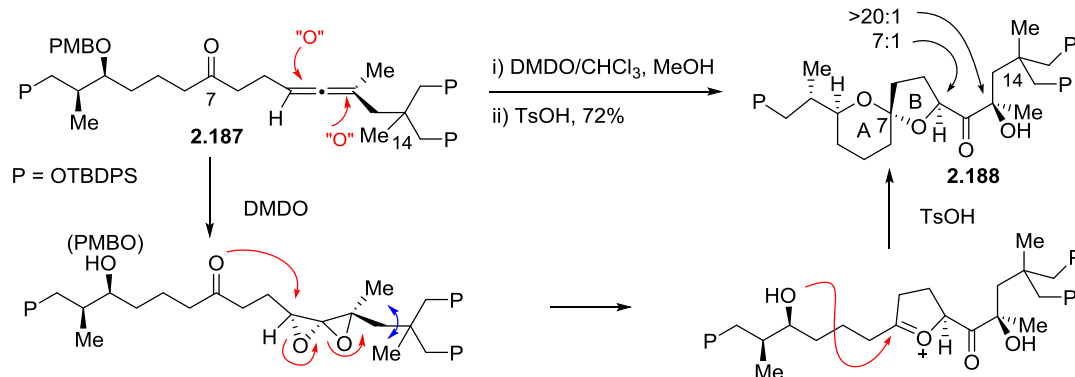
Besides being opened intramolecularly by an alcohol, SDEs can also be opened by a carbonyl group intramolecularly to give cyclic (hemi)ketal/acetal products. The Crandall group had reported studies on DMDO oxidation of simple allenyl ketones/aldehydes.⁴¹ According to their observation, DMDO oxidation of aldehydes to acids is generally slower than diepoxidation of trisubstituted allenes and subsequent nucleophilic addition of aldehydes to the resulting SDEs. The putative oxocarbenium intermediates that would result from carbonyl group addition to a SDE could well be readily trapped by water, methanol, or even the newly generated hydroxyl ketone to form (hemi)ketals/acetals, methoxy ketals/acetals, and bicyclic ketals (Table 2.1). For example, in entry 8, MeOH directed SDEs opening produced α -methoxy- α' -hydroxyl ketone under anhydrous conditions.

Table 2.1 DMDO oxidation of allenyl aldehydes/ketones⁴¹

$ \begin{array}{c} \text{R} \\ \diagup \\ \text{C}=\text{C} \begin{array}{l} \diagup \text{Me} \\ \diagdown \text{Me} \end{array} \\ \diagdown \\ \text{H} \end{array} \xrightarrow[\text{condition}]{\text{DMDO/Acetone,}} \begin{array}{c} \text{(hemi) ketal/acetal} \end{array} $				
entry	R	condition	Product	yield%
1		H ₂ O		83
2		MeOH, K ₂ CO ₃		83
3		MeOH, CH ₂ Cl ₂ TsOH		80
4		H ₂ O		68
5		MeOH		51
6		Anhydrous		17
7		H ₂ O		38
8		MeOH		47(27)

Our group has shown that DMDO oxidation of a properly engineered allenyl ketone can lead to a spiroketal product, providing direct access to the AB spiroketal rings of PTX-4.⁴² As shown in Scheme 2.24, upon treatment of excess DMDO in a mixture of CHCl₃ and MeOH, allenyl ketone **2.187** was converted into spiroketals. Subsequent acid induced ring isomerization gave the thermodynamically more stable (*S*)-spiroketal **2.188** in 72% yield with 7:1 dr at C10. The exceptionally high stereoselectivity at C10 was attributed to the

much more favored conformation of the allene oxide intermediate to avoid *syn*-pentane interactions between the C14 methyl and the C12 methyl substituents. Given that a large excess of DMDO was used, the spiroketal could also be formed by a mechanism different from what has been suggested by the Crandall group. DMDO oxidation could also initiate oxidative deprotection of PMB ether under the employed reaction conditions. Then the C3 alcohol could be released and form a lactol with a C7 ketone. Alternatively, the SDE could be opened by the newly forming lactol, giving the final spiroketal product.

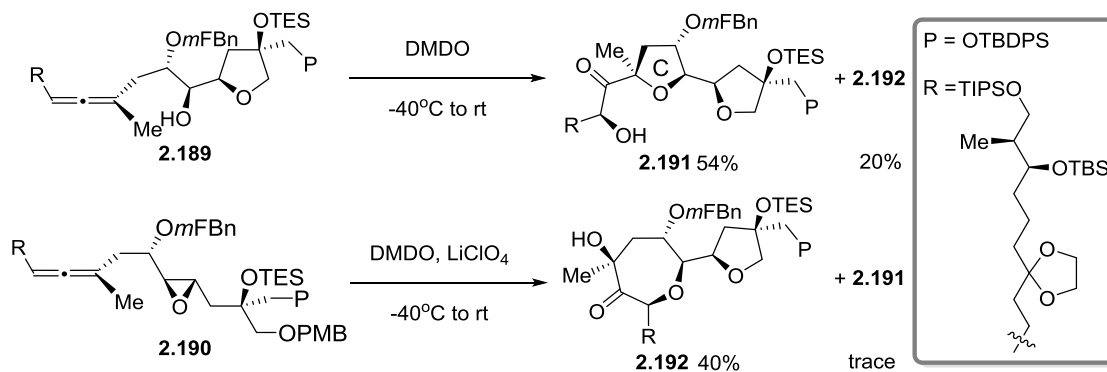


Scheme 2.24 A spirodiepoxide-based strategy to the AB ring system of PTX-4⁴²

3. Spirodiepoxide strategy to the C ring

We have also applied our SDE chemistry to access tetrasubstituted tetrahydrofuran rings, en route to the upper hemisphere of **PTX-4** (Scheme 2.25).⁴³ Exposure of allenyl alcohol **2.189** to DMDO generated an SDE intermediate. Subsequent intramolecular ring opening by C15 alcohols smoothly furnished the α -tetrahydrofuanyl- α' -hydroxyl ketone **2.191** as a single isomer. Based on our previous study, trisubstituted allenes with no α -branching on the more substituted double bond generally give low diastereomeric ratios of SDEs. The second

epoxidation of allene **2.189** was expected to be less selective. We concluded that a pair of diastereoisomers (dr 1.1:1) was formed. Surprisingly the minor diastereoisomeric SDE gave rise to oxepanone **2.192**, as proven by extensive NMR studies. It is still not clear why 7-*endo*-tet cyclization is favored over 5-*exo*-tet cyclization for the minor diastereomer. Remarkably, treatment of allenyl epoxide **2.190** with DMDO and LiClO₄ resulted in major formation of oxepanone **2.192** with 40% yield. DMDO promoted PMB ether cleavage is much slower than diepoxidation of trisubstituted allenes in this series; therefore, it is not surprising that a cascade of in situ PMB deprotection, release of C15 alcohol from hydroxyl group mediated epoxide opening and SDE opening by the newly formed alcohol was not observed. What is especially intriguing is that the oxepanone **2.192** in the second reaction was formed in much higher yield, 40%, and probably reflects rapid decomposition of the major diastereoisomer or the equivalent.

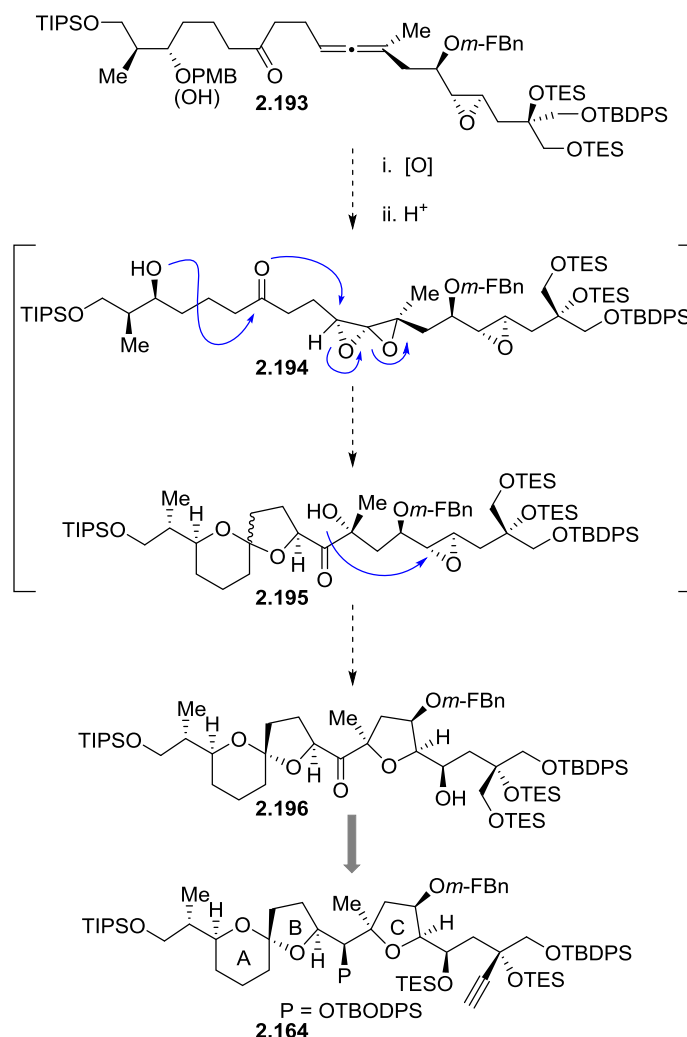


Scheme 2.25 A spirodiepoxide-based strategy to the C ring of **PTX-4**⁴³

4. Spirodiepoxide strategy to the ABC ring

Here we present our extended spirodiepoxide strategy to the ABC ring system of **PTX-4**

(Scheme 2.26). This strategy is a union of a previous AB spiroketal formation sequence (Scheme 2.24) and a reversed C ring formation sequence (Scheme 2.25) via the same C10-C12 SDE. The left to right order in C ring formation requires opposite stereochemistry of allene **2.193** to that of allene **2.189** or **2.190**, and the the C15-C16 epoxide. The stereochemistry of the C14 alcohol is not of importance, since oxidation to ketone will be required later. We used TES instead of PMB as the protecting group for the C19 alcohol to allow it to survive the oxidation reactions and stay intact in the cascade ring opening stage. Ideally, deprotection of C19 primary TES ether can be achieved under relatively mild conditions, leaving other functionalities untouched. The resultant alcohol can be easily oxidized to an aldehyde by, for example, Ley oxidation, and homologation using the Bestmann reagent should deliver the desired alkyne **2.164**. Thus, we aimed to use the epoxy allenyl ketone **2.193** as the key allenic intermediate in our study.



Scheme 2.26 A spirodiepoxide-based strategy to the ABC rings of **PTX-4**

DMDO oxidation of advanced allene intermediate **2.193** would, in principle, give the reactive spirodiepoxide intermediate **2.194** with the stereochemistry as shown in Scheme 2.26. The first epoxidation would occur on the more substituted π -bond on the most accessible face with high stereoselectivity. The second epoxidation would be less selective due to the reduced stereo bias. The SDE could then be opened by the carbonyl group, giving an oxocarbenium cation, followed by intramolecular hydroxyl group capture. Alternatively, the SDE could be also opened intramolecularly by the lactol formed by *in situ* PMB ether

cleavage, resulting in the same α -spiroketal- α' -hydroxyl ketone **2.195**. Finally, epoxide opening by the newly formed C12 alcohol would give the fully substituted C ring system. The formation of C ring derivatives via acid promoted 5-*exo*-tet cyclization of epoxy alcohol had been reported by Murai several years ago and was used in the Fujiwara synthesis of **PTX-2** (\rightarrow **2.152**, Scheme 16). In our system, the use of acid was planned to help promote the isomerization of AB spiroketal and deliver the thermodynamically more stable isomer.

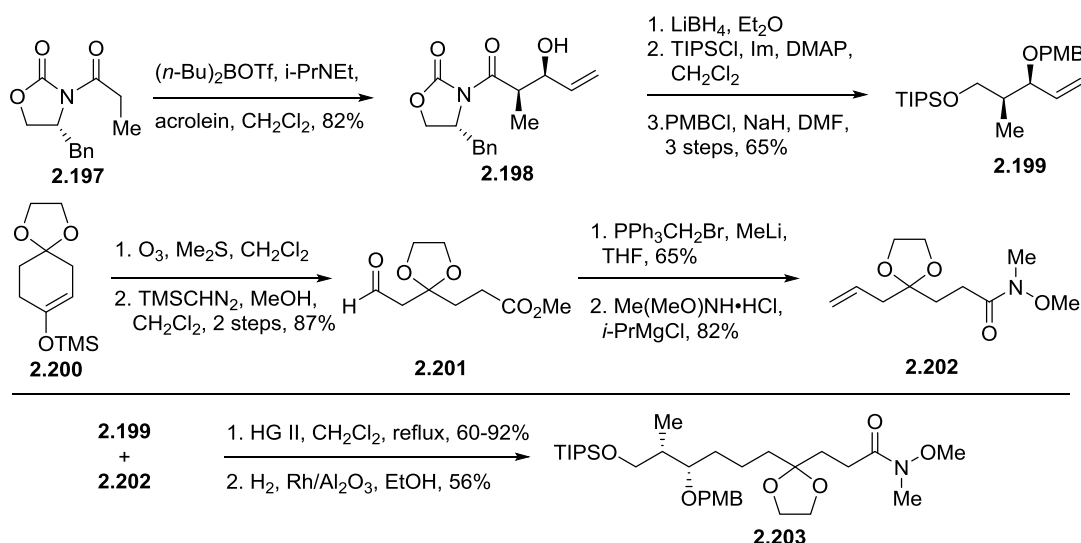
One problem we will need to solve later in this strategy is the stereoselective reduction of the C11 ketone. The Evans group presented a similar reaction earlier, reduction of an enone to alcohol **2.111** (Scheme 2.12). Chelation controlled $\text{Zn}(\text{BH}_4)_2$ reduction delivered hydride to the less hindered face giving C11 alcohol **2.111** in 80% yield with 73:27 dr. In our case, the existence of the C ring and the stereochemistry at C12 makes it difficult to predict the stereochemistry of ketone reduction. In an *anti*-Felkin-Anh model, polar effect of the oxygen in the C ring may stabilize the chelation between C10, C11 oxygen and $\text{Zn}(\text{BH}_4)_2$. The C12 methyl group may adapt a conformation in which the *Si* face of the C11 ketone was blocked. Then the desired alcohol would then be obtained.

2.3 Synthetic approach towards C1-C19 sector of PTX-4

1. Convergent synthesis of C1-C19 epoxy allene **2.211**

As with our earlier work, the synthesis took advantage of copper-mediated stereospecific allene assembly of a propargyl alcohol derived from alkyne Weinreb amide coupling.

Preparation of Weinreb amide **2.203** followed our previous synthesis of a similar compound⁴³ with a change of the C3 alcohol protective group (Scheme 2.27). Hence, instead of the TBS silyl ether, a PMB ether was used in order to evaluate the selective unmasking of the alcohol under oxidative conditions, following our previous AB spiroketal formation strategy (Scheme 2.24). Thus we prepared olefin **2.199** and **2.202** accordingly. Synthesis of olefin **2.199** started from Evans *syn*-aldol product **2.198**, followed by a 3 step sequence including reduction and protection. Known olefin **2.202** was prepared from cyclic enol ether **2.200** via ozonolysis, esterification, Wittig olefination and Merck Weinreb amidation, as before.⁴³



Scheme 2.27 Synthesis of a C1-C10 Weinreb amide

The cross metathesis of olefin **2.199** and **2.202** was then investigated. According to the Grubbs categorization, olefin **2.199** is a type II olefin that undergoes slow homodimerization and olefin **2.202** is a type I olefin, which undergoes fast homodimerization. When the Hoveyda-Grubbs second generation catalyst (**HGII**, Figure 2.4) was employed, the cross

metathesis product and a small amount of homodimer of olefin **2.202** were formed. The reaction yield was improved by portionwise addition of the catalyst. In order to fully consume the homodimer of olefin **2.202**, the reaction was carried out under an extended period of time. Surprisingly, some (~3%) *N*-methoxy bond cleavage of the product was observed (formation of *N*-methyl amide, Figure 2.3). When a more reactive catalyst **Zhan-1B** was used, homodimerization of type II olefin **2.199** was observed, but the yield of desired product was not increased. Hydrogenation of the metathesis product was catalyzed by Rh/Al₂O₃. The reaction was slow (21 hours), and PMB ether was cleaved progressively during the course of the reaction. Gratifyingly, the unmasked alcohol was recovered and effectively protected using a combination of La(OTf)₃ and 4-methoxybenzyl-trichloroacetimidate to give an additional 30% of **2.203** (combined yield 86%). As an alternative, diimide reduction with potassium azodicarboxylate proceeded with no detectable deprotection, but the reaction was even slower (>3 days) and was not pursued.

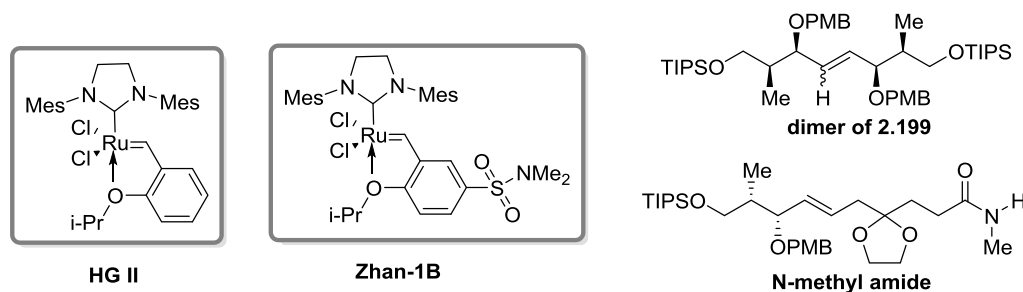
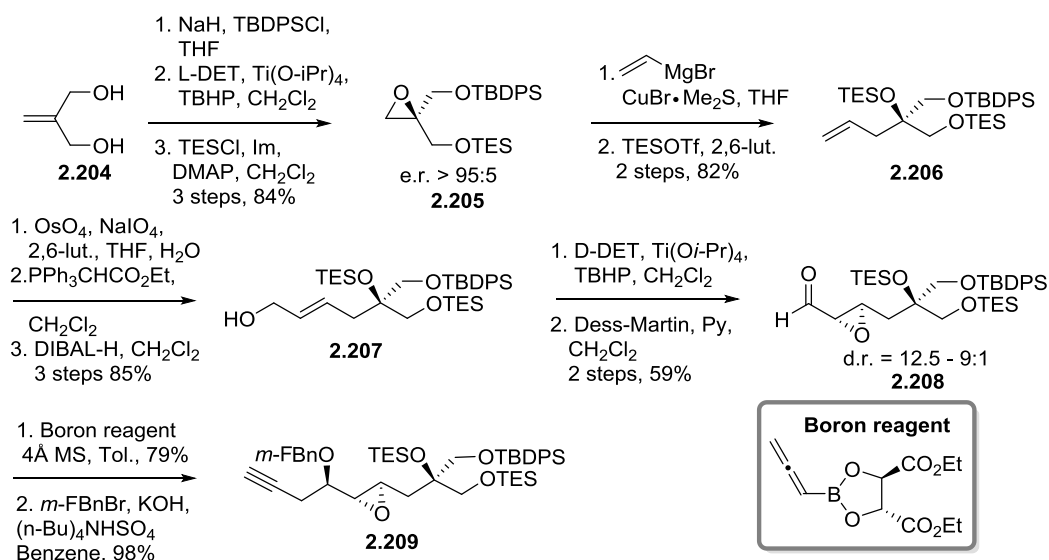


Figure 2.4 Catalysts for olefin cross metathesis and observed side products

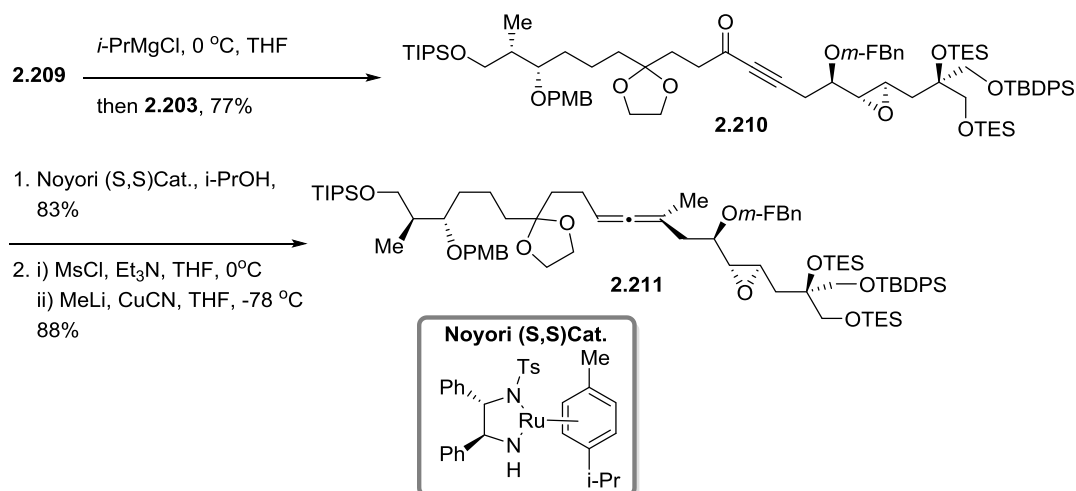
In analogy to our previous synthetic sequence, alkyne **2.209** was prepared with full control of the stereochemistry at C19 via Sharpless epoxidation (*er* > 95:5), and good stereoselectivity at C15-C16 (12.5 – 9:1) (Scheme 2.28). The selectivity of the second

Sharpless epoxidation (\rightarrow **2.208**) in the sequence is also very sensitive to trace amounts of water in the reaction, and high dr requires rigorously dry reaction conditions. Diastereoisomers from this reaction were also inseparable by flash column chromatography and were employed through the remainder of the sequence. Yamamoto homopropargylation of epoxy aldehyde **2.208** smoothly delivered the desired alcohol **2.209** in good yield (79%) and high selectivity (>20:1), whereas reactions using the other enantiomer of the boron reagent gave a low dr (\sim 2:1) as indicated by crude $^1\text{H-NMR}$ analysis.



Scheme 2.28 Synthesis of a C11-C19 alkyne

The synthesis of the C1-C19 epoxy allene **2.211** commenced with coupling of C1-C10 Weinreb amide **2.203** and C11-C19 alkyne **2.209** (Scheme 2.29). Noyori reduction of the coupling product (**2.210**) followed by mesylation and $\text{SN}2'$ displacement of the propargyl alcohol with low order methyl cuprate gave allene **2.211** as single diastereomer.



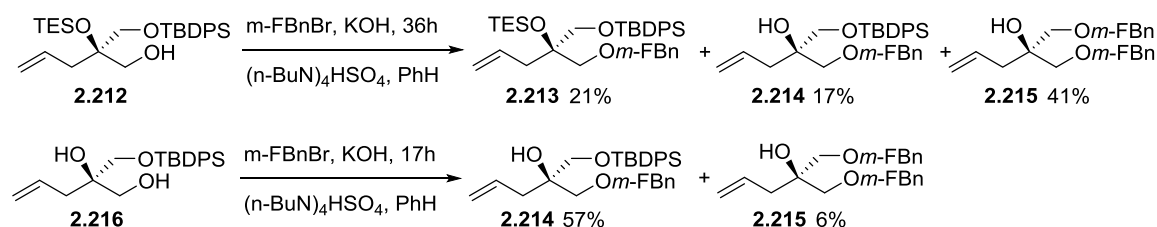
Scheme 2.29 Convergent assembling of a C1-C19 epoxy allene

Surprisingly, deprotection of the 1,3-dioxolane at the C7 ketone turned out to be problematic. Products isolated under various deprotection conditions were accompanied with C19 TES deprotection and C15-C16 epoxide opening. Since both the ketone and the epoxide are essential for the evaluation of our ring opening and forming cascade, we sought a protective group more robust than the TES silyl group upon treatment with Bronsted/Lewis acids. A *m*-FBn ether was considered due to its stability when exposed to acids and oxidative conditions used for SDE formation, but to differentiate it from C14 alcohol, we decided to protect C14 alcohol as a TBS silyl ether.

2. Convergent synthesis of C1-C19 epoxy allenyl ketone 2.227

Initially, we tried to modify the protective group in intermediate olefin **2.206** from our previous alkyne synthesis (Scheme 2.28), however, the results were not satisfying (Scheme 2.30). Both alcohol **2.212** and **2.216** were prepared from acid promoted desilylation of

olefin **2.206**. For protection of alcohol **2.212**, the major product was isolated as a bis-*m*-FBn ether **2.215**, with only 21% of the desired olefin **2.213**. Deprotection of the primary TBDPS silyl ether under such reaction conditions was not entirely expected, but it was observed (*cf.* **2.215**). Comparatively, monoprotection of the less hindered diol **2.216** was faster and gave 57% of desired product. With shorter reaction times, cleavage of the primary TBDPS silyl group was also minimized.

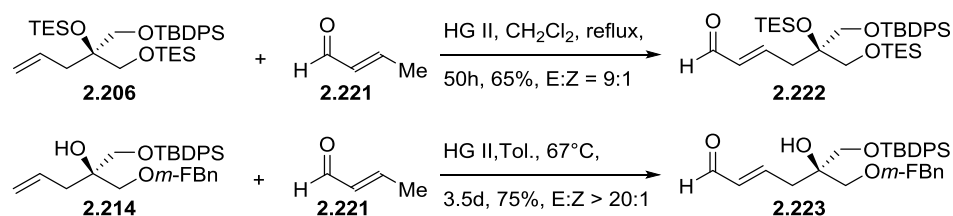


Scheme 2.30 Synthesis of *m*-FBn ether protected olefin **2.213**

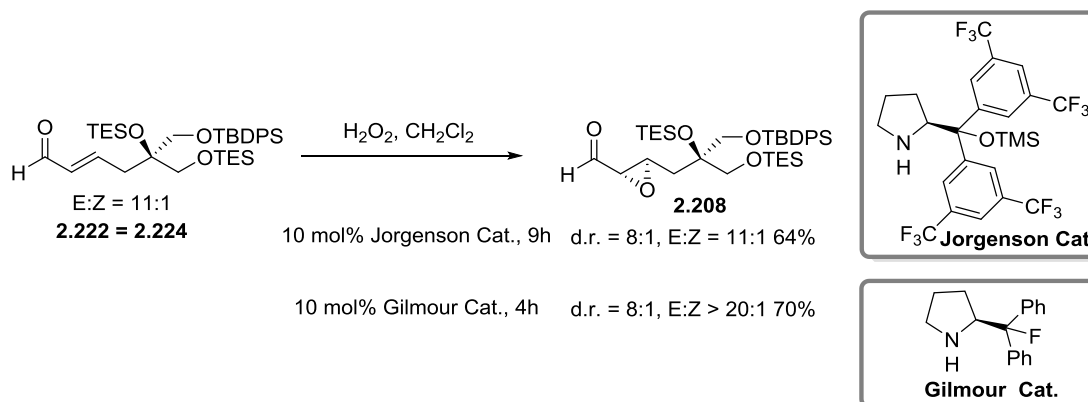
Change of the C19 protective group was then initiated at the beginning of the synthesis (Scheme 3.31). The route to alkyne **2.220** was essentially the same as the sequence we employed before for the preparation of alkyne **2.209** (Scheme 2.28), except for some minor changes as indicated below. Firstly, boronic acid catalyzed monoprotection of diol **2.204**⁴⁴ was employed, instead of a base promoted reaction with phase transfer catalyst (Scheme 2.28, \rightarrow **2.209**). The later gave 58% monoprotection product and 15% di-protected product. Secondly, Sharpless asymmetric epoxidation of the allylic alcohol **2.218** turned out to be less selective than Shi epoxidation, 6.5:1 verse 8:1. Note that the selectivity for Sharpless asymmetric epoxidation on a similar substrate **2.207** was as high as 12.5:1 (Scheme 2.28). Lastly, TBS protection of the C14 alcohol was very slow using TBSCl, presumably due to the steric hindrance generated by the protective groups nearby. A more reactive reagent

Our approach to the epoxy aldehyde intermediate **2.219** appeared to be inefficient with regard to multi-step oxidation and reduction reactions (Scheme 2.31). This sequence includes oxidative cleavage of a terminal olefin to an aldehyde, homologation and reduction to allyl alcohol **2.218**, hydroxyl directed asymmetric epoxidation, and finally oxidation of the primary alcohol. We envisioned alternative routes to **2.208** and **2.219** via cross metathesis to an α,β -unsaturated aldehyde followed by direct epoxidation (see Scheme 2.28 for the structure of **2.208** and Scheme 2.31 for the structure of **2.219**). Indeed, improved efficiency was realized for the synthesis of C19 OTES epoxy aldehyde **2.208** (Schemes 2.32 and 2.33) compared to original 4 steps with 50% yield and 12.5 – 9:1 dr (Scheme 2.31). Cross metathesis of olefin **2.206** with crotonaldehyde **2.221** (Scheme 2.32), followed by organocatalytic epoxidation of **2.222** (= **2.224**) using H₂O₂ and the Gilmour catalyst (Scheme 2.33) delivered aldehyde **2.208** in 2 steps with 46% yield and 8:1 dr. However, metathesis

reaction for fully protected olefin **2.213** with crotonaldehyde gave only a small amount of the desired olefin (not shown). The immediate precursor to **2.213**, olefin **2.214** gratifyingly gave the corresponding α,β -unsaturated aldehyde **2.223** with good yield and excellent stereoselectivity. Unfortunately, epoxidation using either the Jorgensen catalyst or the Gilmour catalyst proved fruitless; the reaction was very slow and conversion to complex mixture was observed over extended reaction time.



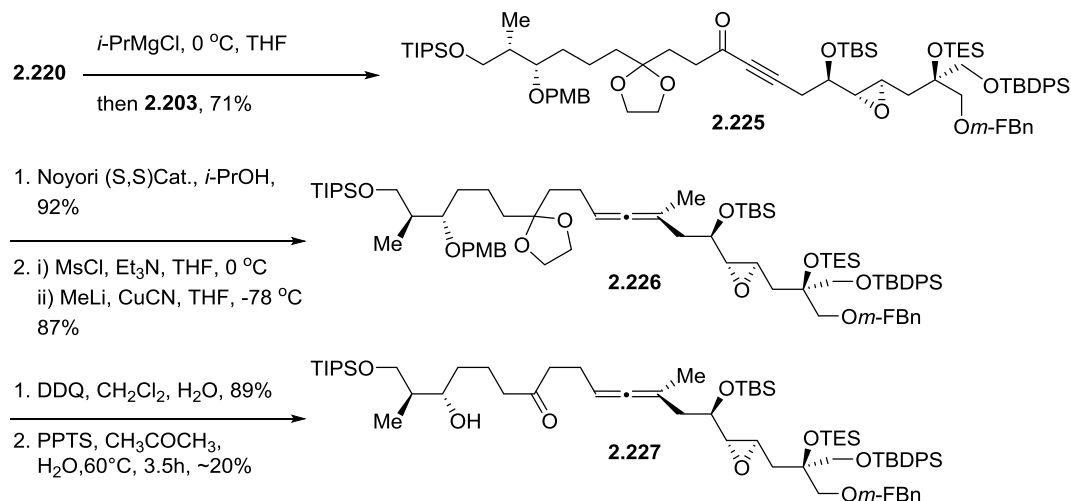
Scheme 2.32 Preparation of α,β -unsaturated aldehydes via olefin metathesis



Scheme 2.33 Catalytic epoxidation of α,β -unsaturated aldehydes

C19 *m*-FBn allene **2.226** was prepared using the same reaction conditions as for C19 TES **2.211** (Scheme 2.34). Various ketone deprotection conditions were then investigated. Epoxy allenyl ketone **2.227** was isolated as a slightly impure product by brief exposure of the corresponding C3 alcohol to PPTS in a mixture of acetone and water at 60°C. All other conditions⁴⁵, including TsOH, Pd(CH₃CN)₂Cl₂, CeCl₃ with NaI, BiCl₃, and In(OTf)₃, resulted in

epoxide opening, *m*-FBn ether cleavage, and/or allene consumption.

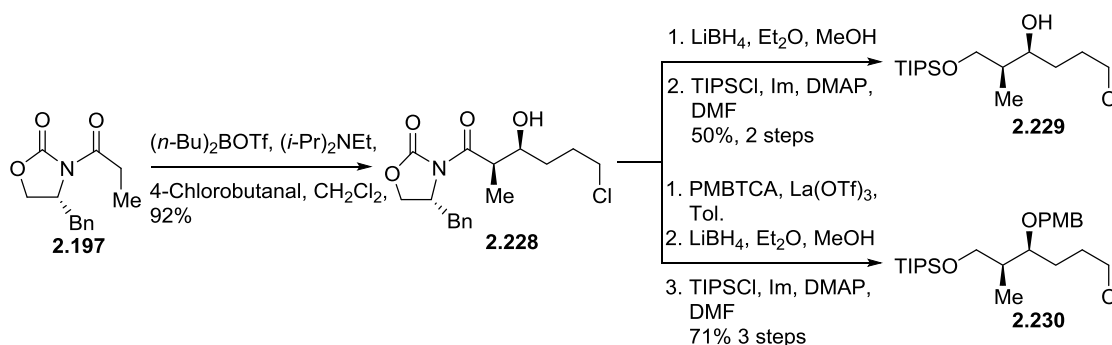


Scheme 2.34 Synthesis of C1-C19 epoxy allenyl ketone **2.227**

3. Direct access to the C1-C19 epoxy allenyl ketone **2.227**

Pleasingly, the removal of the dioxolane (compare **2.211** with **2.226**) of the C1-C19 epoxy allenyl ketone **2.227** was successful after changing the C19 TES protective group to the *m*-FBn protective group. However, the low yield in the last step compromised its application to our study. We started to consider other alternative routes. Inspired by Paquette's convergent synthesis to AB spiroketal **2.43** (Scheme 2.6), we decided to directly couple a C1-C6 lithium alkylide with a C7-C19 Weinreb amide. The stabilities of allenes and epoxides under these types of conditions have already been proven in our previous study.^{42,43} In principle, we could prepare and couple two segments in the same approximate number of steps as in previous route. The results are summarized below.

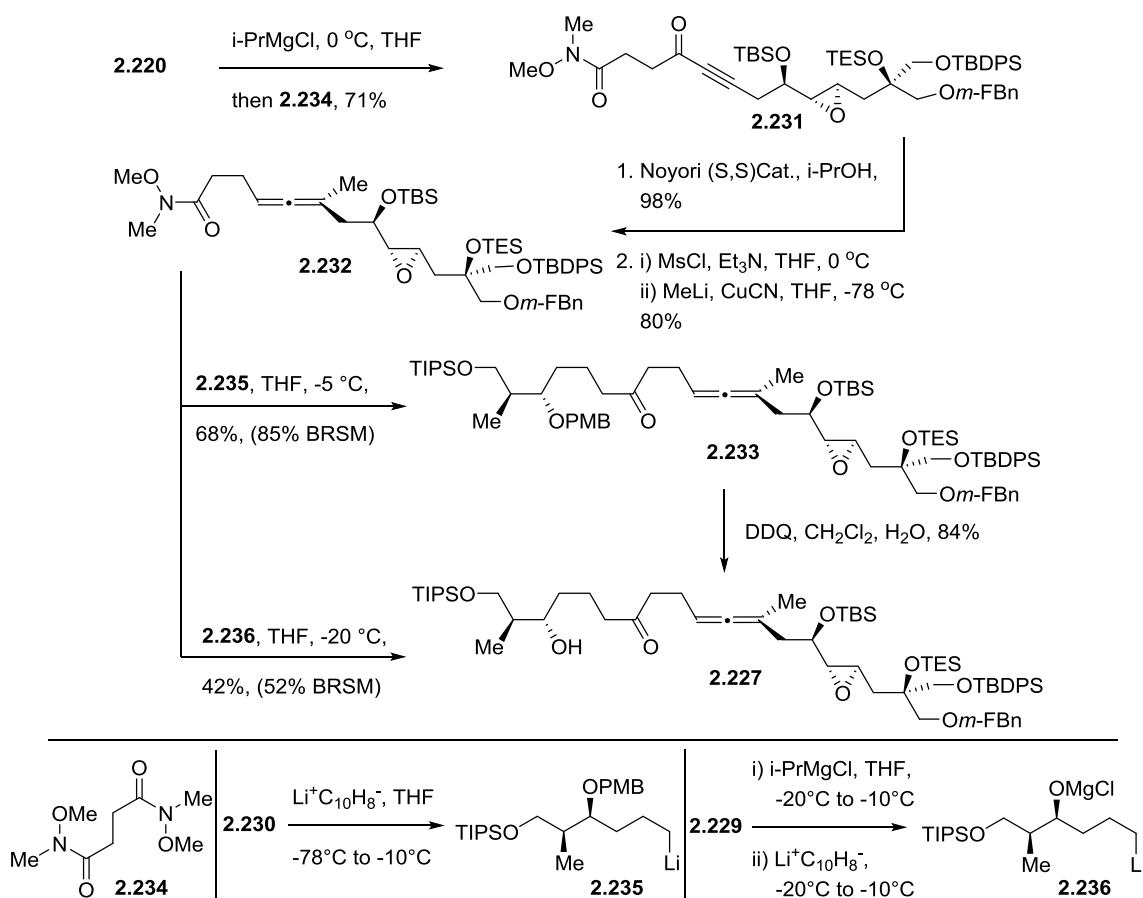
Two alkyl chlorides **2.229** and **2.230** were considered. Both of them were prepared from Evans' *syn*-aldol product **2.228**, followed by cleavage of the chiral auxiliary and protection of the corresponding alcohols (Scheme 2.35). **2.228** was prepared from 4-chlorobutanal. Reaction with 4-bromobutanal gave a tetrahydrofuranyl product as expected. Notably, chlorohydrin **2.229** is susceptible to acid promoted intramolecular displacement of chloride under mild conditions, although the parent compound **2.228** is not. During purification of **2.229** by flash column chromatography, about 20% of the product was cyclized. Complete cyclization was observed when a concentrated solution of chlorohydrin **2.229** was treated with dry silica gel.



Scheme 2.35 Synthesis of the C1-C6 chlorohydrin

The C7-C19 Weinreb amide segment **2.232** was then prepared from coupling alkyne **2.220** with a known bis-Weinreb amide **2.234** readily available from succinyl chloride (Scheme 2.36). The coupling reaction was very effective (71% yield) with only a small amount (<5%) bis-alkynone formed, and the remaining unreacted starting material was fully recovered. Subsequent stereoselective reduction and allene formation (**2.231**→**2.232**) also worked as expected. Final coupling of the Normant's-type Grignard reagent **2.236** with Weinreb amide

2.232 worked moderately (42%). A complex mixture containing allene isomerization products were also observed by crude ^1H -NMR. The other lithium alkylide **2.235**, with the C3 alcohol protected, reacted with Weinreb amide **2.232** giving improved yield (68%). Thus, target allene **2.227** was obtained in 17 steps (longest linear sequence) with 9% overall yield, or 16 steps with 7% overall yield.

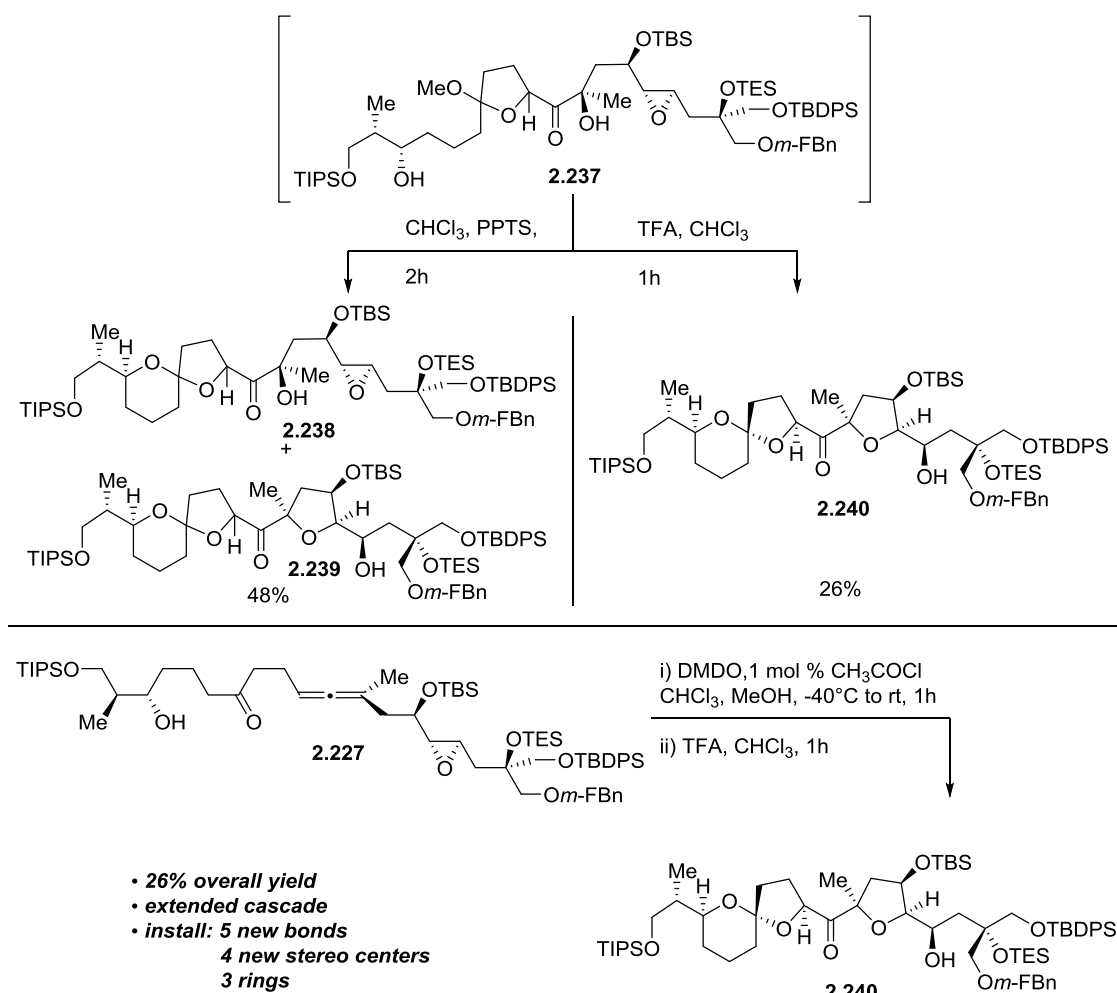


Scheme 2.36 Synthesis of the C1-C19 epoxy allenyl ketone

4. SDEs ring formation and opening cascade

With an efficient route established, we continued with our study to the proposed ring

forming/opening cascade. Firstly, allene oxidation was effected with 4 equiv. of DMDO in a mixture of chloroform and methanol with trace amount of acetone (~5%), and HCl (1 mol %) at -40°C (Scheme 2.37). After removal of solvent, the major immediate was examined by ^1H -NMR and mass spectrometry. As suggested by the mass and the proton signals at 3.19 ppm and 5.06 ppm that could be assigned as the methoxy and C10 proton respectively, the product was the methoxy ketal **2.237** with the epoxide untouched. No further action was taken to elucidate the structure. As discussed in section 2.2, the Crandall group showed that a single isomer of methoxy ketal product was isolated upon DMDO oxidation of some simple allenyl aldehydes/ketones (Table 2.1, entry 2 and 8). Our result is consistent with their observation. However, in our case, the addition of MeOH and trace amount of acid seemed to be essential. In a model study, DMDO oxidations conducted with anhydrous CHCl_3 or with addition of powdered K_2CO_3 gave no detectable spiroketal products (data not shown). We reasoned that the introduction of trace amounts of acid might promote formation of the lactol, which might be a better nucleophile than a ketone or epoxide, thus facilitating SDE opening and spiroketal formation. This is a delicate issue, however, because high acid content could adversely affect the double oxidation. The allene oxide may react under acidic conditions prior to the second oxidation. Moreover, the SDE functionality may also be highly destabilized and thereby compromise the ring opening/ring closing cascade.

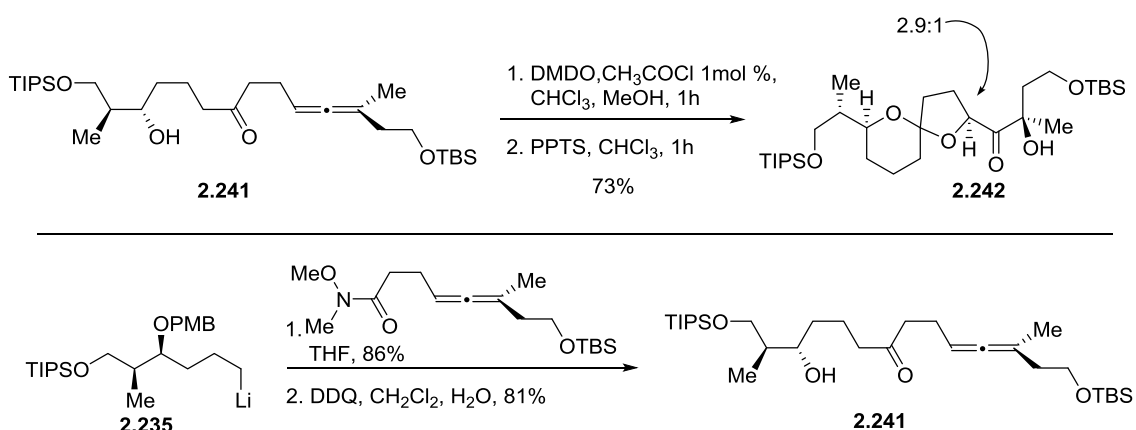


Scheme 2.37 Oxidative cyclization C1-C19 epoxy allenyl ketone **2.227**

Accordingly, we carefully introduced small quantities of acid to promote SDE consumption and found that later addition of more acid for the improved efficiency. MeOH in the oxidation solvent mixture was removed prior to addition of the second portion of acid to avoid possible deprotection of the labile C18 OTES group. In the conversion of **2.227** to **2.240** we initially tried 2 equiv. of PPTS. After 2 hours, the epoxide opening was still not complete, and the spiroketals were a mixture of both isomers. Treatment of the reaction mixture from DMDO oxidation with 1 equiv. of TFA as a 1% solution in CHCl_3 gratifyingly produced the anomeric spiroketal **2.240** with C ring installed. The major product was

isolated as a single isomer in 26% yield. There were also several other minor products that are only partially characterized, but which did not further isomerize to the desired product under these conditions.

Why is this SDE cyclization cascade effective? To better understand this, a brief digression is in order. In the model study allenyl ketone **2.241** was prepared via coupling lithium alkylide **2.235** with the corresponding allenyl Weinreb amide, followed by DDQ deprotection of the PMB ether. We found that DMDO oxidation of allene **2.241** under neutral or basic conditions followed by subsequent PPTS treatment resulted in product formation with low yield (less than 25%). With addition of acid (acetyl chloride, 1 – 2 mol%), we were able to increase the yield of spiroketal **2.243** to 73%. Use of lithium perchlorate (1.0 equiv.) instead of acetyl chloride, **2.242** is only 59% yield. Interestingly, DMDO oxidation of **2.241** in anhydrous chloroform without methanol resulted in only trace product formation (*cf.* Table 2.1 entry 6). Acid and methanol appear to be crucial for the desired product.



Scheme 2.38 Oxidative cyclization of a model allenyl ketone

2.4 Summary

Our SDE based strategy towards C1-C19 sector of **PTX-4** relies on the successful preparation of allene **2.227**. The initial route involves convergent assembly of Weinreb amide **2.203** and terminal alkyne **2.220**. However, deprotection of C7 ketone was low yielding (Scheme 2.34). An improved route was then developed, involving sequential coupling of 3 fragments: terminal alkyne **2.220**, bis-Weinreb amide **2.234**, and lithium alkylide **2.235** (Scheme 2.36). By applying our SDE chemistry, we were able to convert allene **2.227** with 6 stereo centers and one epoxide in one pot to a C1-C19 sector of **PTX-4** with 3 rings and 9 stereo centers in a remarkably efficient 26% yield.

2.5 References

- (1) *Seafood and Freshwater Toxins: Pharmacology, Physiology, and Detection*; Botana, L. M., Ed.; 3rd ed.; CRC Press: Boca Raton, 2014.
- (2) Yasumoto, T.; Murata, M.; Oshima, Y.; Matsumoto, G. K.; Clardy, J. *ACS Symp. Ser.* **1984**, 262, 207.
- (3) Yasumoto, T.; Murata, M.; Oshima, Y.; Sano, M.; Matsumoto, G. K.; Clardy, J. *Tetrahedron* **1985**, 41, 1019.
- (4) Sasaki, K.; Satake, M.; Yasumoto, T. *Biosci. Biotechnol. Biochem.* **1997**, 61, 1783.
- (5) Sasaki, K.; Wright, J. L. C.; Yasumoto, T. *J. Org. Chem.* **1998**, 63, 2475.
- (6) Suzuki, T.; Mackenzie, L.; Stirling, D.; Adamson, J. *Toxicon* **2001**, 39, 507.
- (7) Espina, B.; Louzao, M. C.; Ares, I. R.; Fonfria, E. S.; Vilarino, N.; Vieytes, M. R.; Yasumoto, T.; Botana, L. M. *Chem. Res. Toxicol.* **2010**, 23, 504.
- (8) Allingham, J. S.; Miles, C. O.; Rayment, E. J. *Mol. Biol.* **2007**, 371, 959.

- (9) Kim, G. Y.; Kim, W. J.; Choi, Y. H. *Mar. Drugs* **2011**, *9*, 2176.
- (10) Halim, R.; Brimble, M. A.; Merten, J. *Org. Lett.* **2005**, *7*, 2659.
- (11) Halim, R.; Brimble, M. A.; Merten, J. *Org. Biomol. Chem.* **2006**, *4*, 1387.
- (12) Brimble, M. A.; Halim, R. *Pure Appl. Chem.* **2007**, *79*, 153.
- (13) Heapy, A. M.; Wagner, T. W.; Brimble, M. A. *Synlett* **2007**, 2359.
- (14) Carley, S.; Brimble, M. A. *Org. Lett.* **2009**, *11*, 563.
- (15) Donohoe, T. J.; Lipiński, R. M.; Lipin, R. M. *Angew. Chem. Int. Ed.* **2013**, *52*, 2491.
- (16) Paquette, L. A.; Peng, X. W.; Bondar, D. *Org. Lett.* **2002**, *4*, 937.
- (17) Peng, X. W.; Bondar, D.; Paquette, L. A. *Tetrahedron* **2004**, *60*, 9589.
- (18) Bondar, D.; Liu, J.; Muller, T.; Paquette, L. A. *Org. Lett.* **2005**, *7*, 1813.
- (19) O'Connor, P. D.; Knight, C. K.; Friedrich, D.; Peng, X. W.; Paquette, L. A. *J. Org. Chem.* **2007**, *72*, 1747.
- (20) Pihko, P. M.; Aho, J. E. *Org. Lett.* **2004**, *6*, 3849.
- (21) Helmboldt, H.; Aho, J. E.; Pihko, P. M. *Org. Lett.* **2008**, *10*, 4183.
- (22) Aho, J. E.; Salomaki, E.; Rissanen, K.; Pihko, P. M. *Org. Lett.* **2008**, *10*, 4179.
- (23) Aho, J. E.; Piisola, A.; Krishnan, K. S.; Pihko, P. M. *European J. Org. Chem.* **2011**, 1682.
- (24) Kemppainen, E. K.; Sahoo, G.; Valkonen, A.; Pihko, P. M. *Org. Lett.* **2012**, *14*, 1086.
- (25) Micalizio, G. C.; Roush, W. R. *Org. Lett.* **2001**, *3*, 1949.
- (26) Canterbury, D. P.; Micalizio, G. C. *Org. Lett.* **2011**, *13*, 2384.
- (27) Kubo, O.; Canterbury, D. P.; Micalizio, G. C. *Org. Lett.* **2012**, *14*, 5748.
- (28) Takaoka, L. R.; Buckmelter, A. J.; LaCruz, T. E.; Rychnovsky, S. D. *J. Am. Chem. Soc.* **2005**, *127*, 528.
- (29) Vellucci, D.; Rychnovsky, S. D. *Org. Lett.* **2007**, *9*, 711.

- (30) Evans, D. A.; Rajapakse, H. A.; Chiu, A.; Stenkamp, D. *Angew. Chem. Int. Ed.* **2002**, *41*, 4573.
- (31) Evans, D. A.; Rajapakse, H. A.; Stenkamp, D. *Angew. Chem. Int. Ed.* **2002**, *41*, 4569.
- (32) Amano, S.; Fujiwara, K.; Murai, A. *Synlett* **1997**, 1300.
- (33) Fujiwara, K.; Kobayashi, M.; Yamamoto, F.; Aki, Y.; Kawamura, M.; Awakura, D.; Amano, S.; Okano, A.; Murai, A.; Kawai, H.; Suzuki, T. *Tetrahedron Lett.* **2005**, *46*, 5067.
- (34) Awakura, D.; Fujiwara, K.; Murai, A. *Synlett* **2000**, 1733.
- (35) Fujiwara, K.; Aki, Y. I.; Yamamoto, F.; Kawamura, M.; Kobayashi, M.; Okano, A.; Awakura, D.; Shiga, S.; Murai, A.; Kawai, H.; Suzuki, T. *Tetrahedron Lett.* **2007**, *48*, 4523.
- (36) Fujiwara, K.; Suzuki, Y.; Koseki, N.; Murata, S.; Murai, A.; Kawai, H.; Suzuki, T. *Tetrahedron Lett.* **2011**, *52*, 5589.
- (37) Fujiwara, K.; Suzuki, Y.; Koseki, N.; Aki, Y.; Kikuchi, Y.; Murata, S.; Yamamoto, F.; Kawamura, M.; Norikura, T.; Matsue, H.; Murai, A.; Katoono, R.; Kawai, H.; Suzuki, T. *Angew Chem Int Ed Engl* **2014**, *53*, 780.
- (38) Sharma, R. The spirodiepoxide: a platform for diversity and target oriented synthesis. Ph.D. Dissertation, Rutgers, The State University of New Jersey, 2013.
- (39) Kolakowski, R. V.; Williams, L. J. *Tetrahedron Lett.* **2007**, *48*, 4761.
- (40) Evans, D. A.; Black, W. C. *J. Am. Chem. Soc.* **1993**, *115*, 4497.
- (41) Crandall, J. K.; Rambo, E. *Tetrahedron Lett.* **1994**, *35*, 1489.
- (42) Lotesta, S. D.; Hou, Y. Q.; Williams, L. J. *Org. Lett.* **2007**, *9*, 869.
- (43) Joyasawal, S.; Lotesta, S. D.; Akhmedov, N. G.; Williams, L. J. *Org. Lett.* **2010**, *12*, 988.
- (44) Lee, D.; Williamson, C. L.; Chan, L.; Taylor, M. S. *J. Am. Chem. Soc.* **2012**, *134*, 8260.
- (45) Wuts, P. G. M.; Greene, T. W. *Greene's Protective Groups in Organic Synthesis*; 4th ed.; Wiley: Hoboken, 2006.

Chapter 3 Allene Osmylation

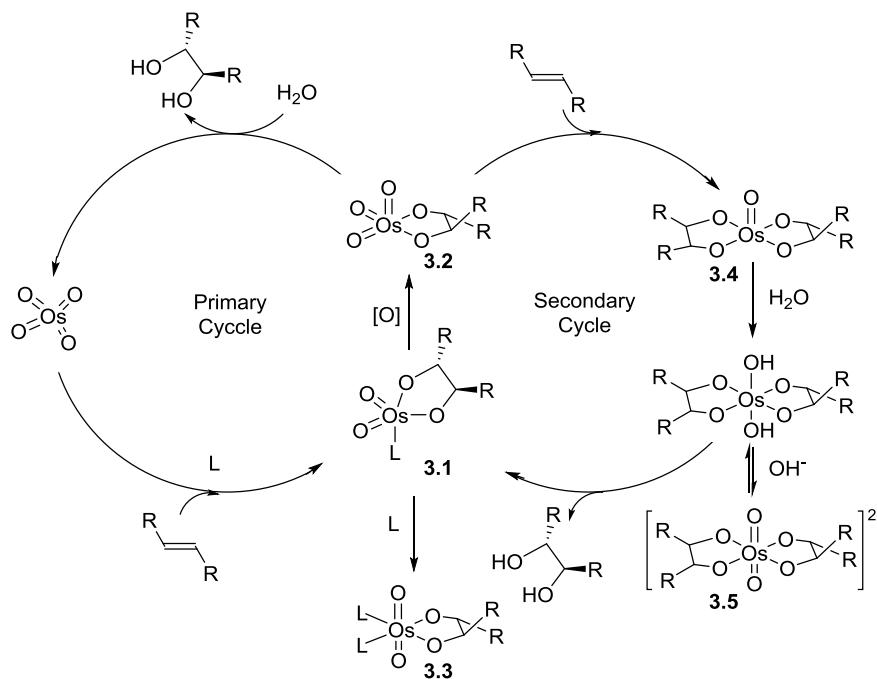
3.1 Background

Olefin osmylation has been well-studied and is now a very important method for the stereoselective oxidation of alkenes. Comparatively, allene osmylation has been explored much less. There are only 7 reports on osmium tetroxide mediated oxidation of allenic compounds, and with few exceptions it's found to be slow, unselective and low yielding. One difference between these two reactions is that the allene osmylation intermediate is an enol ester which is also reactive towards osmium addition. The uncharted behavior of osmate enol esters complicates the development of new reaction methodology. In this chapter we present our studies in this area.

1. Olefin osmylation

That osmium tetroxide reacts with olefins was discovered in the 1900s, and was studied by Hofmann to perform cis-dihydroxylation catalytically in the 1910s, and by Criegge to react stoichiometrically in the 1930s.^{1,2} In 1980s, the Sharpless group made substantial progress on olefin osmylation, and developed asymmetric dihydroxylation.³ The reaction is now usually conducted with AD-mix, which is a commercial premix of $\text{K}_2\text{OsO}_2(\text{OH})_4$ as a nonvolatile osmium source, $\text{K}_3\text{Fe}(\text{CN})_6$ as the oxidant, and a quinine/quinidine derived chiral ligand. In the case of sterically hindered substrates, addition of methanesulfonamide can increase the catalytic turnover and shorten reaction time. There were two critical findings in

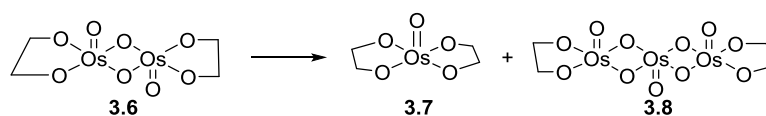
the successful development of catalytic asymmetric dihydroxylation. One was the application of ligand accelerated catalysis, and the other was the identification of two catalytic cycles (Scheme 3.1). Additionally, modifications have been developed that suppress over-oxidation and otherwise improve this methodology.



Scheme 3.1 Proposed mechanism for the Os(VIII)-catalyzed dihydroxylation of olefins⁴⁻⁶

The first critical finding was ligand acceleration, first noted by Criegee. He discovered that certain tertiary amines can accelerate stoichiometric osmylation, due to increased reactivity of the osmium tetroxide-ligand complex. However, ligands can also bind to the intermediate osmium(VI) ester **3.1** and form a six coordinate complex **3.3**, slowing down the hydrolysis/reoxidation, and thereby inhibiting catalytic osmylation in cases of hindered alkene substrates.⁶ Interestingly, the binding affinity of tertiary amines does not

monotonically map to the reactivity of osmium tetroxide-ligand complexes. For example, quinuclidine coordinates to osmium tetroxide more strongly than DHQD-CLB(dihydroquinidine p-chlorobenzoate), but accelerates the rate of osmylation much less than DHQD-CLB.⁷ It was also proposed that the binding pocket resulting from non-covalent interactions between the substrate and the ligand accounts for the rate acceleration in addition to increasing facial selectivity.⁷⁻⁹ Besides the balance of ligands in catalysis, there is another interesting fact. It has been reported that the osmium(VI) ester **3.6**, when left to stand in solution, forms osmium(VI) diester **3.7** and a black, insoluble, presumably trimeric, osmium compound **3.8** (Scheme 3.2).² It is also noted, that in practice sometimes olefin osmylation with large catalyst loading gives moderate yields and forms black precipitates during work up. Since the direct osmium tetroxide and olefin adduct is a d^2 complex, which is not stable, the formation of a five coordinate osmium complex is preferred. Therefore, dimeric osmium complexes **3.6** and osmium diesters **3.7** are formed. It is reasonable to assume that addition of ligands can reduce the possibility of dimeric or trimeric osmium complex formation, rendering the catalytic reaction more efficient.



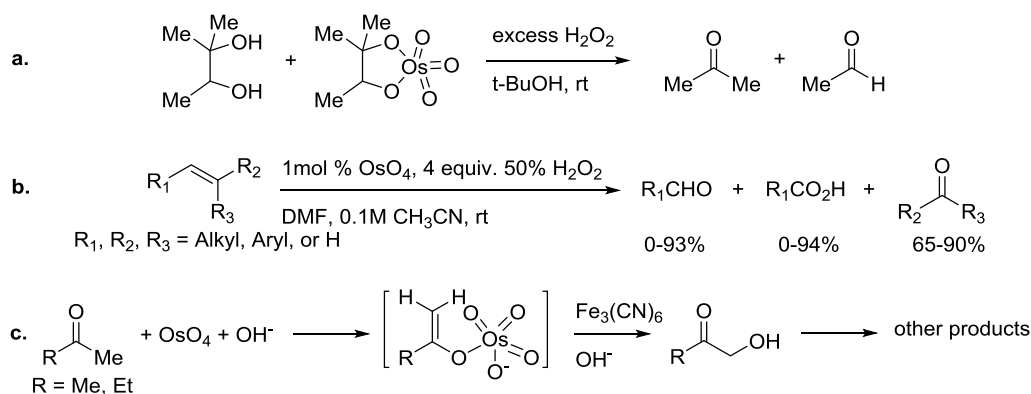
Scheme 3.2 The conversion of monoester to diester in solution²

The second critical finding that enabled the development of catalytic asymmetric alkene osmylation was identification conditions that preclude the secondary cycle in olefin osmylation and lead to greatly improved asymmetric catalysis.⁴ It was found that for some

substrates asymmetric dihydroxylation in the secondary cycle led to products with the opposite stereochemistry of the products from the primary cycle. The second cycle is caused by addition of osmium(VIII) ester **3.2** to a second olefin molecule (Scheme 3.1). Therefore, rapid hydrolysis of osmium esters **3.1** and **3.2** is critical for high ee, not only for increasing turn over. An extensive amount of work on facilitating hydrolysis of osmium esters was reported. Addition of base or phase transfer catalysts and use of aqueous alkaline buffer were reported to facilitate hydrolysis.^{10–12} A New mechanism for osmium ester cleavage was discovered.¹³ These developments provided alternative oxidants, expanded the substrate scope, and improved reaction efficiency. The strategy applied in the Sharpless dihydroxylation was to use $K_3Fe(CN)_6$ with K_2CO_3 in a mixture of *t*-BuOH and water.^{4,14} The biphasic conditions decoupled the two catalytic cycles. Oxidation of osmium(VI) ester **3.1** was minimized, since the oxidant is insoluble in the organic layer. The effect was quite obvious: when catalyzed by DHQD-CLB, the ee% (percent enantiomeric excess) for dihydroxylation of styrene increased from 56 (NMO as the oxidant) to 60 (slow addition of substrate) to 73 ($K_3Fe(CN)_6$ as the oxidant). And even the addition of K_2CO_3 (salting out effect) led the ee% of stoichiometric reaction increased from 58 to 74.¹⁴

Another modification that has been developed to improve this method aimed to suppress over-oxidation of products. It was noted that when hydrogen peroxide was employed as the oxidant, aldehydes and ketones were observed, especially for some aromatic substrates.^{15,16} Sharpless mentioned that over-oxidation was likely related to inefficient hydrolysis of osmium ester. Therefore, conditions that facilitate hydrolysis should help minimize formation of over-oxidation. And reports^{17,18} focused on C-C bond cleavage promoted by

osmylation are mostly studying reactions in acetonitrile or dimethylformamide, which are not the usual hydrolytic conditions (Scheme 3.3). Interestingly, it was also described that osmium tetroxide oxidizes acetone and ethyl methyl ketone with $K_3Fe(CN)_6$ rapidly near pHs 11 and temperatures between 25°C and 45°C, via the enolate osmium tetroxide complex (reaction **c** in Scheme 3.3).¹⁹ Notice that the Sharpless asymmetric dihydroxylation of alkenes call for the use of a constant pH of 12.0 for the best performance.¹² The initial pH of the original Sharpless conditions using AD-mix is 12.2, which slowly drops over the course of the reaction. However, the reaction is carried out at 0°C, conditions that are compatible with methyl ketones. Evidently, comparatively lower temperatures slow down osmium tetroxide promoted decomposition of methyl ketones.



Scheme 3.3 Selected examples for OsO_4 promoted oxidative decomposition^{16,17,20}

Recently, a new series of modifications aimed to improve the method for difficult substrates. The approach focused on employing the secondary cycle by preventing hydrolysis of the osmium monoester with ligands that bind strongly (Figure 3.1).^{21,22} One approach has been found to provide great benefit to reactions with olefins bearing electron-withdrawing

functionality. In this case, the initial osmium substrate complexes are difficult to hydrolyze, possibly being trapped as the dianion **3.5** under basic environment (Scheme 3.1). While hydrolysis of the osmium ester can also be conducted under acidic conditions, acid is known to cause the disproportionation of osmium(VI), so it is not usually suitable for catalytic reactions. In this approach, citric acid was introduced. It binds to osmium strongly, is thought to form complex **3.9** and stabilize osmium in acidic solution. Thus catalytic olefin osmylation appears to enter the secondary cycle and work efficiently.⁵

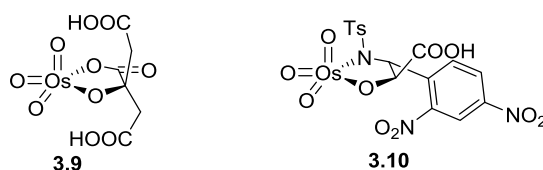


Figure 3.1 Osmium complexes for olefin dihydroxylation in the secondary cycle^{5,23}

The last modification of alkene osmylation, other than using different oxo-metals altogether, focused on methods that allow the osmium reagent to be reused. Due to the volatility and toxicity of osmium tetroxide, immobilized osmium catalysts are highly valued (Figure 3.2). The quinine/quinidine polymer supports, such as **3.11**, have the problem of slow leaching due to insufficient binding affinity. Applying polymer supports that form stable osmium esters, such as **3.12**, seems to be more effective as a reagent. Yet after several uses, osmium is still slowly released into solution, by apparently hydrolysis of osmium esters on the support.²⁴ It is remarkable that these polymer-supports are effective. After all, the Sharpless asymmetric dihydroxylation behaves so well because the employed conditions ensure hydrolysis of osmium esters and minimize the possibility of involving the secondary cycle.

Interestingly, in one case, it was reported that cross-linked poly(4-vinyl pyridine) supported osmium catalysts with hydrogen peroxide as the oxidant succeeded. The authors suggest that other systems fail because they tend to form stable oxo-bridged osmium complexes like **3.13**, which can only be oxidized by hydrogen peroxide.²⁵

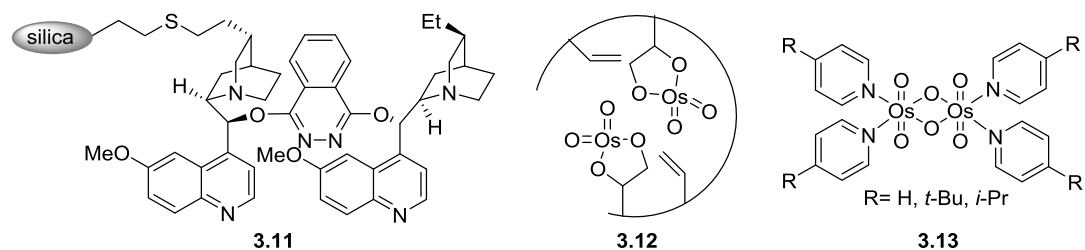


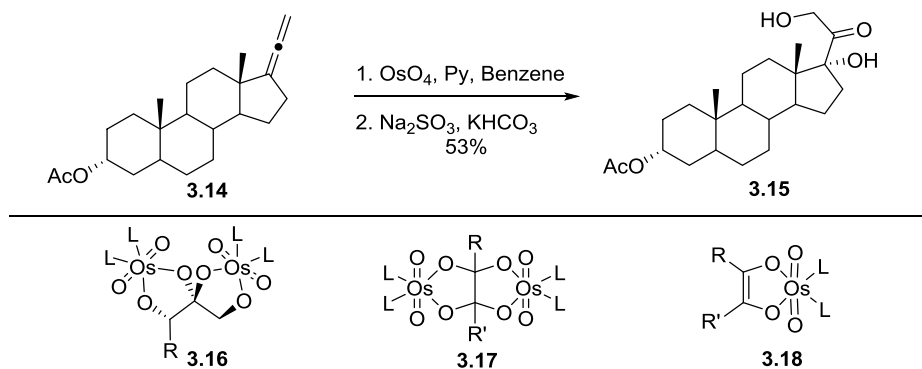
Figure 3.2 Structure of oxo-osmium(VI) pyridine complex (X = H, *tert*-butyl, isopropyl)^{25,26}

2. Allene osmylation

Published allene osmylation work

Compared to the well developed and broadly studied olefin osmylation, there are only sporadic reports about allene osmylation.^{27–30} In 1971, the first allene osmylation was reported by the Crabbe group in their corticoid side chain synthesis, where osmylation of an allenyl steroid **3.14** gave a dihydroxyketone product **3.15** (Scheme 3.4).²⁷ It seemed that in the case of stoichiometric allene osmylation, osmium complex of structure **3.16** might be formed, which upon reductive hydrolysis gave the dihydroxyketone product. It has been proposed the adduct from alkyne and osmium tertiary amine has the structure of **3.17**, which is polymeric in the solid state. However, the corresponding mono-osmium adduct

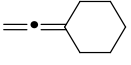
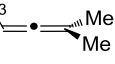
3.18 has not been isolated.²



Scheme 3.4 Stoichiometric allene osmylation by Crabtree and related osmium complexes^{2,27}

The next allene osmylation paper did not appear until 25 years later. In 1996, the Cazes group reported their first catalytic allene osmylation to give α ketols, using 1% osmium tetroxide and NMO as the stoichiometric oxidant without any other ligands.²⁸ Part of their results are shown in **Table 3.1**. They observed that reaction yields decreased while increasing the catalyst loading from 0.2% to 10%. And osmium addition favors the more substituted double bond, except in **entry 4**, where the selectivity for osmium addition was low. Also, dihydroxyketone products were not observed in any case. As will be shown, (see below), the data in entry 1 and 4 is surprising and difficult to rationalize in light of our findings.

Table 3.1 Catalytic allene osmylation²⁸

$ \begin{array}{c} \text{R}_3 \\ \diagup \\ \text{C} = \text{C} \\ \diagdown \quad \diagup \\ \text{R}_1 \quad \text{R}_2 \end{array} \xrightarrow[\text{acetone, H}_2\text{O (1:2)}]{\text{OsO}_4 \text{ 1\%, 4 eq. NMO}} \begin{array}{c} \text{R}_3 \text{---} \text{C} \text{---} \text{C} \text{---} \text{R}_1 \\ \quad \quad \quad \text{O} \quad \quad \quad \text{HO} \\ \text{A} \end{array} + \begin{array}{c} \text{R}_3 \text{---} \text{C} \text{---} \text{C} \text{---} \text{R}_1 \\ \quad \quad \quad \text{OH} \quad \quad \quad \text{R}_2 \\ \text{B} \end{array} $			
entry	allene	ratio (A:B)	yield% (A+B)
1	C_7H_{15}	76:24	60
2	Ph	100:0	35
3		100:0	48
4	C_6H_{13} 	56:44	71

In 2004 and 2005, the Fleming group reported an asymmetric allene osmylation, applying the standard Sharpless dihydroxylation condition using AD-mix.^{29,30} Selected data are presented in Table 3.2 and Table 3.3. Again, osmium addition prefers the more electron rich double bond. Dihydroxyketone products were not observed from any terminal allene substrate. However, all 1,3-disubstituted allenes with an aryl substituent generated dihydroxyketone products. Indeed, the diols became major products for trisubstituted aryl allenes. Product over-oxidation became a serious problem for trisubstituted allenes, and severely limited reaction yields.

Table 3.2 Asymmetric allene osmylation of mono and disubstituted allenes²⁹

entry	allene	recovered SM%(ee%)	yield% of A (ee%)	yield% of B (ee%, de%)
1		--	45(88)	not observed
2		--	30(<5)	not observed
3		<10	72(86)	not observed
4		20 (45)	31 (83)	32 (82, not reported)
5		10(~15)	35 (93)	20 (>90, 90)
6		18 (99)	40 (64) (R ₁ = Ph) 20 (34) (R ₁ = <i>t</i> -Bu)	28 (not reported, 53)

Table 3.3 Asymmetric allene osmylation of trisubstituted aryl allene³⁰

entry	allene	recovered SM% (%ee)	yield% of A (%ee)	yield% of B (%ee)
1		39	38 (51)	unkown
2		69	16 (31)	unkown
3		36 (77)	39 (66)	unkown
4		38 (70)	10 (79) 5 (70)	33 (31)
5		26 (45)	41 (59)	22 (56)

There appears to be another limitation to their study. When a racemic mixture of allenes is subjected to an enantiomerically pure catalyst, both enantiomers should give two diastereoisomers. The ratios of these products should be different reflecting the matched and mismatched cases. These individual ratios cannot be calculated from the overall enantiomer excess of the mixture. Therefore, it is difficult to comment on the enantioselectivity of these reactions.

In summary, stoichiometric allene osmylation gives the dihydroxyketone product presumably via bis-osmylation of both double bonds on the allene. Catalytic allene osmylation of terminal allenes occurs selectively on more substituted bond. For 1,3-disubstituted allenes and trisubstituted aryl allenes, catalytic allene osmylation prefers the more electron rich double bond, and monohydroxyketone and dihydroxyketone products are both observed, at least this catalyst loading (see below). Trisubstituted allenes are generally less reactive, giving more recovered starting material. Generally, the enantioselectivity is poor, diastereoselectivity, though rarely studied, was also poor, the yields for allene osmylation were also usually poor, with a few exceptions.

It was reported that allene dihydroxylation can also be conducted with RuCl_3 as the catalyst and NaIO_4 as the oxidant.³¹ The combination of these two reagents along with other modifications were originally used for olefin double bond cleavage. [The Sharpless group provided an improved procedure for oxidative cleavage of olefins using RuCl_3 and NaIO_4 to give carboxylic acids.³² They proposed that an oxo-triruthenium carboxylate complex generated in the reaction led to catalyst deactivation. The addition of acetonitrile as a ligand

and cosolvent can help to dissolve the inactive ruthenium complex and restore its catalytic activity. The Shing group later found that diols can be isolated from alkenes with good yields when the reaction is properly quenched and the products are not soluble in the aqueous phase.³³ The Plietker group found that addition of protic acid and CeCl_3 can promote hydrolysis of the ruthenium ester and decrease catalyst loading. With these modifications, unreactive tetrasubstituted olefins can be dihydroxylated in good yield.^{34,35} When α -allenic esters were subjected to such conditions, dihydroxyketones were isolated, but with generally low yields (Table 3.4). Diastereoselectivity was substrate dependent. The reactions were still very fast (< 5 minutes). For an aryl allene substrate and a terminal allene substrate, C-C bond cleavage to the ketone was observed as the major isolated product (not shown).³¹ Comparing reaction yields, it seems that allenes are more prone to C-C bond cleavage than olefins when ruthenium was used.

Table 3.4 Ruthenium catalyzed allene dihydroxylation³¹

$ \begin{array}{c} \text{R}_1 \\ \diagup \\ \text{C}=\text{C}=\text{C}-\text{CO}_2\text{Et} \\ \diagdown \quad \quad \quad \diagup \\ \text{R}_2 \quad \quad \quad \text{R}_3 \end{array} \xrightarrow[0^\circ\text{C}]{\text{RuCl}_3 \cdot 3\text{H}_2\text{O}, \text{NaIO}_4, \text{EtOAc}, \text{CH}_3\text{CN}, \text{H}_2\text{O}} \begin{array}{c} \text{O} \\ \parallel \\ \text{R}_1-\text{C}-\text{C}-\text{CO}_2\text{Et} \\ \diagup \quad \diagdown \quad \diagup \\ \text{R}_2 \quad \text{OH} \quad \text{R}_3 \quad \text{OH} \end{array} $			
entry	allene	Yield%	de%
1	$ \begin{array}{c} \text{Me} \\ \diagup \\ \text{C}=\text{C}=\text{C}-\text{CO}_2\text{Et} \\ \diagdown \quad \quad \quad \diagup \\ \text{Me} \end{array} $	32	--
2	$ \begin{array}{c} t\text{-Bu} \\ \diagup \\ \text{C}=\text{C}=\text{C}-\text{CO}_2\text{Et} \\ \diagdown \quad \quad \quad \diagup \\ t\text{-Bu} \end{array} $	24	--
3	$ \begin{array}{c} t\text{-Bu} \\ \diagup \\ \text{C}=\text{C}=\text{C}-\text{CO}_2\text{Et} \\ \diagdown \quad \quad \quad \diagup \\ \text{Me} \end{array} $	72	0
4	$ \begin{array}{c} t\text{-Bu} \\ \diagup \\ \text{C}=\text{C}=\text{C}-\text{CO}_2\text{Et} \\ \diagdown \quad \quad \quad \diagup \\ n\text{-Bu} \end{array} $	38	88
5	$ \begin{array}{c} t\text{-Bu} \\ \diagup \\ \text{C}=\text{C}=\text{C}-\text{CO}_2\text{Et} \\ \diagdown \quad \quad \quad \diagup \\ \text{Me} \quad \quad \quad \text{OEt} \end{array} $	45	48:38:14

Osmium enolate/enol ester

We envisioned that the osmium tetroxide addition to an allene will give an osmium enolate **3.19** (Figure 3.3), and that this enolate could be used as a nucleophile within an oxidative catalytic cycle. Indeed, we wondered whether the use of an electrophile would rescue and improve catalytic allene osmylation. The chemistry of alkali metal enolates and early transition metal enolates has been well studied. Comparatively, the behavior of enolates bound to middle and late transition metals is less understood, especially for osmium enolates. Some low valent enolato osmium complexes **3.20** and **3.21** have appeared in the literature (Figure 3.3)^{36,37}, but their reactivity in the context of an organic reaction is completely unknown. We believe that high valent osmium enolates might share some reactivity common among metal enolates, for example, nucleophilic addition towards good

electrophiles. Many metal catalyzed 1,4-addition to nitroalkenes have been reported. Particularly, it was revealed by the Sodeoka group that enolato nickel complexes can perform conjugated addition to nitroalkenes.³⁸ They proposed a transition structure **3.22**, where both the enolate and the electrophile coordinate to the metal center. Osmium enolates might react in a similar fashion.

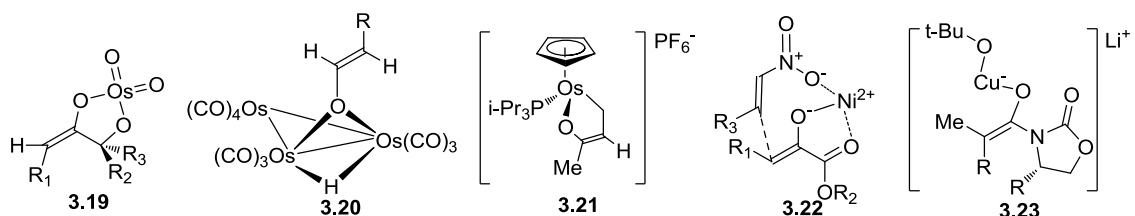


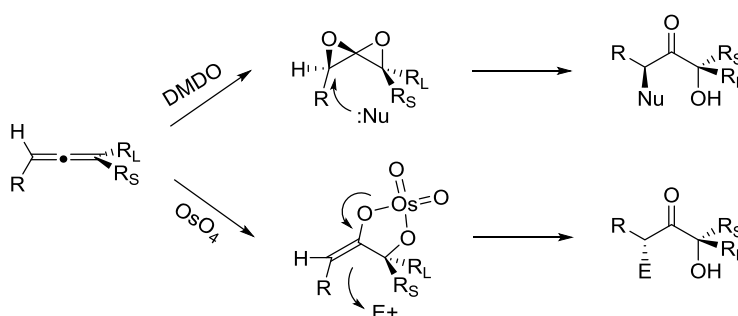
Figure 3.3 Proposed osmium enolate and other reported metal enolates^{36–39}

One concern is the stability of osmium enolates under oxidative conditions. The Marek group has shown a nice example of generating copper enolates **3.23** under oxidative conditions, where a vinyl cuprate was oxidized by lithium *tert*-butylperoxide at -78°C to form a copper enolate which can be further trapped as a silyl enol ether.³⁹ However, enolates generated in the presence of osmium tetroxide are expected to behave differently, since enol ethers,⁴⁰ enol phosphates,⁴¹ and vinyl esters⁴² are all known to react with osmium tetroxide. How to effectively capture osmium enolates (or enol esters) before it reacts with osmium tetroxide was the central challenge that we successfully addressed.

Allene osmylation from the Williams group

Our study on allene osmylation started in 2010. Some of our work^{43–45} is shown below. We

envisioned that allene osmylation followed by enolate capture would give the anti-adduct as illustrated in the lower half of **Scheme 3.5**. As discussed in section 3.1, and based on our experience with allene epoxidation, allene osmylation should favor the more substituted double bond. The face selectivity is expected to be good, given the difference between the two substituents H and R on the non-reacting terminus. The electrophile addition to the enolato osmium complex would be directed by $A^{1,3}$ -strain, thus giving the anti-adduct as the major product. This insight could provide a new method for the stereoselective functionalization of chiral allenes, complementing our spirodiepoxide chemistry,^{46–51} which accesses the syn α -substituted- α' -hydroxyketone by nucleophilic addition to the epoxidized chiral allenes.



Scheme 3.5 Face selective DMDO oxidation and allene osmylation

The result for stoichiometric osmylation of cyclic bis-allenes is shown in Table 3.5. The reaction employed osmium tetroxide in a mixture of *t*-BuOH and H_2O at room temperature and various electrophiles (2-5 equiv.) including SelectFlour®, NCS, NBS, and Brønsted acids (hydrochloric acid, acetic acid, citric acid). Excess osmium tetroxide effected reaction of both allene (entry 1 – 3). When 1.1 – 1.5 equiv of osmium tetroxide is used, evidently, the

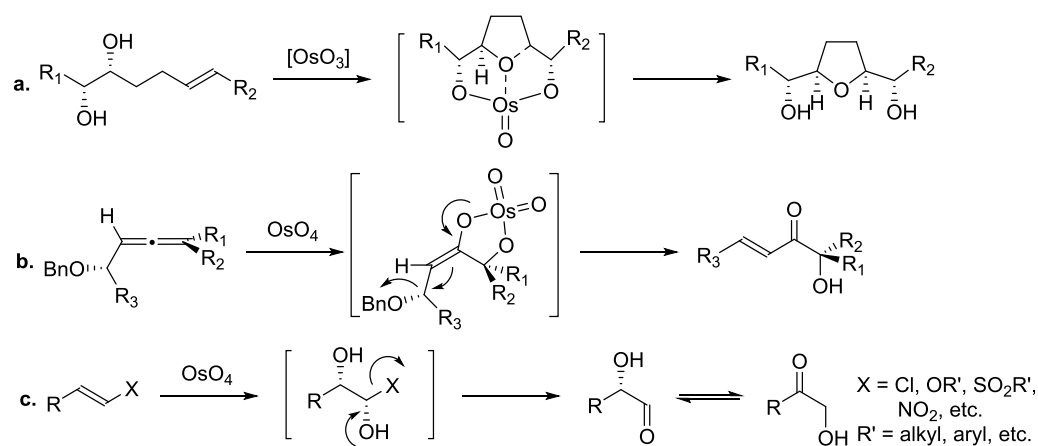
reaction favors osmium addition to one of the most electron rich allenic π -bonds. Hence, the disubstituted allene terminus that is not flanked by an ester react fastest with osmium tetroxide. In all cases, the stereoselectivities are excellent, only one diastereoisomer was observed. More importantly, diols are not observed (*c.f.* Crabee's stoichiometric allene osmylation, scheme 3.4). Indeed, the introduced electrophiles appear to capture the osmium enolate, preventing further oxidation of the osmium enolates. Although the yields are moderate, given the complexity of the transformation, the efficiency of allene oxidation and functionalization is good.

A black precipitate was observed and may indicate ineffective hydrolysis of osmium complex and lead to the low yield. Interestingly, in entry 5, an example of oxidative cyclization of allene was observed. However, this is quite different from Donohoe's oxidative cyclization of diene derivatives (reaction **a** in Scheme 3.6).⁵² A stepwise osmylation, elimination, and conjugated addition sequence (reaction **b**) is more likely to be involved. This is similar to dihydroxylation of vinyl halides and enol ethers, followed by α -elimination (reaction **c**).⁵³ This rational has strong supporting evidence as indicated by entry 6, which is the corresponding masked version of the substrate in entry 5.

Table 3.5 Stoichiometric osmylation of cyclic bisallenes

entry	allene	product	d.r.	yield
1			--	45%
2			>20:1	56%
3			>20:1	52%
4			>20:1	84%
5			>20:1	48%
6			>20:1	32% ^a
7			>20:1	59%

a) partial conversion.



Scheme 3.6 Osmylation elimination^{52,53}

Table 3.6 shows stoichiometric osmylation of some trisubstituted and disubstituted allenes. Compared to cyclic bis-allenes, isolated yields for reactions involving acyclic aliphatic allenes are higher on average, although the diastereoselectivities are inferior. The decrease in stereoselectivity could be explained by the loss of steric bias introduced by the 14-membered ring system of cyclic bis-allenes. By increasing steric bulkiness of one substituent in the allene (entry 7-9), we see improvement in stereoselectivity. In entry 9, one might expect osmium addition to the electron rich double bond distal to the silyl ether substituent. However, osmylation favors reaction at the more accessible double bond. This trend is consistent with the observation that in olefin osmylation and is in contrast to allene epoxidation. The sterically more accessible double bond is sometimes preferred over the electron rich one.⁵⁴

Table 3.6 Stoichiometric osmylation of acyclic allenes

entry	allene	product	d.r.	yield
1			--	62%
2			--	75%
3			--	70%
4			7:1	74%
5			2.5:1	51%
6			1.7:1	55%
7			5.9:1	68%
8			5.3:1	78%
9			>20:1	64%

Electrophile addition to osmium enolates can also be conducted catalytically. The reaction conditions we found most generally effective involve 10% OsO₄ and 2 equiv NMO as the stoichiometric oxidant, solvents and electrophiles are similar to the stoichiometric reaction condition. As shown in Table 3.7, catalytic allene osmylation/electrophile capture proceeds smoothly with yields comparable to stoichiometric reactions. For substrates with *tert*-butyl like substituents, we see excellent stereoselectivities (entry 12-14). One thing worth mentioning is that when NCS and NBS were used as electrophiles in catalytic conditions,

they are added to the reaction mixture slowly via syringe pump, to avoid background reactions. However, SelectFlour® is less reactive and does not require slow addition and, pleasingly, proceeds with excellent stereoselectivity.

Table 3.7 Catalytic osmylation of acyclic allene

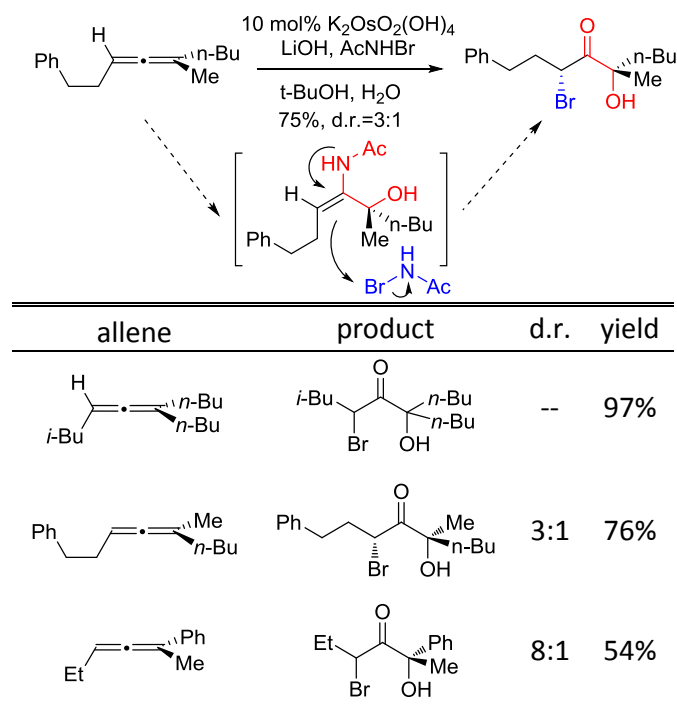
entry	allene	product	d.r.	yield
1			--	75%
2			--	40%
3			--	68%
4			--	68%
5			--	71%
6			1.8:1	58%
7			2:1	64%
8			--	44%
9			5:1	57%
10			2.4:1	55%
11			1.6:1	46%

Table 3.7 Catalytic osmylation of acyclic allene (continued)

entry	allene	product	d.r.	yield
11			1.6:1	46%
12			>20:1	54%
13			>20:1	62%
14			>20:1	69%

Besides general dihydroxylation conditions, we also subjected our allene substrates to the Sharpless aminohydroxylation conditions with the hope of incorporating nitrogen into allenic substrates. Surprisingly, the bromohydroxyketone product was isolated (Table 3.8). The formation of this product was originally rationalized in the following way: The active oxidant imidotrioxoosmium(VIII) intermediate adds to allene, resulting in an enamide after hydrolysis. Subsequent nucleophilic attack on N-bromoacetamide delivers the bromohydroxyketone product. Interestingly, an aryl allene substrate also reacted smoothly under these conditions to give a good yield and very good stereoselectivity (entry 3), catalytic allene osmylation of this substrate using NBS as the electrophile gave a complex mixture that appeared to include this product in low yield.⁴⁵

Table 3.8 Initial mechanistic framework for osmylation of trisubstituted allenes with aminohydroxylation reagent



3.2 Result and discussion

In this section, we describe more detailed studies of allene osmylation, focusing on understanding the stereoselectivity, efforts towards improving catalyst efficiency, and results on allene aminohydroxylation.

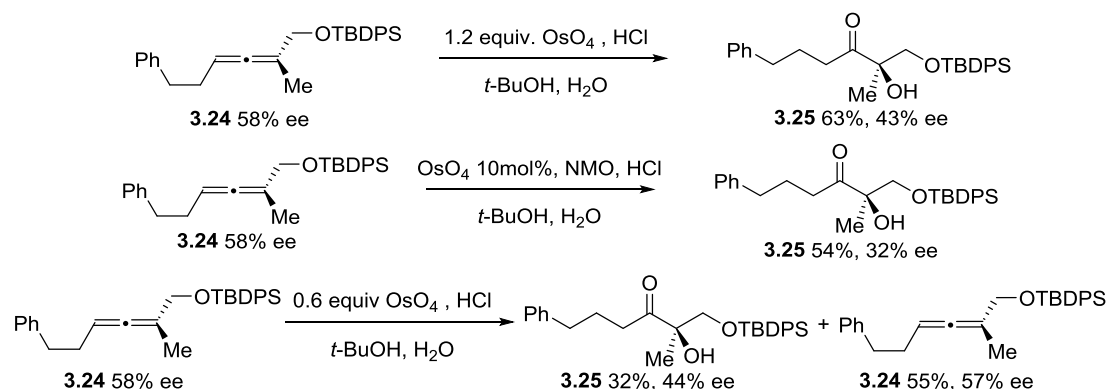
1. Osmium addition to allene and electrophile trapping

As shown by the Fleming group,^{29,30} the enantioselectivity for osmylation of monosubstituted (achiral) aryl allenes using AD-mix is good (88-92 ee%). However, for 1,3-disubstituted (chiral) aryl allenes, the diastereoselectivity is generally poor and gave

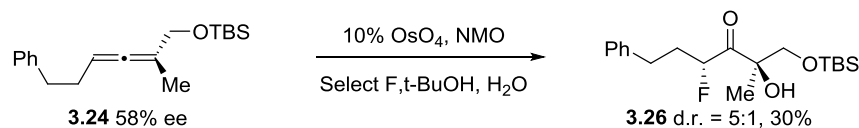
complex mixtures. Moreover, alkyl substituted allenes failed. In our example of allene osmylation/electrophile trapping, cyclic bisallenes gave very excellent diastereoselectivity. For acyclic allenyl substrates, diastereoselectivity was good, especially when the two substituents on one terminus are significantly different in terms of steric bias. Our allene osmylation/electrophile capture sequence includes two key points: face selective osmium addition and face selective electrophile addition to the enolato osmium. The overall diastereoselectivity is the consequence of both sub-processes.

To understand the face selectivity in each step, we first studied the osmium addition to a highly enantiomerically enriched allene (Scheme 3.7). The substrate **3.24** was prepared in 4 steps via the propargyl alcohol, which was generated by way of CBS reduction⁵⁵ of the corresponding alkynone. Reduction using Noyori's asymmetric transfer hydrogenation condition was not successful. Catalyst deactivation and alkyne reduction was observed, and slow addition of the substrate was not helpful.⁵⁶ Applying our one pot allene synthesis procedure, allene **3.24** was prepared in 65% yield with 58% ee. However, the ee% of the osmium addition product after hydrolysis was deteriorated, and the ee% for product isolated under catalytic conditions was even lower. In principle, the decrease in ee% could result from both osmium promoted racemization of chiral allenes and face selectivity of osmium addition. Isomerization of allenes with a low valent triosmium complex at low temperature has been reported before.⁵⁷ It is a concern that allene might racemize under the current reaction conditions. But a sub-stoichiometric osmylation using 0.6 equiv of osmium tetroxide suggests that this is unlikely, because the recovered starting material ee was found to be nearly unchanged. If assuming the face selectivity of osmium addition to

either enantiomer is equal, the calculated face selectivity is approximately 7:1 for this substrate. Considering the simplicity of the system and its amenability to optimization, such face selectivity may be acceptable. The lower selectivity under catalytic conditions is intriguing. It could be related to no stirring during the reaction, or the unknown black precipitate observed in all these reactions, or to the heterogeneity of these systems. We tried to determine the ee% of a fluorine addition product **3.26** (Scheme 3.8). Neither **3.26** nor the corresponding diol were able to be resolved by HPLC. No further effort was taken to determine the enantiomer ratio. Alternative mechanisms cannot be ruled out at this time. For example, osmium addition to the π -bond may be reversible, as noted for alkenes. The ee may therefore reflect the rate of Os(VI) ester hydrolysis/oxidation. Similarly, other isomerization pathways may be relevant, such as oxyallyl zwitterion formation of the osmate ester.



Scheme 3.7 Osmium addition to an enantiomerically enriched allene



Scheme 3.8 Osmium addition to an enantiomerically enriched allene

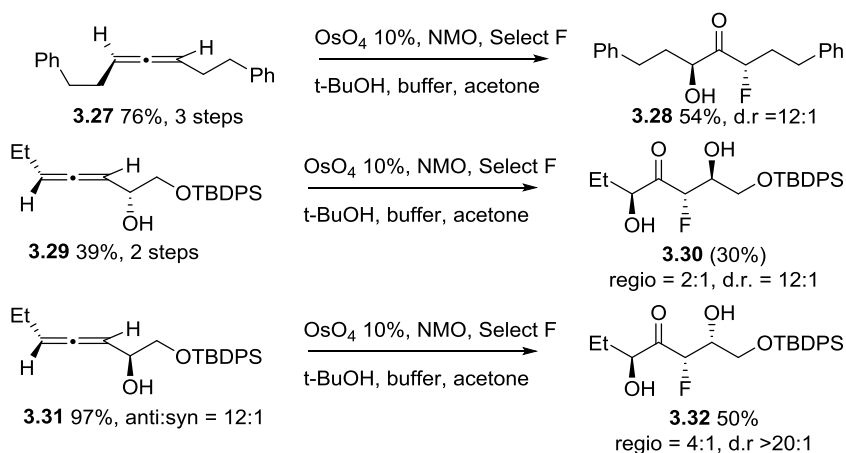
From our previous studies, we had found that the diastereoselectivity can be increased by increasing the steric bulk of one substituent (Table 3.6 and 3.7). We began to wonder about the effect of altering the size of the substituent adjacent to the site of osmium addition. As shown in Table 3.9, the diastereoselectivity indeed increased as the substituent was changed from methylene to *tert*-butyl group. However, the reaction yields dropped significantly. Osmium glycol esters generated from sterically hindered olefins are known to be difficult to hydrolyze, this might also be true for allenes.

Table 3.9 Osmylation/Fluorination of trisubstituted allenes

allene	product	d.r.	yield
		1.8:1	68%
		4.7:1	30%
		4.7:1	25%
		4.7:1	48%
		6.9:1	39%

We also studied 1,3-disubstituted allene, in addition to those shown in Table 3.6 and 3.7. As shown in Scheme 3.9, osmylation of a C_2 symmetric allene **3.27** gave good yield and diastereoselectivity. Hydroxyl group-directed olefin osmylation has been reported before,^{58,59} we also prepared two diastereoisomeric allenes **3.29** and **3.31**. Both the

regioselectivity and diastereoselectivity are much higher for allene **3.29** than for allene **3.31**. We concluded that this reflects a matched and mismatched diastereoselectivity. The corresponding ether of **3.31** gave a complex mixture with little to no selectivity (data not shown).



Scheme 3.9 Osmylation/Fluorination of disubstituted allenes

2. Efforts towards reducing the catalyst loading

The standard Sharpless asymmetric dihydroxylation condition using AD-mix only employs 0.1% $\text{K}_2\text{OsO}_2(\text{OH})_4$. Due to the high toxicity and expense of osmium tetroxide, we wanted to lower catalyst loading in our allene osmylation reactions. Also, it has been shown by the Cazes group that using less osmium tetroxide can improve yields,²⁸ (see Section 3.1). We first started with 2.5% osmium tetroxide. When the original allene osmylation conditions, including 2 equiv. oxidant NMO and 2-5 equiv. electrophile NCS in a 1:1 mixture of *t*-BuOH and H_2O , was applied, significant background reaction (reaction between NCS allene and water to generate chloroalkenes and chlorohydrins) took place and catalyst deactivation

Chemical structures of the reagents and ligands used in the synthesis:

- DABCO: 1,4-diazabicyclo[2.2.2]octane
- quinuclidine: 8-azabicyclo[3.3.1]nonane
- TMEDA: 1,1,3,3-tetramethyl-2,2-bis(2-methylpropan-2-yl)aziridine
- 2,6-Pyridinedimethanol: 2,6-pyridinedimethanol
- sodium citrate: sodium 3-oxopentanoate
- DHQD: 6-methoxy-2-(1-hydroxy-2-ethyl-2-oxobicyclo[2.2.1]hept-5-en-5-yl)quinoline
- DHQDCLB: 6-methoxy-2-(1-(4-chlorobenzoyloxy)-2-ethyl-2-oxobicyclo[2.2.1]hept-5-en-5-yl)quinoline
- (DHQD)₂PHAL: 6-methoxy-2-(1-(2-((6-methoxy-2-(1-hydroxy-2-ethyl-2-oxobicyclo[2.2.1]hept-5-en-5-yl)quinolin-2-yl)oxy)phenyl)-2-oxobicyclo[2.2.1]hept-5-en-5-yl)quinoline

To further promote hydrolysis, we introduced some additives which were shown to assist the hydrolysis of osmium complex in olefin osmylation.^{2,10} The results are shown in Table

3.10. When tetraethylammonium acetate (TENOAc) and tetraethylammonium hydroxide (TENOH) were used, entries 2 and 3, the reaction became faster as indicated by less recovered starting material. However, the product yields were even lower, which might be caused by promotion of an undesired reaction path way. With addition of methanesulfonic acid (MSA), a compound which is known to shorten the reaction time for dihydroxylation of hindered olefin substrates, the recovered starting material was reduced, but the product yields did not increase. In all cases studied, the additives increased the reaction rate but did not increase the overall yield. These data were somewhat perplexing, because the reaction mass balance was low, and yet the TLC data were simple: starting material, desired product, and only trace quantities of the diol and the monohydroxy ketone were observed. There was no evidence of organics in the aqueous phase and no evidence of over-oxidation/cleavage other than the low mass balance.

Table 3.10 The effect of additives on osmylation of trisubstituted allenes

entry	ligand	additive	yield %	recovered allene
1	20% DABCO	none	46%	36%
2	20% DABCO	6% TENOAc	29%	32%
3	20% DABCO	5% TENOH	28%	29%
4	20% DABCO	100% MSA	37%	26%
5	5% DHQDCLB	none	29%	46%
6	5% DHQDCLB	50% MSA	20%	31%
7	100% Sodium citrate	none	19%	47%
8 ^a	20% DABCO	none	78%	0%

a) 10% OsO₄ was used instead of 2.5% OsO₄

As mentioned before, olefin osmylation was suggested to be conducted at a constant pH of 12.0.¹² Under such conditions, product over oxidation can be minimized, reaction times can be greatly shortened, and the usage of methanesulfonic acid becomes unnecessary. Thus we used buffers of pH ranging from 11.0 to 13.0 to perform our allene osmylation. The results are shown in Table 3.11, pH of 12.0 gave the best result, but compared with conditions using K₂CO₃ as the base (entry 1 in Table 3.10), which could also be considered as a weak buffer, pH of 12.0 showed no advantage. The decreased yield and lower ratio of chlorinated products in entry 4 and 5 could be a result of chlorinated product enolization and then decomposition under strong basic conditions.

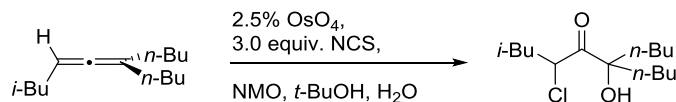
Table 3.11 Osmylation/Chlorination of trisubstituted allenes under basic conditions

entry	pH	recovered SM%	yield %	ratio (Cl:H)
1	11.0	63%	14%	>20:1
2	11.5	53%	26%	>20:1
3	12.0	52%	34%	>20:1
4	12.5	58%	15%	10:1
5	13.0	67%	10%	1.3:1

Perplexed by the above results, we further considered performing these reactions under acidic conditions, since we believed that the low turnover might be related to the difficulties in hydrolyzing osmium complexes, and since the hydrolysis of certain osmium complexes appeared to benefit from acidic conditions.⁵ As shown in Table 3.12, NMO was used as the stoichiometric oxidant because of toxicity issues related to $K_3Fe(CN)_6$ under acidic conditions. In contrast to the conditions described in Table 3.10 and 3.11 ($pH > 8$), allene consumption was fast and complete under neutral and acid conditions ($pH \leq 7$), as summarized in Table 3.12. Under these conditions (Table 3.12) complex mixtures were obtained. Omission of osmium tetroxide revealed that under acidic conditions the background reaction of allene with NCS dominated the product distribution. Use of *t*-BuOMe, instead of *t*-BuOH, resulted in the reaction mixture being biphasic and suppressed osmylation as well as the background reaction, such that the reaction cleanly yielded the desired product, albeit in very low efficiency (< 5%, data not shown). Under the conditions shown in Table 3.12, the background reaction probably generated products containing

chlorinated olefins and chlorohydrins. The desired product apparently formed, but we were surprisingly unable to purify it, since it co-eluted with other several other – presumably chlorinated – compounds. All yields are estimated based on NMR data.

Table 3.12 Osmylation/Chlorination of trisubstituted allenes under acidic conditions

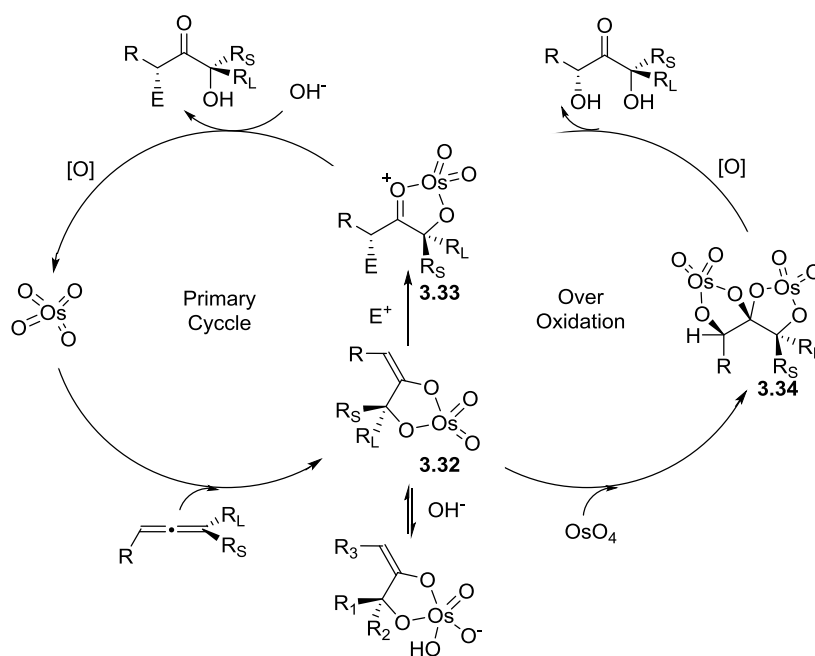


entry	pH	ligand	yield %
1	3.0	Na Citrate	(15%)
2	4.0	Na Citrate	(17%)
3	5.0	Na Citrate	(17%)
4	6.0	Na Citrate	(21%)
5	7.0	Na Citrate	(27%)

Allene osmylation proved problematic under acidic conditions and the decreased yield appears to be a consequence of the increased rate of side reactions. Allene osmylation under basic conditions was clean, but slow and hence impractical. Taken together, of the ligands commonly used to promote alkene osmylation, DABCO emerged as the most efficient. Use of 10% osmium tetroxide in conjunction with DABCO represents a smooth, clean, and efficient method of allene oxidative chlorination. Importantly, under all of these conditions, the dihydroxyl ketone products were not observed or only constituted to a very small portion of the product mixture (< 2%). This finding stands in stark contrast to osmylation of aryl allenes as disclosed by Fleming.

3. Oxidation of osmium enolate/osmate enol ester

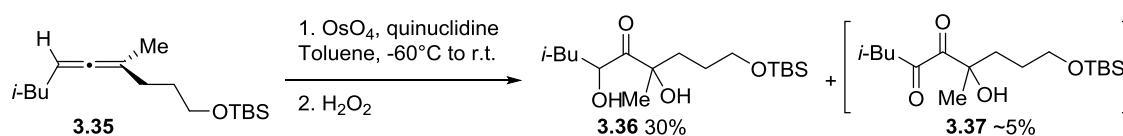
One key point of our study was to capture osmium enolates with electrophiles. Nucleophilic addition to an osmium enolate **3.32** might form an intermediate like **3.33** which should be hydrolyze readily (Scheme 3.10). Also, in most of our allene osmylation examples, the ratio of α -halo- α' -hydroxyketones to α -hydroxyketones is very high, which means electrophile capture is much faster than the hydrolysis of the osmium enolate. The question remains: why is the turnover for these reactions low? One possibility is that over-oxidation of the osmium enolate gives a bis(osmium) complex that is slow to hydrolyze.



Scheme 3.10 Mechanic framework for the Os(VIII)-catalyzed oxidation of allenes

To force the formation of the bisosmium adduct, we performed stoichiometric allene osmylation using 2 equiv of osmium tetroxide (Scheme 3.11). Within 0.5 hours at $-60\text{ }^\circ\text{C}$,

virtually all of the allene was consumed (> 95%). The reaction mixture was then warmed to room temperature to ensure complete consumption of starting material **3.35**. The resulted dark green solution slowly formed a black solid upon standing. Removal of the solvent gave an insoluble fine black powder. Regular reductive treatment of this solid with saturated aqueous Na₂SO₃ gave only trace amounts of product by TLC analysis. Only oxidative workup using hydrogen peroxide, which was accompanied by vigorous oxygen evolution, liberated the dihydroxyketone product **3.36** (30% isolated yield. A single isomer as observed by ¹H-NMR, relative stereochemistry not determined). A minor byproduct (**3.37**) was also isolated and tentatively assigned as α-diketone based on ¹H-NMR.



Scheme 3.11 Stoichiometric allene osmylation using 2 equiv of osmium tetroxide

4. Peroxides as stoichiometric oxidant in osmium tetroxide/allene derivatization cascade

An interesting series of studies were also performed, related to hydrogen peroxide as the stoichiometric oxidant. A former graduate student Kai Liu from our group conducted a preliminary study on allene osmylation using hydrogen peroxide and *t*-BuOOH as the stoichiometric oxidants. The reaction involving hydrogen peroxide is generally fast, and is complete in about 0.5 hours. It is also accompanied by oxygen evolution. The osmium tetroxide catalyzed decomposition of hydrogen peroxide is known, and it was suggested that an osmium(VII) species is involved.⁶¹ Interestingly, when *t*-BuOOH was used, α-*tert*-

butoxyketone **3.39** was isolated as the major product (instead of the dihydroxyketone **3.40** when hydrogen peroxide was used). This led us to speculate that osmium(VII) and the radical cation generated from the enolato ligand by inner shell electron transfer of the osmium(VIII) enolates could be formed and trap solvent to give the ether product (**3.39**). A series of reactions were carried out to test this possibility, as shown in Table 3.13. Varying the ratio of *t*-BuOH to H₂O in the solvent had a limited (~40%) and counterintuitive effect in product yield (the higher ratio of water corresponds to a lower ratio of putative water addition, *c.f.* entries 1 – 3). The isopropyl ether was not observed when *i*-PrOH was used in the solvent. And when cumene hydroperoxide was used, a small amount of the 1,1-dimethyl benzyl ether was isolated (as a mixture containing 1,1-dimethyl benzyl alcohol). We conclude that the osmium(VII) radical species is not involved in the major reaction pathway, and the formation of α -*tert*-butoxyl ketone products must be via another mechanism. Intermolecular (bimolecular) process would seem to be unfavorable and inconsistent with the product distribution. Intramolecular process may be relevant. The product could be formed via an interrupted osmium(VI) to osmium(VIII) oxidation. After *t*-BuOOH coordination, the enolate could capture the coordinated *tert*-butoxy group through a six membered ring transition state.

Table 3.13 Catalytic osmylation using H₂O₂ and *t*-BuOOH

Reaction scheme: Allene **3.38** (with *i*-Bu and *n*-Bu substituents) reacts with OsO₄ (10%) in a solvent [O] to yield osmate ester **3.39** and vicinal diol **3.40**.

entry	oxidant	solvent	ratio of A:B	yield % of A	yield % of B
1	<i>t</i> -BuOOH	<i>t</i> -BuOH : H ₂ O (2:1)	1.1:1	40	38
2	<i>t</i> -BuOOH	<i>t</i> -BuOH : H ₂ O (1:1)	2.7:1	40	15
3	<i>t</i> -BuOOH	<i>t</i> -BuOH : H ₂ O (1:2)	3.3:1	36	11
4	<i>t</i> -BuOOH	<i>i</i> -PrOH : H ₂ O (1:1)	1.5:1	44	29
5	H ₂ O ₂	<i>t</i> -BuOH : H ₂ O (1:1)	1:100	<1	64
6	H ₂ O ₂	<i>i</i> -PrOH : H ₂ O (1:1)	--	--	68
7	PhC(Me) ₂ OOH	<i>t</i> -BuOH : H ₂ O (1:1)	--	(15) ^a	10

a) The corresponding α -(2-phenylpropan-2-yl)oxy- α' -hydroxyketone was isolated.

It was also found that allenes were consumed in 2-4 hours at 0°C when 2.5% osmium tetroxide with hydrogen peroxide was used; however, low yields (< 20%) and mass balance, along with some evidence for oxidative fragmentation (data not shown). The problem of catalyst deactivation seemed to be solved by employing hydrogen peroxide, since using K₂Fe₃(CN)₆ with K₂CO₃ gave much unreacted starting material; hydrogen peroxide is able to oxidize the black osmium containing precipitates generated from stoichiometric osmylation; however, the product yields were too low to be synthetically useful. It is known that hydrogen peroxide can cause C-C bond cleavage when vicinal diols complex with osmium tetroxide. It also has been suggested that over-oxidation products are easier to generate when osmate esters hydrolyze slowly. Therefore, we consider hydrogen peroxide under

these conditions to be a poor choice.

In summary, it seems that an osmium(VI) enolate is generated in our osmium tetroxide/allene functionalization. The osmium enolate bond is vulnerable to hydrolysis similar to other osmate esters, especially after electrophile capture. Low catalyst turn over appears to involve double osmylation of an allene, leading to insoluble complexes when NMO is used, and substrate over-oxidation and cleavage when peroxides are used.

5. Allene aminohydroxylation: substrate scope expansion and product derivatization

Previously, we have shown that when AcNHBr (N-bromoacetamide) was used as the stoichiometric oxidant, the α -bromo- α' -hydroxyketone is isolated as the major product. More examples are shown in Table 3.14, following our optimized reaction conditions: 10 mol% $K_2OsO_2(OH)_4$, 5 equiv. of AcNHBr and 5 equiv. of LiOH in *t*-BuOH : H₂O (2:1). The reaction was usually completed in 30 min. Yields are generally good to excellent except aryl allenes. Diastereoselectivity is moderate at the 1,1-disubstituted site (entry 2-5), but considering the small difference between the methyl group and the other alkyl group, the result is quite good. For aryl allenes, the selectivity is better but yields are lower (entries 6, 7).

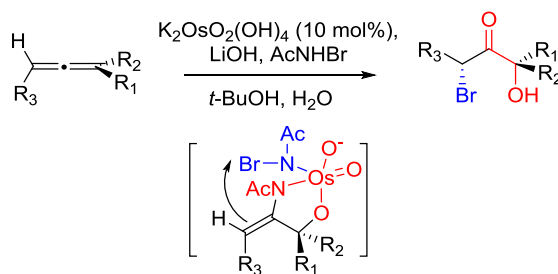
Table 3.14 Osmylation/bromo-addition of trisubstituted allenes^a

entry	Allene	product	d.r.	yield
1			--	98%
2			3:1	68%
3			2:1	50%
4			3:1	58%
5			3.2:1	78%
6			4.7:1	42%
7			5.1:1	32%

a) Conditions: 10 mol% $\text{K}_2\text{OsO}_2(\text{OH})_4$, 5 equiv. of AcNHBr , 5 equiv. of LiOH in $t\text{-BuOH} : \text{H}_2\text{O}$ (2:1), reactions are conducted for around 30 min at room temperature.

One feature of this reaction is that excess (5 equiv) AcNHBr/LiOH (1:1) appears to be required for good efficiency. When 2-3 equiv of these reagents were used the formation of the bromohydrins and bromoolefins became significant. Similar results were observed when the AcNHBr/LiOH ratio was changed to greater than 1:1 or less osmium catalyst was used. The study of olefin aminohydroxylation has shown that using equal ratios of LiOH to AcNHBr is important to avoid direct reaction between AcNHBr and olefins. Given that AcNHBr is highly reactive and the reaction is fast and clean and earlier studies showed that the addition of other electrophiles did not change the reaction outcome,^{44,45} we propose that

bromination occurs intramolecularly via the osmium(VI) coordination complex shown in Scheme 3.12. The bromo group is delivered by way of the 6-membered cyclic transition structure, and parallels our proposal for α -*tert*-butyl ether formation. These intramolecular processes are thermally allowed, 6 π , retro-ene-type pericyclic reactions and not simple 6-endo enolate nucleophilic bromine substitutions.



Scheme 3.12 Revised mechanistic framework for osmylation/bromo-addition of trisubstituted allenes (*c.f.* Table 3.8)

The allene aminohydroxylation products, α -bromo- α' -hydroxyketones, are a class of useful intermediates. As shown in Table 3.15, they can be easily and efficiently converted into other compounds under standard conditions (see supporting information for details). The bromine can be displaced by azides, thiols, thioacetates, and amines as shown in entries 1-4 and 5. The substitution reactions are high yielding with inversion of the stereocenter. Except in entry 4 and 5, epimerization of the bromine substituted carbon was not observed. We attribute epimerization to the basic reaction conditions (sodium hydroxide in dimethyl sulfoxide and dimethyl amine in acetonitrile). In entry 4, oxetanones can be formed via intramolecular displacement of the bromine and the yield is quite good. We also show that E2 elimination under the ionic conditions developed by Paquette,⁶² gave the enone product

(entry 6). Lastly, reduction of the bromo-ketone stereoselectively gave the diol. The stereochemistry was assigned as *syn*, in accord with the polar Felkin-Ahn model and was consistent with by ^1H -NMR analysis of the corresponding epoxide.

Table 3.15 Product derivatization

entry	bromo-ketone	product	d.r.	yield
1			3:1	98%
2			3:1	80%
3			3:1	95%
4			1.3:1	68%
5			1:1	85%
6			--	77%
7			>20:1	82%
8			--	85%

3.3 Summary

In this chapter, we discussed our allene osmylation/electrophile capture which lead to the

generation of α -halo- α' -hydroxyketones efficiently. Osmium addition to allene prefers the more substituted double bond on the less hindered face, and electrophile addition is governed by A^{1,3} strain. The reaction yields and stereoselectivities are good to excellent. Both 1,3-disubstituted allenes and trisubstituted allenes react smoothly under conditions using stoichiometric oxidant and additional electrophiles. However, 1,3-disubstituted allenes failed to give isolable product under conditions using AcNHBr, possibly because of the known proclivity for over-oxidation and oxidative cleavage of these intermediates under these basic conditions. Taken together, we have developed reliable method for allene oxidation/fluorination and allene oxidation/bromination. In the course of developing an understanding of allene oxidative osmylation and catalyst turnover,⁶³ we have developed an optimized procedure for allene oxidation/chlorination, as well, albeit additional studies are warranted. These highly functionalized products are excellent intermediates for further modification and use in organic synthesis.

3.4 References

- (1) Criegee, R.; Marchand, B.; Wannowius, H. *Justus Liebig's Ann. der Chemie* 1942, 550, 99.
- (2) Schroeder, M. *Chem. Rev.* 1980, 80, 187.
- (3) Kolb, H. C.; Vannieuwenhze, M. S.; Sharpless, K. B. *Chem. Rev.* 1994, 94, 2483.
- (4) Wai, J. S. M.; Marko, I.; Svendsen, J. S.; Finn, M. G.; Jacobsen, E. N.; Sharpless, K. B. *J. Am. Chem. Soc.* 1989, 111, 1123.
- (5) Dupau, P.; Epple, R.; Thomas, A. A.; Fokin, V. V.; Sharpless, K. B. *Adv. Synth. Catal.* 2002, 344, 421.
- (6) Jacobsen, E. N.; Marko, I.; France, M. B.; Svendsen, J. S.; Sharpless, K. B. *J. Am. Chem. Soc.* 1989, 111, 737.

- (7) Nelson, D. W.; Gypser, A.; Ho, P. T.; Kolb, H. C.; Kondo, T.; Kwong, H. L.; McGrath, D. V.; Rubin, A. E.; Norrby, P. O.; Gable, K. P.; Sharpless, K. B. *J. Am. Chem. Soc.* 1997, 119, 1840.
- (8) Jacobsen, E. N.; Marko, I.; Mungall, W. S.; Schroder, G.; Sharpless, K. B. *J. Am. Chem. Soc.* 1988, 110, 1968.
- (9) Kolb, H. C.; Andersson, P. G.; Sharpless, K. B. *J. Am. Chem. Soc.* 1994, 116, 1278.
- (10) Sharpless, K. B.; Akashi, K. J. *Am. Chem. Soc.* 1976, 98, 1986.
- (11) Junttila, M. H.; Hormi, O. O. E. *J. Org. Chem.* 2009, 74, 3038.
- (12) Mehlretter, G. M.; Döbler, C.; Sundermeier, U.; Beller, M.; Do, C. *Tetrahedron Lett.* 2000, 41, 8083.
- (13) Hovelmann, C. H.; Muniz, K. *Chem. Eur. J.* 2005, 11, 3951.
- (14) Kwong, H. L.; Sorato, C.; Ogino, Y.; Hou, C.; Sharpless, K. B. *Tetrahedron Lett.* 1990, 31, 2999.
- (15) Milas, N. A.; Sussman, S. J. *Am. Chem. Soc.* 1937, 59, 2345.
- (16) Milas, N. A.; Trepagnier, J. H.; Nolan Jr., J. T.; Iliopoulos, M. I. *J. Am. Chem. Soc.* 1959, 81, 4730.
- (17) Hart, S. R.; Whitehead, D. C.; Travis, B. R.; Borhan, B. *Org. Biomol. Chem.* 2011, 9, 4741.
- (18) Travis, B. R.; Narayan, R. S.; Borhan, B. *J. Am. Chem. Soc.* 2002, 124, 3824.
- (19) Singh, N.; Singh, V.; Singh, M. *Aust. J. Chem.* 1968, 21, 2913.
- (20) Singh, V. N.; Singh, H. S.; Saxena, B. B. L. *J. Am. Chem. Soc.* 1969, 91, 2643.
- (21) Andersson, M. A.; Epple, R.; Fokin, V. V.; Sharpless, K. B. *Angew. Chem. Int. Ed.* 2002, 41, 472.
- (22) Donohoe, T. J.; Harris, R. M.; Butterworth, S.; Burrows, J. N.; Cowley, A.; Parker, J. S. J. *Org. Chem.* 2006, 71, 4481.
- (23) Wu, P.; Hilgraf, R.; Fokin, V. V. *Adv. Synth. Catal.* 2006, 348, 1079.
- (24) Yang, J. W.; Han, H. Y.; Roh, E. J.; Lee, S. G.; Song, C. E. *Org. Lett.* 2002, 4, 4685.

- (25) Herrmann, W. A.; Kratzer, R. M.; Blumel, J.; Friedrich, H. B.; Fischer, R. W.; Apperly, D. C.; Mink, J.; Berkesi, O.; Bliemel, J.; Apperley, D. C. *J. Mol. Catal. a-Chemical* 1997, 120, 197.
- (26) Zaitsev, A. B.; Adolfsson, H. *Synthesis-Stuttgart* 2006, 1725.
- (27) Biollaz, M.; Haefliger, W.; Velarde, E.; Crabb, P.; Fried, J. H. *J. Chem. Soc. D Chem. Commun.* 1971, 1322.
- (28) David, K.; Ariento, C.; Greiner, A.; Goré, J.; Cazes, B. *Tetrahedron Lett.* 1996, 37, 3335.
- (29) Fleming, S. A.; Carroll, S. M.; Hirschi, J.; Liu, R.; Lee Pace, J.; Ty Redd, J. *Tetrahedron Lett.* 2004, 45, 3341.
- (30) Fleming, S. A.; Liu, R.; Redd, J. T. *Tetrahedron Lett.* 2005, 46, 8095.
- (31) Laux, M.; Krause, N. *Synlett* 1997, 1997, 765.
- (32) Carlsen, P. H. J.; Katsuki, T.; Martin, V. S.; Sharpless, K. B. *J. Org. Chem.* 1981, 46, 3936.
- (33) Shing, T. K. M.; Tai, V. W.-F.; Tam, E. K. W. *Angew. Chem. Int. Ed.* 1994, 33, 2312.
- (34) Plietker, B.; Niggemann, M.; Pollrich, A. *Org. Biomol. Chem.* 2004, 2, 1116.
- (35) Plietker, B.; Niggemann, M. *J. Org. Chem.* 2005, 70, 2402.
- (36) Azam, K. A.; Deeming, A. J.; Rothwell, I. P. *J. Chem. Soc. Dalt. Trans.* 1981, 91.
- (37) Esteruelas, M. A.; Hernández, Y. A.; López, A. M.; Oliván, M.; Oñate, E. *Organometallics* 2005, 24, 5989.
- (38) Nakamura, A.; Lectard, S.; Hashizume, D.; Hamashima, Y.; Sodeoka, M. *J. Am. Chem. Soc.* 2010, 132, 4036.
- (39) Minko, Y.; Pasco, M.; Lercher, L.; Botoshansky, M.; Marek, I. *Nature* 2012, 490, 522.
- (40) Marcune, B. F.; Karady, S.; Reider, P. J.; Miller, R. A.; Biba, M.; DiMichele, L.; Reamer, R. A. *J. Org. Chem.* 2003, 68, 8088.
- (41) Krawczyk, E.; Mielniczak, G.; Owsianik, K.; Luczak, J. *Tetrahedron-Asymmetry* 2012, 23, 1480.
- (42) Milas, N. A.; Sussman, S.; Mason, H. S. *J. Am. Chem. Soc.* 1939, 61, 1844.
- (43) Liu, K.; Kim, H.; Ghosh, P.; Akhmedov, N. G.; Williams, L. J. *J. Am. Chem. Soc.* 2011, 133, 14968.

- (44) Sharma, R. The spirodiepoxide: a platform for diversity and target oriented synthesis. Ph.D. Dissertation, Rutgers, The State University of New Jersey, 2013.
- (45) Liu, K. Accessing erythronolide structure space: new reactions and applications. Ph.D. Dissertation, Rutgers, The State University of New Jersey, 2012.
- (46) Lotesta, S. D.; Kiren, S.; Sauers, R. R.; Williams, L. J. *Angew. Chem. Int. Ed.* 2007, 46, 7108.
- (47) Sharma, R.; Manpadi, M.; Zhang, Y.; Kim, H.; Ahkmedov, N. G.; Williams, L. J. *Org. Lett.* 2011, 13, 3352.
- (48) Katukojvala, S.; Barlett, K. N.; Lotesta, S. D.; Williams, L. J. *J. Am. Chem. Soc.* 2004, 126, 15348.
- (49) Ghosh, P.; Lotesta, S. D.; Williams, L. J. *J. Am. Chem. Soc.* 2007, 129, 2438.
- (50) Yue, Z.; Cusick, J. R.; Ghosh, P.; Ning, S. G.; Katukojvala, S.; Inghrim, J.; Emge, T. J.; Williams, L. J. *J. Org. Chem.* 2009, 74, 7707.
- (51) Ghosh, P.; Cusick, J. R.; Inghrim, J.; Williams, L. J. *Org. Lett.* 2009, 11, 4672.
- (52) Pilgrim, B. S.; Donohoe, T. J. *J. Org. Chem.* 2013, 78, 2149.
- (53) Evans, P.; Leffray, M. *Tetrahedron* 2003, 59, 7973.
- (54) Français, A.; Bedel, O.; Haudrechy, A. *Tetrahedron* 2008, 64, 2495.
- (55) Corey, E. J.; Bakshi, R. K.; Shibata, S. *J. Am. Chem. Soc.* 1987, 109, 5551.
- (56) Matsumura, K.; Hashiguchi, S.; Ikariya, T.; Noyori, R. *J. Am. Chem. Soc.* 1997, 119, 8738.
- (57) Arce, A. J.; Chierotti, M.; Sanctis, Y. De; Deeming, A. J.; Gobetto, R. *Inorganica Chim. Acta* 2004, 357, 3799.
- (58) Cha, J. K.; Christ, W. J.; Kishi, Y. *Tetrahedron* 1984, 40, 2247.
- (59) Poli, G. *Tetrahedron Lett.* 1989, 30, 7385.
- (60) Minato, M.; Yamamoto, K.; Tsuji, J. *J. Org. Chem.* 1990, 55, 766.
- (61) Csányi, L. J.; Galbács, Z. M.; Nagy, L.; Marek, N. *Transit. Met. Chem.* 1986, 11, 319.
- (62) King, P. F.; Paquette, L. A. *Synthesis (Stuttg.)* 1977.

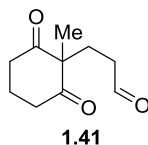
- (63) One major problem we encountered was formation of “osmium black”, which appears to be caused by slow hydrolysis of the osmium/allene adduct and thence cause catalyst deactivation and product decomposition. Electrophilic radical trapping, low valent osmium(V, VI) catalysis (less reactive oxidants that might be less likely to oxidize osmium enolates) and immobilized catalyst (preventing osmium tetroxide from reacting with osmium enolates) might improve the yield.

Chapter 4 Experimental Data

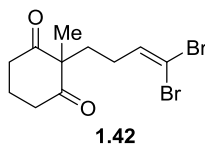
4.1 General

Starting materials, reagents and solvents were purchased from commercial suppliers (Aldrich, TCI, and Fischer) and used without further purification unless otherwise mentioned. All reactions were conducted under dry nitrogen or argon atmosphere unless otherwise mentioned and monitored by thin layer chromatography (thickness 250um with fluorescent indicator, Dynamic Adsorbents' Inc.). Crudes were purified by flash column chromatography on 32-63um silica gel (Dynamic Adsorbents' Inc.). Infrared (FTIR) spectra were recorded on an ATI Mattson Genesis Series FT-Infrared spectrophotometer. Proton nuclear magnetic resonance spectra (^1H NMR) were recorded on either Varian-500 instrument (500 MHz) or Varian-400 instrument (400 MHz). Carbon nuclear magnetic resonance spectra (^{13}C NMR) were recorded on either Varian-500 instrument (126 MHz) or Varian-400 instrument (100 MHz). Optical rotations were recorded at $\sim 24^\circ\text{C}$ using the sodium D line (589 nm), on a JASCO P-2000 polarimeter. Mass spectra were recorded on a Finnigan LCQ-DUO mass spectrometer.

4.2 Chapter 1

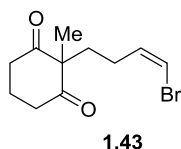


Aldehyde **1.41**: To a 500 ml round-bottomed flask, 2-methylcyclohexane-1,3-dione **1.40** (5.00 g, 38.5 mmol) and 60 ml water were added and the mixture was vigorously stirred. To this was added acetic acid (0.11 ml, 2.0 mmol), and then acrolein (4.3 ml, 58 mmol) was added dropwise. After 18 h, the suspension was partitioned against and washed with ethyl acetate (3x60 mL). The organic fractions were combined, washed with satd. NaCl (aq) (60 mL), dried over Na₂SO₄, filtered, and concentrated in vacuo to give aldehyde **1.41** (7.45 g) as a viscous yellow oil (quantitative crude yield). IR $\nu_{\text{max}}(\text{neat})/\text{cm}^{-1}$ 3435, 2960, 2731, 1722, 1692, 1460; ¹H NMR (500 MHz, CDCl₃) δ 9.67 (1H, t, J = 1.2 Hz), 2.73 – 2.60 (4H, m), 2.39 – 2.28 (2H, m), 2.13 – 2.07 (2H, m), 2.01 – 1.89 (2H, m), 1.28 (3H, s). ¹³C NMR (125 MHz, CDCl₃) δ 210.0, 201.2, 64.6, 39.5, 38.0, 27.4, 21.8, 17.7; m/z (ESI/MS) calculated 205.2 (C₁₀H₁₄NaO₃), observed 205.0 (M+Na)⁺.



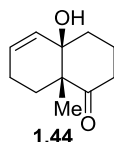
Dibromoalkene **1.42**: In a 25 ml flame-dried round-bottomed flask, carbon tetrabromide (364 mg, 1.10 mmol) was suspended in dry dichloromethane (3 mL), to which was added a solution of triphenylphosphine (576 mg, 2.20 mmol) in dry dichloromethane (3 mL) at 0 °C, and then the reaction mixture was stirred for 30 min. To this, compound **1.41** (100 mg, 0.549 mmol, azeotroped with toluene) dissolved in dry dichloromethane (3 mL) was added

over 30 minutes. After 1.5 h, the reaction mixture was diluted with hexane (50 mL), filtered, concentrated in vacuo, and the resultant oil was purified by FCC (15% ethyl acetate in hexane) to give **1.42** (135 mg, 72%) as a light yellow oil (R_f = 0.80, 50% ethyl acetate in hexane). IR ν_{\max} (neat)/ cm^{-1} 2962, 1725, 1694, 1456, 1025; ^1H NMR (500 MHz, CDCl_3) δ 6.37 – 6.25 (1H, m), 2.74 – 2.60 (4H, m), 2.03 – 1.85 (6H, m), 1.27 (3H, s); ^{13}C NMR (125 MHz, CDCl_3) δ 210.0, 137.6, 90.2, 64.9, 38.2, 33.8, 28.9, 21.4, 17.8; m/z (ESI/MS) calculated 371.9 ($\text{C}_{11}\text{H}_{20}\text{Br}_2\text{NO}_3$), observed 372.0 ($\text{M}+\text{H}_2\text{O}+\text{NH}_4$) $^+$.

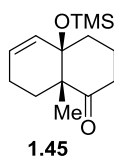


(*Z*)-bromoalkene **1.43**: Tetrakis[triphenylphosphine]palladium(0) (18 mg, 0.016 mmol) was placed in a flame-dried 10 ml round-bottomed flask under a nitrogen atmosphere (in a glove bag). To this was added a solution of dione **1.42** (133 mg, 0.393 mmol, azeotroped with toluene 3 times) in dry toluene (4 mL) with vigorous stirring, and then $n\text{-Bu}_3\text{SnH}$ (110 μL , 0.40 mmol). After 2 h, the reaction mixture was diluted with hexanes (4 mL), washed with water (4 mL), satd. NaCl (aq) (4 mL), and then the organic layer was dried over Na_2SO_4 , filtered, concentrated in vacuo, and the resultant oil was purified by FCC (15% ethyl acetate in hexane) to give **1.43** (135 mg, 67%) as a light yellow oil (R_f = 0.80 50% ethyl acetate in hexane). IR ν_{\max} (neat)/ cm^{-1} 3084, 2960, 1725, 1694, 1278, 671; ^1H NMR (500 MHz, CDCl_3) δ 6.20 – 6.09 (1H, m), 6.01 (1H, apparent dt, J = 8.2, 6.2 Hz), 2.82 – 2.54 (4H, m), 2.08 – 1.85 (6H, m), 1.26 (3H, s); ^{13}C NMR (125 MHz, CDCl_3) δ 210.2, 133.6, 109.2, 65.3, 38.2, 34.9, 25.6, 20.4, 17.9; m/z (ESI/MS) calculated 276.0, 278.0 ($\text{C}_{11}\text{H}_{19}\text{BrNO}_2$), observed 276.1, 278.1

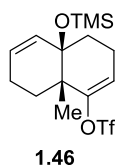
$(M+NH_4)^+$.



Bicyclic alcohol **1.42**: To a 100 ml flame-dried round-bottomed flask, chromium(II) chloride (747 mg, 6.08 mmol), nickel(II) chloride (20 mg, 0.15 mmol), and 4Å activated molecule sieves were suspended in 50 mL DMF at 0 °C. To this mixture, dione **1.41** (350 mg, 1.35 mmol, azeotroped with toluene 3 times), dissolved in DMF (1 mL), was then added. An additional portion of DMF (1 mL) was used to rinse the flask and was then added to the reaction mixture, which was then allowed to warm to room temperature. After 12 h, the reaction mixture was diluted with ethyl ether (500 mL), filtered through Florisil, concentrated in vacuo, and the residue was purified by FCC (20% ethyl acetate in hexane) to give **1.42** (161 mg, 66%) as a light yellow oil (R_f = 0.53 50% ethyl acetate in hexane). IR $\nu_{\max}(\text{neat})/\text{cm}^{-1}$ 3444, 3016, 2941, 2873, 1695, 1053, 1017; ^1H NMR (500 MHz, CDCl_3) δ 5.86 – 5.80 (1H, m), 5.53 (1H, apparent dt, J = 10.0, 2.2 Hz), 2.42 (1H, ddd, J = 15.4, 12.2, 6.4 Hz), 2.27 – 2.15 (2H, m), 2.11 – 2.04 (1H, m), 2.04 – 1.93 (2H, m), 1.88 – 1.80 (1H, m), 1.75 (1H, s), 1.74 – 1.71 (1H, m), 1.53 – 1.43 (2H, m), 1.16 (3H, s); ^{13}C NMR (125 MHz, CD_3CN) δ 213.8, 133.5, 130.5, 72.6, 52.5, 37.3, 34.6, 27.3, 22.8, 20.4, 20.1; m/z (ESI/MS) calculated 203.1 ($\text{C}_{11}\text{H}_{16}\text{O}_2\text{Na}$), observed 203.1 ($M+\text{Na}$) $^+$.

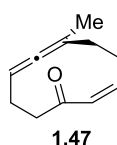


TMS ether **1.45**: In a 25 ml pear shaped flask, bicyclic alcohol **1.44** (150 mg, 0.832 mmol, azeotroped with toluene) was suspended in dry THF (8.3 mL), to which 1-(trimethylsilyl)-1H-imidazole (0.13 mL, 0.83 mmol) and one drop of TBAF (1.0 M in THF) was added. After 2 h, the reaction mixture was quenched with satd. NH_4Cl (aq) (8 mL) and partitioned against and then extracted with ethyl acetate (3x8 mL). The organic fractions were combined, washed with satd. NaCl (aq) (8 mL), dried over Na_2SO_4 , concentrated in vacuo, and the residue was purified by FCC (2% ethyl acetate in hexanes) to give **1.45** (139 mg, 66%) as colorless oil ($R_f=0.76$ 16% ethyl acetate in hexane), and unreacted **1.44** (27 mg, 18%). IR $\nu_{\text{max}}(\text{neat})/\text{cm}^{-1}$ 2950, 1706, 1249, 1100, 1077; ^1H NMR (400 MHz, CDCl_3) δ 5.85 – 5.77 (1H, m), 5.55 (1H, dt, $J = 10.0, 2.2$ Hz), 2.40 (1H, ddd, $J = 15.4, 12.7, 6.5$ Hz), 2.27 – 2.13 (2H, m), 2.07 (1H, td, $J = 13.0, 3.8$ Hz), 2.00 – 1.85 (2H, m), 1.83 – 1.66 (2H, m), 1.57 (1H, ddd, $J = 13.3, 10.1, 6.7$ Hz), 1.44 (1H, qdd, $J = 12.7, 4.9, 3.5$ Hz), 1.10 (3H, s), 0.13 – -0.02 (9H, m); ^{13}C NMR (101 MHz, CDCl_3) δ 214.2, 133.1, 132.5, 74.9, 53.5, 37.6, 35.9, 26.6, 23.3, 21.7, 20.5, 2.5; m/z (ESI/MS) calculated 275.2 ($\text{C}_{14}\text{H}_{24}\text{NaO}_2\text{Si}$), observed 275.3 ($\text{M}+\text{Na}$) $^+$.



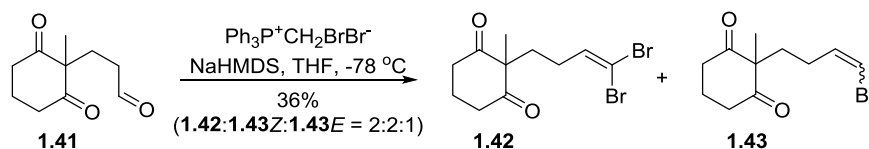
Vinyl triflate **1.46**: In a 10 ml pear shaped flask, **1.45** (138 mg, 0.547 mmol, azeotroped with toluene 3 times) was suspended in dry THF (6 mL) and the mixture was then cooled to $-78\text{ }^\circ\text{C}$. To this was added NaHMDS (0.63 mL, 0.63 mmol, 1.0 M in THF) with vigorous stirring. After 30 min, phenyl triflimide (3.0 mL, 0.60 mmol, 0.20 M in THF) was added in dropwise, and the reaction mixture was warmed to $0\text{ }^\circ\text{C}$. After 1 h, the reaction mixture was quenched by

satd. NH_4Cl (aq) (10 mL) and partitioned against ethyl acetate (3x10 mL). The organic fractions were combined, washed with satd. NaCl (aq) (10 mL), dried over Na_2SO_4 , concentrated in vacuo, and the residue was purified by FCC (pure hexane) to give **1.46** (166 mg, 79%) as colorless oil (R_f = 0.58 1% ethyl acetate in hexane). IR $\nu_{\text{max}}(\text{neat})/\text{cm}^{-1}$ 2952, 1680, 1412, 1248, 1210, 994, 841; ^1H NMR (500 MHz, CDCl_3) δ 5.84 (1H, dt, J = 9.9, 3.6 Hz), 5.68 – 5.58 (1H, m), 5.57 – 5.45 (1H, m), 2.19 – 2.08 (1H, m), 2.07 – 1.94 (3H, m), 1.88 (1H, ddd, J = 12.8, 10.4, 5.7 Hz), 1.74 (1H, ddd, J = 13.6, 9.4, 6.7 Hz), 1.65 (1H, dt, J = 13.5, 4.4 Hz), 1.60 – 1.52 (1H, m), 1.16 (3H, s), 0.15 – 0.06 (9H, m); ^{13}C NMR (125 MHz, CDCl_3) δ 152.9, 131.0, 130.9, 118.6 (q, $J_{\text{C-F}}$ 320Hz), 115.8, 73.9, 43.7, 32.0, 27.7, 22.8, 21.38, 21.3, 2.6; m/z (ESI/MS) calculated 407.1 ($\text{C}_{15}\text{H}_{23}\text{NaF}_3\text{O}_4\text{SSi}$), observed 407.2 ($\text{M}+\text{Na}$) $^+$.



Endocyclic allene **1.47**: In a 25 mL flame-dried flask, vinyl triflate **1.46** (157 mg, 0.408 mmol, azeotroped with toluene 3 times) was suspended in dry THF (13 mL) and to this TBAF (0.4 mL, 0.4 mmol, 1.0 M in THF, stored over molecular sieves for >24 h) was added drop wise. After 10 min, the reaction was quenched with satd. NH_4Cl (aq) (15 mL), and the reaction mixture was partitioned against and extracted with ethyl acetate (3x15 mL). The organic fractions were combined, washed with satd. NaCl (aq) (15 mL), dried over Na_2SO_4 , concentrated in vacuo, and purified by FCC (5% ethyl acetate/hexane) to give **1.47** (43 mg, 64%) as colorless oil (R_f = 0.08 1% ethyl acetate/hexane). IR $\nu_{\text{max}}(\text{neat})/\text{cm}^{-1}$ 2975, 2903, 2851, 1964, 1693, 1440, 1400; ^1H NMR (400 MHz, CDCl_3) δ 6.25 (1H, dd, J = 11.9, 2.2 Hz), 5.70 (1H, td, J = 11.7, 4.2 Hz), 4.95 – 4.85 (1H, m), 2.70 – 2.57 (2H, m), 2.42 – 2.15 (5H, m),

1.76 (1H, ddt, $J = 14.7, 12.1, 2.2$ Hz), 1.63 (3H, d, $J = 2.8$ Hz); ^{13}C NMR (101 MHz, CDCl_3) δ 205.9, 202.1, 140.2, 132.1, 97.8, 89.3, 41.9, 32.7, 26.7, 26.1, 19.9; m/z (ESI/MS) calculated 185.2 ($\text{C}_{11}\text{H}_{14}\text{NaO}$), observed 185.0 ($\text{M}+\text{Na}$) $^+$.



E/Z-bromoalkenes **1.43** and dibromide **1.42**: (Entry 2, see Table 4.1). NaHMDS (0.56 ml, 0.56 mmol, of 1.0 M in THF) was added dropwise to bromomethyl triphenylphosphonium bromide (244 mg, 0.560 mmol) in dry THF (8 mL) at room temperature under vigorous stirring. After 10 min, the dark yellow suspension was cooled to $-78\text{ }^\circ\text{C}$ and stirred for an additional 20 min. Separately, **1.41** (51 mg, 0.28 mmol, azotroped with toluene 3 times and dried under high vacuum) was suspended in dry THF (1 mL) and then added dropwise to the cooled reaction mixture at over 1 min. An additional portion of THF (0.5 mL) was used to rinse the flask that had contained **1.41** and was then added to the reaction mixture. After 0.5 h, the reaction mixture was diluted with hexane (cooled to $-78\text{ }^\circ\text{C}$), warmed to room temperature, filtered, concentrated in vacuo, and the resultant oil was purified by FCC (15% ethyl acetate in hexane) to give monobromo and dibromo products as an inseparable (oil) mixture (22 mg, $R_f = 0.80$ 50% ethyl acetate in hexane, 22% **1.43**, 8% *E* isomer of **1.43**, and 5% **1.42**, the yields are estimated based on ^1H NMR of the mixture).

Table 4.1 Mono bromoolefination of diketone aldehyde **1.41** under different conditions

entry	eq. of wittig reagent ^[a]	solvent	reaction molarity (M)	reaction time (h)	yield ^[b] (%)	yield of 1.43 ^[c] (%)
1	1.0	THF	0.035	1.0	31	26
2	1.5	THF	0.035	0.5	35	22
3	2.0	THF	0.035	0.5	39	20
4	3.0	THF	0.035	0.5	24	17
5	1.0	Toluene	0.07	1.0	55	25
6	1.2	Toluene	0.02	1.0	38	16
7	1.5	Toluene	0.09	0.5	30	13

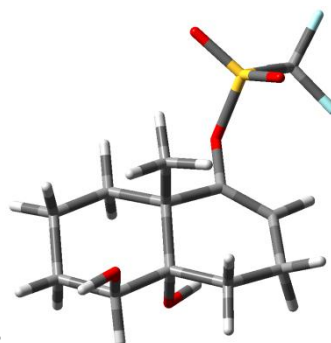
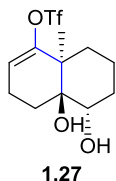
[a] Equal amount of phosphonium salt and base were used to generate the Wittig reagent.

[b] The total yields for a mixture of the product are determined from the ¹H NMR of the mixture.

[c] The yields of **21** are determined from the ¹H NMR of the mixture.

Computational data for Table 1.1:

Entry 1

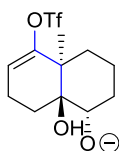


Dihedral angle $\Phi_{((HO)C-C-C-O(Tf))} = 152.5^\circ$

	Atomic Type	Coordinates (Angstroms)		
		X	Y	Z
	C	3.953155	-1.289560	-0.880371
	C	3.875742	0.027384	-0.092344
	C	2.489255	0.691259	-0.242405
	C	1.300716	-0.283095	0.114792
	C	1.423977	-1.552700	-0.770372
	C	2.785452	-2.241423	-0.584128
	H	4.593937	0.739856	-0.526553
	H	3.958954	-1.037232	-1.945413
	H	4.913439	-1.778163	-0.665086
	H	0.612377	-2.244604	-0.526877
	H	1.302758	-1.274966	-1.822462
	H	2.872528	-2.630813	0.436125

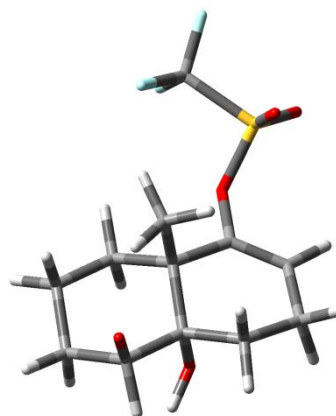
H	2.843732	-3.110733	-1.249004
C	0.032278	0.502708	-0.174390
C	2.364841	2.001626	0.550057
H	2.395403	1.787592	1.620302
H	3.229850	2.634152	0.326304
C	1.068114	2.747005	0.174973
H	0.776155	3.431322	0.981145
H	1.241832	3.388119	-0.700332
C	-0.089614	1.831196	-0.131904
H	-1.058126	2.279992	-0.331962
O	2.461007	0.993858	-1.650066
H	1.552393	1.230383	-1.881904
O	4.151389	-0.142674	1.299744
H	5.051150	-0.484797	1.376670
O	-1.100983	-0.287633	-0.518824
C	1.248940	-0.697858	1.611751
H	2.187109	-1.144770	1.935494
H	1.042594	0.157154	2.258432
H	0.443787	-1.424484	1.762802
S	-2.285866	-0.591505	0.576597
O	-2.482285	-2.029584	0.639202
O	-2.131344	0.232606	1.764869
C	-3.702016	0.115624	-0.421140
F	-4.825083	-0.055328	0.273109
F	-3.793989	-0.509069	-1.590407
F	-3.500188	1.420005	-0.624895

HF = -1541.2591036



1.29

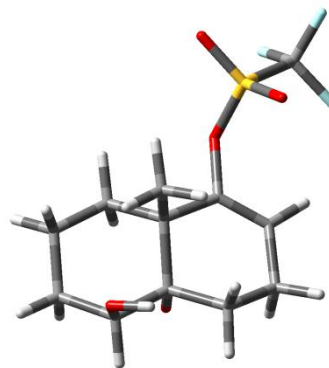
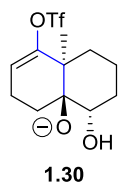
Dihedral angle $\Phi_{((HO)C-C-C-O(Tf))} = 155.3^\circ$



Atomic Type	Coordinates (Angstroms)		
	X	Y	Z
C	3.514036	-1.863272	-0.612627

C	3.709912	-0.559479	0.254034
C	2.564718	0.457540	-0.164300
C	1.137155	-0.153154	0.062156
C	1.012750	-1.441505	-0.792425
C	2.112527	-2.457416	-0.433536
H	4.628257	-0.043763	-0.235393
H	3.689455	-1.670814	-1.683219
H	4.276247	-2.576263	-0.275619
H	0.021509	-1.885300	-0.639346
H	1.092735	-1.174130	-1.851532
H	2.000166	-2.770862	0.610421
H	1.982207	-3.358884	-1.050403
C	0.151056	0.918547	-0.340917
C	2.692386	1.786929	0.584099
H	2.561748	1.605870	1.653074
H	3.716745	2.160176	0.457328
C	1.692188	2.825469	0.040595
H	1.541731	3.643311	0.760184
H	2.103878	3.288824	-0.867000
C	0.355587	2.233019	-0.328144
H	-0.443941	2.906977	-0.628347
O	3.817919	-0.777369	1.551433
O	-1.146470	0.428769	-0.776826
C	0.904224	-0.501067	1.563596
H	1.835118	-0.934022	1.953882
H	0.671514	0.396502	2.143200
H	0.056243	-1.188002	1.667624
S	-2.503301	0.765244	0.022342
O	-3.403580	1.522396	-0.840839
O	-2.268507	1.170590	1.400963
C	-3.180513	-0.975037	0.060440
F	-4.393261	-0.939095	0.629332
F	-3.296414	-1.454873	-1.178767
F	-2.392221	-1.778802	0.773175
O	2.680091	0.741389	-1.582612
H	3.624488	0.601771	-1.760777

HF = -1540.6603569



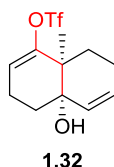
Dihedral angle $\Phi_{((O^-)C-C-C-O(Tf))} = 156.0^\circ$

	Atomic Type	Coordinates (Angstroms)		
		X	Y	Z
	C	4.066694	-1.172988	-0.861928
	C	3.919447	0.062727	0.029631
	C	2.548430	0.755057	-0.276490
	C	1.329664	-0.305908	0.057802
	C	1.524114	-1.449677	-0.963606
	C	2.881596	-2.149093	-0.763263
	H	4.674682	0.803346	-0.280955
	H	4.120415	-0.785887	-1.882647
	H	5.008989	-1.688716	-0.629530
	H	0.709060	-2.182078	-0.891649
	H	1.502037	-0.987998	-1.954932
	H	2.902354	-2.663549	0.205724
	H	2.996812	-2.935340	-1.523475
	C	0.076868	0.482397	-0.179736
	C	2.303397	2.010802	0.633801
	H	2.140751	1.784554	1.700873
	H	3.176706	2.673719	0.561866
	C	1.076896	2.730121	0.056727
	H	0.775705	3.597245	0.660893
	H	1.371942	3.075572	-0.943140
	C	-0.092121	1.799466	-0.130885
	H	-1.078625	2.222006	-0.298703
	O	2.543083	1.101258	-1.561424
	O	4.195145	-0.325033	1.401388
	H	3.827296	0.379693	1.949698
	O	-1.114857	-0.335640	-0.493726
	C	1.243726	-0.880591	1.497892
	H	2.179316	-1.355649	1.792763
	H	1.015980	-0.097129	2.227286
	H	0.442207	-1.629743	1.571427
	S	-2.286976	-0.614784	0.556863

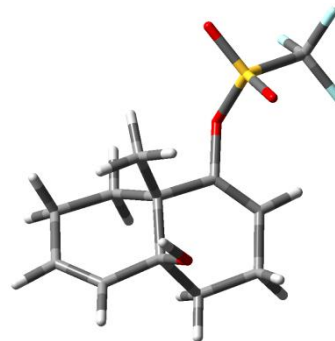
O	-2.577532	-2.043549	0.592253
O	-2.166393	0.163567	1.783100
C	-3.693119	0.146659	-0.407163
F	-4.830807	-0.027557	0.280768
F	-3.818652	-0.434853	-1.601629
F	-3.497555	1.458836	-0.579664

HF=-1540.6634949

Entry 2



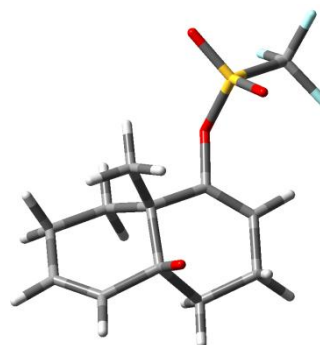
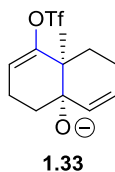
Dihedral angle $\Phi_{((\text{HO})\text{C}-\text{C}-\text{C}-\text{O}(\text{Tf}))} = 175.4^\circ$



Atomic Type	Coordinates (Angstroms)		
	X	Y	Z
C	0.165719	1.738533	-0.493703
C	0.280211	0.423895	-0.324132
C	1.534678	-0.367612	-0.011120
C	2.701722	0.630261	0.342628
O	-0.864633	-0.403609	-0.556295
C	-3.444894	0.177602	-0.393468
F	-4.558077	0.051542	0.326309
F	-3.199888	1.473862	-0.604969
F	-3.589560	-0.443120	-1.560242
S	-2.036749	-0.590547	0.571003
O	-2.330426	-2.010732	0.668024
O	-1.795465	0.245113	1.736925
C	1.264194	-1.315931	1.181322
C	1.930302	-1.198486	-1.266198
C	3.211668	-2.018013	-1.063518
C	4.283276	-1.218896	-0.373838
C	4.049882	-0.052758	0.234389
O	2.552451	1.150492	1.673585
C	2.662547	1.886526	-0.547982
C	1.348506	2.656170	-0.376872
H	-0.809568	2.160227	-0.714528
H	0.838791	-0.771098	2.027217

H	2.186700	-1.804885	1.507574
H	0.558737	-2.101603	0.899611
H	2.075389	-0.513865	-2.109203
H	1.096371	-1.853919	-1.536620
H	3.006303	-2.929975	-0.484018
H	3.578810	-2.372434	-2.035235
H	5.291766	-1.629311	-0.371891
H	4.861236	0.490528	0.716128
H	2.702741	0.426963	2.295755
H	2.788563	1.588242	-1.593379
H	3.514454	2.521471	-0.285323
H	1.328408	3.148707	0.603317
H	1.274741	3.451295	-1.128309

HF = -1464.818396



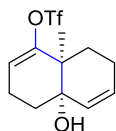
Dihedral angle $\Phi_{((O^-)C-C-O(Trf))} = 176.2^\circ$

Atomic Type	Coordinates (Angstroms)		
	X	Y	Z
C	0.191015	1.732476	-0.400734
C	0.337014	0.420671	-0.232781
C	1.578440	-0.372760	0.049445
C	2.784123	0.692376	0.378544
O	-0.863518	-0.414896	-0.460555
C	-3.429373	0.164032	-0.441996
F	-3.542748	-0.485680	-1.603769
F	-4.584232	0.052393	0.229307
F	-3.207150	1.460343	-0.691395
S	-2.056993	-0.564277	0.596253
O	-1.921111	0.303584	1.756785
O	-2.401252	-1.975293	0.729846
C	1.375107	-1.225173	1.314954
C	1.911706	-1.253246	-1.184795
C	3.200148	-2.070914	-1.010297
C	4.314817	-1.241953	-0.424338

C	4.115898	-0.034491	0.118418
O	2.742577	1.135561	1.630794
C	2.653107	1.888451	-0.642213
C	1.377308	2.646374	-0.274195
H	-0.794370	2.142169	-0.602670
H	1.232247	-0.544729	2.155903
H	2.274823	-1.809962	1.524438
H	0.532277	-1.920483	1.215570
H	2.029785	-0.597682	-2.056641
H	1.073270	-1.926433	-1.411893
H	3.007660	-2.951081	-0.375539
H	3.502366	-2.484295	-1.985797
H	5.313622	-1.685785	-0.431977
H	4.956374	0.510995	0.549793
H	2.630066	1.574004	-1.696997
H	3.528606	2.534661	-0.501764
H	1.498666	2.920871	0.785034
H	1.224243	3.555991	-0.869821

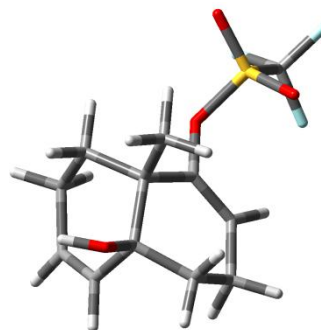
HF=-1464.2166481

Entry 2 (0.16 Kcal lower energy conformer)



1.32

Dihedral angle $\Phi_{((HO)C-C-C-O(Tf))} = 163.4^\circ$

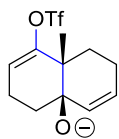


Atomic Type	Coordinates (Angstroms)		
	X	Y	Z

C	0.452196	1.420981	-0.855694
C	0.435583	0.285479	-0.162139
C	1.570952	-0.340095	0.627000
C	2.915817	0.373886	0.207995
O	-0.758574	-0.501649	-0.164529
C	-3.294577	0.045503	-0.605335
F	-3.371285	-1.102422	-1.271687
F	-4.477022	0.334604	-0.065600
F	-2.937015	1.024387	-1.440688
S	-2.040062	-0.098290	0.775211

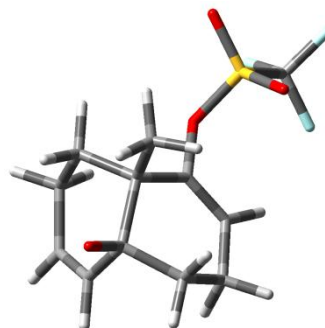
O	-1.875214	1.222438	1.361342
O	-2.406751	-1.264601	1.561225
C	1.296659	-0.178434	2.139319
C	1.680176	-1.854391	0.305349
C	1.936748	-2.139880	-1.176986
C	3.029898	-1.264110	-1.722498
C	3.453554	-0.156623	-1.106669
C	2.719964	1.896295	0.119053
C	1.677021	2.286127	-0.934157
H	-0.445788	1.735021	-1.378649
H	1.148504	0.867467	2.417276
H	2.137223	-0.568899	2.715542
H	0.397626	-0.733374	2.424376
H	0.775419	-2.366797	0.642628
H	2.508359	-2.258567	0.902063
H	2.200696	-3.195800	-1.316182
H	1.016646	-1.987687	-1.759787
H	3.489273	-1.559183	-2.664554
H	4.268062	0.426727	-1.533848
H	3.688747	2.353521	-0.105559
H	2.417166	2.264728	1.104327
H	1.390007	3.337095	-0.808914
H	2.103341	2.209862	-1.944725
O	3.925763	0.192291	1.215678
H	4.287877	-0.696852	1.103258

HF = -1464.8186512



1.33

Dihedral angle $\Phi_{((O^-)C-C-C-O(Tf))} = 163.6^\circ$

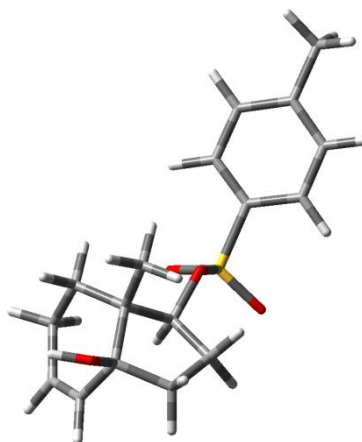
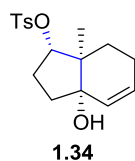


Atomic Type	Coordinates (Angstroms)		
	X	Y	Z
C	0.472268	1.515266	-0.603002
C	0.491973	0.294501	-0.077598
C	1.602218	-0.432079	0.598100
C	3.044085	0.344879	0.332633
O	-0.765594	-0.496078	-0.235074

C	-3.276339	0.201632	-0.581893
F	-4.473051	0.362815	0.000373
F	-2.922634	1.360063	-1.152742
F	-3.380822	-0.732920	-1.529863
S	-2.034356	-0.306992	0.718145
O	-2.489576	-1.610111	1.188490
O	-1.912110	0.827425	1.624581
C	1.380585	-0.493241	2.120636
C	1.780909	-1.868963	0.061749
C	1.995077	-1.932112	-1.455111
C	3.077139	-0.973820	-1.886221
C	3.492863	0.032137	-1.107456
O	3.974019	-0.050592	1.187269
C	2.750139	1.885004	0.415662
C	1.693182	2.396313	-0.574877
H	-0.438225	1.887760	-1.064282
H	1.020083	0.460179	2.519142
H	2.368234	-0.702317	2.547703
H	0.661418	-1.272689	2.404532
H	2.681999	-2.240345	0.563964
H	0.934402	-2.502445	0.356367
H	2.266228	-2.959156	-1.743830
H	1.049267	-1.722563	-1.982926
H	3.549451	-1.155810	-2.854518
H	4.322776	0.656673	-1.446752
H	2.442322	2.104682	1.445293
H	3.704665	2.402207	0.257439
H	1.382278	3.425648	-0.339041
H	2.114853	2.438172	-1.591186

HF = -1464.2178719

Entry 3

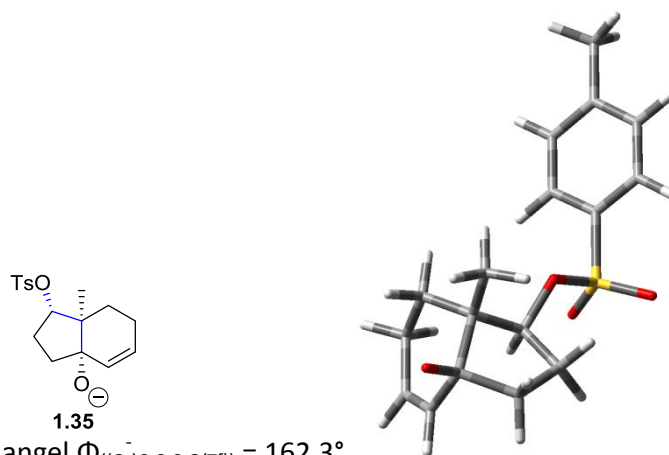


Dihedral angle $\Phi_{((\text{HO})-\text{C}-\text{C}-\text{C}-\text{O}(\text{Tf}))} = 163.9^\circ$

	Atomic Type	Coordinates (Angstroms)		
		X	Y	Z
O	-0.009055	0.008868	0.015554	
C	0.019665	-0.018131	3.903182	
C	2.647406	0.014214	1.010752	
C	0.763323	-2.336722	0.348390	
C	1.757846	-2.960295	1.359261	
C	0.325088	-1.018808	1.001664	
C	1.512386	-0.558859	1.875837	
C	1.935183	-1.930651	2.510215	
C	1.114318	0.473477	2.947246	
C	0.247069	-1.441221	4.333219	
C	1.079727	-2.281778	3.709222	
O	3.313709	-1.980261	2.905578	
H	-0.024142	0.631785	4.786493	
H	-0.969775	0.072021	3.431980	
H	2.974041	-0.682631	0.234065	
H	2.321422	0.935505	0.521161	
H	3.517292	0.232618	1.633960	
H	1.253358	-2.114078	-0.603450	
H	-0.094442	-2.975496	0.127204	
H	1.415320	-3.924067	1.746452	
H	2.737670	-3.127762	0.904794	
H	-0.551915	-1.180763	1.632191	
H	0.799766	1.403397	2.460763	
H	2.015259	0.717565	3.527389	
H	-0.319464	-1.798013	5.192111	
H	1.203691	-3.299341	4.077211	
H	3.383289	-1.523141	3.755129	
O	-2.213068	0.773240	0.975178	
S	-1.609343	0.244439	-0.251394	
O	-2.169889	-0.954036	-0.876839	
C	-1.468973	1.545522	-1.459831	
C	-1.453929	2.875021	-1.037126	
C	-1.388718	1.212841	-2.812282	
C	-1.344987	3.882883	-1.991694	
H	-1.535506	3.108234	0.018572	
C	-1.280374	2.235420	-3.750999	
H	-1.419373	0.172598	-3.116518	
C	-1.256888	3.581586	-3.358546	
H	-1.331386	4.920894	-1.671072	
H	-1.215801	1.984921	-4.806242	
C	-1.172097	4.682788	-4.386952	
H	-0.627305	4.357488	-5.277640	

H	-2.173484	4.991397	-4.711422
H	-0.672728	5.568772	-3.984922

HF = -1360.0986911



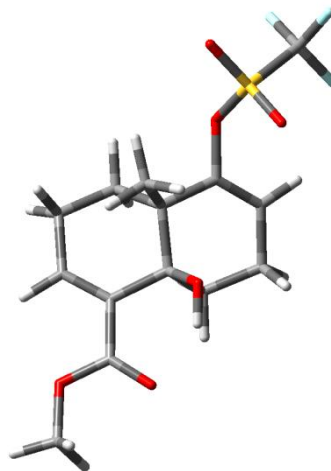
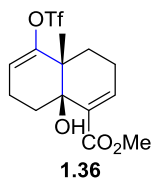
Atomic Type	Coordinates (Angstroms)		
	X	Y	Z

O	-0.011197	0.549685	0.265487
C	2.383853	-2.052078	-1.397424
C	1.779598	-0.639773	2.190224
C	2.157623	1.846162	0.338228
C	3.586853	1.434759	0.774343
C	1.472230	0.526422	-0.057124
C	2.152553	-0.592295	0.705549
C	3.731192	-0.141000	0.616169
C	2.008072	-1.989580	0.090674
C	3.679424	-1.327143	-1.671930
C	4.224412	-0.459934	-0.807301
O	4.525472	-0.727209	1.493578
H	2.470673	-3.104683	-1.708292
H	1.567995	-1.640514	-2.017576
H	1.664905	0.359143	2.625500
H	0.843200	-1.184953	2.363271
H	2.616952	-1.131481	2.698375
H	1.600380	2.304584	1.161474
H	2.132343	2.559876	-0.492916
H	4.367303	1.966700	0.215868
H	3.752550	1.639353	1.836866
H	1.525655	0.362584	-1.133089
H	0.995714	-2.392640	0.245482
H	2.707535	-2.623114	0.652721

H	4.184689	-1.560013	-2.612350
H	5.190661	-0.009787	-1.045372
O	-0.695280	1.021607	-2.119623
S	-1.017721	1.323376	-0.718468
O	-1.185523	2.725978	-0.316871
C	-2.520673	0.447344	-0.281366
C	-2.772492	-0.806204	-0.840855
C	-3.420178	1.024273	0.613063
C	-3.936954	-1.484718	-0.491487
H	-2.062786	-1.234887	-1.539916
C	-4.582065	0.332190	0.951985
H	-3.202480	2.001971	1.028323
C	-4.859032	-0.928280	0.407146
H	-4.133809	-2.463697	-0.921640
H	-5.284305	0.778059	1.652352
C	-6.134353	-1.658831	0.755926
H	-6.488025	-1.390971	1.756223
H	-6.938591	-1.414127	0.050002
H	-5.995176	-2.743813	0.724684

HF = -1359.4909522

Entry 4

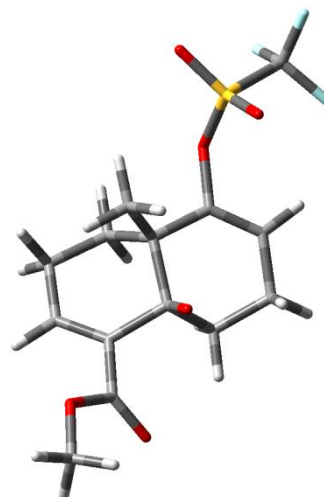
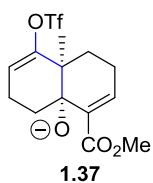


Dihedral angle $\Phi_{((\text{HO})\text{C}-\text{C}-\text{C}-\text{O}(\text{Tf}))} = 174.4^\circ$

Atomic Type	Coordinates (Angstroms)		
	X	Y	Z
C	-0.486232	-2.389065	-0.978028
C	0.759435	-1.562482	-0.845200
C	0.711314	-0.285480	-0.476702
C	-0.516216	0.548891	-0.159876
C	-1.761276	-0.400371	-0.047062

C	-1.725418	-1.502321	-1.136759
O	1.919143	0.479117	-0.472802
C	4.443927	-0.254738	-0.235998
F	5.496857	-0.348547	0.574330
F	4.716717	0.581646	-1.233380
F	4.159253	-1.462386	-0.731807
S	2.995177	0.386851	0.759557
O	3.336153	1.743496	1.154075
O	2.626402	-0.644448	1.715517
C	-0.304041	1.304801	1.173656
C	-0.723422	1.560410	-1.320371
C	-1.958821	2.441387	-1.117855
C	-3.141397	1.659894	-0.638302
C	-3.068372	0.405444	-0.160025
C	-4.305094	-0.288992	0.293975
O	-4.324663	-1.404081	0.803709
O	-5.435314	0.414468	0.089337
C	-6.648899	-0.215956	0.534568
H	-0.592159	-3.020890	-0.087137
H	-0.393521	-3.067092	-1.834592
H	1.723265	-2.021140	-1.041424
H	-1.731535	-1.041889	-2.131248
H	-2.634481	-2.105997	-1.057069
H	-0.020680	0.612252	1.966116
H	0.474692	2.064474	1.065029
H	-1.224501	1.801921	1.487901
H	0.173628	2.179021	-1.417248
H	-0.826457	1.010234	-2.262104
H	-2.216884	2.957972	-2.051472
H	-1.758255	3.244965	-0.393922
H	-4.109793	2.151571	-0.665105
H	-6.609655	-0.410242	1.608760
H	-6.805190	-1.161021	0.009565
H	-7.445187	0.489720	0.300349
O	-1.675038	-1.017278	1.235622
H	-2.507969	-1.508624	1.348617

HF = -1692.7032593



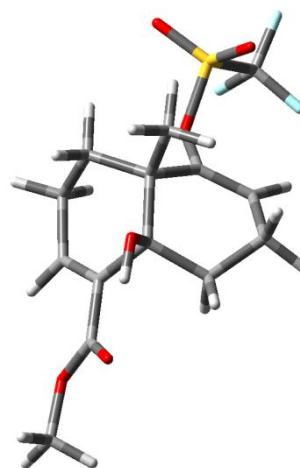
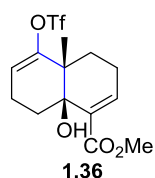
Dihedral angle $\Phi_{((O^-)C-C-C-O(Tf))} = 176.8^\circ$

	Atomic Type	Coordinates (Angstroms)		
		X	Y	Z
C		0.493142	2.513527	-0.544625
C		-0.752513	1.672966	-0.527712
C		-0.665706	0.353123	-0.387503
C		0.555263	-0.510002	-0.239638
C		1.846572	0.478841	-0.063875
C		1.673069	1.684865	-1.053110
O		-1.921168	-0.413821	-0.480707
C		-4.428080	0.312163	-0.148831
F		-5.505369	0.238108	0.644522
F		-4.701087	-0.297027	-1.305497
F		-4.164966	1.601990	-0.389638
S		-2.989820	-0.514543	0.711583
O		-3.396076	-1.906522	0.864868
O		-2.662013	0.320733	1.857111
C		0.437745	-1.349544	1.046390
C		0.702058	-1.409569	-1.495023
C		1.931638	-2.325116	-1.424483
C		3.148787	-1.602437	-0.915698
C		3.104016	-0.352591	-0.427135
O		2.005070	0.892935	1.193367
C		4.367870	0.303452	0.024336
O		4.777262	1.397656	-0.314397
O		5.118953	-0.511220	0.830665
C		6.345681	0.065776	1.273188
H		0.744754	2.796519	0.488125
H		0.326902	3.426001	-1.131840
H		-1.728896	2.141054	-0.613177
H		1.501486	1.371838	-2.094603

H	2.596411	2.267827	-1.020914
H	0.382359	-0.667801	1.895768
H	-0.430211	-2.019847	1.020388
H	1.334980	-1.957655	1.185313
H	-0.202264	-2.015060	-1.641759
H	0.792561	-0.763274	-2.376713
H	2.132015	-2.752237	-2.419703
H	1.724076	-3.192680	-0.778471
H	4.091708	-2.149981	-0.928385
H	6.162619	0.984896	1.837482
H	7.001566	0.308172	0.430034
H	6.816361	-0.683534	1.913699

HF = -1692.1008936

Entry 4 (8.55 Kcal higher energy conformer)



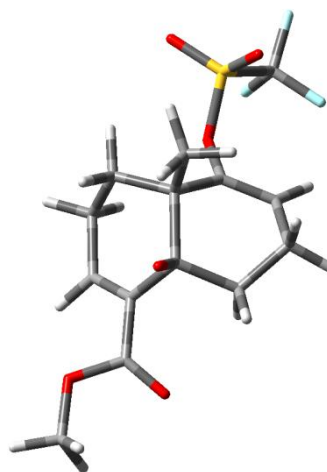
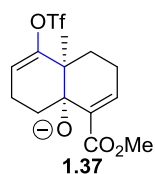
Dihedral angle $\Phi_{((\text{HO})\text{C}-\text{C}-\text{C}-\text{O}(\text{Tf}))} = 141.4^\circ$

Atomic Type	Coordinates (Angstroms)		
	X	Y	Z

C	0.623461	1.981985	-1.750082
C	-0.524922	1.073609	-1.414082
C	-0.519566	0.460170	-0.233856
C	0.506846	0.711836	0.865400
C	1.959896	0.851837	0.225316
C	1.934962	1.346996	-1.266409
O	-1.558099	-0.463471	0.078593
C	-4.025900	-0.702611	-0.839555
F	-5.316743	-0.473375	-0.608789
F	-3.805865	-2.011687	-0.912321
F	-3.670798	-0.124971	-1.989863
S	-3.041574	0.035116	0.571067
O	-3.383912	-0.718795	1.765216

O	-3.172902	1.481404	0.489102
C	0.102805	2.035215	1.573321
C	0.496644	-0.402921	1.934644
C	0.932718	-1.766488	1.399157
C	2.253847	-1.649371	0.708270
C	2.729074	-0.484250	0.240210
O	2.654273	1.792700	1.044713
C	4.129627	-0.405650	-0.257441
O	4.767576	0.637830	-0.337815
O	4.661965	-1.595338	-0.597046
C	6.043482	-1.565103	-0.997054
H	0.474784	2.970435	-1.296164
H	0.675673	2.148039	-2.830890
H	-1.333541	0.910120	-2.118111
H	2.131022	0.492573	-1.923671
H	2.767260	2.042466	-1.395249
H	0.151496	2.893730	0.901996
H	-0.923731	1.954688	1.940971
H	0.769086	2.231390	2.413202
H	1.192271	-0.095305	2.722667
H	-0.495777	-0.470849	2.388080
H	0.179577	-2.180457	0.714493
H	1.015788	-2.489743	2.219452
H	2.874232	-2.537416	0.625525
H	6.305826	-2.599901	-1.214646
H	6.668625	-1.169480	-0.193223
H	6.171807	-0.940969	-1.884227
H	3.572394	1.782971	0.722325

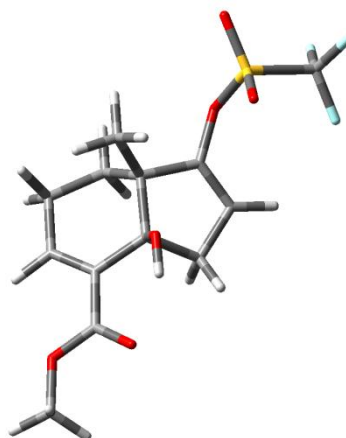
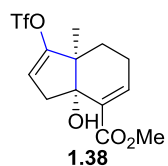
HF = -1692.6896301



Dihedral angle $\Phi_{((O^-)C-C-C-O(Tf))} = 138.3^\circ$

Atomic Type	Coordinates (Angstroms)		
	X	Y	Z
C	0.534884	2.671645	-0.425951
C	-0.614111	1.714870	-0.586969
C	-0.546717	0.556339	0.066095
C	0.507409	0.165984	1.048929
C	2.062555	0.716804	0.546995
C	1.869286	1.909968	-0.488566
O	-1.614613	-0.420701	-0.215221
C	-4.114808	-0.144994	-0.973512
F	-5.397951	-0.165620	-0.588281
F	-3.913020	-1.123893	-1.857895
F	-3.863293	1.030755	-1.559902
S	-3.033980	-0.379030	0.532061
O	-3.354804	-1.710230	1.032553
O	-3.213409	0.809244	1.355421
C	0.234968	0.870669	2.396424
C	0.568725	-1.346475	1.317143
C	1.009024	-2.178270	0.110051
C	2.356908	-1.713205	-0.359708
C	2.779768	-0.447231	-0.202076
O	2.804682	1.012435	1.593532
C	4.169841	-0.114810	-0.633362
O	4.556899	0.909990	-1.161876
O	5.045318	-1.155352	-0.416600
C	6.376887	-0.905459	-0.856776
H	0.452588	3.203110	0.533141
H	0.494416	3.441507	-1.207492
H	-1.462852	1.949391	-1.221522
H	1.982098	1.545361	-1.516348
H	2.703037	2.587135	-0.295327
H	-0.103535	1.902029	2.264410
H	-0.533311	0.341160	2.974449
H	1.193807	0.889970	2.925178
H	1.307183	-1.483614	2.115814
H	-0.395061	-1.709140	1.697232
H	0.256889	-2.118930	-0.691249
H	1.060793	-3.240490	0.387565
H	3.030271	-2.455579	-0.784858
H	6.950670	-1.799604	-0.601857
H	6.798546	-0.029284	-0.355083
H	6.416222	-0.727820	-1.937105
HF = -1692.0872292			

Entry 5

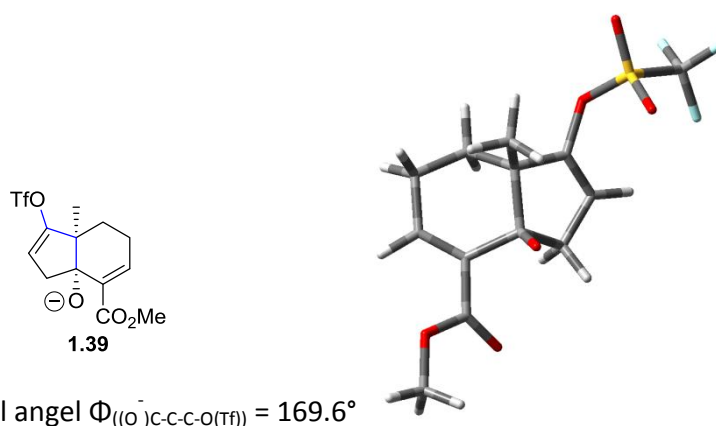


Dihedral angle $\Phi_{((\text{HO})\text{C}-\text{C}-\text{C}-\text{O}(\text{Tf}))} = 171.3^\circ$

Atomic Type	Coordinates (Angstroms)		
	X	Y	Z
C	0.314432	-1.088452	-0.999010
C	0.633724	0.080986	-0.452553
C	-0.536360	0.892759	0.066824
C	-1.639750	-0.226985	0.130739
O	1.909986	0.671843	-0.487625
C	4.189120	-0.699681	-0.450371
F	4.599550	0.040170	-1.475827
F	5.235543	-1.081951	0.278645
F	3.548354	-1.779233	-0.906394
S	3.046762	0.301843	0.643823
O	2.513239	-0.593688	1.655436
O	3.742503	1.536476	0.957707
C	-0.260464	1.549061	1.427940
C	-0.906523	1.959314	-0.999124
C	-2.270145	2.604233	-0.737612
C	-3.325191	1.572344	-0.477608
C	-3.051159	0.303845	-0.127991
C	-1.171571	-1.305912	-0.906547
H	1.010082	-1.774200	-1.466607
H	0.067898	0.809434	2.157471
H	-1.161142	2.025746	1.823508
H	0.513744	2.316513	1.322809
H	-0.932473	1.482689	-1.986398
H	-0.118705	2.718891	-1.037401
H	-2.227870	3.295718	0.116602
H	-2.567987	3.222687	-1.593801
H	-4.364255	1.873316	-0.578447
H	-1.443845	-2.306266	-0.557250

H	-1.646580	-1.167738	-1.888049
C	-4.148447	-0.673214	0.104366
O	-3.975239	-1.800888	0.551576
O	-5.371006	-0.217262	-0.229617
C	-6.459514	-1.125100	0.014637
H	-6.518149	-1.378153	1.075748
H	-7.356740	-0.595698	-0.304179
H	-6.329232	-2.043973	-0.561335
O	-1.577993	-0.784706	1.438491
H	-2.264799	-1.472719	1.458469

HF = -1695.37974860

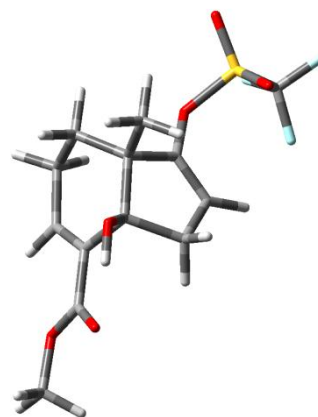
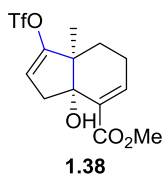


Atomic Type	Coordinates (Angstroms)		
	X	Y	Z
C	0.352606	-1.190884	-0.774519
C	0.604928	0.054425	-0.378992
C	-0.566451	0.902577	0.005052
C	-1.710629	-0.279852	0.194529
O	1.921236	0.652456	-0.430820
C	4.201391	-0.712282	-0.382752
F	4.532423	-0.080184	-1.511936
F	5.317070	-0.966518	0.314269
F	3.615929	-1.873996	-0.690378
S	3.071087	0.352706	0.658821
O	2.620371	-0.479907	1.762043
O	3.812137	1.589627	0.871444
C	-0.361004	1.634958	1.331700
C	-0.914611	1.863278	-1.157678
C	-2.287859	2.525467	-0.994234
C	-3.356624	1.512524	-0.685293
C	-3.074055	0.253199	-0.306809

C	-1.120079	-1.462834	-0.706027
H	1.109018	-1.899616	-1.098047
H	-0.304996	0.887323	2.125240
H	-1.217924	2.276461	1.558660
H	0.539721	2.262996	1.314931
H	-0.921735	1.288550	-2.093290
H	-0.135283	2.631969	-1.268615
H	-2.255330	3.291768	-0.203461
H	-2.544355	3.074985	-1.913554
H	-4.393102	1.838804	-0.764105
H	-1.363574	-2.406219	-0.207800
H	-1.555985	-1.500300	-1.715786
C	-4.182199	-0.721581	-0.109819
O	-4.172812	-1.894447	-0.432370
O	-5.311121	-0.149460	0.424620
C	-6.409671	-1.043895	0.577752
H	-6.145455	-1.881300	1.230471
H	-7.215955	-0.457127	1.024146
H	-6.730595	-1.453602	-0.386269
O	-1.900449	-0.633556	1.451495

HF = -1652.7776413

Entry 5^(1.04 Kcal lower energy conformer)

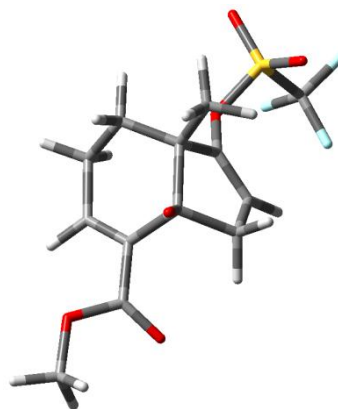
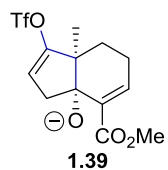


Dihedral angle $\Phi_{((\text{HO})\text{C}-\text{C}-\text{C}-\text{O}(\text{Tf}))} = 163.7^\circ$

Atomic Type	Coordinates (Angstroms)		
	X	Y	Z
C	1.269058	0.282842	2.410785
C	2.458016	-0.283676	1.697992
C	2.731718	-0.034833	0.406829
C	1.838001	0.783753	-0.536128
C	0.546427	1.325459	0.191471
C	0.749396	1.535162	1.702675

C	1.273688	-0.166229	-1.653585
C	-0.063923	-0.599585	-1.121399
C	-0.427729	0.206353	-0.128174
O	2.566463	1.877501	-1.066313
O	-1.614707	0.118936	0.622052
C	-3.781867	-1.266233	-0.060021
F	-5.016110	-1.211408	-0.555080
F	-3.811628	-1.748715	1.178013
F	-3.029109	-2.056582	-0.829670
S	-3.078054	0.468445	-0.051271
O	-3.827166	1.222709	0.936647
O	-2.932800	0.891561	-1.433851
C	0.054036	2.643083	-0.443909
C	3.992291	-0.535334	-0.204795
O	4.420358	-0.155886	-1.288950
O	4.645996	-1.445563	0.542183
C	5.898954	-1.904895	0.005564
H	0.481420	-0.482732	2.472593
H	1.539270	0.510583	3.448771
H	3.144474	-0.906534	2.264828
H	1.470194	2.350301	1.834719
H	-0.193955	1.861252	2.152170
H	1.159858	0.411698	-2.579984
H	1.943795	-1.000620	-1.879861
H	-0.656093	-1.411159	-1.525524
H	3.363550	1.488403	-1.466800
H	0.792823	3.432567	-0.293000
H	-0.888093	2.951679	0.021006
H	-0.113709	2.536611	-1.517687
H	6.283925	-2.616747	0.734947
H	5.747298	-2.389110	-0.961724
H	6.592192	-1.070232	-0.121483

HF = -1653.3814056



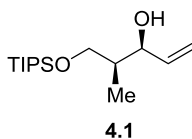
Dihedral angle $\Phi_{((O-)C-C-C-O(Tf))} = 156.6^\circ$

	Atomic Type	Coordinates (Angstroms)		
		X	Y	Z
C		1.270292	1.041539	2.112543
C		2.461782	0.249546	1.648319
C		2.685544	-0.047652	0.355968
C		1.915228	0.511420	-0.878468
C		0.543206	1.290124	-0.325946
C		0.786830	1.993516	1.013755
C		1.232794	-0.704457	-1.673935
C		-0.072897	-0.944752	-0.972910
C		-0.402938	0.136907	-0.269823
O		2.748732	1.266188	-1.548756
O		-1.568802	0.167413	0.603893
C		-3.817536	-1.177344	0.194473
F		-5.115353	-1.081522	-0.125011
F		-3.712305	-1.641400	1.441639
F		-3.233117	-2.039508	-0.642894
S		-3.039336	0.516278	0.056494
O		-3.716445	1.330638	1.057507
O		-3.058367	0.862835	-1.357329
C		0.164655	2.326230	-1.394659
C		3.916569	-0.814507	0.010827
O		4.028224	-1.697527	-0.820087
O		4.989530	-0.464918	0.796715
C		6.177364	-1.209228	0.540714
H		0.449925	0.371023	2.414531
H		1.532404	1.610633	3.015661
H		3.181745	-0.061407	2.404004
H		1.563386	2.748219	0.834008
H		-0.116411	2.526211	1.342961
H		1.071624	-0.338858	-2.697456
H		1.878678	-1.583253	-1.731313

H	-0.667304	-1.852307	-1.022898
H	1.089116	2.847813	-1.667216
H	-0.590458	3.036686	-1.032945
H	-0.227895	1.849264	-2.297582
H	6.933065	-0.812823	1.222858
H	6.027843	-2.278867	0.723919
H	6.502302	-1.085975	-0.496747

HF = -1652.781674

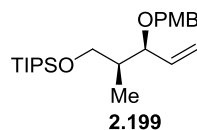
4.3 Chapter 2



Reduction of **2.198**: In a 250 mL round-bottomed flask, the Evans syn-aldol product **2.198** (3.62 g, 12.5 mmol) was dissolved in 115 mL dry THF. The mixture was then cooled to 0°C under vigorous stirring. To this was added a suspension of LiBH₄ (272 mg, 12.5 mmol) in 10 mL dry THF slowly. After 40 min, the reaction was quenched by addition of NH₄Cl (aq.) (40 mL). The reaction mixture was then partitioned against ethyl acetate (3x60 mL). The organic fractions were combined, washed with satd. NaCl (aq) (30 mL), dried over Na₂SO₄, filtered, and concentrated in vacuo to give a crude mixture containing the corresponding diol and Evans-type auxiliary. The mixture was difficult to separate and was used directly for the next step.

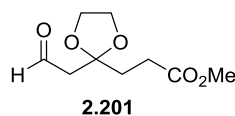
Terminal olefin **4.1**: In a 100 mL round-bottomed flask, the above crude mixture, azeotroped with toluene (3x10 mL), was dissolved in 60 mL dry DCM. To this, imidazole (2.55 g, 37.5 mmol), 4-dimethylaminopyridine (153 mg, 1.25 mmol) and TIPSCl (3.13 g, 16.2 mmol) were added in. After 16 h, 1 mL methanol was added, the reaction mixture was concentrated in vacuo, and purified by FCC (2% ethyl acetate/hexane) to give **4.1** (2.70 g, 79%) as a colorless yellow liquid (*R*_f = 0.9 40% ethyl acetate/hexane). [α]_D²³ -14.9 (*c* = 0.67, CHCl₃); IR ν_{max} (neat)/cm⁻¹ 3447, 3079, 2941, 2867, 1644, 1464, 1425, 1249, 882, 681; ¹H NMR (500 MHz, CDCl₃) δ 5.90 (1H, dd, *J* = 6.5, 5.5 Hz), 5.31 (1H, dt, *J* = 17.2, 1.8 Hz), 5.19 (1H, dt, *J* = 10.5, 1.7 Hz), 4.34 – 4.28 (1H, m), 3.83 – 3.72 (2H, m), 3.54 (1H, s), 3.42 (1H, d, *J* = 5.2 Hz), 2.01 – 1.94 (1H, m), 1.10 – 1.03 (21H, m), 0.89 (3H, d, *J* = 7.1 Hz); ¹³C NMR (126 MHz, CDCl₃) δ 138.7, 115.3, 76.1, 67.9, 39.8, 18.1, 12.0, 11.3; *m/z* (ESI/MS) calculated 273.2

(C₁₅H₃₃O₂Si), observed 273.2 (M+H)⁺.

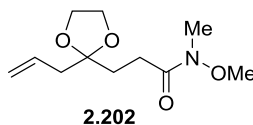


Terminal olefin **2.199**: To a flame dried 100 mL round-bottomed flask, sodium hydride 60 % dispersion in mineral oil (467 mg, 11.7 mmol) was added. It was then washed with dry hexane (3x10 mL) and dried under argon flow. 50 mL dry DMF were then added and the mixture was cooled to 0°C and vigorously stirred. Allylic alcohol **4.1** (1.27 g, 4.67 mmol) was azeotroped with toluene (3x10 mL), dissolved in 5 mL dry DMF, and added to this. After 20 min, the cooling bath was removed, and a catalytic amount of tetrabutylammonium iodide (173 mg, 0.467 mmol) was added in. Another 10 min later, 4-Methoxybenzyl chloride (1.10 g, 7.01 mmol) was added in. The reaction was then monitored by TLC. After 4 h, the reaction was cooled to 0°C, quenched by addition of water. The reaction mixture was diluted with water (3x60 mL) and partitioned against diethyl ether (4x60 mL). The organic fractions were combined, washed with satd. NaCl (aq) (60 mL), dried over Na₂SO₄, filtered, concentrated in vacuo, and purified by FCC (2% ethyl acetate/hexane) to give **2.199** (1.51 g, 82%) as a light yellow liquid (*R*_f = 0.65 5% ethyl acetate/hexane). [α]_D²³ 29.7 (*c* = 0.74, CHCl₃); IR ν_{max} (neat)/cm⁻¹ 3074, 2940, 2866, 1614, 1587, 1514, 1421, 1247, 882, 681; ¹H NMR (500 MHz, CDCl₃) δ 7.29 – 7.22 (2H, m), 6.90 – 6.83 (2H, m), 5.79 (1H, ddd, *J* = 17.6, 10.5, 7.5 Hz), 5.28 – 5.19 (2H, m), 4.53 (1H, d, *J* = 11.4 Hz), 4.27 (1H, d, *J* = 11.4 Hz), 3.89 – 3.83 (1H, m), 3.81 (3H, s), 3.70 (1H, dd, *J* = 9.6, 6.0 Hz), 3.55 (1H, dd, *J* = 9.6, 5.9 Hz), 1.81 – 1.74 (1H, m), 1.10 – 1.05 (21H, m), 0.98 (3H, d, *J* = 6.9 Hz); ¹³C NMR (126 MHz, CDCl₃) δ 159.1, 138.1, 131.4, 129.3, 117.2, 113.8, 80.9, 70.3, 65.4, 55.4, 41.4, 18.2, 12.2 (2); *m/z* (ESI/MS)

calculated 393.3 ($C_{23}H_{41}O_3Si$), observed 393.3 ($M+H$)⁺.



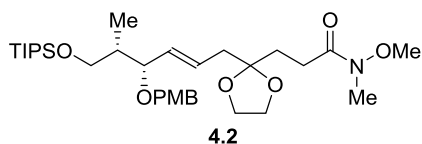
Aldehyde **2.201**: In a 100 mL round-bottomed flask, silyl enol ether **2.200** (2.00 g, 8.76 mmol) was dissolved in 45 mL DCM. The mixture was then cooled to -78°C under vigorous stirring. Dry O₃ was bubbled in until a faint blue color developed. Argon was then bubbled in for 10 min, followed by addition of PPh₃ (9.19 g, 35.0 mmol), and the cooling bath was removed. After 20 h, the solvent was removed and crude mixture was dissolved in a mixture of 10 mL methanol and 24 mL diethyl ether. At 0°C, a 2.0 M solution of TMSCHN₂ in ether (5.91 mL, 11.8 mmol) was added in dropwise. After 10 min, the reaction was quenched by addition of 20 mL water and partitioned against diethyl ether (3x30 mL). The organic fractions were combined, washed with satd. NaCl (aq) (20 mL), dried over Na₂SO₄, filtered, concentrated in vacuo, and purified by FCC (20% ethyl acetate/hexane) to give **2.201** (1.54 g, 87%) as a light yellow liquid (*R*_f = 0.60 70% ethyl acetate/hexane). ¹H NMR (500 MHz, CDCl₃) δ 9.69 (1H, t, *J* = 2.9 Hz), 3.97 (4H, s), 3.63 (3H, s), 2.64 (2H, d, *J* = 2.9 Hz), 2.36 (2H, t, *J* = 7.5 Hz), 2.06 (2H, t, *J* = 7.5 Hz); ¹³C NMR (126 MHz, CDCl₃) δ 199.8, 173.4, 108.4, 65.2, 51.7, 50.6, 33.2, 28.3; *m/z* (ESI/MS) calculated 225.1 (C₉H₁₄NaO₅), observed 225.1 ($M+Na$)⁺.



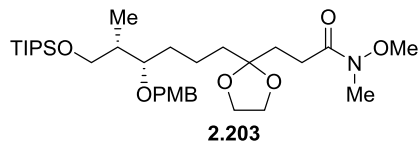
Wittig reaction of **2.201**: In a 100 mL round-bottomed flask, PPh₃CH₃⁺Br⁻ (2.12 g, 5.93 mmol) was dissolved in dry Et₂O (50 mL). An excess of sodium amide (50 wt.% suspension in

toluene) was added in. The resultant mixture was stirred at room temperature for 12h. The clear solution from the upper layer was cannulated to **2.201** (1.00 g, 4.95 mmol) dissolved in 25 mL dry Et₂O at -20°C under vigorous stirring. After 30 min, the reaction was quenched by addition of 20 mL NH₄Cl (aq.) and partitioned against diethyl ether (3x40 mL). The organic fractions were combined, washed with satd. NaCl (aq) (30 mL), dried over Na₂SO₄, filtered, concentrated in vacuo, and purified by FCC (10% diethyl ether/pentane) to give the volatile olefin product (~666 mg, ~67%) as a colorless liquid (*R*_f = 0.80 40% ethyl acetate/hexane). 393 mg unreacted starting material was also collected.

Winreb amide **2.201**: In a 50 mL round-bottomed flask, the above olefin ester (255 mg, 1.27 mmol) was dissolved in 12 mL THF, to which HNCH₃(OCH₃)·HCl (186 mg, 1.90 mmol) was added. The mixture was then cooled to -10°C under vigorous stirring, to which a 2.0 M solution of *i*-PrMgCl (1.90 mL, 3.80 mmol) was added. After 30 min, the reaction was quenched by addition of 5 mL NH₄Cl (aq.) and partitioned against ether acetate (3x10 mL). The organic fractions were combined, washed with satd. NaCl (aq) (5 mL), dried over Na₂SO₄, filtered, concentrated in vacuo, and purified by FCC (15% diethyl ether/pentane) to give **2.202** (238 mg, 82%) as a colorless liquid (*R*_f = 0.90 50% ethyl acetate/hexane). ¹H NMR (500 MHz, CDCl₃) δ 5.81 (1H, ddt, *J* = 17.4, 10.2, 7.2 Hz), 5.15 – 5.04 (2H, m), 3.95 (4H, s), 3.67 (3H, s), 3.16 (3H, s), 2.49 (2H, t, *J* = 8.0 Hz), 2.38 (2H, dt, *J* = 7.2, 1.2 Hz), 2.03 – 1.95 (2H, m); ¹³C NMR (126 MHz, CDCl₃) δ 133.1, 118.4, 110.5, 65.1, 61.3, 42.2, 32.4, 31.7, 26.3 (Carbon peak in Winreb amide was not observed.); *m/z* (ESI/MS) calculated 252.1 (C₁₁H₂₀NO₄), observed 230.1 (M+H)⁺.

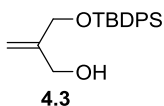


Olefin **3.2**: In a 50 mL round-bottomed flask, olefin **2.199** (2.46 g, 6.26 mmol) and olefin **2.202** (718 mg, 3.13 mmol) were dissolved in 20 mL bulk DCM, to which Hoveyda-Grubbs 2nd generation catalyst (10 mg, 0.0160 mmol) in 0.75 mL DCM was added. After 12 h, Hoveyda-Grubbs 2nd generation catalyst (10 mg, 0.0160 mmol) in 0.75 mL DCM was added in. After another 12 h, Hoveyda-Grubbs 2nd generation catalyst (15 mg, 0.0239 mmol) in 1.0 mL DCM was added in. After another 2 d, the reaction mixture was passed through a short pad of florisil and then treated with activated charcoal powder (100 mg) for 1 h. Then the solid was filtered, and the solution was concentrated in vacuo, purified by FCC (30% ethyl acetate/hexane) to give **4.2** (1.10 g, 59%) as a pale yellow oil (R_f = 0.55 60% ethyl acetate/hexane). 214 mg of olefin **2.202** was also collected. $[\alpha]_D^{23}$ (c = 0, CHCl_3); IR $\nu_{\text{max}}(\text{neat})/\text{cm}^{-1}$ 2957, 2907, 1613, 1586, 1513, 1464, 1251, 1129, 841, 749; ^1H NMR (500 MHz, CDCl_3) δ 7.30 – 7.21 (2H, m), 6.92 – 6.82 (2H, m), 5.65 (1H, dt, J = 15.7, 7.1 Hz), 5.51 (1H, ddt, J = 15.4, 7.8, 1.1 Hz), 4.51 (1H, d, J = 11.4 Hz), 4.24 (1H, d, J = 11.5 Hz), 4.00 – 3.93 (4H, m), 3.85 – 3.78 (4H, m), 3.76 – 3.65 (4H, m), 3.51 (1H, dd, J = 9.6, 6.2 Hz), 3.17 (3H, s), 2.55 – 2.38 (4H, m), 2.07 – 2.00 (2H, m), 1.83 – 1.72 (1H, m), 1.14 – 0.98 (21H, m), 0.96 (3H, dd, J = 6.9, 1.8 Hz); ^{13}C NMR (126 MHz, CDCl_3) δ 159.0, 133.6, 131.4, 129.3, 127.9, 113.7, 110.6, 80.2, 70.0, 65.4, 65.2, 61.3, 55.4, 41.6, 40.7, 32.4, 31.9, 26.4, 18.2, 12.3, 12.1 (Carbon peak in Winreb aminde was not observed.); m/z (ESI/MS) calculated 616.4 ($\text{C}_{32}\text{H}_{55}\text{NNaO}_7\text{Si}$), observed 616.4 ($\text{M}+\text{Na}$)⁺.

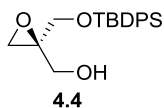


C1-C10 Winreb amide **2.203**: In a 50 mL round-bottomed flask, olefin **4.2** (1.10 g, 1.85 mmol) was dissolved in 21 mL dry ethanol, to which a powder of rhodium on alumina (5 wt.% loading, 152 mg, 0.0740 mmol) was added. Hydrogenation was then conducted with hydrogen filled balloons. After 21 h, the reaction mixture was filtered, concentrated in vacuo, and purified by FCC (30% ethyl acetate/hexane) to give **2.203** (614 mg, 56%) as a pale yellow oil (R_f = 0.55 60% ethyl acetate/hexane). A mixture containing PMB ether cleavage product was also collected.

Protection of the secondary alcohol: In a 50 mL round-bottomed flask, the above crude mixture was dissolved in 20mL toluene, to which PMB trichloroacetimidate (712 mg, 2.52 mmol) and $\text{La}(\text{OTf})_3$ (36 mg, 0.063 mmol) were added. After 1 d, the reaction mixture was concentrated in vacuo, and purified by FCC (30% ethyl acetate/hexane) to give **2.203** (336 mg, 30%) as a pale yellow oil. $[\alpha]_D^{23}$ 2.6 (c = 0.21, CHCl_3); IR $\nu_{\text{max}}(\text{neat})/\text{cm}^{-1}$ 3072, 2957, 2867, 1618, 1592, 1463, 1255, 835, 742; ^1H NMR (500 MHz, CDCl_3) δ 7.28 – 7.20 (2H, m), 6.88 – 6.80 (2H, m), 4.51 – 4.41 (2H, m), 3.97 – 3.87 (4H, m), 3.78 (3H, s), 3.73 – 3.63 (4H, m), 3.56 – 3.49 (2H, m), 3.17 (3H, s), 2.52 – 2.44 (2H, m), 2.01 – 1.94 (2H, m), 1.88 – 1.78 (1H, m), 1.69 – 1.29 (6H, m), 1.14 – 0.99 (21H, m), 0.90 (3H, d, J = 6.9 Hz); ^{13}C NMR (126 MHz, CDCl_3) δ 174.5, 159.1, 131.6, 129.4, 113.7, 111.1, 79.3, 72.1, 65.7, 65.1, 61.3, 55.3, 39.4, 37.5, 31.9, 31.6, 26.6, 20.5, 18.2, 12.1, 11.6; m/z (ESI/MS) calculated 618.4 ($\text{C}_{32}\text{H}_{57}\text{NNaO}_7\text{Si}$), observed 618.4 ($\text{M}+\text{Na}$) $^+$.

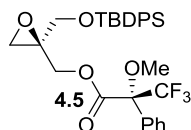


Allylic alcohol **4.3**: In a 500 mL round-bottomed flask, sodium hydride 60 % dispersion in mineral oil (4.54 g, 11.3 mmol) was suspended in dry THF (280 mL) and cooled to 0°C, to which diol **2.204** (10.0 g, 113.5 mmol) was added. After addition, the reaction was warmed to room temperature and kept for 30 min before it was cooled back to 0°C. Then TBDPSCI (31.2 g, 113.5 mmol) was added in, and the cooling bath was removed afterwards. After 2.5 h, the reaction was quenched by addition of 50 mL water and partitioned against diethyl ether (3x100 mL). The organic fractions were combined, dried over Na₂SO₄, filtered, concentrated in vacuo, and purified by FCC (10% ethyl acetate/hexane) to give **4.3** (29.1 g, 81%) as a colorless oil (*R*_f = 0.85 30% ethyl acetate/hexane). $\nu_{\text{max}}(\text{neat})/\text{cm}^{-1}$ 3355, 3071, 2932, 2857, 1660, 1589, 1428, 826, 741; ¹H NMR (500 MHz, CDCl₃) δ 7.73 – 7.63 (4H, m), 7.48 – 7.33 (6H, m), 5.19 – 5.10 (2H, m), 4.27 (2H, s), 4.19 (2H, d, *J* = 6.0 Hz), 1.82 (1H, t, *J* = 6.1 Hz), 1.08 (9H, s); ¹³C NMR (126 MHz, CDCl₃) δ 147.4, 135.8, 133.4, 130.0, 128.0, 111.4, 65.8, 64.7, 27.0, 19.4; *m/z* (ESI/MS) calculated 349.2 (C₂₀H₂₆NaO₂Si), observed 349.2 (M+Na)⁺.

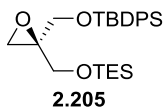


Epoxy alcohol **4.4**: In a 100 mL round-bottomed flask, 4 Å molecular sieves powder was activated, dispensed in dry DCM (30 mL), and cooled down to -30°C. (*L*)-diethyl tartrate (0.379 g, 1.84 mmol) and Ti(*Oi*-Pr)₄ (0.278 g, 0.980 mmol) were added in and aged for 45 min. Then anhydrous *t*-BuOOH (4.30 mL, 23.7 mmol) was added in and aged for 45 min.

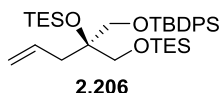
Allylic alcohol **4.3** (2.00 g, 6.13 mmol), dried over 4 Å molecular sieves, was then added in, and the reaction was kept at -30°C for 17h. The reaction was quenched by addition of water and 20 mL NaOH (30% in saturated NaCl solution), filtered, and partitioned against dichloromethane (3x20 mL). The organic fractions were combined, dried over Na₂SO₄, filtered, concentrated in vacuo, and used for the next step. An aliquot was taken and purified as a colorless oil. ee% of this product was determined as >20:1 by Mosher ester analysis. $[\alpha]_D^{23}$ -3.2 (c = 0.50, CHCl₃); IR ν_{\max} (neat)/cm⁻¹ 3447, 3071, 2932, 2858, 1589, 1428, 824, 741, 703; ¹H NMR (400 MHz, CDCl₃) δ 7.72 – 7.63 (4H, m), 7.51 – 7.33 (6H, m), 3.95 (1H, dd, *J* = 12.3, 4.8 Hz), 3.90 – 3.74 (3H, m), 2.86 (1H, d, *J* = 4.8 Hz), 2.67 (1H, d, *J* = 4.8 Hz), 1.85 (1H, dd, *J* = 8.2, 4.8 Hz), 1.07 (9H, s); ¹³C NMR (101 MHz, CDCl₃) δ 135.7 (2), 133.1, 133.0, 130.0 (2), 127.9, 65.0, 62.0, 59.7, 49.0, 26.9, 19.4 (Both phenyl groups in TBDPS were observed.); m/z (ESI/MS) calculated 365.2 (C₂₀H₂₆NaO₃Si), observed 365.2 (M+Na)⁺.



IR ν_{\max} (neat)/cm⁻¹ 3428, 3072, 2933, 2858, 1756, 1716, 1667, 1589, 1452, 1270, 911, 824, 704; ¹H NMR (500 MHz, CDCl₃) δ 7.66 – 7.54 (4H, m), 7.54 – 7.48 (3H, m), 7.46 – 7.31 (8H, m), 4.68 (1H, d, *J* = 11.8 Hz), 4.45 (1H, d, *J* = 11.8 Hz), 3.75 (1H, d, *J* = 11.5 Hz), 3.64 (1H, d, *J* = 11.5 Hz), 3.51 (3H, s), 2.72 (1H, d, *J* = 4.7 Hz), 2.63 (1H, d, *J* = 4.7 Hz), 1.04 (9H, s); ¹³C NMR (126 MHz, CDCl₃) δ 166.3, 135.7, 135.6, 133.0, 132.9, 132.1, 130.0 (2), 129.8, 128.6, 127.9, 127.5, 123.4 (d, *J* = 288.4 Hz), 65.4, 63.8, 57.4, 55.6, 49.4, 26.9, 19.4 (Both phenyl groups in TBDPS were observed, the quaternary carbon next to the ester was not observed.); m/z (ESI/MS) calculated 581.3 (C₃₀H₃₃F₃NaO₅Si), observed 581.2 (M+Na)⁺.



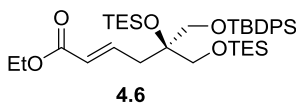
Epoxide **2.205**: In a 100 mL round-bottomed flask, the above crude product, azeotroped with toluene (3x10 mL), was dissolved in dry DCM (60 mL), to which was added imidazole (834 mg, 12.3 mmol), 4-dimethylaminopyridine (187 mg, 1.53 mmol) and TESI (1.30 mL, 7.66 mmol). After 20 min, the reaction was quenched by addition of water (30 mL) and partitioned against dichloromethane (3x40 mL). The organic fractions were combined, dried over Na₂SO₄, filtered, concentrated in vacuo, and purified by FCC (2% ethyl acetate/hexane) to give **2.205** (2.60 g, 93% two steps) as a light yellow liquid (R_f = 0.75 10% ethyl acetate/hexane). $[\alpha]_D^{23}$ -0.8 (c = 0.28, CHCl₃); IR ν_{\max} (neat)/cm⁻¹ 3073, 2956, 2876, 1659, 1428, 1239, 822, 738, 701; ¹H NMR (500 MHz, CDCl₃) δ 7.70 – 7.66 (4H, m), 7.47 – 7.34 (6H, m), 3.90 – 3.78 (4H, m), 2.76 (1H, d, J = 5.2 Hz), 2.69 (1H, d, J = 5.1 Hz), 1.06 (9H, s), 0.95 (9H, t, J = 8.0 Hz), 0.60 (6H, q, J = 8.0 Hz); ¹³C NMR (126 MHz, CDCl₃) δ 135.8 (2), 133.5 (2), 129.9 (2), 127.9 (2), 64.1, 62.9, 60.2, 49.0, 27.0, 19.5, 6.9, 4.6 (Both phenyl groups in TBDPS groups were observed.); m/z (ESI/MS) calculated 479.3 (C₂₆H₄₀NaO₃Si₂), observed 479.2 (M+Na)⁺.



Epoxide opening of **2.205**: In a flame dried 500 mL round-bottomed flask, CuBr·Me₂S (9.00 g, 43.8 mmol) was dispersed in dry Et₂O (200 mL), to which 10 mL Me₂S was added. The suspension was then cooled down to -40°C. To this, 1.0 M vinyl magnesium bromide in THF (109 mL, 109 mmol) was added. After 40 min, the suspension was cooled down to -78°C. To

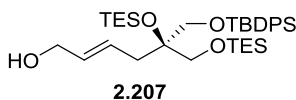
this, epoxide **2.205** (5.00 g, 11.0 mmol), azeotroped with toluene (3x20 mL), was added in. The reaction was then slowly warmed to -15°C and monitored by TLC. Upon full consumption of starting material, the reaction was quenched by 100 mL NH_4Cl (aq) and partitioned against diethyl ether (2x100 mL). The organic fractions were combined, washed with satd. NaCl (aq) (100 mL), dried over Na_2SO_4 , filtered, concentrated in vacuo, and used for the next step directly.

Olefin 2.206: In a 500 mL round-bottomed flask, the above crude material was azeotroped with toluene (3x20 mL) and dissolved in dry DCM (200 mL), to which 2,6-lutidine (10.2 mL, 88.0 mmol) and TESOTf (8.0 mL, 35.4 mmol) were added. After 1 h, the reaction was quenched by 100 mL water and partitioned against dichloromethane (3x50 mL). The organic fractions were combined, dried over Na_2SO_4 , filtered, concentrated in vacuo, and purified by FCC (2% ethyl acetate/hexane) to give **2.206** (5.35 g, 82% two steps) as a light yellow liquid ($R_f = 0.90$ 5% ethyl acetate/hexane). $[\alpha]_D^{23} 4.3$ ($c = 0.43$, CHCl_3); IR $\nu_{\text{max}}(\text{neat})/\text{cm}^{-1}$ 3072, 2956, 2876, 1640, 1590, 1428, 1239, 822, 738, 700; ^1H NMR (500 MHz, CDCl_3) δ 7.72 – 7.65 (4H, m), 7.46 – 7.34 (6H, m), 5.90 – 5.81 (1H, m), 5.08 – 4.98 (2H, m), 3.63 (1H, d, $J = 9.9$ Hz), 3.59 – 3.46 (3H, m), 2.36 (2H, qd, $J = 14.1, 7.1$ Hz), 1.07 (9H, s), 0.95 (9H, t, $J = 8.0$ Hz), 0.86 (9H, t, $J = 8.0$ Hz), 0.61 (6H, q, $J = 7.9$ Hz), 0.56 (6H, q, $J = 7.9$ Hz); ^{13}C NMR (126 MHz, CDCl_3) δ 136.0, 135.9, 134.8, 133.8 (2), 129.7 (2), 127.7, 117.2, 78.6, 67.0, 66.7, 39.6, 27.2, 19.5, 7.4, 7.1, 6.9, 4.6 (Both phenyl groups in TBDPS were observed.); m/z (ESI/MS) calculated 621.4 ($\text{C}_{34}\text{H}_{58}\text{NaO}_3\text{Si}_3$), observed 621.3 ($\text{M}+\text{Na}$) $^+$.

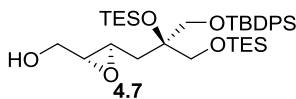


Oxidative cleavage of olefin **2.206**: In a 100 mL round-bottomed flask, olefin **2.206** (2.80 g, 4.67 mmol) was dispensed in a mixture of 1,4-dioxane (36 mL) and water (12 mL), to which 2,6-lutidine (1.1 mL, 9.34 mmol), sodium periodate (4.00 g, 18.7 mmol), 4 wt.% osmium tetroxide in water (1.2 mL, .186 mmol) were added. After 24 h, the solid was filtered off, and the reaction was quenched by 50 mL $\text{Na}_2\text{S}_2\text{O}_3$ (aq.) and partitioned against dichloromethane (3x80 mL). The organic fractions were combined, dried over Na_2SO_4 , filtered, concentrated in vacuo, and used for the next step directly.

Ester **4.4**: In a 50 mL round-bottomed flask, the above crude material was azeotroped with toluene (3x10 mL) and dissolved in dry DCM (24 mL), to which $\text{Ph}_3\text{PCHCO}_2\text{Et}$ (4.50 g, 11.7 mmol) was added. After 36 h, the solvent was partially removed, the syrup like crude material was dispensed in 300 mL diethyl ether, the resultant solid was filtered off, the organic fraction was concentrated in vacuo, and purified by FCC (2% ethyl acetate/hexane) to give **2.206** (2.84 g, 90% two steps) as a colorless thick oil (R_f = 0.95 10% ethyl acetate/hexane). $[\alpha]_D^{23}$ 2.6 (c = 0.31, CHCl_3); IR ν_{max} (neat)/ cm^{-1} 3072, 2956, 2876, 1723, 1654, 1590, 1428, 1265, 1181, 822, 739; ^1H NMR (500 MHz, CDCl_3) δ 7.70 – 7.61 (4H, m), 7.46 – 7.29 (6H, m), 7.04 (1H, dt, J = 15.6, 7.5 Hz), 5.83 (1H, dt, J = 15.7, 1.4 Hz), 4.18 (2H, q, J = 7.1 Hz), 3.61 (1H, d, J = 10.0 Hz), 3.57 – 3.42 (3H, m), 2.53 – 2.44 (2H, m), 1.28 (3H, t, J = 7.1 Hz), 1.07 (9H, s), 0.94 (9H, t, J = 7.9 Hz), 0.86 (9H, t, J = 7.9 Hz), 0.59 (6H, q, J = 7.8 Hz), 0.55 (6H, q, J = 7.8 Hz); ^{13}C NMR (126 MHz, CDCl_3) δ 166.5, 146.0, 135.9 (2), 133.5 (2), 129.9 (2), 127.8, 123.7, 78.7, 67.1, 66.8, 60.2, 38.0, 27.1, 19.4, 14.5, 7.3, 7.0, 6.8, 4.6 (Both phenyl groups in TBDPS were observed.); m/z (ESI/MS) calculated 693.4 ($\text{C}_{37}\text{H}_{62}\text{NaO}_5\text{Si}_3$), observed 693.4 ($\text{M}+\text{Na}$) $^+$.

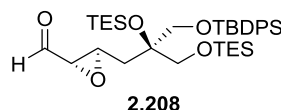


Allylic alcohol **2.207**: In a 50 mL round-bottomed flask, ester **4.6** (2.84 g, 4.23 mmol) was azeotroped with toluene (3x10 mL), dissolved in dry DCM (60 mL), and cooled to -78°C , to which 1.0 M DIBAL-H in hexane (8.46 mL, 8.46 mmol) was added slowly. After 1 h, the reaction was quenched by 50 mL saturated Rochelle salt solution and partitioned against dichloromethane (3x50 mL). The organic fractions were combined, dried over Na_2SO_4 , filtered, concentrated in vacuo, and purified by FCC (10% ethyl acetate/hexane) to give **2.207** (2.54 g, 95%) as a colorless oil ($R_f = 0.20$ 10% ethyl acetate/hexane). $[\alpha]_D^{23}$ 2.8 ($c = 0.29$, CHCl_3); IR $\nu_{\text{max}}(\text{neat})/\text{cm}^{-1}$ 3331, 3072, 2956, 2876, 1428, 1239, 822, 7398, 702; ^1H NMR (500 MHz, CDCl_3) δ 7.69 – 7.64 (4H, m), 7.46 – 7.35 (6H, m), 5.74 – 5.59 (2H, m), 4.02 (2H, t, $J = 5.6$ Hz), 3.62 (1H, d, $J = 9.9$ Hz), 3.54 (2H, dd, $J = 9.3, 4.3$ Hz), 3.45 (1H, d, $J = 9.8$ Hz), 2.41 – 2.28 (2H, m), 1.07 (9H, s), 0.96 (9H, t, $J = 7.9$ Hz), 0.88 (9H, t, $J = 8.0$ Hz), 0.61 (6H, q, $J = 8.2$ Hz), 0.55 (6H, q, $J = 8.1$ Hz); ^{13}C NMR (126 MHz, CDCl_3) δ 135.9 (2), 133.7 (2), 131.7, 129.8, 129.7, 129.1, 127.7 (2), 78.6, 66.7 (2), 64.1, 37.7, 27.1, 19.4, 7.3, 7.0, 6.8, 4.5 (Both phenyl groups in TBDPS were observed.); m/z (ESI/MS) calculated 651.4 ($\text{C}_{35}\text{H}_{60}\text{NaO}_4\text{Si}_3$), observed 651.3 ($\text{M}+\text{Na}$) $^+$.



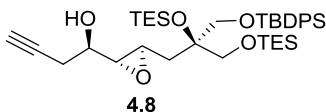
Epoxy alcohol **4.7**: In a 100 mL round-bottomed flask, 3 Å molecular sieves pellets was activated, dispensed in extra dry DCM (20 mL), and cooled down to -30°C . (*D*)-diisopropyl tartrate (0.240 g, 1.03 mmol) and $\text{Ti}(\text{O}i\text{-Pr})_4$ (0.224 g, 0.789 mmol) were added in and aged

for 45 min. Then anhydrous *t*-BuOOH in DCM (0.72 ml, 3.16 mmol) was added in and aged for 40 min. Allylic alcohol **2.207** (993 mg, 1.58 mmol), dried over 3 Å molecular sieves pellets, was then added in. The reaction was kept at -35°C for 3h, then placed in a -30°C freezer and kept for 36h. The reaction was quenched by addition of water and 10 mL NaOH (30 wt.% in saturated NaCl solution), filtered, and partitioned against diethyl ether (3x30 mL). The organic fractions were combined, dried over Na₂SO₄, filtered, concentrated in vacuo, and purified by FCC (10-15% ethyl acetate/hexane) to give **4.6** (694 mg, 69%) as a colorless oil (*R*_f = 0.40 15% ethyl acetate/hexane, 9:1 d.r.). $[\alpha]_D^{23}$ 9.9 (*c* = 0.36, CHCl₃); IR $\nu_{\max}(\text{neat})/\text{cm}^{-1}$ 3447, 3072, 2956, 2876, 1590, 1428, 1239, 822, 739, 702; ¹H NMR (500 MHz, CDCl₃) δ 7.70 – 7.65 (4H, m), 7.47 – 7.34 (6H, m), 3.84 (1H, ddd, *J* = 12.5, 5.7, 2.6 Hz), 3.68 – 3.62 (2H, m), 3.60 – 3.54 (2H, m), 3.50 (1H, ddd, *J* = 12.1, 6.8, 4.6 Hz), 3.05 (1H, td, *J* = 6.2, 2.3 Hz), 2.89 (1H, dt, *J* = 4.8, 2.5 Hz), 1.97 (1H, dd, *J* = 14.1, 5.5 Hz), 1.74 (1H, dd, *J* = 14.1, 6.4 Hz), 1.68 – 1.61 (1H, m), 1.08 (9H, s), 0.94 (9H, t, *J* = 7.9 Hz), 0.89 (9H, t, *J* = 7.9 Hz), 0.64 – 0.49 (12H, m); ¹³C NMR (126 MHz, CDCl₃) δ 136.0, 135.9, 133.6, 133.5, 129.9 (2), 127.8 (2), 78.4, 67.2 (2), 62.1, 58.7, 52.9, 37.4, 27.2, 19.5, 7.3, 7.1, 6.8, 4.6 (Both phenyl groups in TBDPS were observed.); *m/z* (ESI/MS) calculated 667.4 (C₃₅H₆₀NaO₅Si₃), observed 667.4 (M+Na)⁺.



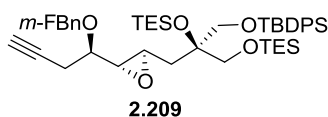
Epoxy aldehyde 2.208: In a 100 mL round-bottomed flask, epoxy alcohol **4.6** (694 mg, 1.08 mmol) was azeotroped with toluene (3x10 mL), dissolved in dry DCM (31 mL), to which pyridine (0.53 mL, 6.46 mmol) and Dess-Martin periodinane (1.37 g, 3.23 mmol) were added. After 2 h, the reaction was quenched by 20 mL Na₂S₂O₃ (aq.) and partitioned against

dichloromethane (3x30 mL). The organic fractions were combined, dried over Na_2SO_4 , filtered, concentrated in vacuo, and purified by FCC (5% ethyl acetate/hexane) to give **2.208** (656 mg, 95%) as a colorless oil ($R_f = 0.95$ 20% ethyl acetate/hexane). $[\alpha]_D^{23} -16.5$ ($c = 0.42$, CHCl_3); IR $\nu_{\text{max}}(\text{neat})/\text{cm}^{-1}$ 3072, 2956, 2876, 1732, 1428, 1239, 822, 739, 702; ^1H NMR (500 MHz, CDCl_3) δ 8.90 (1H, d, $J = 6.4$ Hz), 7.70 – 7.61 (4H, m), 7.48 – 7.34 (6H, m), 3.67 – 3.49 (4H, m), 3.32 (1H, td, $J = 5.7, 2.0$ Hz), 3.10 (1H, dd, $J = 6.4, 2.0$ Hz), 1.95 (1H, dd, $J = 14.3, 6.0$ Hz), 1.86 (1H, dd, $J = 14.2, 5.5$ Hz), 1.08 (9H, s), 0.93 (9H, t, $J = 7.9$ Hz), 0.87 (9H, t, $J = 7.9$ Hz), 0.65 – 0.49 (12H, m); ^{13}C NMR (126 MHz, CDCl_3) δ 198.8, 136.0, 135.9, 133.4, 133.3, 130.0 (2), 127.9 (2), 78.2, 67.2 (2), 59.3, 53.8, 36.7, 27.2, 19.5, 7.3, 7.0, 6.8, 4.5 (Both phenyl groups in TBDPS were observed.); m/z (ESI/MS) calculated 665.4 ($\text{C}_{35}\text{H}_{58}\text{NaO}_5\text{Si}_3$), observed 665.4 ($\text{M}+\text{Na}$) $^+$.



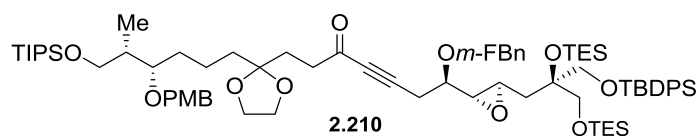
Alkyne **4.8**: To a 50 mL flame dried round-bottomed flask, activated 4 Å molecular sieves pellets (100 mg) and allenyl boronic acid (200 mg, 2.38 mmol) were added under argon. To this, dry toluene (10 mL) and (*D*)-diisopropyl tartrate (0.681 g, 2.85 mmol) were added. After 36 h, the reaction was cooled to -78°C . To this, epoxy aldehyde **2.208** (656 mg, 1.02 mmol) was added. After another 12 h, the cooling bath was removed. After another 12 h, the reaction mixture was passed through a short pad of celite. The organic fraction was concentrated in vacuo, and purified by FCC (10% ethyl acetate/hexane) to give **4.8** (552 mg, 79%) as a colorless oil ($R_f = 0.40$ 10% ethyl acetate/hexane). $[\alpha]_D^{23} -1.7$ ($c = 0.27$, CHCl_3); IR $\nu_{\text{max}}(\text{neat})/\text{cm}^{-1}$ 3451, 3313, 3072, 2955, 2876, 1590, 1428, 1239, 822, 740, 701; ^1H NMR

(400 MHz, CDCl₃) δ 7.70 – 7.63 (4H, m), 7.47 – 7.32 (6H, m), 3.80 – 3.70 (1H, m), 3.67 (2H, dd, J = 10.0, 5.5 Hz), 3.58 (2H, dd, J = 10.0, 2.0 Hz), 3.16 (1H, td, J = 5.9, 2.3 Hz), 2.86 (1H, dd, J = 4.3, 2.3 Hz), 2.47 – 2.41 (2H, m), 2.07 – 1.99 (2H, m), 1.88 – 1.81 (2H, m), 1.06 (9H, s), 0.94 (9H, t, J = 7.9 Hz), 0.89 (9H, t, J = 7.9 Hz), 0.59 (6H, q, J = 8.1 Hz), 0.56 (6H, q, J = 8.1 Hz); ¹³C NMR (101 MHz, CDCl₃) δ 136.0, 135.9, 133.7, 133.6, 129.9, 129.8, 127.8 (2), 80.0, 78.5, 71.1, 68.5, 67.3, 66.9, 59.5, 52.9, 37.5, 27.2, 24.0, 19.5, 7.3, 7.0, 6.9, 4.6; m/z (ESI/MS) calculated 705.4 (C₃₈H₆₂NaO₅Si₃), observed 705.4 (M+Na)⁺.



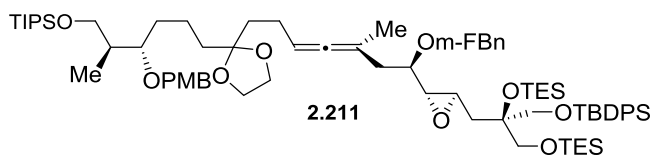
Alkyne **2.209**: In a 25 mL round bottomed flask, alkyne **4.8** (367 mg, 0.537 mmol) was dispensed in a mixture of benzene (4 mL) and potassium hydroxide (30 wt.% aqueous solution, 4 mL). To this, 3-fluorobenzyl bromide (0.305 g, 1.61 mmol) and *n*-Bu₄HSO₄ (36 mg, 0.107 mmol) were added. After 2 d, the reaction was diluted with 20 mL water and partitioned against dichloromethane (3x40 mL). The organic fractions were combined, dried over Na₂SO₄, filtered, concentrated in vacuo, and purified by FCC (20% dichloromethane/hexane) to give **2.209** (419 mg, 98%) as a colorless liquid (R_f = 0.80 15% ethyl acetate/hexane). $[\alpha]_D^{23}$ 8.7 (c = 0.53, CHCl₃); IR ν_{\max} (neat)/cm⁻¹ 3313, 3072, 2957, 2876, 1618, 1428, 1256, 825, 741, 641; ¹H NMR (500 MHz, CDCl₃) δ 7.76 – 7.65 (4H, m), 7.51 – 7.34 (6H, m), 7.33 – 7.25 (1H, m), 7.16 – 7.05 (2H, m), 6.98 (1H, tdd, J = 8.3, 2.6, 1.0 Hz), 4.61 (2H, dd, J = 38.0 Hz, J = 12.2 Hz), 3.76 – 3.58 (4H, m), 3.41 (1H, q, J = 5.6 Hz), 3.20 (1H, ddd, J = 6.9, 4.9, 2.2 Hz), 2.88 (1H, dd, J = 5.4, 2.2 Hz), 2.54 (2H, dd, J = 5.8, 2.7 Hz), 2.04 (1H, t, J = 2.6 Hz), 1.91 (1H, dd, J = 14.4, 4.8 Hz), 1.82 (1H, dd, J = 14.4, 6.6 Hz), 1.09 (9H, s), 0.96 (9H, t,

$J = 7.9$ Hz), 0.91 (9H, t, $J = 7.9$ Hz), 0.67 – 0.52 (12H, m); ^{13}C NMR (126 MHz, CDCl_3) δ 163.0 (d, $J = 245.7$ Hz), 140.9 (d, $J = 7.1$ Hz), 135.9, 135.8, 133.5 (2), 129.9 (d, $J = 8.2$ Hz), 129.7 (2), 127.7, 122.9 (d, $J = 2.9$ Hz), 114.6 (d, $J = 17.9$ Hz), 114.4 (d, $J = 18.5$ Hz), 80.4, 78.5, 76.9, 71.44 (d, $J = 1.9$ Hz), 70.4, 67.2, 66.8, 58.2, 54.1, 37.4, 27.1, 22.5, 19.4, 7.3, 7.0, 6.7, 4.5 (Both phenyl groups in TBDPS were observed.); m/z (ESI/MS) calculated 813.4 ($\text{C}_{45}\text{H}_{67}\text{FNaO}_5\text{Si}_3$), observed 813.4 ($\text{M}+\text{Na}$) $^+$.



Alkynone **2.210**: In a flame dried 25 mL round-bottomed flask, alkyne 2.209 (380 mg, 0.480 mmol) was dissolved in 10 mL dry THF and cooled down to -25°C . To this, 2.0 M isopropylmagnesium chloride solution in THF (0.31 mL, 0.62 mmol) was added. The reaction was then slowly warmed to room temperature over 20 min. After another 10 min, the reaction was cooled back to -25°C . To this, amide **2.203** (205 mg, 0.344 mmol) in 2 mL dry THF was added. The reaction was slowly warmed to 0°C over 2h, then quenched by 5 mL NH_4Cl (aq.) and partitioned against dichloromethane (3x15 mL). The organic fractions were combined, dried over Na_2SO_4 , filtered, concentrated in vacuo, and purified by FCC (12% ethyl acetate/hexane) to give **2.210** (353 mg, 77%) as a colorless oil ($R_f = 0.70$ 25% ethyl acetate/hexane). $[\alpha]_D^{23}$ 5.8 ($c = 0.38$, CHCl_3); IR ν_{max} (neat)/ cm^{-1} 3071, 2956, 2876, 2216, 1675, 1591, 1514, 1464, 1248, 821, 742, 505; ^1H NMR (500 MHz, CDCl_3) δ 7.72 – 7.65 (4H, m), 7.46 – 7.33 (6H, m), 7.32 – 7.23 (3H, m), 7.07 (2H, td, $J = 9.4, 8.9, 1.9$ Hz), 7.00 – 6.93 (1H, m), 6.90 – 6.83 (2H, m), 4.64 (1H, d, $J = 12.1$ Hz), 4.53 (1H, d, $J = 12.1$ Hz), 4.48 (2H, s), 3.94 – 3.86 (4H, m), 3.80 (3H, s), 3.75 – 3.50 (7H, m), 3.41 – 3.34 (1H, m), 3.12 (1H, ddd, $J = 6.9, 4.8,$

2.2 Hz), 2.78 (1H, dd, $J = 5.9, 2.1$ Hz), 2.69 – 2.64 (2H, m), 2.61 (2H, t, $J = 7.4$ Hz), 2.02 (2H, t, $J = 7.5$ Hz), 1.92 – 1.81 (2H, m), 1.78 (1H, dd, $J = 14.4, 6.8$ Hz), 1.64 – 1.49 (3H, m), 1.51 – 1.40 (2H, m), 1.41 – 1.30 (1H, m), 1.10 – 1.05 (30H, m), 0.98 – 0.85 (21H, m), 0.64 – 0.53 (12H, m); ^{13}C NMR (126 MHz, CDCl_3) δ 187.2, 163.0 (d, $J = 246.0$ Hz), 159.1, 140.6 (d, $J = 7.2$ Hz), 135.9, 135.8, 133.5, 133.4, 131.6, 130.0 (d, $J = 8.1$ Hz), 129.8 (2), 129.4, 127.7, 122.9 (d, $J = 2.9$ Hz), 114.7 (d, $J = 21.1$ Hz), 114.3 (d, $J = 21.8$ Hz), 113.8, 110.8, 89.6, 82.0, 79.2, 78.4, 77.1, 72.1, 71.7 (d, $J = 1.9$ Hz), 67.2, 66.9, 65.7, 65.2, 57.9, 55.4, 54.6, 40.2, 39.5, 37.8, 37.3, 31.9, 31.3, 27.1, 23.4, 20.5, 19.4, 18.2, 12.1, 11.7, 7.3, 7.0, 6.8, 4.5 (Both phenyl groups in TBDPS were observed.); m/z (ESI/MS) calculated 1347.8 ($\text{C}_{75}\text{H}_{117}\text{FNaO}_{11}\text{Si}_4$), observed 1347.8 ($\text{M}+\text{Na}$) $^+$.



Preparation of the (*S,S*)-Noyori catalyst: In a 5 mL vial, dichloro(*p*-cymene)ruthenium(II) dimer (35 mg, 0.057 mmol), (1*S*,2*S*)-(-)-*N*-*p*-tosyl-1,2-diphenylethylenediamine (42 mg, 0.125 mmol), and potassium hydroxide powder (64 mg, 1.14 mmol) were dispensed in 2 mL dry DCM. Under vigorous stirring, the suspension turned from orange to dark purple (about 5 min). The reaction mixture was filtered, concentrated in vacuo, and dissolved in 10 mL oxygen free *i*-PrOH to give an orange solution.

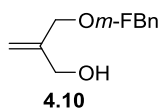
Reduction to propargyl alcohol **4.9**: In a flame dried 25 mL round-bottomed flask, alkynone **2.210** (71 mg, 0.0535 mmol) was azeotroped with toluene (3x5 mL) and dissolved in 2 mL oxygen free *i*-PrOH. To this, the above (*S,S*)-Noyori catalyst (0.5 mL) was added. The reaction turned to purple and then shortly back to orange, which was concentrated in vacuo, and purified by FCC (14% ethyl acetate/hexane) to give the corresponding propargyl alcohol **4.9**

(59 mg, 83%) as a colorless oil (R_f = 0.55 25% ethyl acetate/hexane) and 12 mg unreacted starting material.

Preparation of the methyl cuprate: In a flame dried 25 mL round-bottomed flask, CuCN (60 mg, 0.666 mmol), activated by gentle heating, was dispensed in dry THF (6.6 mL) and cooled to -40°C . To this, 1.6 M MeLi in Et₂O (0.42 mL, 0.666 mmol) was added. In about 5 min, the reaction mixture became a faint yellow solution and was transferred via syringe to the next step.

Allene **2.211**: In a flame dried 25 mL round-bottomed flask, the above propargyl alcohol **4.9** (59 mg, 0.0444 mmol) was azeotroped with toluene (3x2 mL), dissolved in 2 mL dry THF and cooled down to 0°C . To this, triethylamine (19 μL , 0.13 mmol) and methanesulfonyl chloride (5.2 μL , 0.067 mmol) were added. After 20 min, upon full consumption of starting material, the reaction was cooled down to -78°C . To this, the above methyl cuprate solution (0.93 mL) was added slowly. The reaction was then slowly warmed to -20°C over 20 min, then quenched by 3 mL NH₄Cl (aq.) and partitioned against diethyl ether (3x10 mL). The organic fractions were combined, dried over Na₂SO₄, filtered, concentrated in vacuo, and purified by FCC (10% ethyl acetate/hexane) to give **2.211** (52 mg, 88%) as a colorless oil (R_f = 0.70 20% ethyl acetate/hexane). $[\alpha]_D^{23}$ 19.3 (c = 0.36, CHCl₃); IR $\nu_{\text{max}}(\text{neat})/\text{cm}^{-1}$ 3072, 2956, 2876, 1966, 1734, 1615, 1591, 1514, 1463, 1248, 822, 741, 504; ¹H NMR (500 MHz, CDCl₃) δ 7.72 – 7.63 (4H, m), 7.45 – 7.32 (7H, m), 7.30 – 7.21 (3H, m), 7.07 – 7.00 (2H, m), 6.97 – 6.89 (1H, m), 6.90 – 6.82 (2H, m), 5.11 – 5.01 (1H, m), 4.63 (1H, d, J = 11.9 Hz), 4.52 – 4.40 (3H, m), 3.89 (4H, s), 3.79 (3H, s), 3.76 – 3.66 (3H, m), 3.67 – 3.51 (4H, m), 3.44 (1H, dt, J = 8.7, 4.3 Hz), 3.19 (1H, ddd, J = 6.8, 4.8, 2.2 Hz), 2.72 (1H, dd, J = 4.9, 2.2 Hz), 2.28 (1H, dt, J = 15.2, 3.6 Hz), 2.20 (1H, ddd, J = 15.1, 8.5, 2.4 Hz), 2.08 – 2.00 (2H, m), 1.92 – 1.81 (2H, m), 1.77 (1H,

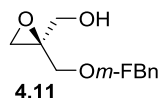
dd, $J = 14.4, 6.6$ Hz), 1.74 – 1.64 (5H, m), 1.66 – 1.52 (3H, m), 1.52 – 1.40 (2H, m), 1.41 – 1.33 (1H, m), 1.03 – 1.10 (30H, m), 0.97 – 0.85 (21H, m), 0.64 – 0.51 (12H, m); ^{13}C NMR (126 MHz, CDCl_3) δ 202.0, 163.0 (d, $J = 245.3$ Hz), 159.1, 141.7 (d, $J = 7.2$ Hz), 135.9, 135.8, 133.6, 133.5, 131.6, 129.8 (d, $J = 7.5$ Hz), 129.7 (2), 129.4, 127.7, 122.7 (d, $J = 2.9$ Hz), 114.3 (d, $J = 3.6$ Hz), 114.1 (d, $J = 3.0$ Hz), 113.8, 111.5, 96.6, 90.6, 79.3, 78.5, 77.4, 72.1, 71.7 (d, $J = 1.9$ Hz), 67.2, 66.9, 65.7, 65.2, 59.5, 55.4 (2), 53.4, 39.5, 37.7 (2), 37.6, 37.1, 31.9, 27.1, 23.8, 20.4, 20.0, 19.4, 18.2, 12.2, 11.6, 7.3, 7.0, 6.8, 4.5 (Both ketal carbons were observed, both phenyl groups in TBDPS were observed.); m/z (ESI/MS) calculated 1347.8 ($\text{C}_{76}\text{H}_{121}\text{FNaO}_{10}\text{Si}_4$), observed 1347.8 ($\text{M}+\text{Na}$) $^+$.



Allylic alcohol **4.10**: In a 500 mL round-bottomed flask, sodium hydride 60 % dispersion in mineral oil (2.38 g, 59.6 mmol) was washed with dry hexane (3x20 mL), suspended in dry THF (250 mL) and cooled to 0°C, to which a dry THF solution of diol **2.204** (5.00 g in 50 mL, 56.8 mmol) was added in slowly. After 1 h, the reaction was warmed to room temperature and kept for 30 min before it was cooled back to 0°C. To this, 3-fluorobenzyl bromide (11.3 g, 59.6 mmol) and dry tetrabutylammonium iodide (2.10 g, 5.68 mmol) were added in, and the cooling bath was removed. After 2 d, the reaction was filtered, concentrated in vacuo, and purified by FCC (30% ethyl acetate/hexane) to give **4.10** (6.26 g, 58%) as a light yellow oil (R_f = 0.50 50% ethyl acetate/hexane). 4.44 g of bis-3-fluorobenzylether was also collected.

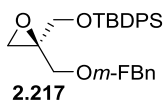
Boronic acid catalyzed approach to allylic alcohol **4.10**: In a 25 mL round-bottomed flask, potassium iodide (188 mg, 1.14 mmol), potassium carbonate (188 mg, 1.36 mmol), and 2-

aminoethyl diphenylborinate (26 mg, 0.114 mmol) were suspended in dry acetonitrile (6 mL). To this, diol **2.204** (100 mg, 1.14 mmol) and 3-fluorobenzyl bromide (322 mg, 1.70 mmol) were added. The reaction was then warmed to 60 °C and kept for 16 h before it was cooled back to room temperature. After another 8 h, the reaction was filtered, concentrated in vacuo, and purified by FCC (30% ethyl acetate/hexane) to give **4.10** (169 mg, 76%) as a colorless liquid ($R_f = 0.50$ 50% ethyl acetate/hexane). IR $\nu_{\max}(\text{neat})/\text{cm}^{-1}$ 3384, 3081, 2862, 1167, 1592, 1487, 1450, 1257, 1139, 1068, 917, 785, 685; ^1H NMR (500 MHz, CDCl_3) δ 7.34 – 7.27 (1H, m), 7.13 – 7.01 (2H, m), 7.02 – 6.94 (1H, m), 5.28 – 5.10 (2H, m), 4.51 (2H, s), 4.20 (2H, s), 4.10 (2H, s), 1.81 (1H, s); ^{13}C NMR (126 MHz, CDCl_3) δ 163.1 (d, $J = 246.1$ Hz), 145.0, 140.8 (d, $J = 7.1$ Hz), 130.1 (d, $J = 8.2$ Hz), 123.1 (d, $J = 2.8$ Hz), 114.7 (d, $J = 20.9$ Hz), 114.4, 113.8, 72.0, 71.8 (d, $J = 44.0$ Hz), 64.6; m/z (ESI/MS) calculated 219.1 ($\text{C}_{11}\text{H}_{13}\text{FNaO}_2$), observed 219.1 ($\text{M}+\text{Na}$) $^+$.



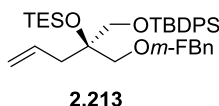
Epoxy alcohol **4.11**: In a 250 mL round-bottomed flask, 4 Å molecular sieves powder (8 g) was activated, dispensed in dry DCM (160 mL), and cooled down to -25°C. (*D*)-diisopropyl tartrate (0.822 g, 3.51 mmol) and $\text{Ti}(\text{O}i\text{-Pr})_4$ (0.90 g, 3.19 mmol) were added in and aged for 1 h. Then anhydrous *t*-BuOOH in decane (14.5 mL, 79.8 mmol) was added in and aged for 1 h. Allylic alcohol **4.10** (6.26 g, 31.9 mmol), dried over 4 Å molecular sieves, was added in, and the reaction was kept in a -30°C freezer. After 18 h, the reaction was quenched by tartaric acid (10 wt.% in water, 80 mL), filtered, and partitioned against dichloromethane (3x100 mL). The organic fractions were combined, dried over Na_2SO_4 , filtered, concentrated in

vacuo, and used for the next step. An aliquot (200 mg) was taken and purified as a colorless oil. ee% was determined as >20:1 by Mosher ester (R) analysis. $[\alpha]_D^{23}$ 14.5 ($c = 0.63$, CHCl_3); ^1H NMR (500 MHz, CDCl_3) δ 7.55 – 7.49 (2H, m), 7.45 – 7.34 (3H, m), 7.33 – 7.27 (1H, m), 7.10 – 6.94 (3H, m), 4.60 (1H, d, $J = 12.0$ Hz), 4.53 – 4.45 (3H, m), 3.62 – 3.52 (2H, m), 3.53 (3H, s), 2.82 (1H, d, $J = 4.7$ Hz), 2.77 (1H, d, $J = 4.7$ Hz); ^{13}C NMR (126 MHz, CDCl_3) δ 166.3, 163.1 (d, $J = 246.3$ Hz), 140.4 (d, $J = 7.1$ Hz), 132.2, 130.2 (d, $J = 8.3$ Hz), 130.0, 128.7, 127.6, 123.5 (d, $J = 288.5$ Hz), 123.16 (d, $J = 2.9$ Hz), 114.9 (d, $J = 21.2$ Hz), 114.5 (d, $J = 21.7$ Hz), 72.9 (d, $J = 1.9$ Hz), 70.4, 65.1, 56.3, 55.6, 49.1 (The quaternary carbon next to the ester was not observed.); m/z (ESI/MS) calculated 451.1 ($\text{C}_{21}\text{H}_{20}\text{F}_4\text{NaO}_5$), observed 451.1 ($\text{M}+\text{Na}$) $^+$.



Epoxide 2.217: In a 250 mL round-bottomed flask, the above crude product, azeotroped with toluene (3x50 mL), was dissolved in a mixture of DCM (100 mL) and DMF (10 mL), to which was added imidazole (6.50 g, 95.7 mmol), 4-dimethylaminopyridine (390 mg, 3.19 mmol) and TBDPSCI (13.2 g, 47.9 mmol). After 1 h, 1 mL methanol was added in. The reaction was filtered, concentrated in vacuo, diluted with satd. NaCl (aq) (90 mL), and partitioned against diethyl ether (3x80 mL). The organic fractions were combined, washed with satd. NaCl (aq) (50 mL), dried over Na_2SO_4 , filtered, and concentrated in vacuo, and purified by FCC (3% ethyl acetate/hexane) to give **2.217** (11.3 g, 79% two steps) as a colorless liquid ($R_f = 0.75$ 40% ethyl acetate/hexane). $[\alpha]_D^{23}$ 32.5 ($c = 0.55$, CHCl_3); IR $\nu_{\text{max}}(\text{neat})/\text{cm}^{-1}$ 3071, 2931, 2858, 1617, 1591, 1428, 1256, 823, 703, 505; ^1H NMR (500 MHz, CDCl_3) δ 7.70 – 7.63 (4H, m), 7.48 – 7.31 (6H, m), 7.31 – 7.25 (1H, m), 7.10 – 6.93 (3H, m),

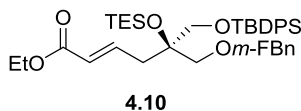
4.53 (2H, d, $J = 3.2$ Hz), 3.92 – 3.77 (2H, m), 3.77 – 3.67 (2H, m), 2.78 – 2.69 (2H, m), 1.05 (9H, s); ^{13}C NMR (126 MHz, CDCl_3) δ 140.8 (d, $J = 7.1$ Hz), 135.8, 135.7, 133.3, 133.2, 130.0 (d, $J = 8.3$ Hz), 129.9 (2), 127.9 (2), 123.1 (d, $J = 2.8$ Hz), 114.7 (d, $J = 18.1$ Hz), 114.6 (d, $J = 17.6$ Hz), 72.8 (d, $J = 1.9$ Hz), 70.3, 64.0, 58.9, 48.9, 26.9, 19.4 (Both phenyl groups on TBDPS were observed, one carbon on 4-fluorobenzyl ether ring was not observed.); m/z (ESI/MS) calculated 473.2 ($\text{C}_{27}\text{H}_{31}\text{FNaO}_3\text{Si}$), observed 473.2 ($\text{M}+\text{Na}$) $^+$.



Epoxide opening: In a flame dried 500 mL round-bottomed flask, $\text{CuBr}\cdot\text{Me}_2\text{S}$ (9.81 g, 47.5 mmol) was dispersed in dry Et_2O (100 mL), to which 10 mL Me_2S was added. The resultant dark solution was then cooled down to -40°C . To this, vinyl magnesium bromide 1.0 M in THF (119 mL, 109 mmol) was added. After 20 min, the suspension was cooled down to -75°C . To this, epoxide **2.217** (5.36 g, 11.9 mmol), dissolved in dry Et_2O (50 mL), was added in slowly. The black suspension was then warmed up to -20°C over 20 min. The reaction was then quenched by 50 mL NH_4Cl (aq) and filtered through a short pad of celite. The filtrate was partitioned against diethyl ether (3x80 mL). The organic fractions were combined, washed with satd. NaCl (aq) (100 mL), dried over Na_2SO_4 , filtered, concentrated in vacuo, and used for the next step directly.

Olefin **2.213**: In a 250 mL round-bottomed flask, the above crude material was azeotroped with toluene (3x50 mL), dissolved in dry DCM (120 mL) and cooled down to -20°C , to which 2,6-lutidine (8.3 mL, 71.3 mmol) and TESOTf (3.5 mL, 15.4 mmol) were added. The reaction was then warmed up to room temperature over 1 h. To this, 1 mL methanol was added. The

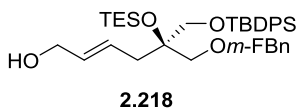
reaction was then concentrated in vacuo, and purified by FCC (1% ethyl acetate/hexane) to give **2.213** (6.69 g, 95% two steps) as a light yellow liquid (R_f = 0.80 9% ethyl acetate/hexane). $[\alpha]_D^{23}$ 37.8 (c = 0.50, CHCl_3); IR $\nu_{\text{max}}(\text{neat})/\text{cm}^{-1}$ 3072, 2956, 2876, 1640, 1618, 1592, 1415, 1258, 823, 738, 505; ^1H NMR (500 MHz, CDCl_3) δ 7.67 – 7.62 (4H, m), 7.42 – 7.36 (2H, m), 7.35 – 7.23 (5H, m), 7.07 – 6.92 (3H, m), 5.86 (1H, ddt, J = 17.3, 10.3, 7.1 Hz), 5.10 – 4.99 (2H, m), 4.46 (2H, s), 3.66 (1H, d, J = 9.5 Hz), 3.53 (1H, d, J = 9.4 Hz), 3.47 (1H, d, J = 3.4 Hz), 3.45 (1H, d, J = 3.7 Hz), 2.38 (2H, d, J = 7.4), 1.04 (9H, s), 0.85 (9H, t, J = 7.9 Hz), 0.51 (6H, q, J = 8.1 Hz); ^{13}C NMR (126 MHz, CDCl_3) δ 163.0 (d, J = 245.4 Hz), 141.2 (d, J = 7.3 Hz), 135.8 (2), 134.2, 133.6 (2), 129.8 (d, J = 8.3 Hz), 129.7, 127.7 (2), 123.1 (d, J = 2.9 Hz), 117.5, 114.5 (d, J = 21.7 Hz), 114.3 (d, J = 21.3 Hz), 77.8, 74.2, 72.8 (d, J = 2.0 Hz), 66.6, 40.5, 27.0, 19.4, 7.2, 6.8 (Both phenyl groups in TBDPS were observed.); m/z (ESI/MS) calculated 615.3 ($\text{C}_{35}\text{H}_{49}\text{FNaO}_3\text{Si}_2$), observed 615.3 ($\text{M}+\text{Na}$) $^+$.



Oxidative cleavage of olefin **2.213**: In a 100 mL round-bottomed flask, olefin **2.213** (3.09 g, 5.21 mmol) was dissolved in 40 mL 1,4-dioxane, to which 2,6-lutidine (1.20 mL, 10.4 mmol), sodium periodate (4.46 g in 13.5 mL water, 20.9 mmol), $\text{K}_2\text{OsO}_2(\text{OH})_4$ (7.7 mg, .021 mmol) were added. After 4.5 h, the reaction was filtered, quenched by 50 mL $\text{Na}_2\text{S}_2\text{O}_3$ (aq.) and partitioned against ethyl acetate (3x80 mL). The organic fractions were combined, dried over Na_2SO_4 , filtered, concentrated in vacuo, and used for the next step directly.

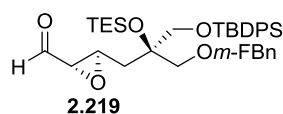
Ester **4.10**: In a 50 mL round-bottomed flask, the above crude material was azeotroped with toluene (3x10 mL) and dissolved in dry DCM (26 mL), to which $\text{Ph}_3\text{PCHCO}_2\text{Et}$ (4.54 g, 13.0

mmol) was added. After 17.5 h, the reaction was concentrated in vacuo, and purified by FCC (5% ethyl acetate/hexane) to give **4.10** (3.10 g, 89% two steps) as a colorless oil ($R_f = 0.55$ 9% ethyl acetate/hexane). $[\alpha]_D^{23} 42.8$ ($c = 0.44$, CHCl_3); IR $\nu_{\text{max}}(\text{neat})/\text{cm}^{-1}$ 3072, 2957, 2876, 1718, 1655, 1618, 1592, 1451, 1258, 823, 738, 506; ^1H NMR (500 MHz, CDCl_3) δ 7.66 – 7.60 (4H, m), 7.44 – 7.38 (2H, m), 7.37 – 7.24 (5H, m), 7.11 – 6.95 (4H, m), 5.86 (1H, d, $J = 15.7$ Hz), 4.47 (2H, s), 4.19 (2H, q, $J = 7.1$ Hz), 3.67 (1H, d, $J = 9.7$ Hz), 3.52 (1H, d, $J = 9.3$ Hz), 3.47 (1H, d, $J = 9.4$ Hz), 3.43 (1H, d, $J = 9.7$ Hz), 2.52 (2H, d, $J = 7.5$ Hz), 1.29 (3H, t, $J = 7.1$ Hz), 1.05 (9H, s), 0.86 (9H, t, $J = 7.9$ Hz), 0.52 (6H, q, $J = 7.8$ Hz); ^{13}C NMR (126 MHz, CDCl_3) δ 166.5, 163.1 (d, $J = 245.9$ Hz), 145.2, 140.9 (d, $J = 7.2$ Hz), 135.9 (2), 133.3 (2), 130.0, 129.9, 127.9, 127.8, 124.1, 123.2 (d, $J = 2.9$ Hz), 114.7 (d, $J = 11.5$ Hz), 114.5 (d, $J = 11.0$ Hz), 77.9, 74.2, 72.9 (d, $J = 1.9$ Hz), 66.7, 60.3, 38.9, 27.1, 19.4, 14.5, 7.3, 6.7 (Both phenyl groups in TBDPS were observed.); m/z (ESI/MS) calculated 687.3 ($\text{C}_{38}\text{H}_{53}\text{FNaO}_5\text{Si}_2$), observed 687.3 ($\text{M}+\text{Na}$) $^+$.



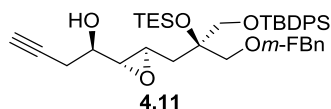
Allylic alcohol **2.218**: In a 100 mL round-bottomed flask, ester **2.218** (3.05 g, 4.59 mmol) was azeotroped with toluene (3x20 mL), dissolved in dry DCM (54 mL), and cooled to -78°C , to which 1.0 M DIBAL-H in hexane (9.2 mL, 9.2 mmol) was added slowly. After 50 min, the reaction was quenched by 50 mL saturated Rochelle salt solution and partitioned against dichloromethane (3x50 mL). The organic fractions were combined, dried over Na_2SO_4 , filtered, concentrated in vacuo, and purified by FCC (10% ethyl acetate/hexane) to give **2.218** (2.73 g, 96%) as a colorless oil $[\alpha]_D^{23} 2.7$ ($c = 0.42$, CHCl_3); IR $\nu_{\text{max}}(\text{neat})/\text{cm}^{-1}$ 3355, 3071, 2956, 2876, 1695, 1591, 1428, 1256, 824, 738, 504; ^1H NMR (500 MHz, CDCl_3) δ 7.68 –

7.61 (4H, m), 7.45 – 7.38 (2H, m), 7.38 – 7.25 (5H, m), 7.09 – 6.95 (3H, m), 5.76 – 5.61 (2H, m), 4.49 (2H, s), 4.03 (2H, d, $J = 5.2$ Hz), 3.55 (2H, dd, $J = 118.3, 9.5$ Hz), 3.52 (2H, dd, $J = 40.4, 9.3$ Hz), 2.37 (2H, dd, $J = 6.7, 3.7$ Hz), 1.06 (9H, s), 0.87 (9H, t, $J = 7.9$ Hz), 0.53 (6H, q, $J = 8.0$ Hz); ^{13}C NMR (126 MHz, CDCl_3) δ 163.0 (d, $J = 245.7$ Hz), 141.1 (d, $J = 7.2$ Hz), 135.8 (2), 133.5 (2), 132.1, 129.9, 129.8 (2), 128.4, 127.7 (2), 123.1 (d, $J = 2.8$ Hz), 114.5 (d, $J = 17.6$ Hz), 114.4 (d, $J = 17.1$ Hz), 77.9, 74.2, 72.8 (d, $J = 1.9$ Hz), 66.3, 64.0, 38.6, 27.0, 19.4, 7.2, 6.7 (Both phenyl groups in TBDPS were observed.); m/z (ESI/MS) calculated 645.3 ($\text{C}_{36}\text{H}_{51}\text{FNaO}_4\text{Si}_2$), observed 645.3 ($\text{M}+\text{Na}$) $^+$.



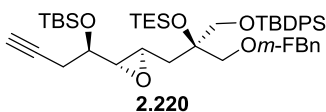
Epoxidation of allylic alcohol **2.218**: In a 250 mL round-bottomed flask, allylic alcohol **2.219** (3.41 g, 5.47 mmol), (*D*)-fructose derived Shi catalyst (1.41 g, 5.47 mmol), and tetrabutylammonium hydrogensulfate (372 mg, 1.10 mmol) were dispensed in a mixture of sodiumtetraborate buffer (0.05 M in 0.4 mM Na_2EDTA water solution, 55 mL) and CH_3CN (82 mL). Under vigorous stirring, Oxone[®] (130 g/L in 0.4 mM Na_2EDTA water solution, 35.6 mL) and K_2CO_3 (0.89 M water solution, 35.6 mL) were added over 1 h 45 min via a syringe pump. The internal temperature of the reaction was maintained at -2°C . After 15 min, the reaction mixture was partitioned against diethyl ether (3x100 mL). The organic fractions were combined, dried over Na_2SO_4 , filtered, concentrated in vacuo, and purified by FCC (20% ethyl acetate/hexane) to give a mixture of the epoxy alcohol and (*D*)-Shi catalyst as a colorless oil ($R_f = 0.35$ 20% ethyl acetate/hexane, 8:1 d.r.), which was used directly for the next steps.

Epoxy aldehyde **2.219**: In a 250 mL round-bottomed flask, the above mixture was azeotroped with toluene (3x20 mL), dissolved in dry DCM (40 mL), and cooled down to 0°C. To this, pyridine (1.44 g, 18.2 mmol) and Dess-Martin periodinane (3.85 g in 40 mL DCM, 9.08 mmol) were added. Then the cooling bath was removed. After 2.5 h, the reaction was quenched by Na₂S₂O₃ (40 mL in satd. NaHCO₃ solution) and partitioned against dichloromethane (3x40 mL). The organic fractions were combined, dried over Na₂SO₄, filtered, concentrated in vacuo, and purified by FCC (10% ethyl acetate/hexane) to give **2.219** (2.52 g, 87% two steps) as a colorless oil (*R*_f = 0.60 20% ethyl acetate/hexane). ¹H NMR (500 MHz, CDCl₃) δ 8.93 (1H, d, *J* = 6.4 Hz), 7.68 – 7.60 (4H, m), 7.46 – 7.40 (2H, m), 7.39 – 7.26 (5H, m), 7.07– 6.95 (3H, m), 4.52 – 4.40 (2H, m), 3.74 (1H, d, *J* = 9.9 Hz), 3.58 (1H, d, *J* = 9.9 Hz), 3.50 (2H, s), 3.38 (1H, td, *J* = 5.7, 2.0 Hz), 3.11 (1H, dd, *J* = 6.4, 2.0 Hz), 2.00 (1H, dd, *J* = 14.3, 6.0 Hz), 1.88 (1H, td, *J* = 14.6, 5.5 Hz), 1.06 (9H, s), 0.85 (9H, t, *J* = 7.9 Hz), 0.52 (6H, q, *J* = 7.9 Hz); ¹³C NMR (126 MHz, CDCl₃) δ 198.6, 163.0 (d, *J* = 245.8 Hz), 140.6 (d, *J* = 7.3 Hz), 135.8 (2), 133.2, 133.1, 130.0 (2), 129.9 (d, *J* = 8.1 Hz), 127.8 (2), 123.2 (d, *J* = 3.0 Hz), 114.7 (d, *J* = 4.0 Hz), 114.5 (d, *J* = 3.5 Hz), 77.3, 74.2, 72.9 (d, *J* = 1.9 Hz), 66.8, 59.2, 53.5, 37.6, 27.0, 19.4, 7.2, 6.6 (Both phenyl groups in TBDPS were observed.); *m/z* (ESI/MS) calculated 659.3 (C₃₆H₄₉FO₅Si₂), observed 659.3 (M+Na)⁺.



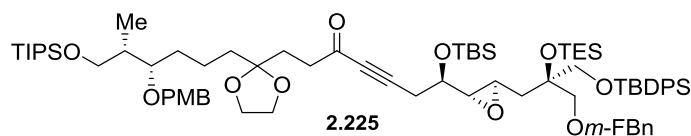
Alkyne **4.11**: Alkyne **4.11** was prepared using the same procedure as described above for the synthesis of alkyne **4.8**. The product was obtained as a colorless oil in 84% yield [α]_D²³ 30.0 (*c* = 0.50, CHCl₃); IR ν_{max} (neat)/cm⁻¹ 3455, 3310, 3072, 2956, 1618, 1591, 1428, 1258, 823,

739, 506; ^1H NMR (400 MHz, CDCl_3) δ 7.71 – 7.63 (4H, m), 7.46 – 7.38 (2H, m), 7.38 – 7.25 (5H, m), 7.09 – 6.96 (3H, m), 4.56 – 4.45 (2H, m), 3.84 – 3.73 (2H, m), 3.66 – 3.57 (3H, m), 3.24 (1H, td, J = 5.9, 2.3 Hz), 2.90 (1H, dd, J = 4.3, 2.2 Hz), 2.47 (2H, ddd, J = 5.9, 5.1, 2.7 Hz), 2.16 (1H, d, J = 3.5 Hz), 2.03 (1H, t, J = 2.7 Hz), 1.95 (1H, dd, J = 14.2, 5.9 Hz), 1.85 (1H, dd, J = 14.3, 5.8 Hz), 1.07 (9H, s), 0.94 – 0.84 (9H, m), 0.61 – 0.50 (6H, m); ^{13}C NMR (126 MHz, CDCl_3) δ 163.0 (d, J = 245.9 Hz), 140.8 (d, J = 7.1 Hz), 135.9, 135.8, 133.4, 133.3, 129.9 (d, J = 8.2 Hz), 129.8 (2), 127.7 (2), 123.1 (d, J = 2.9 Hz), 114.6 (d, J = 9.7 Hz), 114.4 (d, J = 9.1 Hz), 79.8, 77.6, 74.1, 72.8 (d, J = 2.0 Hz), 71.1, 68.3, 67.2, 59.5, 52.6, 38.3, 27.0, 24.0, 19.4, 7.2, 6.7 (Both phenyl groups in TBDPS were observed.); m/z (ESI/MS) calculated 699.3 ($\text{C}_{39}\text{H}_{53}\text{FNaO}_5\text{Si}_2$), observed 699.3 ($\text{M}+\text{Na}$) $^+$.

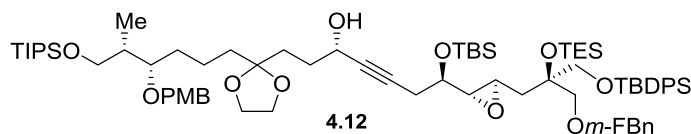


Alkyne **2.220**: In a 100 mL round-bottomed flask, alkyne **4.11** (2.05 g, 3.03 mmol) was azeotroped with toluene (3x10 mL), dissolved in dry DCM (55 mL), and cooled down to -78°C, to which 2,6-lutidine (1.06 mL, 9.09 mmol) and TBSOTf (1.04 mL, 4.55 mmol) were added. The reaction was then slowly warmed up over 40 min, before it was cooled back to -78°C. To this, 30 mL *satd.* NaHCO_3 (aq.) was added. The reaction mixture was partitioned against dichloromethane (3x50 mL). The organic fractions were combined, dried over Na_2SO_4 , filtered, concentrated in vacuo, and purified by FCC (2% ethyl acetate/hexane) to give **2.220** (2.20 g, 92%) as a colorless oil (R_f = 0.80 10% ethyl acetate/hexane). $[\alpha]_D^{23}$ -7.6 (c = 0.43, CHCl_3); IR ν_{max} (neat)/ cm^{-1} 3643, 3312, 3072, 2956, 1618, 1592, 1428, 1256, 837, 741, 505; ^1H NMR (500 MHz, CDCl_3) δ 7.70 – 7.61 (4H, m), 7.46 – 7.36 (2H, m), 7.35 – 7.23 (5H, m),

7.06 – 6.94 (3H, m), 4.48 (2H, q, $J = 12.0$ Hz), 3.82 – 3.72 (2H, m), 3.63 (1H, d, $J = 9.7$ Hz), 3.60 – 3.53 (2H, m), 3.22 – 3.16 (1H, m), 2.84 – 2.80 (1H, m), 2.43 – 2.35 (2H, m), 1.97 – 1.94 (1H, m), 1.91 (1H, dd, $J = 14.3, 4.6$ Hz), 1.78 (1H, dd, $J = 14.3, 6.8$ Hz), 1.04 (9H, s), 0.95 – 0.75 (18H, m), 0.54 (6H, q, $J = 7.9$ Hz), 0.06 (6H, d, $J = 16.7$ Hz); ^{13}C NMR (126 MHz, CDCl_3) δ 163.0 (d, $J = 245.8$ Hz), 140.8 (d, $J = 7.2$ Hz), 135.9, 135.8, 133.5 (2), 129.8 (d, $J = 8.0$ Hz), 129.7, 127.7, 123.1 (d, $J = 2.9$ Hz), 114.5 (d, $J = 13.7$ Hz), 114.4 (d, $J = 13.3$ Hz), 80.9, 77.7, 74.1, 72.7 (d, $J = 1.9$ Hz), 70.5, 69.8, 67.0, 59.6, 52.2, 38.4, 27.0, 25.9, 25.4, 19.4, 18.3, 7.3, 6.7, -4.4, -4.8 (Both phenyl groups in TBDPS were observed, both methyl groups in TBS were observed.); m/z (ESI/MS) calculated 813.4 ($\text{C}_{45}\text{H}_{67}\text{FNaO}_5\text{Si}_3$), observed 813.4 ($\text{M}+\text{Na}$) $^+$.

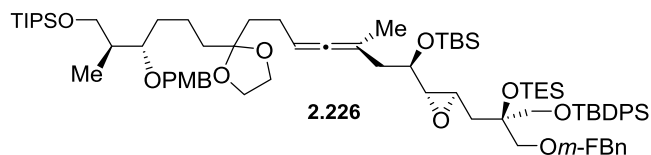


Alkynone 2.225: Alkynone **2.225** was prepared using the same procedure as described above for the synthesis of alkynone **2.210**. The product was obtained as a colorless oil in 71% yield oil ($R_f = 0.60$ 20% ethyl acetate/hexane) and used for the next step.



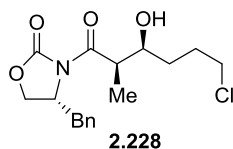
Propargyl alcohol 4.12: Propargyl alcohol **4.12** was prepared using the same procedure as described above for the synthesis of propargyl alcohol **4.9**. The product was obtained as a colorless thick oil in 92% yield ($R_f = 0.50$ 20% ethyl acetate/hexane). $[\alpha]_D^{23} -9.0$ ($c = 0.44$, CHCl_3); IR ν_{max} (neat)/ cm^{-1} 3447, 3072, 2956, 2865, 2219, 1676, 1615, 1591, 1464, 1250, 835,

741, 506; ^1H NMR (500 MHz, CDCl_3) δ 7.73 – 7.64 (4H, m), 7.45 – 7.24 (9H, m), 7.08 – 6.95 (3H, m), 6.92 – 6.85 (2H, m), 4.56 – 4.43 (4H, m), 4.40 – 4.33 (1H, m), 4.00 – 3.87 (4H, m), 3.81 (3H, s), 3.80 – 3.53 (7H, m), 3.49 – 3.40 (1H, m), 3.20 (1H, ddd, J = 6.8, 4.2, 2.1 Hz), 2.81 (1H, dd, J = 4.0, 2.1 Hz), 2.50 – 2.39 (3H, m), 1.95 (1H, dd, J = 14.4, 4.3 Hz), 1.92 – 1.73 (6H, m), 1.70 – 1.32 (6H, m), 1.11 – 1.04 (30H, m), 0.97 – 0.84 (21H, m), 0.56 (6H, q, J = 8.0 Hz), 0.09 (6H, d, J = 19.4 Hz); ^{13}C NMR (126 MHz, CDCl_3) δ 163.0 (d, J = 245.8 Hz), 159.1, 140.9 (d, J = 7.2 Hz), 135.9, 135.8, 133.5, 133.4, 131.6, 129.8 (d, J = 8.2 Hz), 129.7, 129.4, 127.7, 123.0 (d, J = 2.8 Hz), 114.5 (d, J = 11.6 Hz), 114.3 (d, J = 11.0 Hz), 113.8, 111.5, 83.2, 81.7, 79.2, 77.7, 74.2, 72.7 (d, J = 1.8 Hz), 72.1, 70.2, 67.0, 65.7, 65.1, 62.6, 59.5, 55.3, 52.1, 39.5, 38.4, 37.4, 32.8, 32.3, 31.8, 27.0, 25.9, 25.7, 20.5, 19.4, 18.3, 18.2, 12.1, 11.7, 7.2, 6.7, -4.4, -4.7 (Both phenyl groups in TBDPS were observed, both methyl groups in TBS were observed.); m/z (ESI/MS) calculated 1349.8 ($\text{C}_{75}\text{H}_{119}\text{FNaO}_{11}\text{Si}_4$), observed 1349.8 ($\text{M}+\text{Na}$) $^+$



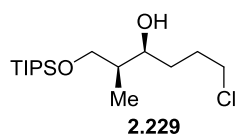
Allene 2.226: Allene **2.226** was prepared using the same procedure as described above for the synthesis of allene **2.211**. The product was obtained as a colorless oil in 87% yield (R_f = 0.75 20% ethyl acetate/hexane). $[\alpha]_D^{23}$ 5.5 (c = 0.33, CHCl_3); IR ν_{max} (neat)/ cm^{-1} 3072, 2956, 2865, 1964, 1615, 1591, 1514, 1428, 1250, 836, 741, 703; ^1H NMR (500 MHz, CDCl_3) δ 7.76 – 7.67 (4H, m), 7.46 – 7.26 (9H, m), 7.10 – 6.96 (3H, m), 6.89 (2H, d, J = 8.3 Hz), 5.12 – 5.03 (1H, m), 4.57 – 4.47 (4H, m), 3.98 – 3.90 (4H, m), 3.87 (1H, td, J = 6.4, 3.3 Hz), 3.81 (3H, s), 3.79 – 3.55 (7H, m), 3.24 (1H, td, J = 4.1, 1.9 Hz), 2.74 (1H, dd, J = 3.6, 2.0 Hz), 2.29 (1H, ddd, J = 14.4, 6.3, 2.6 Hz), 2.16 (1H, ddd, J = 14.2, 6.5, 2.0 Hz), 2.13 – 2.04 (2H, m), 2.00 (1H, ddd, J =

12.0, 7.7, 4.3 Hz), 1.85 – 1.94 (2H, m), 1.82 – 1.34 (11H, m), 1.13 – 1.07 (30H, m), 0.98 – 0.88 (21H, m), 0.59 (6H, q, $J = 7.9$ Hz), 0.08 (6H, d, $J = 7.1$ Hz); ^{13}C NMR (126 MHz, CDCl_3) δ 202.3, 163.0 (d, $J = 245.7$ Hz), 159.1, 141.0 (d, $J = 7.1$ Hz), 135.9, 135.8, 133.5 (2), 131.6, 129.8 (d, $J = 8.1$ Hz), 129.7, 129.4, 127.7, 123.0 (d, $J = 2.9$ Hz), 114.5 (d, $J = 16.6$ Hz), 114.3 (d, $J = 16.0$ Hz), 113.8, 111.5, 96.2, 90.2, 79.2, 74.2, 72.8 (d, $J = 1.9$ Hz), 72.1, 69.7, 66.9, 65.7, 65.1, 65.1, 60.2, 55.3, 51.4, 40.3, 39.5, 38.6, 37.6, 37.2, 31.9, 27.0, 26.0, 23.8, 20.4, 20.2, 19.4, 18.3, 18.2, 12.1, 11.6, 7.2, 6.7, -4.4, -4.8 (Both phenyl groups in TBDPS were observed, both methyl groups in TBS were observed.); m/z (ESI/MS) calculated 1347.8 ($\text{C}_{76}\text{H}_{121}\text{FNaO}_{10}\text{Si}_4$), observed 1347.8 ($\text{M}+\text{Na}$) $^+$.



Chlorohydrin **2.228**: In a flame dried 50 mL round-bottomed flask, functionalized oxazolidinone **2.197** (238 mg, 1.02 mmol) was azeotroped with toluene (3x10 mL), dissolved in 8 mL dry DCM, and cooled down to -5°C , to which dibutylboryl trifluoromethanesulfonate 1.0 M in DCM (1.10 mL, 1.10 mmol) was added. After 3 min, triethylamine (163 μL , 1.22 mmol) was added in slowly to give a colorless solution. The reaction was kept at 0°C for 1 h before cooled down to -78°C . To this, 4-chlorobutanol (163 mg in 2 mL dry DCM, 1.53 mmol) was added slowly over 15 min. After 3 h, the reaction was warmed to 0°C and kept for 0.5 h. To this, a cold solution of methanol (1 mL) and aqueous buffer (pH = 7.4, 3 mL) were added. After 5 min, a cold solution of hydrogen peroxide (30 wt.%, 1 mL) and methanol (2 mL) were added in. The reaction mixture was then partitioned against dichloromethane (3x20 mL). The organic fractions were combined, washed

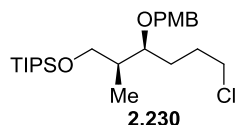
with satd. NaCl (aq) (60 mL), dried over Na₂SO₄, filtered, concentrated in vacuo, and purified by FCC (30% ethyl acetate/hexane) to give **2.228** (318 mg, 92%) as a colorless viscous liquid (R_f = 0.25 30% ethyl acetate/hexane). $[\alpha]_D^{23}$ -45.2 (c = 0.40, CHCl₃); IR ν_{\max} (neat)/cm⁻¹ 3527, 3029, 2959, 2871, 1779, 1695, 1604, 1456, 1212, 763, 648; ¹H NMR (500 MHz, CDCl₃) δ 7.37 – 7.24 (3H, m), 7.23 – 7.16 (2H, m), 4.71 (1H, ddt, J = 9.2, 7.6, 3.2 Hz), 4.27 – 4.13 (2H, m), 4.00 – 3.92 (1H, m), 3.76 (1H, qd, J = 7.1, 2.9 Hz), 3.65 – 3.49 (2H, m), 3.23 (1H, dd, J = 13.5, 3.4 Hz), 3.01 (1H, s), 2.80 (1H, dd, J = 13.5, 9.3 Hz), 2.07 – 1.95 (1H, m), 1.90 – 1.76 (2H, m), 1.71 – 1.53 (2H, m), 1.27 (3H, d, J = 7.0 Hz); ¹³C NMR (126 MHz, CDCl₃) δ 177.3, 153.1, 135.0, 129.5, 129.0, 127.5, 70.9, 66.3, 55.1, 45.1, 42.4, 37.8, 31.2, 29.3, 10.7; m/z (ESI/MS) calculated 362.1 (C₁₇H₂₂ClNNaO₄), observed 362.1 (M+Na)⁺.



Reduction of 2.228: In a 25 mL round-bottomed flask, chlorohydrins **2.229** (340 mg, 1.00 mmol) was dissolved in 5 mL THF and cooled to 0°C, to which LiBH₄ (44 mg, 2.00 mmol) and methanol (0.1 mL) were added. After 1 h, the reaction was quenched by addition of NH₄Cl (aq.) (10 mL). The reaction mixture was then partitioned against dichloromethane (3x40 mL). The organic fractions were combined, dried over Na₂SO₄, filtered, and concentrated in vacuo to give a crude mixture which was used directly for the next step.

Chlorohydrin 2.229: In a 25 mL round-bottomed flask, the above crude mixture, azeotroped with toluene (3x5 mL), was dissolved in 5 mL dry DMF and cooled down to 0°C, to which triethylamine (303 mg, 3.00 mmol), 4-dimethylaminopyridine (7.0 mg, 0.10 mmol) and TIPSCI (289 mg, 1.50 mmol) were added in. After 20 h, the reaction was diluted with satd.

NaCl (aq) (25 mL) and partitioned against a 1:1 mixture of ethyl acetate and hexane (3x30 mL). The organic fractions were combined, washed with satd. NaCl (aq) (20 mL), dried over Na₂SO₄, filtered, concentrated, and purified by FCC (2% ethyl acetate/hexane. Crude material was diluted with a small amount of hexane before loading to the column to minimize cyclization.) to give **2.229** (167 mg, 52%) as a light yellow liquid (*R*_f = 0.95 50% ethyl acetate/hexane). [α]_D²³ -7.9 (*c* = 0.50, CHCl₃); IR ν_{max} (neat)/cm⁻¹ 3447, 2940, 2867, 1464, 1384, 1249, 1100, 1014, 883, 787, 681; ¹H NMR (500 MHz, CDCl₃) δ 3.85 (1H, dd, *J* = 9.8, 3.8 Hz), 3.83 – 3.74 (2H, m), 3.66 – 3.51 (2H, m), 3.30 (1H, s), 2.06 – 1.95 (1H, m), 1.86 – 1.73 (2H, m), 1.64 – 1.52 (2H, m), 1.06 (21H, s), 0.93 (3H, d, *J* = 7.1 Hz); ¹³C NMR (126 MHz, CDCl₃) δ 74.5, 68.9, 45.4, 39.3, 31.3, 29.6, 18.0, 11.9, 10.7; *m/z* (ESI/MS) calculated 323.2 (C₁₆H₃₆ClO₂Si), observed 323.2 (M+H)⁺.

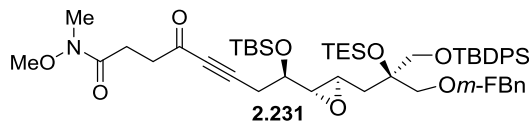


Protection of chlorohydrin **2.228**: In a 50 mL round-bottomed flask, chlorohydrin **2.228** (804 mg, 2.36 mmol) was dissolved in 20 mL toluene, to which PMB trichloroacetimidate (936 mg, 3.31 mmol) and La(OTf)₃ (69 mg, 0.118 mmol) were added. After 14 h, the reaction mixture was concentrated in vacuo, and purified by FCC (15% ethyl acetate/hexane) to give the impure PMB ether 1.54 g as a white solid.

Reduction to diol: In a 100 mL round-bottomed flask, the above impure product was dissolved in 25 mL Et₂O and cooled down to 0°C, to which LiBH₄ (110 mg, 5.05 mmol) and methanol (0.5 mL) were added. After 20 min, the reaction was quenched by slow addition of NH₄Cl (aq.) (10 mL). The reaction mixture was then partitioned against diethyl ether (4x50

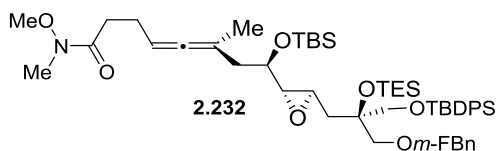
mL). The organic fractions were combined, washed with satd. NaCl (aq) (50 mL), dried over Na₂SO₄, filtered, and concentrated in vacuo to give a crude mixture which was used directly for the next step.

Alkyl chloride 2.230: In a 50 mL round-bottomed flask, the above crude mixture, azeotroped with toluene (3x10 mL), was dissolved in 15 mL dry DMF and cooled down to 0°C, to which imidazole (500 mg, 7.34 mmol), 4-dimethylaminopyridine (28 mg, 0.229 mmol) and TIPSCI (690 mg, 3.58 mmol) were added in. After 20 h, satd. NaCl (aq) (10 mL) and water (50 mL) were added in. The reaction mixture was partitioned against diethyl ether (4x75 mL). The organic fractions were combined, washed with satd. NaCl (aq) (50 mL), dried over Na₂SO₄, filtered, concentrated, and purified by FCC (2% ethyl acetate/hexane) to give **2.230** (826 mg, 78% three steps) as a colorless liquid (*R*_f = 0.80 10% ethyl acetate/hexane). [α]_D²³ -1.8 (*c* = 0.45, CHCl₃); IR ν_{max} (neat)/cm⁻¹ 2940, 2866, 1613, 1587, 1514, 1464, 1301, 1249, 1108, 827, 821, 682; ¹H NMR (500 MHz, CDCl₃) δ 7.26 (2H, d, *J* = 7.1 Hz), 6.88 (2H, d, *J* = 8.7 Hz), 4.49 (2H, dd, *J* = 18.6 Hz, *J* = 11.1 Hz), 3.81 (3H, s), 3.72 (1H, dd, *J* = 9.7, 6.6 Hz), 3.62 – 3.47 (4H, m), 1.94 – 1.83 (2H, m), 1.83 – 1.72 (1H, m), 1.70 – 1.63 (2H, m), 1.12 – 1.04 (21H, m), 0.95 (3H, d, *J* = 6.9 Hz); ¹³C NMR (126 MHz, CDCl₃) δ 159.2, 131.3, 129.5, 113.9, 78.8, 72.1, 65.5, 55.4, 45.4, 39.6, 29.4, 29.0, 18.2, 12.1, 12.0; *m/z* (ESI/MS) calculated 465.3 (C₂₄H₄₃ClNaO₃Si), observed 465.3 (M+Na)⁺.

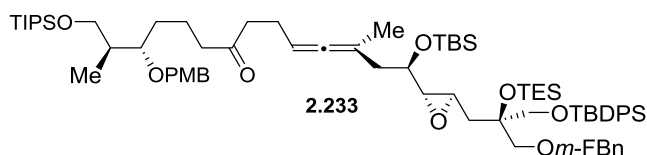


Alkynone 2.231: In a flame dried 25 mL round-bottomed flask, alkyne 2.220 (940 mg, 1.19 mmol) was dissolved in 7 mL dry THF and cooled down to -20°C. To this, 2.0 M

isopropylmagnesium chloride solution in THF (0.65 mL, 1.30 mmol) was added. The reaction was then kept at room temperature for 30 min before it was used for the next step. In another flame dried 25 mL round-bottomed flask, bis-Winreb amide **2.234** (727 mg, 3.56 mmol) was dissolved in 5 mL dry THF and cooled down to -20°C. (Lower temperature will cause compound to precipitate out from solution.) To this, the above alkynide solution was added in. The reaction mixture was slowly warmed to room temperature over 3 h. After 15 h, the reaction was quenched by 6 mL NH₄Cl (aq.), diluted with 50 mL water, and partitioned against ethyl acetate (3x100 mL). The organic fractions were combined, dried over Na₂SO₄, filtered, concentrated in vacuo, and purified by FCC (40% ethyl acetate/hexane) to give **2.231** (785 mg, 71%) as a colorless oil (*R*_f = 0.60 40% ethyl acetate/hexane). [α]_D²³ -36.0 (*c* = 1.3, CHCl₃); IR ν_{max} (neat)/cm⁻¹ 3072, 2924, 2856, 2217, 1790, 1724, 1592, 1463, 1378, 1258, 1129, 837, 741; ¹H NMR (500 MHz, CDCl₃) δ 7.62 – 7.71 (4H, m), 7.45 – 7.25 (7H, m), 7.07 – 6.94 (3H, m), 4.55 – 4.43 (2H, m), 3.82 – 3.67 (5H, m), 3.70 – 3.60 (1H, m), 3.60 – 3.51 (2H, m), 3.22 – 3.11 (4H, m), 2.96 – 2.87 (2H, m), 2.80 – 2.71 (3H, m), 2.58 (2H, d, *J* = 5.9 Hz), 1.97 (1H, dd, *J* = 14.4, 4.0 Hz), 1.75 (1H, dd, *J* = 14.4, 7.3 Hz), 1.06 (9H, s), 0.93 – 0.82 (18H, m), 0.55 (6H, q, *J* = 7.9 Hz), 0.09 (6H, d, *J* = 21.3 Hz); ¹³C NMR (126 MHz, CDCl₃) δ 186.0, 162.9 (d, *J* = 245.7 Hz), 140.8 (d, *J* = 7.2 Hz), 135.9, 135.8, 133.4 (2), 129.8 (d, *J* = 8.3 Hz), 129.7, 127.7 (2), 123.1 (d, *J* = 2.9 Hz), 114.5 (d, *J* = 12.5 Hz), 114.4 (d, *J* = 12.0 Hz), 90.6, 82.1, 77.6, 74.2, 72.7 (d, *J* = 1.8 Hz), 69.9, 66.9, 61.3, 59.2, 52.7, 39.8, 38.3, 32.3, 27.0, 26.1, 26.0, 25.8, 19.3, 18.2, 7.2, 6.7, -4.4, -4.8 (Winreb amide carbon was not observed, both phenyl groups in TBDPS were observed, both methyl groups in TBS were observed.); *m/z* (ESI/MS) calculated 956.5 (C₅₁H₇₆FNNaO₈Si₃), observed 956.5 (M+Na)⁺.

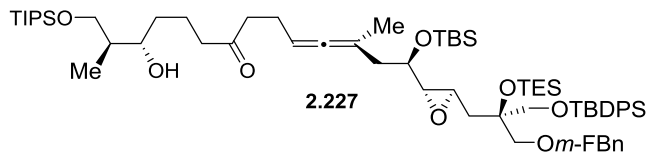


Winreb amide **2.232**: Winreb amide **2.232** was prepared using the same procedure as described above for the synthesis of allene **2.211**. The product was obtained as a colorless oil in two steps 78% yield from alkynone **2.231** ($R_f = 0.25$ 25% ethyl acetate/hexane). $[\alpha]_D^{23}$ 13.5 ($c = 0.47$, CHCl_3); IR $\nu_{\text{max}}(\text{neat})/\text{cm}^{-1}$ 3072, 2956, 2857, 1965, 1671, 1618, 1592, 1428, 1255, 835, 741, 506; ^1H NMR (500 MHz, CDCl_3) δ 7.72 – 7.61 (4H, m), 7.46 – 7.23 (7H, m), 7.08 – 6.94 (3H, m), 5.16 – 5.08 (1H, m), 4.54 – 4.44 (2H, m), 3.85 – 3.75 (2H, m), 3.71 – 3.60 (4H, m), 3.63 – 3.55 (2H, m), 3.23 – 3.15 (4H, m), 2.70 (1H, dd, $J = 3.7, 2.2$ Hz), 2.57 – 2.45 (2H, m), 2.36 – 2.27 (2H, m), 2.24 (1H, ddd, $J = 14.3, 6.3, 2.7$ Hz), 2.12 (1H, ddd, $J = 14.4, 6.4, 2.3$ Hz), 1.96 (1H, ddd, $J = 11.7, 7.7, 4.0$ Hz), 1.76 – 1.68 (4H, m), 1.05 (9H, s), 0.91 – 0.84 (18H, m), 0.55 (6H, q, $J = 7.9$ Hz), 0.04 (6H, d, $J = 6.5$ Hz); ^{13}C NMR (126 MHz, CDCl_3) δ 202.4, 163.0 (d, $J = 245.7$ Hz), 141.0 (d, $J = 7.2$ Hz), 135.9, 135.8, 133.5 (2), 129.8 (d, $J = 8.2$ Hz), 129.7, 127.7, 123.1 (d, $J = 2.8$ Hz), 114.5 (d, $J = 13.5$ Hz), 114.3 (d, $J = 12.9$ Hz), 97.0, 89.7, 77.8, 74.3, 72.8 (d, $J = 1.9$ Hz), 70.0, 66.9, 61.3, 60.2, 51.6, 40.2, 38.6, 31.6, 27.0, 26.2, 25.9, 24.2, 20.3, 19.4, 18.3, 7.2, 6.7, -4.3, -4.8 (Winreb amide carbon was not observed, both methyl groups in TBS were observed.); m/z (ESI/MS) calculated 956.5 ($\text{C}_{52}\text{H}_{80}\text{FNNaO}_7\text{Si}_3$), observed 956.5 ($\text{M}+\text{Na}$) $^+$.

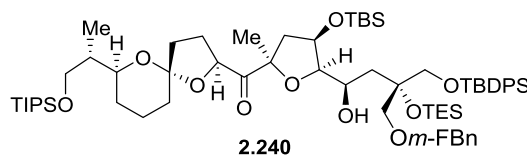


Allene **2.233**: To a flamed dried 10 mL round-bottomed flask, alkyl chloride **2.230** (35 mg in

1.7 mL THF, 0.79 mmol), dried over 4 Å molecular sieves pellets, was added. The solution was cooled down to -78°C, to which lithium naphthalenide (0.27 mL about 0.5 M solution in THF, about 0.135 mmol) was added. After 40 min, the reaction was warmed up to -5°C, to which Winreb amide **2.232** (50 mg in 2.5 mL THF, 0.54 mmol), dried over 4 Å molecular sieves pellets, was added. After 5 min, the reaction was quenched by 2 mL satd. NH₄Cl (aq.), diluted with 10 mL water, and partitioned against diethyl ether (3x20 mL). The organic fractions were combined, washed with satd. NaCl (aq) (10 mL), dried over Na₂SO₄, filtered, concentrated, and purified by FCC (5% ethyl acetate/hexane) to give **2.233** (47 mg, 69%) as a colorless oil (*R*_f = 0.80 10% ethyl acetate/hexane). [α]_D²³ 7.2 (*c* = 0.34, CHCl₃); IR $\nu_{\text{max}}(\text{neat})/\text{cm}^{-1}$ 3072, 2956, 2864, 1956, 1716, 1614, 1591, 1514, 1463, 1249, 1112, 834, 741, 614, 505; ¹H NMR (500 MHz, CDCl₃) δ 7.70 – 7.59 (4H, m), 7.42 – 7.21 (9H, m), 7.05 – 6.92 (3H, m), 6.88 – 6.81 (2H, m), 5.07 – 4.98 (1H, m), 4.52 – 4.42 (4H, m), 3.81 – 3.60 (7H, m), 3.59 – 3.49 (4H, m), 3.20 – 3.14 (1H, m), 2.67 (1H, dd, *J* = 3.8, 2.1 Hz), 2.50 – 2.40 (2H, m), 2.40 – 2.31 (2H, m), 2.26 – 2.15 (3H, m), 2.09 (1H, ddd, *J* = 14.2, 6.5, 2.1 Hz), 1.96 (1H, dd, *J* = 14.4, 4.0 Hz), 1.88 – 1.80 (1H, m), 1.74 – 1.40 (8H, m), 1.14 – 1.01 (30H, m), 0.95 – 0.79 (21H, m), 0.53 (6H, q, *J* = 7.9 Hz), 0.02 (6H, d, *J* = 4.6 Hz); ¹³C NMR (101 MHz, CDCl₃) δ 210.1, 202.5, 163.0 (d, *J* = 245.7 Hz), 159.2, 141.0 (d, *J* = 7.2 Hz), 135.9, 135.8, 133.5 (2), 131.5, 129.8 (d, *J* = 7.9 Hz), 129.7, 129.4, 127.7, 123.1 (d, *J* = 2.9 Hz), 114.5 (d, *J* = 10.4 Hz), 114.3 (d, *J* = 9.7 Hz), 113.8, 97.1, 89.3, 79.1, 74.3, 72.8 (d, *J* = 1.6 Hz), 72.1, 70.0, 66.9, 65.6, 60.2, 55.4, 51.7, 42.9, 42.1, 40.2, 39.5, 38.6, 31.3, 29.8, 27.0, 25.9, 23.4, 20.5, 20.2, 19.4, 18.3, 18.2, 12.1, 11.7, 7.3, 6.7, -4.3, -4.8 (Both phenyl groups in TBDPS were observed, methyl groups in TBS were observed.); *m/z* (ESI/MS) calculated 1303.8 (C₇₄H₁₁₇FN₃O₉Si₄), observed 1303.8 (M+Na)⁺.



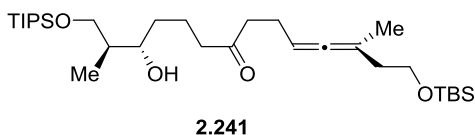
Allene **2.227**: In a 25 mL round-bottomed flask, allene **2.233** (47 mg, 0.037 mmol) was dipenssed in a mixture of DCM (2.5 mL) and phosphate buffer (pH = 7.4, 0.63 mL) and cool to 0°C. To this, DDQ (25 mg, 0.11 mmol) was added. After 30 min, the reaction was quenched by 3 mL *satd.* NaHCO₃ (aq.), diluted with 20 mL water, and partitioned against diethyl ether (3x40 mL). The organic fractions were combined, washed with *satd.* NaCl (aq) (10 mL), dried over Na₂SO₄, filtered, concentrated, and purified by FCC (8% ethyl acetate/hexane) to give **2.227** (36 mg, 85%) as a colorless oil (*R*_f = 0.50 10% ethyl acetate/hexane). $[\alpha]_D^{23}$ -4.8 (*c* = 0.20, CHCl₃); IR ν_{\max} (neat)/cm⁻¹ 3509, 3072, 2926, 2857, 1965, 1716, 1618, 1593, 1463, 1376, 1258, 1112, 835, 741, 702; ¹H NMR (400 MHz, CDCl₃) δ 7.70 – 7.62 (4H, m), 7.45 – 7.20 (7H, m), 7.07 – 6.91 (3H, m), 5.07 – 4.97 (1H, m), 4.52 – 4.42 (2H, m), 3.91 – 3.70 (5H, m), 3.63 (1H, d, *J* = 9.7 Hz), 3.61 – 3.50 (2H, m), 3.20 (1H, d, *J* = 3.5 Hz), 3.17 (1H, ddd, *J* = 6.1, 4.1, 2.0 Hz), 2.67 (1H, dd, *J* = 3.8, 2.2 Hz), 2.55 – 2.35 (4H, m), 2.28 – 2.15 (3H, m), 2.09 (1H, ddd, *J* = 14.4, 6.5, 2.2 Hz), 1.95 (1H, dd, *J* = 14.4, 3.9 Hz), 1.79 – 1.60 (7H, m), 1.54 – 1.32 (2H, m), 1.18 – 0.98 (30H, m), 0.93 (3H, d, *J* = 7.1 Hz), 0.90 – 0.78 (18H, m), 0.53 (6H, q, *J* = 7.7 Hz), 0.02 (6H, d, *J* = 3.8 Hz); ¹³C NMR (126 MHz, CDCl₃) δ 210.3, 202.5, 163.0 (d, *J* = 245.7 Hz), 141.0 (d, *J* = 7.2 Hz), 135.9, 135.8, 133.5 (2), 129.8 (d, *J* = 8.1 Hz), 129.7, 127.7, 123.1 (d, *J* = 2.9 Hz), 114.5 (d, *J* = 13.8 Hz), 114.3 (d, *J* = 13.4 Hz), 97.1, 89.3, 77.8, 74.7, 74.3, 72.8 (d, *J* = 1.8 Hz), 70.0, 69.1, 66.9, 60.2, 51.7, 42.9, 42.1, 40.2, 39.0, 38.6, 33.7, 27.0, 26.0, 23.4, 20.6, 20.2, 19.4, 18.1 (2), 11.9, 10.4, 7.3, 6.7, -4.3, -4.8 (Both phenyl groups in TBDPS were observed, both methyl groups in TBS were observed.); *m/z* (ESI/MS) calculated 1183.7 (C₆₆H₁₀₉FNaO₈Si₄), observed 1183.7 (M+Na)⁺.



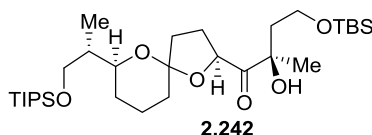
Preparation of **Dimethyldioxirane (DMDO)**: To a 3-neck 3 L round-bottomed flask, sodium bicarbonate (180 g, 2.14 mol), water (330 mL), and acetone (240 mL) was added. The contents were mixed by several quick swirls. To this, OXONE® (375g, 1.22 mol) was quickly added. Then two of the three necks were closed off. One neck were connected a cold finger, a 500 mL round-bottomed flask, and then a vacuum pump. After complete addition of OXONE®, the reaction flask was continuously swirled by hands for 40 min with the vacuum pump turned on. During the process, the cold finger was kept at -78°C using a mixture of acetone and dry ice. The 500 mL round-bottomed flask was kept in a small bucket filled with dry ice. And the vacuum in the system was between 140 Torr and 110 Torr. After 40 min, the 500 mL collection flask was removed from the cooling bucket. The solution was transferred to a pre-cooled 500 mL separatory funnel. To this, 175 mL cold DI water was added carefully. After evolution of oxygen ceased, the solution was extract with ice cold chloroform (7.5 mL and 3x5 mL). The organic fractions were combined, washed with ice cold phosphate buffer (pH = 7.4, 5x75 mL), dried over anhydrous sodium sulfate and then activated 4 Å molecular sieve pellets, and used immediately. The concentration of this DMDO in CHCl₃ solution was determined as about 0.30 M by reacting with PPh₃ at -40 °C.

Allene oxidation to tricycle **2.240**: In a 10 mL round-bottomed flask, dry allene **2.227** (49 mg, 0.042 mmol) was dissolved in a mixture of anhydrous CHCl₃ (1 mL) and CH₃COCl in anhydrous MeOH (1.0 mM, 0.5 mL. Note: the concentration of prepared CH₃COCl solution

may be as high as 1.5 mM on occasion). The solution was then cool to -40°C . To this, freshly prepared DMDO in CHCl_3 ($\sim 0.30\text{ M}$, 0.56 mL) was added. After 20 min, the reaction was slowly warmed up to -20°C in 40 min, then warmed up to room temperature. After removal of solvents, trifluoroacetic acid in CHCl_3 ($0.2\%\text{ v/v}$, 3 mL) was added in. After another 1.5 h, the solvent was removed. The crude product was purified by FCC ($2\%\text{ ethyl acetate/hexane}$) to give **2.240** (13 mg , 26%) as a colorless viscous oil ($R_f = 0.80\text{ }10\%\text{ ethyl acetate/hexane}$). $[\alpha]_D^{23} -1.8$ ($c = 0.19$, CHCl_3); IR $\nu_{\text{max}}(\text{neat})/\text{cm}^{-1}$ 3508, 3072, 2957, 2866, 1728, 1618, 1592, 1463, 1382, 1363, 1259, 1112, 882, 836, 741, 702, 689; ^1H NMR (500 MHz , CDCl_3) δ 7.67 – 7.59 (4H, m), 7.45 – 7.20 (7H, m), 7.03 – 6.93 (3H, m), 5.30 (1H, dd, $J = 10.2, 4.1\text{ Hz}$), 4.51 – 4.41 (2H, m), 4.36 (1H, t, $J = 2.9\text{ Hz}$), 4.15 (1H, t, $J = 9.8\text{ Hz}$), 3.92 (1H, s), 3.88 (1H, d, $J = 9.2\text{ Hz}$), 3.75 – 3.60 (3H, m), 3.62 – 3.49 (3H, m), 3.37 (1H, d, $J = 9.2\text{ Hz}$), 2.45 – 2.34 (3H, m), 1.99 – 1.84 (3H, m), 1.79 – 1.69 (1H, m), 1.67 – 1.15 (11H, m), 1.12 – 0.98 (30H, m), 0.97 – 0.75 (21H, m), 0.57 – 0.39 (6H, m), 0.07 (6H, d, $J = 19.2\text{ Hz}$); ^{13}C NMR (126 MHz , CDCl_3) δ 214.1, 163.0 (d, $J = 245.7\text{ Hz}$), 140.5 (d, $J = 7.3\text{ Hz}$), 135.9 (2), 133.3 (2), 129.9, 129.8 (d, $J = 8.2\text{ Hz}$), 127.8 (2), 123.3 (d, $J = 2.8\text{ Hz}$), 114.7 (d, $J = 21.6\text{ Hz}$), 114.5 (d, $J = 21.1\text{ Hz}$), 107.0, 87.8, 87.2, 80.4, 80.3, 73.2 (2), 73.0 (d, $J = 1.9\text{ Hz}$), 72.1, 67.8, 66.2, 65.3, 49.7, 41.6, 40.9, 36.9, 33.3, 28.5, 27.8, 27.0, 26.8, 25.9, 20.6, 19.4, 18.3, 18.2, 14.8, 12.1, 7.0, 6.6, -4.8 , -5.1 (Both phenyl groups in TBDPS were observed, both methyl groups in TBS were observed.); m/z (ESI/MS) calculated 1215.7 ($\text{C}_{66}\text{H}_{109}\text{FNaO}_{10}\text{Si}_4$), observed 1215.7 ($\text{M}+\text{Na}$) $^+$.



Allene **2.241**: Allene **2.241** was prepared (174 mg, 70% in two steps) as a colorless oil ($R_f = 0.40$ 10% ethyl acetate/hexane) using the same procedure as allene **2.227**. $[\alpha]_D^{23} 14.8$ ($c = 0.41$, CHCl_3); IR $\nu_{\text{max}}(\text{neat})/\text{cm}^{-1}$ 3509, 2938, 2866, 2728, 1966, 1716, 1463, 1384, 1255, 1100, 882, 836, 776, 681; ^1H NMR (500 MHz, CDCl_3) δ 5.08 – 5.00 (1H, m), 3.85 (1H, dd, $J = 9.7, 3.8$ Hz), 3.82 – 3.79 (1H, m), 3.77 (1H, dd, $J = 9.7, 5.5$ Hz), 3.66 (2H, t, $J = 7.1$ Hz), 3.21 (1H, d, $J = 3.6$ Hz), 2.56 – 2.39 (4H, m), 2.29 – 2.17 (2H, m), 2.16 – 2.10 (2H, ,m), 1.78 – 1.69 (2H, m), 1.69 – 1.58 (4H, m), 1.52 – 1.34 (2H, m), 1.16 – 1.01 (21H, m), 0.93 (3H, d, $J = 7.0$ Hz), 0.88 (9H, s), 0.05 (6H, s); ^{13}C NMR (126 MHz, CDCl_3) δ 210.5, 201.5, 97.9, 89.3, 74.7, 69.1, 62.1, 43.0, 41.7, 39.0, 37.4, 33.7, 26.1, 23.3, 20.6, 19.7, 18.5, 18.1, 11.9, 10.4, -5.1 (2) (Both other methyl groups in TBS were observed.); m/z (ESI/MS) calculated 577.4 ($\text{C}_{31}\text{H}_{62}\text{NaO}_4\text{Si}_2$), observed 577.4 ($\text{M}+\text{Na}$) $^+$.



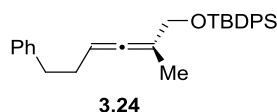
Spiroketal **2.242**: DMDO oxidation of allene **2.241** in the presence of CH_3COCl followed the same procedure as DMDO oxidation of allene **2.227**. For DMDO oxidation in the presence of LiClO_4 : In a 10 mL round-bottomed flask, dry LiClO_4 (6.1 mg, 0.057 mmol) was dissolved in a mixture of anhydrous CHCl_3 (1 mL) and MeOH (0.5 mL), followed by addition of allene **2.241** (32 mg, 0.058 mmol). The suspension was then cool to -40°C . To this, freshly prepared DMDO in CHCl_3 (~ 0.25 M, 1.0 mL) was added. After 20 min, the reaction was slowly warmed up to -20°C in 40 min, then warmed up to room temperature. After removal of solvents, the crude product was dissolved in CF_3COOH in CHCl_3 (0.029 M, 1.0 mL). After another 1 h, the solvent was removed. The crude product was purified by FCC (2% ethyl acetate/hexane) to

give **2.242** (20 mg as a ~3:1 mixture of diastereomers, 59%) as a colorless oil ($R_f = 0.80$ 10% ethyl acetate/hexane). $[\alpha]_D^{23} 8.2$ ($c = 0.22$, CHCl_3); IR $\nu_{\text{max}}(\text{neat})/\text{cm}^{-1}$ 3481, 2938, 2866, 1728, 1704, 1464, 1386, 1367, 1256, 1224, 1100, 836, 780, 681; ^1H NMR (500 MHz, CDCl_3 , * indicates diastereomer signals) δ 5.09 (1H, dd, $J = 10.3, 7.1$ Hz)*, 5.00 (1H, dd, $J = 9.3, 5.5$ Hz), 4.06 (1H, ddd, $J = 11.9, 5.9, 2.1$ Hz)*, 3.88 – 3.77 (1H, m), 3.70 – 3.76 (1H, m), 3.68 (1H, dd, $J = 9.6, 4.8$ Hz), 3.57 (1H, dd, $J = 9.7, 6.4$ Hz), 3.49 (1H, dd, $J = 9.8, 8.2$ Hz)*, 2.47 – 2.35 (1H, m), 2.36 – 2.05 (2H, m), 2.05 – 1.94 (1H, m), 1.93 – 1.75 (3H, m), 1.75 – 1.56 (8H, m), 1.39 (3H, s), 1.33 (3H, s)*, 1.08 – 1.03 (21H, m), 0.96 (3H, d, $J = 6.7$ Hz), 0.87 – 0.90 (9H, m), 0.05 (6H, d, $J = 3.0$ Hz); ^{13}C NMR (126 MHz, CDCl_3 , * indicates diastereomer signals) δ 214.0, 213.1*, 107.4, 106.9*, 79.9, 79.1, 72.4, 65.6, 61.1*, 60.0, 41.7*, 41.2, 40.9, 39.7*, 38.9*, 37.0, 33.5*, 32.9, 28.1, 27.7, 26.3*, 26.1, 26.0, 25.9, 20.7, 18.2, 13.2, 12.2, -5.5 (2) (Both oth methyl groups in TBS were observed.); m/z (ESI/MS) calculated 609.4 ($\text{C}_{31}\text{H}_{62}\text{NaO}_6\text{Si}_2$), observed 609.4 ($\text{M}+\text{Na}$) $^+$.

4.4 Chapter 3

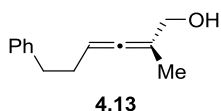
General Procedure for Preparation of Allenes:

At -78°C, alkyne (1.0 equiv, 0.2 M) in dry diethyl ether was treated with *n*-BuLi (1.05 equiv) for 1.5 h. To this, dry aldehyde (1.05 equiv) was added in slowly. After 30 min, the reaction was warmed up to 0°C. After 30 min (upon full consumption of starting material as monitored by TLC), methanesulfonyl chloride (1.5 equiv) and a small amount of triethylamine were added. After 2 h, the reaction was cooled down to -50°C. A cold solution of alkyl cuprate in dry THF, prepared from CuCN (3.0 equiv) and the corresponding alkyllithium reagent (3.0 equiv), was cannulated into the reaction flask. activated by gentle heating, upon full consumption of starting material, the reaction was cooled down to -78°C. The reaction was then slowly warmed to 0°C over 30 min, then quenched by *satd.* NH₄Cl solution (with 10% NH₃·H₂O), and partitioned against diethyl ether. The organic fractions were combined, dried over Na₂SO₄, filtered, concentrated in vacuo, and purified by FCC. In case of the preparation of enantiomeric rich allenes, the corresponding enantiomeric rich propargyl alcohols were used, instead of preparing it from alkyne and aldehyde coupling.

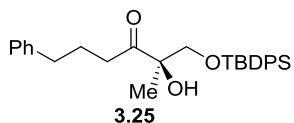


Allene **3.24**: 65% (718 mg); $[\alpha]_D^{23}$ 19.7 (*c* = 0.37, CHCl₃); IR ν_{\max} (neat)/cm⁻¹ 3070, 2931, 2856, 1968, 1472, 1112, 825, 739, 700; ¹H NMR (500 MHz, CDCl₃) δ 7.69 (4H, d, *J* = 8.0 Hz), 7.44 – 7.32 (6H, m), 7.28 – 7.19 (2H, m), 7.10 – 7.16 (3H, m), 5.16 – 5.06 (1H, m), 4.09 (2H, s), 2.68 (2H, t, *J* = 7.5 Hz), 2.27 (2H, q, *J* = 7.0 Hz), 1.66 (3H, d, *J* = 2.9 Hz), 1.06 (9H, s); ¹³C NMR (126

MHz, CDCl₃) δ 201.3, 142.0, 135.7, 134.0, 129.7, 128.6, 128.3, 127.7, 125.9, 100.0, 90.9, 65.9, 35.6, 30.8, 27.0, 19.5, 15.9; m/z (ESI/MS) calculated 449.2 (C₂₉H₃₄NaOSi), observed 449.2 (M+Na)⁺.

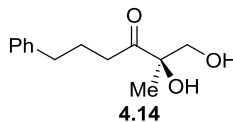


Allene **4.13**: $[\alpha]_D^{23}$ -8.3 ($c = 0.46$, CHCl₃); IR ν_{\max} (neat)/cm⁻¹ 3354, 2921, 1966, 1603, 1496, 1007, 699; ¹H NMR (400 MHz, CDCl₃) δ 7.34 – 7.21 (2H, m), 7.26 – 7.14 (3H, m), 5.35 – 5.23 (1H, m), 3.86 (2H, s), 2.82 – 2.65 (2H, m), 2.46 – 2.26 (2H, m), 1.63 (3H, d, $J = 2.9$ Hz), 1.22 – 1.13 (1H, m); ¹³C NMR (101 MHz, CDCl₃) δ 199.7, 141.7, 128.6, 128.4, 126.0, 101.2, 93.5, 63.9, 35.2, 30.5, 15.8; m/z (ESI/MS) calculated 211.1 (C₁₃H₁₆NaO), observed 211.1 (M+Na)⁺.

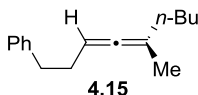


Hydroxyl ketone **3.25**: In 10 mL round-bottomed flask, allene **3.24** (95 mg, 0.22 mmol) was dissolved in 1.9 mL *tert*-butanol and 0.5 mL water. To this, hydrochloric acid (111 μ L, 1.0 M in water, 0.111 mmol) was added, followed by slow addition of osmium tetroxide (1.40 mL, 4 wt.% in water, 0.22 mmol) over 30 min. After another 30 min, hydrochloric acid (111 μ L, 1.0 M in water, 0.111 mmol) and osmium tetroxide (0.28 mL, 4 wt.% in water, 0.044 mmol) were added. After 30 min, the reaction was quenched by *satd.* Na₂S₂O₃ solution (5 mL), diluted with water (10 mL), and partitioned against ethyl acetate (3x20 mL). The organic fractions were combined, dried over Na₂SO₄, filtered, concentrated in vacuo, and purified by FCC (5% ethyl acetate/hexane) to give **3.25** (65 mg, 63%) as a pale yellow oil ($R_f = 0.30$ 10%

ethyl acetate/hexane). $[\alpha]_D^{23}$ -11.8 ($c = 0.70$, CHCl_3); IR $\nu_{\text{max}}(\text{neat})/\text{cm}^{-1}$ 3482, 3026, 2932, 2858, 1713, 1603, 1589, 1497, 1029, 940, 743, 701, 622; ^1H NMR (500 MHz, CDCl_3) δ 7.67 – 7.55 (4H, m), 7.48 – 7.35 (6H, m), 7.31 – 7.24 (2H, m), 7.23 – 7.14 (3H, m), 3.90 (1H, s), 3.85 (1H, d, $J = 10.3$ Hz), 3.59 (1H, d, $J = 10.3$ Hz), 2.72 – 2.53 (4H, m), 2.04 – 1.92 (2H, m), 1.20 (3H, s), 1.00 (9H, s); ^{13}C NMR (126 MHz, CDCl_3) δ 213.5, 141.7, 135.9, 135.8, 133.0, 132.8, 130.1 (2), 128.6 (2), 128.1, 128.0, 126.2, 80.0, 69.9, 36.5, 35.4, 27.0, 25.1, 21.4, 19.5; m/z (ESI/MS) calculated 483.2 ($\text{C}_{29}\text{H}_{36}\text{NaO}_3\text{Si}$), observed 483.2 ($\text{M}+\text{Na}$) $^+$.

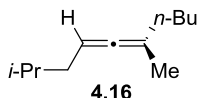


Diol **4.14**: Hydroxyl ketone **3.25** was converted to the corresponding diol using TBAF. $[\alpha]_D^{23}$ 0.5 ($c = 0.80$, CHCl_3); IR $\nu_{\text{max}}(\text{neat})/\text{cm}^{-1}$ 3441, 3026, 2934, 1706, 1603, 1456, 1373, 1054, 747, 700; ^1H NMR (500 MHz, CDCl_3) δ 7.32 – 7.24 (2H, m), 7.24 – 7.15 (3H, m), 3.81 (1H, d, $J = 11.7$ Hz), 3.61 (1H, d, $J = 11.7$ Hz), 2.64 (2H, td, $J = 7.4, 3.4$ Hz), 2.59 (2H, t, $J = 7.2$ Hz), 1.92 – 2.05 (2H, m), 1.24 (3H, s); ^{13}C NMR (126 MHz, CDCl_3) δ 213.1, 141.5, 128.7, 126.3, 79.9, 68.1, 35.3, 35.2, 25.0, 21.7; m/z (ESI/MS) calculated 245.1 ($\text{C}_{13}\text{H}_{18}\text{NaO}_3$), observed 245.1 ($\text{M}+\text{Na}$) $^+$.

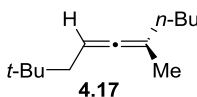


Allene **4.27**: 78 % (4.67 g); IR $\nu_{\text{max}}(\text{neat})/\text{cm}^{-1}$ 3027, 2957, 2931, 2857, 1964, 1604, 1496, 1454, 1369, 1078, 744, 698; ^1H NMR (500 MHz, CDCl_3) δ 7.35 – 7.25 (2H, m), 7.25 – 7.15 (3H, m), 5.11 – 5.01 (1H, m), 2.71 (2H, t, $J = 7.8$ Hz), 2.36 – 2.25 (2H, m), 1.96 – 1.86 (2H, m), 1.74 – 1.59 (3H, m), 1.45 – 1.22 (4H, m), 0.89 (3H, t, $J = 7.0$ Hz); ^{13}C NMR (126 MHz, CDCl_3) δ

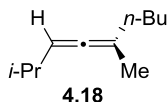
201.5, 142.3, 128.6, 128.3, 125.8, 100.0, 89.5, 35.8, 33.9, 31.2, 29.9, 22.5, 19.4, 14.1; m/z (ESI/MS) calculated 214.2 ($C_{16}H_{22}$), not observed by ESI.



Allene **4.16**: 86% (3.48 g); IR ν_{\max} (neat)/ cm^{-1} 2957, 2930, 2871, 1966, 1728, 1466, 1382, 1367, 1167, 834; ^1H NMR (500 MHz, CDCl_3) δ 4.98 – 4.92 (1H, m), 1.93 (2H, td, J = 7.4, 2.9 Hz), 1.82 – 1.87 (2H, m), 1.67 (3H, d, J = 2.9 Hz), 1.65 – 1.59 (1H, m), 1.44 – 1.28 (4H, m), 0.94 – 0.88 (9H, m); ^{13}C NMR (126 MHz, CDCl_3) δ 202.0, 98.6, 88.8, 39.2, 34.0, 30.0, 28.8, 22.6, 22.6, 19.4, 14.2; m/z (ESI/MS) calculated 166.2 ($C_{12}H_{22}$), not observed by ESI.

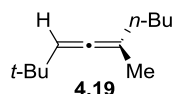


Allene **4.17**: 91% (3.00 g); IR ν_{\max} (neat)/ cm^{-1} 2956, 2873, 1965, 1466, 1364, 1242, 1198, 814; ^1H NMR (400 MHz, CDCl_3) δ 5.00 – 4.91 (1H, m), 1.92 (2H, td, J = 7.3, 2.9 Hz), 1.84 (2H, d, J = 7.8 Hz), 1.66 (3H, d, J = 2.8 Hz), 1.46 – 1.25 (4H, m), 0.92 – 0.88 (12H, s); ^{13}C NMR (101 MHz, CDCl_3) δ 202.8, 97.9, 86.9, 44.6, 34.0, 31.2, 30.0, 29.3, 22.5, 19.4, 14.2; m/z (ESI/MS) calculated 180.2 ($C_{13}H_{24}$), not observed by ESI.



Allene **4.18**: 60% (1.65 g); IR ν_{\max} (neat)/ cm^{-1} 2959, 2927, 2872, 1965, 1459, 1379, 1228, 809; ^1H NMR (500 MHz, CDCl_3) δ 5.04 – 4.99 (1H, m), 2.23 (1H, hd, J = 6.8, 5.7 Hz), 1.96 – 1.88 (2H,

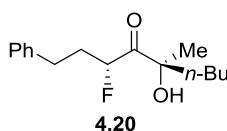
m), 1.67 (3H, d, $J = 3.1$ Hz), 1.46 – 1.27 (4H, m), 0.98 (6H, d, $J = 6.8$ Hz), 0.90 (3H, t, $J = 7.2$ Hz); ^{13}C NMR (126 MHz, CDCl_3) δ 199.6, 100.7, 97.9, 34.0, 30.0, 28.6, 22.9, 22.6, 19.6, 14.2; m/z (ESI/MS) calculated 152.2 ($\text{C}_{11}\text{H}_{20}$), not observed by ESI.



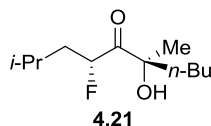
Allene **4.19**: 70% (2.75 g); IR ν_{max} (neat)/ cm^{-1} 2959, 2863, 1956, 1460, 1361, 1263, 1183, 814; ^1H NMR (500 MHz, CDCl_3) δ 5.03 – 4.96 (1H, m), 1.93 (2H, td, $J = 7.9, 7.4, 3.0$ Hz), 1.67 (3H, d, $J = 2.9$ Hz), 1.45 – 1.24 (4H, m), 1.01 (9H, s), 0.90 (3H, t, $J = 7.1$ Hz); ^{13}C NMR (126 MHz, CDCl_3) δ 198.3, 102.4, 101.3, 34.1, 32.2, 30.5, 30.1, 22.6, 19.7, 14.2; m/z (ESI/MS) calculated 166.2 ($\text{C}_{12}\text{H}_{22}$), not observed by ESI.

General Procedure for Allene Osylation with Selectfluor®:

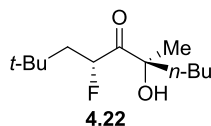
To a solution of Selectfluor® (4.0 equiv, 0.473 M in phosphate buffer pH = 7.4) were added N-Methylmorpholine N-oxide (2.0 equiv) and *t*-BuOH (equal volume). After 5 min, allene was added in, followed by osmium tetroxide (10 mol%, 4 wt.% in water). Slowly, a pale brown mixture formed. Upon full consumption of allene (monitored by TLC), the reaction was quenched by *satd.* $\text{Na}_2\text{S}_2\text{O}_3$ solution, and partitioned against diethyl ether. The organic fractions were combined, dried over Na_2SO_4 , filtered, concentrated in vacuo, and purified by FCC.



Fluorohydrin **4.20** (Table 3.9, entry 1): For yield and characterization of **4.20**, see reference 45 in chapter III.

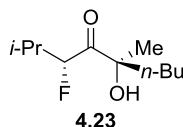


Fluorohydrin **4.21** (Table 3.9, entry 2): 30% (39 mg as a 1.3:1 mixture of hydroxyketone and fluoroketones (4.7:1) as indicated by ^1H NMR); IR $\nu_{\text{max}}(\text{neat})/\text{cm}^{-1}$ 3489, 2958, 2873, 1707, 1468, 1369, 1168, 1062, 973, 840; ^1H NMR (500 MHz, CDCl_3 , * indicates monohydroxyketone signals) δ 5.19 (1H, ddd, $J = 50.0, 9.9, 3.1$ Hz), 3.88 (1H, s), 3.42 (1H, s)*, 2.58 – 2.40 (2H, m)*, 2.06 – 1.15 (12H, m), 0.99 – 0.95 (6H, m), 0.92 – 0.84 (3H, m); (Carbon count for the 1.3:1 mixture) ^{13}C NMR (126 MHz, CDCl_3) δ 214.9, 212.4 (d, $J = 21.3$ Hz), 93.3 (d, $J = 182.6$ Hz), 79.6 (d, $J = 2.6$ Hz), 78.9, 40.9 (d, $J = 20.6$ Hz), 40.8, 39.5, 38.8 (d, $J = 4.1$ Hz), 33.8, 32.6, 27.8, 25.9, 25.7 (d, $J = 2.2$ Hz), 25.0 (d, $J = 3.8$ Hz), 24.7 (d, $J = 2.0$ Hz), 23.3, 23.0, 22.5, 22.4, 21.4, 14.0; m/z (ESI/MS) calculated 241.2 ($\text{C}_{12}\text{H}_{23}\text{FNaO}_2$), observed 241.2 ($\text{M}+\text{Na}$) $^+$.

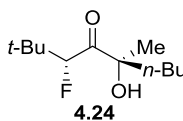


Fluorohydrin **4.22** (Table 3.9, entry 3): 25% (32 mg as a 0.6:1 mixture of hydroxyketone and fluoroketones (4.7:1) as indicated by ^1H NMR); IR $\nu_{\text{max}}(\text{neat})/\text{cm}^{-1}$; ^1H NMR (500 MHz, CDCl_3 , * indicates monohydroxyketone signals) δ 5.25 (1H, ddd, $J = 50.6, 9.6, 2.0$ Hz), 3.86 (1H, s)*, 3.43 (1H, d, $J = 1.4$ Hz), 2.53 – 2.35 (2H, m)*, 1.90 – 1.64 (4H, m), 1.44 – 1.24 (7H, m), 1.00 (9H, s), 0.92 – 0.85 (3H, m); (Carbon count for the 0.6:1 mixture) ^{13}C NMR (126 MHz, CDCl_3)

δ 215.2, 212.7 (d, $J = 22.1$ Hz), 93.2 (d, $J = 183.2$ Hz), 79.7 (d, $J = 2.6$ Hz), 79.1, 45.5 (d, $J = 19.7$ Hz), 39.5, 38.7 (d, $J = 4.2$ Hz), 37.6, 31.4, 30.4 (d, $J = 1.2$ Hz), 30.0, 29.8 (d, $J = 1.6$ Hz), 29.3, 29.2, 25.9, 25.7 (d, $J = 7.4$ Hz), 25.0 (d, $J = 4.0$ Hz), 23.0 (2), 14.1 (2); m/z (ESI/MS) calculated 255.2 ($C_{13}H_{25}FNaO_2$), observed 255.2 ($M+23$)⁺.

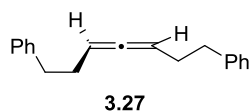


Fluorohydrin **4.23** (Table 3.9, entry 4): 48% (64 mg as a 1.2:1 mixture of hydroxyketone and fluoroketones (4.7:1) as indicated by 1H NMR); IR $\nu_{max}(\text{neat})/\text{cm}^{-1}$ 3482, 2959, 2874, 1706, 1468, 1370, 1290, 1165, 1007, 943, 828, 786; 1H NMR (500 MHz, $CDCl_3$, * indicates monohydroxyl ketone signals) δ 4.92 (1H, dd, $J = 48.3, 4.1$ Hz), 3.88 (1H, s)*, 3.38 (1H, s), 2.46 – 2.26 (2H, m)*, 2.26 – 2.17 (1H, m), 1.79 – 1.59 (2H, m), 1.39 (3H, s), 1.30 (3H, s)*, 1.31 – 1.21 (4H, m), 1.08 – 0.78 (9H, m); (Carbon count for the 1.2:1 mixture of diastereomers) ^{13}C NMR (126 MHz, $CDCl_3$) δ 214.1, 211.4 (d, $J = 21.3$ Hz), 98.0 (d, $J = 185.5$ Hz), 79.6 (d, $J = 2.6$ Hz), 78.7, 44.8, 39.2, 38.5 (d, $J = 4.0$ Hz), 30.4 (d, $J = 20.4$ Hz), 25.7, 25.5 (3), 24.6 (d, $J = 3.3$ Hz), 24.1, 23.0, 22.7 (d, $J = 3.6$ Hz), 18.9 (d, $J = 4.2$ Hz), 16.3 (d, $J = 5.4$ Hz), 14.0; m/z (ESI/MS) calculated 227.2 ($C_{11}H_{21}FNaO_2$), observed 227.2 ($M+Na$)⁺.

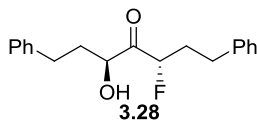


Fluorohydrin **4.24** (Table 3.9, entry 5): 39% (41 mg as a 3.4:1 mixture of hydroxyketone and fluoroketones (6.9:1) as indicated by 1H NMR); IR $\nu_{max}(\text{neat})/\text{cm}^{-1}$ 3481, 2957, 2873, 1707, 1466, 1366, 1249, 1060, 911, 804, 731; 1H NMR (500 MHz, $CDCl_3$, * indicates

monohydroxyketone signals) δ 4.75 (1H, dd, $J = 46.6, 1.3$ Hz), 3.93 (1H, s)*, 3.48 (1H, s), 2.39 (2H, ddd, $J = 84.2, 17.5, 1.3$ Hz)*, 1.72 (2H, t, $J = 8.4$ Hz), 1.68 – 1.57 (2H, m)*, 1.43 – 1.22 (7H, m), 1.06 (9H, s), 1.04 (9H, s)*, 0.90 – 0.84 (3H, m); (Carbon count for the 3.4:1 mixture of diastereomers) ^{13}C NMR (126 MHz, CDCl_3) δ 213.9, 211.5 (d, $J = 23.5$ Hz), 99.3 (d, $J = 185.3$ Hz), 80.0 (d, $J = 2.9$ Hz), 78.8, 47.6, 39.4, 38.6 (d, $J = 4.7$ Hz), 35.9 (d, $J = 19.1$ Hz), 30.8, 29.8, 26.2 (d, $J = 5.0$ Hz), 26.0 (d, $J = 5.1$ Hz), 25.5 (2), 24.3 (d, $J = 3.5$ Hz), 23.1 (2), 14.1 (2); m/z (ESI/MS) calculated 241.2 ($\text{C}_{12}\text{H}_{23}\text{FNaO}_2$), observed 241.2 ($\text{M}+\text{Na}$) $^+$.

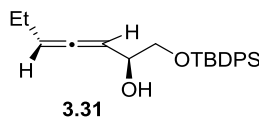


Allene **3.27**: 80 % (686 mg); IR ν_{max} (neat)/ cm^{-1} 3085, 2921, 1962, 1603, 1496, 745, 698; ^1H NMR (500 MHz, CDCl_3) δ 7.29 – 7.22 (4H, m), 7.20 – 7.13 (6H, m), 5.17 – 5.09 (2H, m), 2.65 (4H, t, $J = 7.8$ Hz), 2.33 – 2.18 (4H, m); ^{13}C NMR (126 MHz, CDCl_3) δ 204.2, 142.0, 128.6, 128.4, 125.9, 91.0, 35.5, 30.7; m/z (ESI/MS) calculated 248.2 ($\text{C}_{19}\text{H}_{20}$), not observed by ESI.

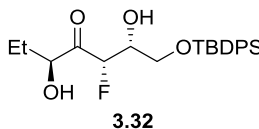


Fluorohydrin **3.28**: 54% (65 mg); IR ν_{max} (neat)/ cm^{-1} 3500, 3027, 2927, 1723, 1603, 1074, 749, 699; ^1H NMR (400 MHz, CDCl_3) δ 7.34 – 7.09 (10H, m), 4.91 (1H, ddd, $J = 49.0, 9.4, 3.7$ Hz), 4.56 – 4.49 (1H, m), 3.22 (1H, d, $J = 6.3$ Hz), 2.90 – 2.66 (4H, m), 2.29 – 2.01 (3H, m), 1.80 – 1.64 (1H, m); ^{13}C NMR (75 MHz, CDCl_3) δ 211.0 (d, $J = 24.9$ Hz), 141.0, 139.8, 128.8, 128.7, 128.6 (2), 126.6, 126.3, 94.3 (d, $J = 183.1$ Hz), 73.9, 77.4 (d, $J = 32.1$ Hz), 35.1 (d, $J = 2.4$ Hz), 34.0 (d, $J = 20.6$ Hz), 31.3 (d, $J = 50.2$ Hz); m/z (ESI/MS) calculated 323.2 ($\text{C}_{19}\text{H}_{21}\text{FNaO}_2$),

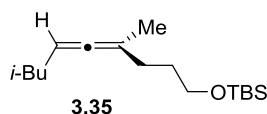
observed 323.0 (M+Na)⁺.



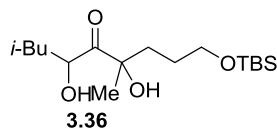
Allene **3.31**: In a flame dried 50 mL round-bottomed flask, CuBr·Me₂S (1.26 g, 6.13 mmol) was dispersed in dry Et₂O (17 mL) and Me₂S (11 mL). The resultant dark solution was then cooled down to -60°C. To this, ethyl magnesium bromide 1.0 M in THF (13.9 mL, 13.9 mmol) was added. After 10 min, to this yellow-greenish solution, trans-2,3-epoxy-pent-4-yn-1-ol (546 mg, 5.57 mmol) was added in slowly. After 1.5 h, the reaction was quenched by 20 mL NH₄Cl (aq) and filtered through a short pad of celite. The filtrate was partitioned against diethyl ether (3x30 mL). The organic fractions were combined, washed with satd. NaCl (aq) (20 mL), dried over Na₂SO₄, filtered, concentrated in vacuo, and purified by FCC (30% ethyl acetate/hexane) to give the corresponding allenyl diol (370 mg, 52%) as a colorless oil (R_f = 0.30 50% ethyl acetate/hexane). The diol was then protected as the TBDPS silyl ether in 97% yield. IR ν_{max}(neat)/cm⁻¹ 3418, 2998, 2858, 1963, 1428, 1113, 701; ¹H NMR (400 MHz, CDCl₃) δ 7.86 – 7.72 (4H, m), 7.54 – 7.36 (6H, m), 5.42 – 5.35 (1H, m), 5.33 – 5.27 (1H, m), 4.33 (1H, tdd, *J* = 6.5, 4.2, 2.3 Hz), 3.79 (1H, dd, *J* = 10.2, 4.1 Hz), 3.70 (1H, dd, *J* = 10.1, 6.8 Hz), 2.71 (1H, s), 2.08 – 1.98 (2H, m), 1.15 (9H, s), 1.00 (3H, t, *J* = 7.4 Hz); ¹³C NMR (101 MHz, CDCl₃) δ 203.0, 135.6, 133.2, 129.9, 127.8, 95.6, 92.4, 70.5, 68.1, 26.9, 21.6, 19.3, 13.3; *m/z* (ESI/MS) calculated 384.2 (C₂₃H₃₄NO₂Si), observed 383.9 (M+NH₄)⁺.



Fluorohydrin **3.32**: 65% (62 mg, a mixture of regioisomers 4:1 as indicated by ^{19}F -NMR, a dd peak, $J = 47.4, 27.1$ Hz for the major product, and a ddd peak, $J = 48.9, 30.7, 22.1$ Hz for the other product); the major isomer is isolated in 50% yield (47 mg) and characterized as: IR $\nu_{\text{max}}(\text{neat})/\text{cm}^{-1}$ 3445, 2933, 1732, 1590, 1112, 614; ^1H NMR (500 MHz, CDCl_3) δ 7.68 – 7.63 (4H, m), 7.50 – 7.37 (6H, m), 5.17 (1H, dd, $J = 47.3, 1.9$ Hz), 4.51 (1H, dtd, $J = 7.5, 3.9, 1.9$ Hz), 4.32 – 4.18 (1H, m), 3.78 (2H, dd, $J = 6.7, 3.6$ Hz), 3.11 (1H, d, $J = 6.6$ Hz), 2.41 (1H, d, $J = 6.5$ Hz), 2.07 – 1.95 (1H, m), 1.61 – 1.50 (1H, m), 1.07 (9H, s), 1.00 (3H, t, $J = 7.4$ Hz); ^{13}C NMR (126 MHz, CDCl_3) δ 209.8 (d, $J = 24.4$ Hz), 135.6, 132.7, 130.2, 128.0, 94.1 (d, $J = 190.2$ Hz), 75.9, 71.6 (d, $J = 18.4$ Hz), 63.3 (d, $J = 4.8$ Hz), 26.9, 26.1 (d, $J = 2.6$ Hz), 19.3, 9.4; m/z (ESI/MS) calculated 436.2 ($\text{C}_{23}\text{H}_{35}\text{FNO}_4\text{Si}$), observed 436.0 ($\text{M} + \text{NH}_4$) $^+$.

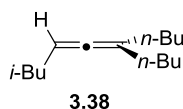


Allene **3.35**: 72 % (4.94 g); IR $\nu_{\text{max}}(\text{neat})/\text{cm}^{-1}$ 2955, 2930, 2897, 2858, 1966, 1464, 1384, 1362, 1255, 1103, 836, 775; ^1H NMR (500 MHz, CDCl_3) δ 5.00 – 4.92 (1H, m), 3.65 – 3.60 (2H, m), 2.00 – 1.94 (2H, m), 1.87 – 1.82 (2H, m), 1.67 (3H, d, $J = 2.8$ Hz), 1.66 – 1.58 (3H, m), 0.93 – 0.86 (15H, m), 0.07 – 0.02 (6H, m); ^{13}C NMR (126 MHz, CDCl_3) δ 201.9, 98.4, 89.3, 63.1, 39.2, 31.1, 30.4, 28.7, 26.2, 22.5 (2), 19.7, 18.6, -5.1 (Both methyl groups in *iso*-butyl group were observed.); m/z (ESI/MS) calculated 305.2 ($\text{C}_{17}\text{H}_{34}\text{NaOSi}$), observed 305.2 ($\text{M} + \text{Na}$) $^+$.



Dihydroxyl ketone **3.36**: In 25 mL round-bottomed flask, quinuclidine (55 mg, 0.49 mmol)

and osmium tetroxide (10.0 mL, 0.049 M in toluene) were added. The resultant red-orange solution was cooled down to -70°C . To this, allene **3.35** (69 mg, 0.24 mmol) was added. The reaction was then slowly warmed up to -60°C over 1 h, then to room temperature over 0.5 h. Half of the resultant dark green solution was concentrated in vacuo, suspended in 10 mL water. Hydrogen peroxide (30 wt.% in water) was then added dropwise until a colorless solution was formed. After 10 min, the reaction was quenched by *satd.* $\text{Na}_2\text{S}_2\text{O}_3$ solution (5 mL), and partitioned against diethyl ether (3x20 mL). The organic fractions were combined, dried over Na_2SO_4 , filtered, concentrated in vacuo, and purified by FCC (15% ethyl acetate/hexane) to give **3.36** (12 mg, 30%) as a colorless oil (R_f = 0.20 10% ethyl acetate/hexane). IR $\nu_{\text{max}}(\text{neat})/\text{cm}^{-1}$ 3417, 2957, 2858, 1709, 1471, 1387, 1257, 1100, 973, 838, 776; ^1H NMR (500 MHz, CDCl_3) δ 4.66 (1H, ddd, J = 10.1, 7.2, 2.6 Hz), 4.59 (1H, s), 3.65 (1H, t, J = 5.5 Hz), 3.26 (1H, d, J = 7.2 Hz), 2.16 (1H, d, J = 1.0 Hz), 2.10 – 2.02 (1H, m), 2.00 – 1.90 (1H, m), 1.81 – 1.71 (1H, m), 1.71 – 1.51 (3H, m), 1.38 – 1.23 (4H, m), 0.98 (3H, d, J = 6.6 Hz), 0.95 (3H, d, J = 6.8 Hz), 0.91 (9H, s), 0.09 (6H, s); ^{13}C NMR (126 MHz, CDCl_3) δ 217.9, 79.4, 72.3, 64.0, 42.9, 37.4, 27.0, 26.6, 26.1, 24.9, 23.8, 21.2, 18.5, -5.3 (Both methyl groups in *iso*-butyl group were observed.); m/z (ESI/MS) calculated 355.2 ($\text{C}_{17}\text{H}_{36}\text{NaO}_4\text{Si}$), observed 355.2 ($\text{M}+\text{Na}$) $^{+}$.

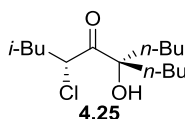


Allene **3.38**: 87% (4.39 g); IR $\nu_{\text{max}}(\text{neat})/\text{cm}^{-1}$ 2957, 2931, 2872, 1962, 1466, 1381, 1366; ^1H NMR (500 MHz, CDCl_3) δ 5.04 – 4.96 (1H, m), 1.95 – 1.89 (4H, m), 1.86 (2H, td, J = 7.0, 1.3 Hz), 1.70 – 1.58 (1H, m), 1.44 – 1.27 (8H, m), 0.98 – 0.83 (12H, m); ^{13}C NMR (126 MHz, CDCl_3)

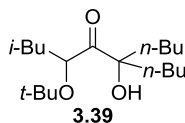
δ 201.4, 103.4, 90.3, 39.4, 32.6, 30.1, 28.9, 22.6, 22.5, 14.2; the spectrums match published results.

General Procedure for Allene Osymlation with N-Chlorosuccinimide®:

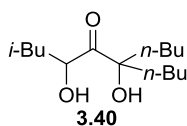
To a yellow solution of potassium carbonate (3.0 equiv), potassium ferricyanide (3.0 equiv), and potassium osmate(VI) dihydrate (2.5 mol%) and ligand (20 mol%) in water were added N-Chlorosuccinimide (3.0 equiv). After 5 min, allene **3.38** in *t*-BuOH (1.0 equiv, 0.19 M) was added in. After 24 h (12 h for Table 3.12), the reaction was quenched by *satd.* Na₂S₂O₃ solution, and partitioned against diethyl ether. The organic fractions were combined, dried over Na₂SO₄, filtered, concentrated in vacuo, and purified by FCC.



Chlorohydrin **4.25**: IR ν_{max} (neat)/cm⁻¹ 3509, 2958, 2873, 1717, 1467, 1386, 1262, 1140, 1052, 884, 731; ¹H NMR (500 MHz, CDCl₃) δ 4.77 (1H, dd, *J* = 10.0, 3.8 Hz), 2.99 (1H, s), 1.93 – 1.81 (2H, m), 1.81 – 1.63 (4H, m), 1.57 – 1.48 (2H, m), 1.46 – 1.20 (8H, m), 1.21 – 1.00 (2H, m), 0.99 – 0.84 (9H, m); ¹³C NMR (126 MHz, CDCl₃) δ 209.0, 82.9, 54.4, 42.1, 38.8, 38.6, 25.7, 25.6, 24.9, 23.2 (2), 23.0, 21.2, 14.0 (2) (Both methyl groups in *iso*-butyl group were observed, both *n*-butyl groups were observed.); *m/z* (ESI/MS) calculated 299.2 (C₁₅H₂₉ClNaO₂), observed 299.2 (M+Na)⁺.

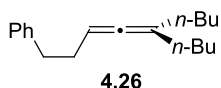


tert-butyl ether **3.39**: In 25 mL round-bottomed flask, allene **3.38** (100 mg, 0.48 mmol) was dissolved in 3 mL *tert*-butanol and 3 mL water. To this milky solution, osmium tetroxide (0.30 mL, 4 wt.% in water, 0.048 mmol) was added, followed by addition of *tert*-butyl hydroperoxide (0.60 mL, 70 wt.% in water, 4.3 mmol). After 20 min, the reaction was quenched by *satd.* Na₂S₂O₃ solution (5 mL), diluted with water (10 mL), and partitioned against ethyl acetate (3x20 mL). The organic fractions were combined, dried over Na₂SO₄, filtered, concentrated in vacuo, and purified by FCC (4% ethyl acetate/hexane) to give **3.39** (64 mg, 42%) as a colorless oil (*R*_f = 0.60 10% ethyl acetate/hexane). IR ν_{max} (neat)/cm⁻¹ 3508, 2958, 2870, 1720, 1468, 1197, 1052, 885, 755, 732; ¹H NMR (500 MHz, CDCl₃) δ 4.89 (1H, dd, *J* = 9.9, 3.1 Hz), 3.32 (1H, s), 1.89 – 1.70 (2H, m), 1.73 – 1.60 (3H, m), 1.56 (1H, ddd, *J* = 14.5, 9.9, 4.5 Hz), 1.45 – 1.18 (17H, m), 1.16 – 1.06 (1H, m), 0.94 (6H, dd, *J* = 19.3, 6.6 Hz), 0.86 (6H, td, *J* = 7.2, 3.3 Hz); ¹³C NMR (126 MHz, CDCl₃) δ 213.4, 82.3 (2), 81.0, 39.2, 38.3, 38.0, 26.5, 25.6, 25.2, 25.1, 23.5, 23.2 (2), 21.9, 14.1 (Both methyl groups in *iso*-butyl group were observed, both *n*-butyl groups were observed, and their methyl signals overlapped.); *m/z* (ESI/MS) calculated 337.3 (C₁₉H₃₈NaO₃), observed 337.3 (M+Na)⁺.

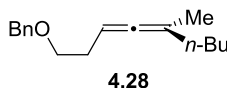


Diol **3.40**: Diol **3.40** was isolated from the above reaction in 15% yield (19 mg) as a colorless oil (*R*_f = 0.15 10% ethyl acetate/hexane). IR ν_{max} (neat)/cm⁻¹ 3447, 2958, 2870, 1706, 1467, 1389, 1228, 1142, 1044, 963; ¹H NMR (500 MHz, CDCl₃) δ 4.53 (1H, ddd, *J* = 10.5, 8.1, 2.3 Hz), 2.85 (1H, d, *J* = 8.1 Hz), 2.58 (1H, s), 2.01 – 1.91 (1H, m), 1.85 – 1.49 (6H, m), 1.49 – 1.16 (7H, m), 1.14 – 1.01 (1H, m), 0.97 (6H, dd, *J* = 12.1, 6.6 Hz), 0.88 (6H, td, *J* = 7.3, 3.1 Hz); ¹³C NMR

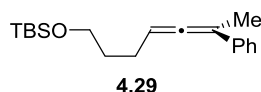
(126 MHz, CDCl₃) δ 217.4, 82.7, 72.5, 43.1, 39.8, 39.2, 25.7, 25.6, 25.0, 23.9, 23.2 (2), 21.3, 14.1 (2) (Both methyl groups in *iso*-butyl group were observed, both *n*-butyl groups were observed.); m/z (ESI/MS) calculated 281.2 (C₁₅H₃₀NaO₃), observed 281.2 (M+Na)⁺.



Allene **4.26**: 89 % (4.15 g); IR ν_{\max} (neat)/cm⁻¹ 3027, 2957, 2857, 1961, 1497, 1454, 1377, 744, 697; ¹H NMR (500 MHz, CDCl₃) δ 7.34 – 7.25 (2H, m), 7.26 – 7.18 (3H, m), 5.20 – 5.09 (1H, m), 2.78 – 2.71 (2H, m), 2.37 – 2.29 (2H, m), 1.96 – 1.90 (4H, m), 1.44 – 1.30 (8H, m), 0.94 (6H, t, *J* = 7.1 Hz); ¹³C NMR (126 MHz, CDCl₃) δ 201.0, 142.3, 128.6, 128.3, 125.8, 104.9, 91.1, 35.9, 32.6, 31.5, 30.0, 22.6, 14.2; the spectrums match published results.

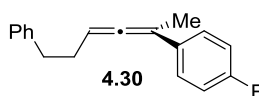


Allene **4.28** (Table 3.13, entry 3): 49 % (2.80 g); IR ν_{\max} (neat)/cm⁻¹ 2956, 2929, 2857, 1964, 1454, 1362, 1104, 734, 696; ¹H NMR (500 MHz, CDCl₃) δ 7.48 – 7.16 (m, 5H), 5.08 – 4.99 (1H, m), 4.53 (2H, s), 3.54 (2H, t, *J* = 6.9 Hz), 2.29 (2H, q, *J* = 6.9 Hz), 1.98 – 1.87 (2H, m), 1.71 – 1.61 (3H, m), 1.48 – 1.24 (4H, m), 0.89 (3H, t, *J* = 7.2 Hz); ¹³C NMR (126 MHz, CDCl₃) δ 202.1, 138.8, 128.5, 127.8, 127.7, 99.9, 86.7, 73.1, 70.4, 33.9, 30.1, 29.9, 22.6, 19.4, 14.2; m/z (ESI/MS) calculated 245.3 (C₁₇H₂₅O), observed 245.3 (M+H)⁺.



Allene **4.29** (Table 3.13, entry 6): 96 % (7.11 g); IR ν_{\max} (neat)/cm⁻¹ 2929, 2895, 2857, 1949,

1597, 1494, 1463, 1256, 1104, 836, 692; ^1H NMR (500 MHz, CDCl_3) δ 7.40 (2H, d, $J = 7.8$ Hz), 7.31 (2H, t, $J = 7.7$ Hz), 7.18 (1H, t, $J = 7.3$ Hz), 5.50 – 5.44 (1H, m), 3.66 (2H, t, $J = 6.4$ Hz), 2.21 – 2.10 (2H, m), 2.09 (3H, t, $J = 6.7$ Hz), 1.74 – 1.63 (2H, m), 0.95 – 0.79 (9H, s), 0.04 (6H, s); ^{13}C NMR (126 MHz, CDCl_3) δ 204.3, 137.9, 128.4, 126.5, 125.8, 100.8, 92.9, 62.8, 32.5, 26.2, 25.5, 18.6, 17.4, -5.1; m/z (ESI/MS) calculated 303.2 ($\text{C}_{19}\text{H}_{31}\text{OSi}$), observed 303.2 ($\text{M}+\text{H}$) $^+$.

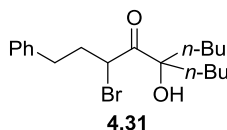


Allene **4.29** (Table 3.13, entry 7): 98 % (2.05 g); IR ν_{max} (neat)/ cm^{-1} 2937, 1951, 1505, 1229, 1099, 1005, 813, 698, 664; ^1H NMR (500 MHz, CDCl_3) δ 7.37 – 7.28 (2H, m), 7.28 – 7.17 (5H, m), 6.98 (2H, m), 5.54 – 5.43 (1H, m), 2.91 – 2.75 (2H, m), 2.57 – 2.40 (2H, m), 2.03 (3H, d, $J = 2.7$ Hz); ^{13}C NMR (126 MHz, CDCl_3) δ 204.3, 161.9 (d, $J = 245.4$ Hz), 141.8, 133.7 (d, $J = 3.2$ Hz), 128.9, 128.6, 127.3 (d, $J = 7.9$ Hz), 126.1, 115.3 (d, $J = 21.5$ Hz), 100.2, 92.8, 35.6, 31.0, 17.5; m/z (ESI/MS) calculated 252.1 ($\text{C}_{18}\text{H}_{17}\text{Fi}$), not observed by ESI.

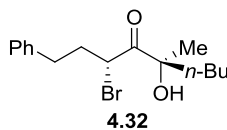
General Procedure for Allene Osylation with N-bromoacetamide:

To a solution of lithium hydroxide (5.0 equiv, 1.36 M) and potassium osmate(VI) dihydrate (10 mol%) in water was added *t*-BuOH (3:2 *t*-BuOH:H₂O) and N-bromoacetamide (5.0 equiv). After 5 min, a pale yellow to colorless solution formed. To this, allene in *t*-BuOH (1.0 equiv, 0.098 M) was added in dropwise. Upon full consumption of allene (monitored by TLC), the reaction was cooled down to 0°C, quenched by *satd.* $\text{Na}_2\text{S}_4\text{O}_3$ solution, and partitioned against diethyl ether. The organic fractions were combined, dried over Na_2SO_4 , filtered,

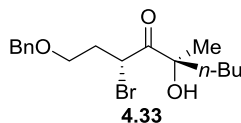
concentrated in vacuo, and purified by FCC.



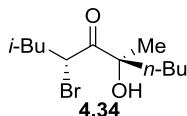
Bromohydrin **4.31** (Table 3.13, entry 1): For yield and characterization of **4.31**, see reference 44 in chapter III.



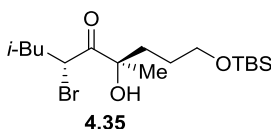
Bromohydrin **4.32** (Table 3.13, entry 2): For yield and characterization of **4.32**, see reference 44 in chapter III.



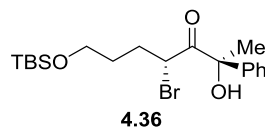
Bromohydrin **4.33** (Table 3.13, entry 3): 50 % (73 mg as a ~2:1 mixture of diastereomers as indicated by ^1H NMR of the crude); IR ν_{max} (neat)/ cm^{-1} 3501, 2957, 2863, 1715, 1455, 1361, 1174, 1104, 736, 698; ^1H NMR (500 MHz, C_6D_6 , * indicates diastereomer signals) δ 7.16 – 7.07 (4H, m), 7.07 – 7.01 (1H, m), 5.15 – 5.02 (1H, m), 4.16 – 4.04 (2H, m), 3.32 – 3.22 (1H, m), 3.15 – 3.03 (1H, m), 2.74 (1H, s)*, 2.56 (1H, s), 2.30 – 2.16 (1H, m), 2.11 – 1.99 (1H, m), 1.63 – 1.46 (1H, m), 1.45 – 1.36 (1H, m), 1.36 – 1.25 (1H, m), 1.23 (3H, m), 1.16 (3H, s)*, 1.15 – 1.05 (3H, m), 0.84 – 0.69 (3H, m); (Carbon count for the major diastereomers) ^{13}C NMR (126 MHz, C_6D_6) δ 208.5, 138.3, 128.4, 127.8, 127.7, 79.4, 72.9, 66.9, 42.9, 40.0, 34.4, 26.3, 25.7, 23.1, 14.0; m/z (ESI/MS) calculated 379.1, 381.1 ($\text{C}_{17}\text{H}_{25}\text{BrO}_3\text{Na}$), observed 379.1, 381.1 ($\text{M}+\text{Na}$) $^+$.



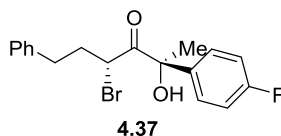
Bromohydrin **4.33** (Table 3.13, entry 4): 58 % (146 mg as a 3:1 mixture of diastereomers as indicated by ^1H NMR of the crude); IR ν_{max} (neat)/ cm^{-1} 3508, 2958, 2872, 1716, 1467, 1370, 1172, 1060, 874, 774; ^1H NMR (500 MHz, CDCl_3 , * indicates diastereomer signals) δ 4.86 (1H, dd, $J = 9.2, 5.6$ Hz), 4.83 (1H, dd, $J = 9.2, 5.6$ Hz)*, 3.03 (1H, s)*, 2.92 (1H, s), 1.96 – 1.85 (1H, m), 1.78 – 1.54 (4H, m), 1.44 (3H, s), 1.42 – 1.32 (1H, m), 1.32 – 1.21 (2H, m), 1.17 – 1.07 (1H, m), 0.98 – 0.81 (9H, m); (Carbon count for the major diastereomers) ^{13}C NMR (126 MHz, CDCl_3) δ 209.2, 79.9, 44.6, 42.2, 40.2, 27.0, 26.2, 25.7, 23.0, 22.9, 21.8, 14.1 (Both methyl groups in the *iso*-butyl group were observed.); m/z (ESI/MS) calculated 301.1, 303.1 ($\text{C}_{12}\text{H}_{23}\text{BrO}_2\text{Na}$), observed 301.1, 303.1 ($\text{M}+\text{Na}$) $^+$.



Bromohydrin **4.35** (Table 3.13, entry 5): 78 % (221 mg as a 3.2:1 mixture of diastereomers as indicated by ^1H NMR of the crude); IR ν_{max} (neat)/ cm^{-1} 3507, 2957, 2858, 1716, 1471, 1388, 1369, 1256, 1100, 814, 777; ^1H NMR (500 MHz, C_6D_6 , * indicates diastereomer signals) δ 5.17 (1H, dd, $J = 8.3, 6.7$ Hz)*, 5.07 (1H, dd, $J = 8.7, 6.0$ Hz), 4.17 (1H, s)*, 3.43 – 3.23 (3H, m), 1.97 – 1.79 (2H, m), 1.79 – 1.38 (5H, m), 1.31 (3H, s), 1.22 (3H, s)*, 0.93 – 0.87 (9H, m), 0.74 – 0.67 (6H, m), -0.01 – -0.06 (6H, m); (Carbon count for the major diastereomer) ^{13}C NMR (126 MHz, C_6D_6) δ 208.7, 79.1, 63.5, 44.5, 42.4, 37.4, 27.2, 27.1, 26.2, 25.9, 22.4, 21.6, 18.3, -5.5 (Both methyl groups in the *iso*-butyl group were observed.); m/z (ESI/MS) calculated 417.2, 419.2 ($\text{C}_{17}\text{H}_{35}\text{BrO}_3\text{SiNa}$), observed 417.2, 419.2 ($\text{M}+\text{Na}$) $^+$.

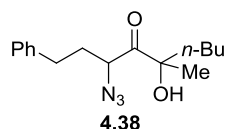


Bromohydrin **4.36** (Table 3.13, entry 6): 42 % (112 mg as a 4.2:1 mixture of diastereomers as indicated by ^1H NMR of the crude); IR $\nu_{\text{max}}(\text{neat})/\text{cm}^{-1}$ 3500, 2929, 2857, 1722, 1472, 1447, 1256, 1108, 836, 776, 699; ^1H NMR (500 MHz, CDCl_3 , * indicates diastereomer signals) δ 7.52 – 7.43 (2H, m), 7.40 – 7.27 (3H, m), 4.80 (1H, dd, $J = 7.9, 6.9$ Hz), 4.55 (1H, dd, $J = 7.9, 6.6$ Hz)*, 4.31 (1H, s)*, 3.53 – 3.34 (2H, m), 3.19 (1H, s), 1.97 – 1.86 (2H, m), 1.84 (3H, s), 1.39 – 1.12 (2H, m), 0.89 – 0.79 (9H, m), 0.02 – -0.05 (6H, m); (Carbon count for the major diastereomer) ^{13}C NMR (126 MHz, CDCl_3) δ 205.8, 140.1, 128.9, 128.4, 125.9, 80.8, 62.1, 45.4, 30.7, 30.2, 27.3, 26.1, 18.5, -5.2; m/z (ESI/MS) calculated 437.1, 439.1 ($\text{C}_{19}\text{H}_{31}\text{BrO}_3\text{SiNa}$), observed 437.1, 439.1 ($\text{M}+\text{Na}$) $^+$.

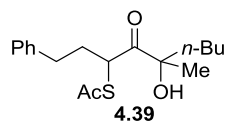


Bromohydrin **4.36** (Table 3.13, entry 7): 32 % (75 mg as a 5.1:1 mixture of diastereomers as indicated by ^1H NMR of the crude); IR $\nu_{\text{max}}(\text{neat})/\text{cm}^{-1}$ 3501, 3027, 2933, 2860, 1716, 1602, 1505, 1455, 1228, 1160, 838, 700; ^1H NMR (500 MHz, CDCl_3 , * indicates diastereomer signals, ** indicates the inseparable bromohydrin side product) δ 7.46 – 7.35 (2H, m), 7.35 – 7.16 (4H, m), 7.07 – 6.89 (3H, m), 6.13 (1H, t, $J = 6.8$ Hz)**, 4.67 (1H, dd, $J = 7.2, 7.2$ Hz), 4.36 (1H, dd, $J = 8.8, 4.4$ Hz)*, 4.25 (1H, s)*, 3.15 (1H, s), 2.90 – 2.74 (2H, m)**, 2.69 – 2.57 (2H, m)**, 2.56 – 2.37 (2H, m), 2.28 – 2.13 (1H, m), 2.13 – 2.01 (1H, m), 1.84 (3H, s)*, 1.78 (3H, s);

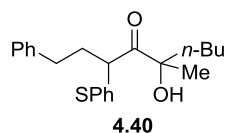
(Carbon count for the major diastereomer) ^{13}C NMR (126 MHz, CDCl_3) δ 205.5, 162.8 (d, J = 247.6 Hz), 140.0, 135.9 (d, J = 3.1 Hz), 128.8, 128.5, 127.8 (d, J = 8.3 Hz), 126.6, 115.8 (d, J = 21.5 Hz), 80.5, 44.4, 35.5, 33.0, 27.6; m/z (ESI/MS) calculated 387.0, 489.0 ($\text{C}_{18}\text{H}_{18}\text{BrFO}_2\text{Na}$), observed 387.0, 489.0 ($\text{M}+\text{Na}$) $^+$.



Azide **4.38** (Table 3.14, entry 1): In 10 mL round-bottomed flask, bromohydrin **4.32** (90 mg, 0.28 mmol) was dissolved in 3 mL acetone. To this, sodium azide (89 mg, 1.4 mmol) was added. The reaction mixture was then brought to reflux. After 1 h 40 min, the solids were filtered, the filtrate was concentrated in vacuo, and purified by FCC (2% ethyl acetate/hexane) to give **4.38** (65 mg, a 3:1 mixture of diastereomers, 98%) as a colorless liquid (R_f = 0.80 10% ethyl acetate/hexane). IR ν_{max} (neat)/ cm^{-1} 3501, 2958, 2105, 1726, 1455, 748, 700; ^1H NMR (500 MHz, CDCl_3 , * indicates diastereomer signals) δ 7.35 – 7.28 (2H, m), 7.25 – 7.18 (3H, m), 4.08 (1H, dd, J = 8.2, 5.6 Hz), 4.00 (1H, t, J = 6.9 Hz)*, 2.91 – 2.82 (1H, m), 2.76 – 2.67 (2H, m), 2.16 – 2.05 (2H, m), 1.76 – 1.51 (2H, m), 1.44 – 1.32 (4H, m), 1.32 – 1.21 (2H, m), 1.13 – 1.01 (1H, m), 0.88 (3H, t, J = 7.3 Hz); (Carbon count for the major diastereomer) ^{13}C NMR (126 MHz, CDCl_3) δ 211.1, 140.2, 128.8, 128.6, 126.6, 79.6, 60.8, 39.6, 32.2, 31.8, 25.6, 25.4, 23.0, 14.0; m/z (ESI/MS) calculated 312.2 ($\text{C}_{16}\text{H}_{23}\text{N}_3\text{NaO}_2$), observed 312.2 ($\text{M}+\text{Na}$) $^+$.

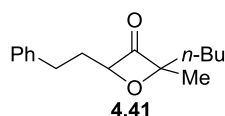


Thioester **4.39** (Table 3.14, entry 2): In 10 mL round-bottomed flask, bromohydrin **4.32** (50 mg, 0.15 mmol) was dissolved in 1.5 mL dichloromethane. To this, N,N-Diisopropylethylamine (59 mg, 0.46 mmol) and thioacetic acid (23 mg, 0.31 mmol) were added. After stirring at room temperature for 12 h, the reaction was concentrated in vacuo, and purified by FCC (5% ethyl acetate/hexane) to give **4.39** (40 mg, a 3:1 mixture of diastereomers, 81%) as a yellow oil ($R_f = 0.65$ 15% ethyl acetate/hexane). IR $\nu_{\max}(\text{neat})/\text{cm}^{-1}$ 3508, 3027, 2957, 2862, 1699, 1604, 1456, 1129, 700, 628; ^1H NMR (500 MHz, CDCl_3 , * indicates diastereomer signals) δ 7.33 – 7.24 (2H, m), 7.25 – 7.13 (3H, m), 4.81 (1H, t, $J = 5.5$ Hz), 3.43 (1H, s)*, 3.40 (1H, s), 2.80 – 2.69 (1H, m), 2.62 – 2.53 (1H, m), 2.38 (3H, s), 2.21 – 2.10 (1H, m), 2.09 – 1.96 (1H, m), 1.68 – 1.61 (2H, m), 1.43 – 1.20 (6H, m), 1.15 – 1.01 (1H, m), 0.87 (3H, t, $J = 7.3$ Hz); (Carbon count for the major diastereomer) ^{13}C NMR (126 MHz, CDCl_3) δ 212.2, 194.5, 140.7, 128.7, 128.6, 126.5, 80.1, 44.8, 39.2, 33.9, 33.1, 30.4, 25.7, 24.9, 23.1, 14.2; m/z (ESI/MS) calculated 345.2 ($\text{C}_{18}\text{H}_{26}\text{NaO}_3\text{S}$), observed 345.2 ($\text{M}+\text{Na}$) $^+$.



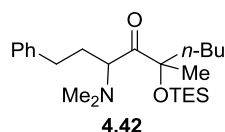
Thioether **4.40** (Table 3.14, entry 3): In 10 mL round-bottomed flask, bromohydrin **4.32** (50 mg, 0.15 mmol) was dissolved in 1.5 mL dry dimethylformamide. To this, N,N-Diisopropylethylamine (59 mg, 0.46 mmol) and thiophenol (34 mg, 0.31 mmol) were added. After stirring at room temperature for 24 h, the reaction was diluted with 10 mL water and partitioned against diethyl ether (3x20 mL). The organic fractions were combined, washed with satd. NaCl (aq) (10 mL), dried over Na_2SO_4 , filtered, concentrated in vacuo, and purified by FCC (3% ethyl acetate/hexane) to give **4.40** (53 mg, a 3:1 mixture of diastereomers, 95%)

as a colorless oil ($R_f = 0.70$ 15% ethyl acetate/hexane). IR $\nu_{\max}(\text{neat})/\text{cm}^{-1}$ 3493, 2956, 1699, 1455, 746, 699; ^1H NMR (500 MHz, CDCl_3 , * indicates diastereomer signals) δ 7.43 – 7.38 (2H, m), 7.36 – 7.24 (6H, m), 7.23 – 7.12 (2H, m), 4.16 (1H, t, $J = 7.1$ Hz)*, 4.06 (1H, t, $J = 7.1$ Hz), 3.15 (1H, s), 2.92 (1H, s)*, 2.65 – 2.80 (2H, m), 2.16 – 1.95 (2H, m), 1.70 – 1.50 (2H, m), 1.40 – 1.08 (7H, m), 0.88 (3H, t, $J = 7.2$ Hz); (Carbon count for the major diastereomer) ^{13}C NMR (126 MHz, CDCl_3) δ 209.9, 140.8, 134.4, 131.4, 129.2, 128.8, 128.6, 128.5, 126.3, 79.7, 48.5, 39.6, 33.0, 32.3, 25.6, 25.3, 23.0, 14.1; m/z (ESI/MS) calculated 379.2 ($\text{C}_{22}\text{H}_{28}\text{NaO}_2\text{S}$), observed 379.2 ($\text{M}+\text{Na}$) $^+$.

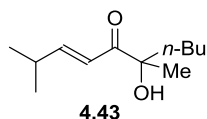


Oxetan-3-one **4.40** (Table 3.14, entry 4): In 25 mL round-bottomed flask, bromohydrin **4.32** (99 mg, 0.302 mmol) was dissolved in 1.5 mL dimethyl sulfoxide. To this, potassium hydroxide in water (48 mg, 39 wt.%, 0.33 mmol) was added. After stirring at room temperature for 50 min, potassium hydroxide in water (87 mg, 39 wt.%, 0.60 mmol) was added. After 10 min, the reaction was diluted with 10 mL water and partitioned against a 1:1 mixture of ethyl acetate and hexane (3x20 mL). The organic fractions were combined, washed with satd. NaCl (aq) (10 mL), dried over Na_2SO_4 , filtered, concentrated in vacuo, and purified by FCC (3% ethyl acetate/hexane) to give **4.41** (51 mg, a 1.3:1 mixture of diastereomers, 68%) as a colorless oil ($R_f = 0.85$ 10% ethyl acetate/hexane). IR $\nu_{\max}(\text{neat})/\text{cm}^{-1}$ 3028, 2957, 2872, 1948, 1812, 1738, 1604, 1456, 1378, 1140, 749, 700; ^1H NMR (500 MHz, CDCl_3 , * indicates diastereomer signals) δ 7.32 – 7.26 (2H, m), 7.23 – 7.17 (3H, m), 5.24 (1H, dd, $J = 8.5, 6.0$ Hz), 5.19 (1H, dd, $J = 7.8, 6.1$ Hz)*, 2.85 – 2.69 (2H, m), 2.20

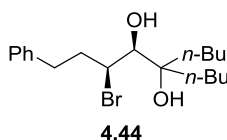
– 2.02 (2H, m), 1.82 – 1.69 (2H, m), 1.57 – 1.43 (4H, m), 1.41 – 1.26 (3H, m), 0.91 (3H, t, $J = 7.1\text{Hz}$); (Carbon count for the 1.3:1 mixture of diastereomers) ^{13}C NMR (126 MHz, CDCl_3) δ 209.3, 209.1, 140.7 (2), 128.6 (2), 128.5, 126.3 (2), 105.6, 105.3, 96.0, 95.2, 36.8, 36.6, 33.9, 32.8, 30.9, 26.0, 25.9, 23.0 (2), 22.0, 21.6, 14.0 (2); m/z (ESI/MS) calculated 269.2 ($\text{C}_{16}\text{H}_{22}\text{NaO}_2$), observed 269.2 ($\text{M}+\text{Na}$) $^+$.



Amine **4.42** (Table 3.14, entry 5): In 10 mL round-bottomed flask, triethylsilyl ether protected bromohydrin (81 mg, 0.18 mmol) was dissolved in 2 mL acetonitrile solution (25 wt.%) of dimethyl amine. After stirring under argon for 7 d, the reaction was concentrated in vacuo, and purified by FCC (2% acetone/hexane with 1% triethyl amine) to give **4.38** (65 mg, a 1:1 mixture of diastereomers, 98%) as a yellow liquid ($R_f = 0.90$ 5% ethyl acetate/hexane). IR $\nu_{\text{max}}(\text{neat})/\text{cm}^{-1}$ 3027, 2957, 2786, 1713, 1604, 1456, 1238, 1083, 1005, 745; ^1H NMR (400 MHz, CDCl_3) δ 7.31 – 7.23 (2H, m), 7.21 – 7.14 (3H, m), 3.98 (1H, dd, $J = 7.0, 6.2\text{ Hz}$), 2.51 – 2.66 (2H, m), 2.38 (3H, s), 2.35 (3H, s), 2.08 – 1.88 (2H, m), 1.88 – 1.71 (2H, m), 1.60 – 1.48 (1H, m), 1.41 – 1.09 (6H, m), 1.05 – 0.78 (12H, m), 0.68 – 0.52 (6H, m); (Carbon count for the 1:1 mixture of diastereomers) ^{13}C NMR (101 MHz, CDCl_3) δ 216.5, 215.6, 142.4, 142.3, 128.6, 128.5 (2), 128.4, 125.9 (2), 83.2, 82.8, 65.0, 64.7, 41.5 (2), 41.4, 40.9, 32.6, 32.4, 28.6, 27.6, 27.4, 26.7, 26.4, 26.2, 23.2, 23.1, 14.1 (2), 7.3 (2), 6.9, 6.8; m/z (ESI/MS) calculated 428.3 ($\text{C}_{24}\text{H}_{43}\text{NNaO}_2\text{Si}$), observed 428.3 ($\text{M}+\text{Na}$) $^+$.

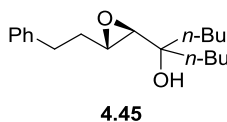


Enone **4.43** (Table 3.14, entry 6): In flame dried 10 mL round-bottomed flask, lithium bromide (160 mg, 1.84 mmol) and lithium carbonate (270 mg, 3.65 mmol) were suspended in 5 mL dry dimethylformamide. To this, bromohydrin **4.34** (125 mg, 0.448 mmol) was added. The reaction mixture was then warmed up to 90°C. After 8 h, the reaction was diluted with 30 mL water and partitioned against a 3:7 mixture of ethyl acetate and hexane (3x25 mL). The organic fractions were combined, dried over Na₂SO₄, filtered, concentrated in vacuo, and purified by FCC (10% ethyl acetate/hexane) to give **4.43** (69 mg, 77%) as a colorless liquid (*R*_f = 0.40 10% ethyl acetate/hexane). IR $\nu_{\text{max}}(\text{neat})/\text{cm}^{-1}$ 3474, 2959, 2873, 1686, 1625, 1467, 1297, 1045, 987, 791; ¹H NMR (500 MHz, CDCl₃) δ 7.11 (1H, dd, *J* = 15.8, 7.2 Hz), 6.34 (1H, d, *J* = 15.4 Hz), 4.03 (1H, s), 2.58 – 2.45 (1H, m), 1.73 – 1.66 (2H, m), 1.44 – 1.33 (4H, m), 1.32 – 1.21 (2H, m), 1.10 (6H, d, *J* = 6.8 Hz), 1.05 – 0.93 (1H, m), 0.87 (3H, t, *J* = 7.3 Hz); ¹³C NMR (126 MHz, CDCl₃) δ 202.9, 156.9, 119.6, 77.9, 39.1, 31.6, 25.6, 25.5, 23.0, 21.4 (2), 14.0 (Both methyl groups in the *iso*-propyl group were observed.); *m/z* (ESI/MS) calculated 221.2 (C₁₂H₂₂NaO₂), observed 221.2 (M+Na)⁺.



Diol **4.44** (Table 3.14, entry 7): In 25 mL round-bottomed flask, bromohydrin **4.31** (210 mg, 0.569 mmol) was dissolved in 5.7 mL methanol and cooled down to 0°C. To this, sodium borohydride (42 mg, 1.1 mmol) was added. After 2 h, the reaction was quenched by H₂O₂ in water (2 mL, 30 wt.%), diluted with *satd.* NH₄Cl solution (20 mL), and partitioned against diethyl ether (3x30 mL). The organic fractions were combined, dried over Na₂SO₄, filtered, concentrated in vacuo, and purified by FCC (7% ethyl acetate/hexane) to give **4.44** (174 mg,

82%) as a colorless oil ($R_f = 0.50$ 15% ethyl acetate/hexane). IR $\nu_{\max}(\text{neat})/\text{cm}^{-1}$ 3528, 3027, 2957, 2869, 1604, 1497, 1457, 1264, 919, 749, 700; ^1H NMR (500 MHz, CDCl_3) δ 7.32 – 7.23 (2H, m), 7.23 – 7.14 (3H, m), 4.07 (1H, ddd, $J = 9.6, 4.6, 1.5$ Hz), 3.32 (1H, d, $J = 9.3$ Hz), 2.93 – 2.84 (2H, m), 2.80 – 2.71 (1H, m), 2.49 – 2.38 (1H, m), 2.24 – 2.14 (1H, m), 2.12 (1H, s), 1.63 – 1.52 (2H, m), 1.52 – 1.43 (1H, m), 1.41 – 1.09 (8H, m), 0.98 – 0.86 (4H, m), 0.83 (3H, t, $J = 7.2$ Hz); ^{13}C NMR (126 MHz, CDCl_3) δ 140.7, 128.8, 128.7, 126.5, 77.0, 74.8, 58.7, 38.8, 35.6, 35.2, 33.5, 25.8, 25.6, 23.4 (2), 14.3, 14.2 (Both *n*-butyl groups were observed.); m/z (ESI/MS) calculated 393.2, 395.2 ($\text{C}_{19}\text{H}_{31}\text{BrNaO}_2$), observed 393.2, 395.2 ($\text{M}+\text{Na}$) $^+$.

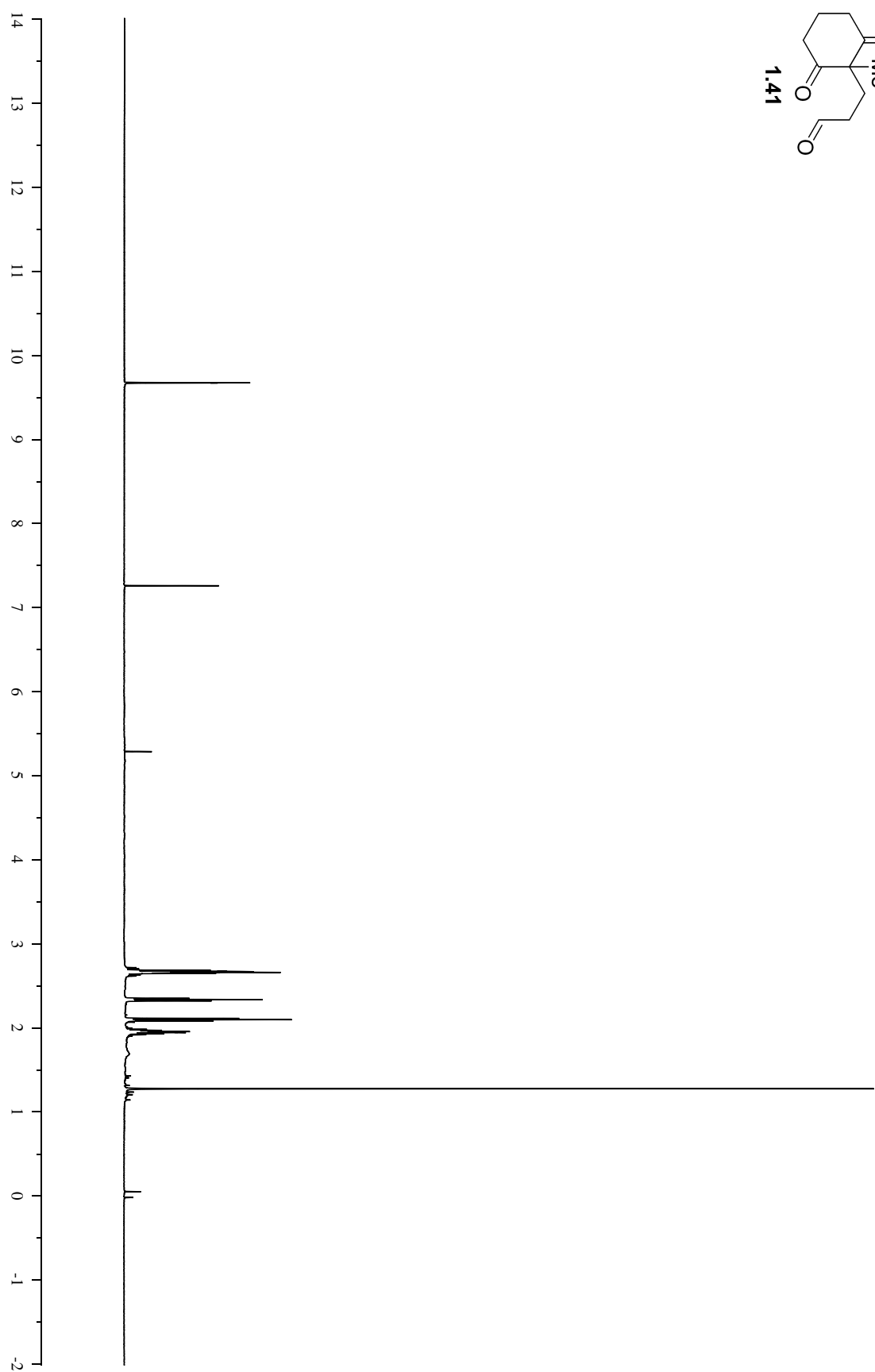
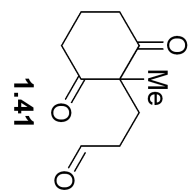


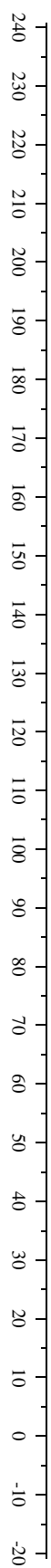
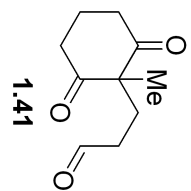
Epoxide **4.45**: In 25 mL round-bottomed flask, diol **4.44** (81 mg, 0.22 mmol) was dissolved in 4.4 mL methanol. To this, potassium carbonate (60 mg, 0.44 mmol) was added. After 16 h, the reaction was diluted with *satd.* NaCl solution (20 mL), and partitioned against diethyl ether (3x30 mL). The organic fractions were combined, dried over Na_2SO_4 , filtered, concentrated in vacuo, and purified by FCC (4% ethyl acetate/hexane) to give **4.44** (54 mg, 84%) as a colorless oil ($R_f = 0.60$ 15% ethyl acetate/hexane). IR $\nu_{\max}(\text{neat})/\text{cm}^{-1}$ 3490, 3027, 2957, 2862, 1603, 1497, 1456, 1142, 915, 748, 699; ^1H NMR (500 MHz, CDCl_3) δ 7.32 – 7.26 (2H, m), 7.25 – 7.15 (3H, m), 2.96 (1H, dt, $J = 8.5, 4.2$ Hz), 2.91 – 2.81 (2H, m), 2.76 (1H, ddd, $J = 13.7, 9.1, 7.0$ Hz), 2.35 – 2.24 (1H, m), 2.15 – 2.05 (1H, m), 1.98 (1H, s), 1.68 – 1.50 (4H, m), 1.46 – 1.24 (8H, m), 0.92 (6H, q, $J = 6.9$ Hz); ^{13}C NMR (126 MHz, CDCl_3) δ 141.5, 128.7, 128.6, 126.2, 71.8, 62.3, 57.8, 41.2, 37.2, 33.7, 29.7, 25.9, 25.6, 23.6, 23.5, 14.3 (2) (Both *n*-butyl groups were observed.); m/z (ESI/MS) calculated 313.2 ($\text{C}_{19}\text{H}_{30}\text{NaO}_2$), observed 313.2

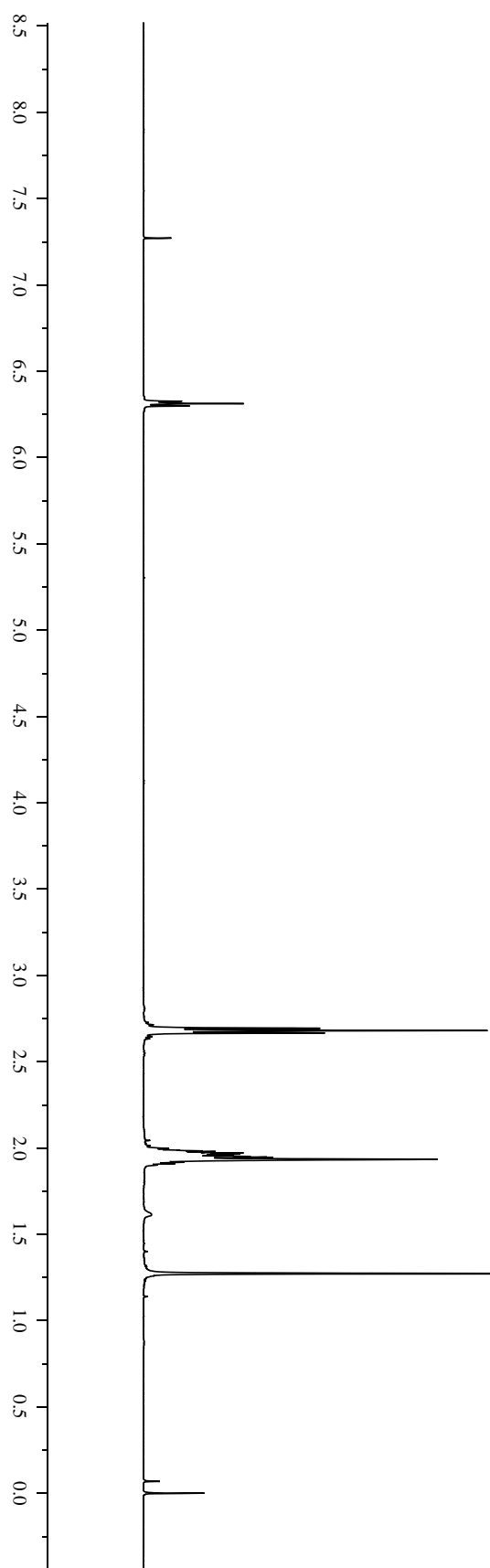
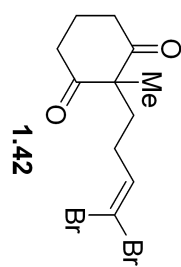
$(M+Na)^+$.

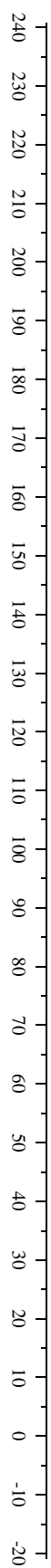
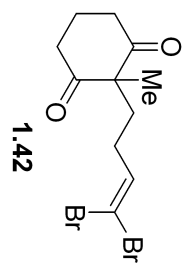
Appendix: Spectral Data

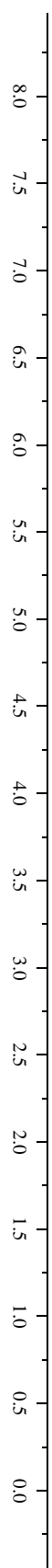
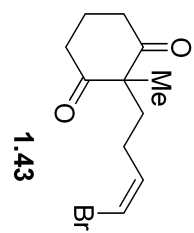
Spectra of Compounds

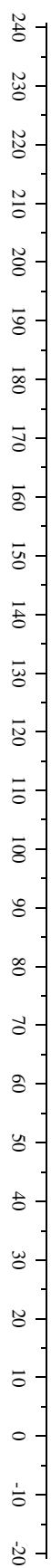
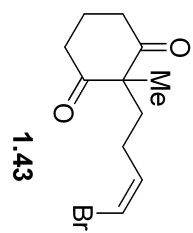


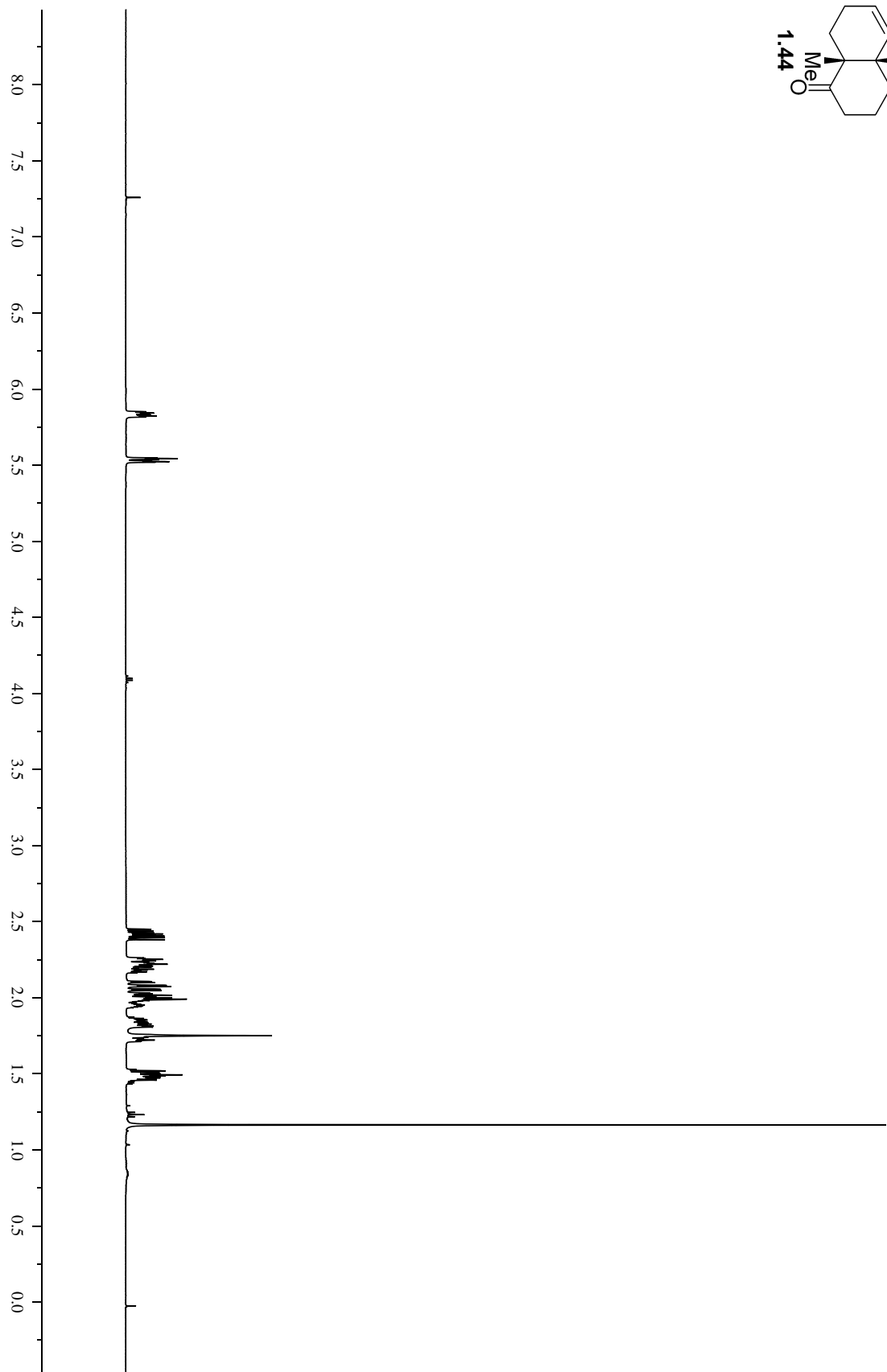
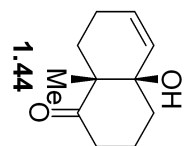


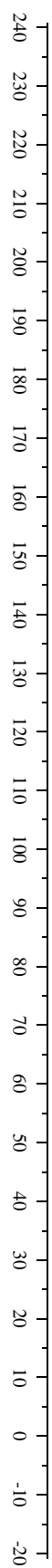
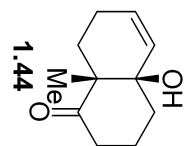


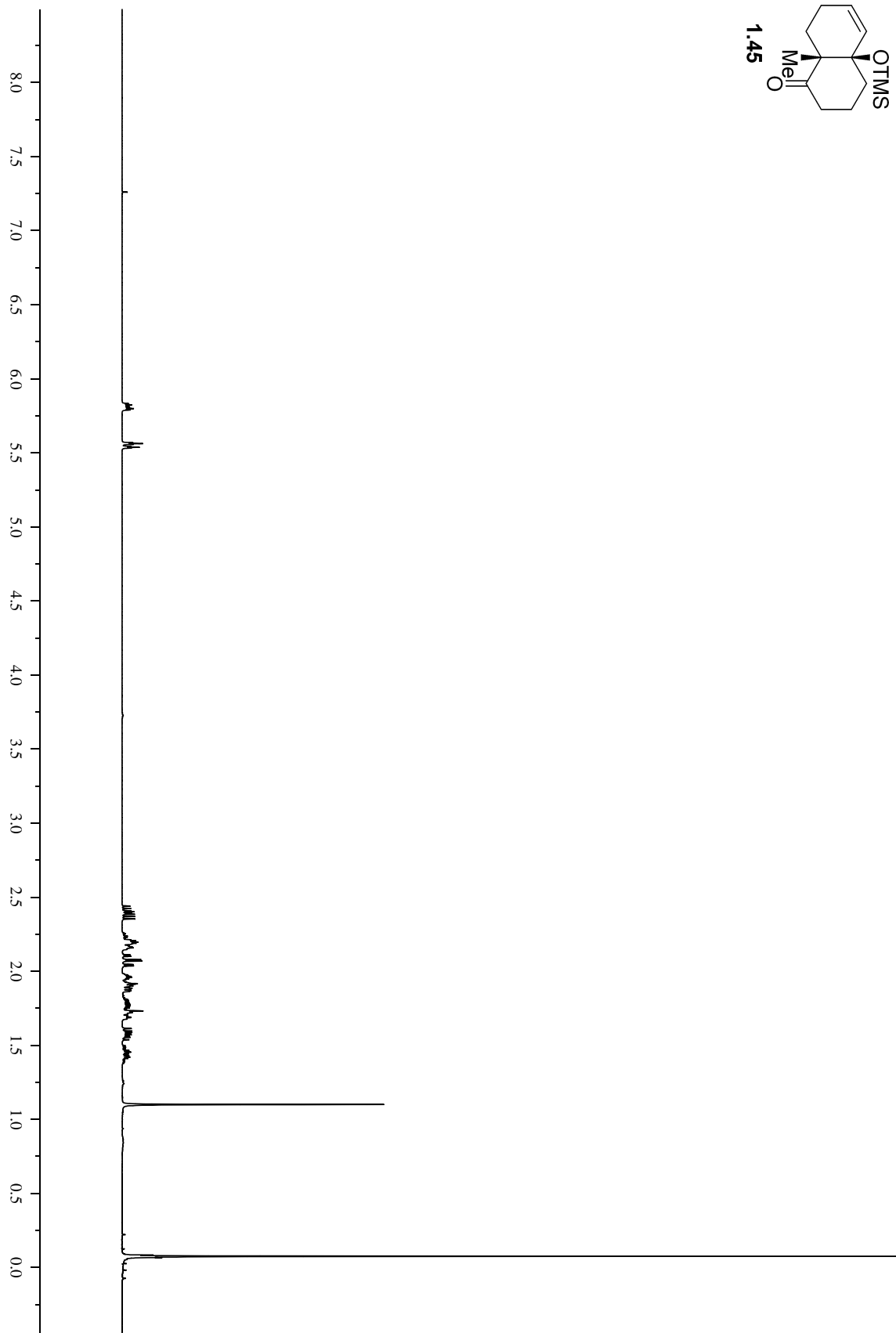
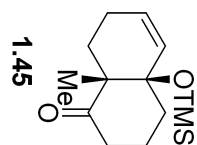


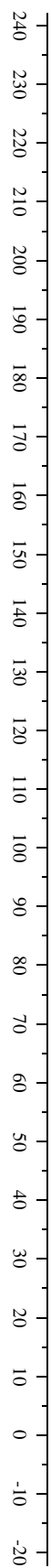
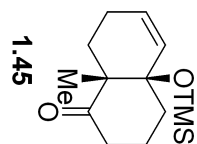


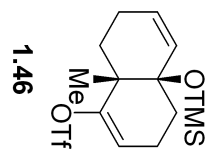




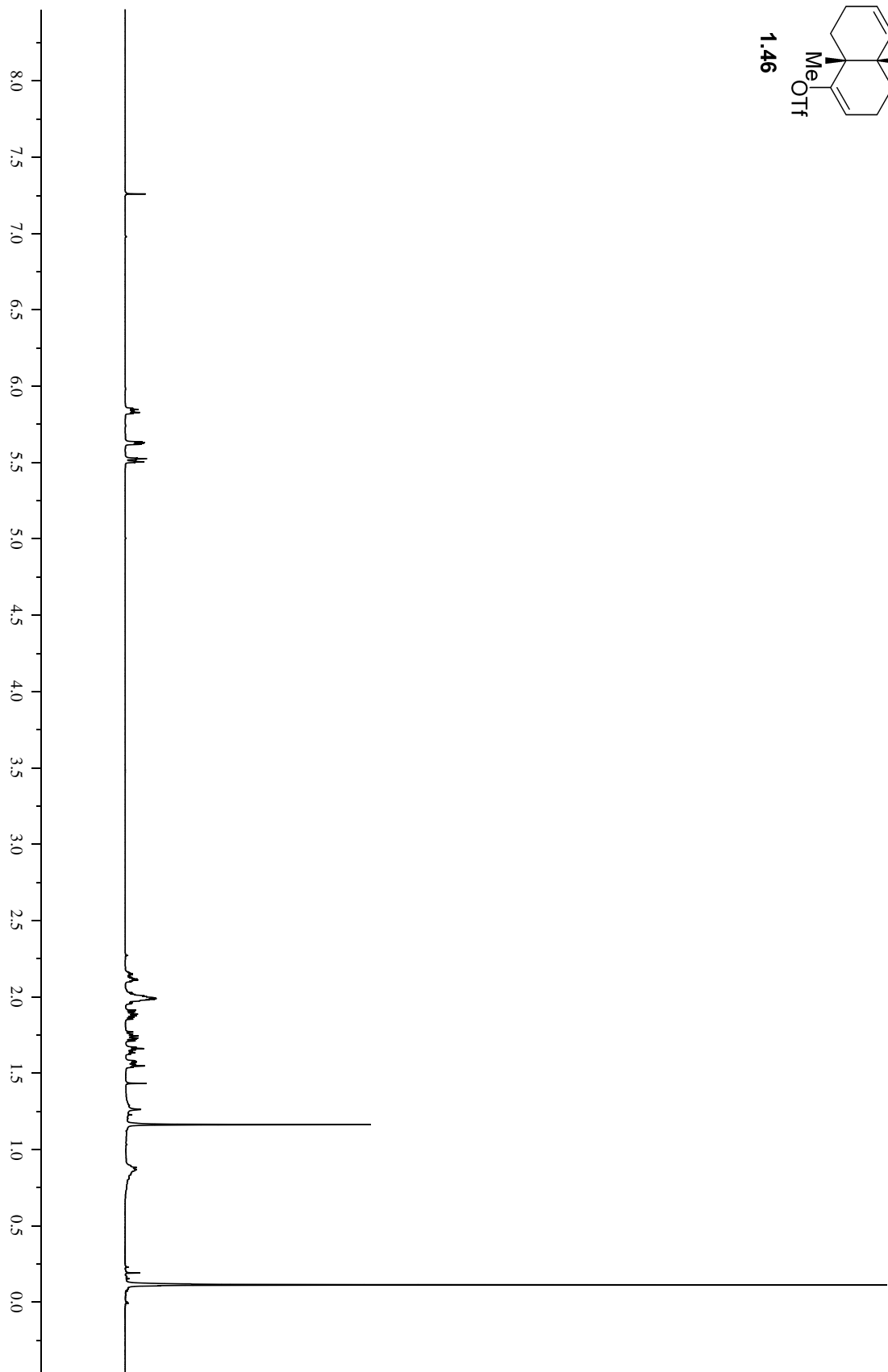


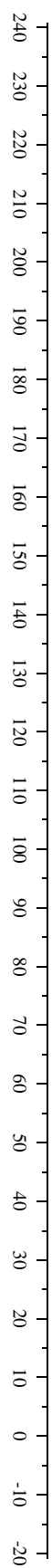
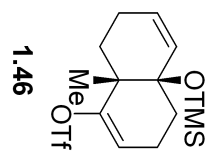


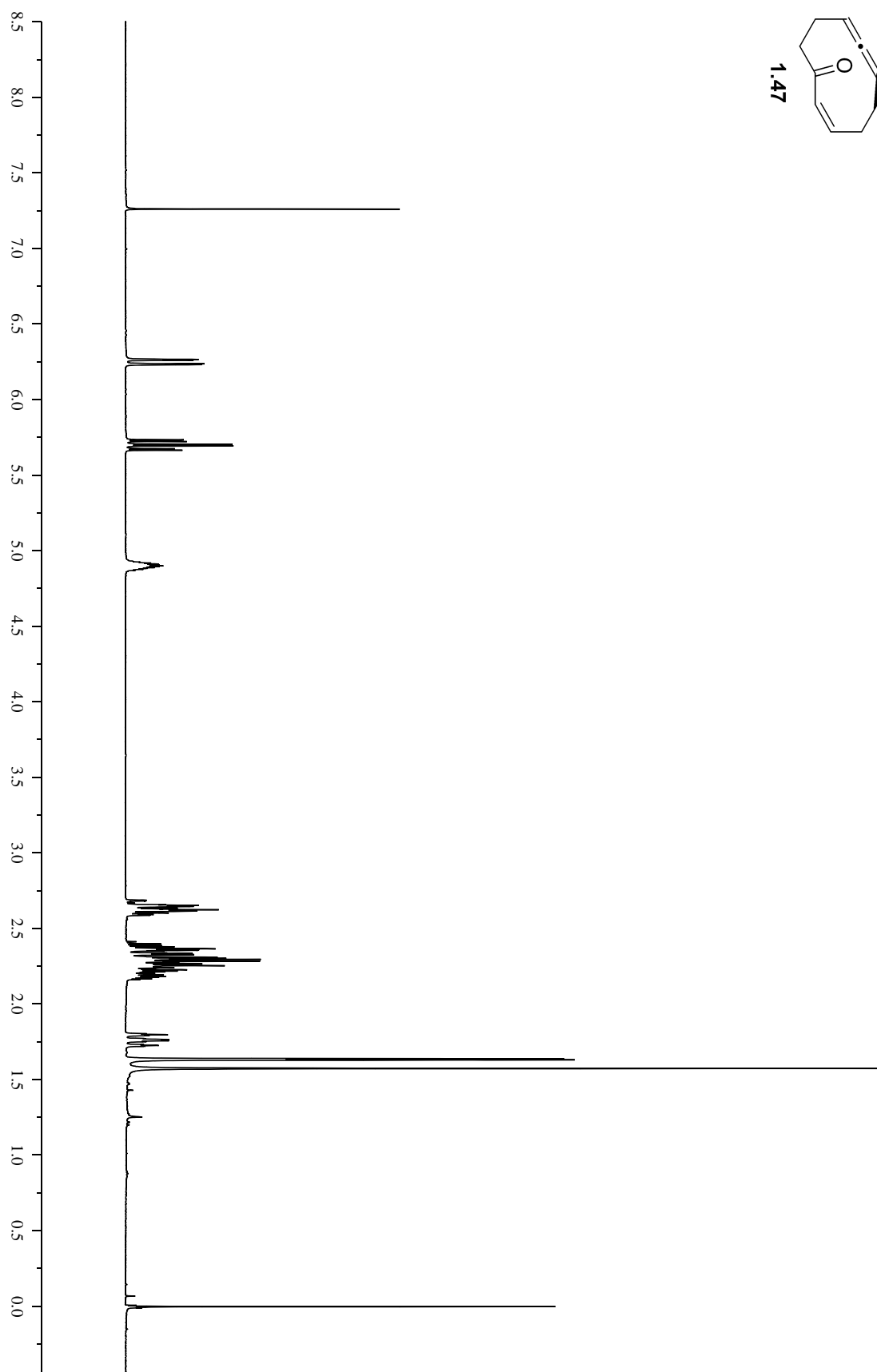
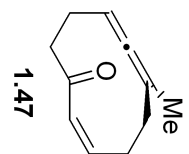


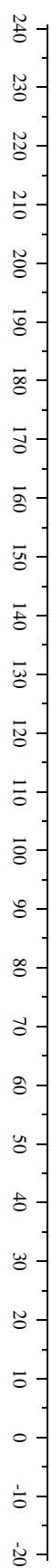
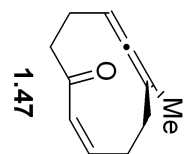


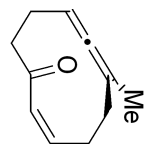
1.46



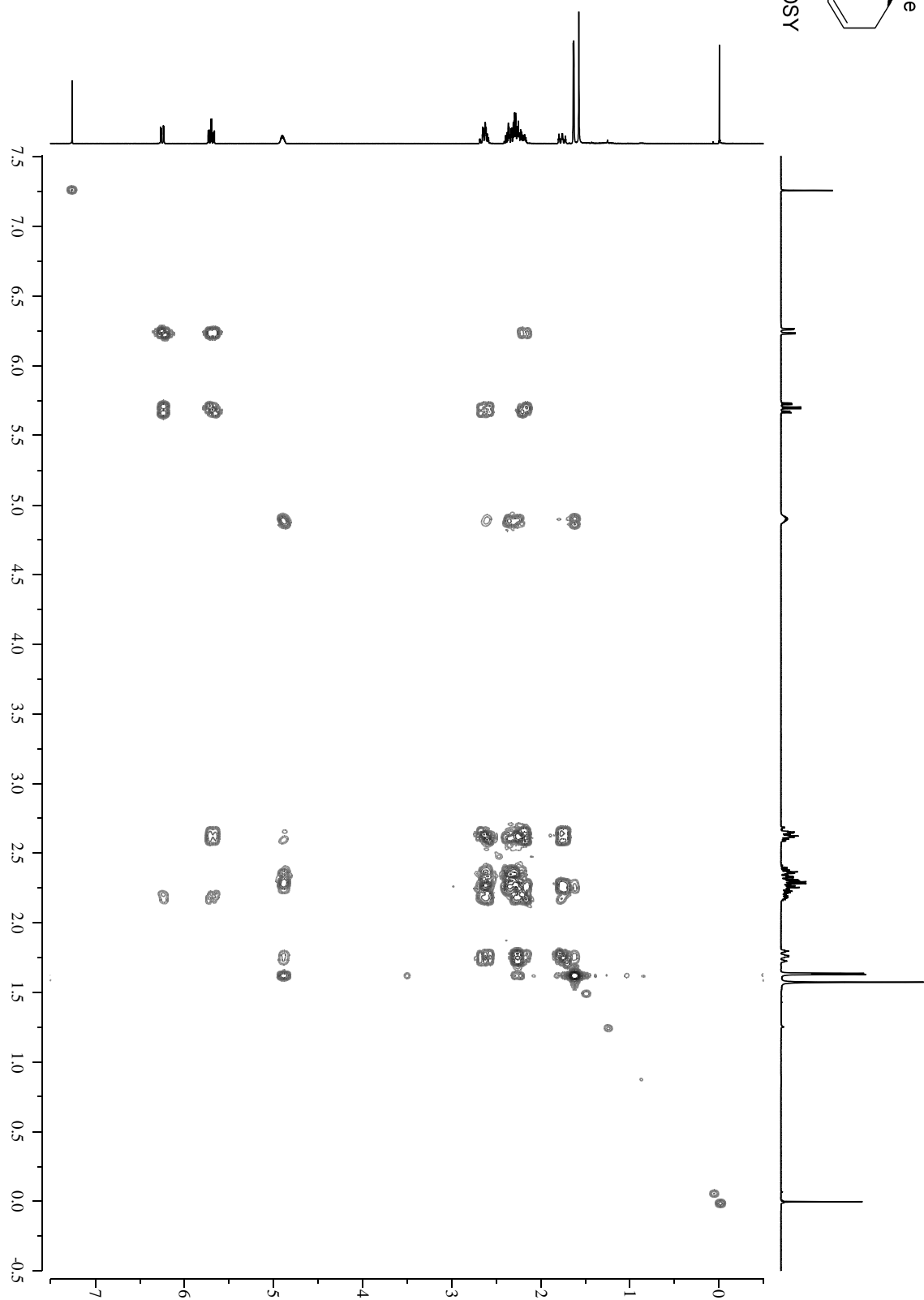


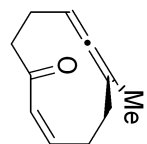




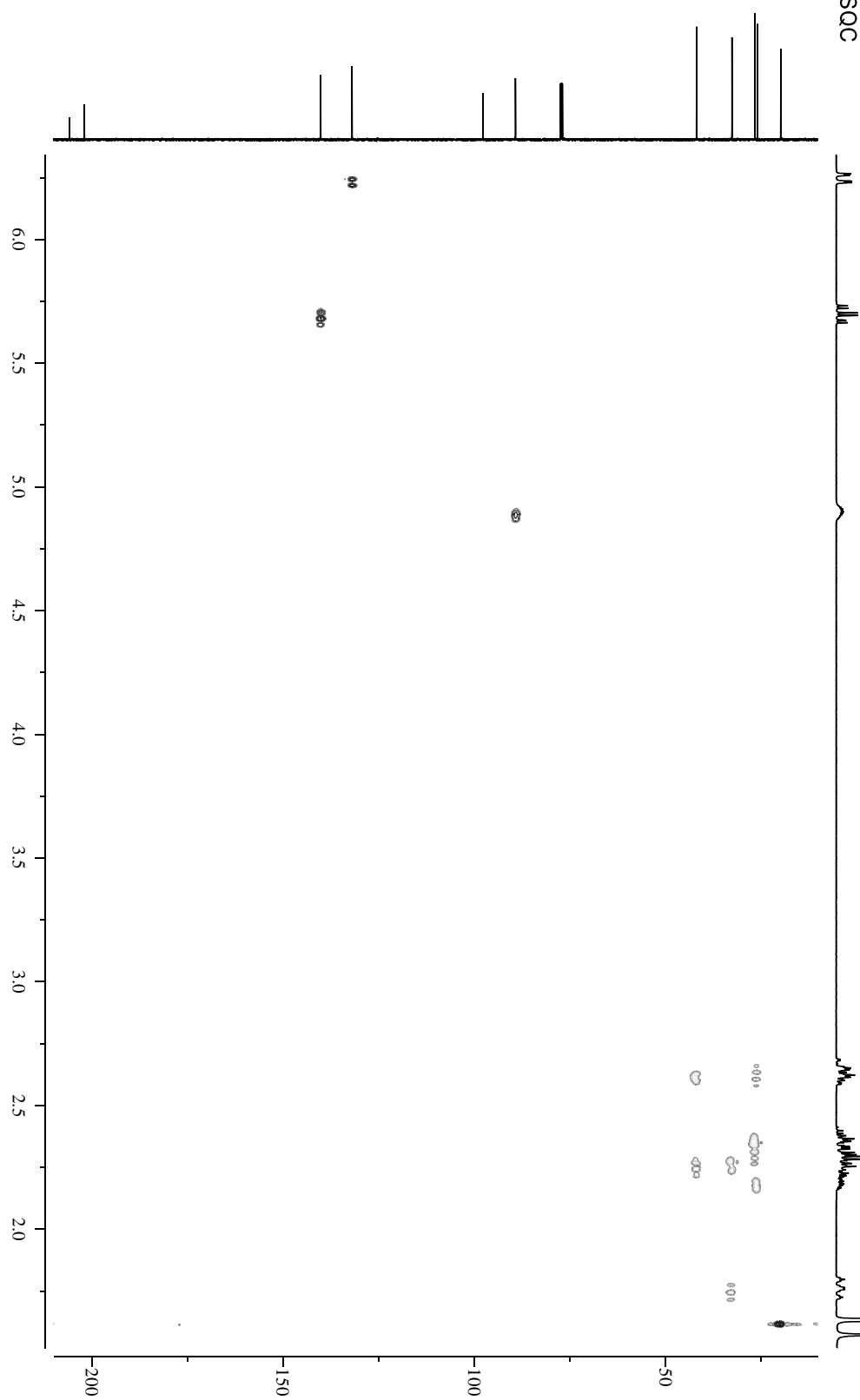


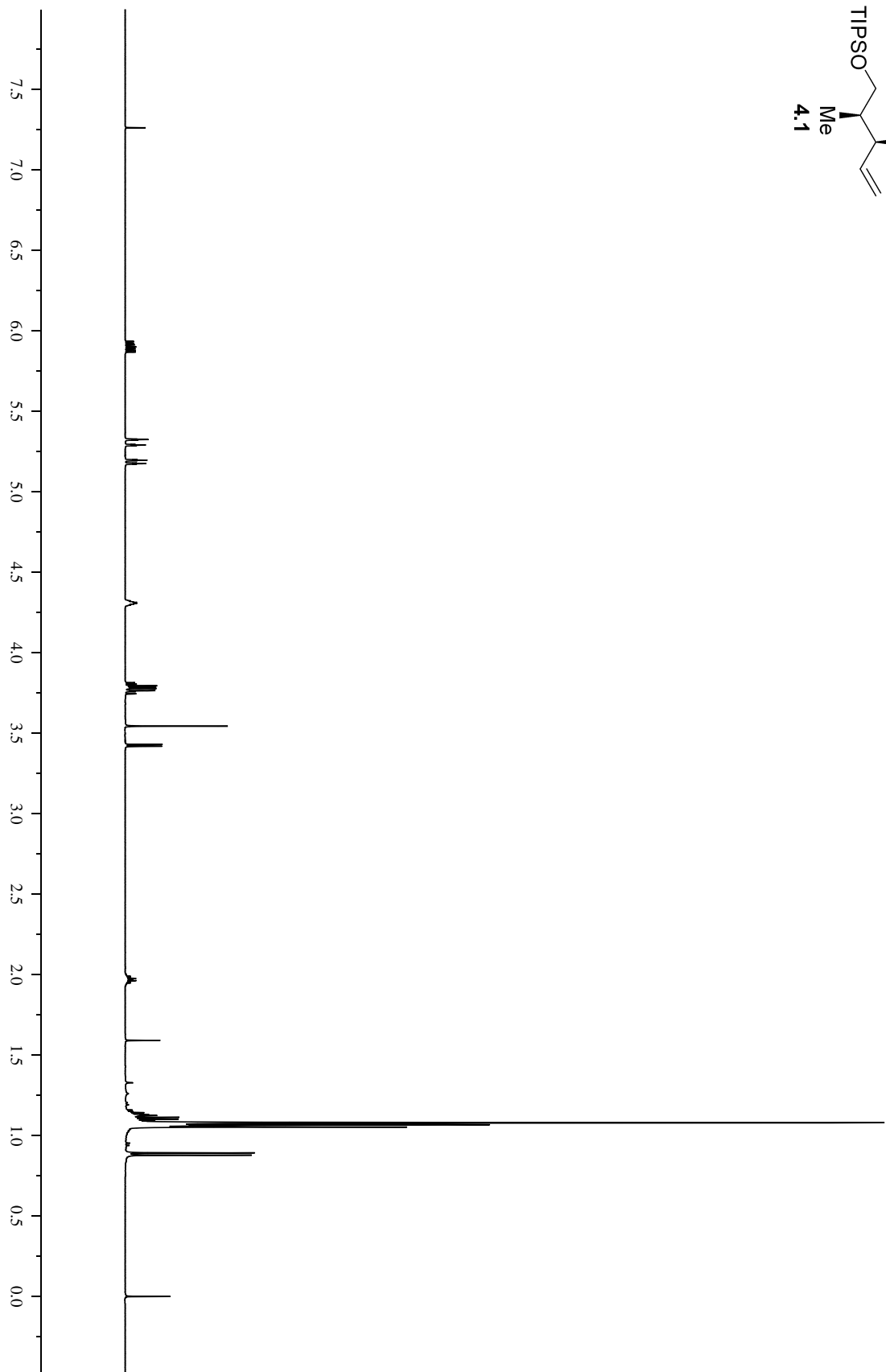
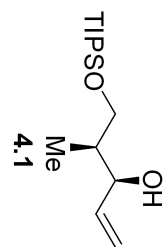
1.47 gcOSY

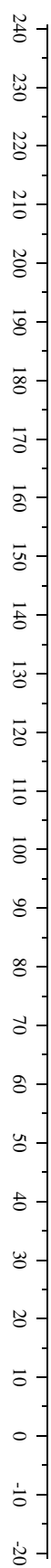
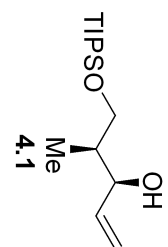


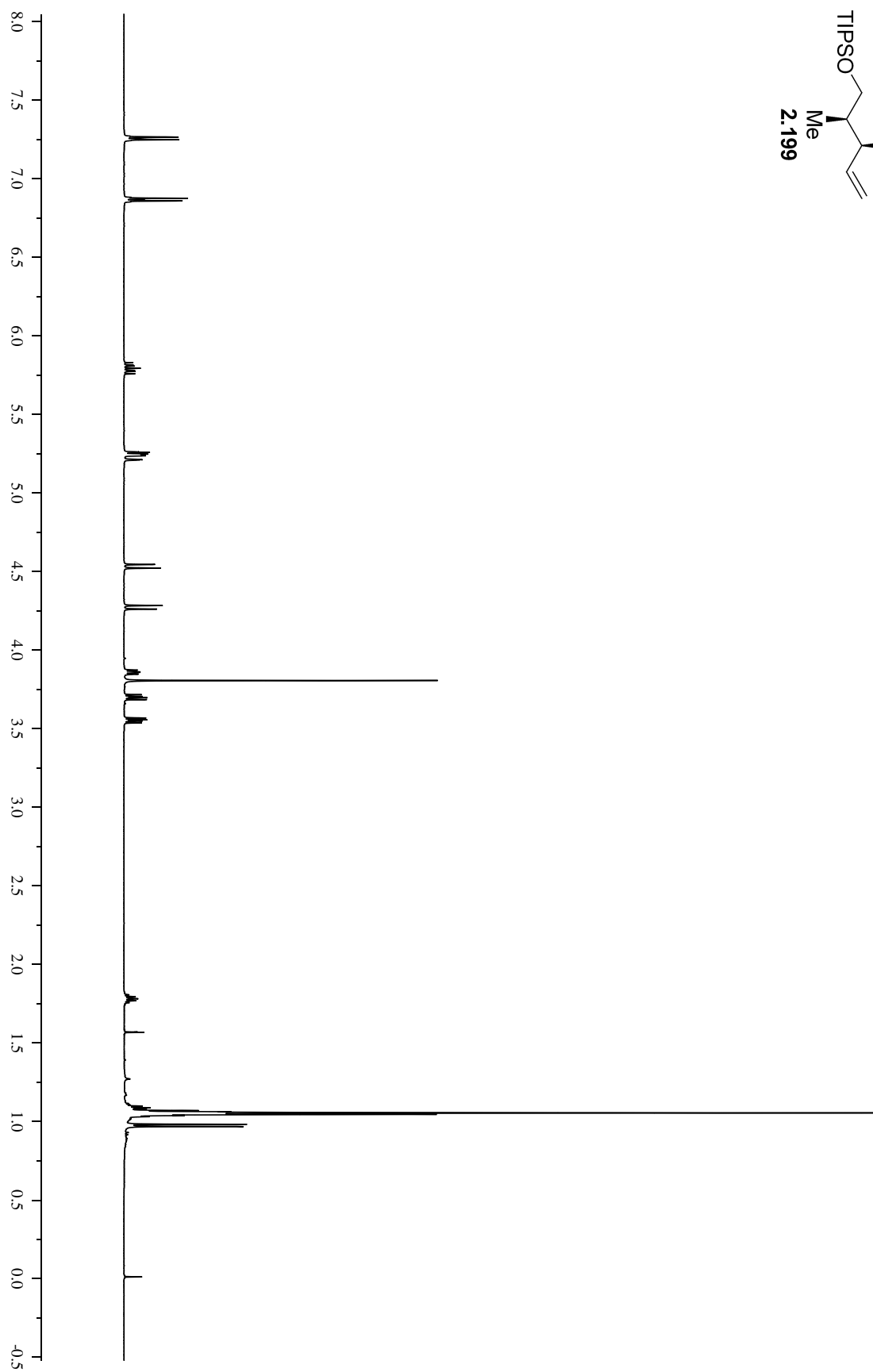
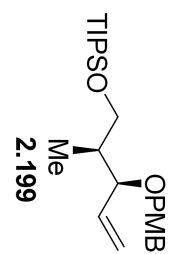


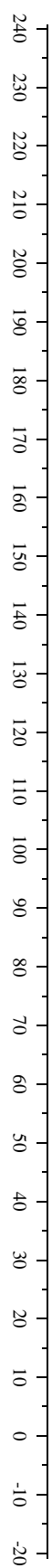
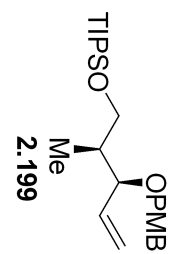
1.47 gHSQC

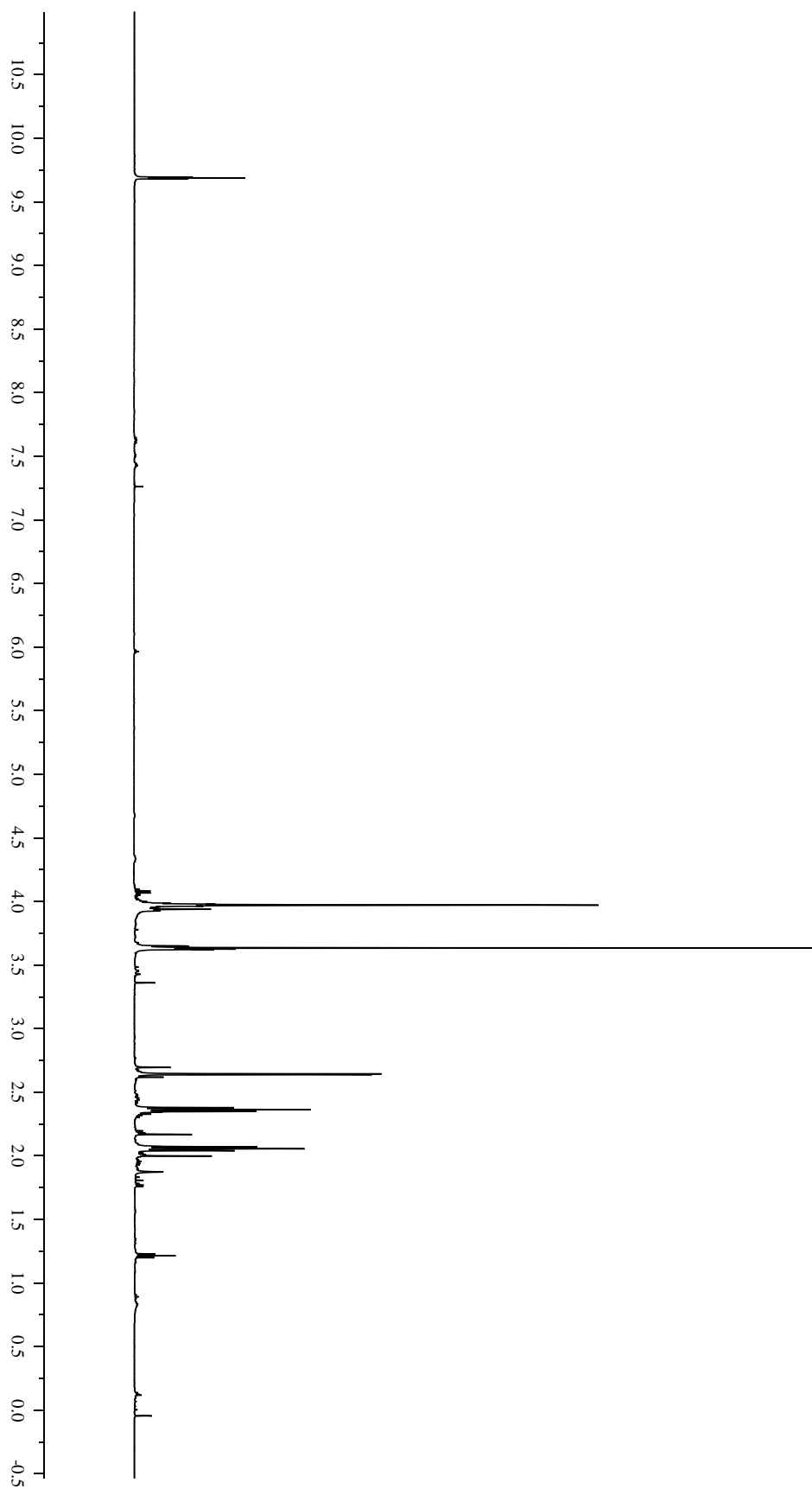
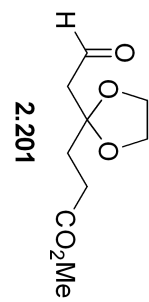


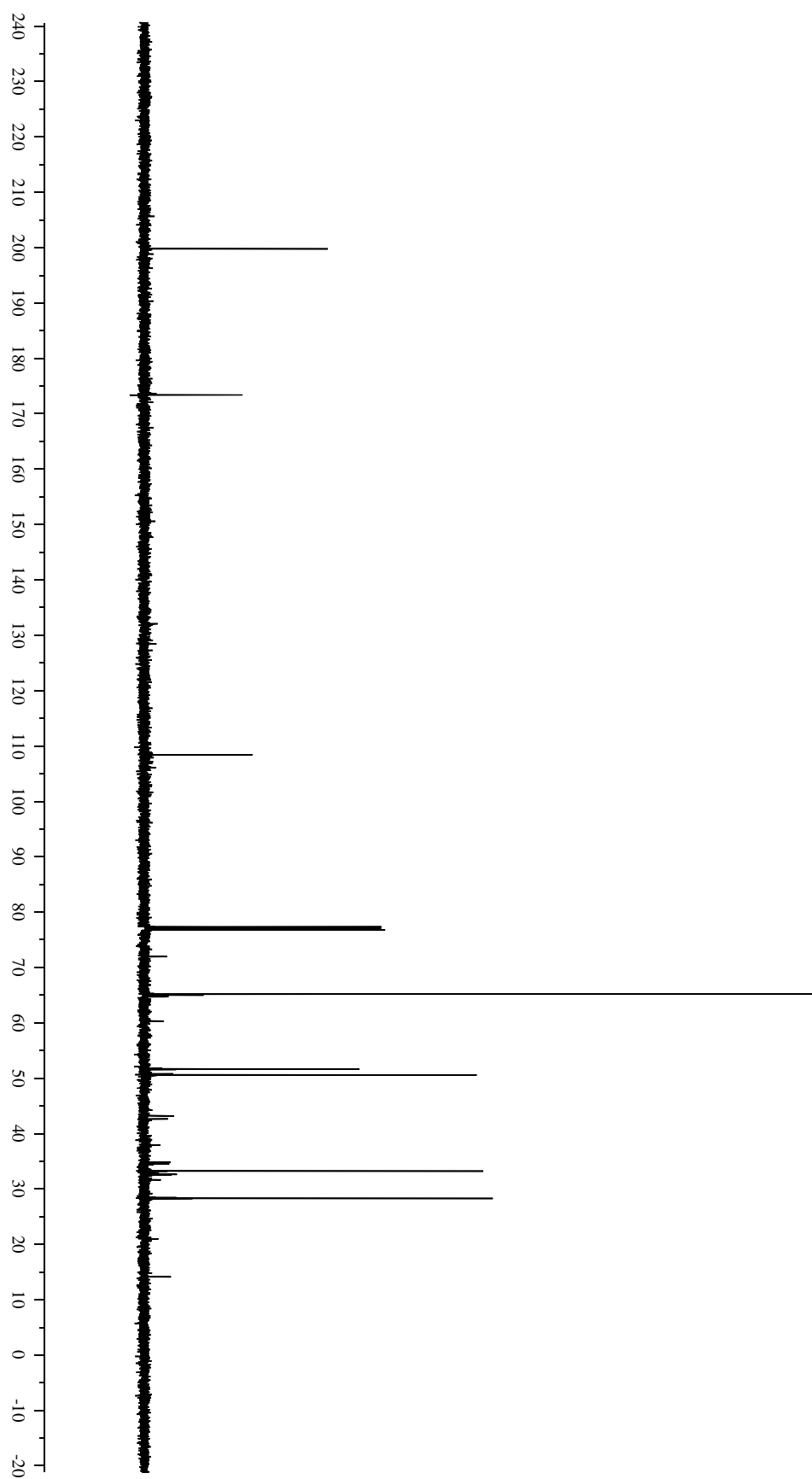
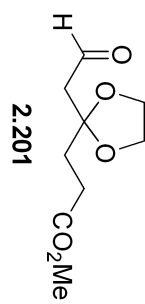


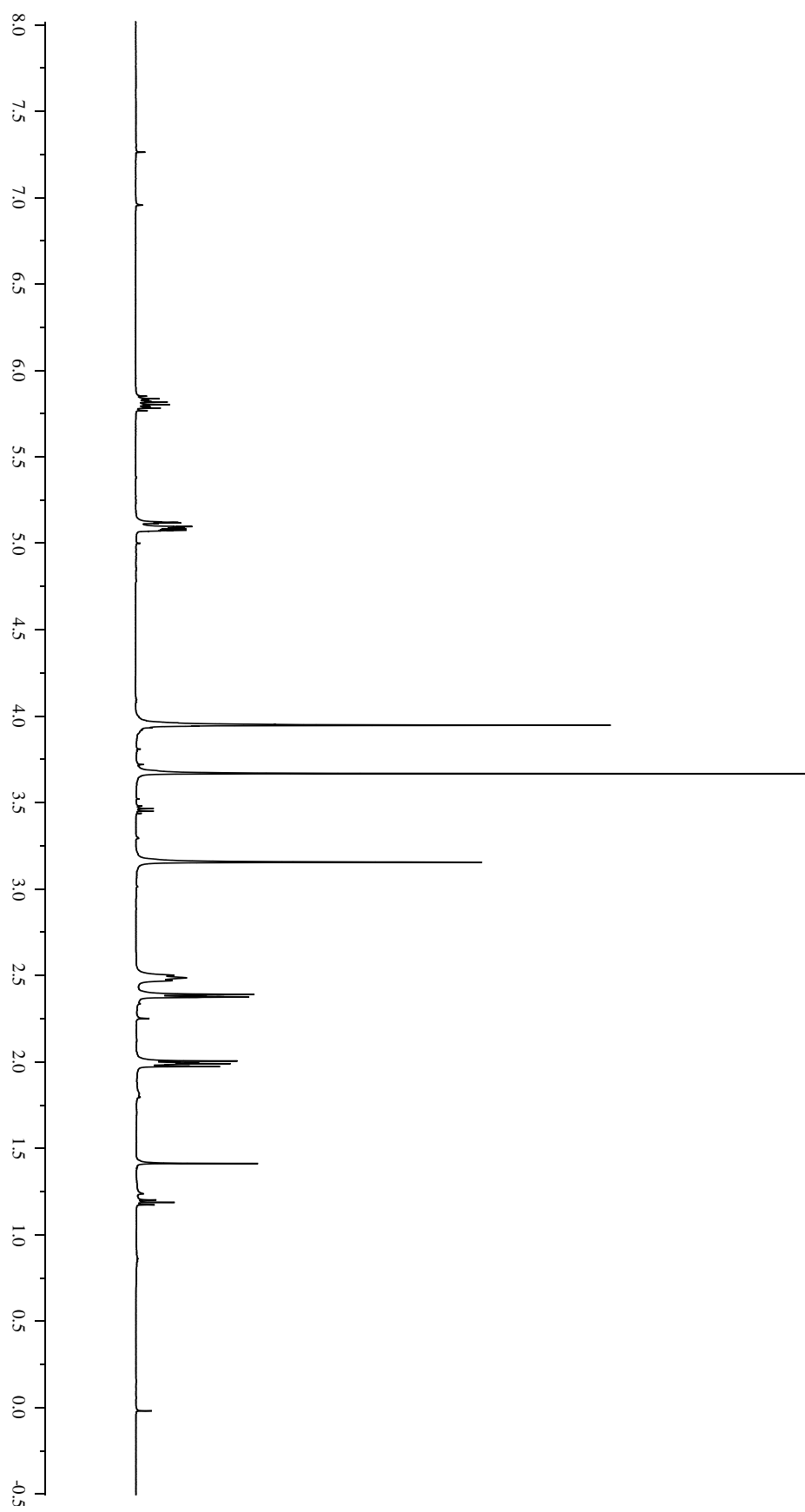
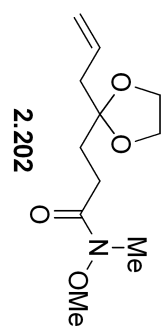


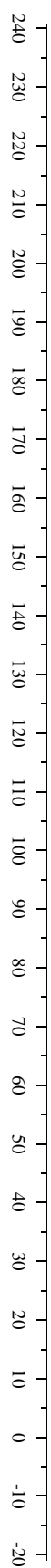
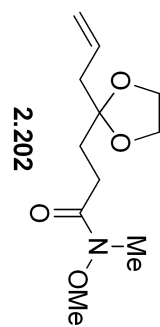


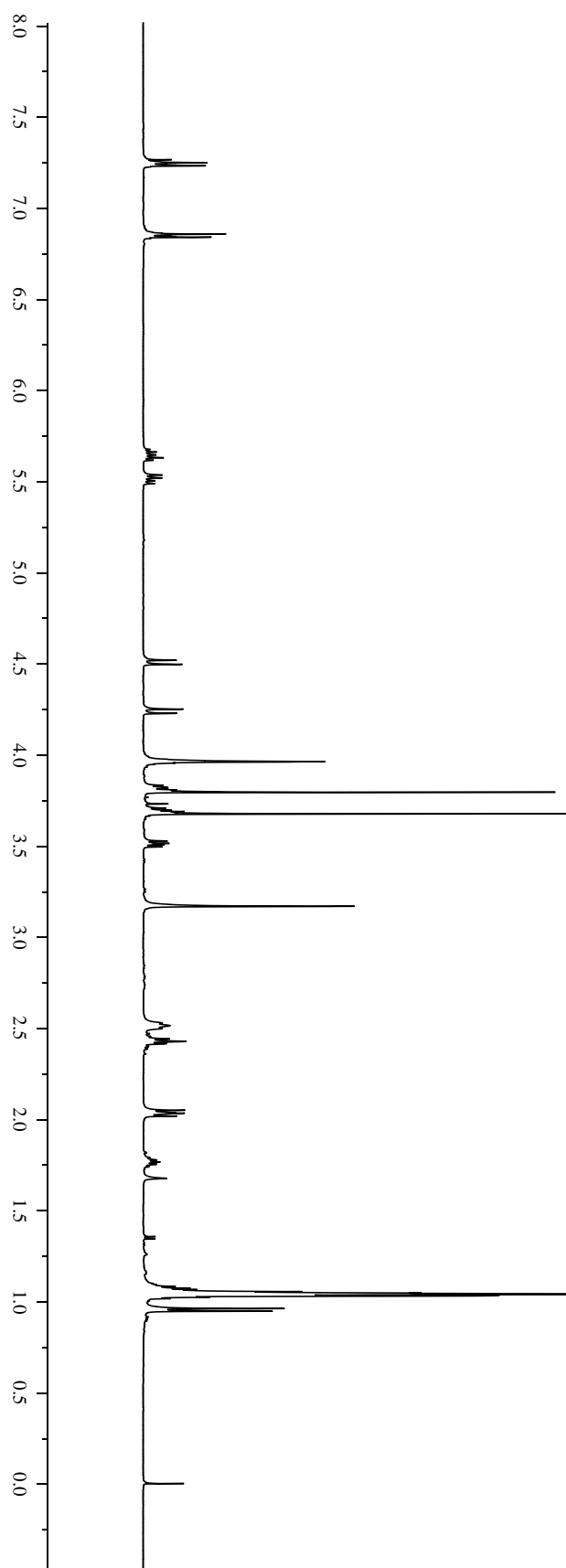
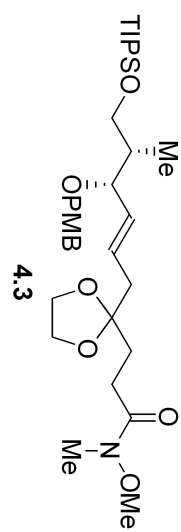


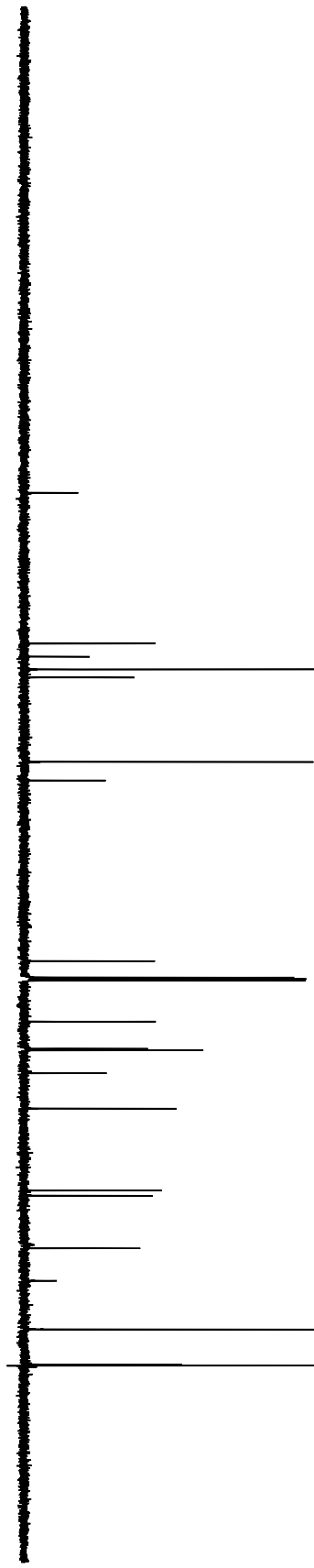


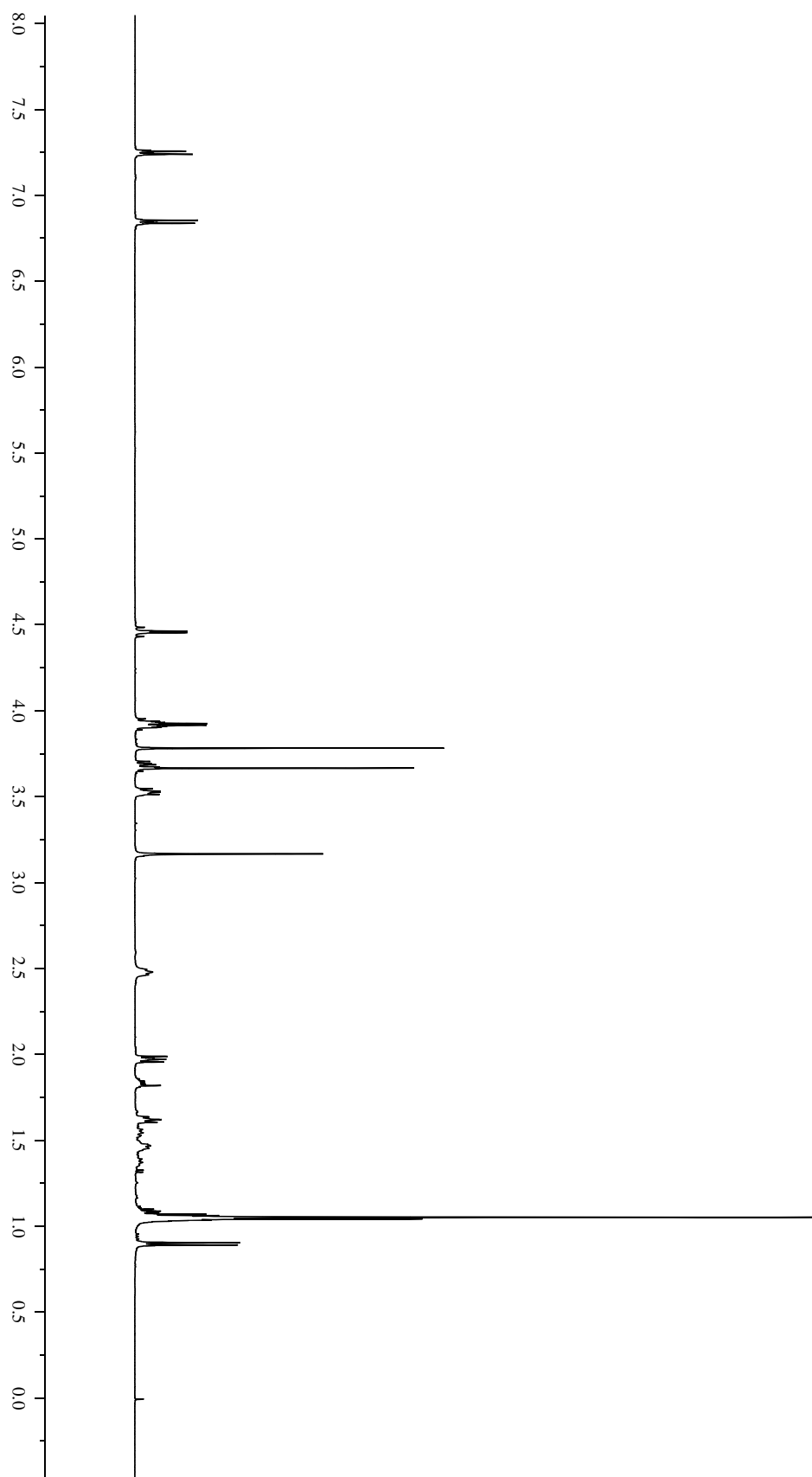
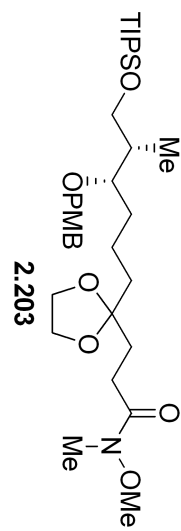


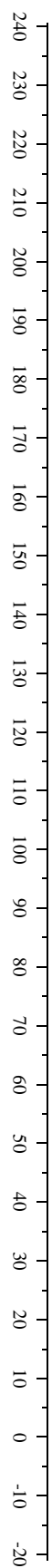


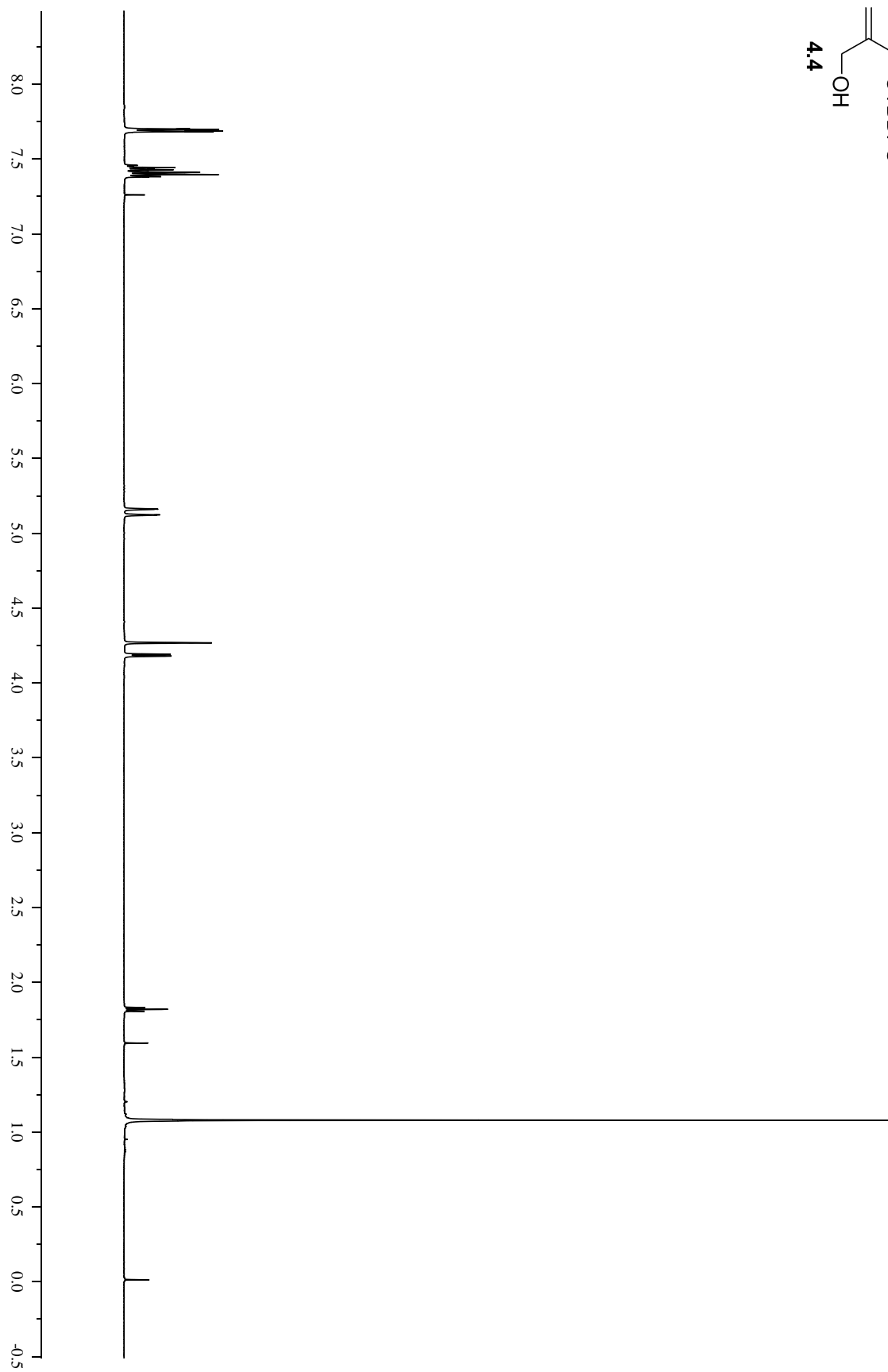
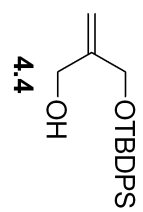


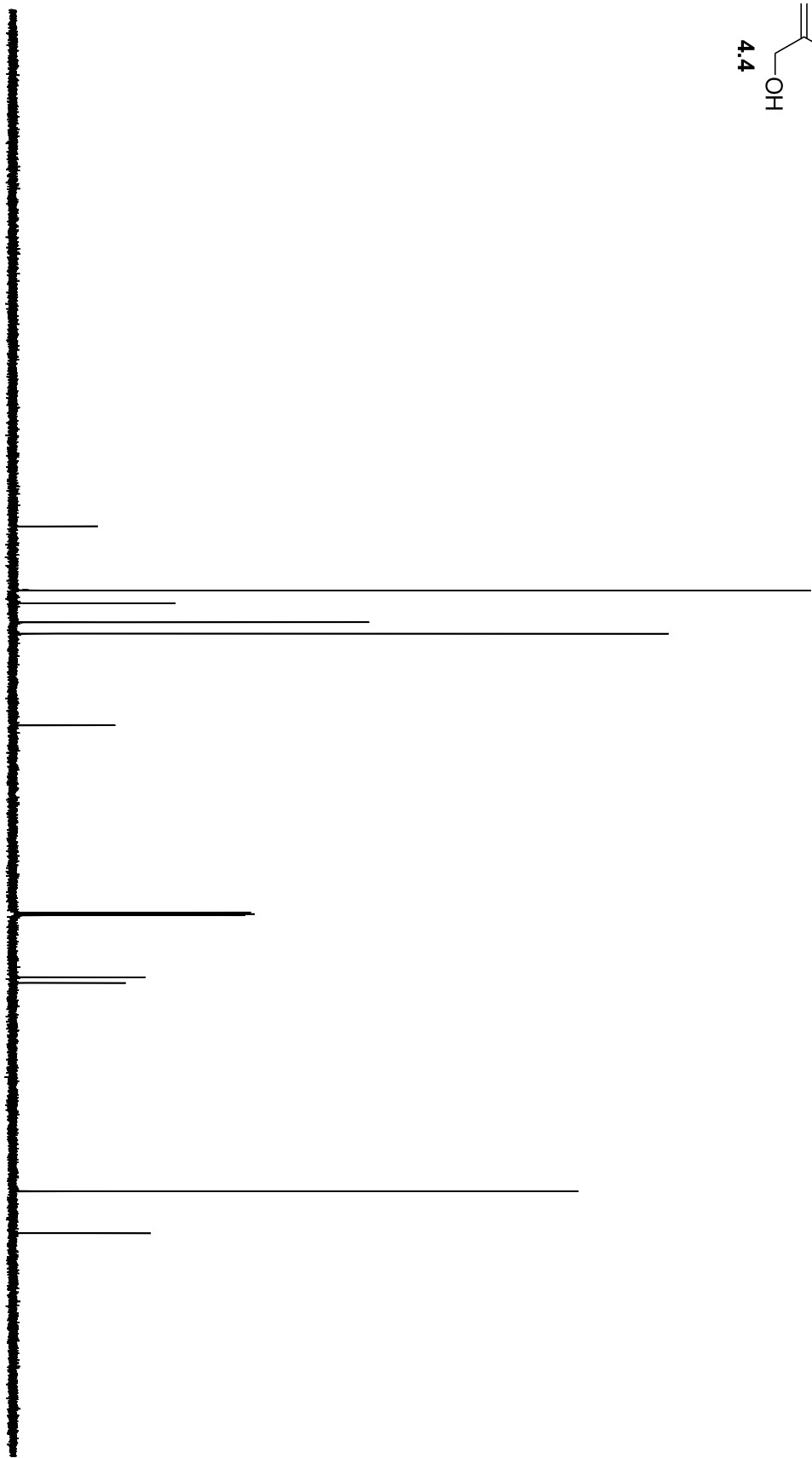


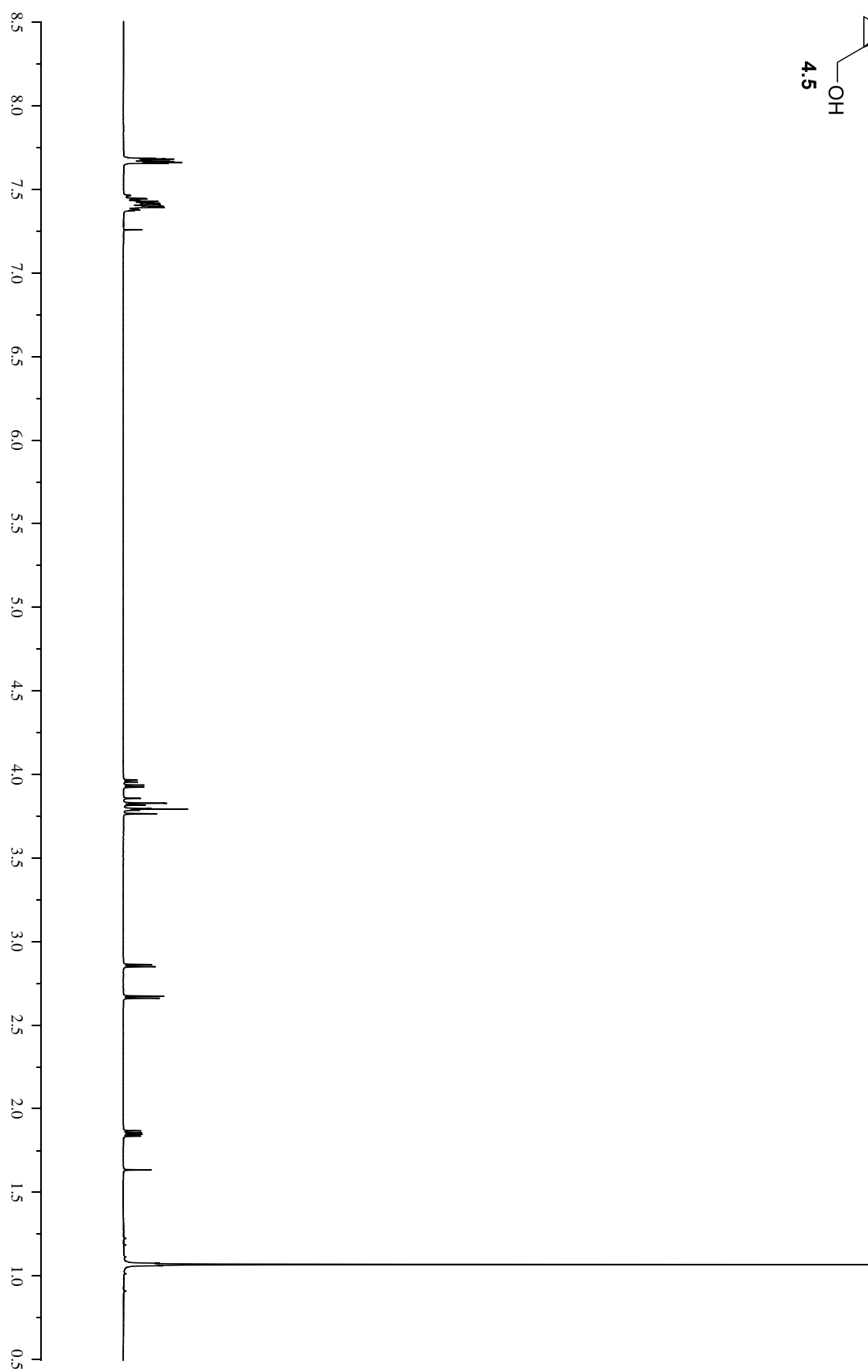
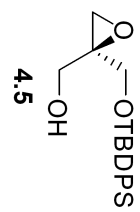


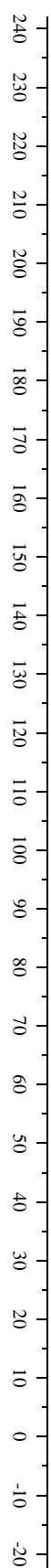
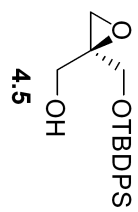


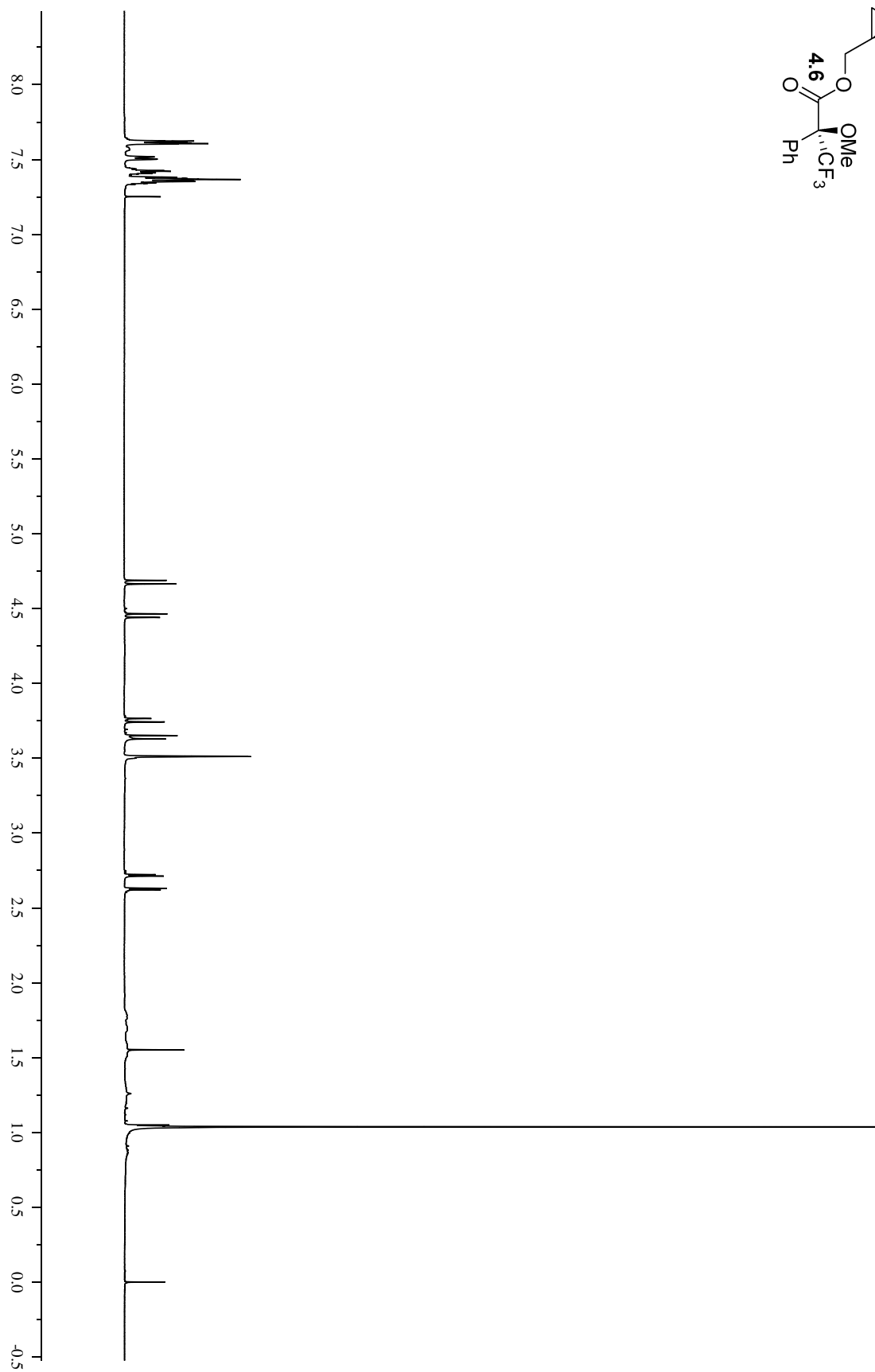
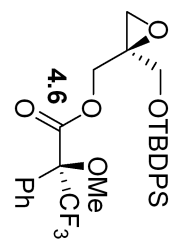


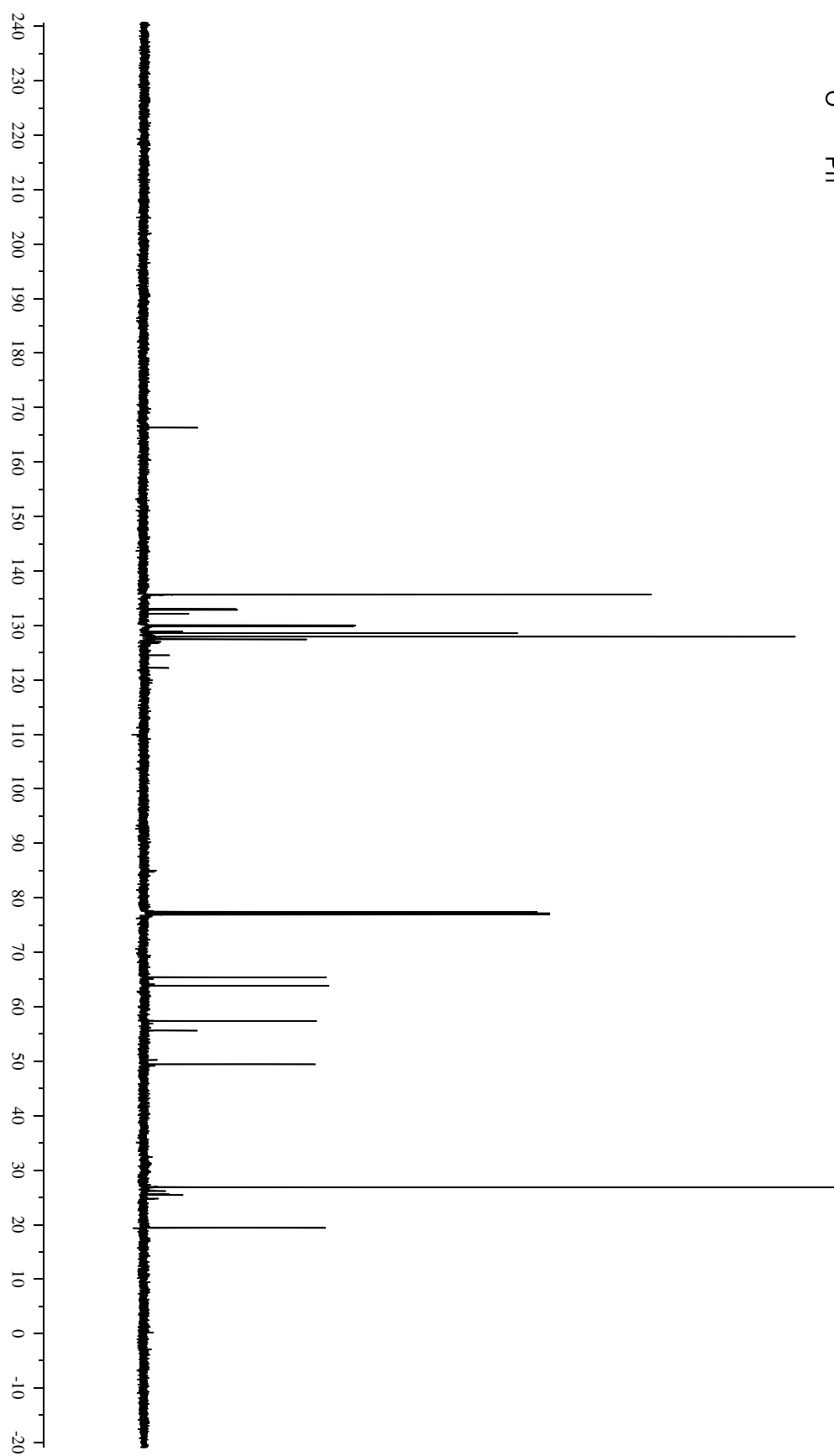
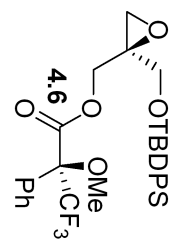


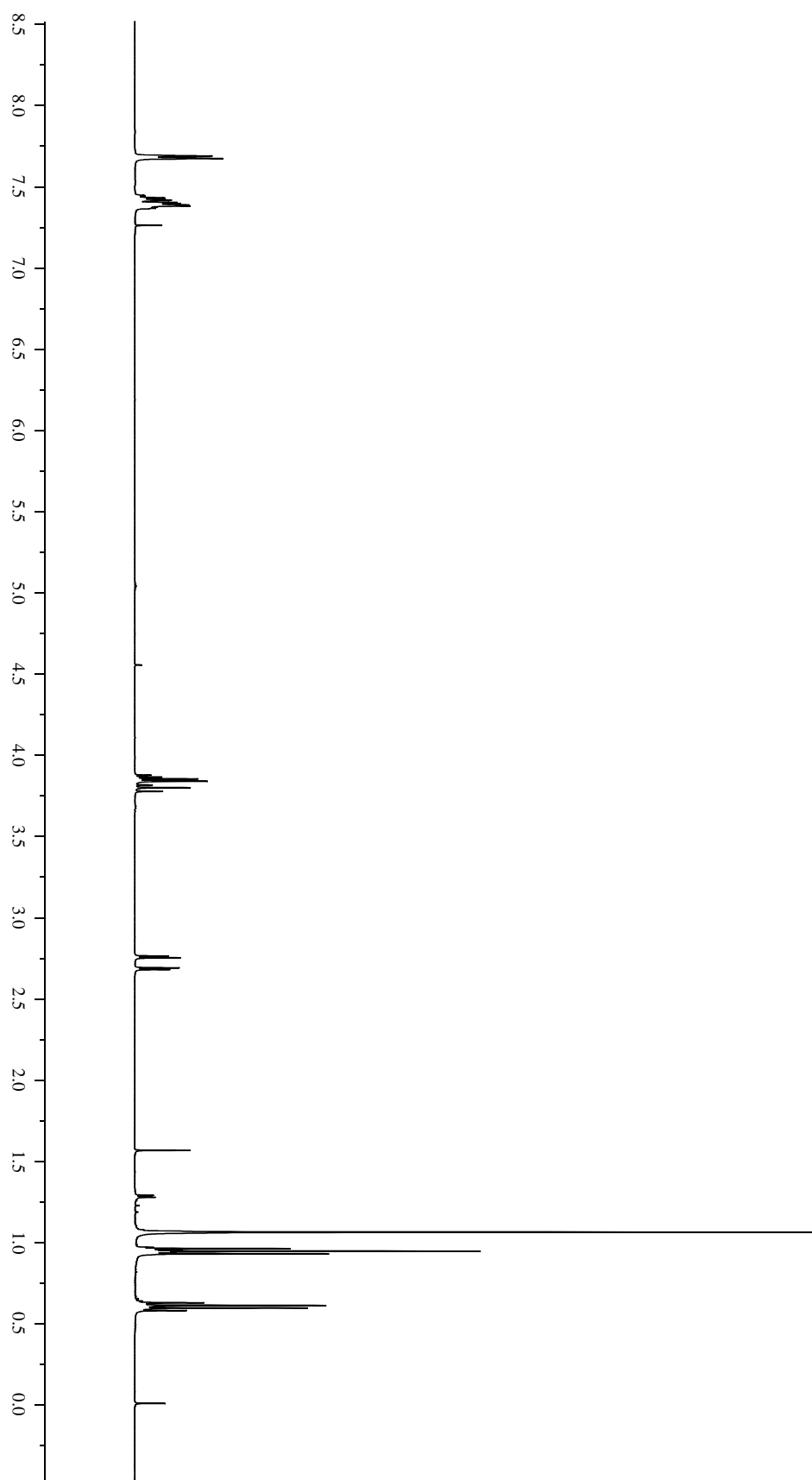
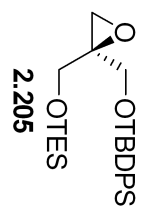


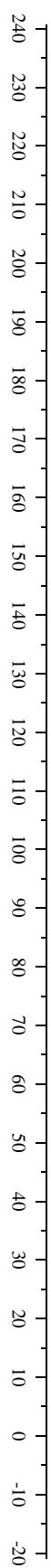
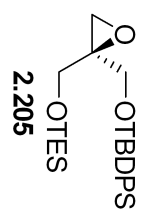


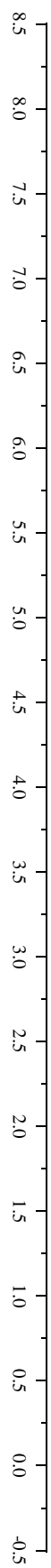
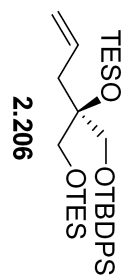


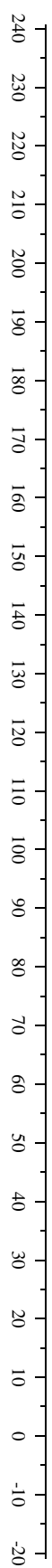
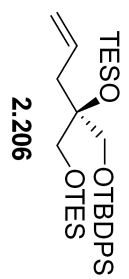


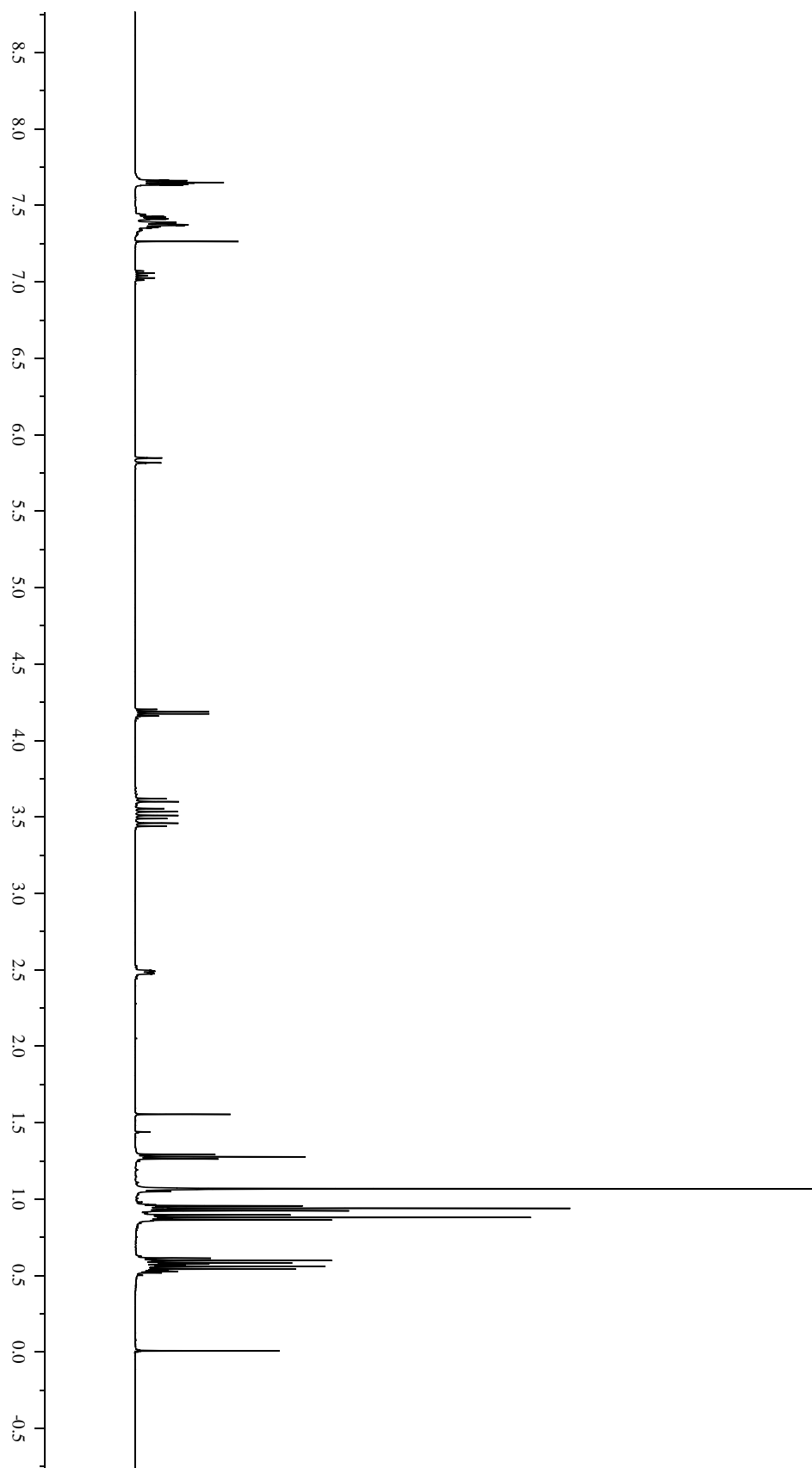
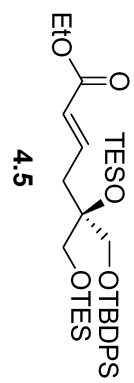


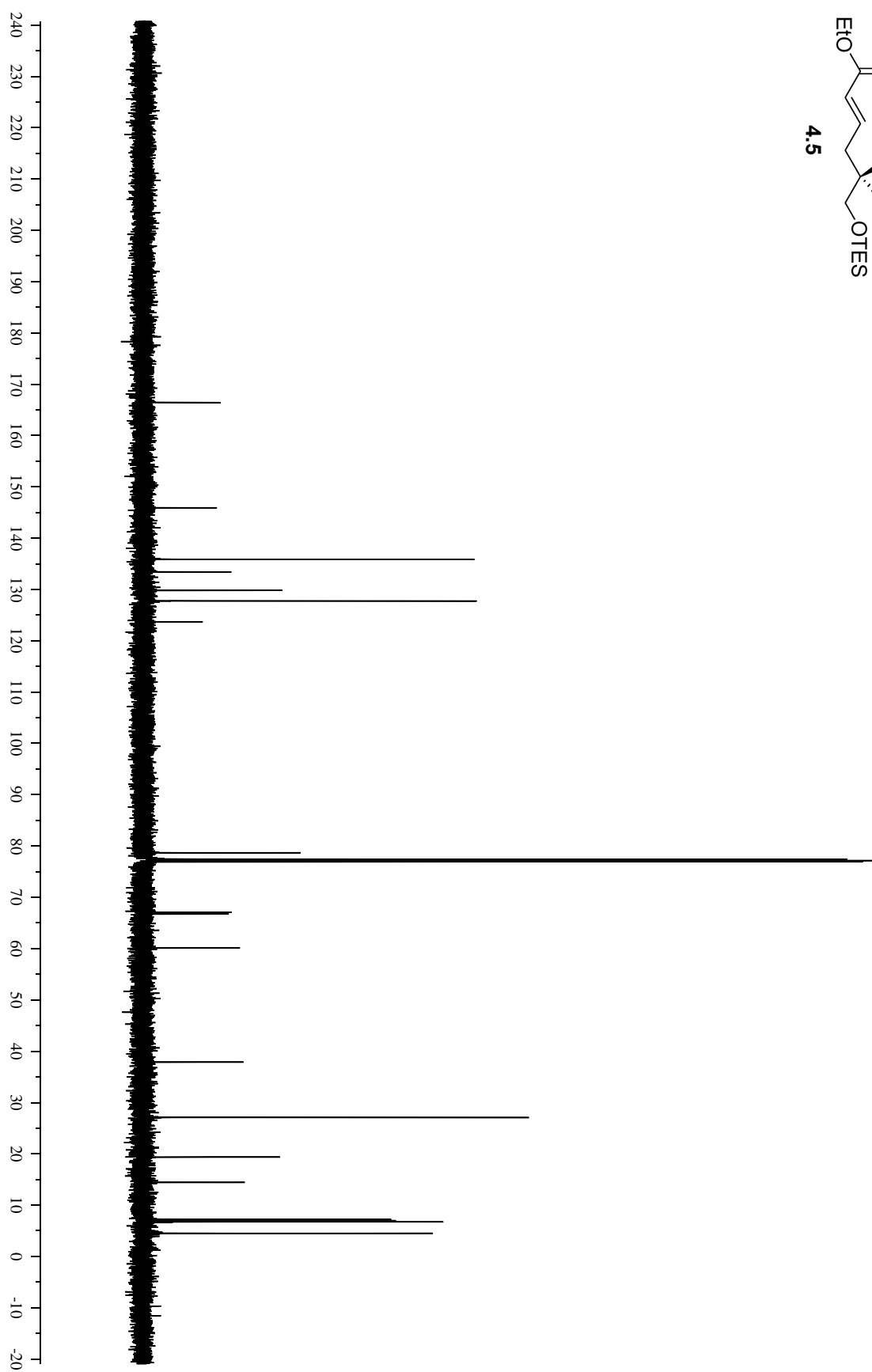
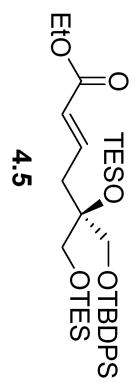


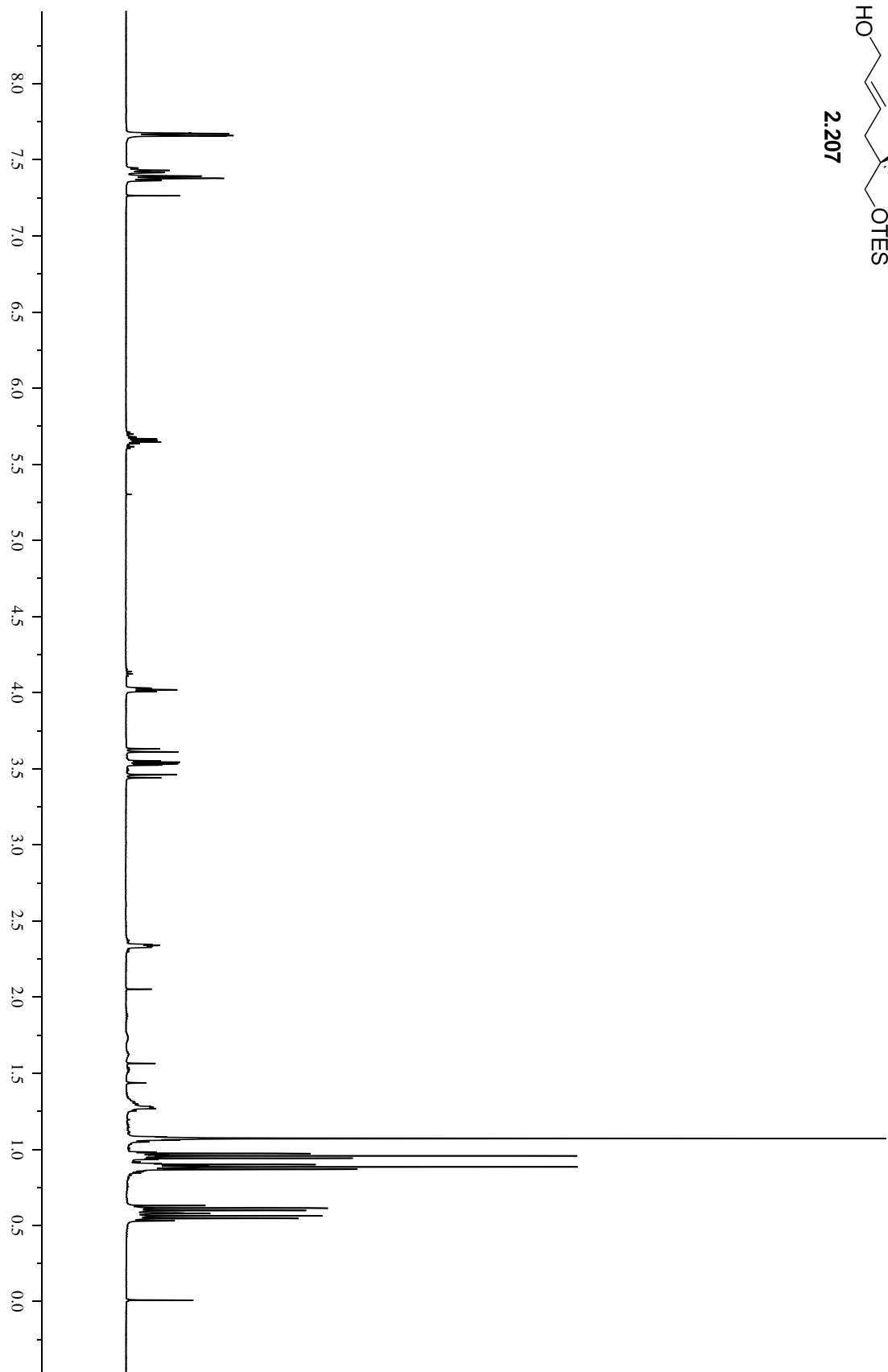


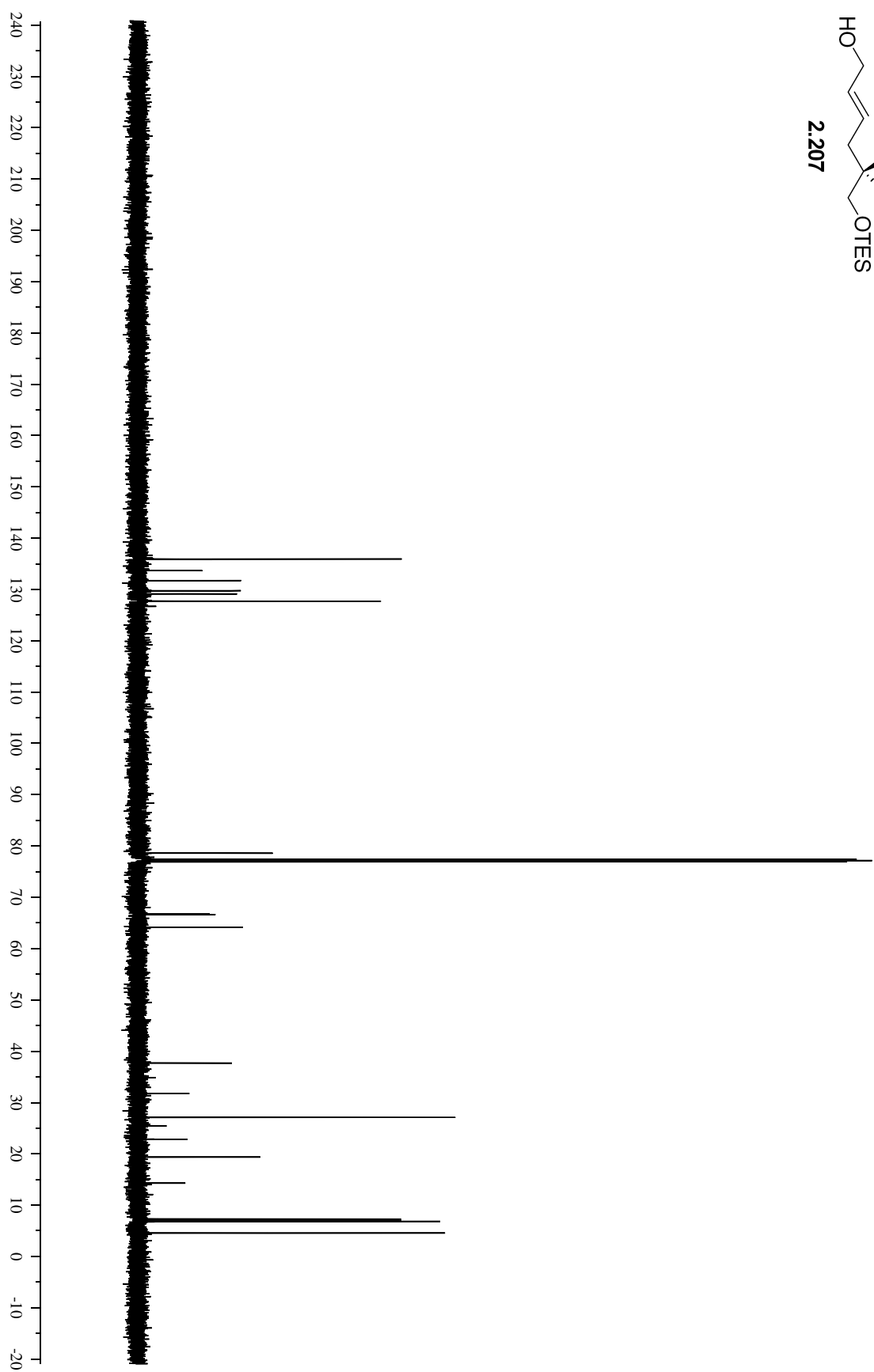


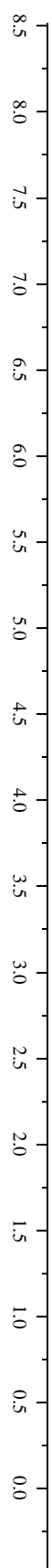
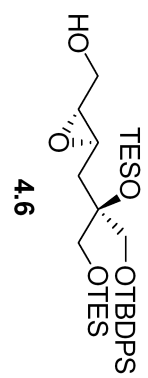


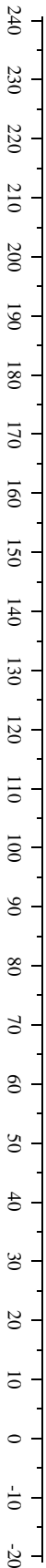
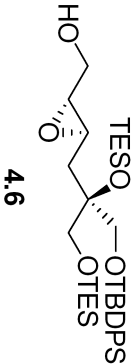


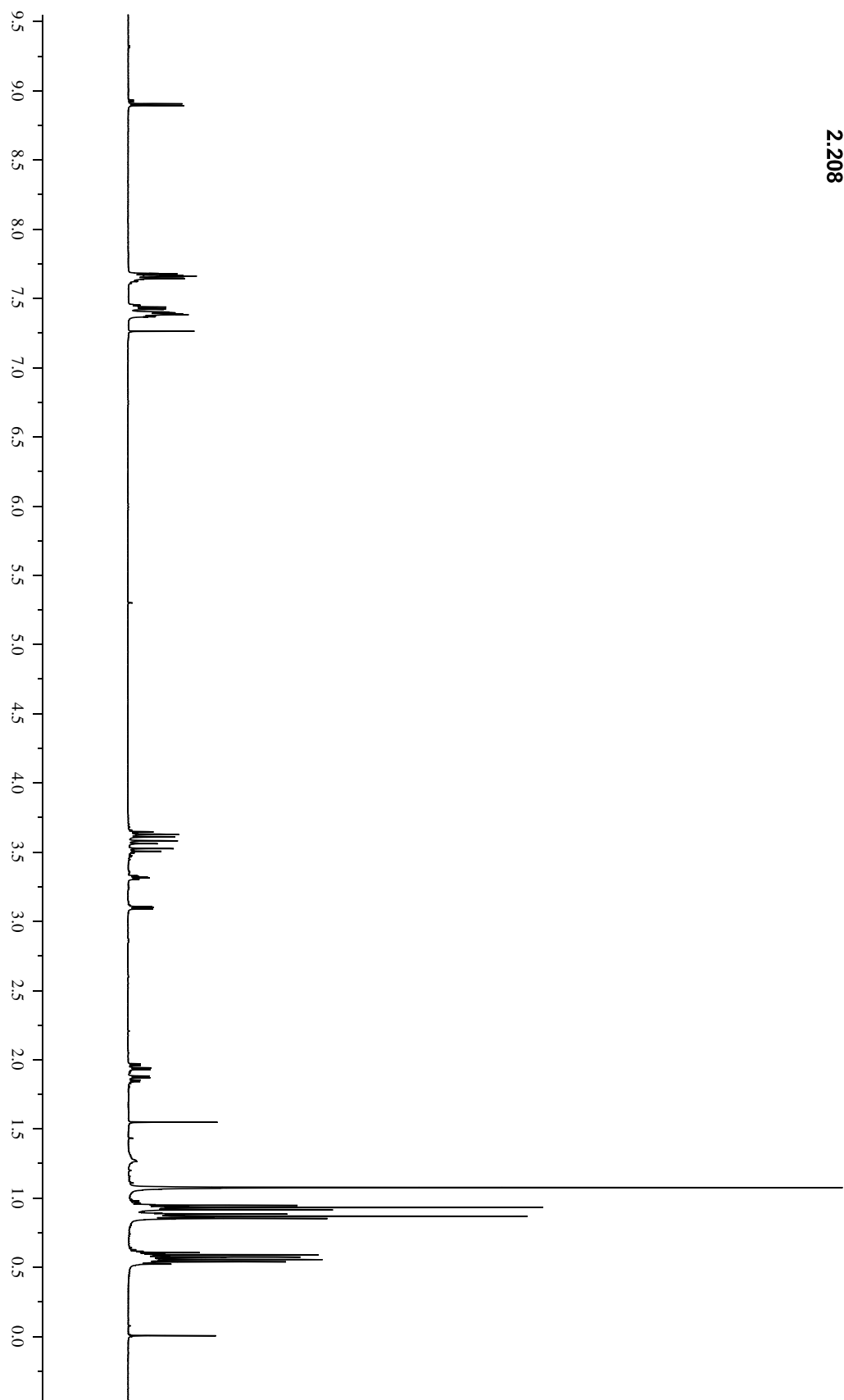
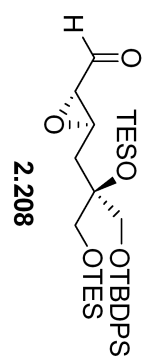


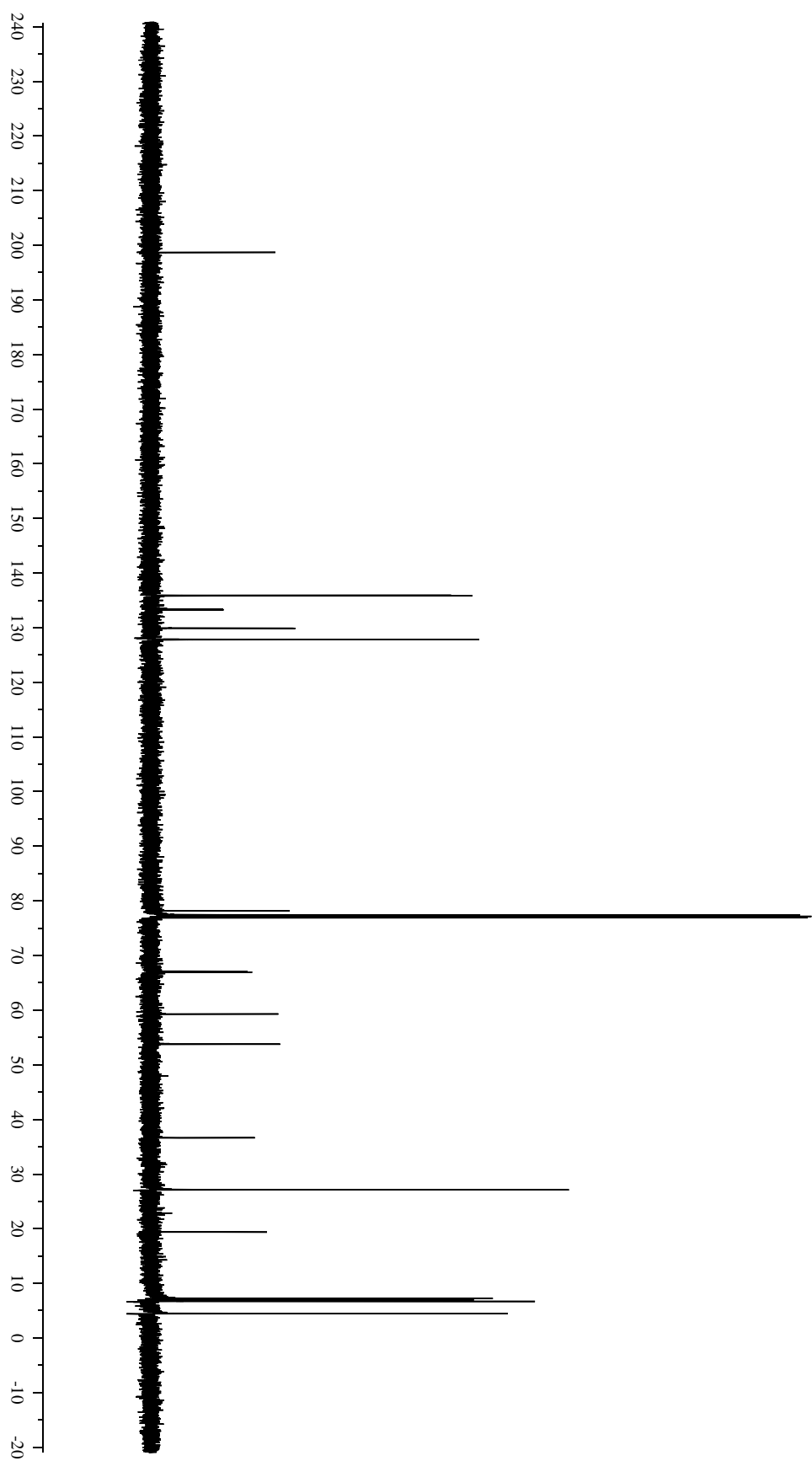
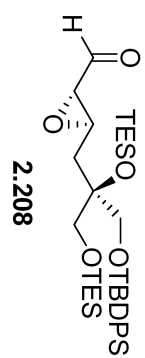


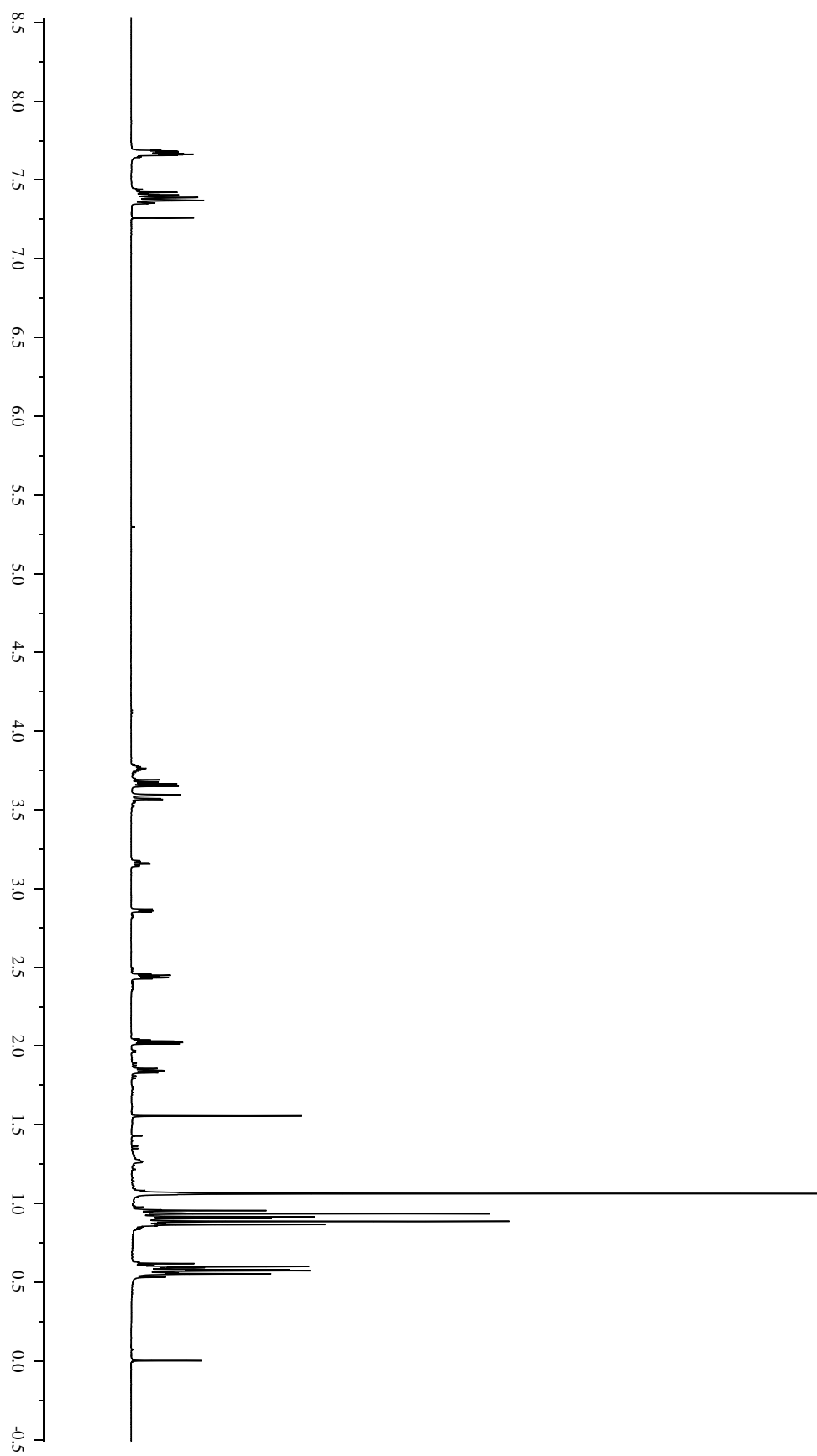
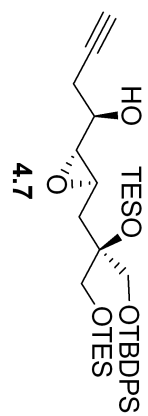


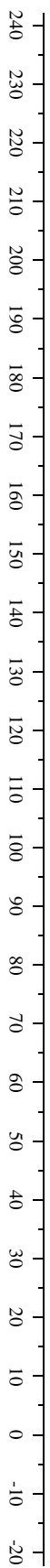
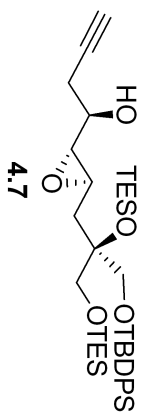


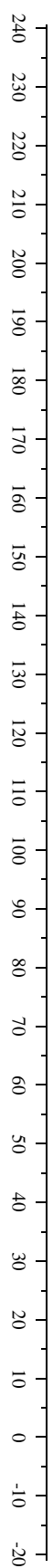
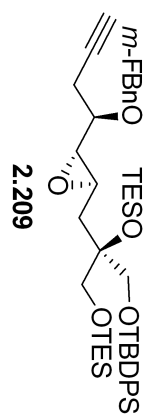


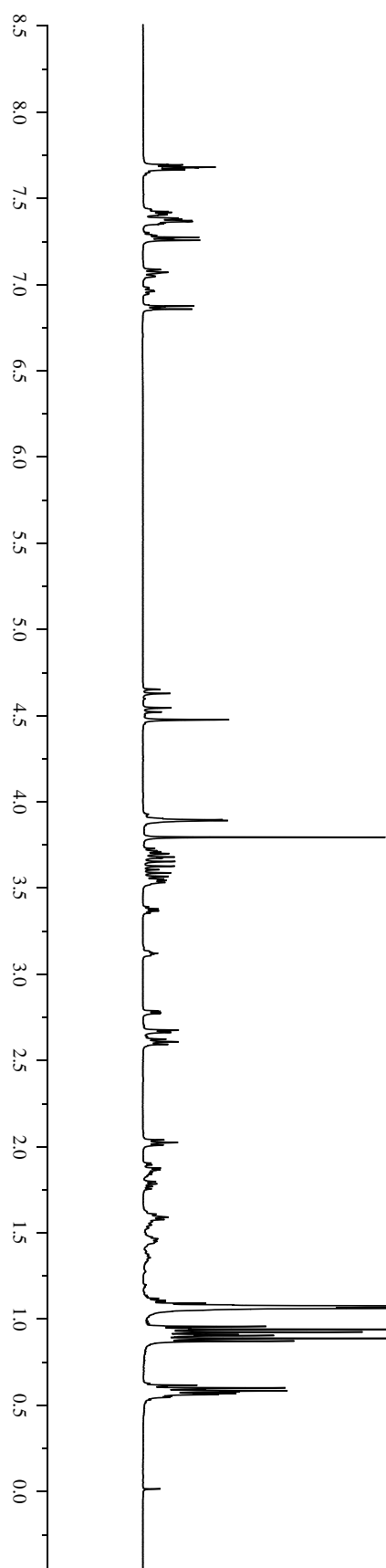
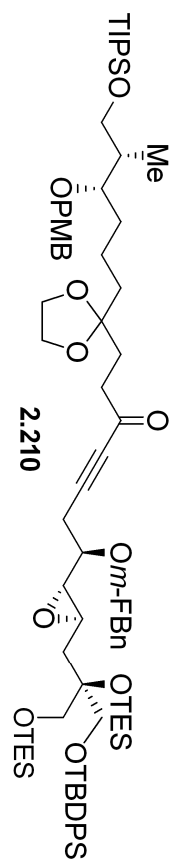


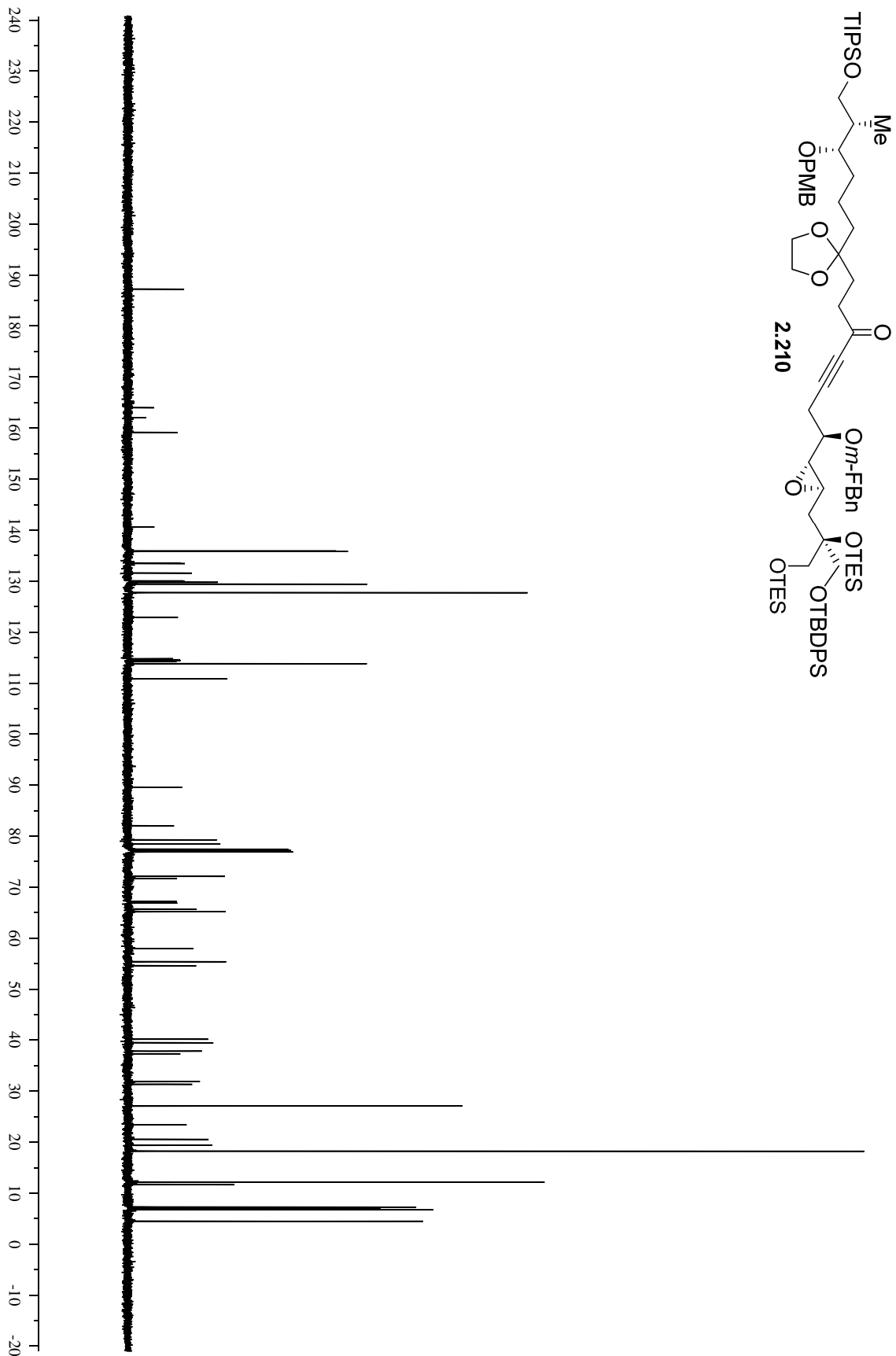


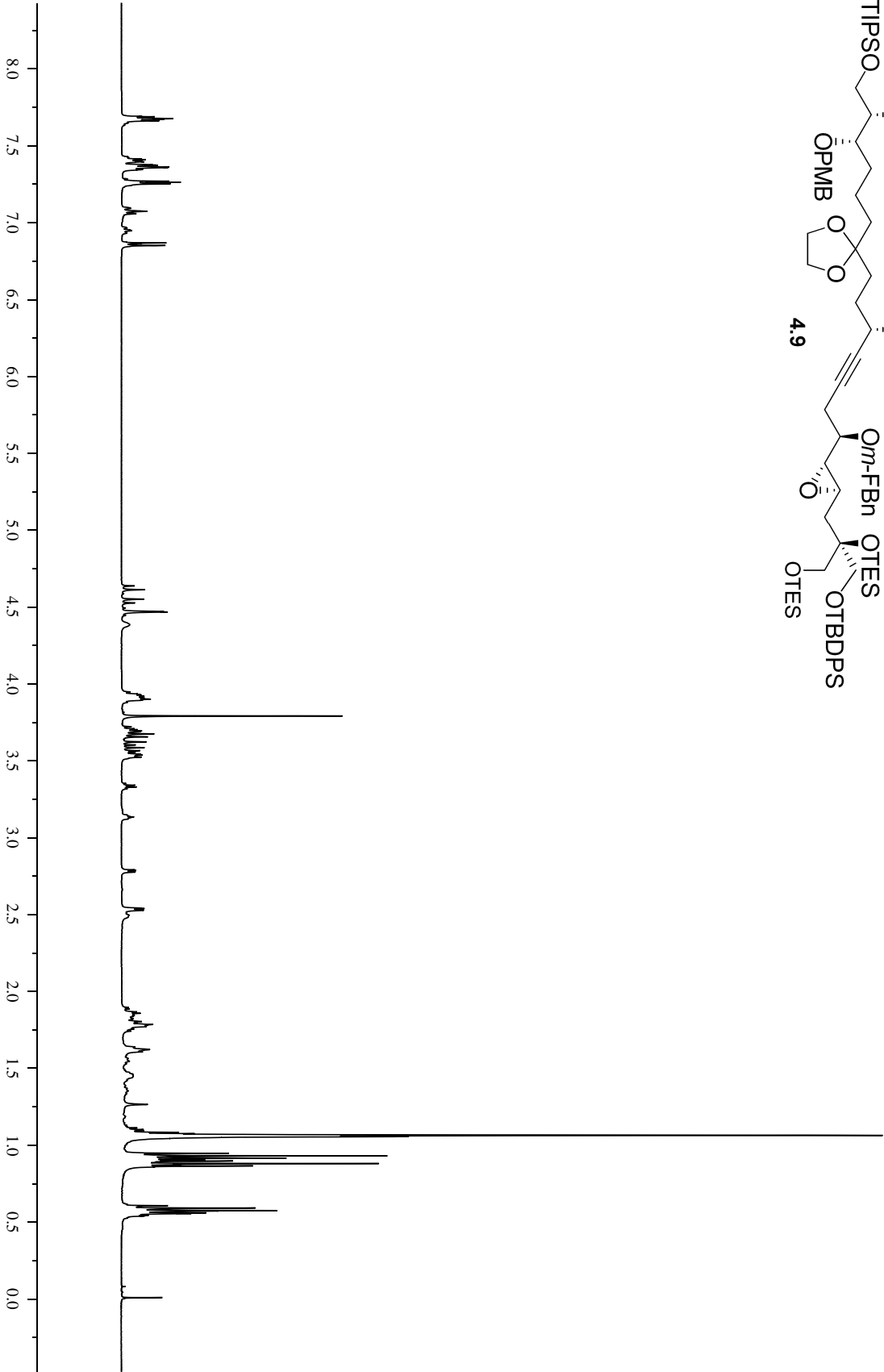
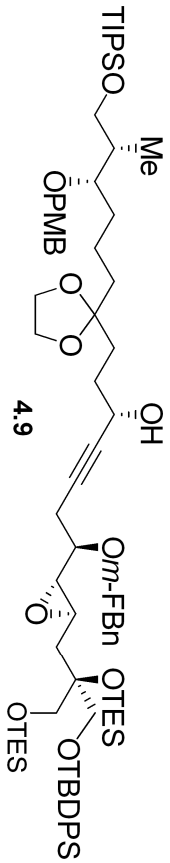


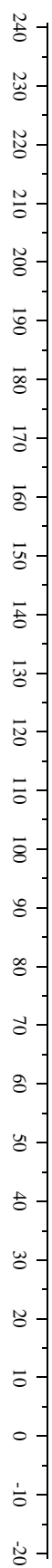
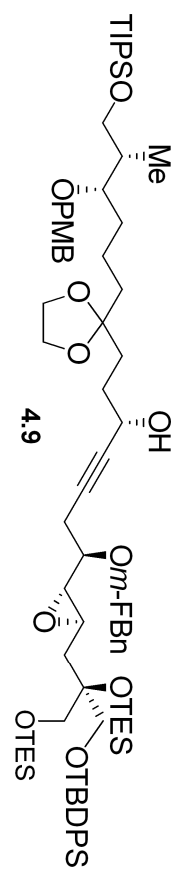


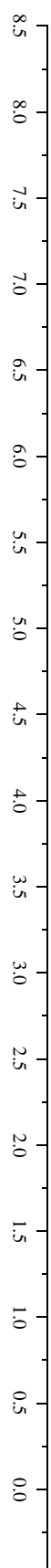
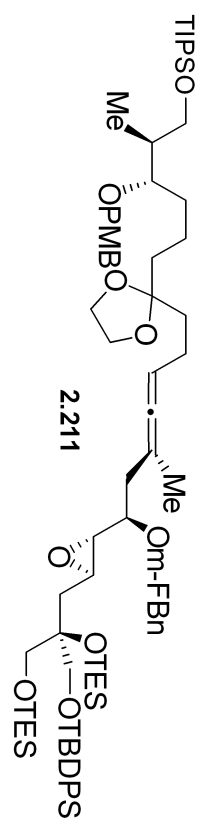


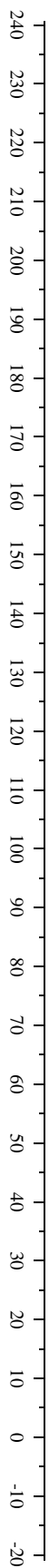


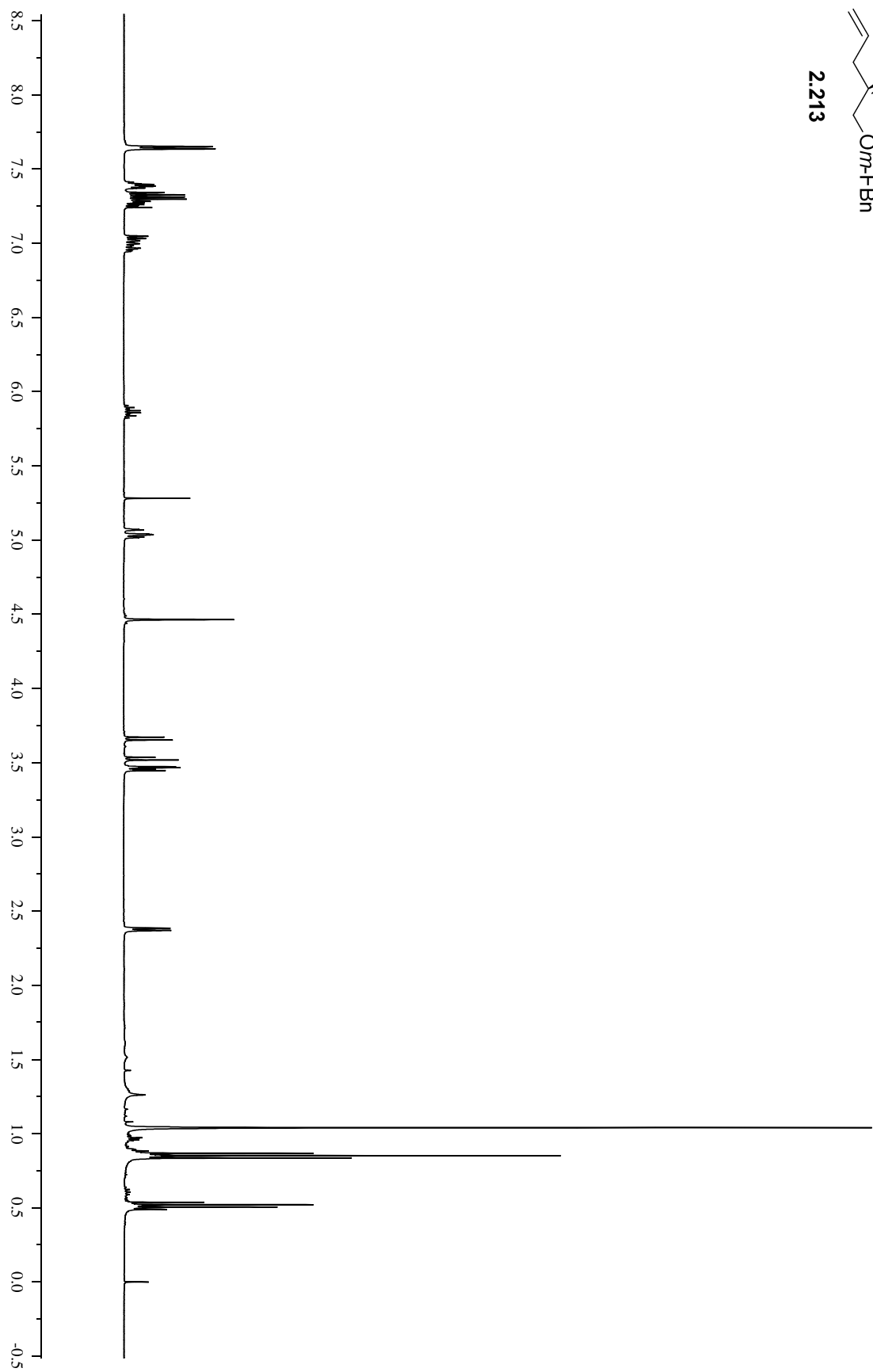
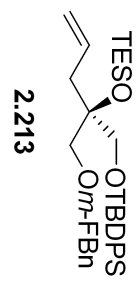


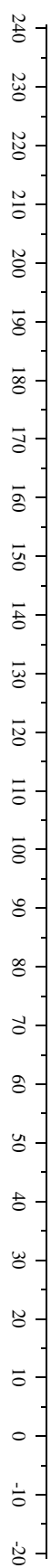
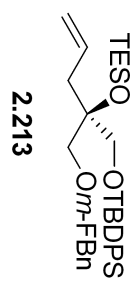


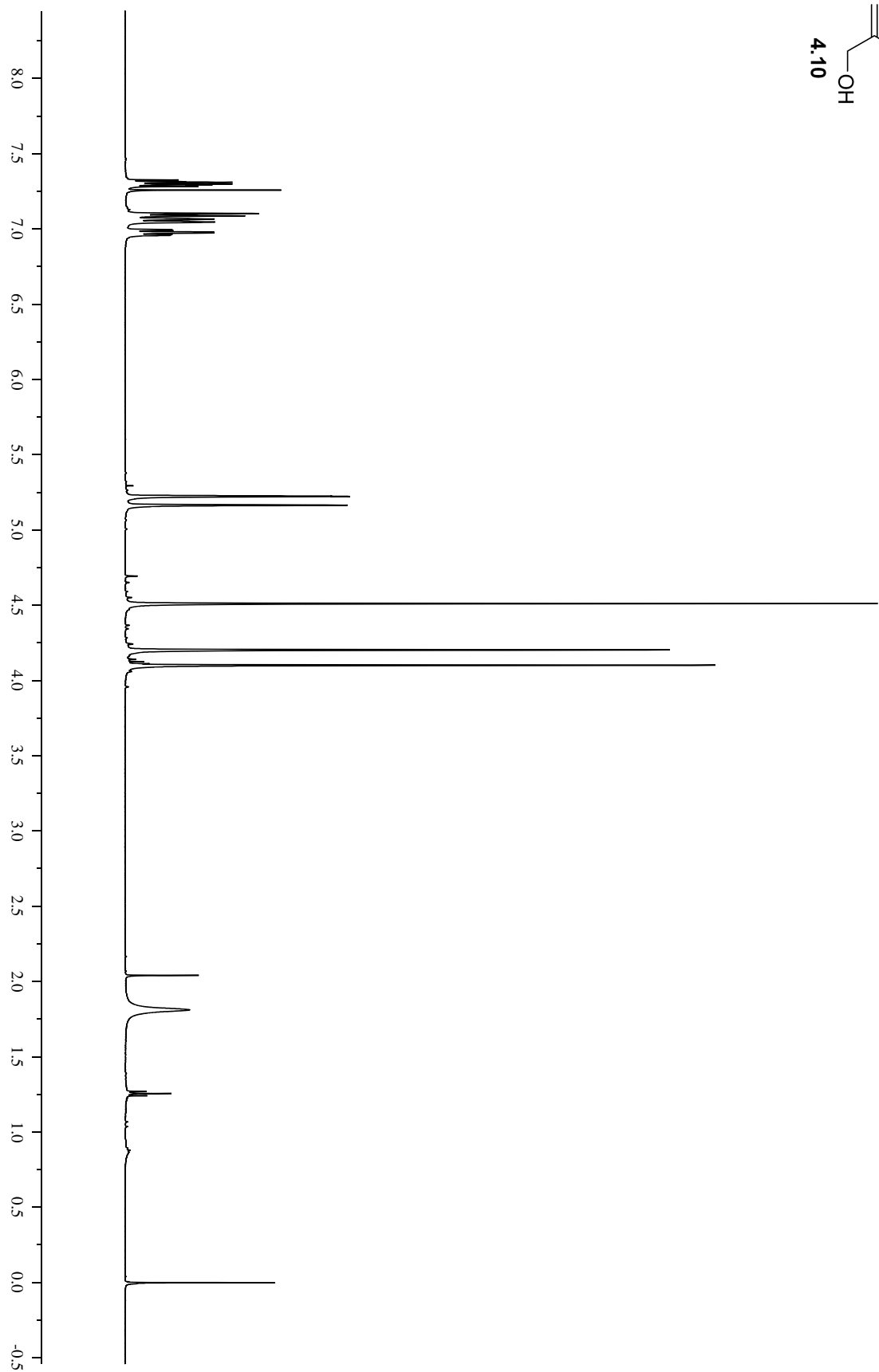
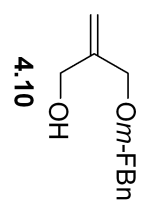


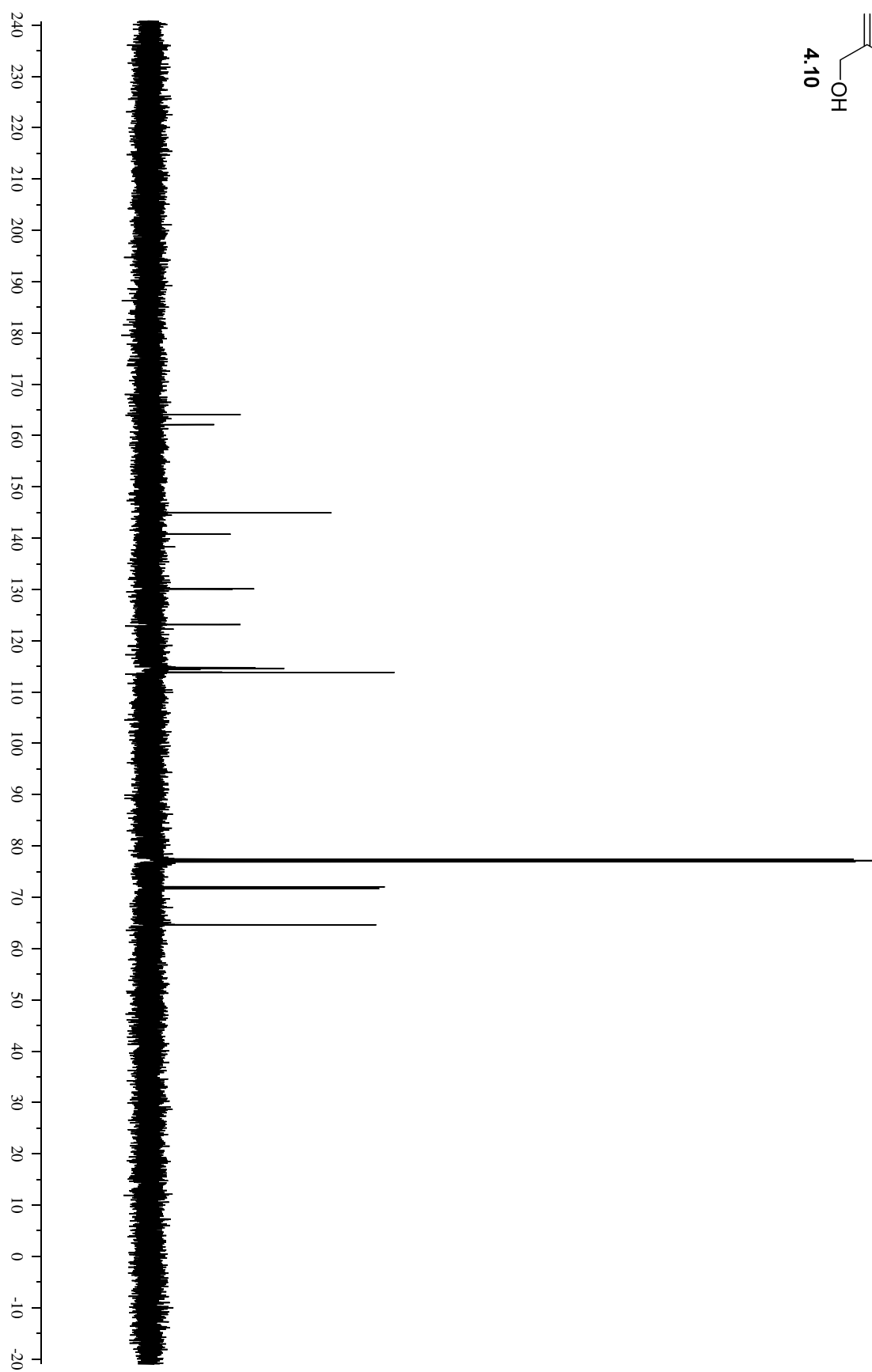
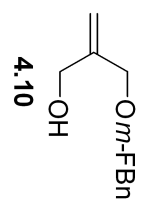


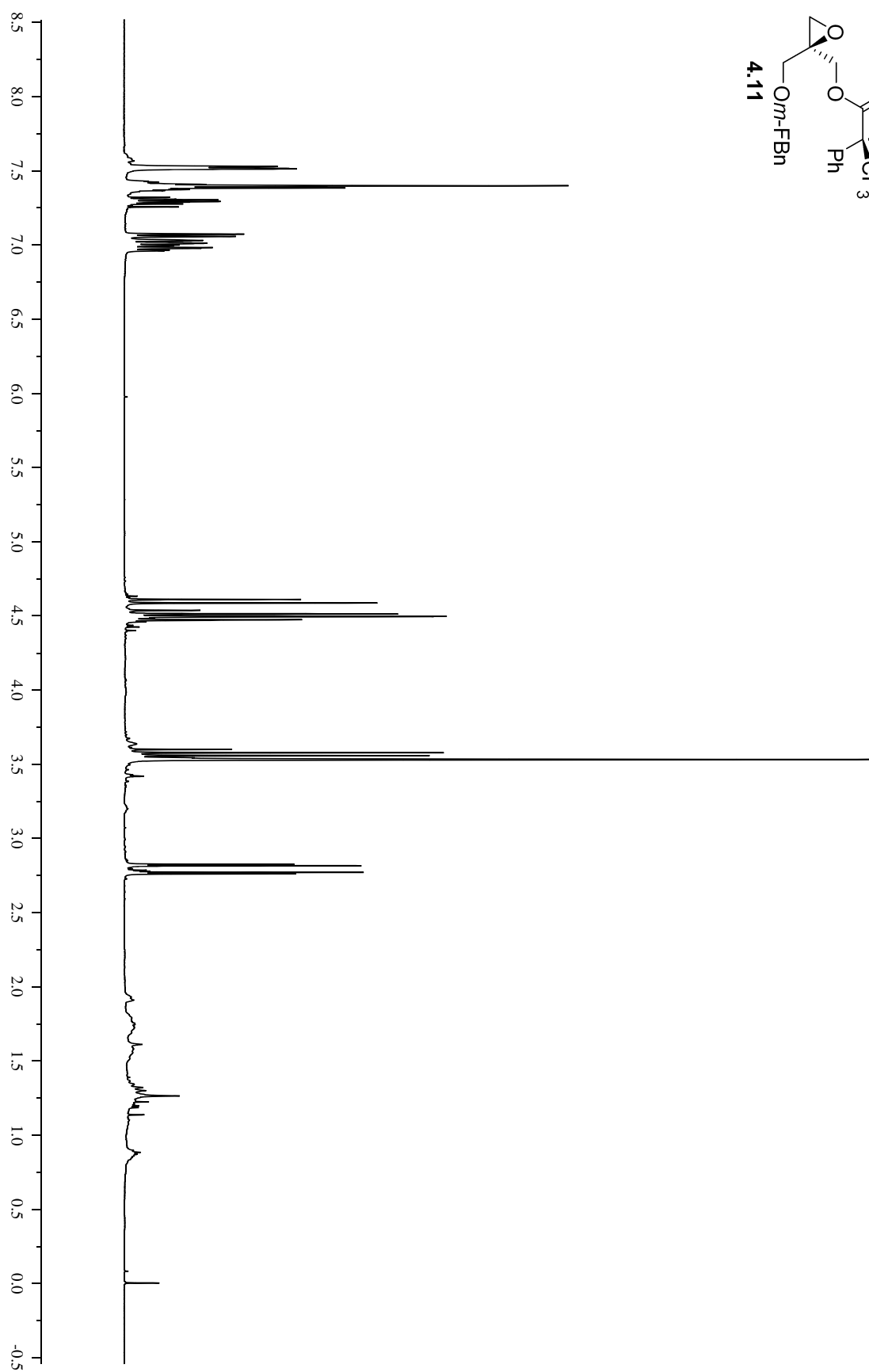
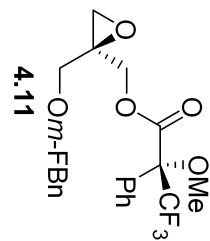


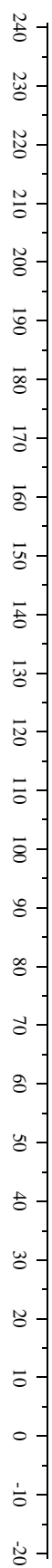
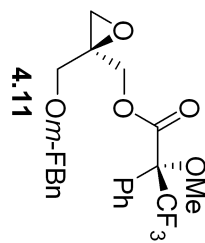


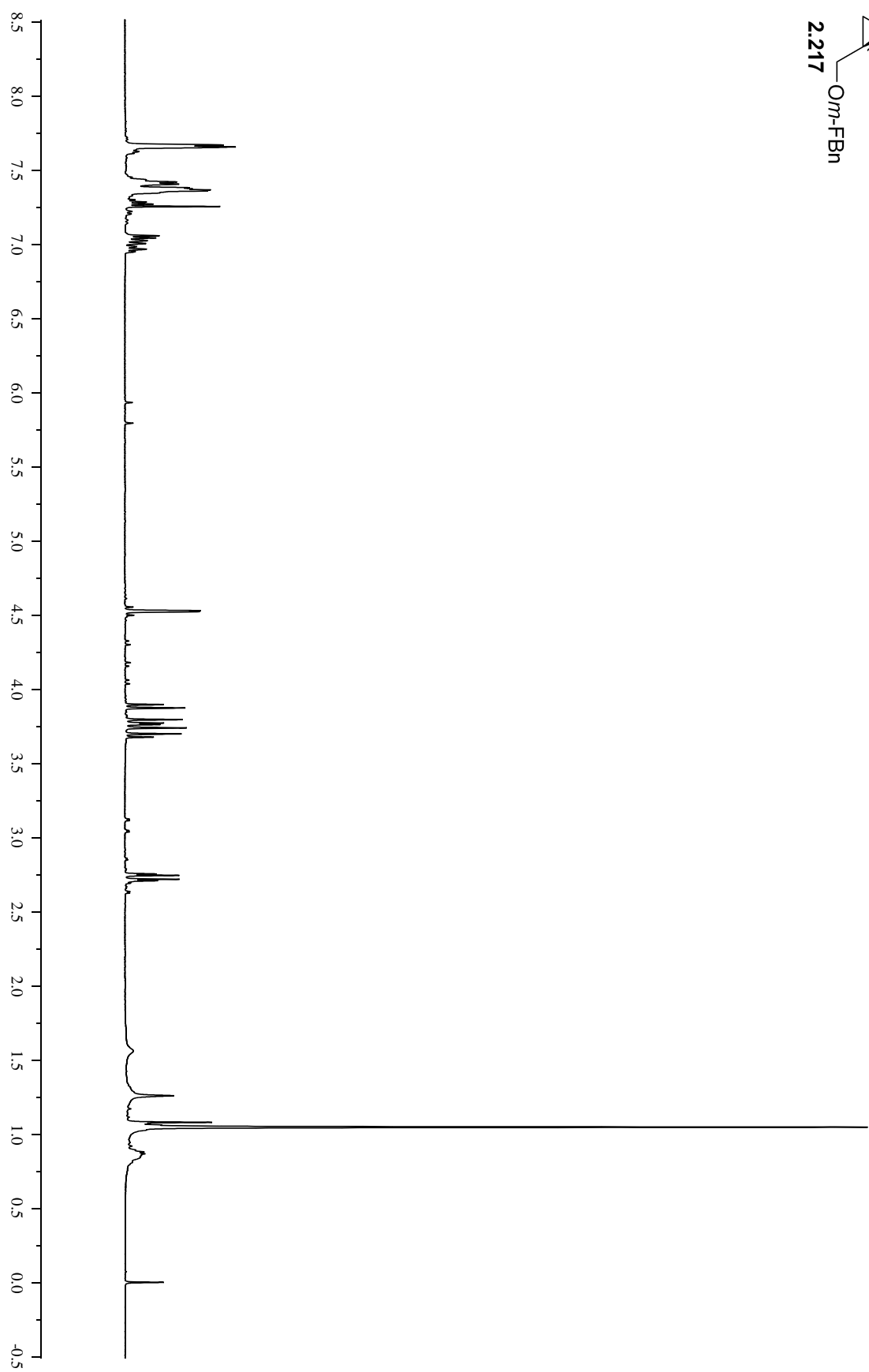
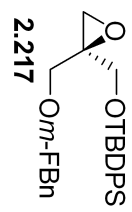


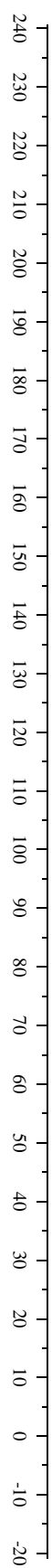
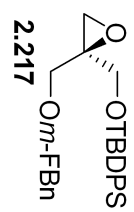


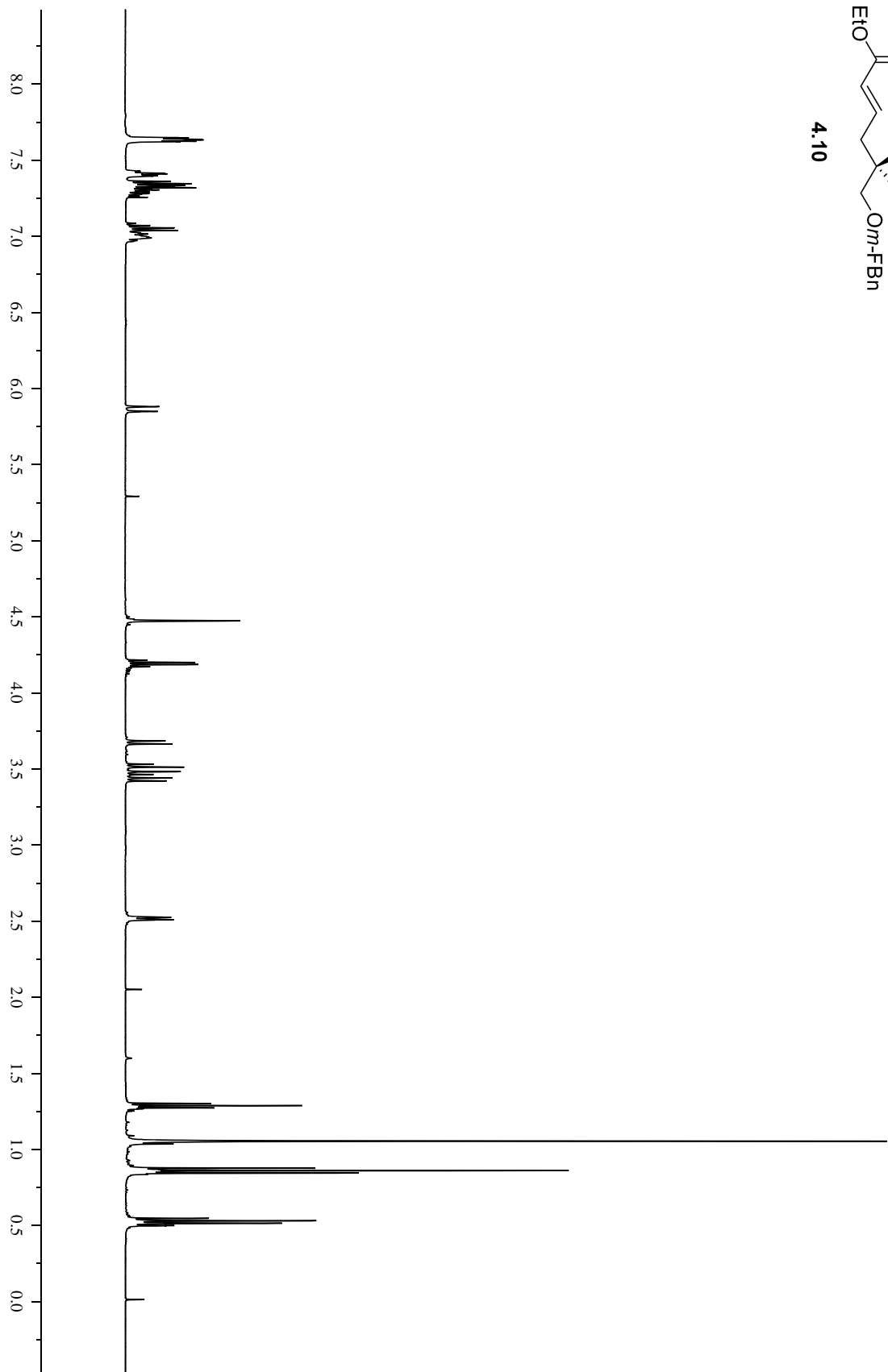
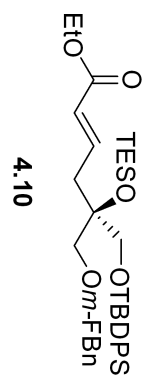






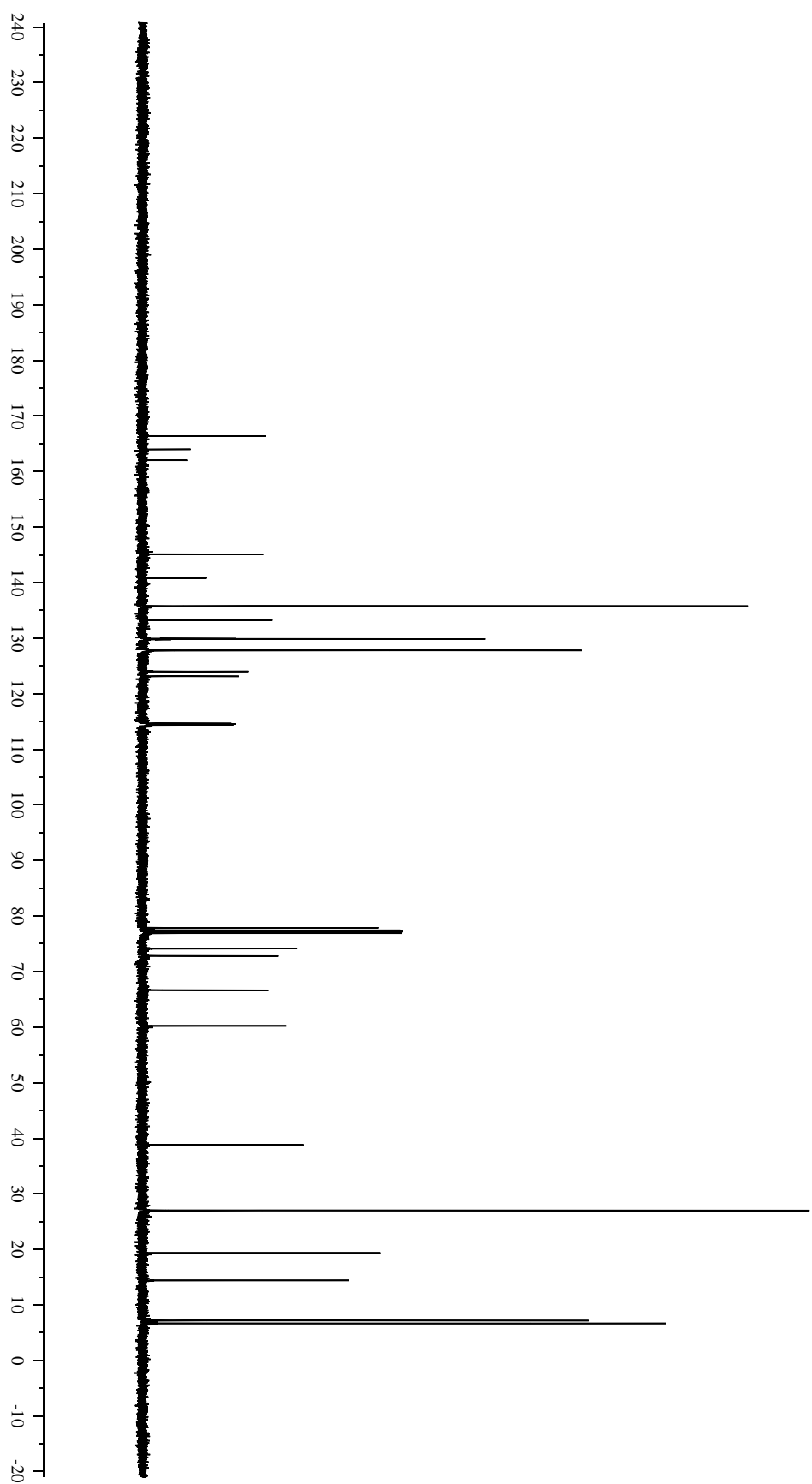


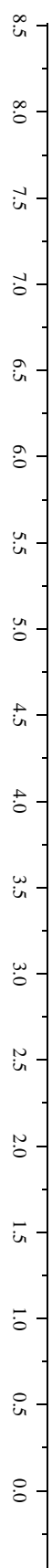
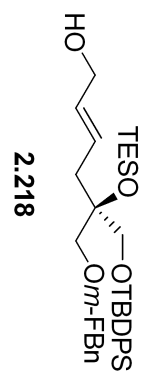






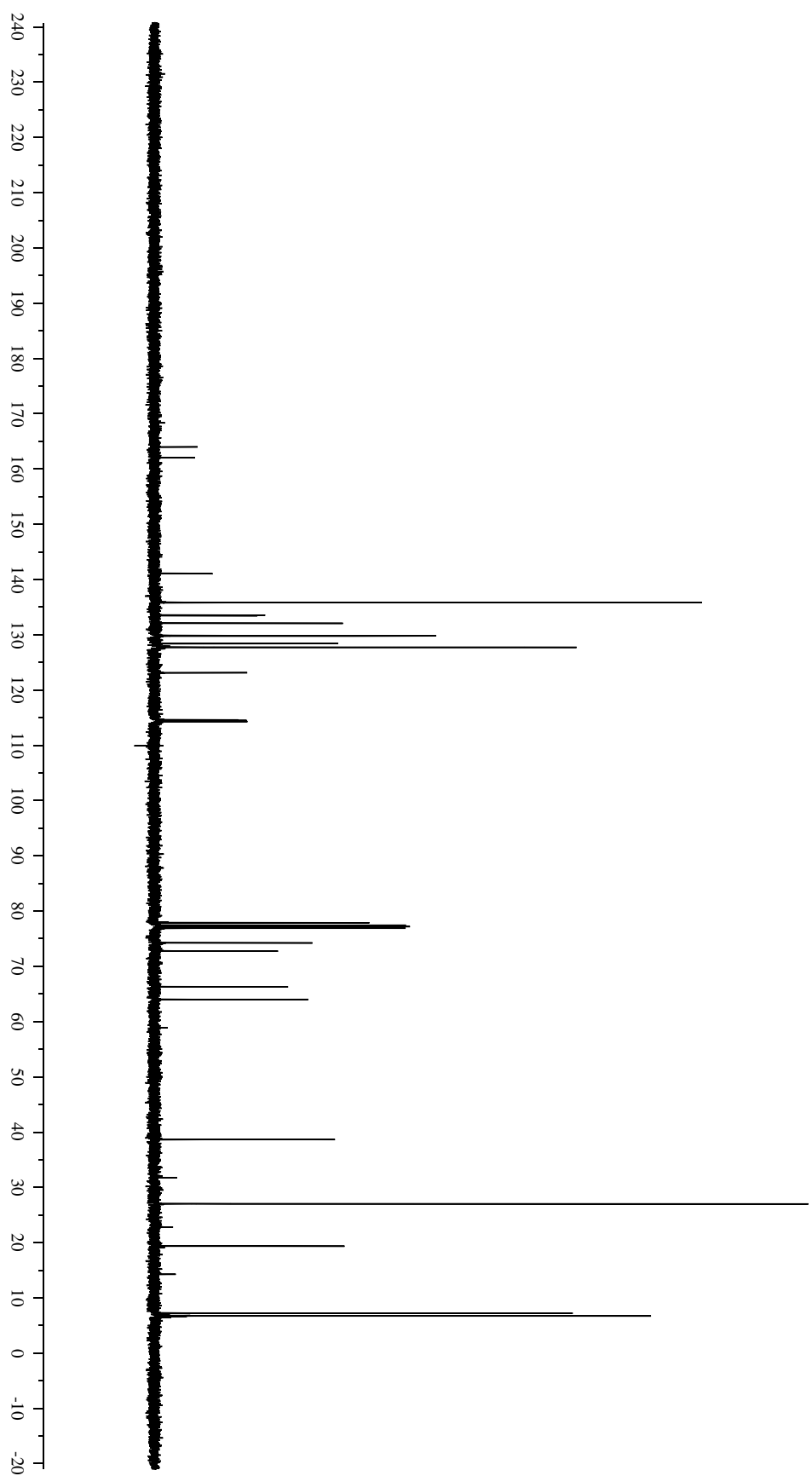
4.10

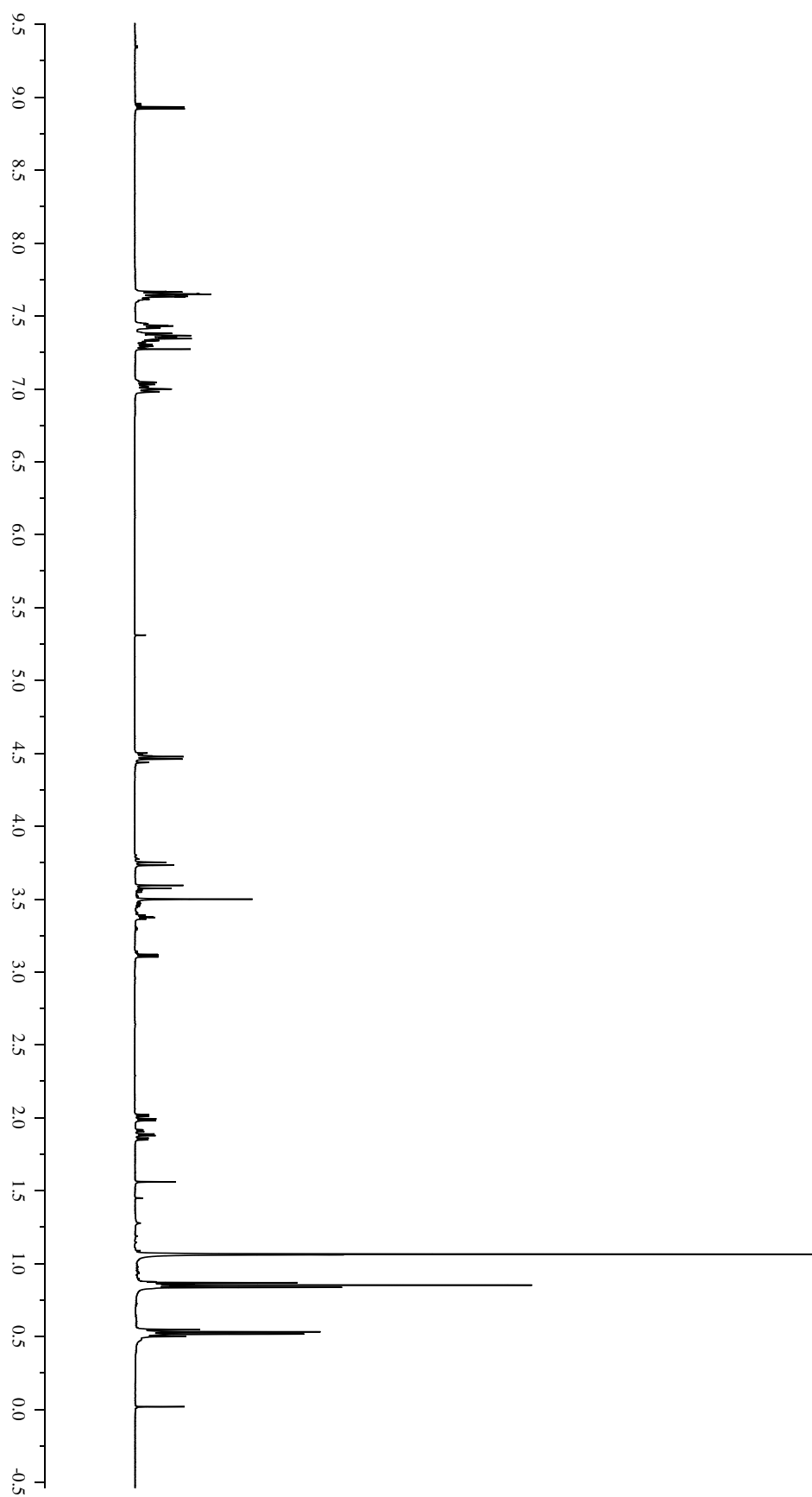
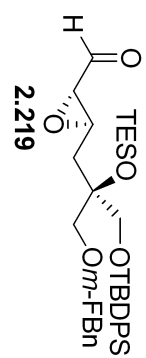


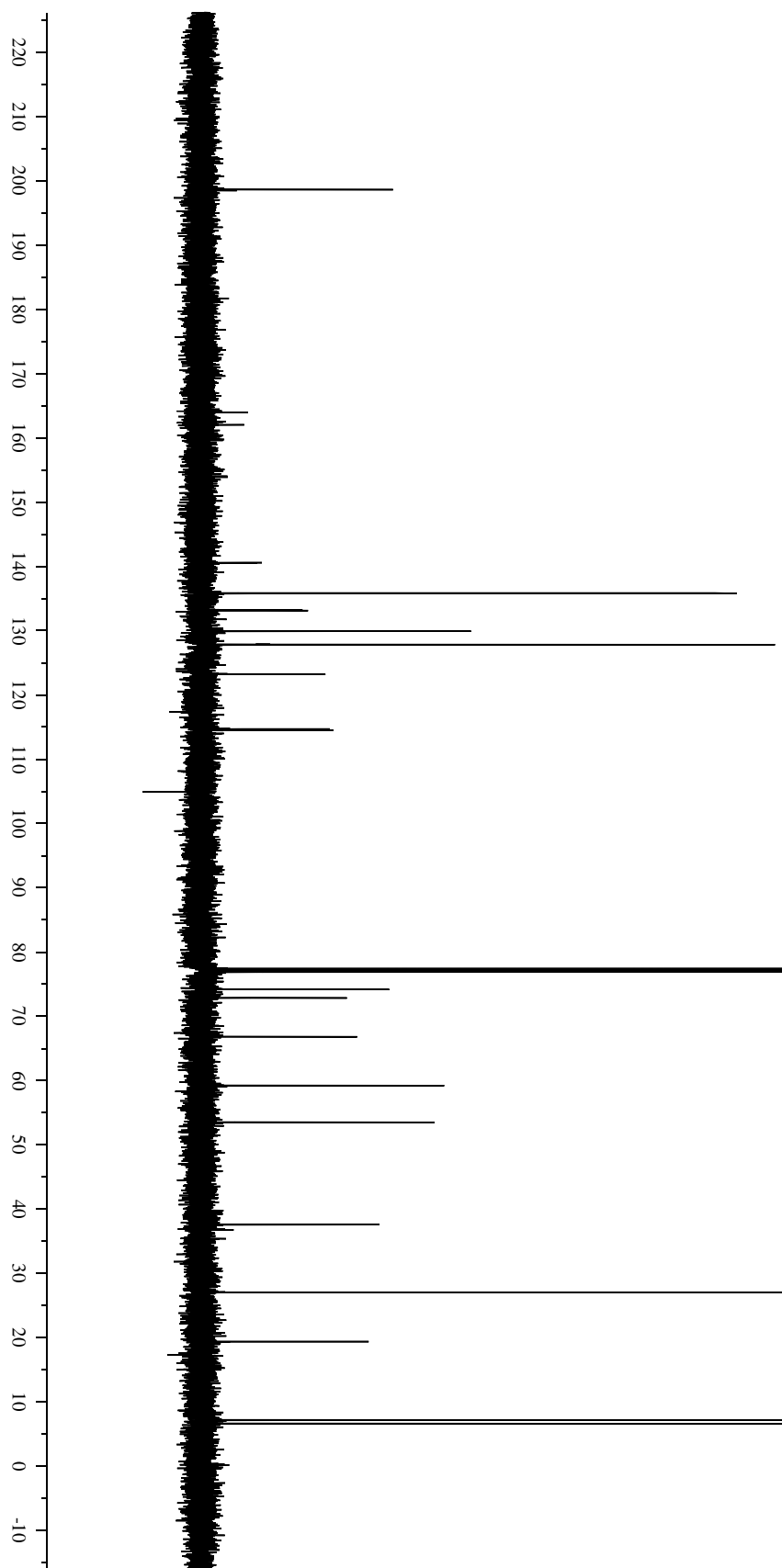
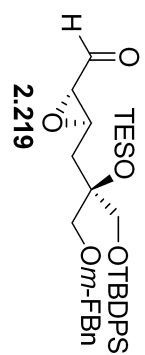


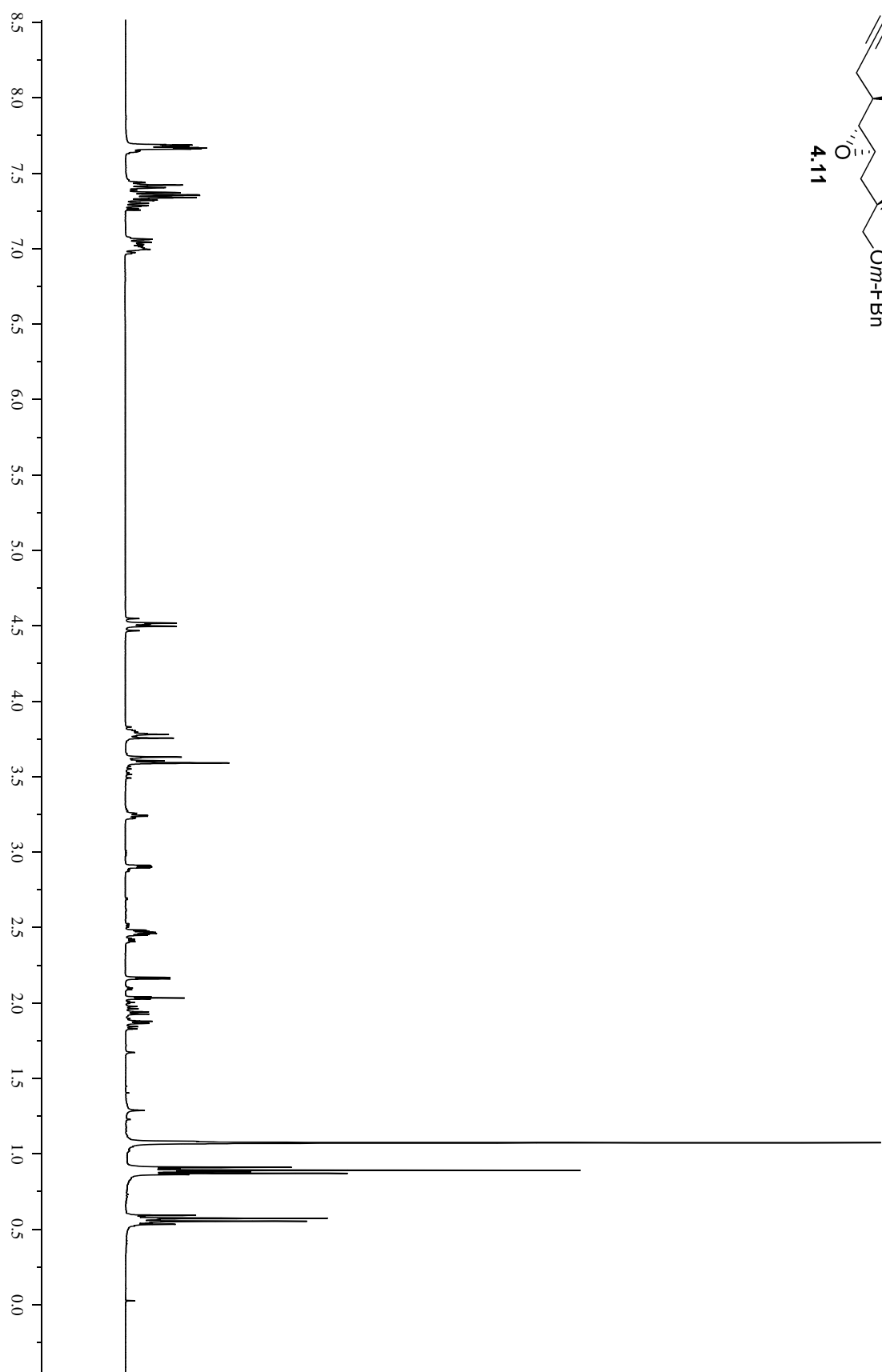


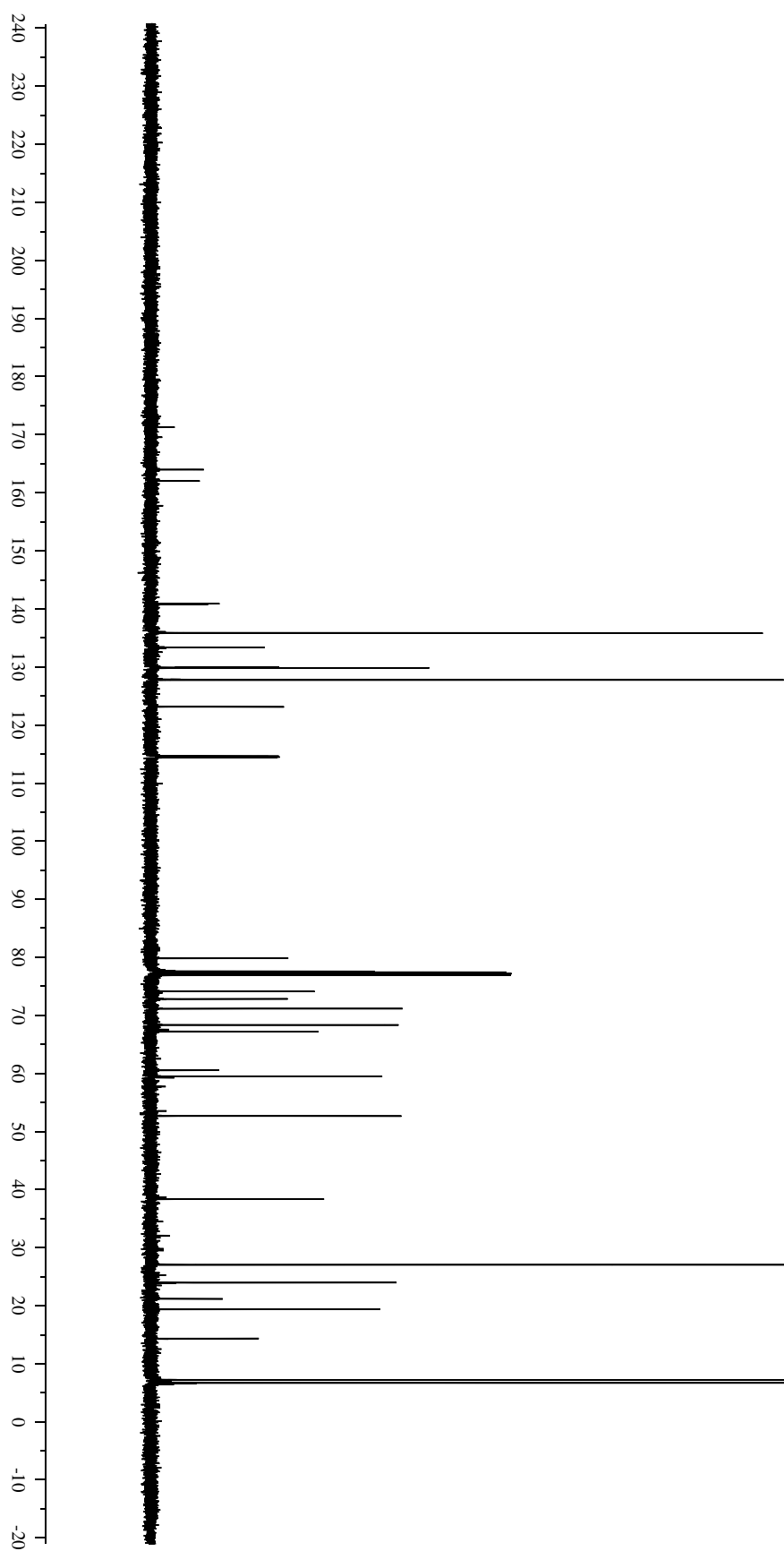
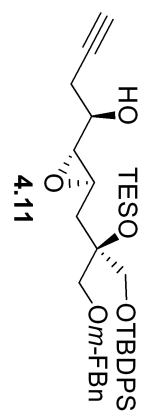
2.218

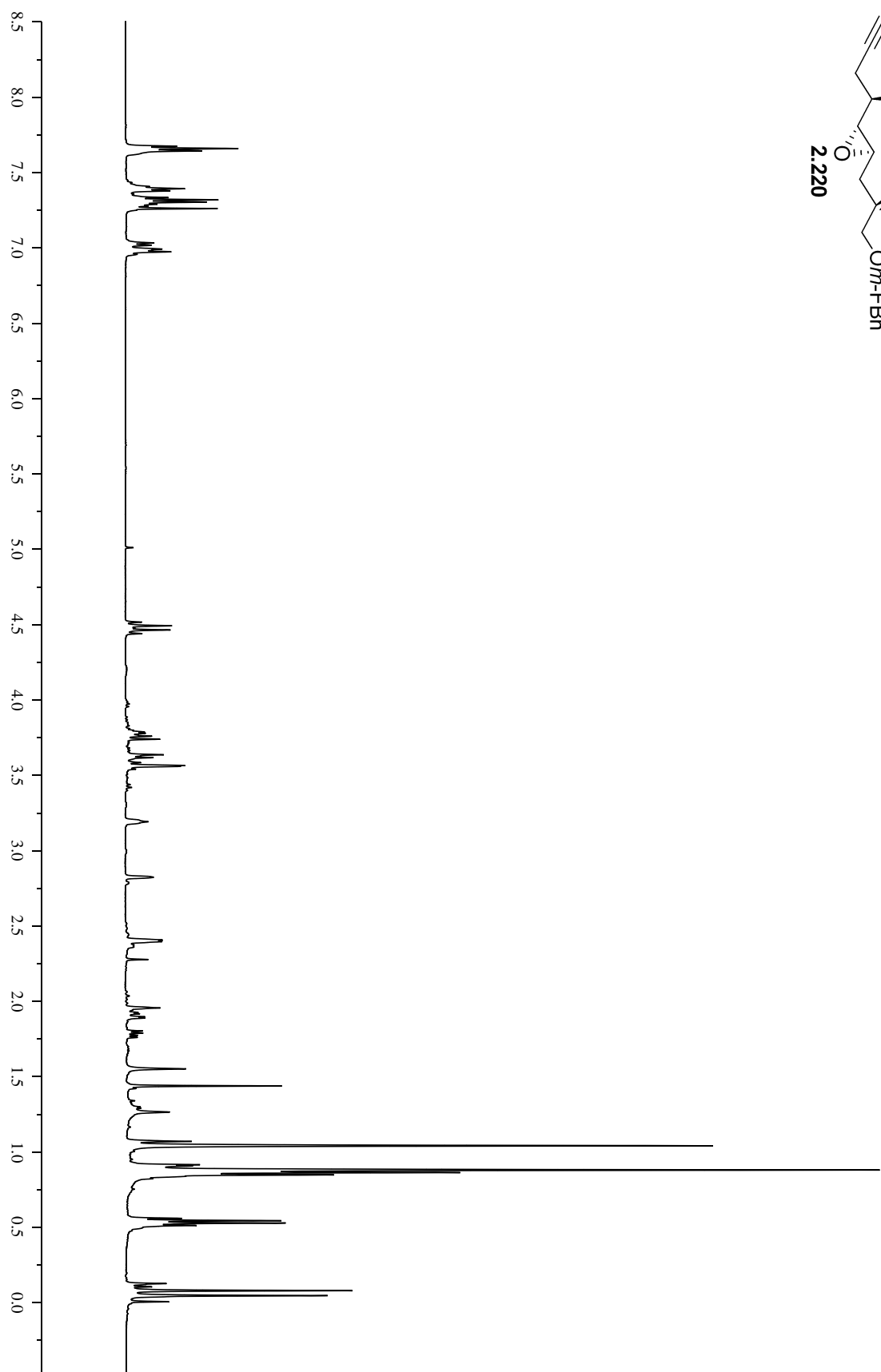
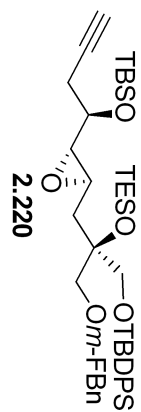


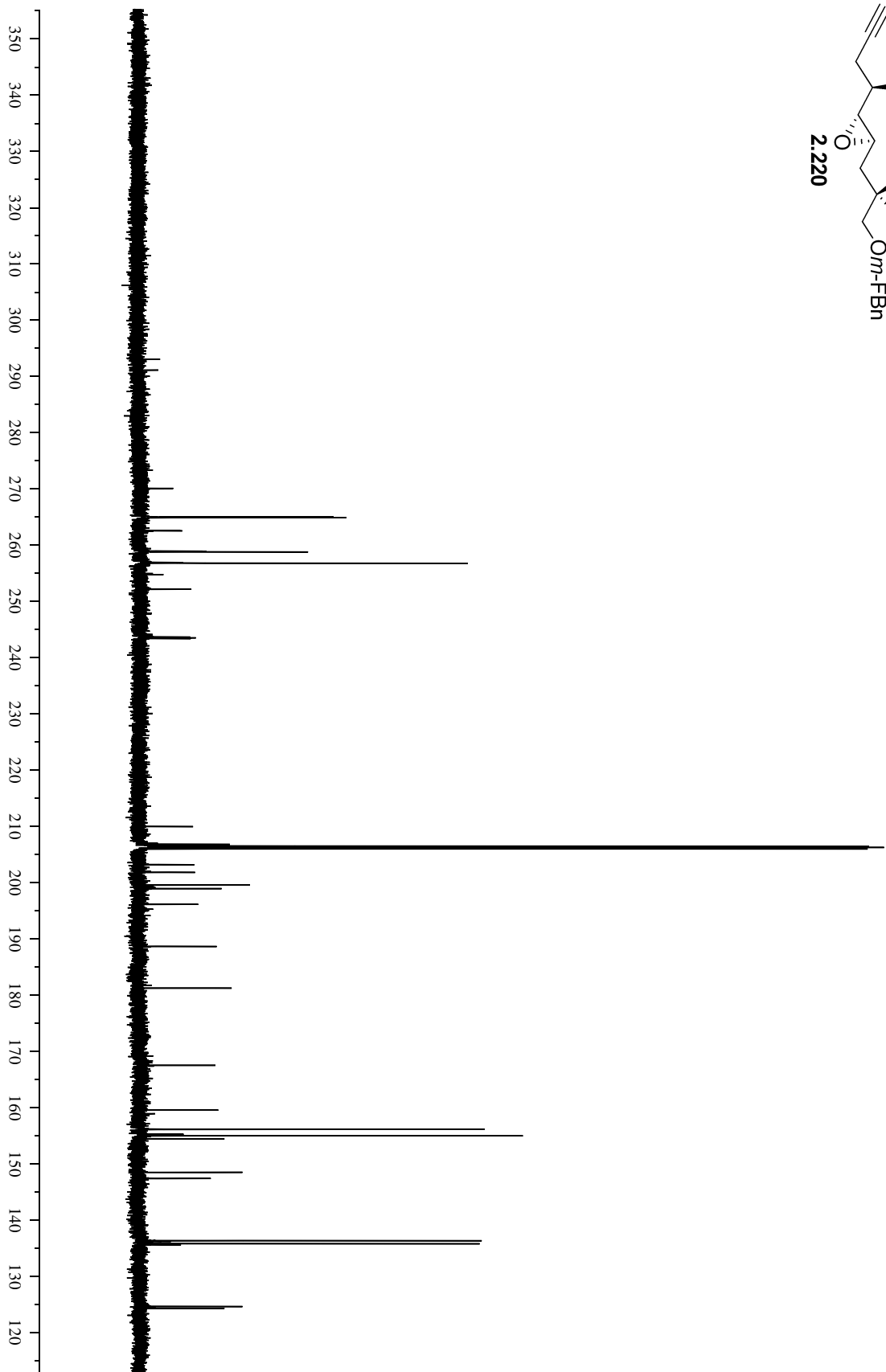
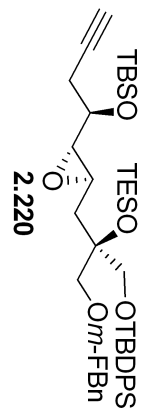


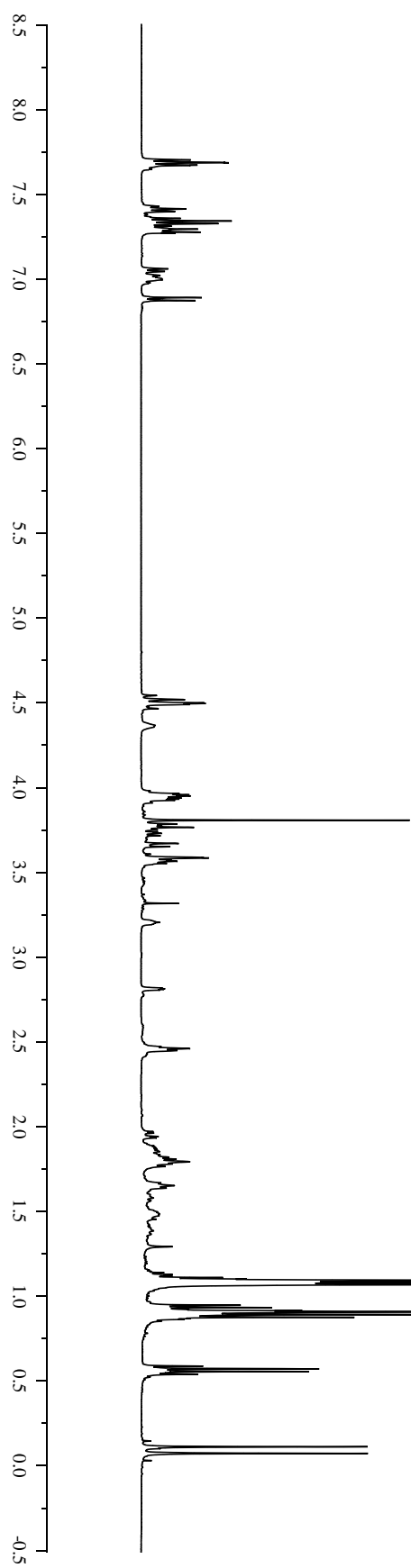
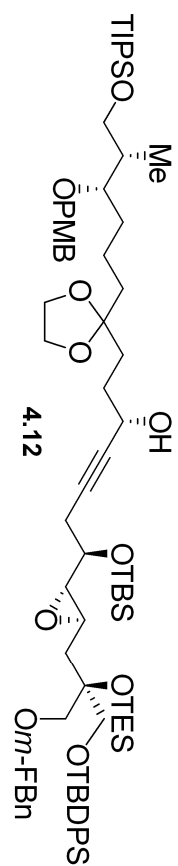


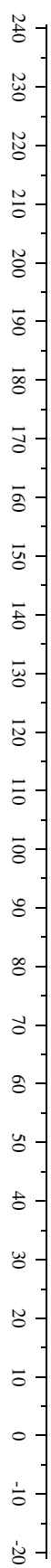
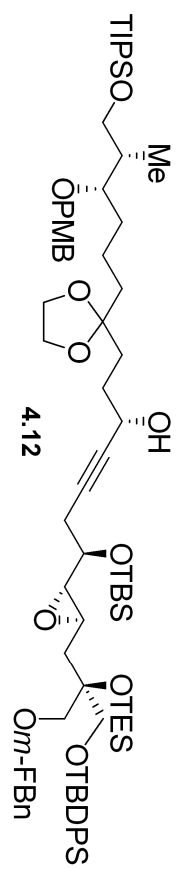


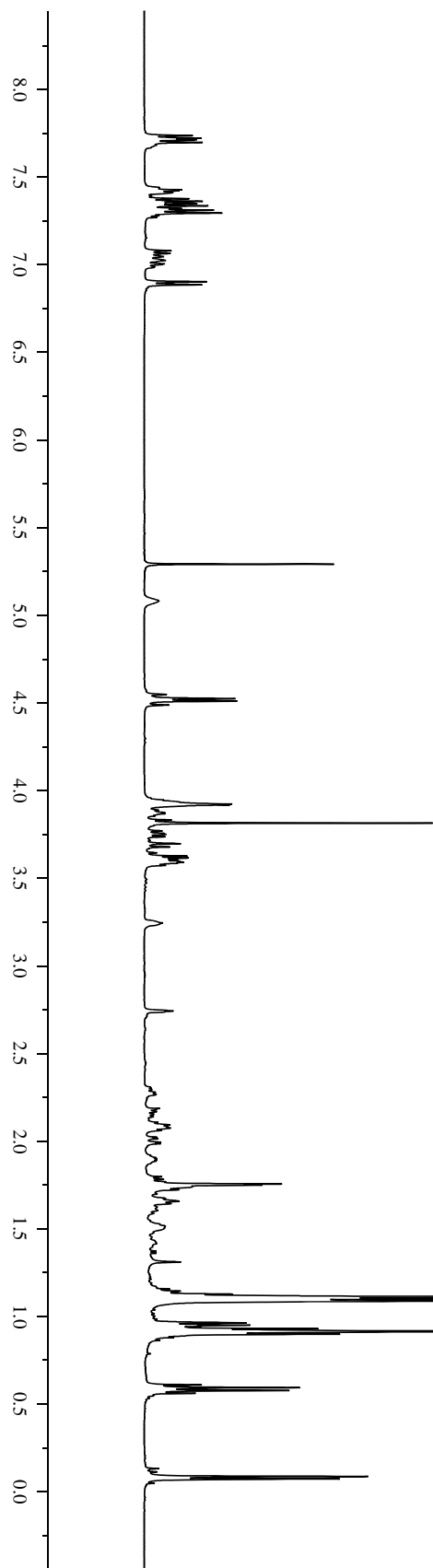
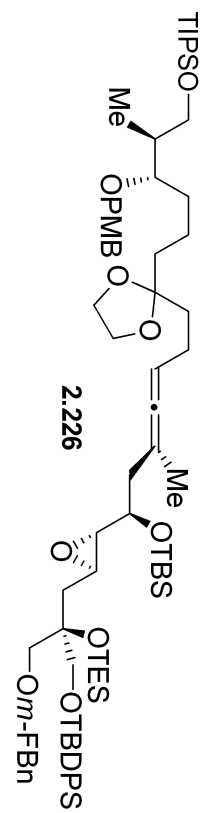


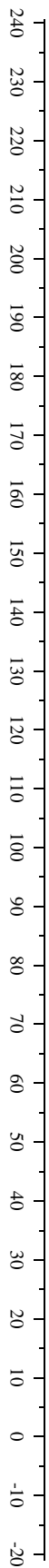


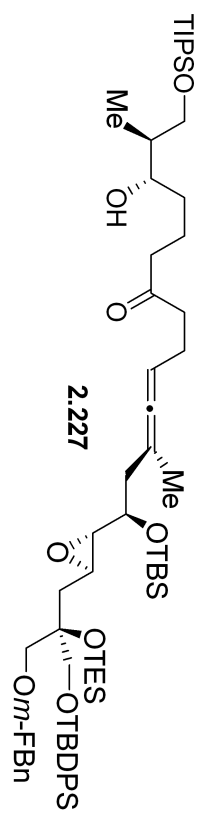


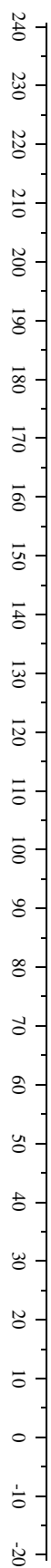
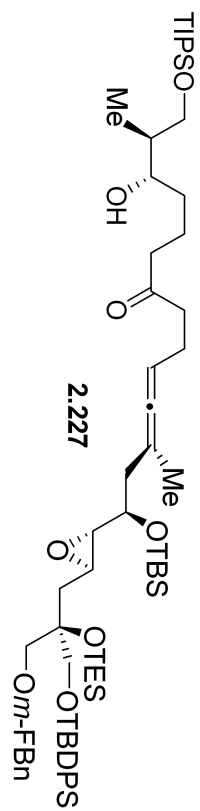


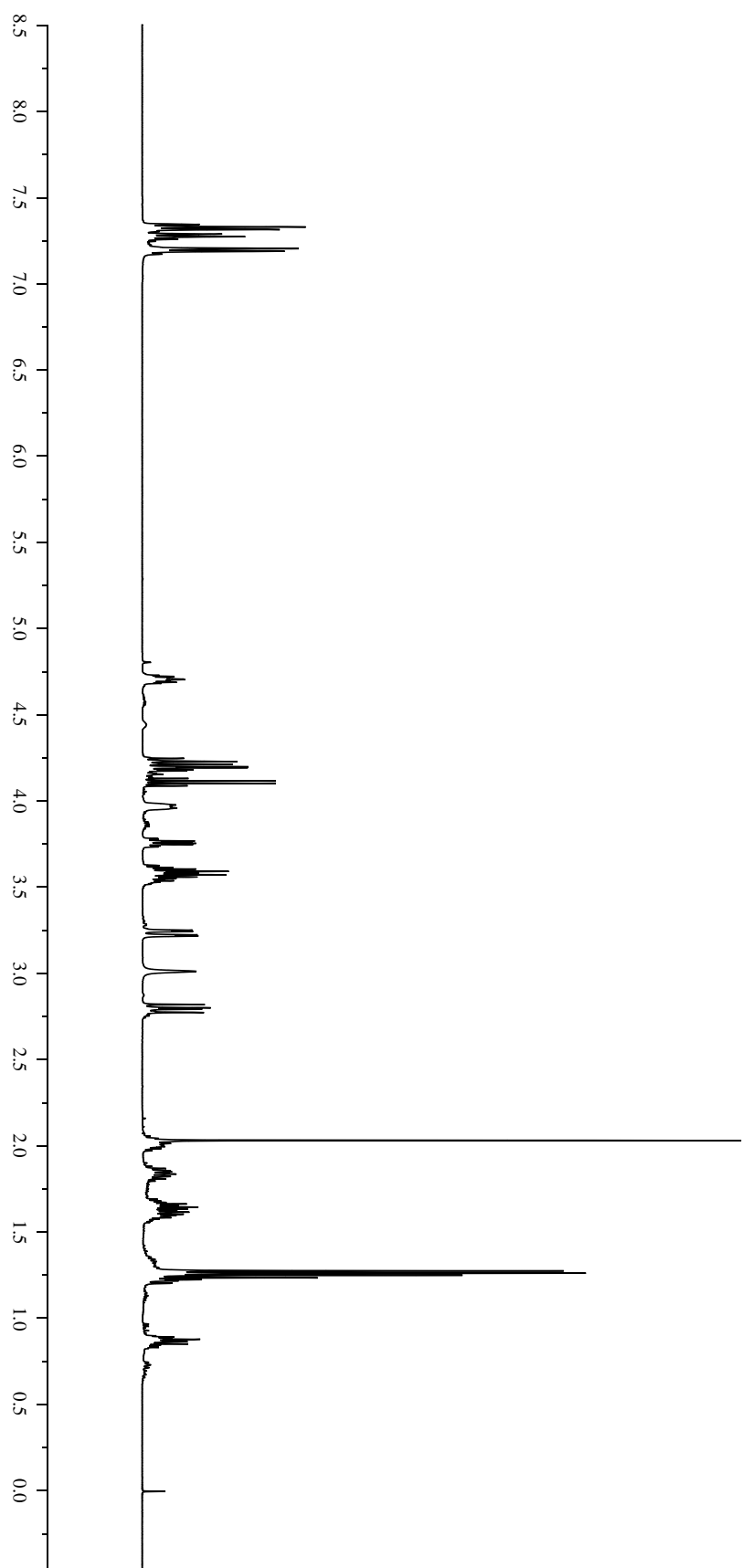
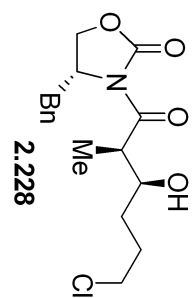


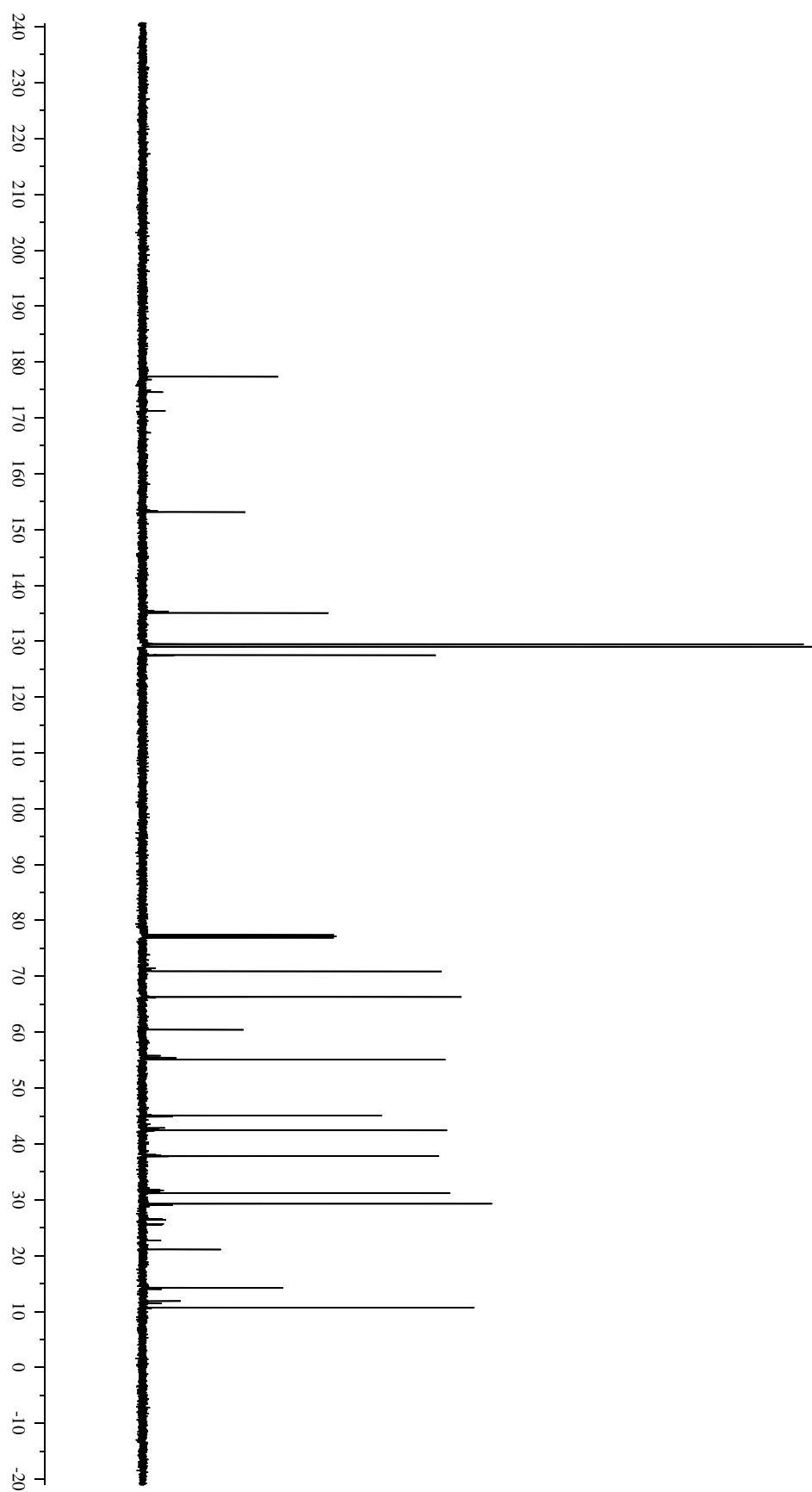
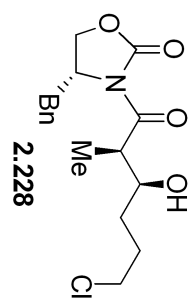


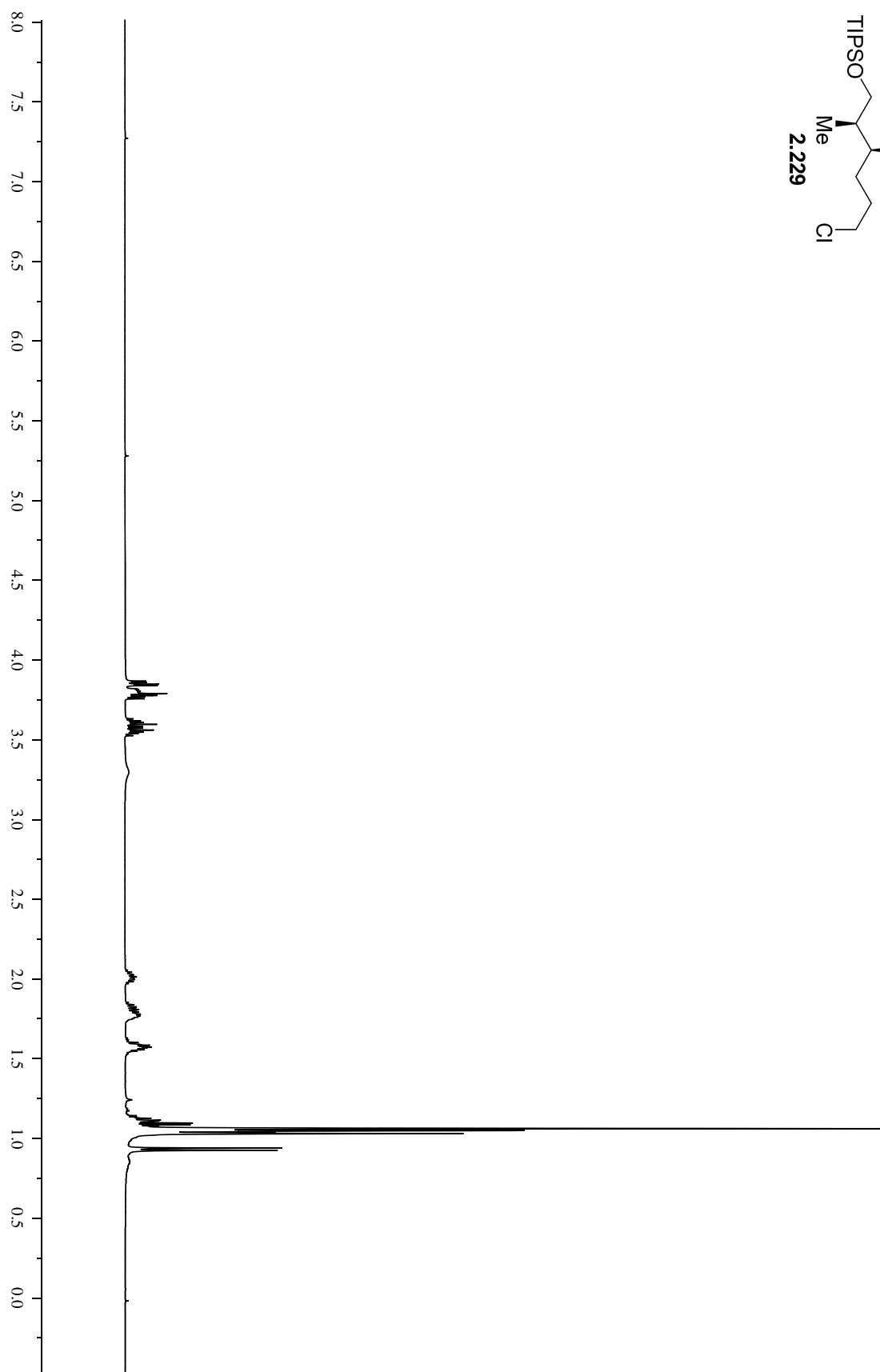
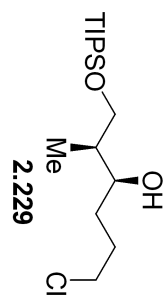


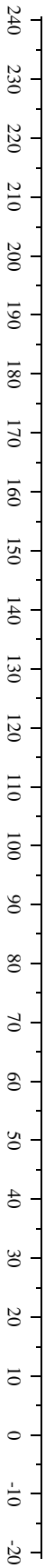


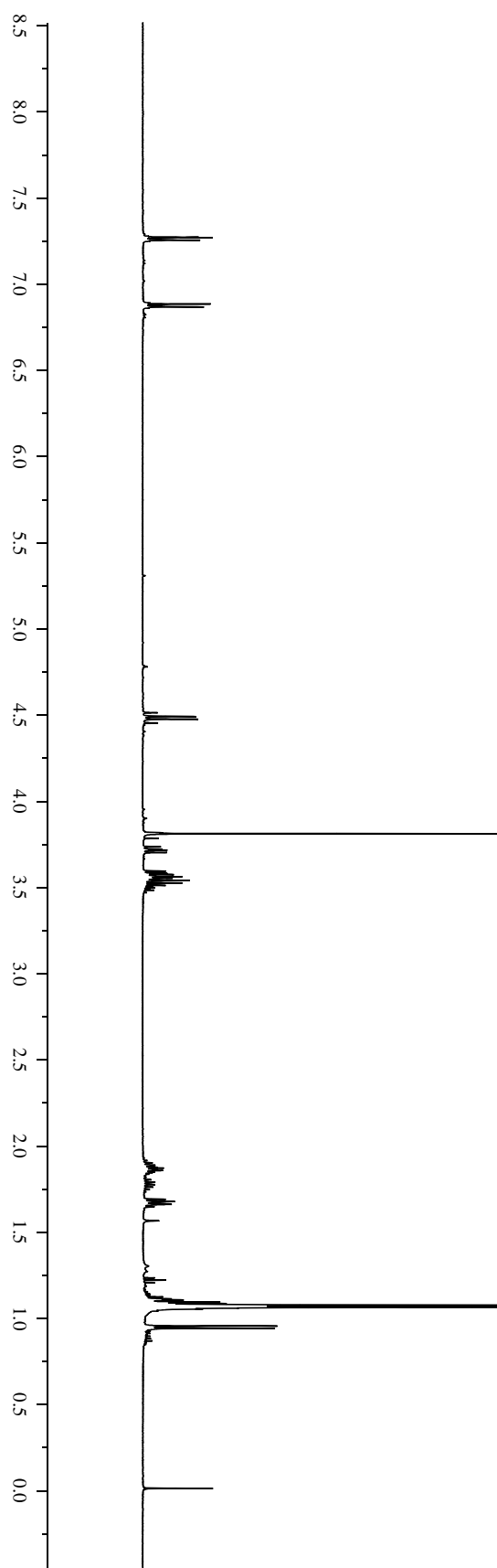
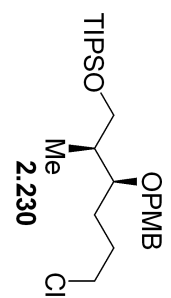


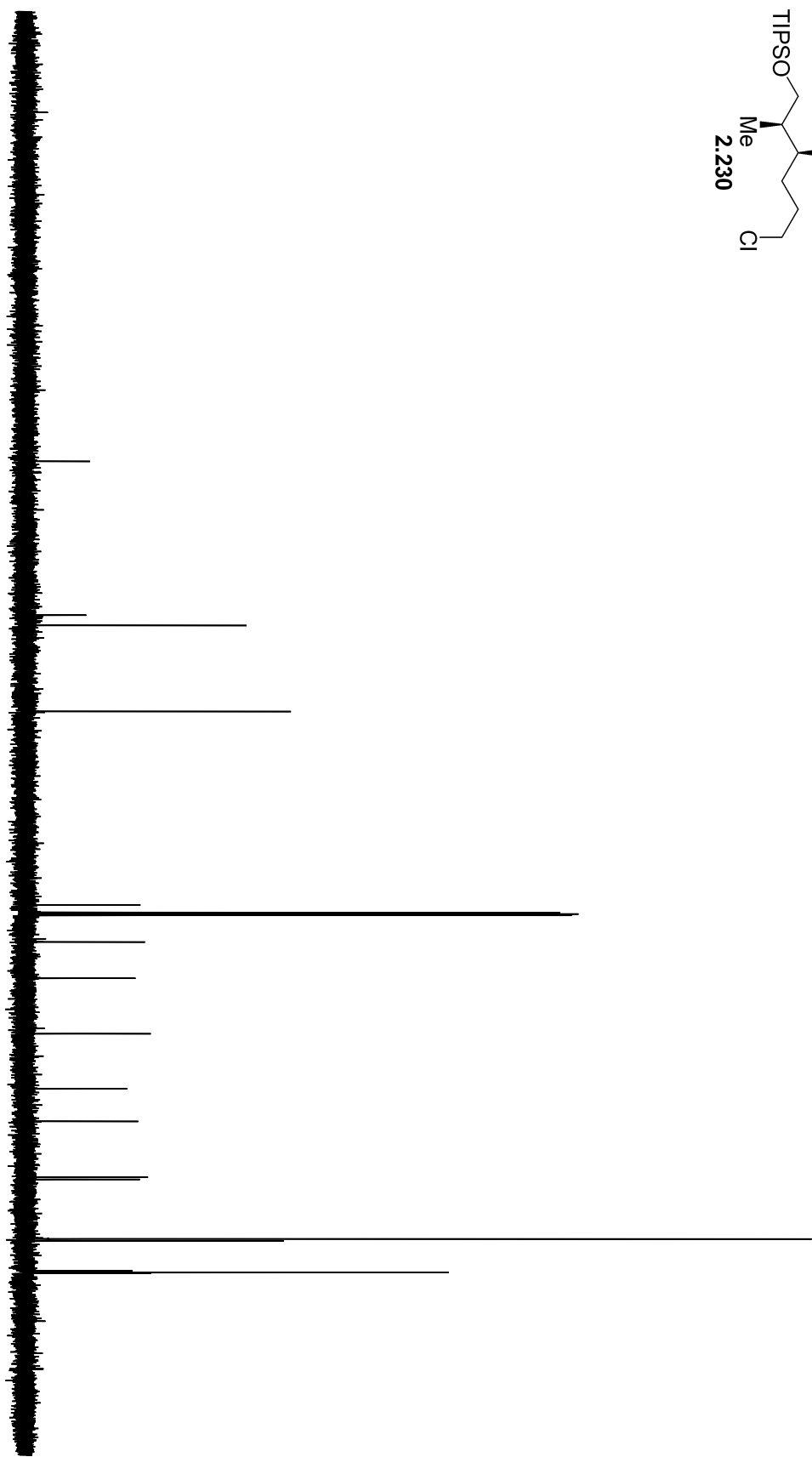
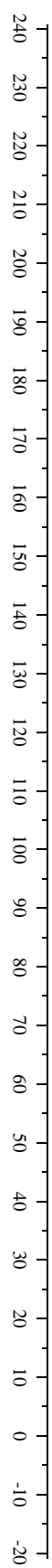
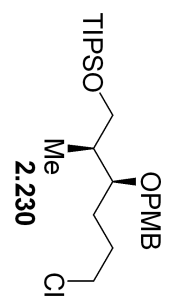


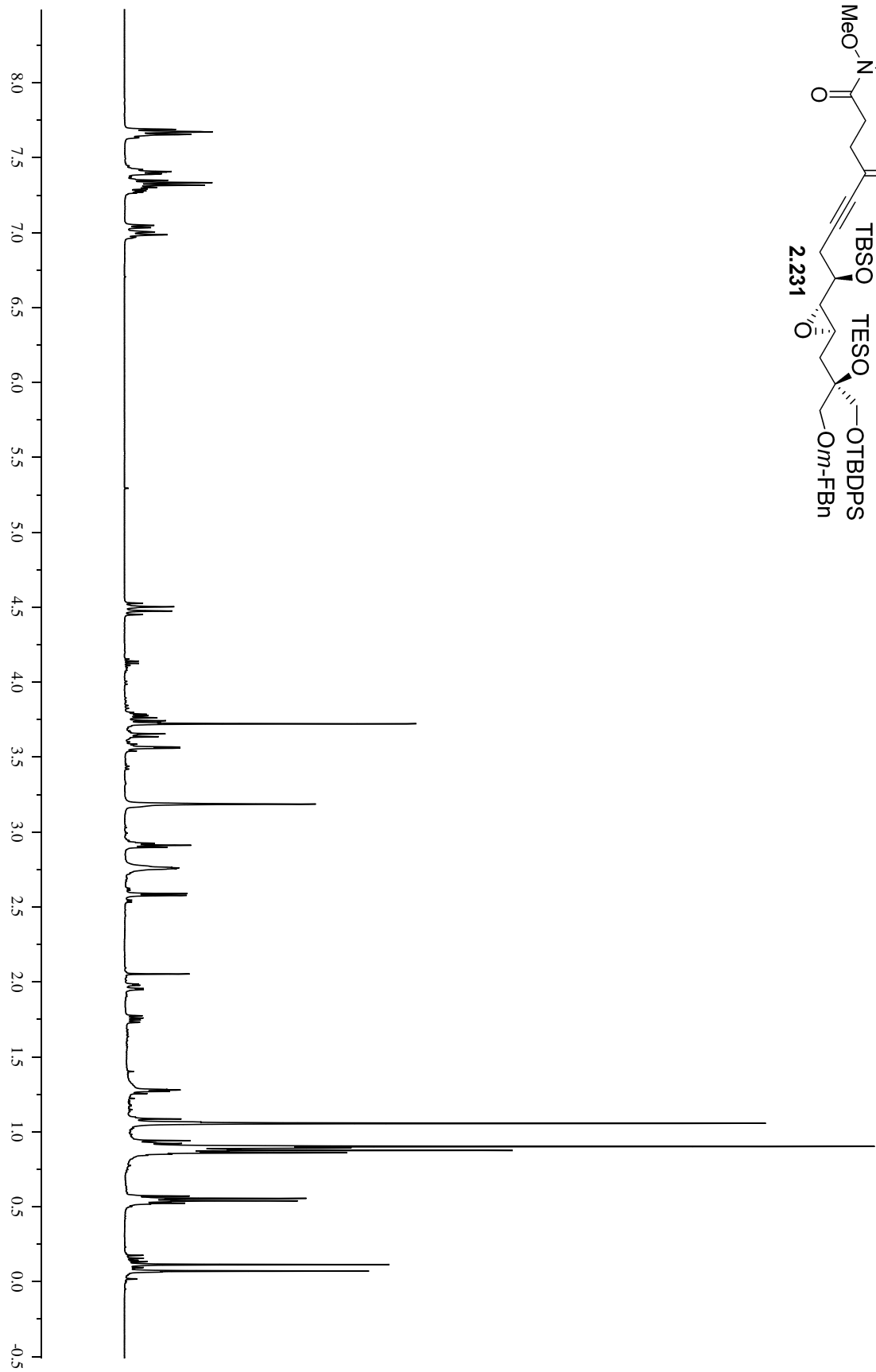
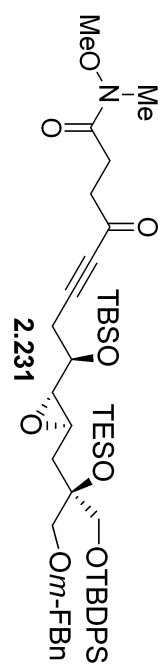


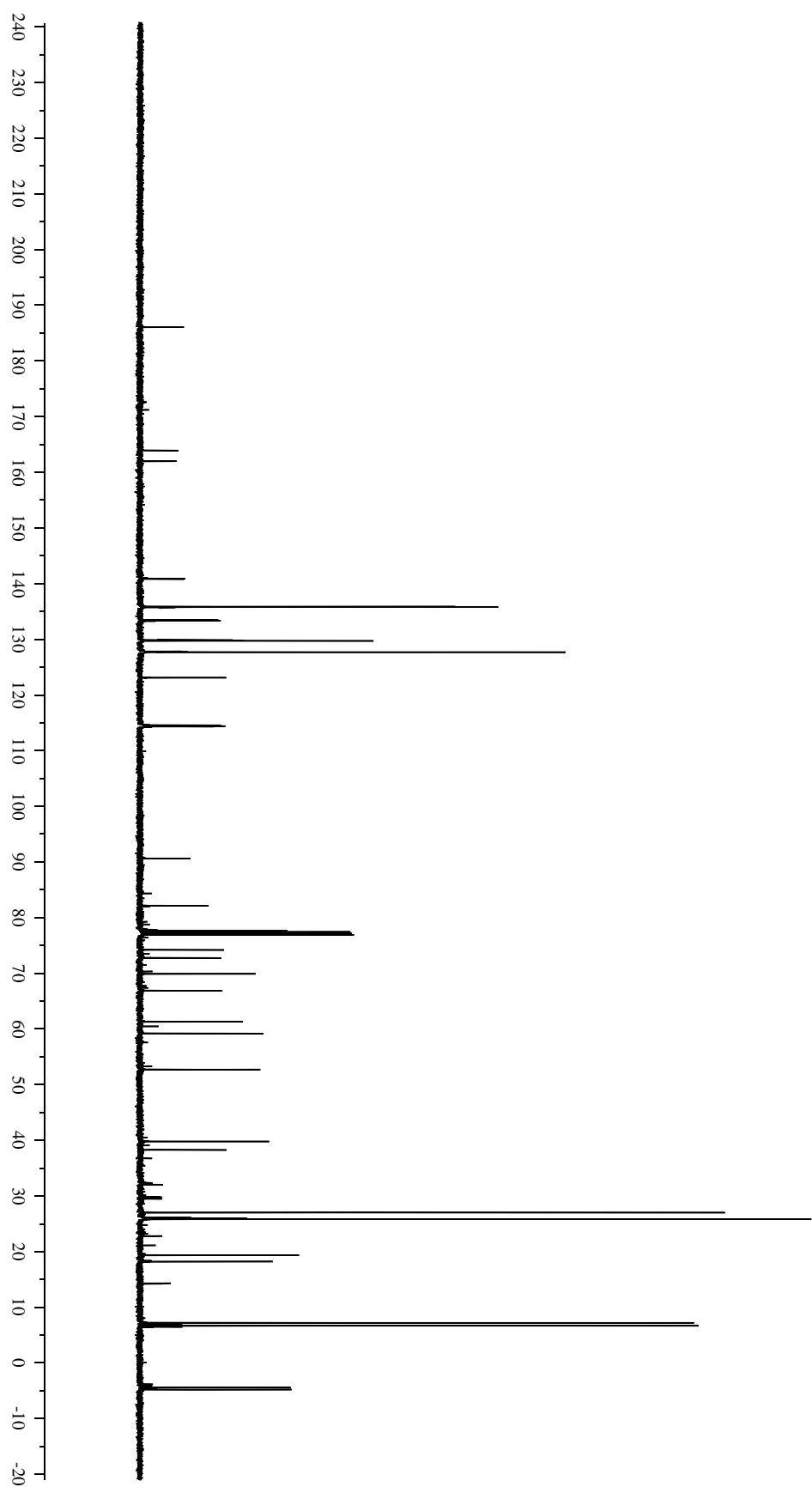
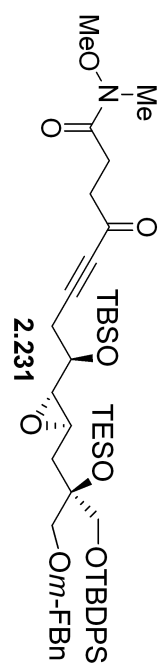


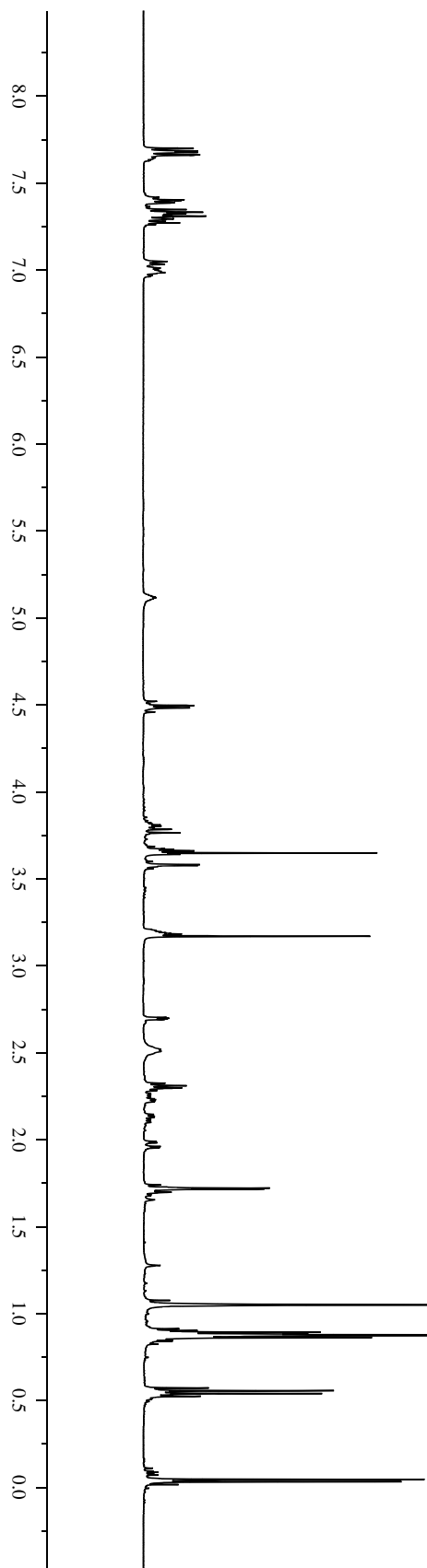
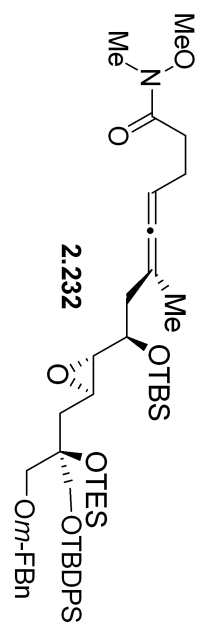


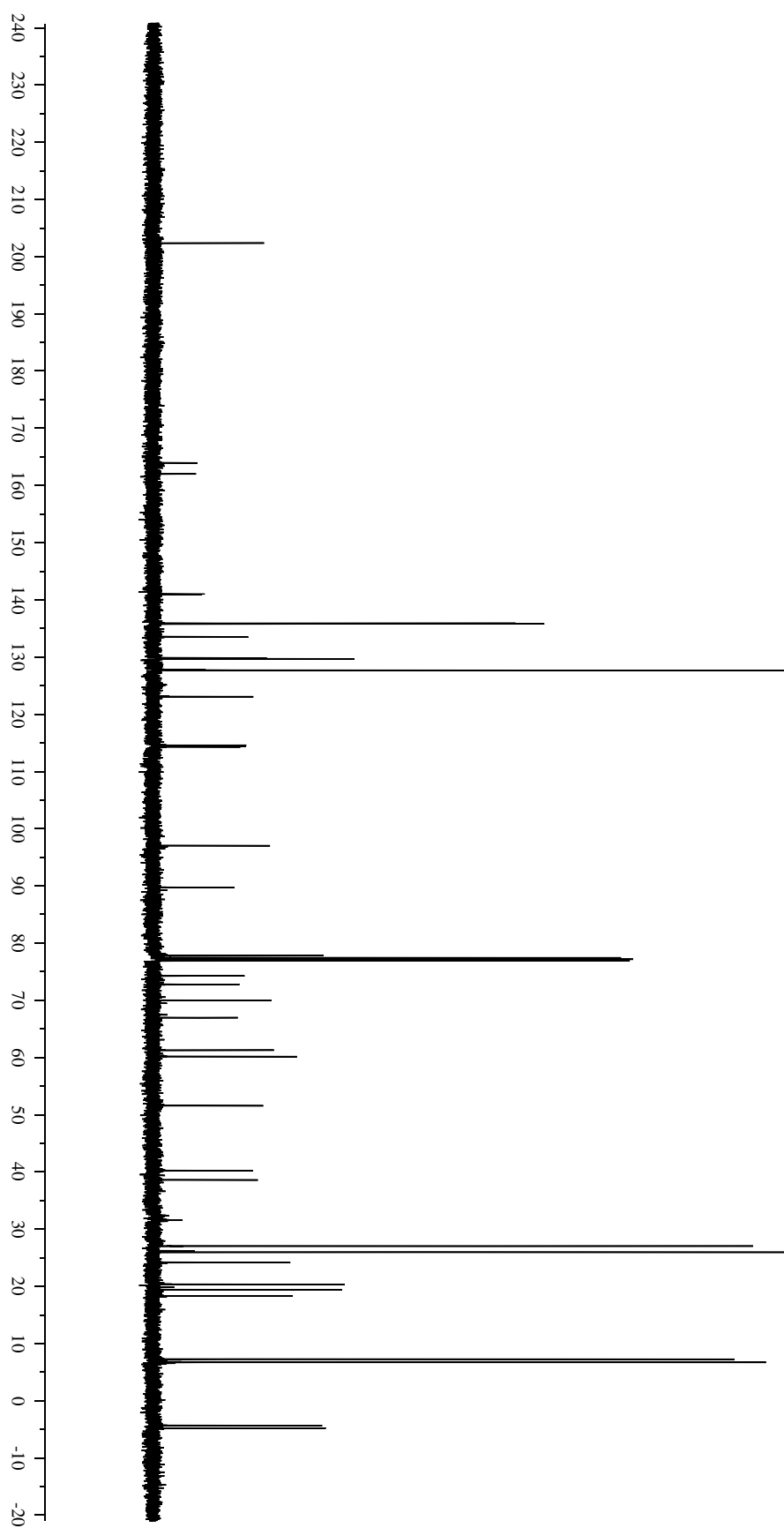
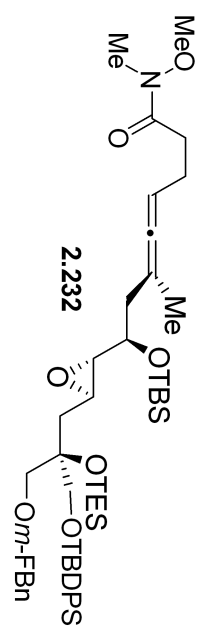


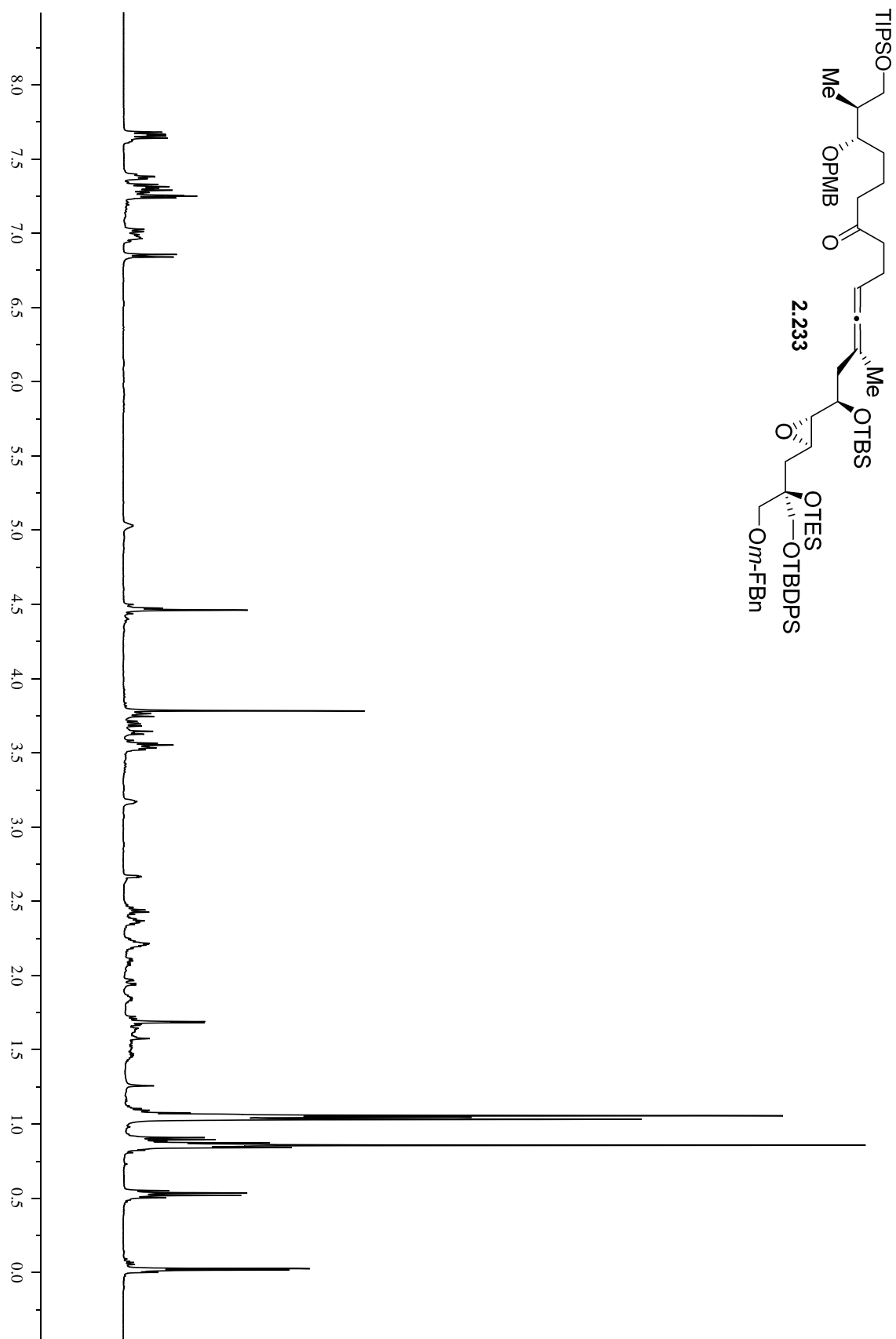


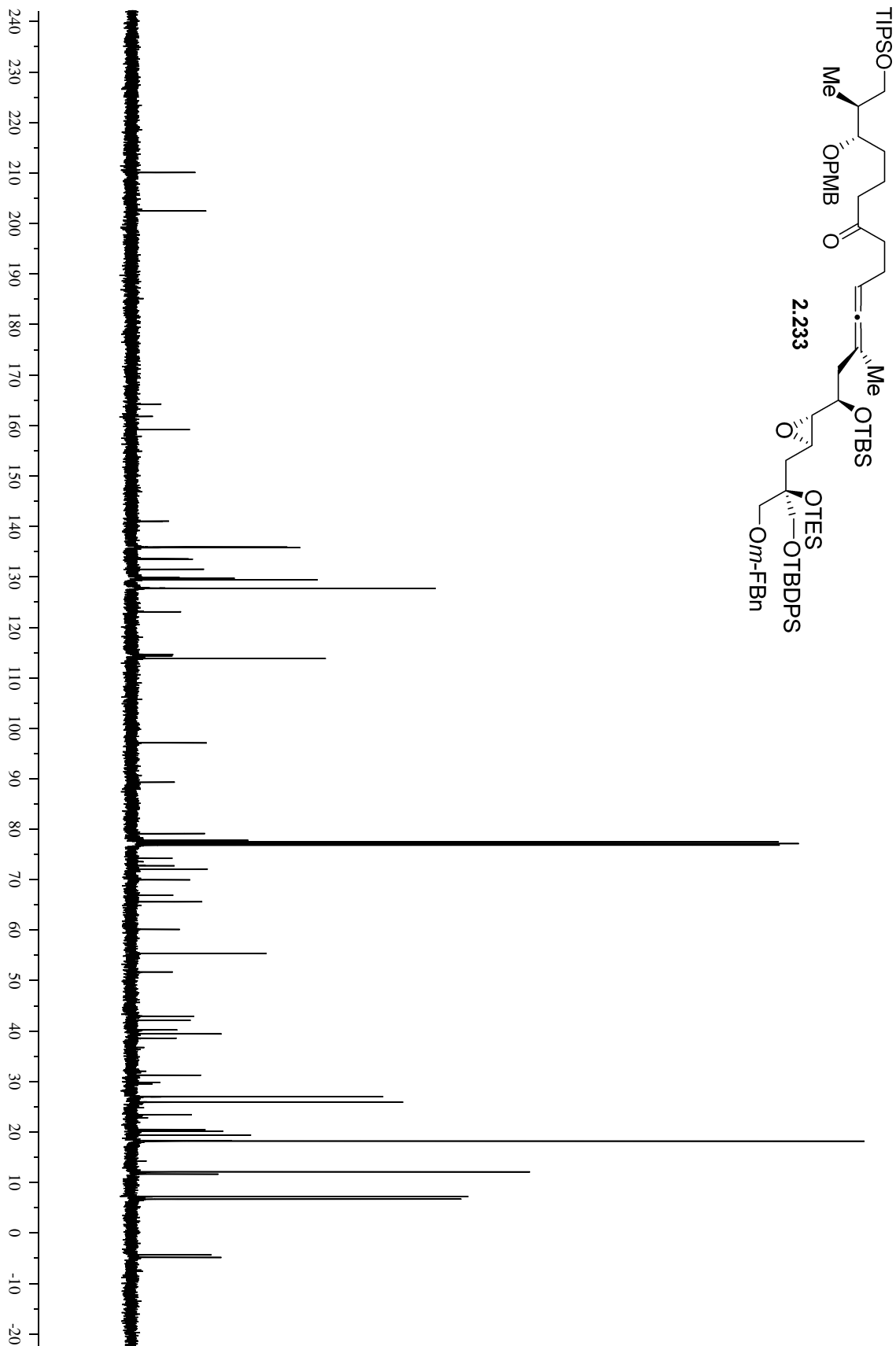


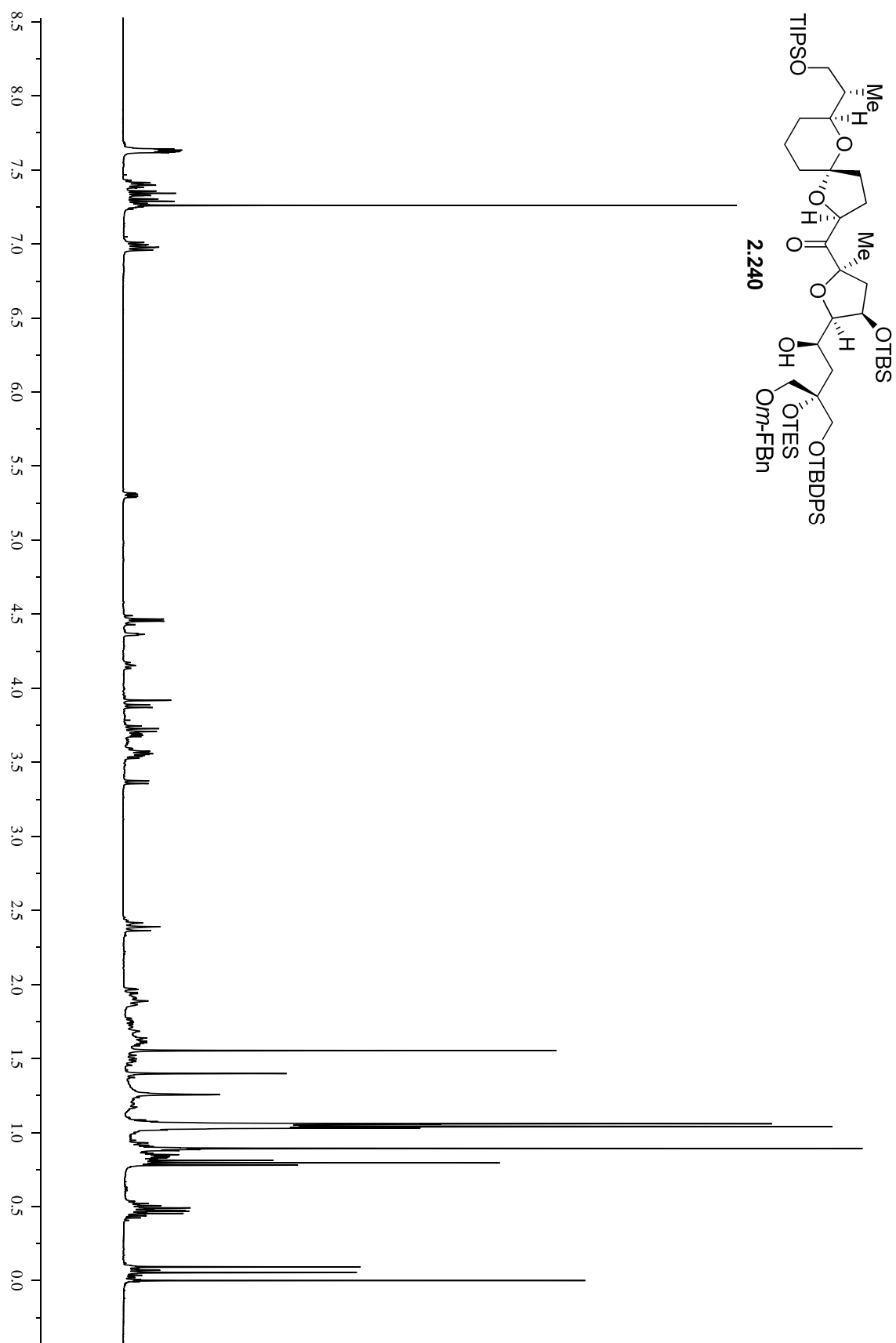


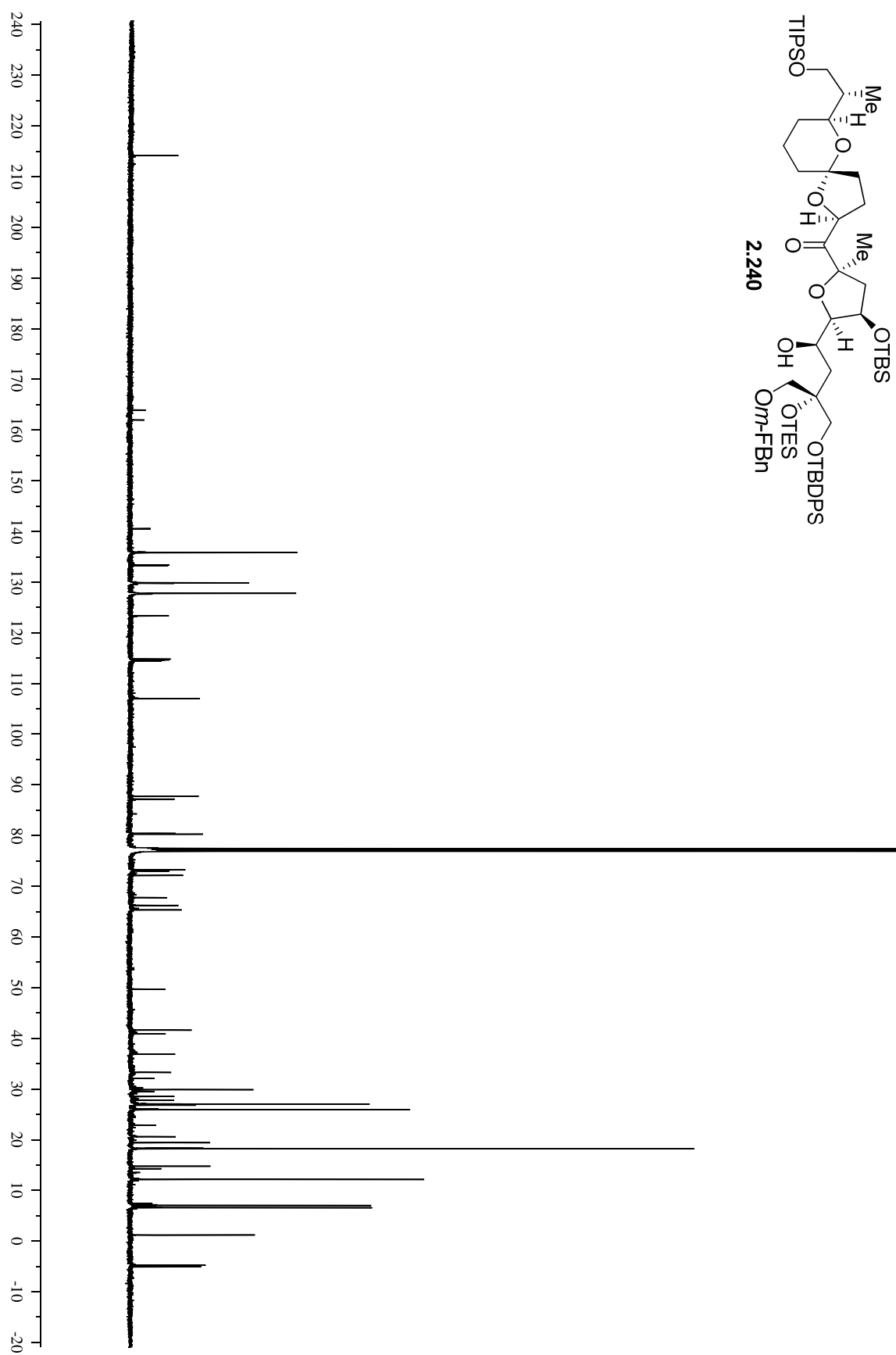
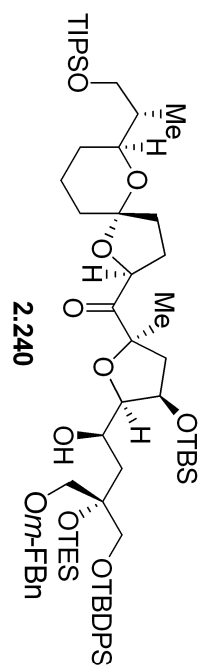


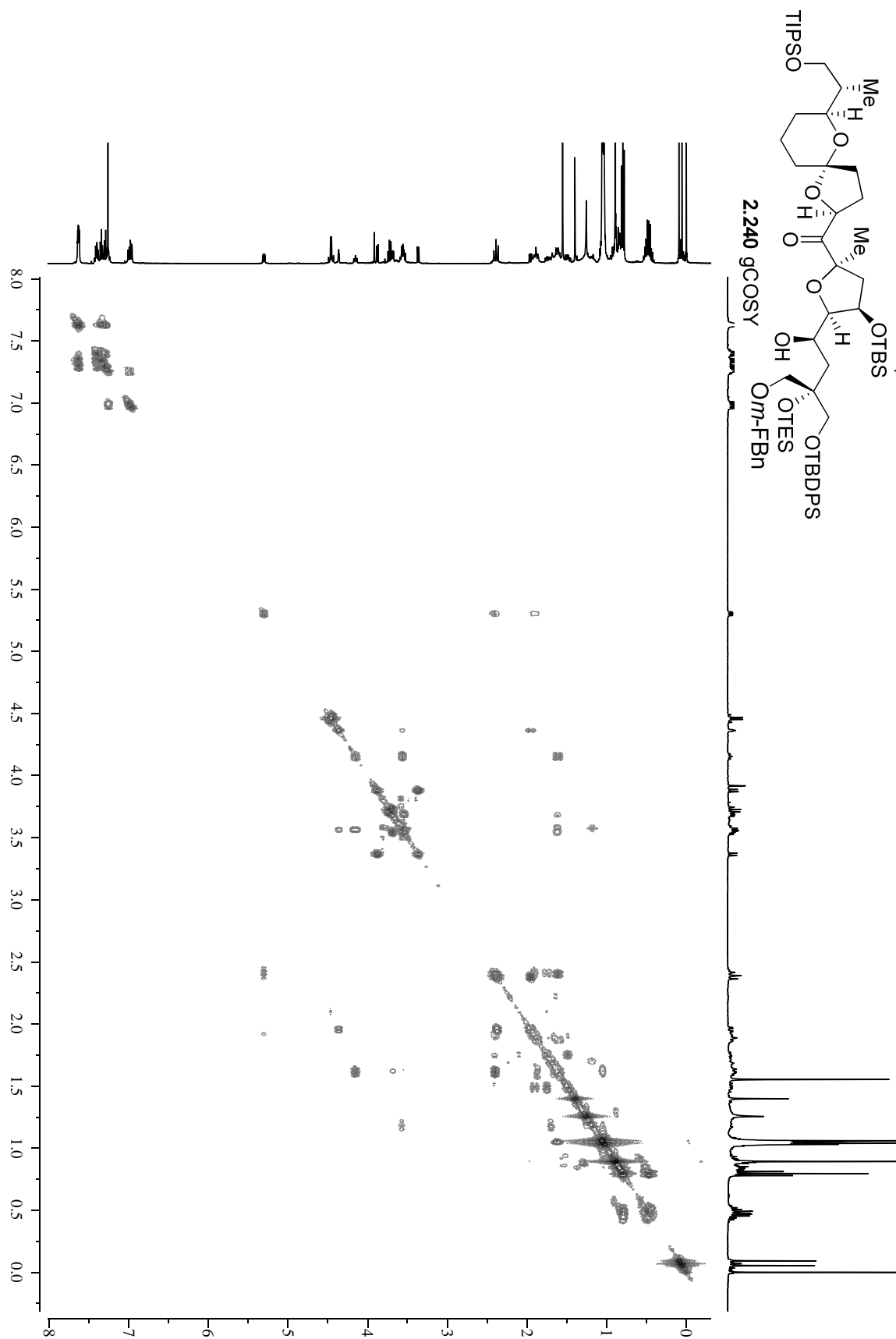


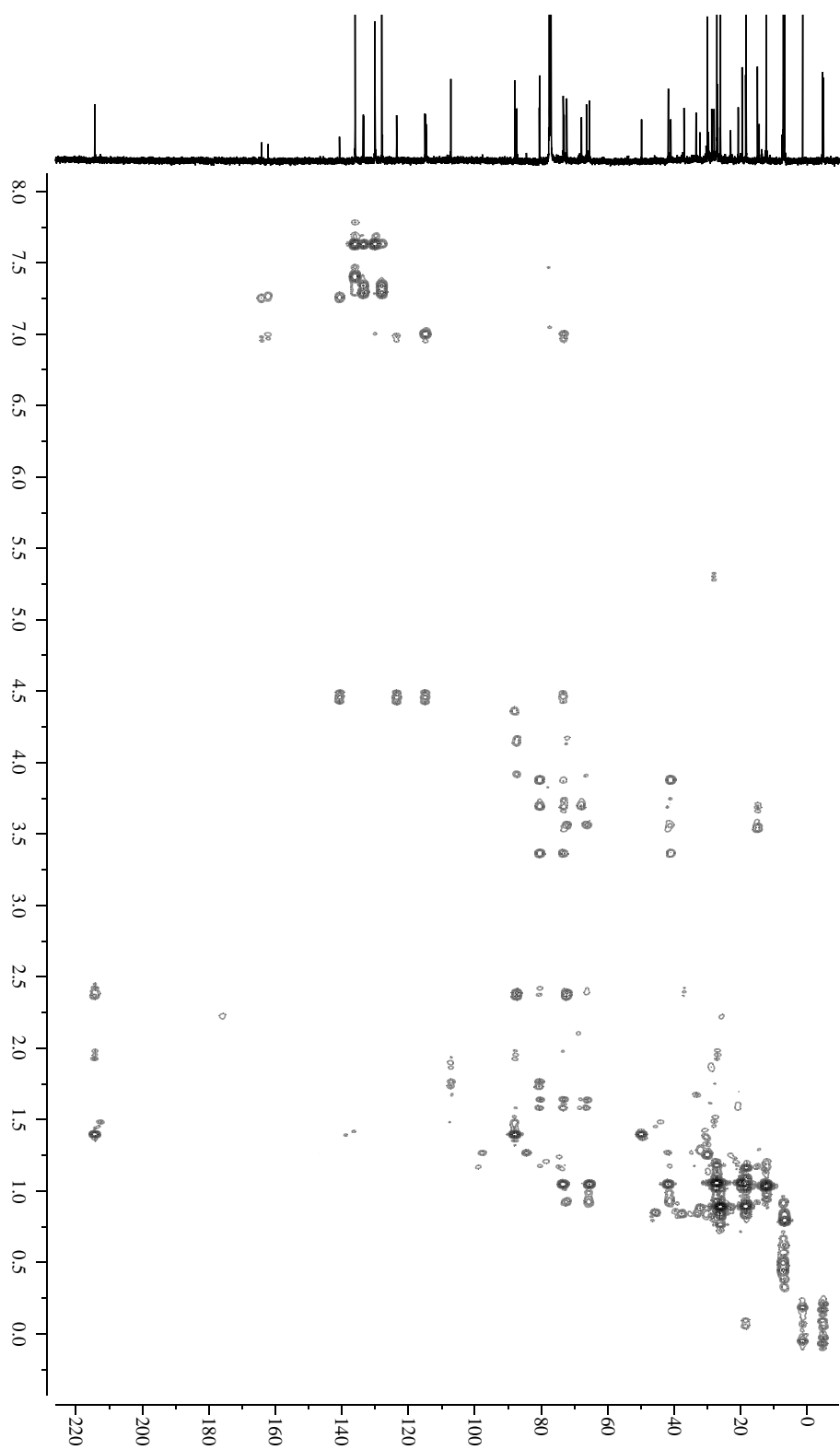


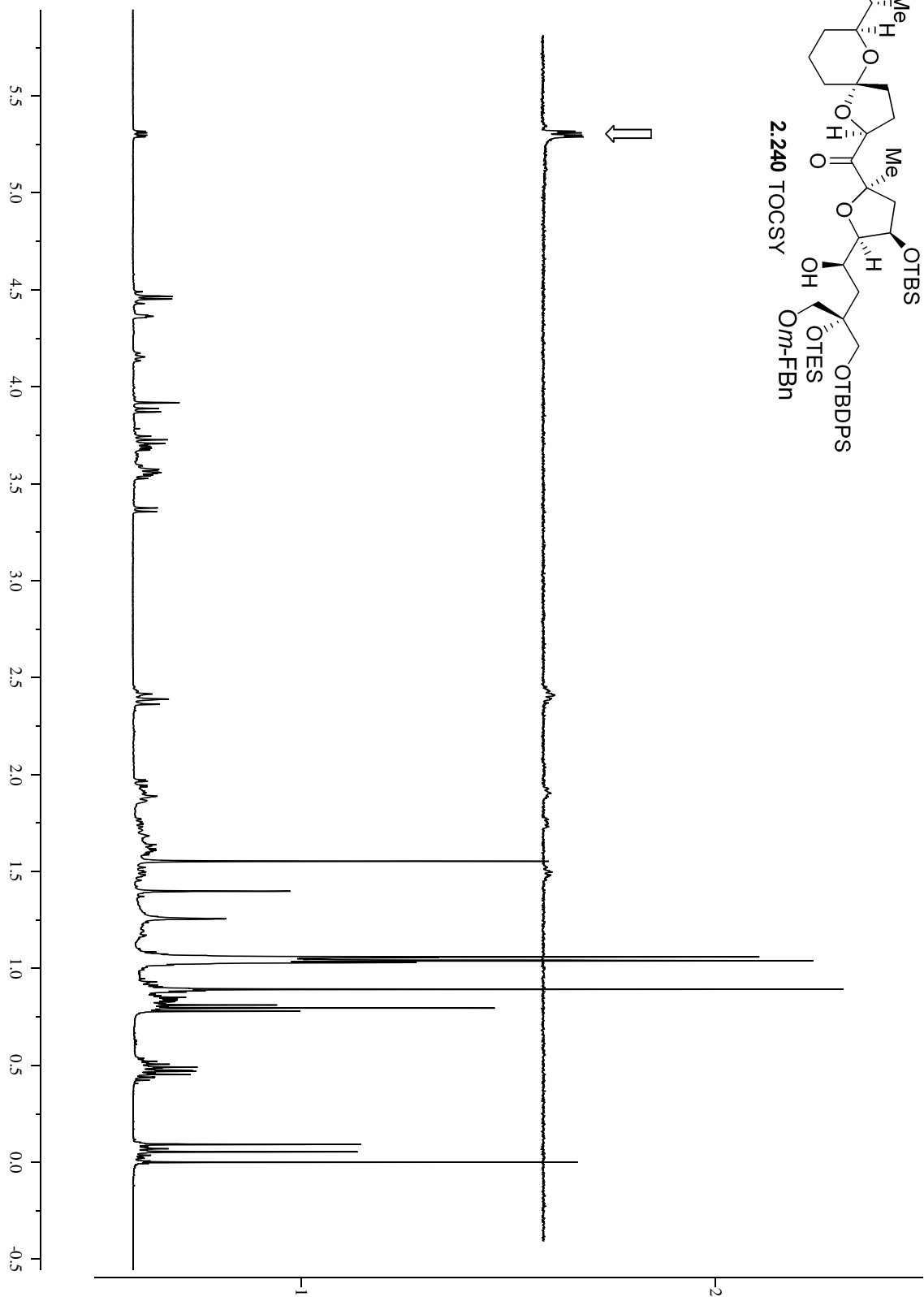


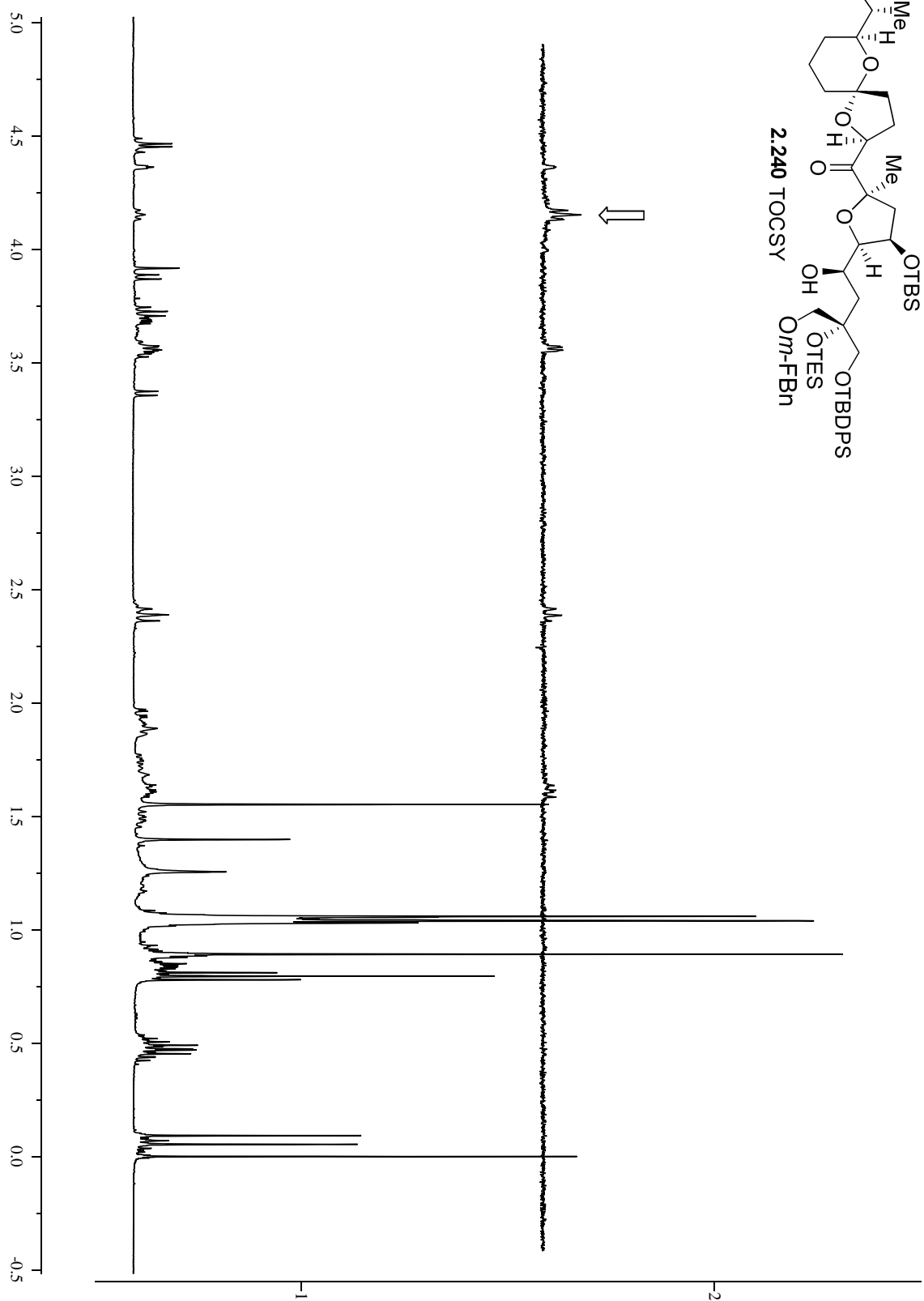
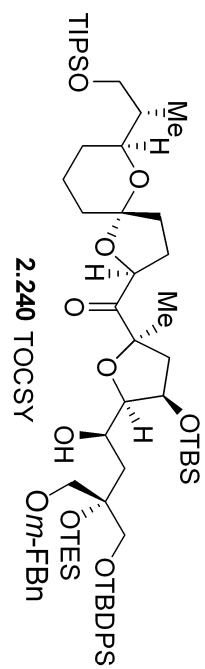


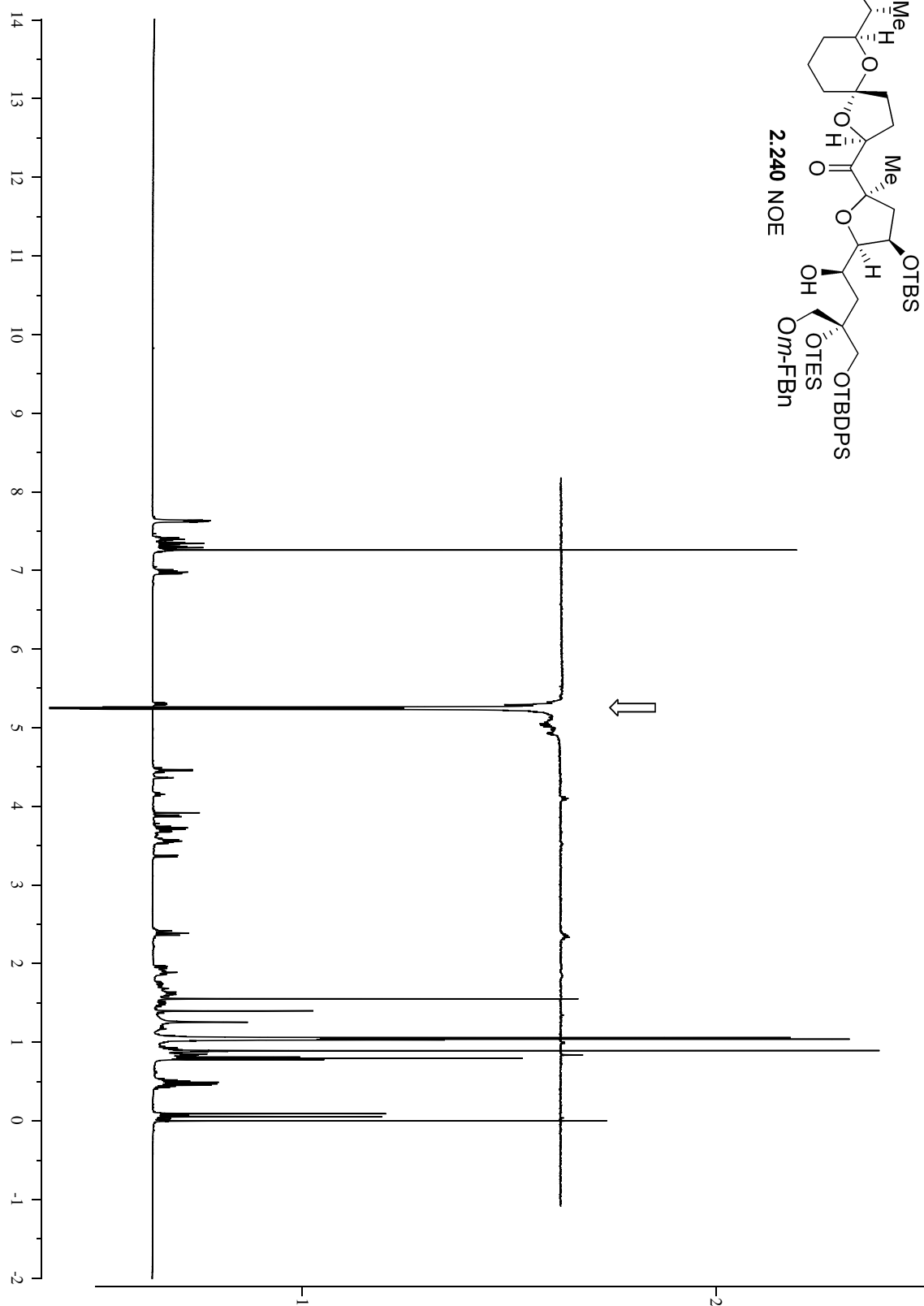
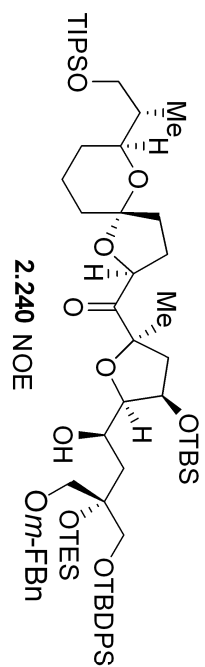


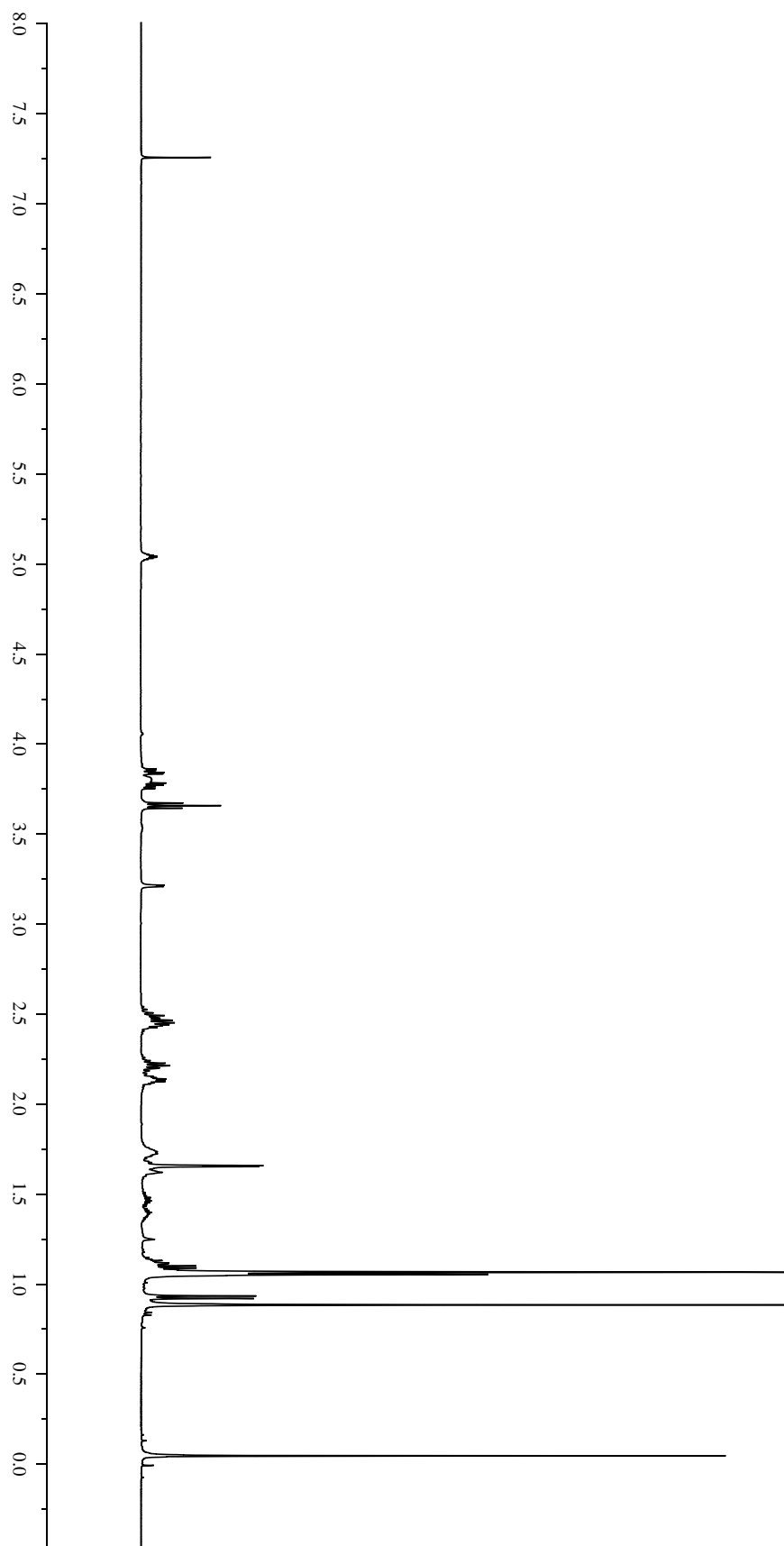


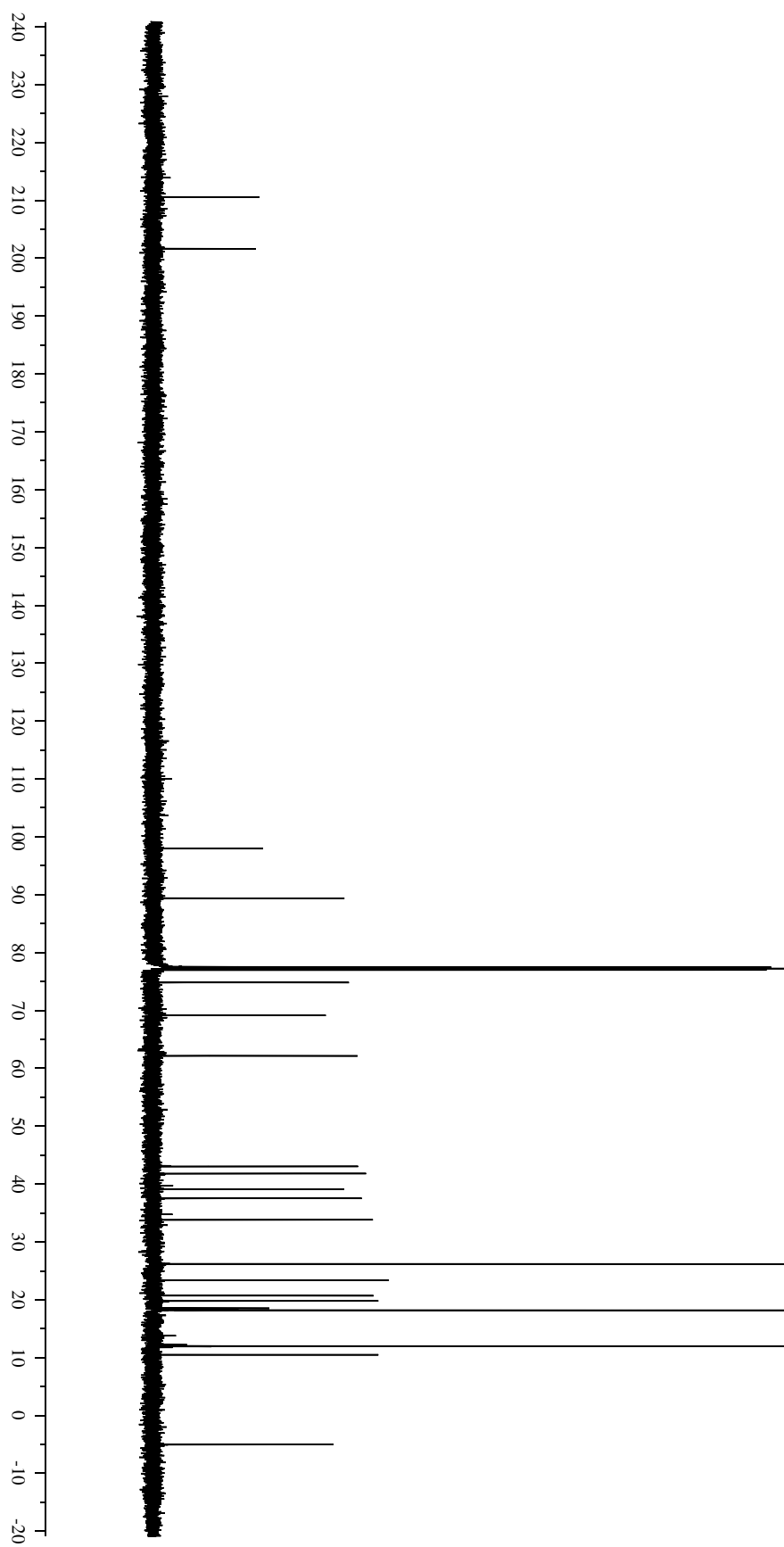
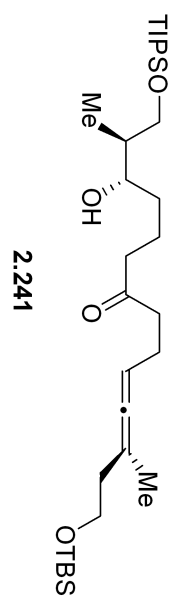


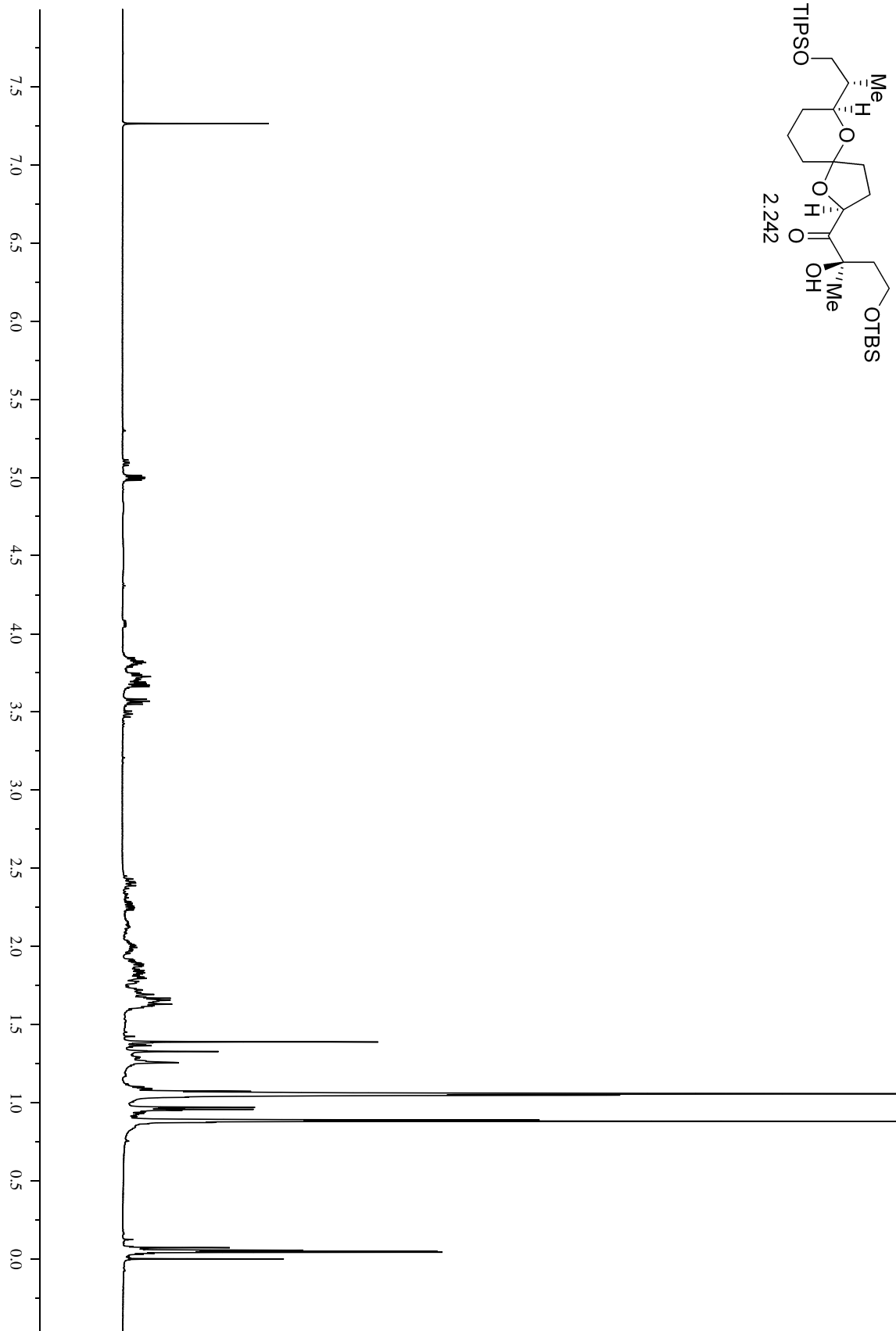
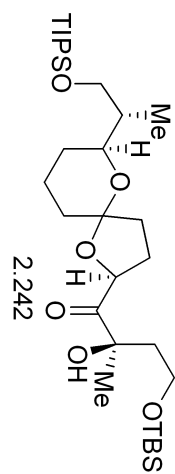


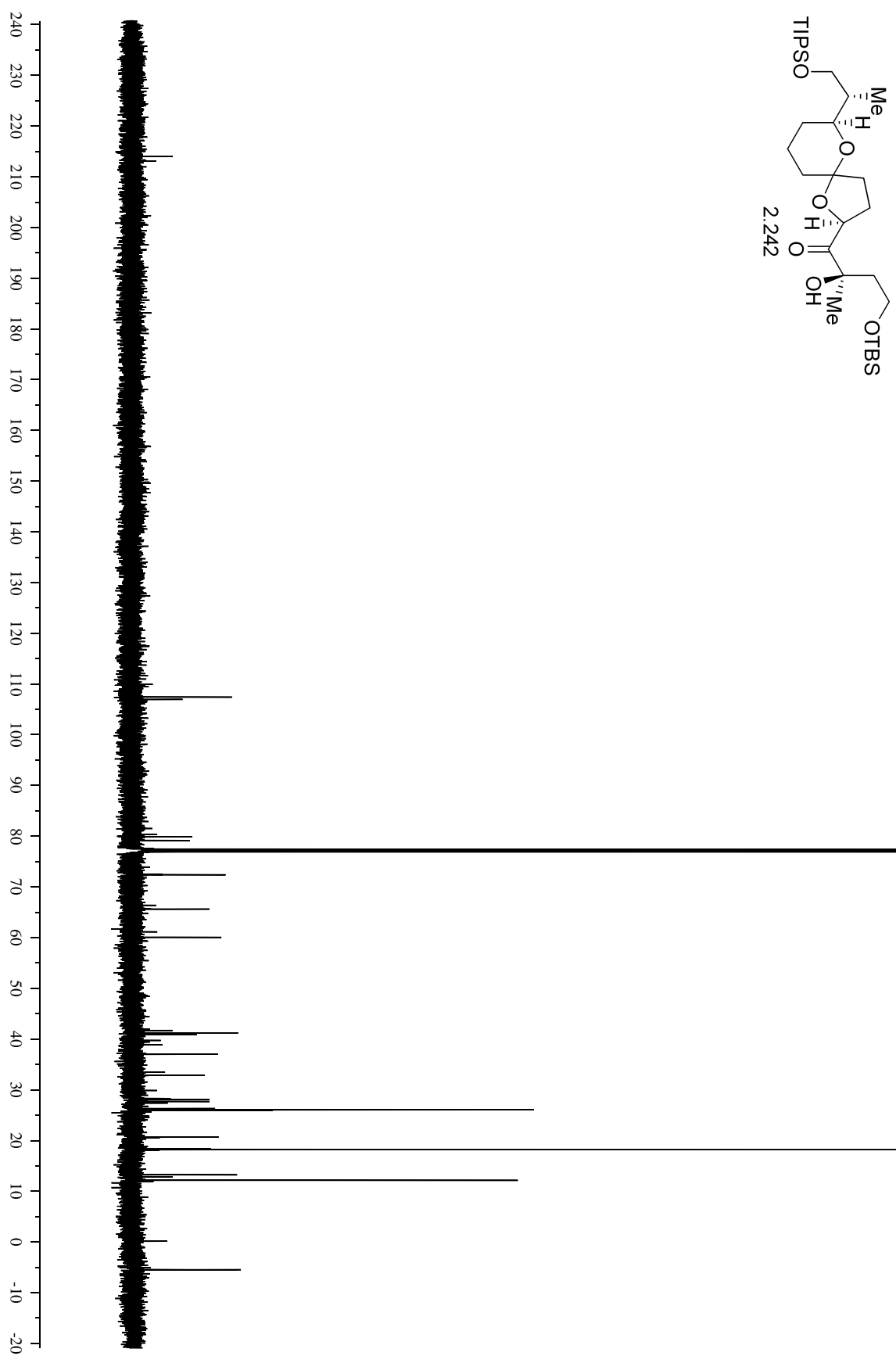
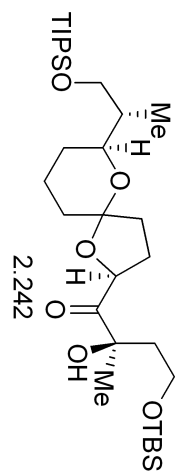


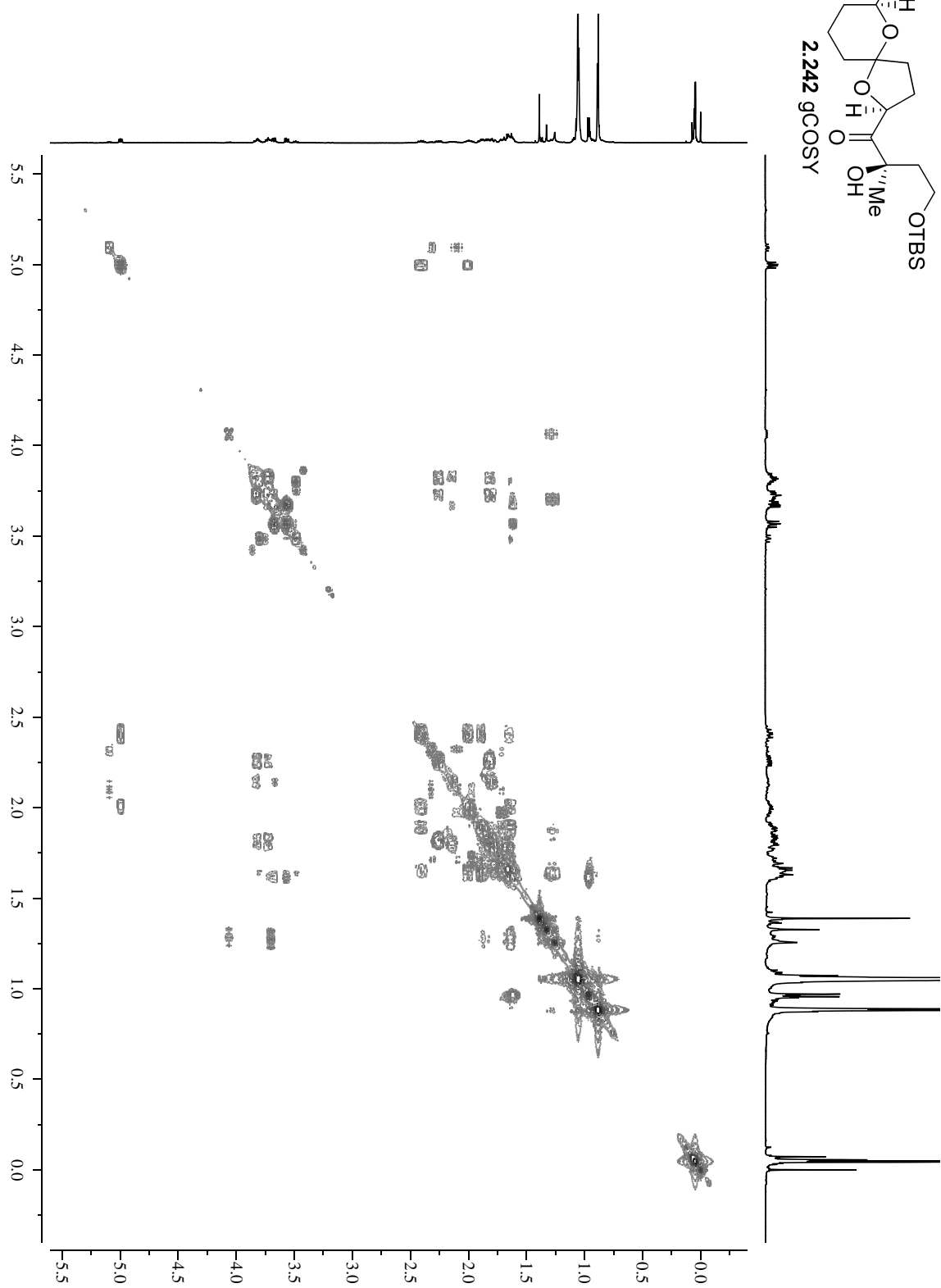


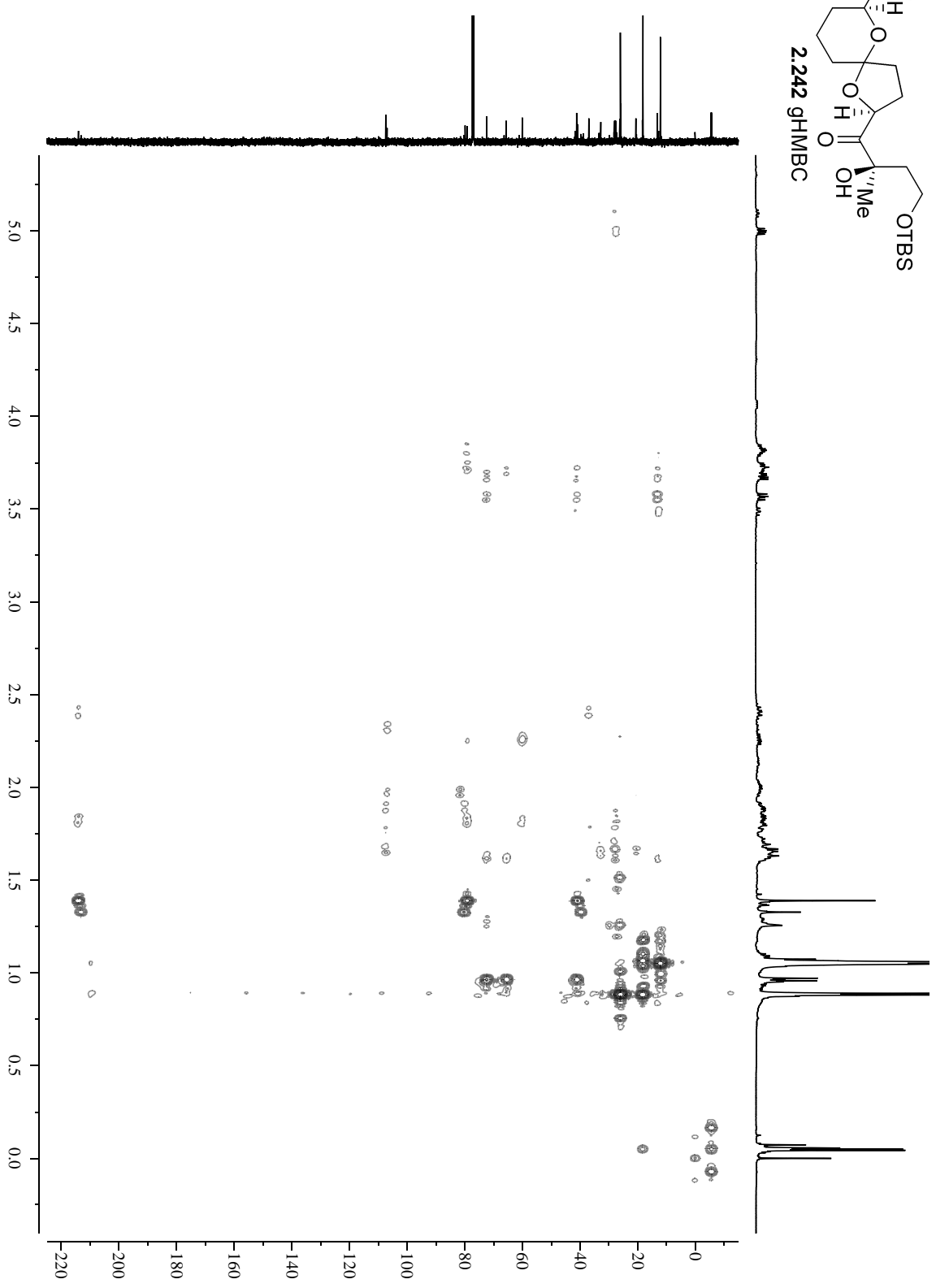
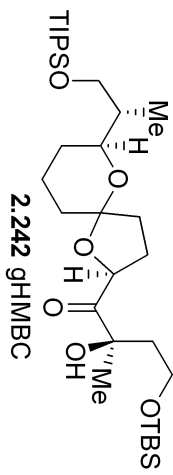


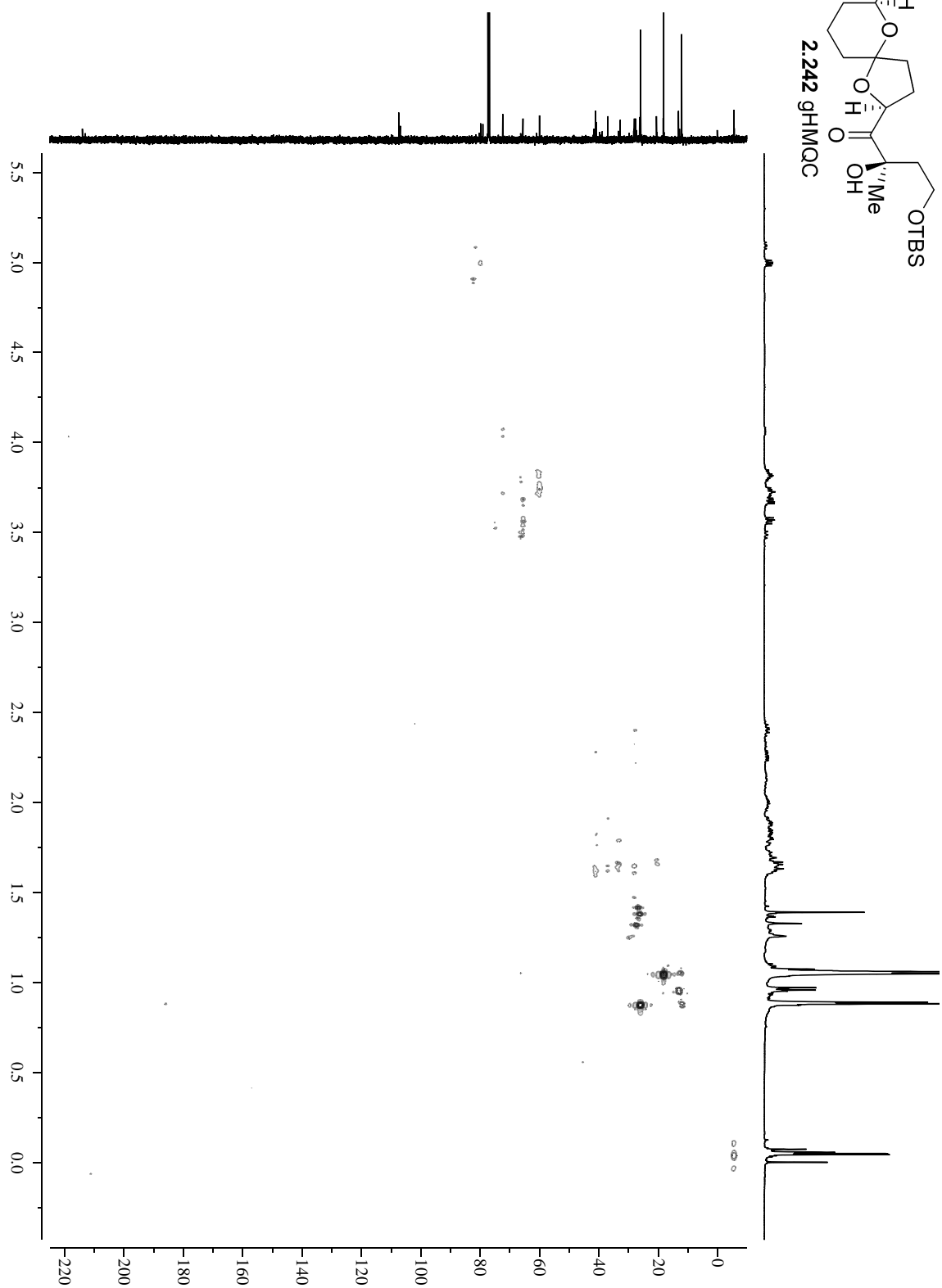
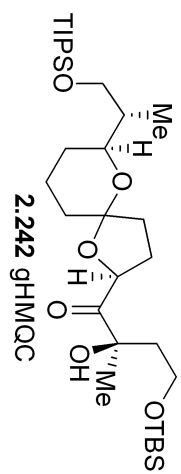


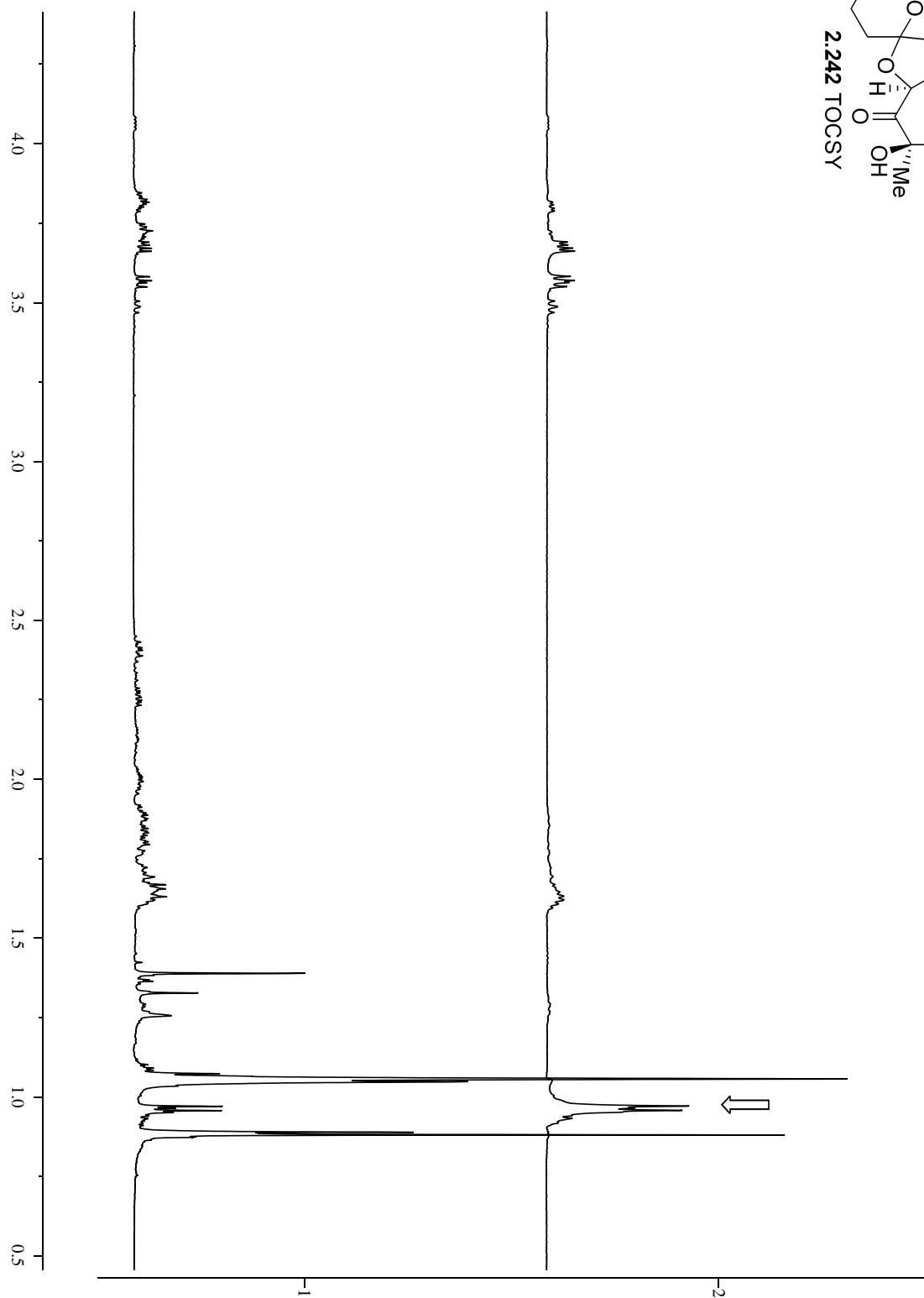
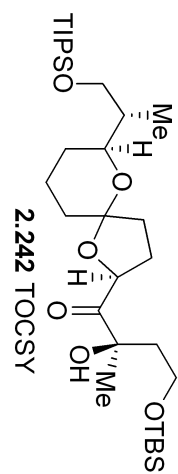


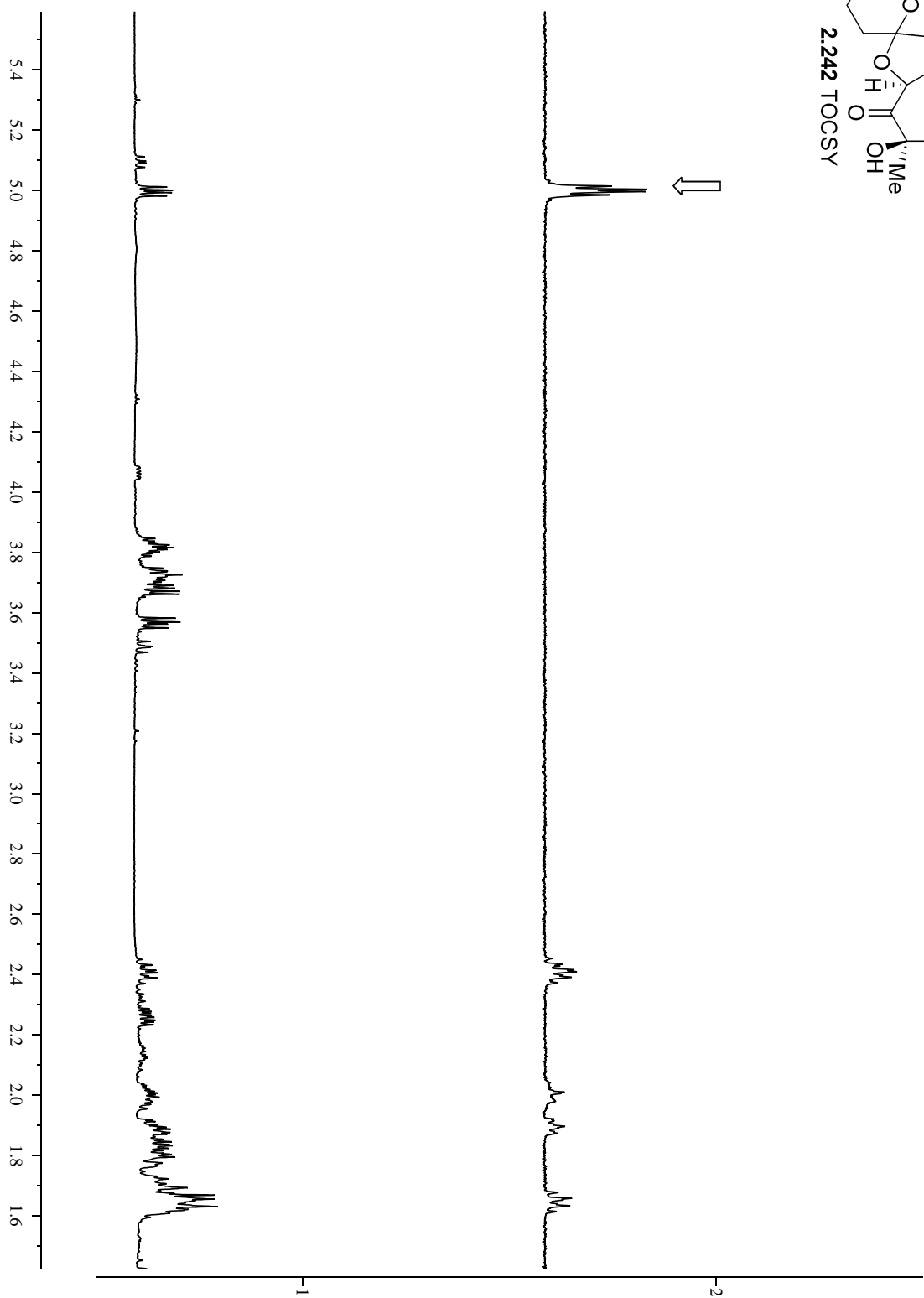
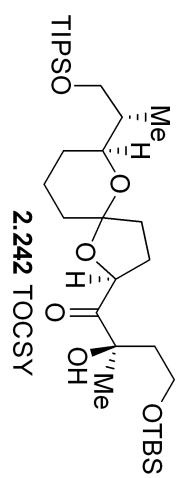


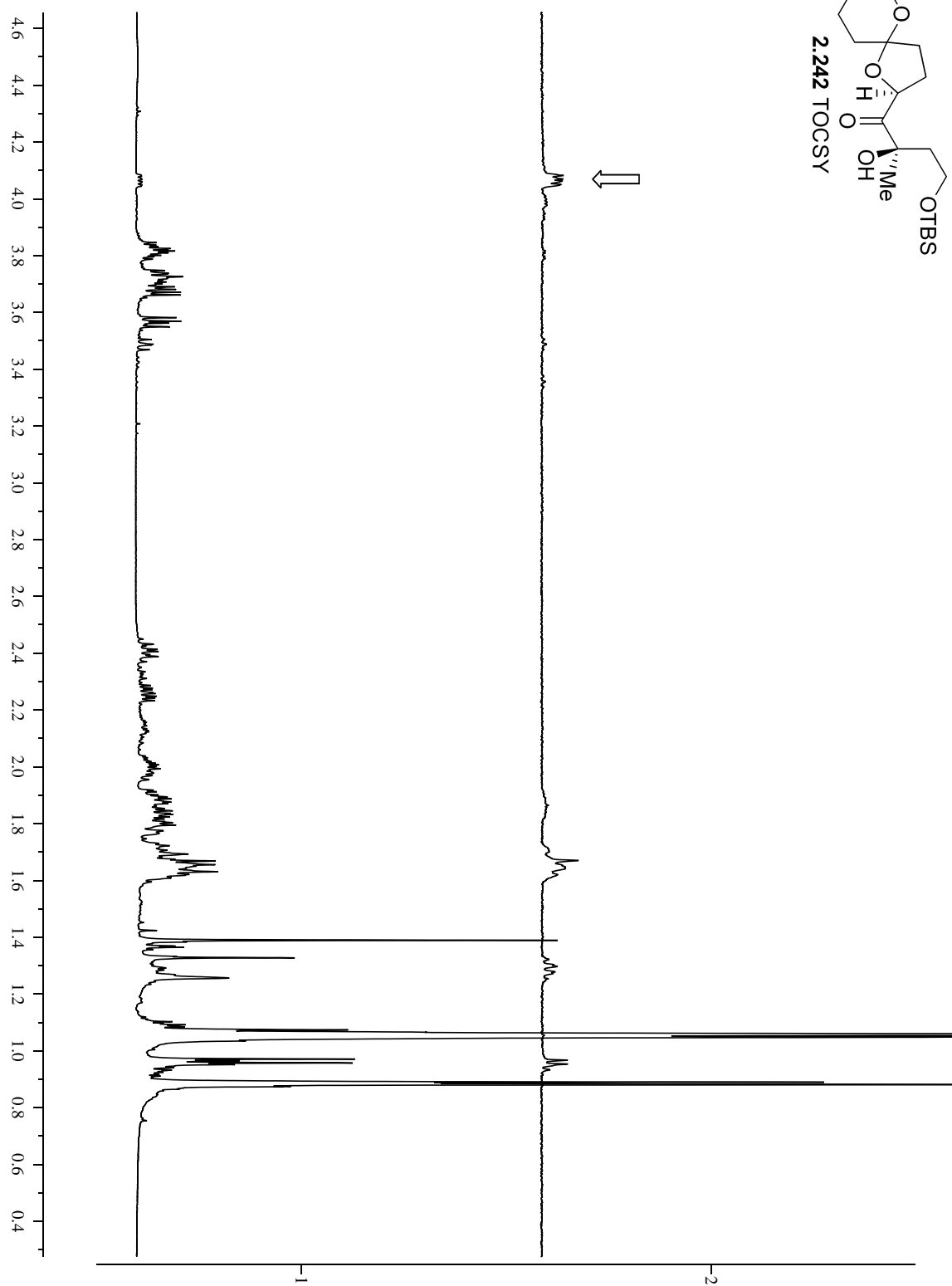
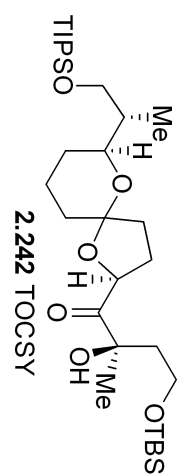


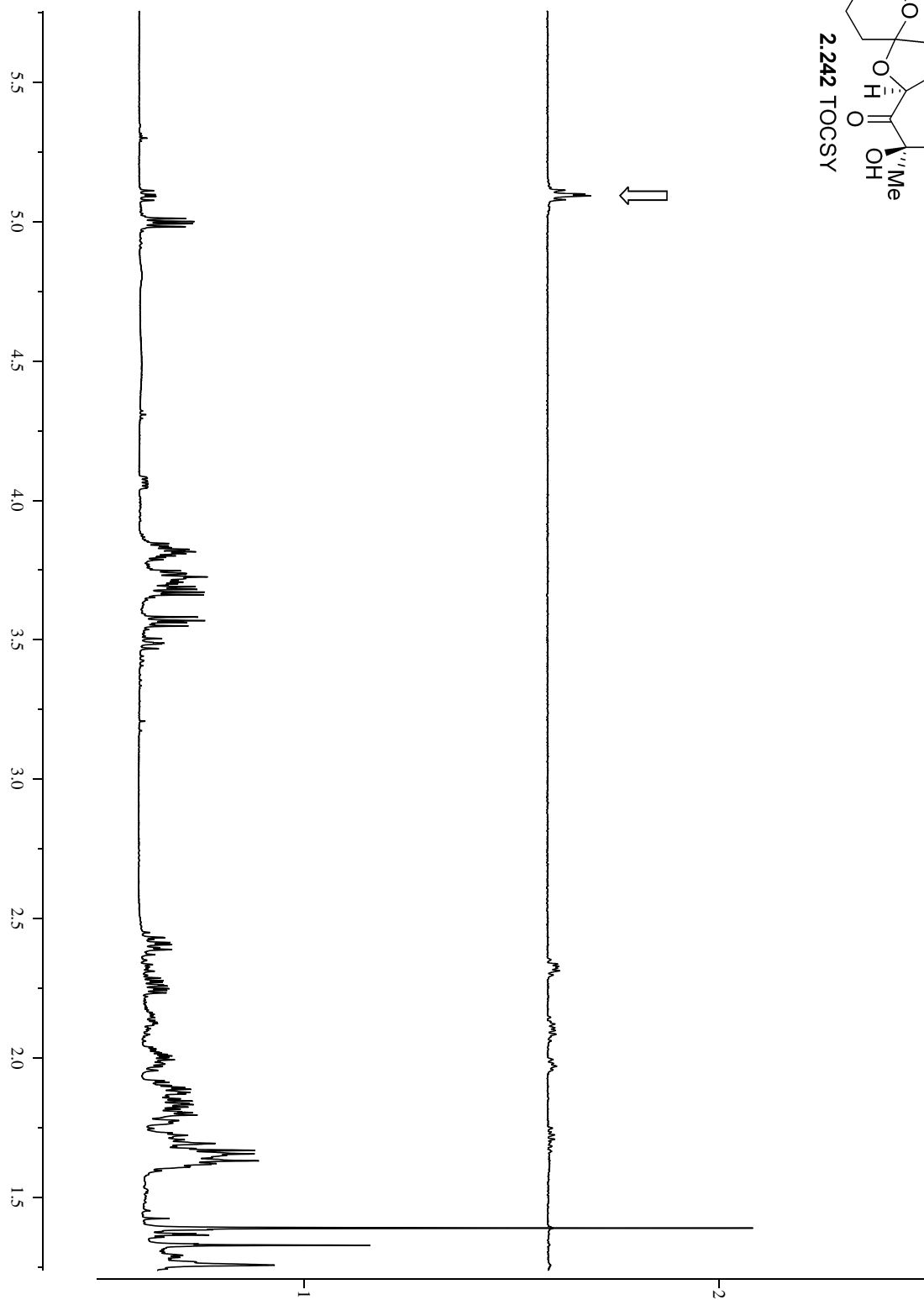
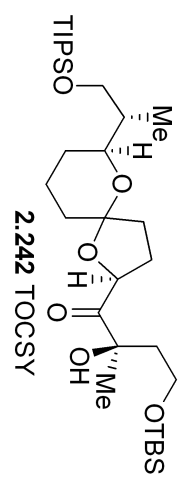


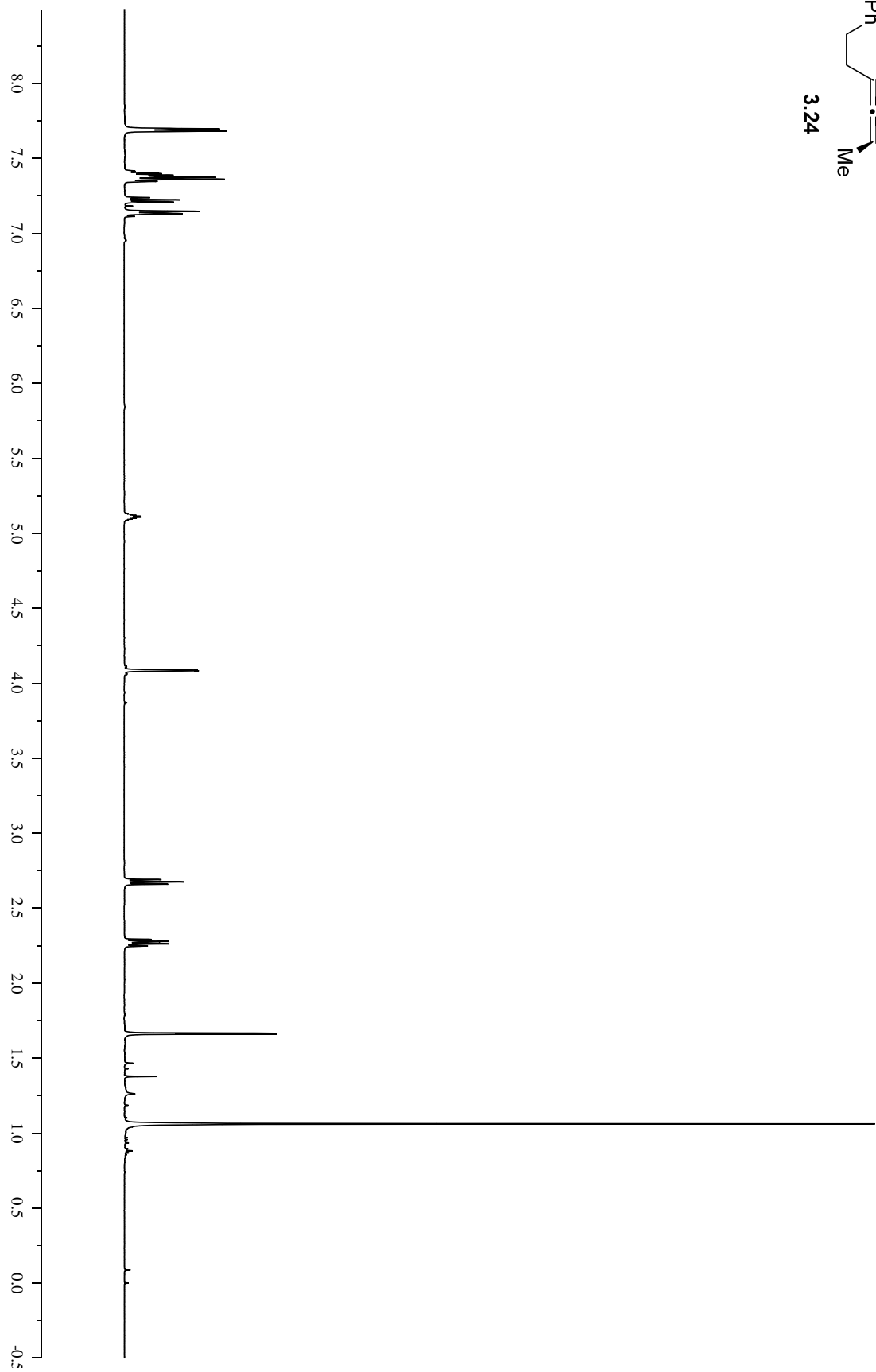
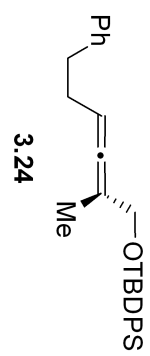


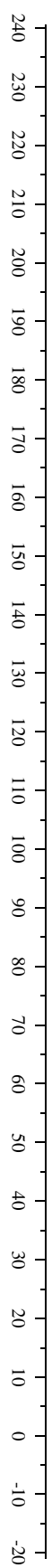
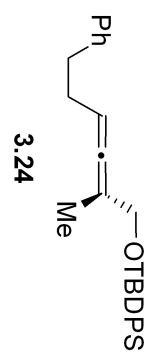


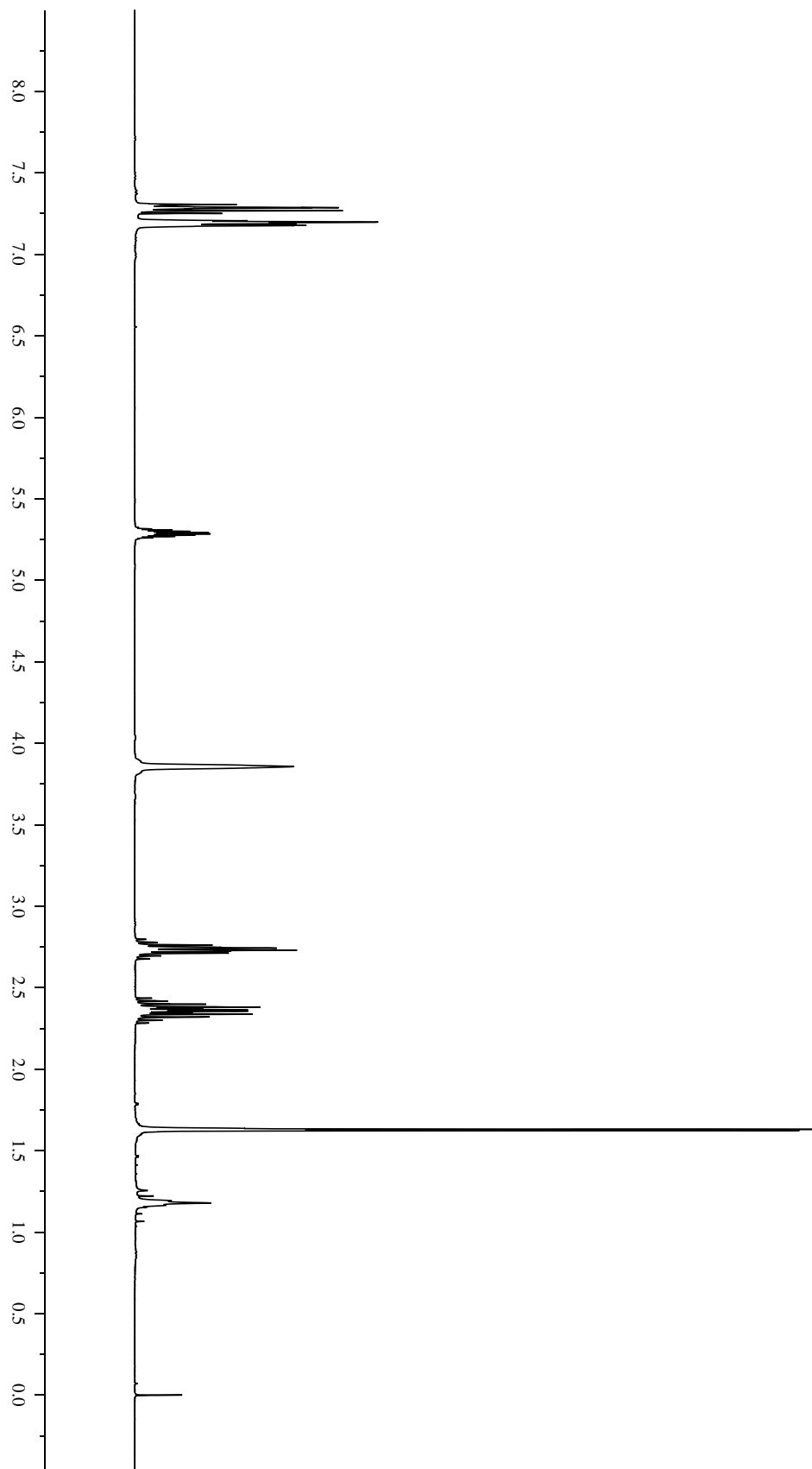
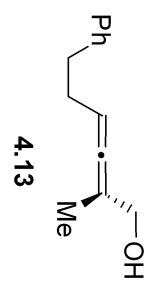


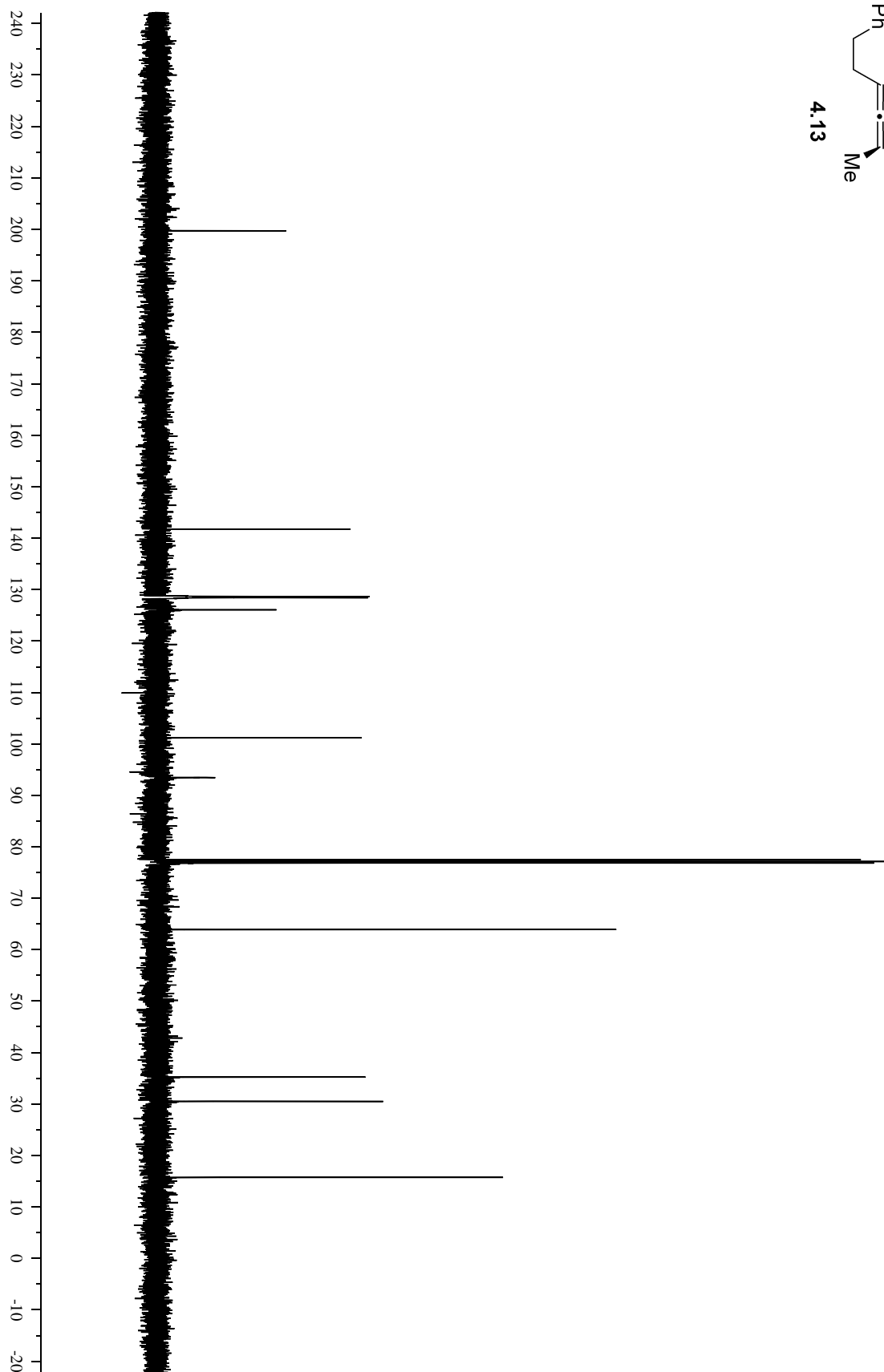
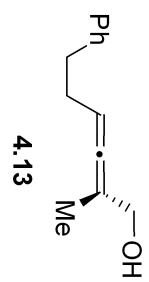


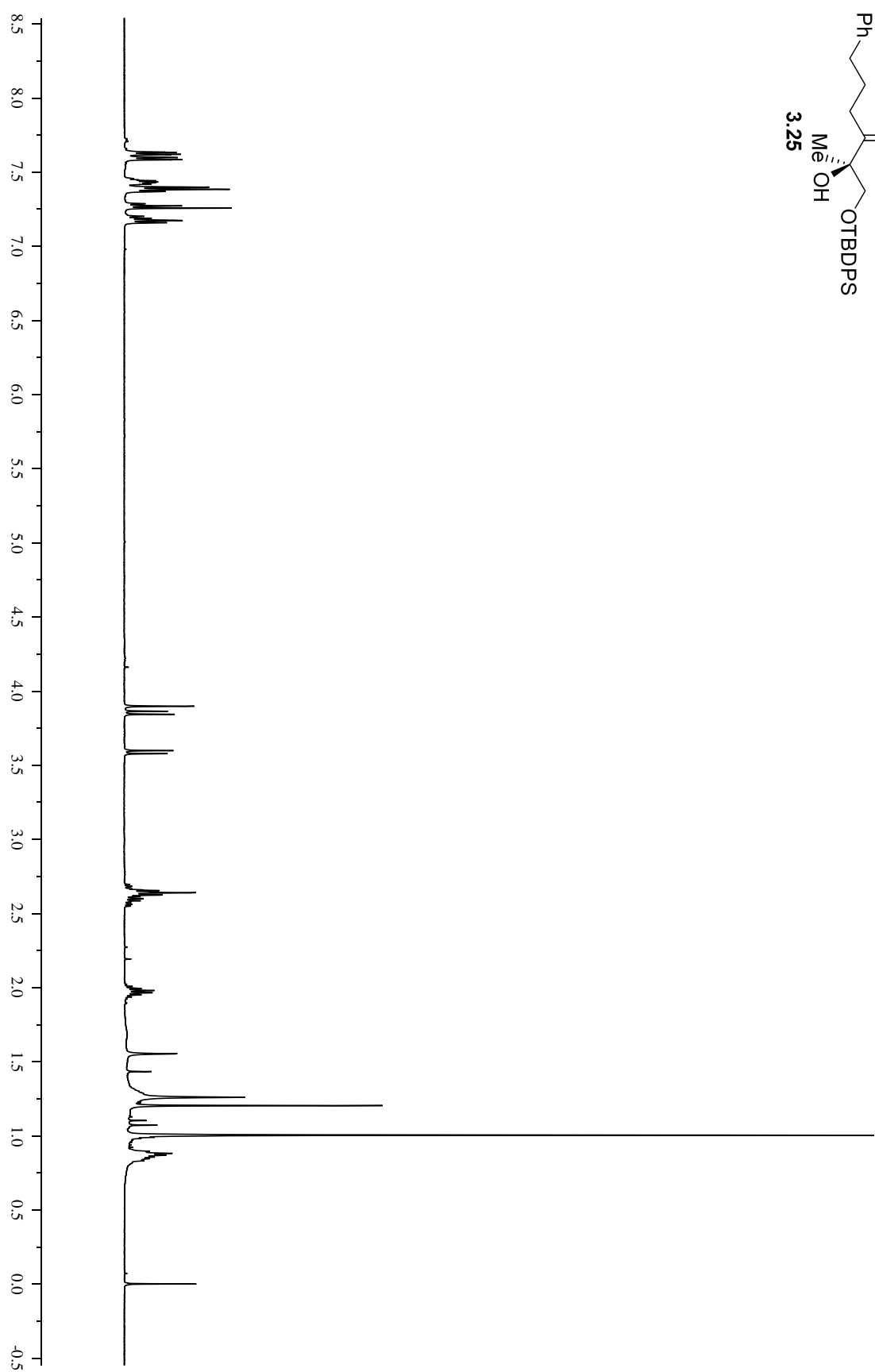
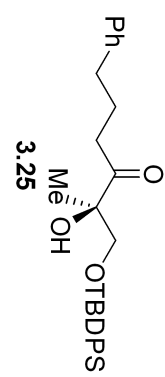


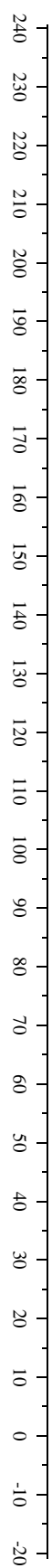
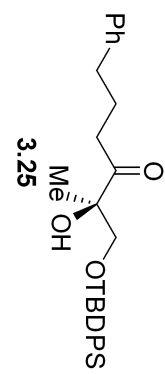


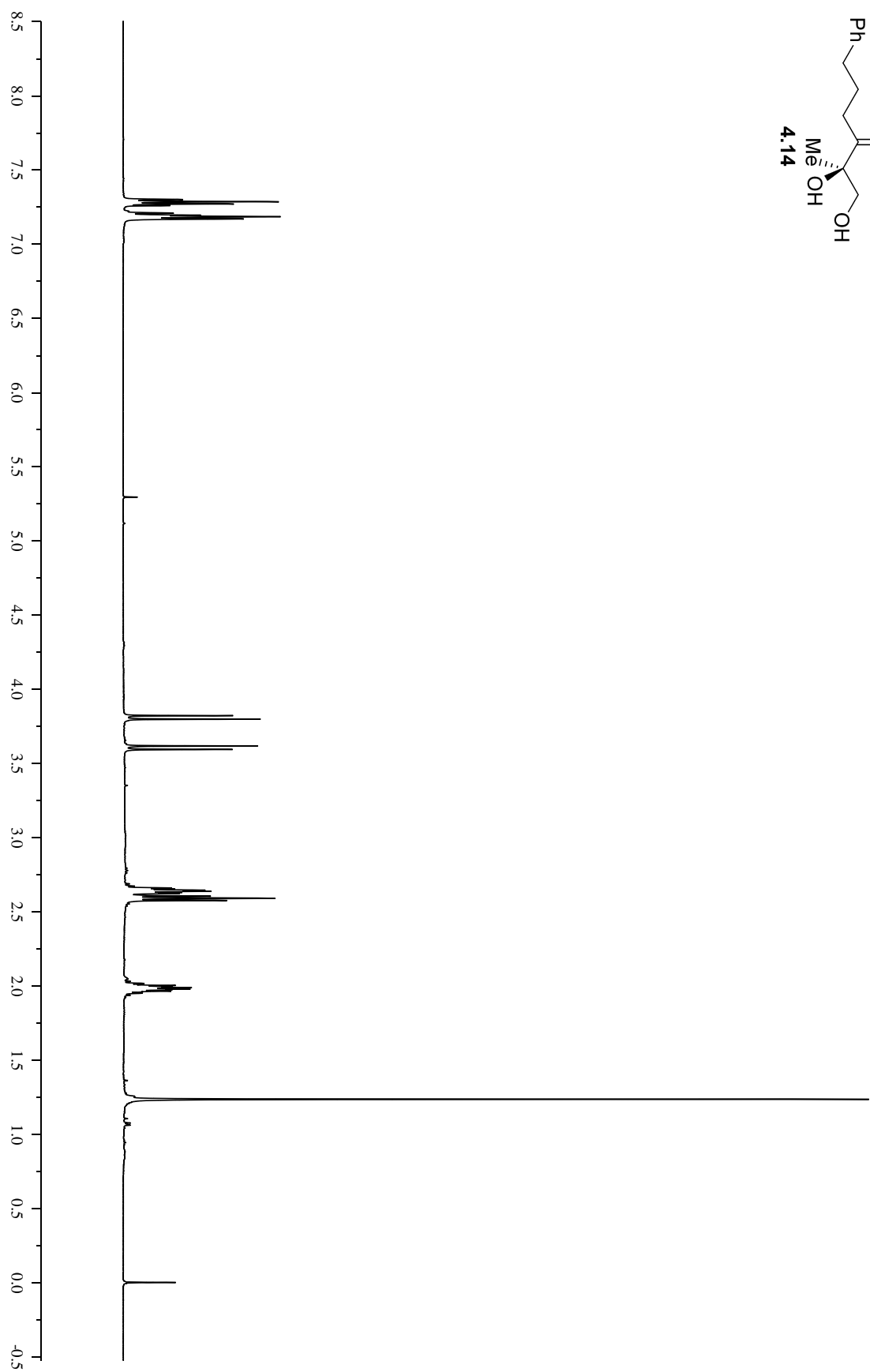
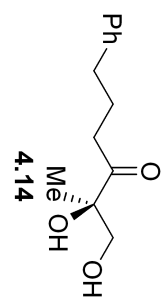


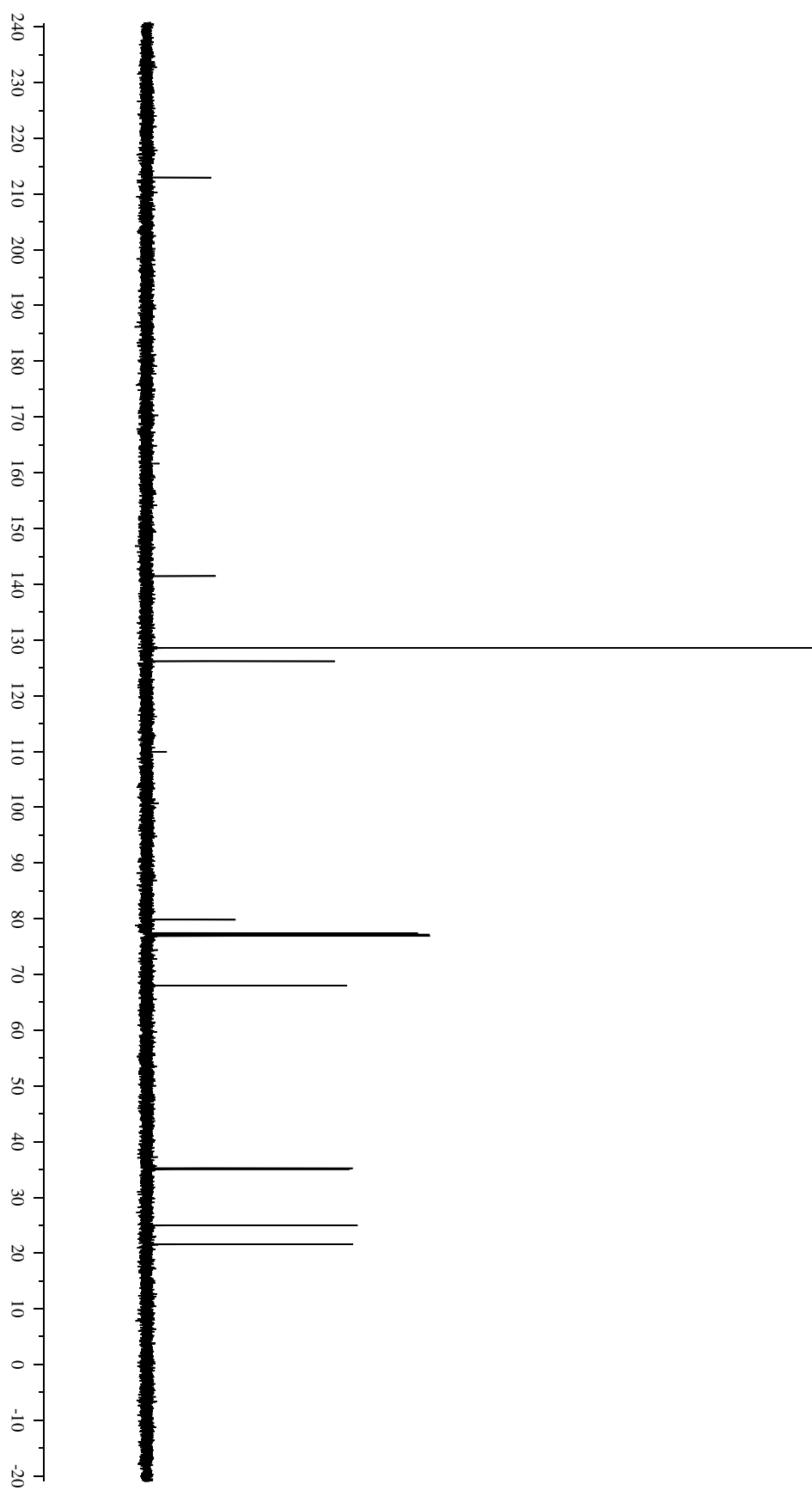
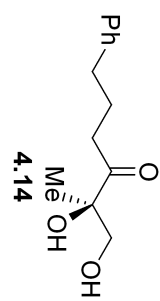


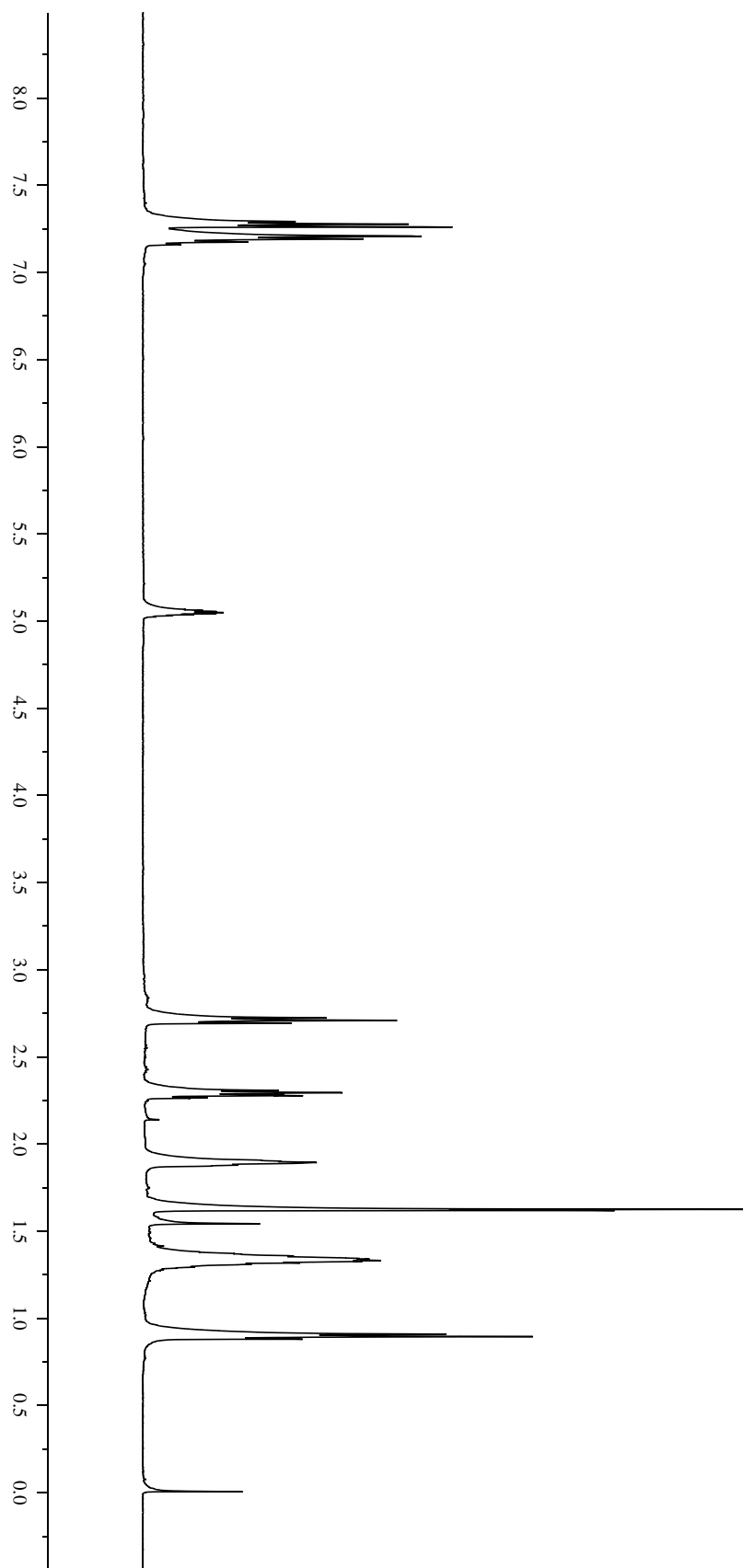
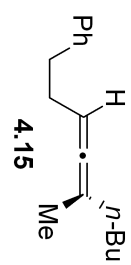


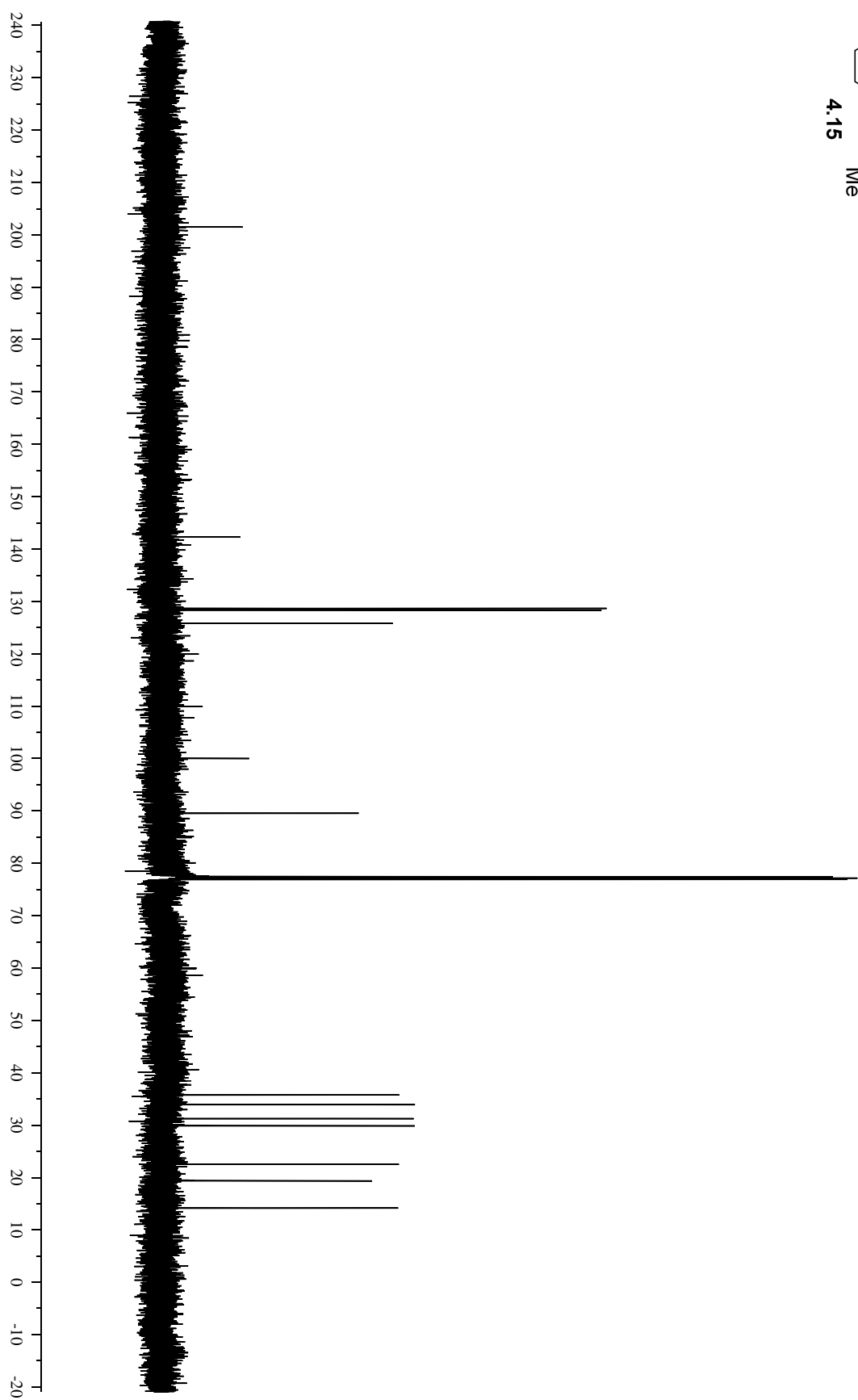
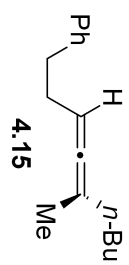


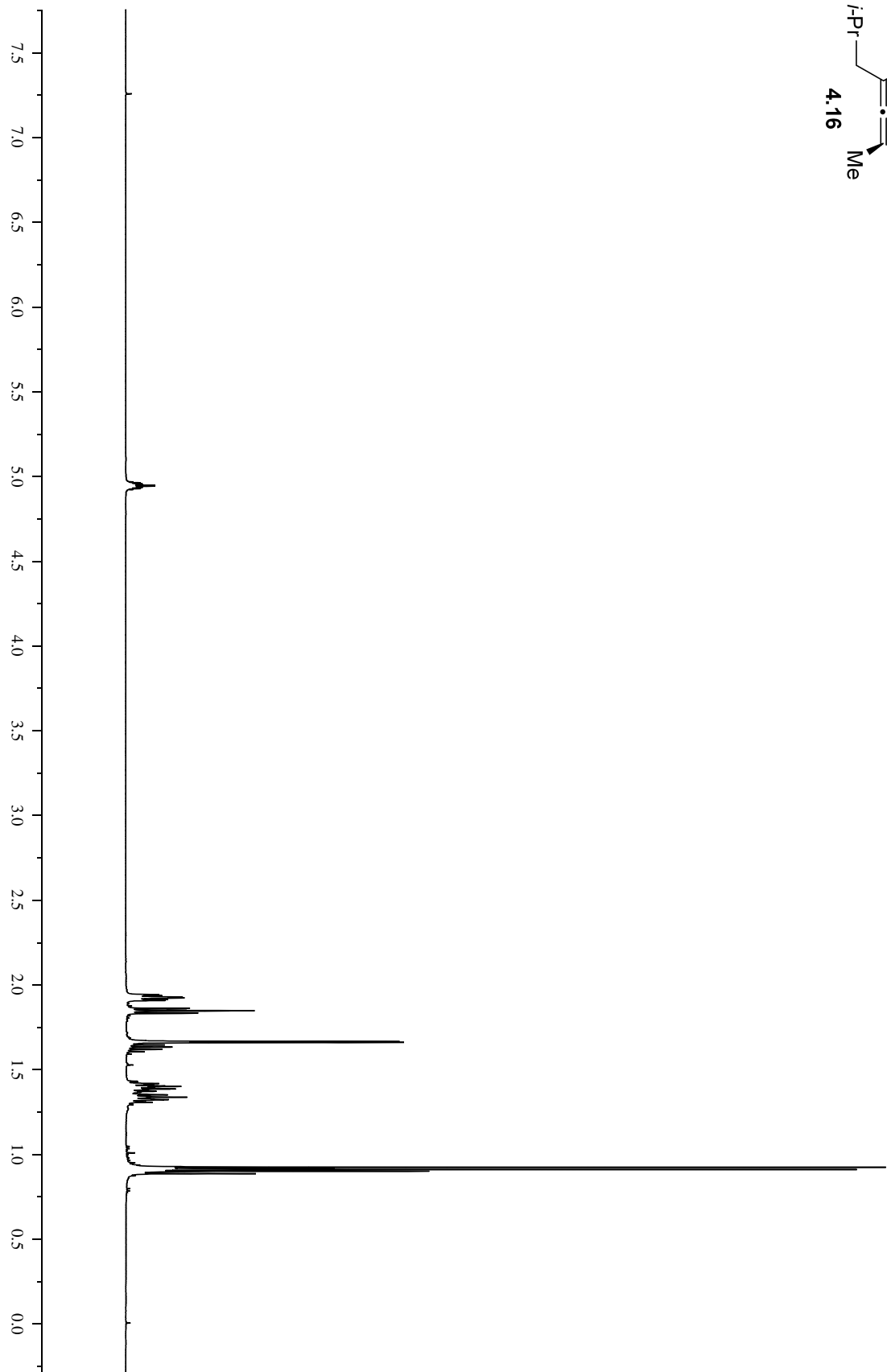
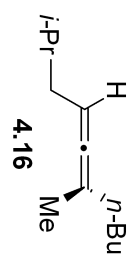


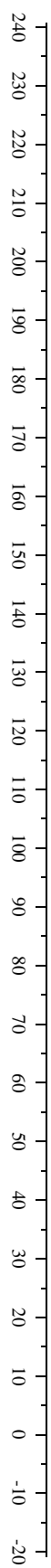
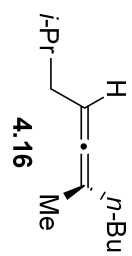


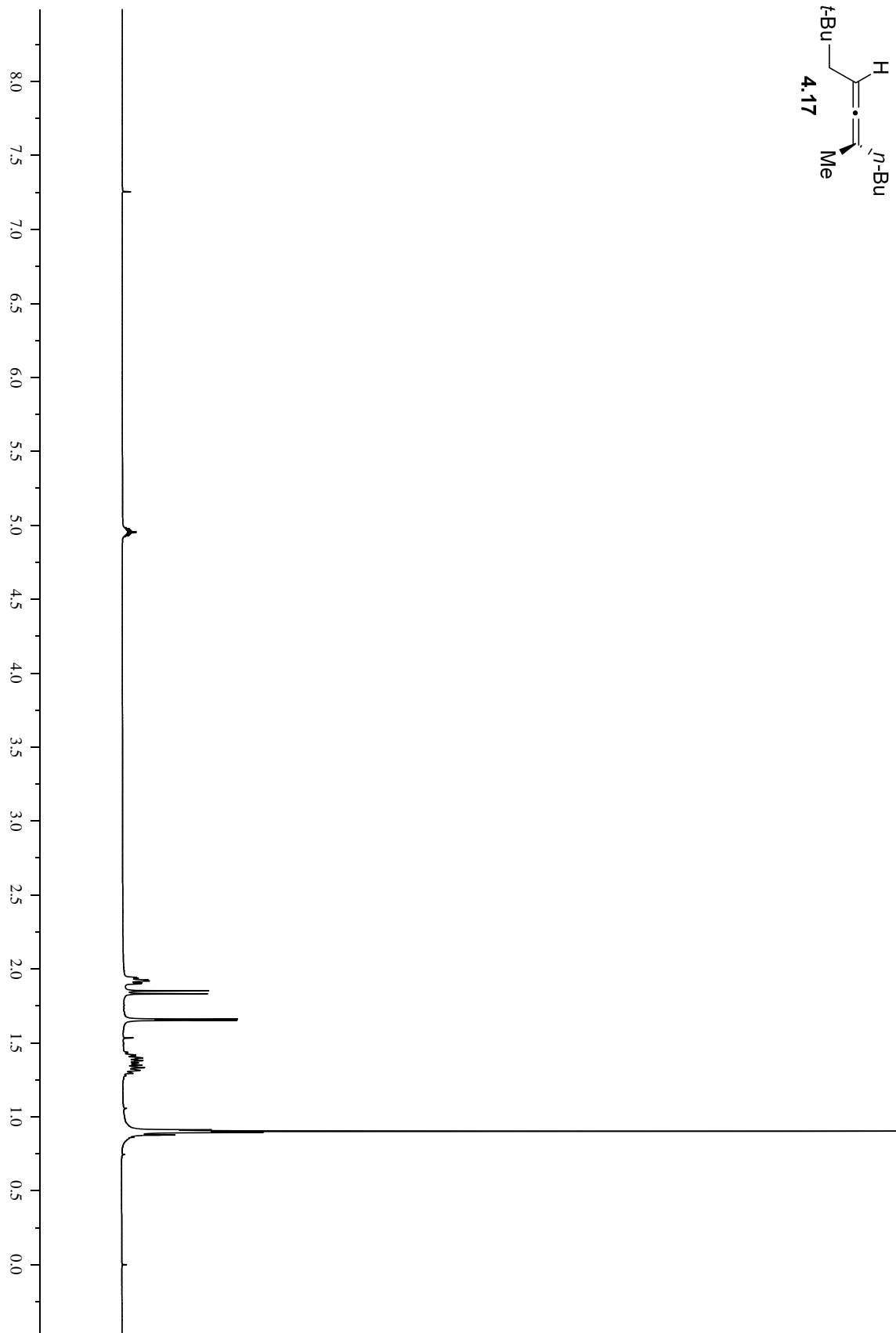
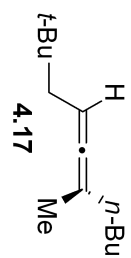


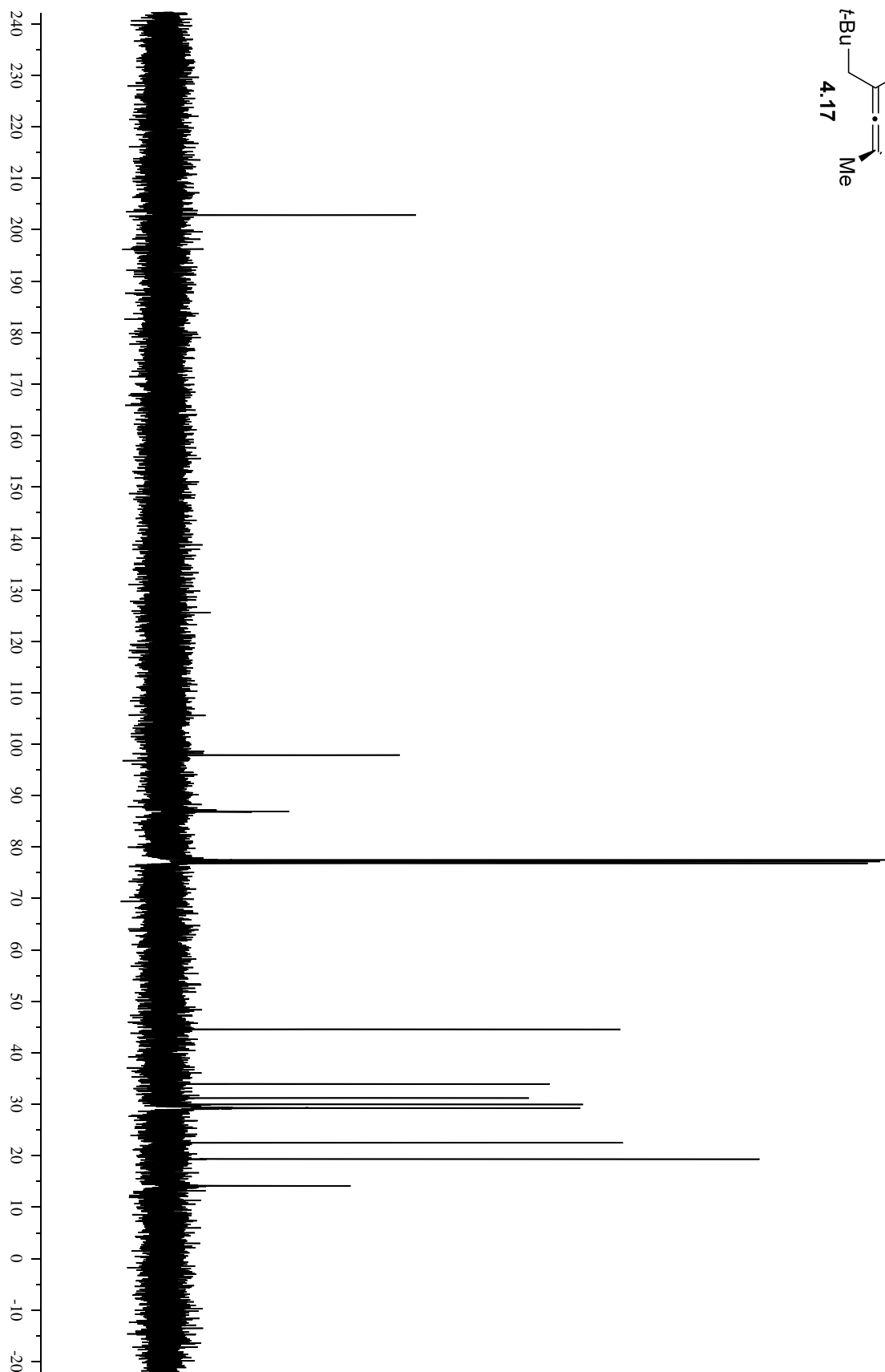
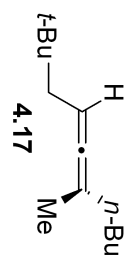


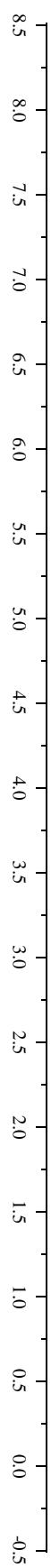
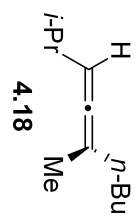


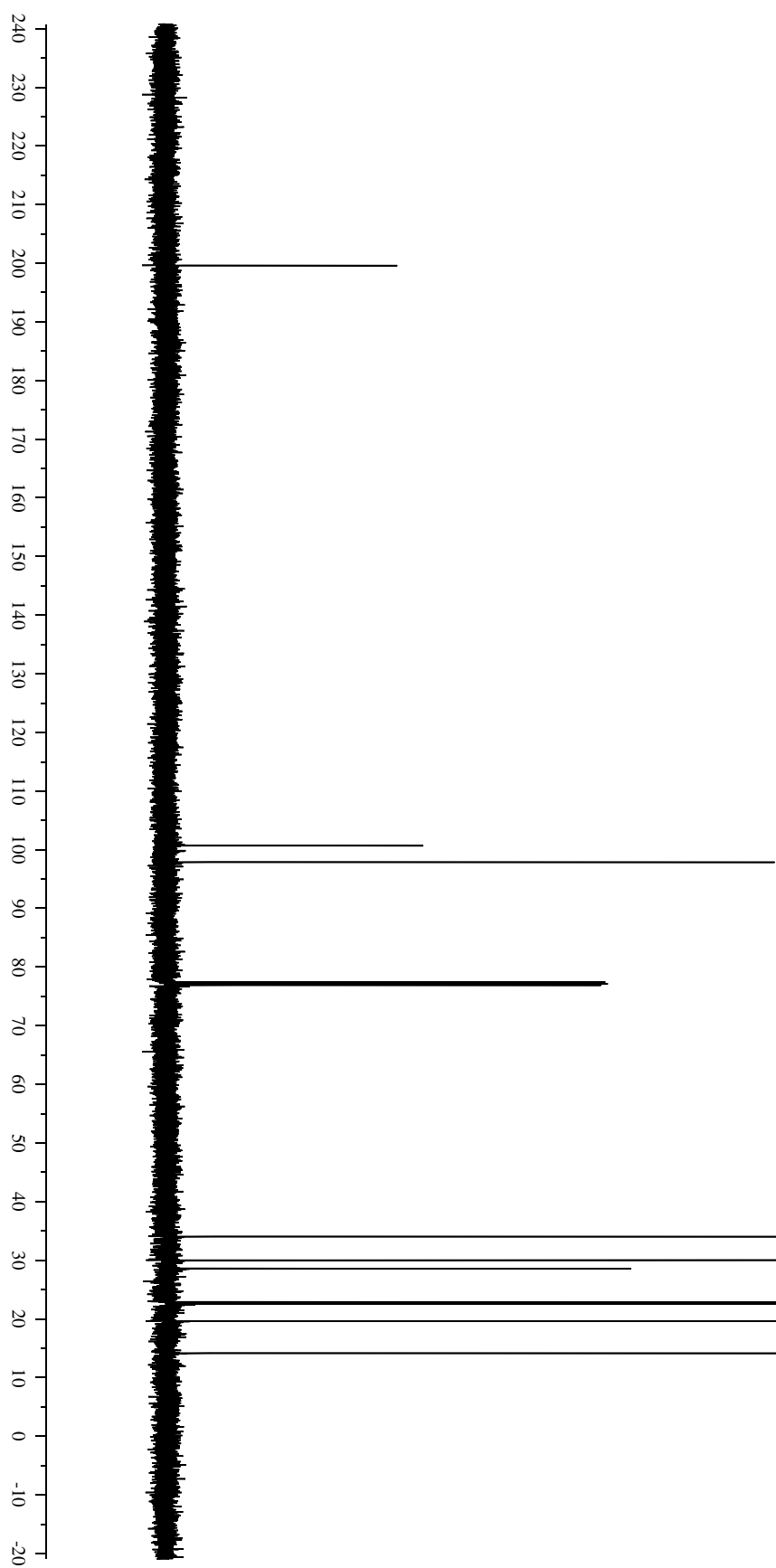
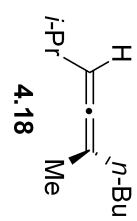


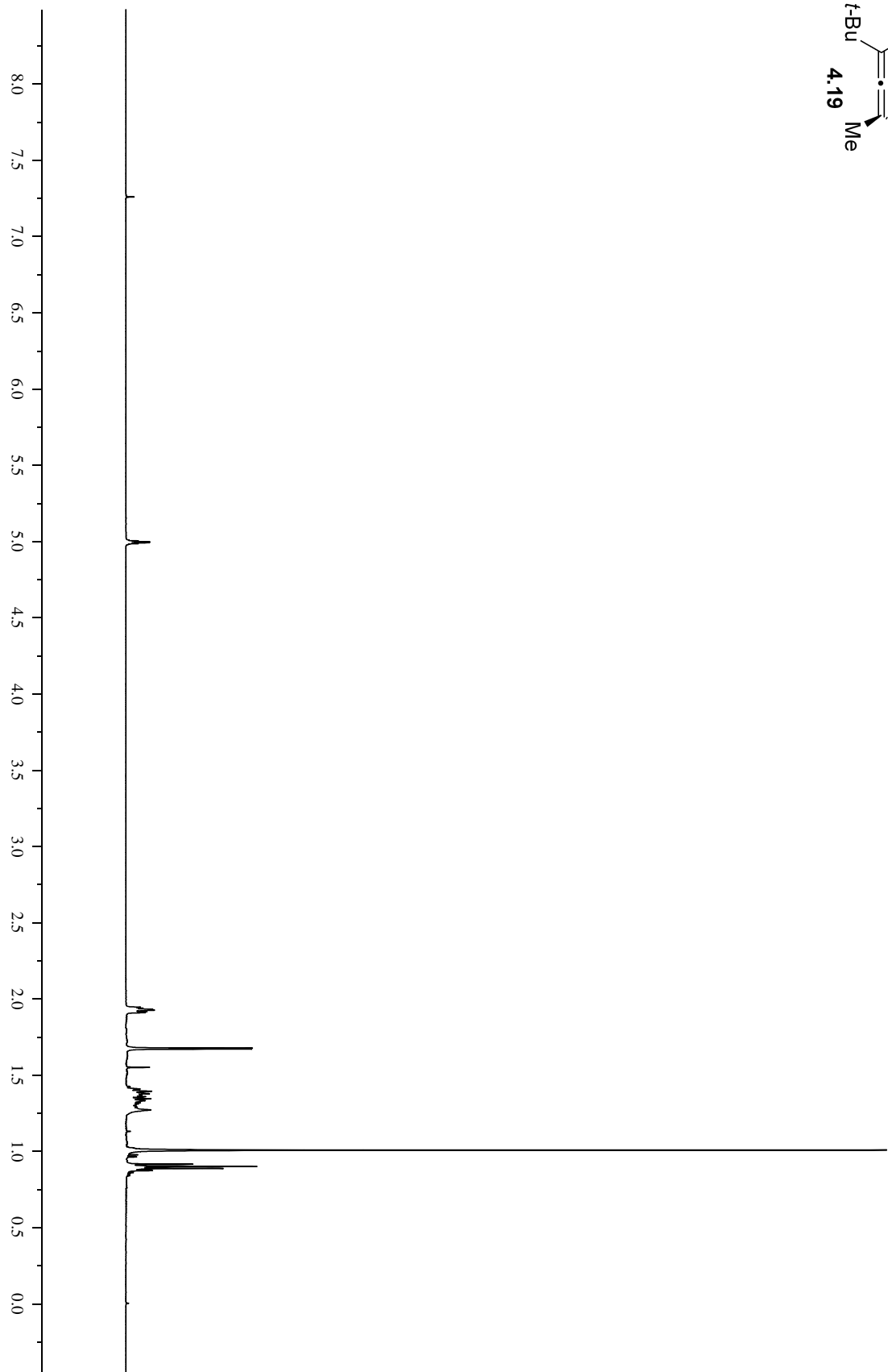
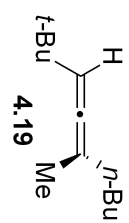


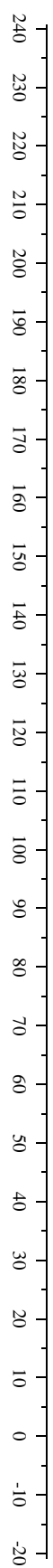


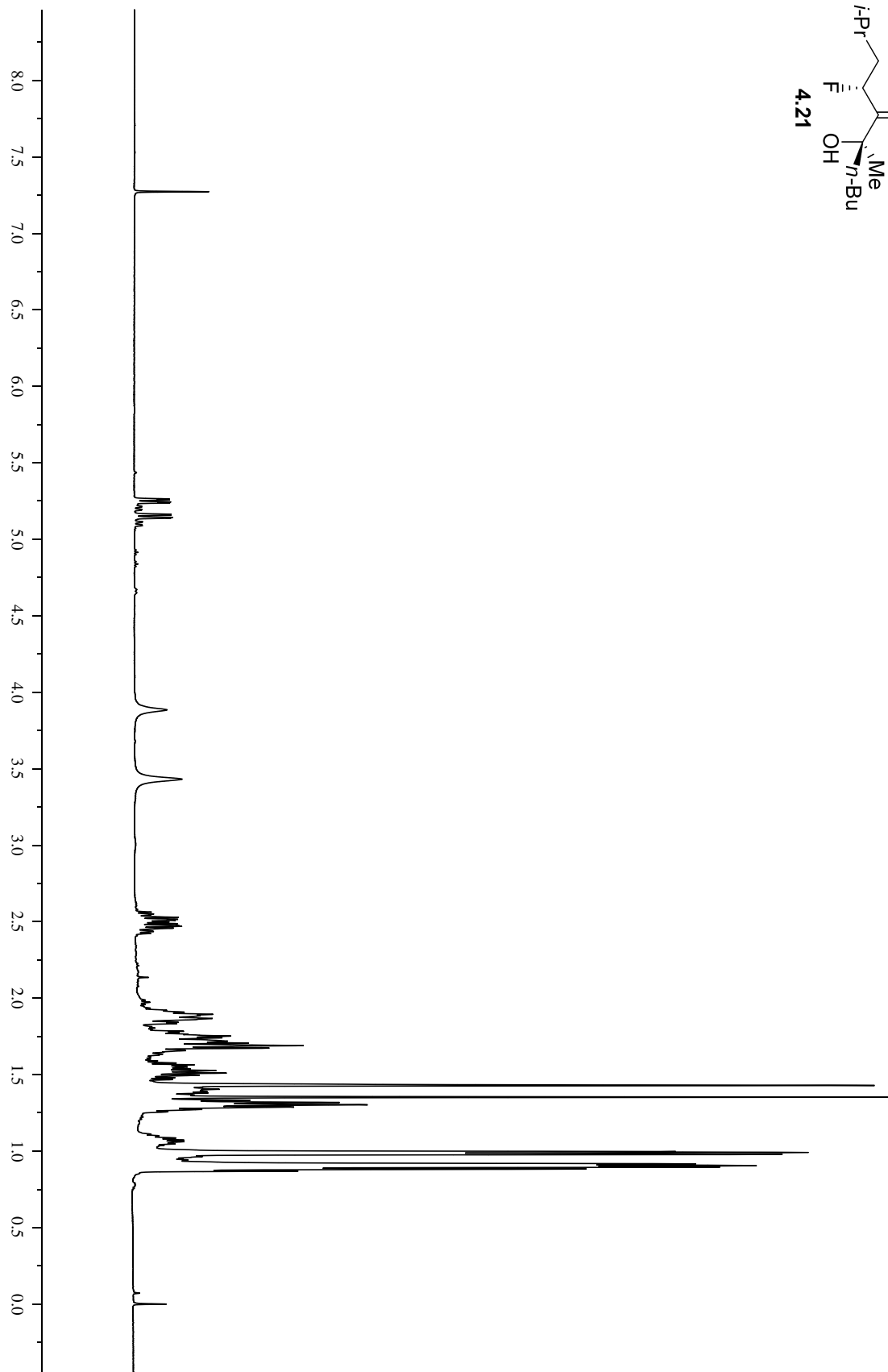
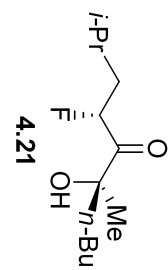


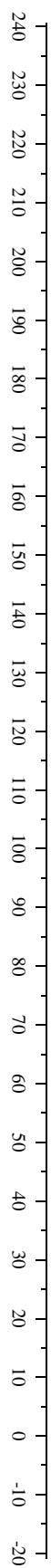
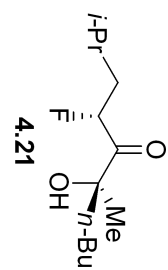


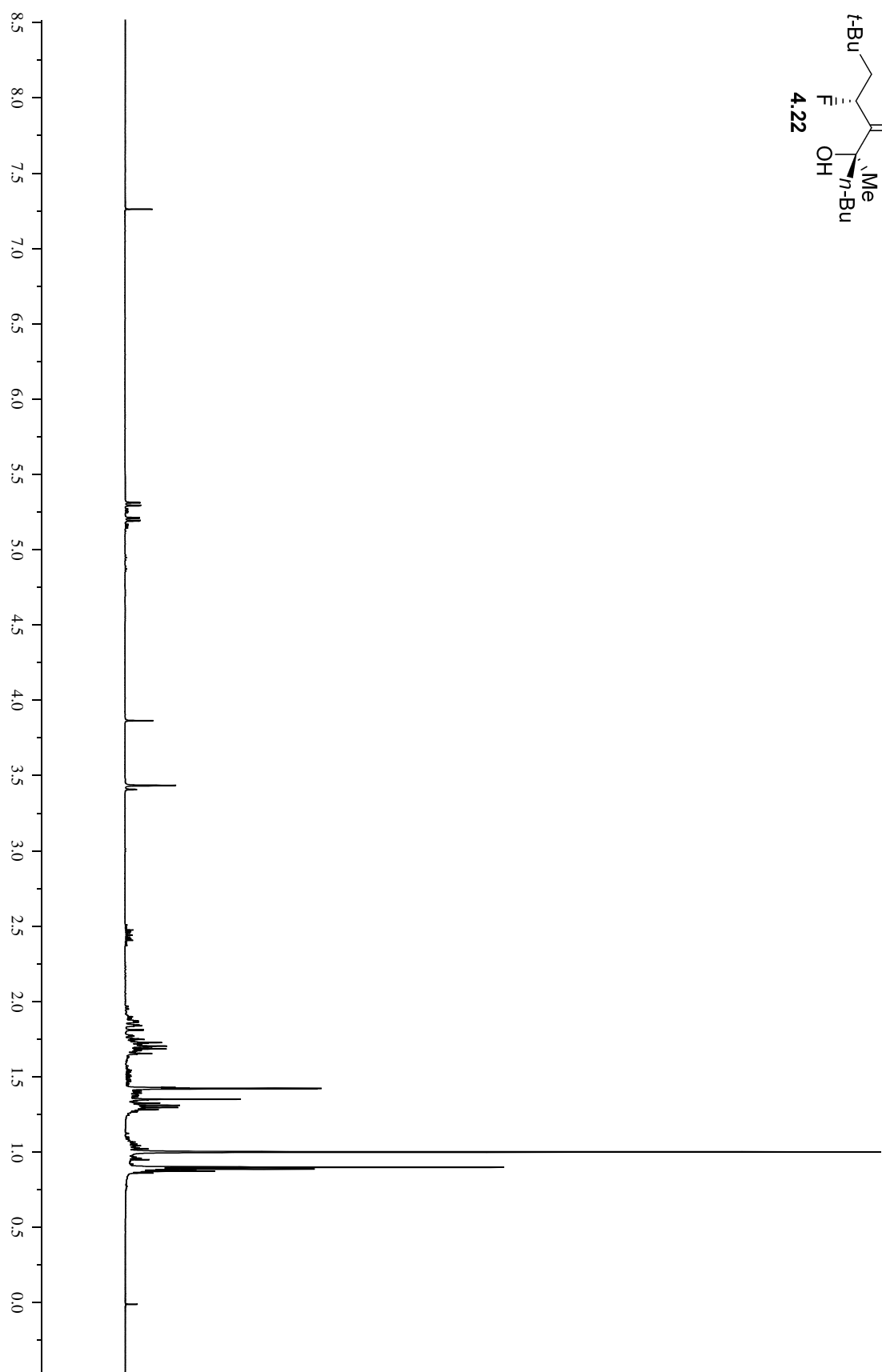
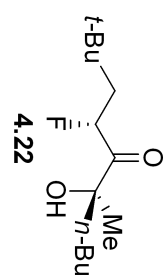


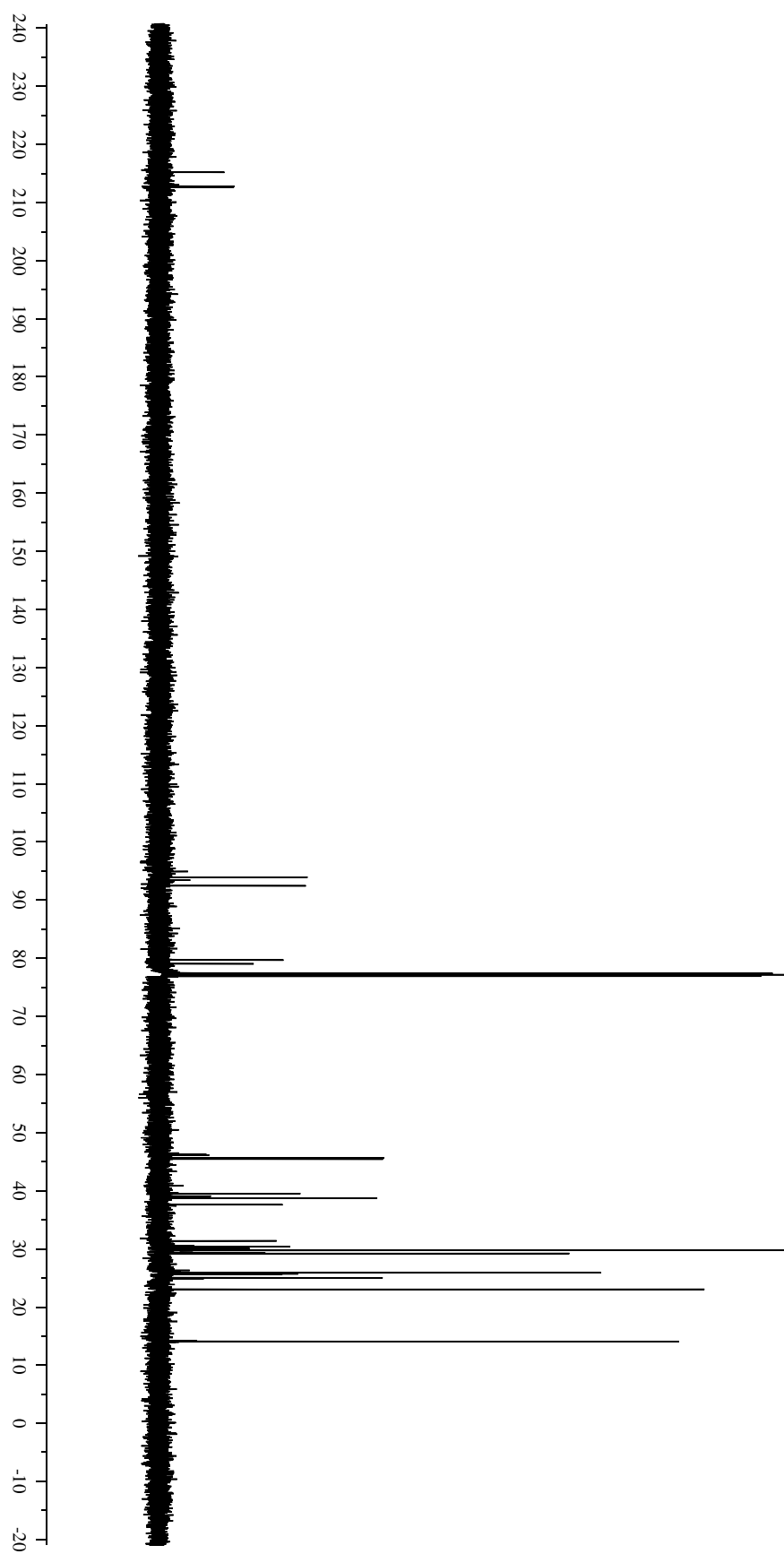
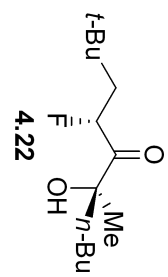


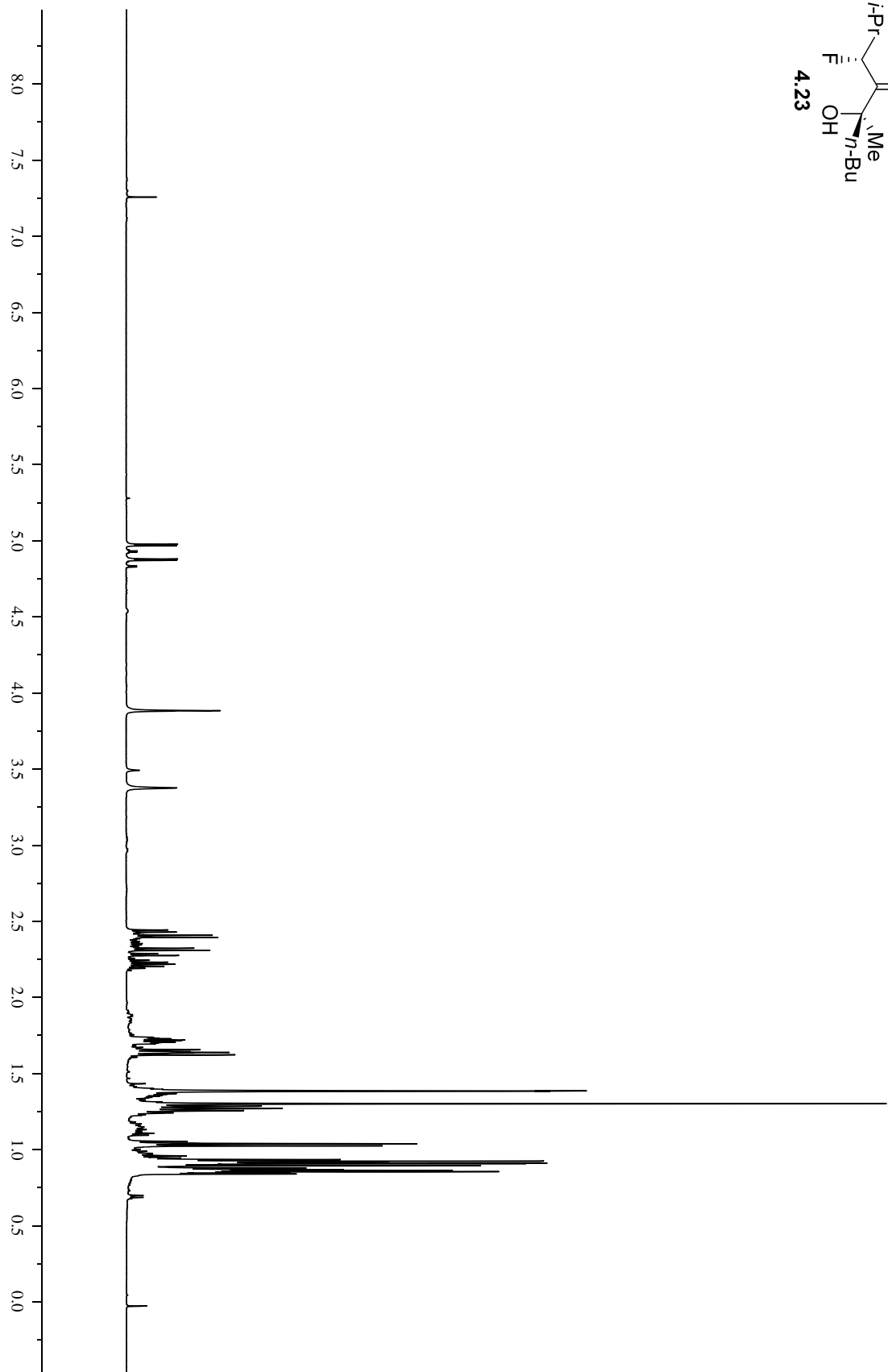
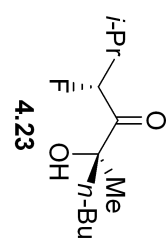


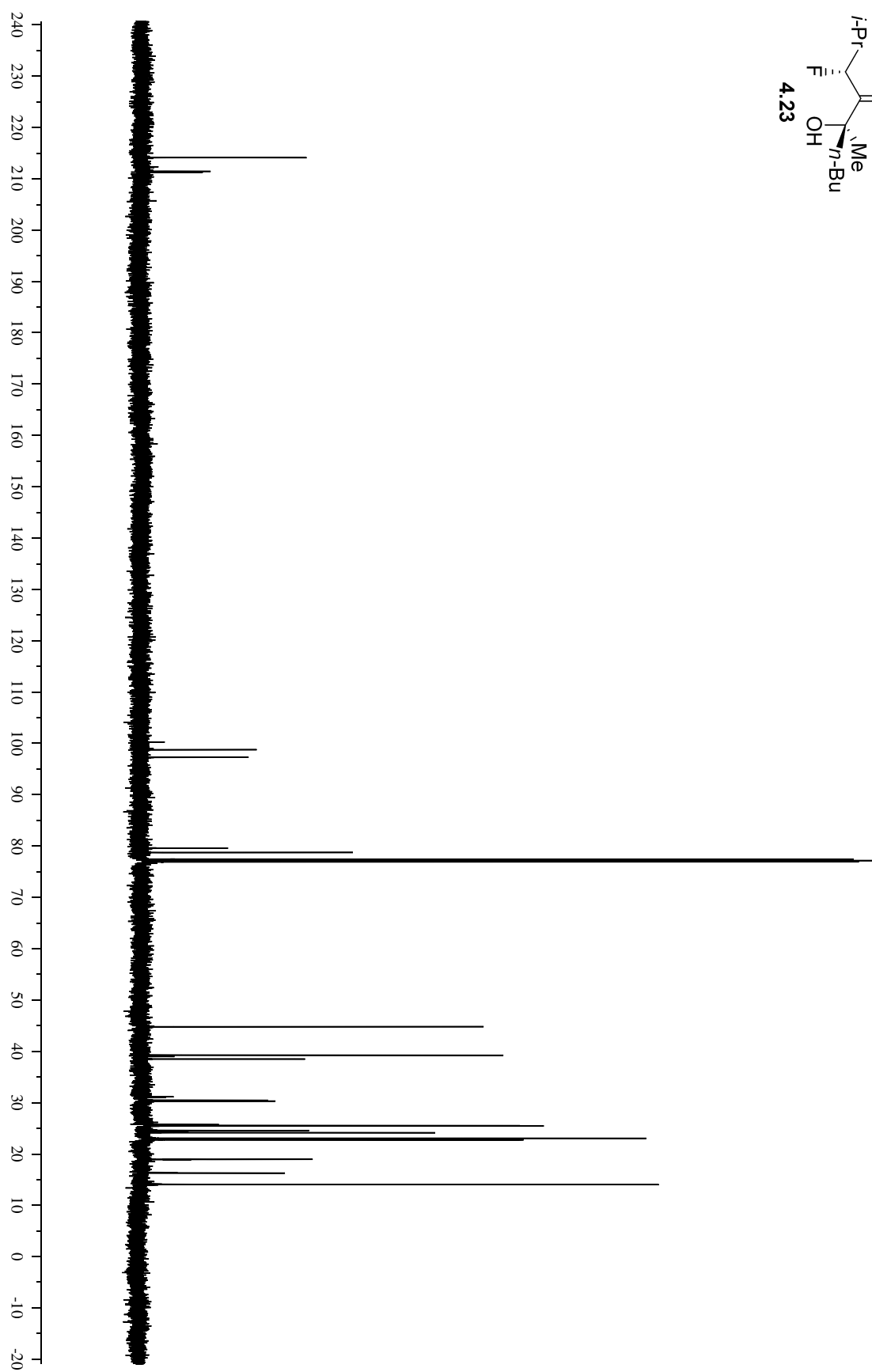
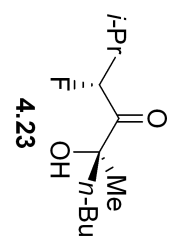


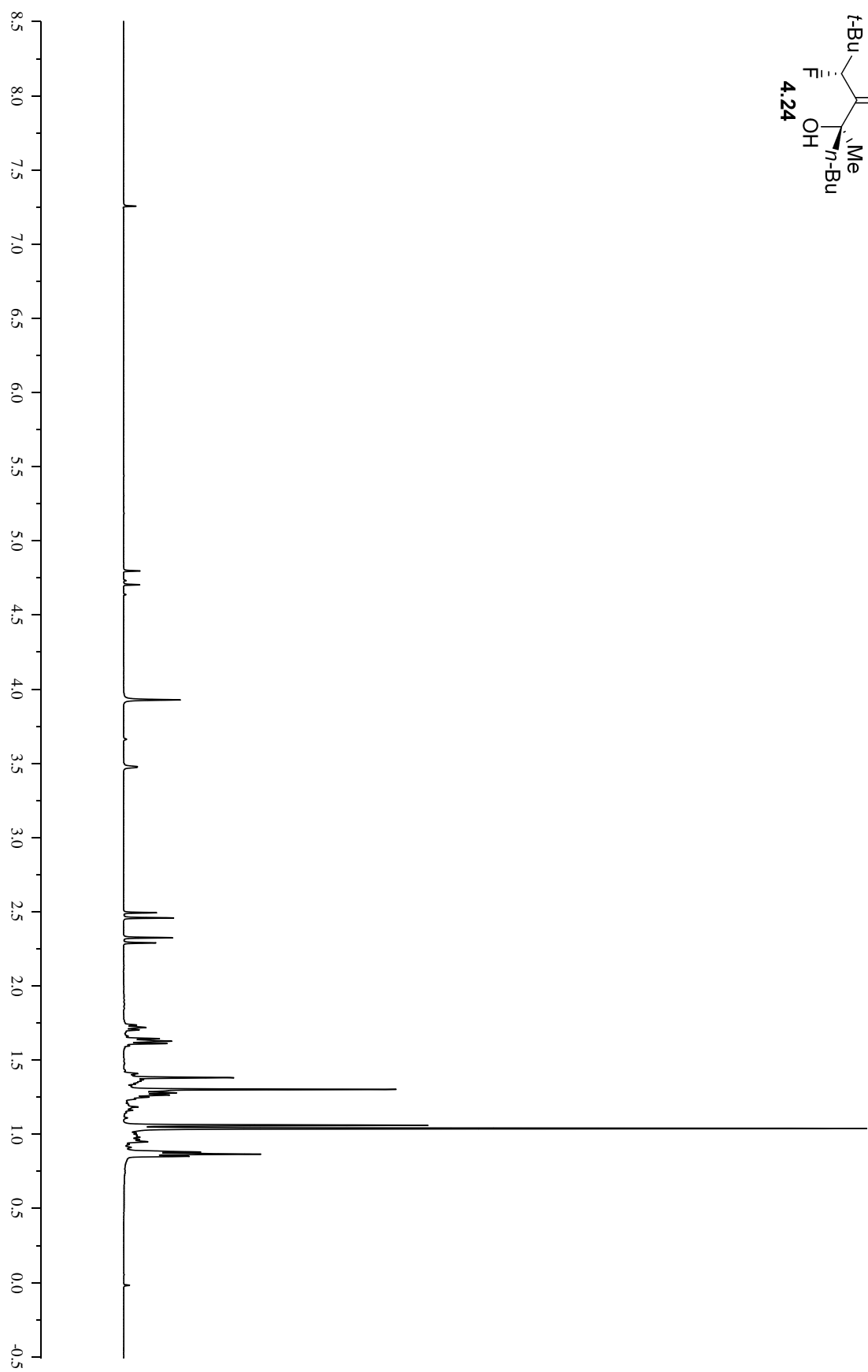
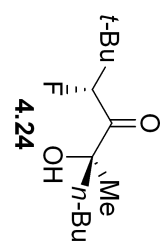


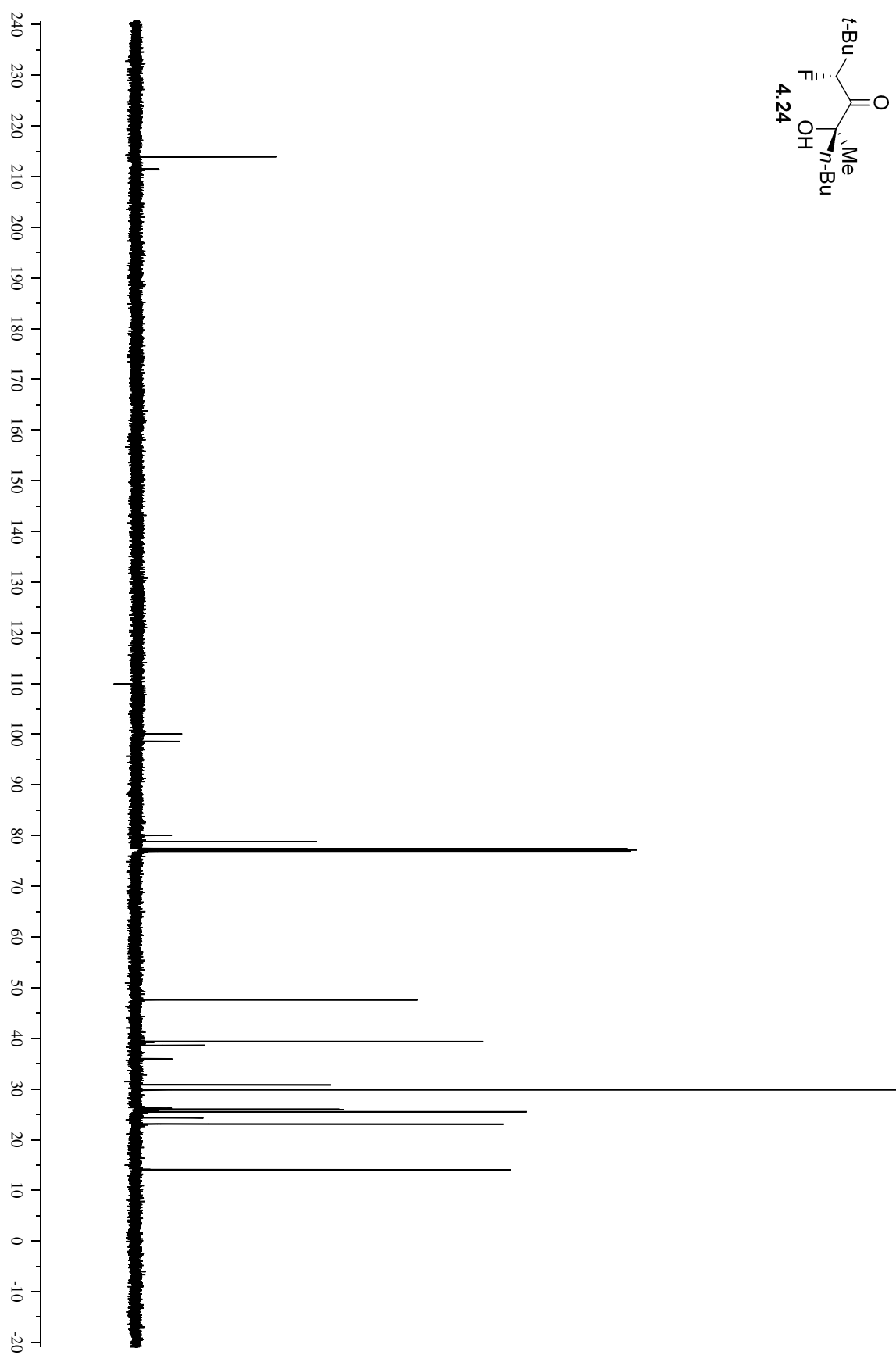
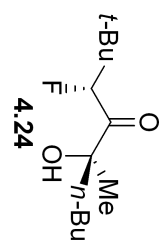


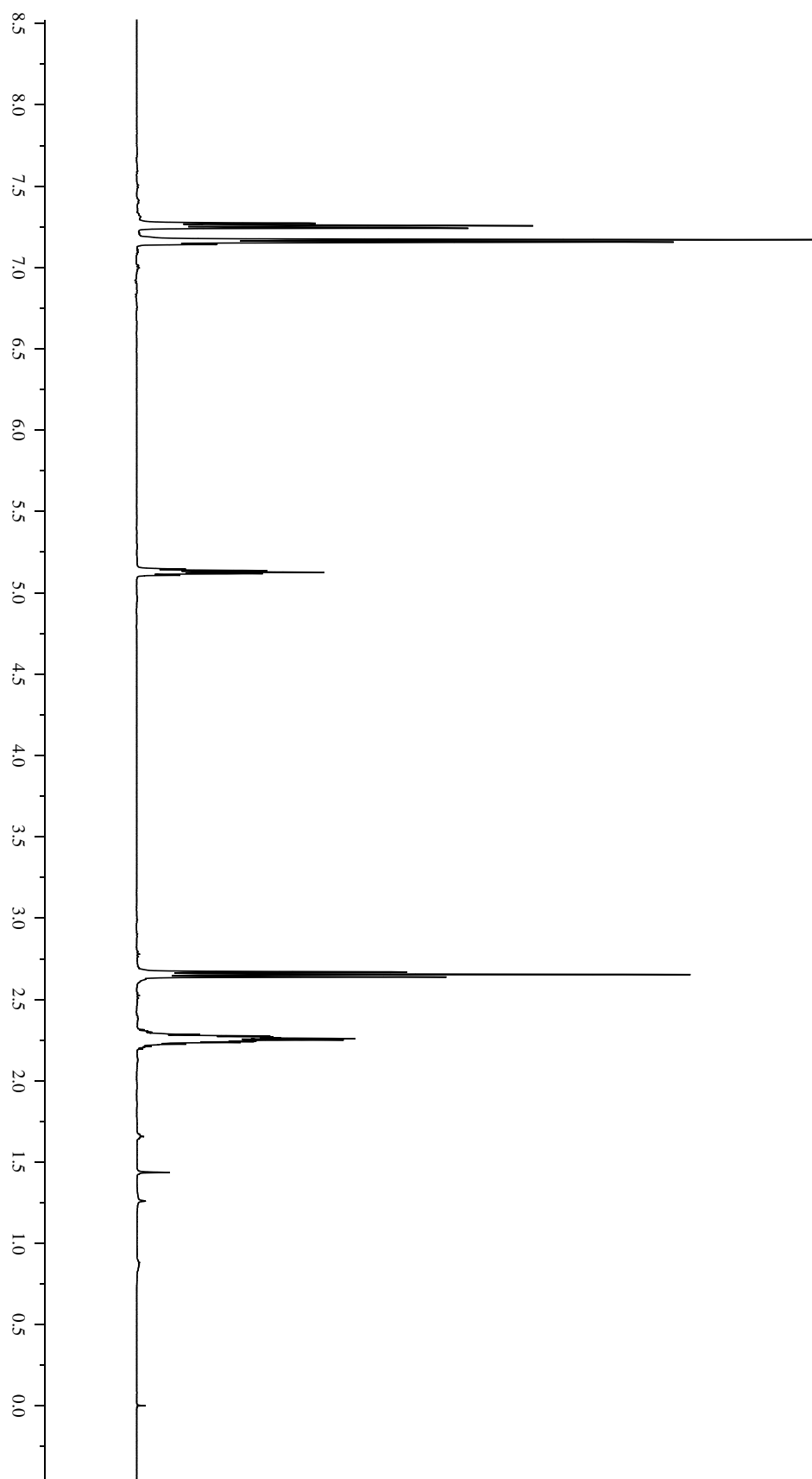
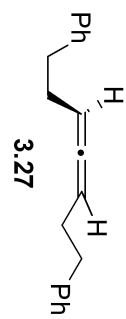


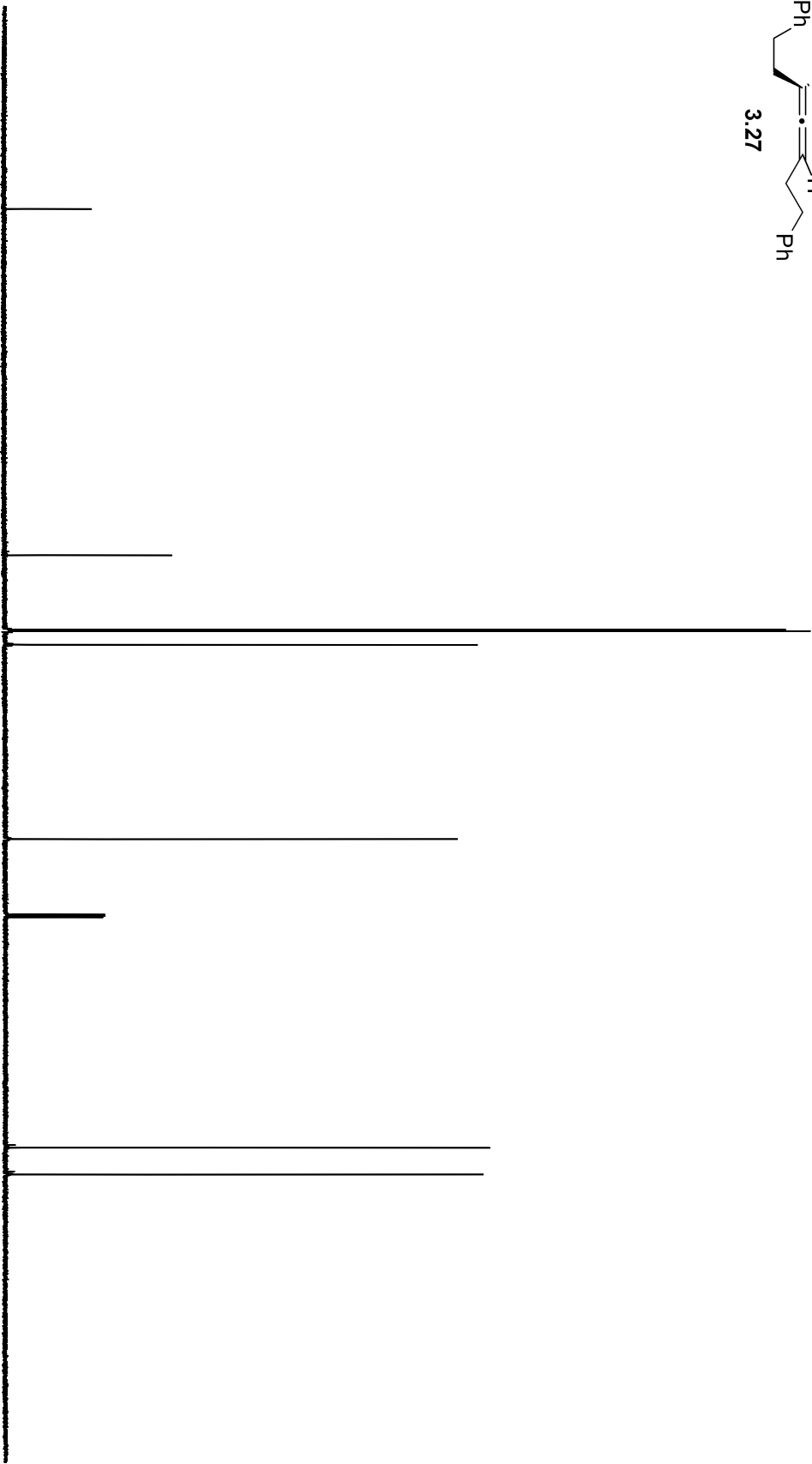


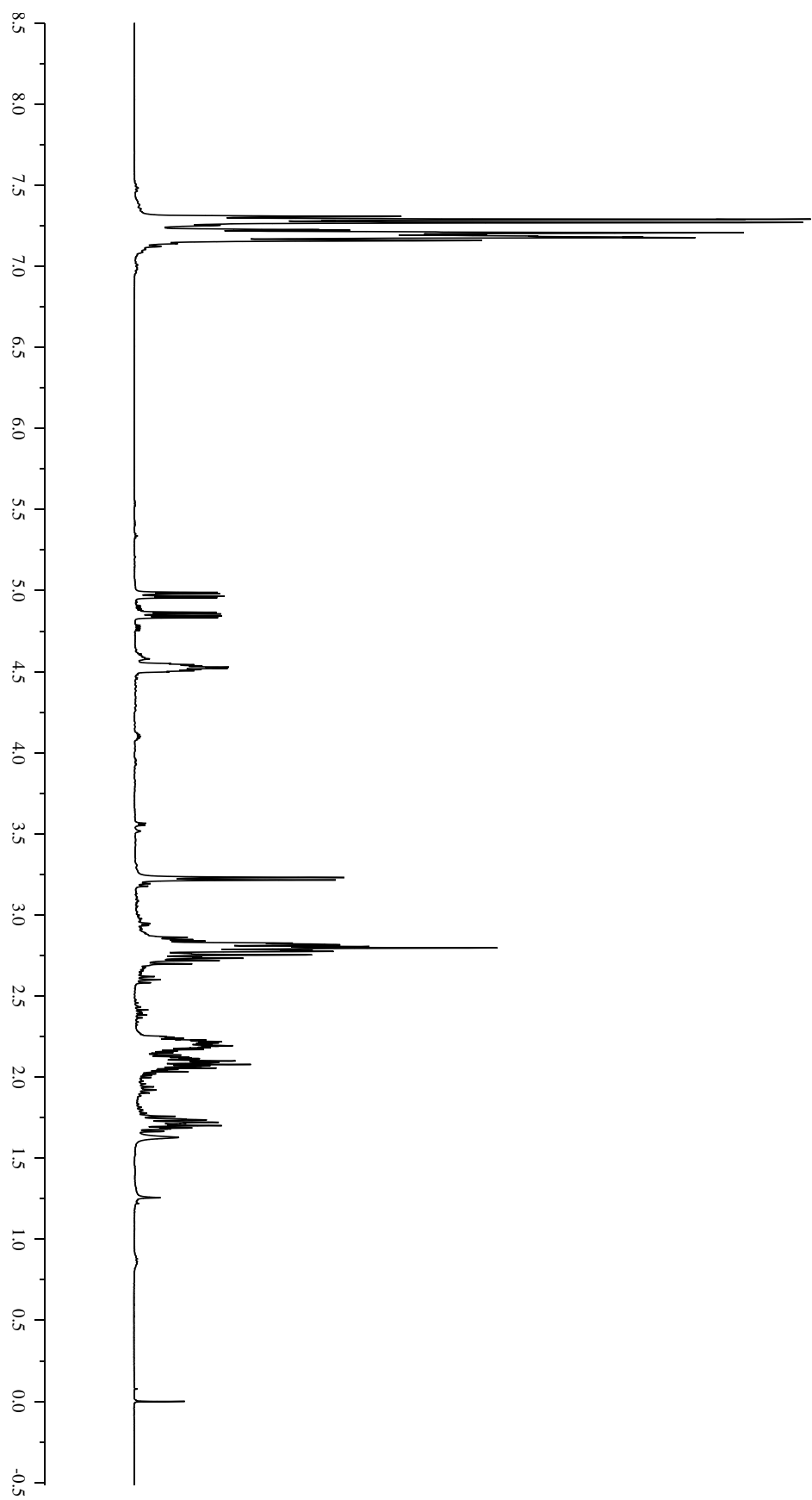
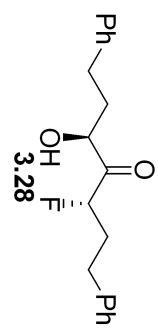


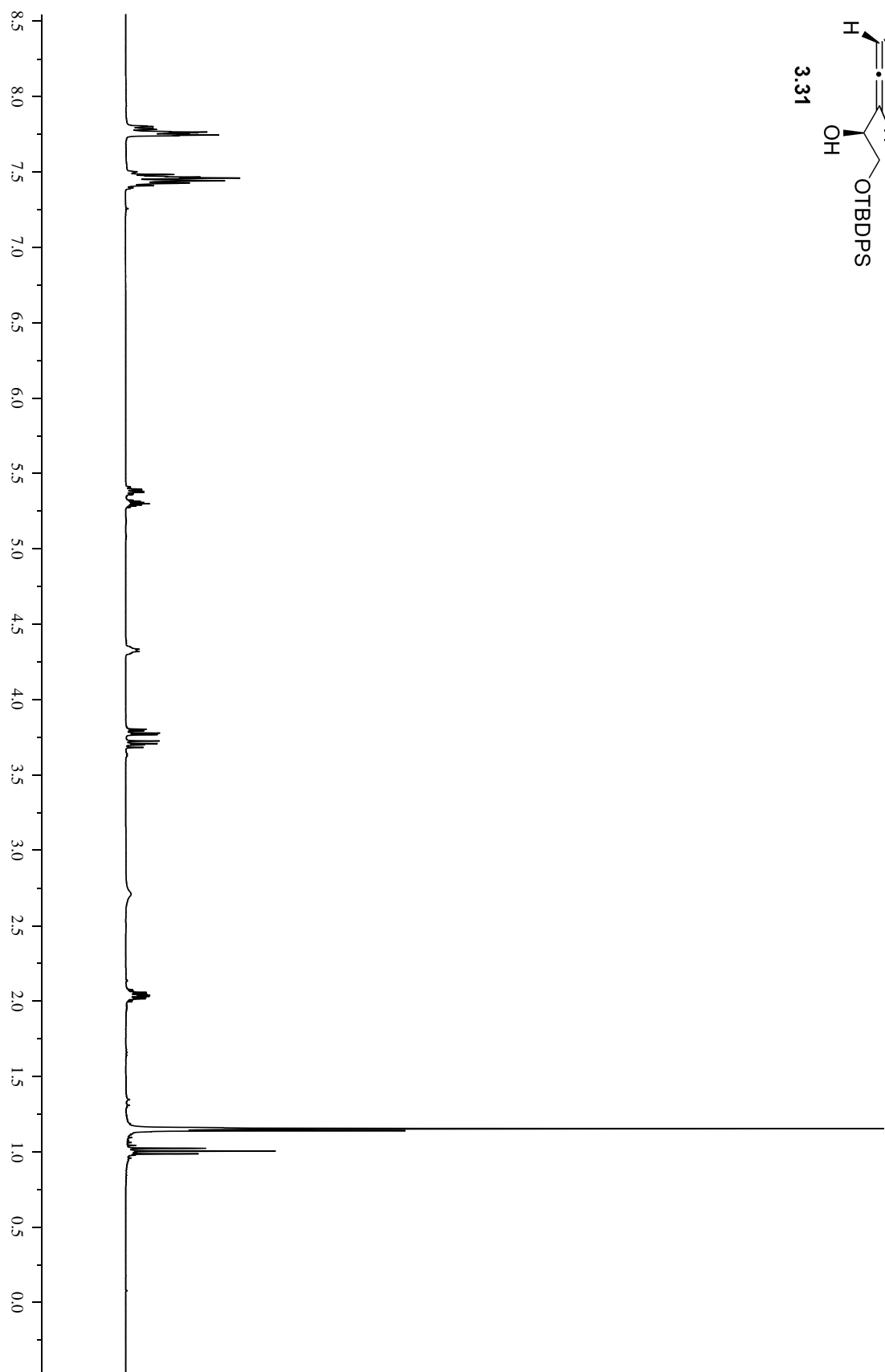
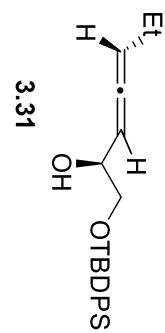


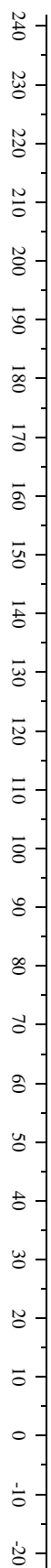
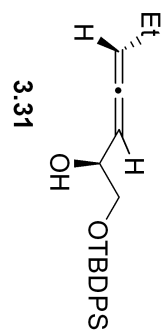


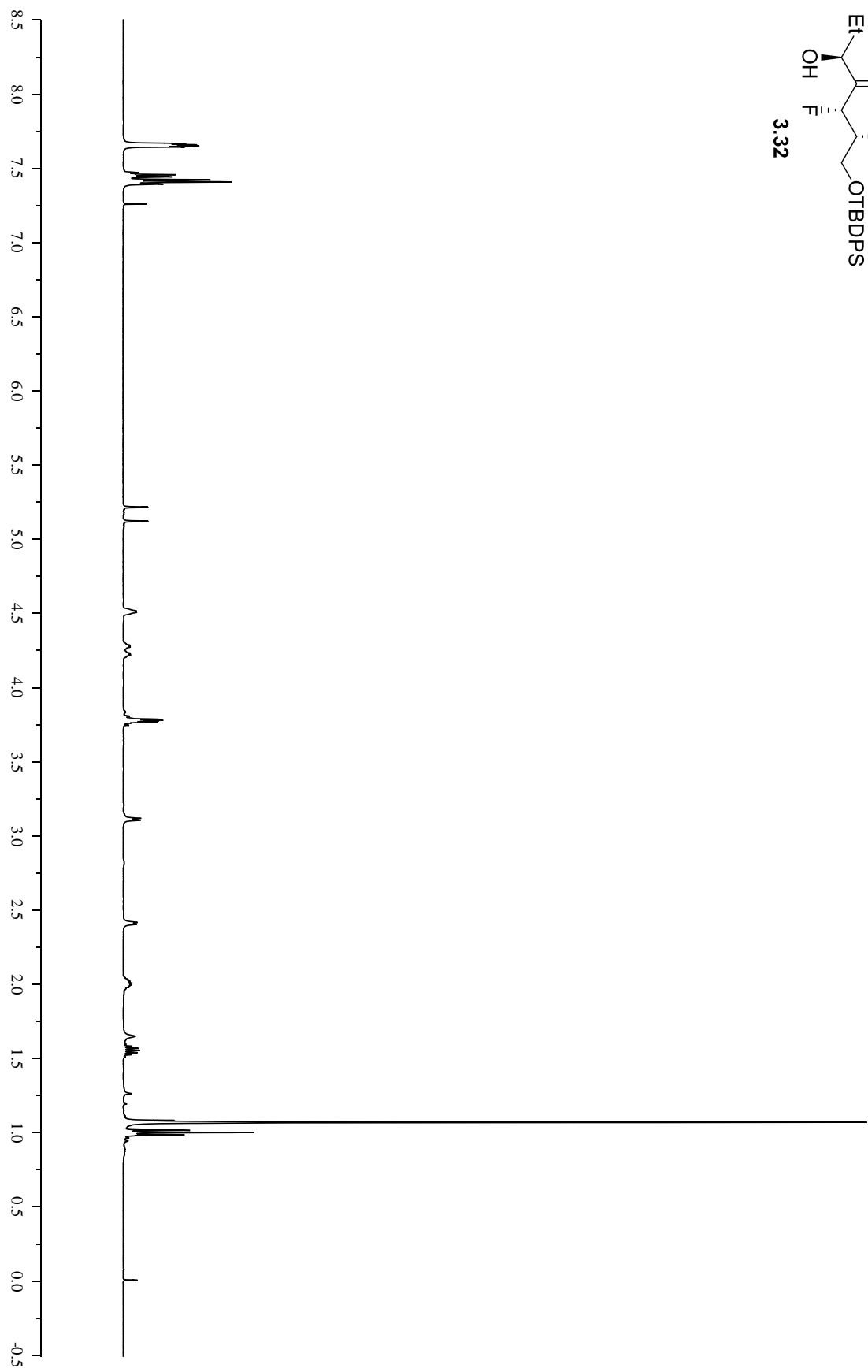
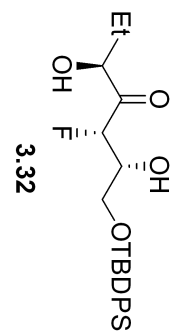


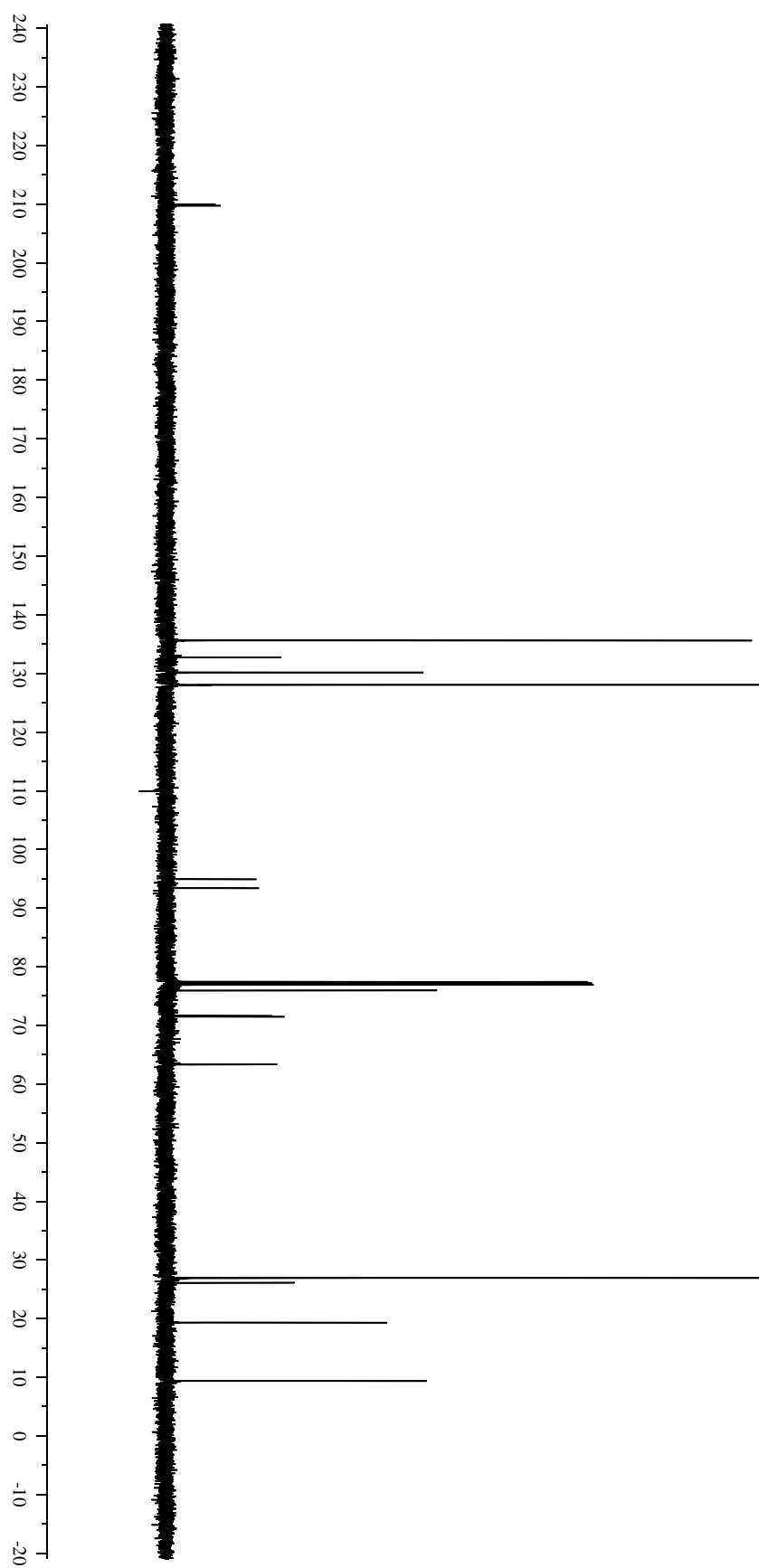
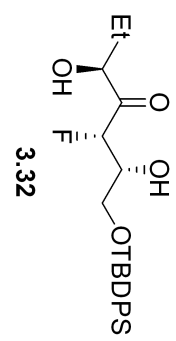


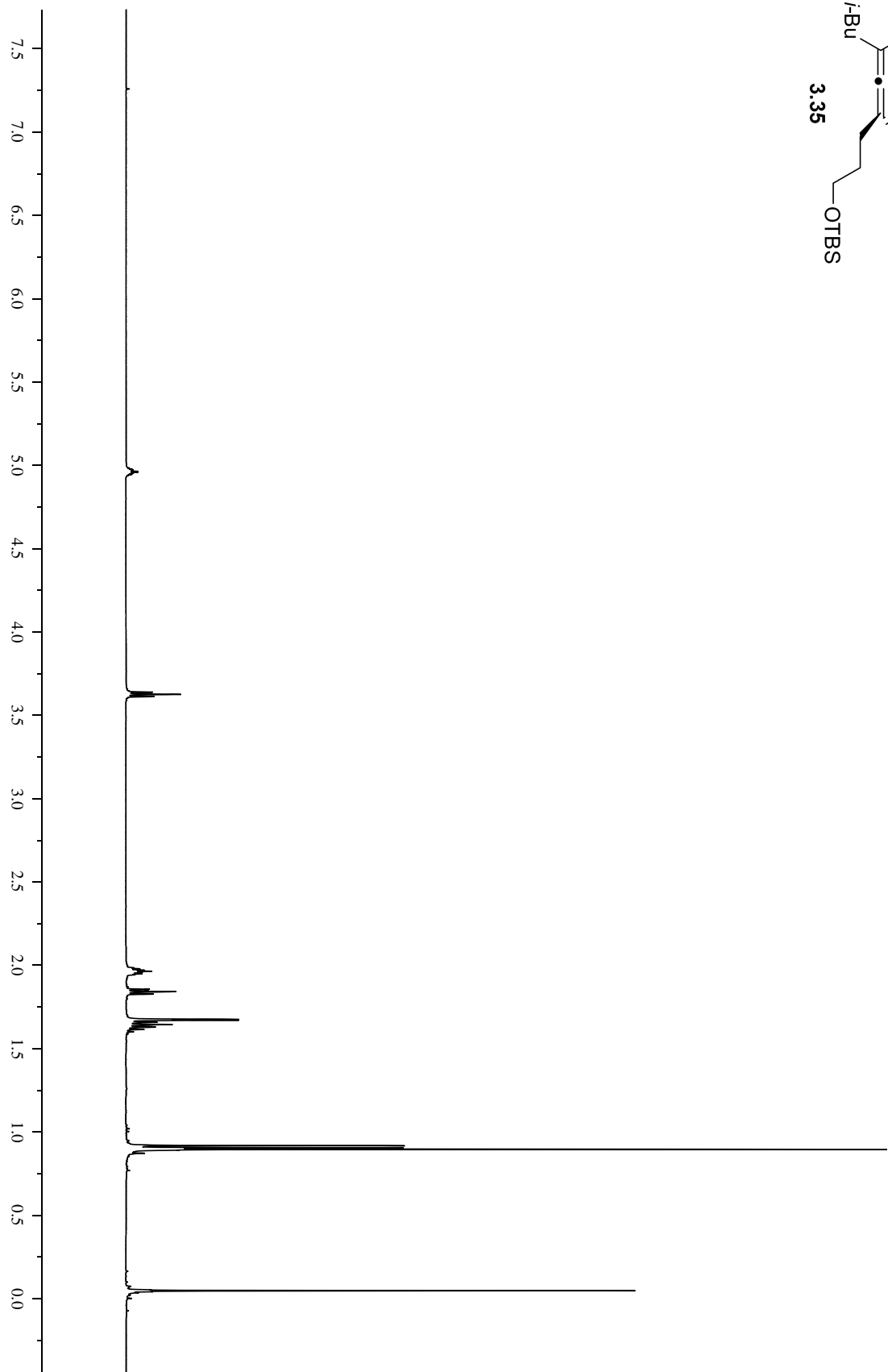
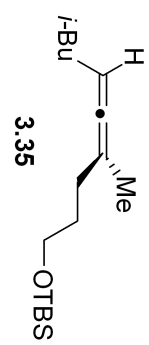


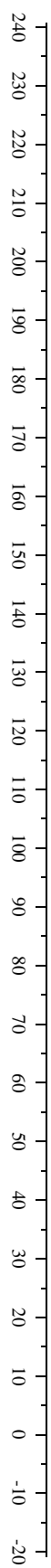
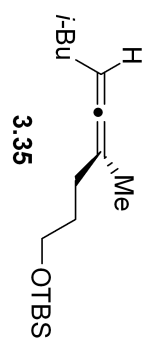


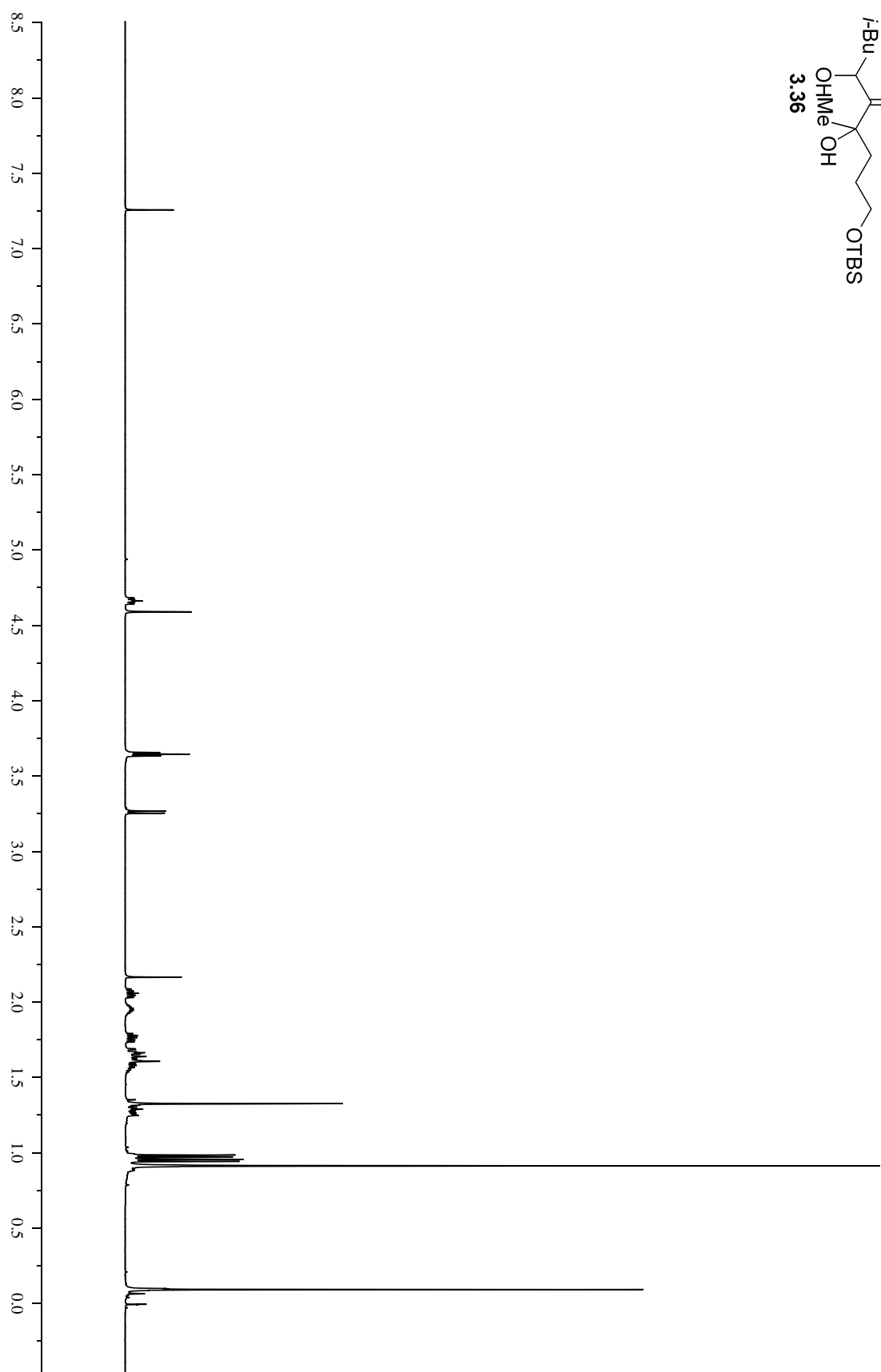
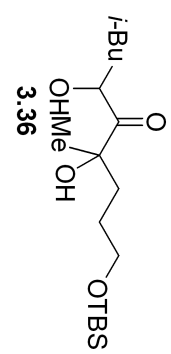


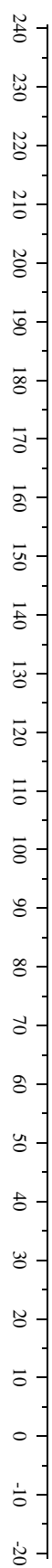
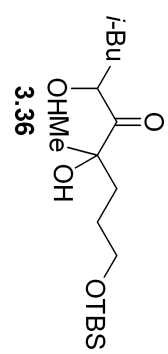


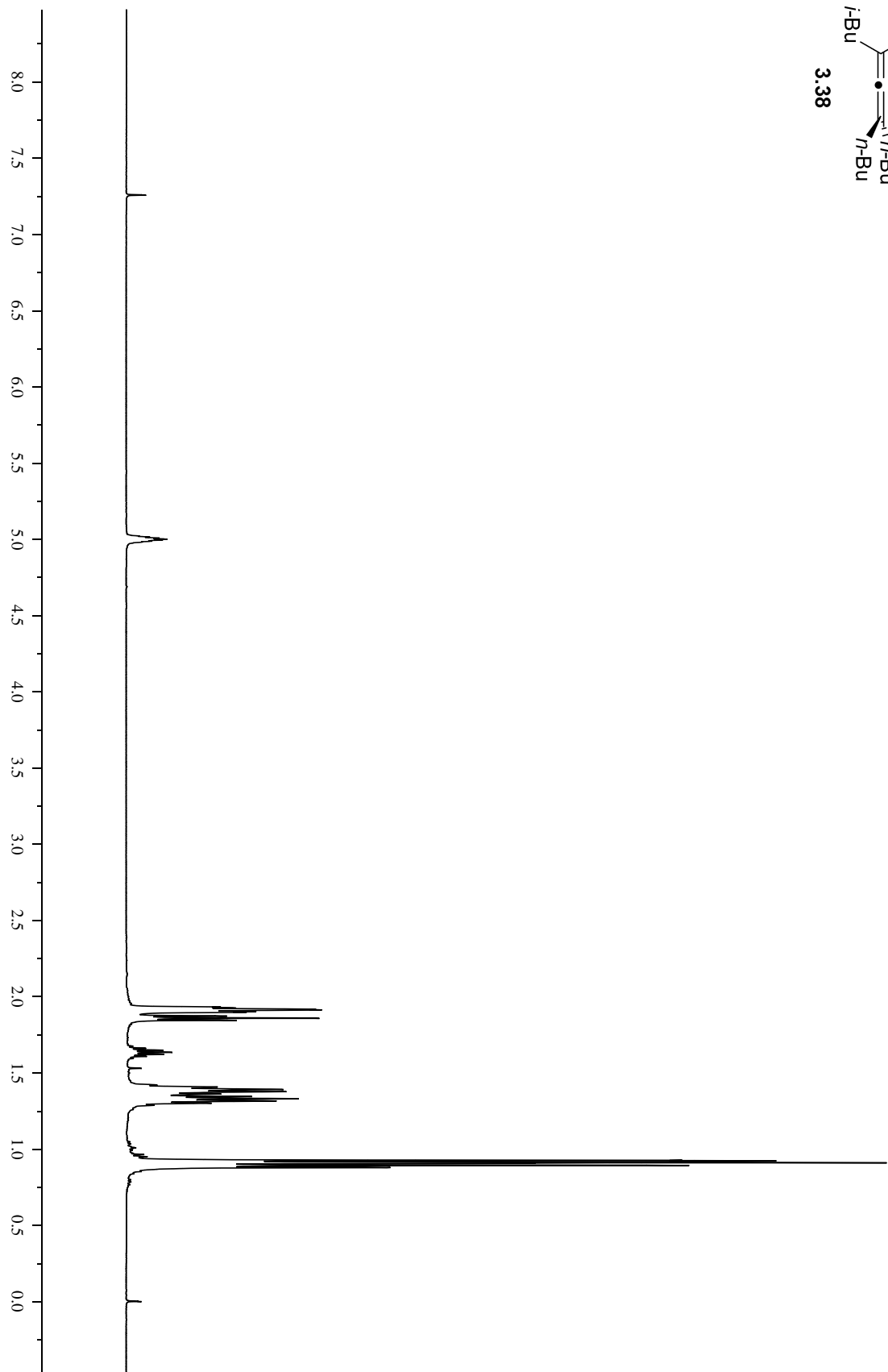
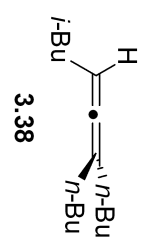


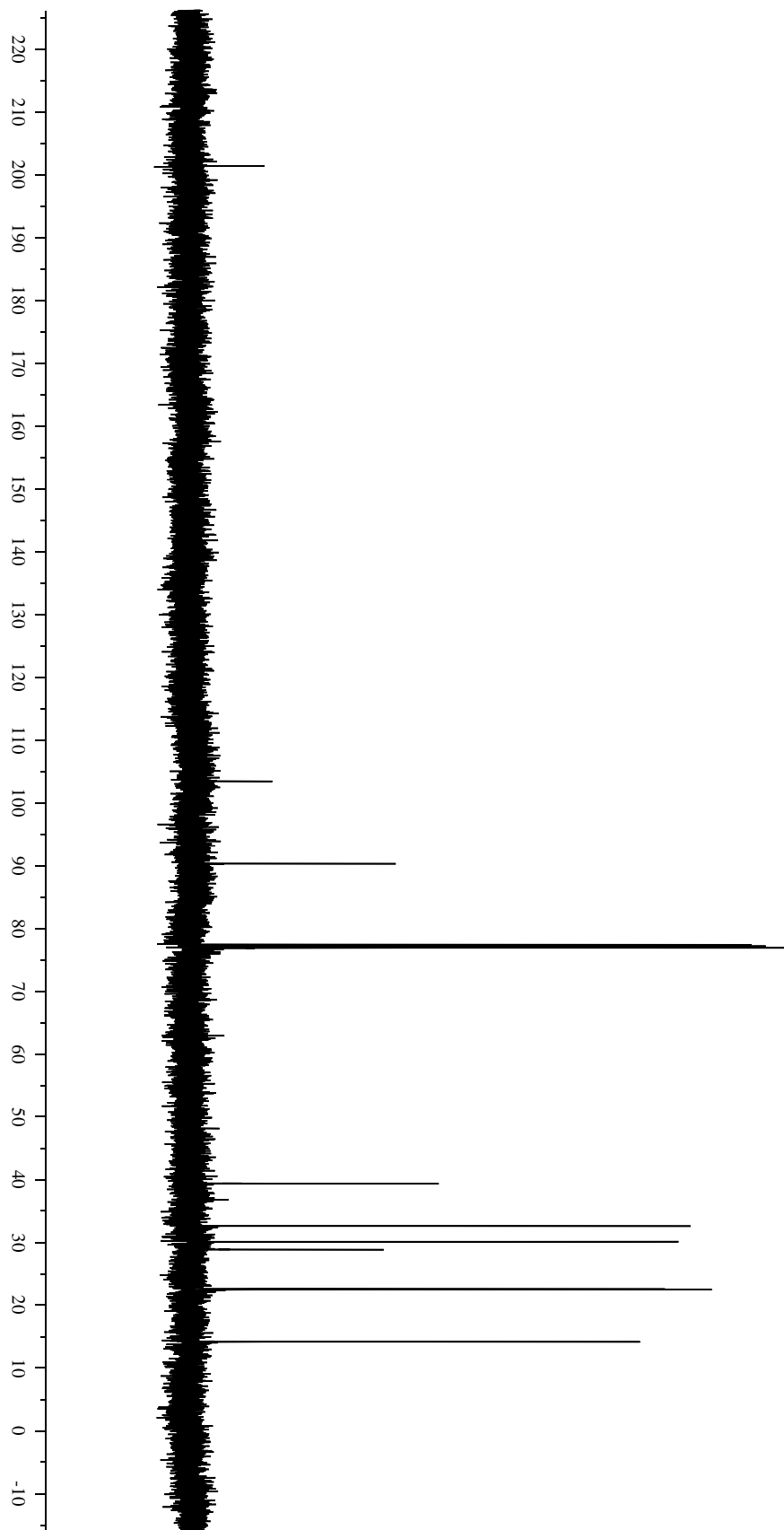
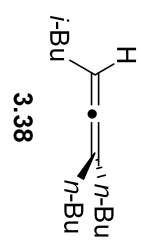


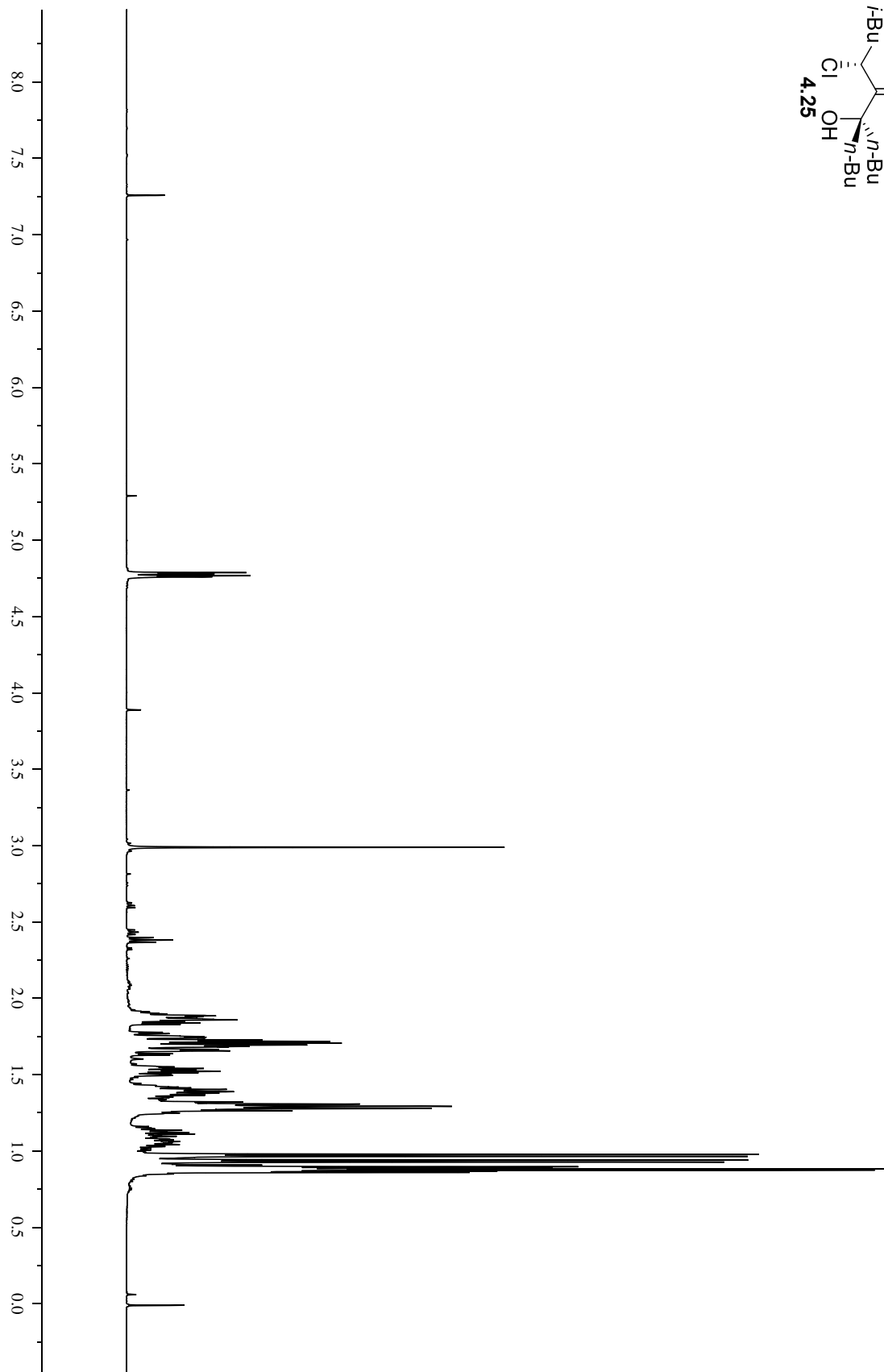
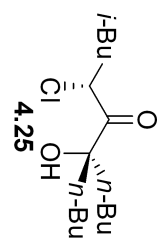


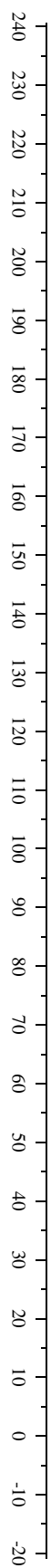
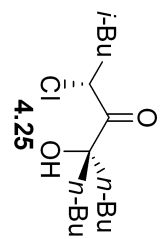


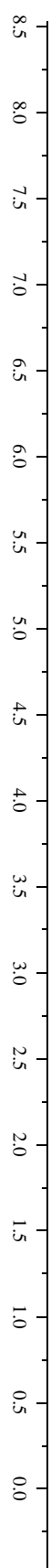
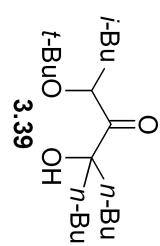


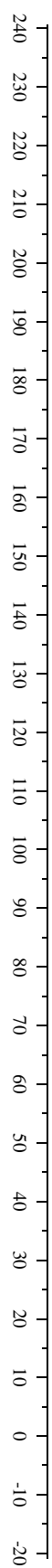
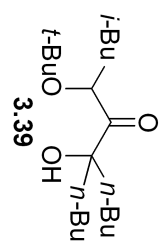


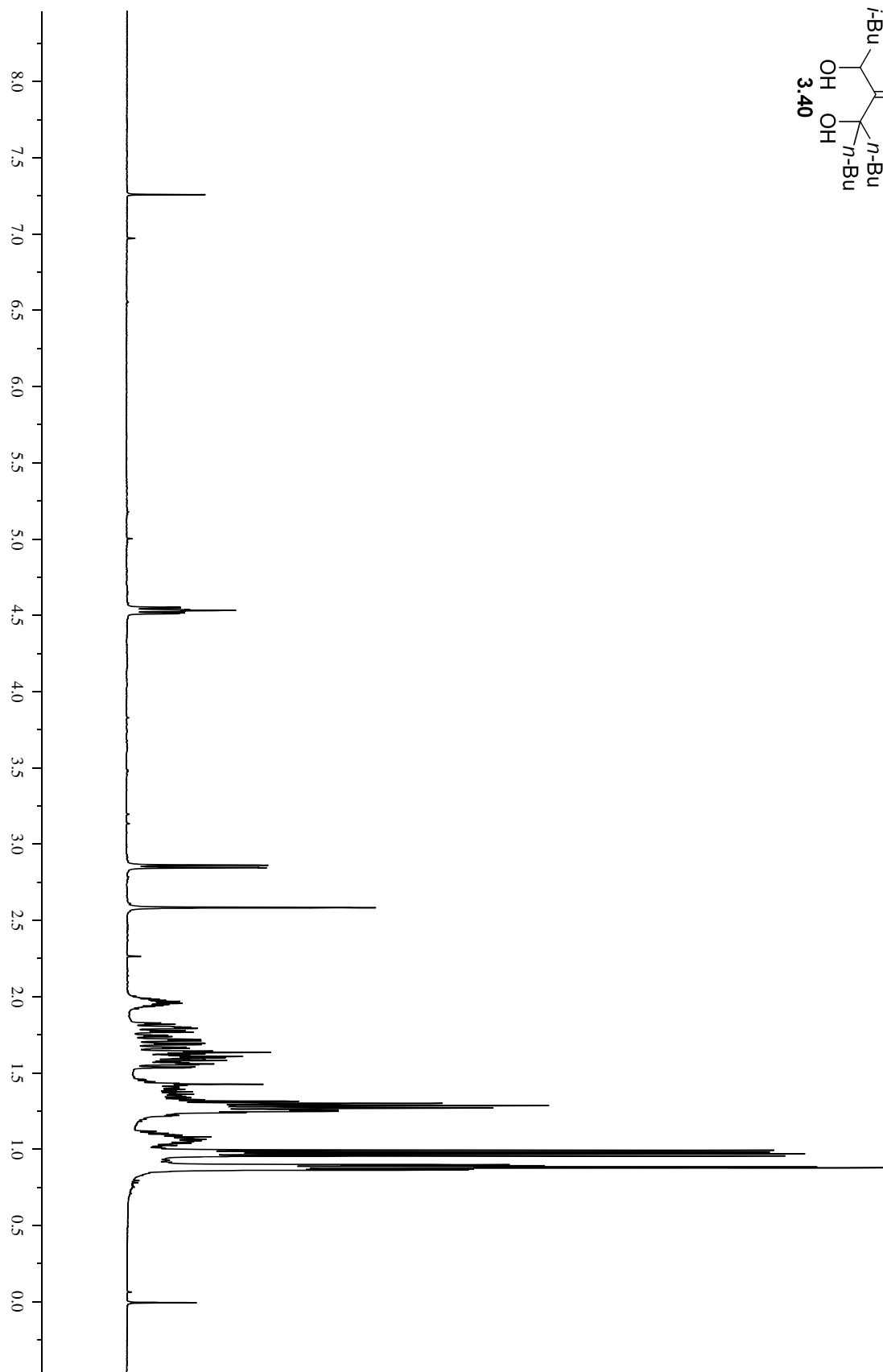
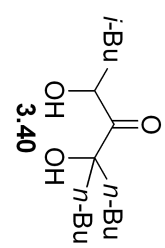


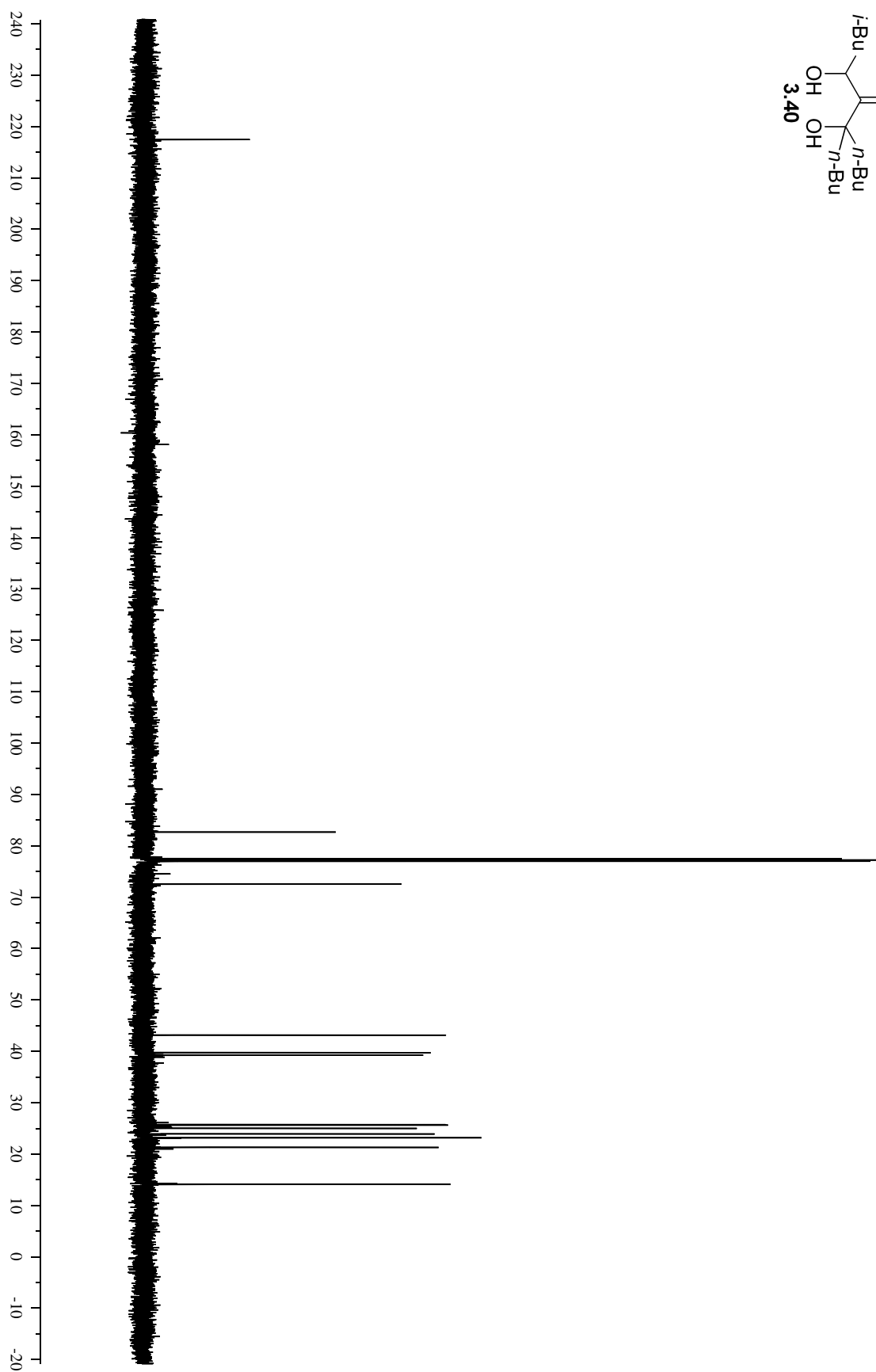
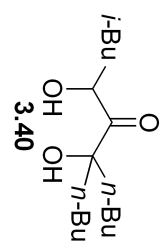


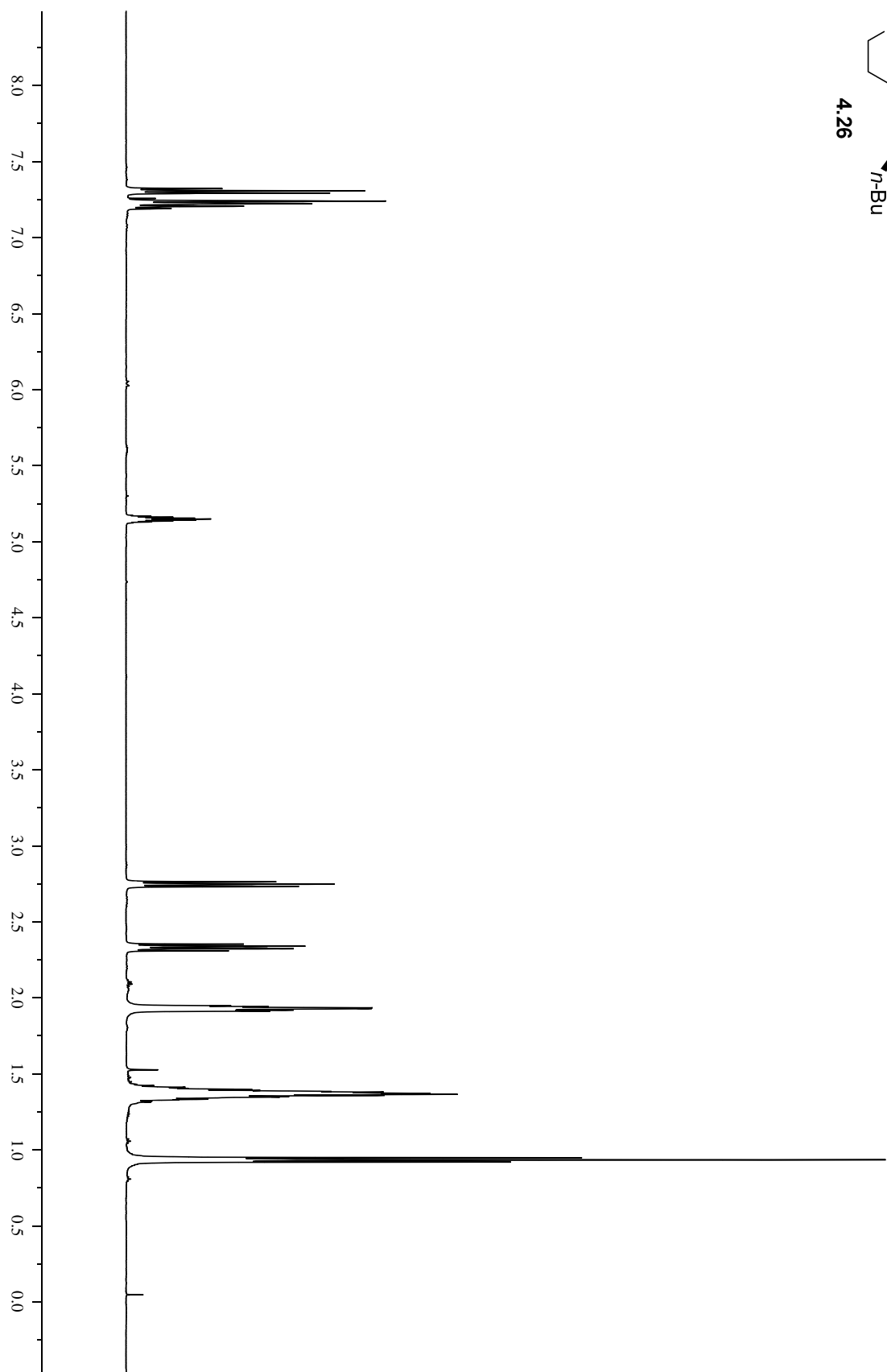
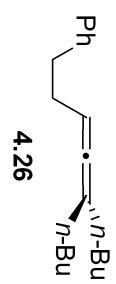


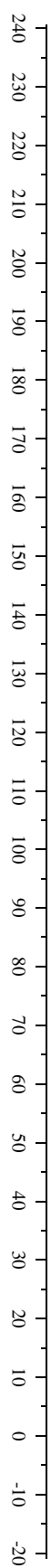
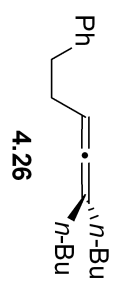


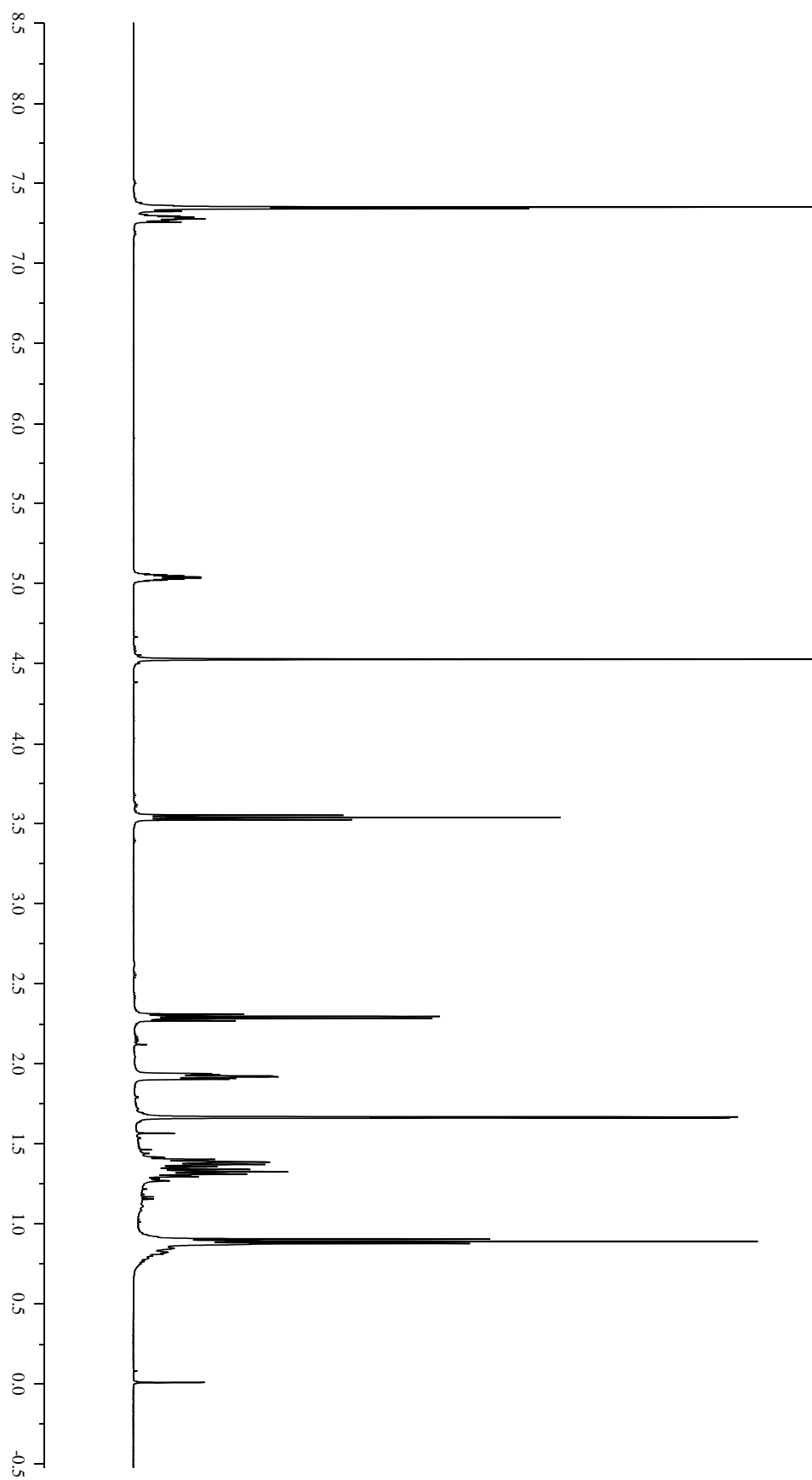
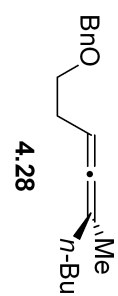


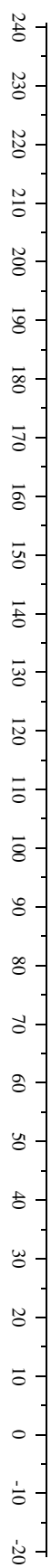
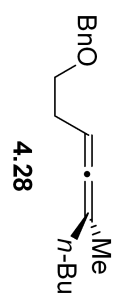


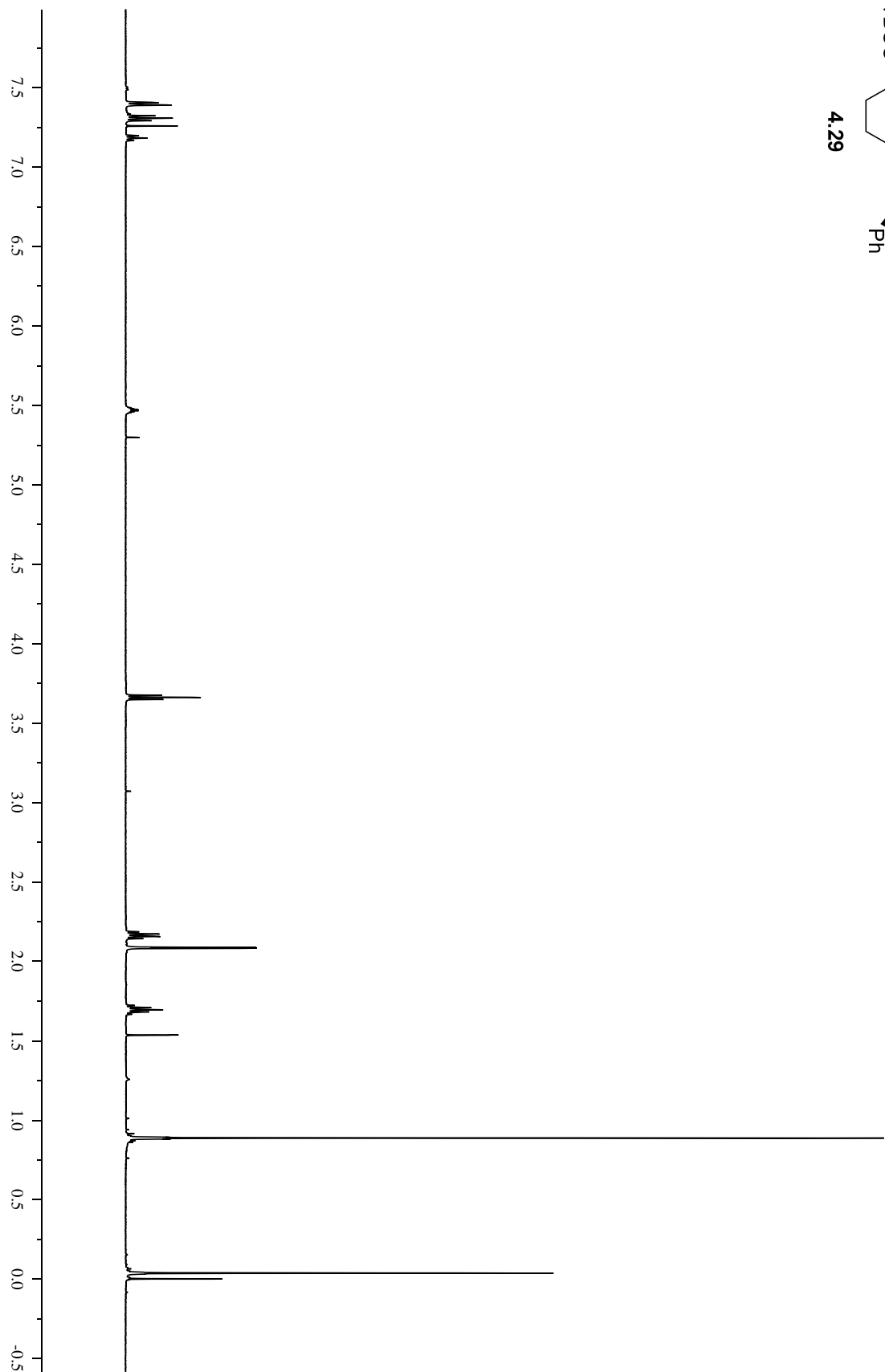
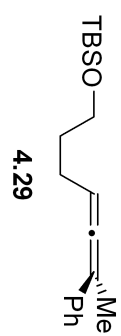












CC(C)(C)C(C)C/C=C/[C@H](C)C1=CC=CC=C1
4.29

